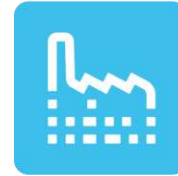




ICEBE
IMAGINEERING
NATURE



Industrial Plant
Engineering and
Application of
Digital Methods

DISSERTATION

**From Digital Model to Digital Predictive Twin:
Development of a digital framework for the creation of
virtual representations in the process development
of energy technologies**

carried out for the purpose of obtaining the degree of

Doctor technicae (Dr. techn.),

submitted at TU Wien, Faculty of Mechanical and Industrial Engineering

Institute of Chemical, Environmental and Bioscience Engineering, by

Dipl.-Ing. Martin Hammerschmid

Mat. Nr.: 01325871

under the supervision of

Ing. Dipl.-Ing. Dr.techn. Stefan Müller

and co-supervision of

Univ.Prof. Dipl.-Ing. Dr.techn. Hermann Hofbauer

Vienna, January 2024

reviewed by

Ao. Univ.Prof. DI Dr.techn. Martin Kozek

Institute of Mechanics & Mechatronics

TU Wien

Getreidemarkt 9/325, 1060 Vienna

Univ.Prof. DI Dr.techn. Tobias Pröll

Institute of Chemical & Energy Engineering

BOKU Wien

Muthgasse 107/I, 1190 Vienna

Imprint

© Martin Hammerschmid, 2024,
all rights reserved

martin.hammerschmid@tuwien.ac.at
Institute of Chemical, Environmental and Bioscience Engineering
TU Wien
Getreidemarkt 9/166
1060 Vienna
Austria

Dissertation:
“From Digital Model to Digital Predictive Twin: Development of a digital framework for the creation of virtual representations in the process development of energy technologies”

ORCID: 0000-0002-1155-926X

Printed by:
Institute of Chemical, Environmental and Bioscience Engineering in Vienna, January 20th, 2024
Reproduction requires color print

Distributed by:
TU Wien
Institute of Chemical, Environmental and Bioscience Engineering
Getreidemarkt 9/166
1060 Vienna
Austria

+43 1 58801 166856
www.vt.tuwien.ac.at

Affidavit

I declare in lieu of oath, that I wrote this thesis and performed the associated research myself, using only literature cited in this volume. If text passages from sources are used literally, they are marked as such.

I confirm that this work is original and has not been submitted elsewhere for any examination, nor is it currently under consideration for a thesis elsewhere.

I acknowledge that the submitted work will be checked electronically-technically using suitable and state-of-the-art means (plagiarism detection software). On the one hand, this ensures that the submitted work was prepared according to the high-quality standards within the applicable rules to ensure good scientific practice "Code of Conduct" at the TU Wien. On the other hand, a comparison with other student theses avoids violations of my personal copyright.

City and Date

Signature

Danksagung

An dieser Stelle möchte ich mich bei allen Personen bedanken, die mich auf dem Weg bis hin zum Abschluss der vorliegenden Dissertation unterstützt, motiviert und inspiriert haben.

Allen voran möchte ich mich sehr herzlich bei meinen beiden Betreuern Stefan Müller und Hermann Hofbauer bedanken. Die Möglichkeit an vielen verschiedenen Forschungsprojekten mitzuarbeiten gekoppelt mit den vielen konstruktiven Diskussionen ermöglichte mir, mich fachlich als auch persönlich weiterzuentwickeln.

Weiters möchte ich mich bei allen Kolleginnen und Kollegen unseres Forschungsbereiches bedanken. Vielen Dank für die stets gute Zusammenarbeit, bei der auch abseits der Arbeit Freundschaften entstanden sind. Ein besonderer Dank gilt meinem Kollegen Stefan Jankovic für den immer exzellenten fachlichen Austausch und für das Korrekturlesen meiner Arbeit.

Auch möchte ich mich bei allen Projektpartnern bedanken. Durch die Mitarbeit an diversen Forschungsprojekten in Kooperation mit einer Vielzahl an Firmenpartnern war es mir möglich, das geforderte Know-How in diesem Themenfeld aufzubauen.

Zu guter Letzt möchte ich mich bei meiner Familie bedanken die mich auf meinem ganzen Lebensweg bis hin zur Fertigstellung dieser Arbeit begleitet haben. Ganz besonders möchte ich mich bei dir, Christina, bedanken für die immerwährende Geduld, Motivation und dein Verständnis, dass du mir gegenüber während der letzten Jahre aufgebracht hast. Hervorheben möchte ich zuletzt die Geburt unseres Sohnes Emil, die mich im Endspurt dieser Arbeit nochmals beflügelt hat.

" Automation applied to an inefficient process magnifies the inefficiency. "

Bill Gates

Abstract

The climate crisis and the associated need for the development and optimization of climate-friendly and efficient energy technologies requires the digitization of the energy sector. Furthermore, digitization can help to speed up the energy transition process by forming a smart interconnected energy system linkage energy provider, distributor and consumer. In order to ensure sustainable digitization in the energy sector, it is necessary to start already at the process development stage. Consequently, a digital reflection of the physical facility, called virtual representation shall be developed along the process development life-cycle besides the physical facility itself. For the development of virtual representations, a standardized framework is needed to define the requirements for virtual representations along the process development of energy technologies. Different frameworks exemplary with the focus on manufacturing, pharmaceutical industry, product life-cycle management and robotics are available in the literature. However, no framework with focus on the development of energy technologies exists.

For this reason, in this doctoral thesis, a framework for the development of virtual representations with a focus on the process development environment of energy technologies was developed. In addition to the continuous development of the physical plant, the novel framework also enables the virtual representation to be co-developed. Furthermore, exchangeable modelling blocks are defined in each virtual representation dimension, which should be addressed and developed along the process development life-cycle. Moreover, required property levels for virtual representations in each process development phase have been defined to enable the widest possible application. Consequently, the process development stages from concept to commercial-scale phase are accompanied by the virtual representation types „Digital Model” to „Digital Predictive Twin”.

To test the applicability of the novel framework, four applications have been elaborated at different process development stages:

- **Digital Model** of a Power-to-Liquid plant for the production of synthetic fuel
 - ➔ Core is a steady-state simulation model with offline data communication to find a suitable conceptual plant design for a to be constructed pilot plant with a nominal power of 1 MW_{el}
- **Digital Shadow** of an OxySER plant for the production of reducing gas for the steel industry
 - ➔ Core is a quasistatic simulation model in ad-hoc mode with uni-directional data communication to enable real-time monitoring of the 100 kW_{th} pilot plant at TU Wien
- **Digital Twin** of a Biomass-to-Gas process for the production of synthetic natural gas
 - ➔ Core is beside the quasistatic simulation model, a model predictive controller with bi-directional real-time data communication to enable a fully automated operation of the 100 kW_{th} pilot plant at TU Wien
- **Digital Predictive Twin** concept of a commercial-scale hazardous waste incineration plant
 - ➔ Core is a predictive simulation model with bi-directional real-time data communication to determine not entirely analysed waste streams by analysing historical data and finally to optimize the plant operation, maintenance and waste management

Furthermore, the developed virtual representations can be used during process development to explore energy system integration scenarios either from the perspective of the developed energy technology or from the perspective of a sector or region. For that reason, the virtual representations of a Biomass-to-Liquid and Biomass-to-Gas process were used to find suitable scenarios for the integration in the Austrian energy system. Moreover, the novel tool ENECO₂Calc was developed to investigate possible energy transition scenarios for any municipality in Austria.

Concluding, the novel virtual representation framework has been successfully applied in different process development stages and the arising virtual representations can contribute to a smart interconnected energy system.

Kurzfassung

Die Klimakrise und der damit verbundene Bedarf an der Entwicklung und Optimierung klimafreundlicher und effizienter Energietechnologien erfordert die Digitalisierung des Energiesektors. Die Digitalisierung kann dazu beitragen, die Energiewende zu beschleunigen, indem sie ein intelligent vernetztes Energiesystem zwischen Energiebereitsteller, -verteiler und -verbraucher bildet. Um eine nachhaltige Digitalisierung im Energiesektor zu gewährleisten, ist es notwendig, bereits bei der Prozessentwicklung anzusetzen. Folglich muss neben der physischen Anlage auch ein digitales Abbild der physischen Anlage, die so genannte virtuelle Repräsentation, mitentwickelt werden. Für die Entwicklung von virtuellen Repräsentationen wird ein standardisiertes Framework benötigt, welche die Anforderungen an virtuelle Repräsentationen entlang der Prozessentwicklung von Energietechnologien definiert. In der Literatur sind verschiedene Frameworks mit unterschiedlichen Branchenschwerpunkten verfügbar. Es existiert jedoch kein Framework mit Fokus auf die Entwicklung von Energietechnologien.

Folglich wurde in dieser Dissertation ein Framework für die Entwicklung virtueller Repräsentationen mit dem Fokus auf die Entwicklung von Energietechnologien erarbeitet. Das neuartige Framework ermöglicht neben der kontinuierlichen Entwicklung der physischen Anlage auch die Mitentwicklung der virtuellen Repräsentation. Zudem werden in jeder Dimension der virtuellen Repräsentation austauschbare Modellierungsblöcke und Eigenschaften definiert, die entlang des Lebenszyklus der Prozessentwicklung entwickelt werden sollten, um eine möglichst breite Anwendung zu ermöglichen. Demzufolge werden die Prozessentwicklungsphasen von der Konzept- bis zur kommerziellen Phase von den virtuellen Repräsentationstypen „Digital Model“ bis „Digital Predictive Twin“ begleitet.

Um die Anwendbarkeit des neuartigen Frameworks zu testen, wurden vier Anwendungen von „Digital Model“ bis „Digital Predictive Twin“ in unterschiedlichen Prozessentwicklungsphasen erarbeitet:

- **„Digital Model“** einer Power-to-Liquid-Anlage für die Erzeugung von synthetischem Treibstoff
→ Kernstück ist ein stationäres Simulationsmodell mit Offline-Datenkommunikation für die Findung eines geeigneten Anlagenkonzeptes für eine zu errichtende Pilotanlage mit einer Nennleistung von 1 MW_{el}
- **„Digital Shadow“** einer OxySER-Anlage zur Reduktionsgaserzeugung für die Stahlindustrie
→ Kernstück ist ein quasistatisches Simulationsmodell im Ad-hoc Modus mit unidirektionaler Datenkommunikation für die Überwachung der 100 kW_{th} Pilotanlage an der TU Wien
- **„Digital Twin“** eines Biomass-to-Gas-Prozesses für die Erzeugung von synthetischem Erdgas
→ Kernstück ist neben dem quasistatischen Simulationsmodell ein modellprädiktiver Regler mit bidirektionaler Echtzeit-Datenkommunikation zur Realisierung der Automatisierung der 100 kW_{th} Pilotanlage an der TU Wien
- **„Digital Predictive Twin“** Konzept einer großtechnischen Sondermüllverbrennungsanlage
→ Kernstück ist ein prädiktives Simulationsmodell mit bidirektionaler Echtzeit-Datenkommunikation zur Bestimmung von nicht analysierten Abfallströmen durch die Analyse historischer Daten, um in weiterer Folge eine umfassende Prozessoptimierung zu ermöglichen

Darüber hinaus können die entwickelten virtuellen Repräsentationen während der Prozessentwicklung genutzt werden, um Szenarien der Energiesystemintegration entweder aus der Perspektive der entwickelten Energietechnologie oder aus der Perspektive eines Sektors oder einer Region zu untersuchen. Aus diesem Grund wurden die virtuellen Repräsentationen eines Biomass-to-Liquid und Biomass-to-Gas Prozesses verwendet, um geeignete Szenarien für die Integration in das österreichische Energiesystem zu finden. Darüber hinaus wurde das neuartige Tool ENECO₂Calc entwickelt, um mögliche Defossilisierungsszenarien für beliebige Gemeinden in Österreich zu untersuchen.

Zusammenfassend lässt sich sagen, dass das neuartige Framework erfolgreich in verschiedenen Phasen der Prozessentwicklung eingesetzt wurde und die entstehenden virtuellen Repräsentationen zu einem intelligenten, vernetzten Energiesystem beitragen können.

List of publications relevant for this thesis

The work is based on the following six peer-reviewed journal papers. The main results of the papers will be presented in the following thesis. Further details are given in the corresponding journal papers.

Paper I “Methodology for the Development of Virtual Representations within the Process Development Framework of Energy Plants: From Digital Model to Digital Predictive Twin - A Review”

Hammerschmid, M., Rosenfeld, D.C., Bartik, A., Benedikt, F., Fuchs, J., Müller, S. *Energies*, 2023, 16(6), 2641, SI Digital Twin Technology in Energy and Environmental Sector. <https://doi.org/10.3390/en16062641>

Author’s contribution: Martin Hammerschmid conducted the comprehensive literature research for the review paper and developed the new framework for virtual representations in the process development of energy technologies. Finally, he wrote the main part of the manuscript (including most figures) with significant inputs from the whole team of authors.

Paper II “Simulation of a Pilot Scale Power-to-Liquid Plant Producing Synthetic Fuel and Wax by Combining Fischer–Tropsch Synthesis and SOEC”

Pratschner, S., Hammerschmid, M., Müller, F.J., Müller, S., Winter, F. *Energies*, 2022, 15(11), 4134. <https://doi.org/10.3390/en15114134>

Author’s contribution: Martin Hammerschmid was part of the research team for the development of a Power-to-Liquid plant. He determined together with Simon Pratschner (corresponding author) the underlying process route with its operating conditions based on a comprehensive literature study. He led the development of the simulation models and simulation flowsheet, which was performed by Simon Pratschner.

Paper III "Evaluation of biomass-based production of below zero emission reducing gas for the iron and steel industry"

Hammerschmid, M., Müller, S., Fuchs, J., Hofbauer, H. *Biomass Conversion and Biorefinery*, 2020, 11, 169-187. <https://doi.org/10.1007/s13399-020-00939-z>

Author’s contribution: Martin Hammerschmid was part of the research team and conducted the underlying literature research. Furthermore, he was in charge of the techno-economic analysis for the comparison of the technology with fossil counterparts. The simulation and experimental work were conducted by Stefan Müller and Josef Fuchs. Martin Hammerschmid wrote the main part of the manuscript and generated most figures.

Paper IV “Thermal Twin 4.0: Digital Support Tool for Optimizing Hazardous Waste Rotary Kiln Incineration Plants”

Hammerschmid, M., Aguiari, C., Kirnbauer, F., Zerobin, E., Brenner, M., Eisl, R., Nemeth, J., Buchberger, D., Ogris, G., Kolroser, R., Goia, A., Beyweiss, R., Kalch, K., Müller, S., Hofbauer, H.

Waste and Biomass Valorization, 2023, 14, 2745-2766. <https://doi.org/10.1007/s12649-022-02028-w>

Author’s contribution: Martin Hammerschmid was part of the research team and developed the underlying balance equations for the process simulation. He also developed the framework for interlinking the hazardous waste incineration plant with the simulation model. He wrote the main part of the manuscript and generated most figures and tables.

Paper V “Economic and ecological impacts on the integration of biomass-based SNG and FT diesel in the Austrian energy system”

Hammerschmid, M., Bartik, A., Benedikt, F., Veress, M., Pratschner, S., Müller, S., Hofbauer, H.

Energies, 2023, 16(16), 6097. <https://doi.org/10.3390/en16166097>

Author’s contribution: Martin Hammerschmid was part of the research team which investigated whether biomass-based DFB gasification technology can replace significant shares of fossil gas and diesel in the Austrian energy system. He was primarily responsible for developing the environmental and techno-economic analysis of both process routes. The simulation work was carried out by Alexander Bartik, Florian Benedikt, Marton Veress and Simon Pratschner. Finally, Martin Hammerschmid wrote the main part of the manuscript (including most figures) with significant inputs from the whole research team.

Paper VI “ENECO₂Calc – A Modeling Tool for the Investigation of Energy Transition Paths toward Climate Neutrality within Municipalities”

Hammerschmid, M., Konrad, J., Werner, A., Popov, T., Müller, S.

Energies, 2022, 15(19), 7162, SI Environmental Assessment and Optimization of Energy Systems and Technologies. <https://doi.org/10.3390/en15197162>

Author’s contribution: Martin Hammerschmid was responsible for the development of the novel simulation tool to evaluate different defossilization scenarios in Austrians municipalities. Furthermore, he conducted the simulation work for the evaluation of the different scenarios for a specific municipality in Carinthia. The main part of the manuscript as well as most figures and tables were generated by Martin Hammerschmid.

Other scientific publications of relevance

- 2019** „Evaluation of Sorption Enhanced Reforming in Combination with Oxyfuel Combustion for the Sequestration of CO₂”
Hammerschmid, M., Müller, S., Fuchs, J., Hofbauer, H.,
Proceedings of the ICPS 19 - International Conference on Polygeneration Strategies, 60-70, Vienna, Austria, 18th-20th November 2019,
ISBN: 978-3-9503671-1-9
- 2020** „Development and Techno-Economical Evaluation of an Optimized Concept for Industrial Bio-SNG Production from Sewage Sludge”
Veress, M., Bartik, A., Benedikt, F., Hammerschmid, M., Fuchs, J., Müller, S.,
Hofbauer, H.,
Proceedings of the 28th European Biomass Conference and Exhibition, 901-911,
Virtual, 6th-9th July 2020
- 2021** „Dual fluidized bed based technologies for carbon dioxide reduction – example hot metal production”
Müller, S., Theiss, L., Fleiß, B., Hammerschmid, M., Fuchs, J., Penthor, S., Rosenfeld, D.,
Lehner, M., Hofbauer, H.,
Biomass Conversion and Biorefinery, 2021, 11, 159-168,
<https://doi.org/10.1007/s13399-020-01021-4>
- 2022** “Digital Twin for the optimization of a special waste rotary kiln incineration plant”
Hammerschmid, M., Müller, S., Hofbauer, H.,
IEA IETS Annex 18 - Digitalisierung, KI und verwandte Technologien für industrielle Energieeffizienz THG-Emissionsreduktion, Task 2: Methods and Applications of Digital Twins (DT), Virtual, 26th January 2022
- 2022** „Thermal Twin 4.0: Next-generation hazardous waste incineration”
Hammerschmid, M., Kilian, M., Kirnbauer, F., Aguiari, C., Eisl, R., Nemeth, J., Ogris, G.,
Beyweiss, R., Dittmer, V., Müller, S., Hofbauer, H.,
9th International Conference on Engineering for Waste and Biomass Valorisation (WasteEng22), Keynote lecture, Kopenhagen, Denmark, 27th-30th June 2022
- 2023** „Design of a digital twin for a pilot plant for synthetic natural gas production”
Jankovic, S., Hammerschmid, M., Stanger, L., Bartik, A., Benedikt, F., Müller, S.,
7th Central European Biomass Conference (CEBC), Graz, Austria, 18th-20th January 2023
- 2023** „CO₂ Footprint of Fischer-Tropsch Products produced by a Power-to-Liquid Plant”
Pratschner, S., Hammerschmid, M., Müller, S., Winter, F.,
15th Mediterranean Congress of Chemical Engineering (MECCE), Barcelona, Spain,
30th May - 02nd June 2023
<https://doi.org/10.48158/McCCE-15.T4-O-16>
- 2023** „Implementation of a Digital Twin for a Pilot Plant for Synthetic Natural Gas Production from Biomass”
Jankovic, S., Hammerschmid, M., Stanger, L., Bartik, A., Benedikt, F., Müller, S.,
31st European Biomass Conference & Exhibition (EUBCE), Bologna, Italy,
05th-09th June 2023

- 2023** „Experimental Investigation and Techno-Economic Analysis of Synthetic Natural Gas Production from Woody Biomass”
Bartik, A., Hammerschmid, M., Benedikt, F., Müller, S., Hofbauer, H.,
31st European Biomass Conference & Exhibition (EUBCE), Bologna, Italy,
05th-09th June 2023
- 2023** „Evaluation of CO₂ sources for Power-to-Liquid plants producing Fischer-Tropsch products”
Pratschner, S., Hammerschmid, M., Müller, S., Winter, F.,
Journal of CO₂ Utilization, 2023, 72, 102508,
<https://doi.org/10.1016/j.jcou.2023.102508>
- 2023** „Converting CO₂ and H₂O into Fischer-Tropsch products – A Techno-economic Assessment”
Pratschner, S., Hammerschmid, M., Müller, S., Winter, F.,
27th International Symposia on Chemical Reaction Engineering (ISCRE),
11th-14th June 2023
- 2024** „Off-grid vs. grid-based: Techno-economic assessment of a power-to-liquid plant combining solid-oxide electrolysis and Fischer-Tropsch synthesis”
Pratschner, S., Hammerschmid, M., Müller, S., Winter, F.,
Chemical Engineering Journal, 2024, 148413,
<https://doi.org/10.1016/j.cej.2023.148413>

List of supervised and co-supervised theses

- 2020** "Marktanalyse zu Holzgas-KWK-Anlagen im kleinen Leistungsbereich"
Diermaier, R., supervision: Hammerschmid, M., Popov, T., Hofbauer, H.,
Bachelor thesis, TU Wien, 2020
- 2021** "Potentialanalyse zu biogenen Roh- und Reststoffen zum Einsatz in Holzgas-
Blockheizkraftwerken im regionalen Kontext"
Poliakov, A., supervision: Hammerschmid, M., Popov, T., Hofbauer, H.,
Bachelor thesis, TU Wien, 2021
- 2021** "Automatisierung des Basic Engineering einer Produktgasaufbereitungsstrecke für die
weitere Verwertung"
Bakosch, C., supervision: Benedikt, F., Hammerschmid, M., Müller, S., Hofbauer, H.,
Diploma thesis, TU Wien, 2021
- 2021** "Datenanalyse von Reststoffen und Abfällen hinsichtlich des Zusammenhangs von
Fixed Carbon und Kohlenstoffgehalt"
Buchberger, C., supervision: Hammerschmid, M., Hofbauer, H.,
Bachelor thesis, TU Wien, 2021
- 2022** "Research Information System for a Smart Lab Use Case Scaling Up of Bio-Fuel
Plant Models"
Grzymek, A., supervision: Hammerschmid, M., Rinker, F., Müller, S., Biffl, S.,
Diploma thesis, TU Wien, 2022
- 2023** "Development of a tool for rapid sustainability assessment in the biopharmaceutical
industry"
De March, F., supervision: Hammerschmid, M., Rosenfeld, D.C., Hofbauer, H.,
Diploma thesis, TU Wien, 2023
- 2023** "Entwicklung und Validierung eines digitalen Zwillings einer
Sondermüllverbrennungsanlage"
Nemeth, J., supervision: Hammerschmid, M., Müller, S., Hofbauer, H.,
Diploma thesis, TU Wien, 2023
- 2023** "Optimierung von Biomasseheizkraftwerken im Bereich regenerativer Stromerzeugung"
Russwurm, M., supervision: Hammerschmid, M., Müller, S.,
Bachelor thesis, TU Wien, 2023

Acknowledgements

The following listed projects have been conducted within several research programs funded on the national level. Most of the listed projects are funded by the Austrian Climate and Energy Fund and processed by the Austrian Research Promotion Agency (FFG). One project was funded by the DaFNE research program, which is the research platform from the federal ministry from the Republic of Austria of agriculture, forestry, regions and water management:

- Comprehensive Automation, Digitalization & Optimization of Renewable & Sustainable SNG-production - ADORe-SNG - FFG
- Innovation Flüssige Energie - IFE - FFG
- Optimierung von „Sorption Enhanced Reforming“ zur Verbesserung der CO₂-Bilanz in der Roheisenerzeugung mittels Biomasse - ERBA II - FFG
- Reallabor zur Herstellung von FT-Treibstoffen und SNG aus Biomasse und biogenen Reststoffen für die Land- und Forstwirtschaft - DaFNE



 Federal Ministry
Republic of Austria
Agriculture, Forestry, Regions
and Water Management



Furthermore, one additional project within this thesis contains results from a research program funded on the state level, which was processed by the Vienna Business Agency:

- Thermal Twin 4.0 - Vienna Business Agency



Additionally, the results are based on developments supported by direct research funds from industry:

- Studie: Ökologische und ökonomische Energieversorgung einer Modellregion mit Betrachtung von CO₂-Bilanz, Wertschöpfungskette, Stromnetzstabilität und Versorgungssicherheit
- GLOCK Research Lab für nachhaltige, emissionsarme Energie- und Mobilitätssysteme



Table of contents

1	INTRODUCTION AND MOTIVATION	1
1.1	AIM & SCOPE.....	2
1.2	METHODOLOGY OF THE THESIS.....	3
<u>SECTION I: STATE OF KNOWLEDGE</u>		
2	VIRTUAL REPRESENTATIONS IN THE ENERGY SECTOR.....	5
2.1	DEFINITIONS OF VIRTUAL REPRESENTATIONS.....	5
2.2	GENERAL SUPERORDINATE FRAMEWORK OF VIRTUAL REPRESENTATIONS	8
2.3	APPLICATIONS OF VIRTUAL REPRESENTATIONS	9
2.4	VIRTUAL REPRESENTATION ARCHITECTURE	10
2.5	PROPERTIES OF VIRTUAL REPRESENTATIONS	12
2.6	VIRTUAL REPRESENTATION CHALLENGES.....	14
3	EVALUATION AND VERIFICATION OF PROCESS DEVELOPMENT	16
3.1	TECHNOLOGY VS. MODELLING READINESS LEVEL	16
3.2	SUSTAINABILITY INDICATORS IN THE ENERGY SECTOR	17
4	FUNDAMENTALS OF INVESTIGATED ENERGY TECHNOLOGIES.....	19
4.1	THERMAL COMBUSTION OF HAZARDOUS WASTE	20
4.2	FLUIDIZED BED GASIFICATION OF BIOMASS AND WASTE	22
4.3	SOLID-OXIDE ELECTROLYZER OPERATING IN CO-ELECTROLYSIS MODE	23
4.4	GAS CLEANING AND COOLING.....	25
4.5	GAS UTILIZATION	25
4.5.1	STEAM TURBINE	25
4.5.2	METHANATION.....	26
4.5.3	FISCHER-TROPSCH SYNTHESIS.....	26
4.6	RAW PRODUCT UPGRADING.....	27
<u>SECTION II: FRAMEWORK</u>		
5	FRAMEWORK FOR THE DEVELOPMENT OF VIRTUAL REPRESENTATIONS	28
5.1	TEN-POINT PLAN FOR THE DEVELOPMENT OF VIRTUAL REPRESENTATIONS	28
5.2	NOVEL DEFINITION FOR VIRTUAL REPRESENTATIONS IN PROCESS DEVELOPMENT.....	29
5.3	INTERACTION OF PHYSICAL AND VIRTUAL PROCESS DEVELOPMENT ENVIRONMENT	29
5.4	MODELLING FRAMEWORK IN THE ENERGY PROCESS DEVELOPMENT ENVIRONMENT.....	31
<u>SECTION III: USE-CASES</u>		
6	VIRTUAL REPRESENTATION USE-CASES WITHIN THE ENERGY SECTOR.....	35
6.1	DIGITAL MODEL OF A POWER-TO-LIQUID PRODUCTION PLANT	36
6.1.1	FRAMEWORK OF DIGITAL MODEL.....	37
6.1.2	PROPERTIES OF DIGITAL MODEL.....	38
6.1.3	PROCESS SIMULATION OF DIGITAL MODEL	39
6.1.4	RESULTS OF DIGITAL MODEL USE-CASE.....	39

6.2	DIGITAL SHADOW OF A ZERO-EMISSION REDUCING GAS PRODUCTION PLANT	42
6.2.1	FRAMEWORK OF DIGITAL SHADOW.....	44
6.2.2	PROPERTIES OF DIGITAL SHADOW.....	44
6.2.3	PROCESS SIMULATION OF DIGITAL SHADOW.....	46
6.2.4	RESULTS OF DIGITAL SHADOW USE-CASE.....	46
6.3	DIGITAL TWIN OF A BIOMASS-TO-GAS PRODUCTION PLANT	49
6.3.1	FRAMEWORK OF DIGITAL TWIN	50
6.3.2	PROPERTIES OF DIGITAL TWIN	51
6.3.3	PROCESS SIMULATION OF DIGITAL TWIN.....	53
6.3.4	RESULTS OF DIGITAL TWIN USE-CASE	53
6.4	DIGITAL PREDICTIVE TWIN OF A HAZARDOUS WASTE INCINERATION PLANT	55
6.4.1	FRAMEWORK OF DIGITAL PREDICTIVE TWIN.....	56
6.4.2	PROPERTIES OF DIGITAL PREDICTIVE TWIN.....	57
6.4.3	PROCESS SIMULATION OF DIGITAL PREDICTIVE TWIN.....	59
6.4.4	RESULTS OF DIGITAL PREDICTIVE TWIN USE-CASE.....	59

SECTION IV: ENERGY SYSTEM INTEGRATION

7	ENERGY SYSTEM INTEGRATION BASED ON VIRTUAL REPRESENTATIONS.....	64
7.1	DEFOSSILIZATION OF THE ENERGY SYSTEM THROUGH INTEGRATION OF DFB PLANTS.....	64
7.1.1	METHODOLOGY FOR THE INVESTIGATION OF ENERGY SYSTEM INTEGRATION SCENARIOS	65
7.1.2	RESULTS OF THE TECHNO-ECONOMIC AND ECOLOGICAL IMPACT OF INTEGRATION SCENARIOS.....	66
7.2	DEFOSSILIZATION OF MUNICIPALITIES THROUGH INTEGRATION OF RES TECHNOLOGIES....	68
7.2.1	METHODOLOGY FOR INVESTIGATION OF DEFOSSILIZATION SCENARIOS OF A SELECTED MUNICIPALITY..	68
7.2.2	RESULTS OF THE TECHNO-ECONOMIC AND ECOLOGICAL IMPACT OF DEFOSSILIZATION SCENARIOS.....	69
8	DISCUSSION OF RESULTS.....	71
9	CONCLUSION AND OUTLOOK.....	76
	LIST OF ABBREVIATIONS.....	78
	LIST OF SYMBOLS.....	81
	REFERENCES	83
	APPENDIX	96

PROCESS AND ENERGY FLOW DIAGRAMS (6 pages)

PUBLICATIONS RELEVANT FOR THIS DOCTORAL THESIS

PAPER I (30 pages)

PAPER II (22 pages)

PAPER III (19 pages)

PAPER IV (22 pages)

PAPER V (29 pages)

PAPER VI (32 pages)

CURRICULUM VITAE MARTIN HAMMERSCHMID (2 pages)

1 Introduction and Motivation

At least since the publication of the Kyoto Protocol in the year 1997, climate change was widely recognized and climate policies formulated [1]. The Paris Agreement 2015 adapted and specified the global framework for avoiding dangerous climate change by limiting the global warming to below 2°C compared to pre-industrial level [2]. The Renewable Energy Directive I and II (RED I and II) from the years 2009 and 2018 respectively are building the European guidelines to set climate actions in order to fulfil the overall climate change prevention target set out in the Paris Agreement [3, 4]. The European Green Deal builds up the latest European climate prevention concept to reach climate neutrality until 2050 in Europe [5]. The European Climate Law is the core of the European Green Deal and sets out ambitious European climate policy goals [6]. In Tab. 1, the most important European and Austrian Climate Policy Goals by 2020 and 2030 are listed. The numbers in brackets and value ranges indicate proposed climate policy goals, which are not fixed yet. The climate policy goals can be grouped into mandatory shares of renewable-based energy carriers in different sectors, energy efficiency and greenhouse gas reduction targets. To achieve these climate policy goals and to reach climate neutrality in the year 2050, a transition of big parts of the energy system has to be realized. Consequently, the flexibility of the energy system has to increase to deal with the implementation of volatile renewable energy carriers [7].

Tab. 1: European and National Climate Policy Goals by 2020 and 2030

European and National Climate Policy Goals by 2020 and 2030	2020		2030		Ref.
	EU	AUT	EU	AUT	
Share of renewable energy carriers* (Percentage of gross final energy consumption)	20%	34%	32% (40%)	46-50%	[8, 9]
Share of electricity from renewable sources - national balanced (Percentage of final energy consumption)	-	-	-	100%	[9]
Share of renewable energy carriers in the mobility sector* (Percentage of final energy consumption)	10%	10%	14%	14%	[9]
Share of advanced biofuels in the mobility sector* (Percentage of final energy consumption)	-	-	3.5%	3.5%	[9]
Energy efficiency** (Cap/Percentage of end energy consumption)	20%	1 050PJ (cap)	32.5% (36-37%)	25-30%	[8, 9]
Greenhouse gas emissions Non-EU ETS*** (Reduction since 2005 – areas not captured by EU ETS)	- 10%	- 16%	-30% (- 40%)	-36% (- 48%)	[8, 9]
Greenhouse gas emissions EU ETS**** (Reduction since 2005 – areas captured by EU ETS)	- 21%	-	- 43% (- 61%)	-	[8]
Legal foundation					
* Renewable Energy Directive from the European Parliament (RED I – RL 2009/28/EG [3] & RED II – RL 2018/2001 [4] & adaption of RED II – RL 2021/0218 [10])					
** Energy Efficiency Directive from the European Parliament (RL 2012/27/EU [11]) and Energy Efficiency Act from the Austrian Parliament (EEff-G; BGBl. I Nr. 72/2014 [12])					
*** Effort-Sharing Decision (Nr. 406/2009/EG [13]) and Climate Protection Law from the Austrian Parliament (KSG; BGBl. I Nr. 106/2011 [14])					
**** European Union Emission Trading System from the European Parliament (EU-ETS, RL 2009/29/EG [15]) and Emission Certificate Act from the Austrian Parliament (EZG; BGBl. I Nr. 118/2011 [16])					

Furthermore, the energy efficiency has to be improved to reduce the end energy consumption. Besides the expansion of storage capacities and the flexibilization of the energy system, energy efficiency improvements can be reached through the interconnection of energy market actors. Digitization can help to speed up the energy transition process by the formation of a smart interconnected energy system linkage of energy provider, distributor and consumer [17, 18]. Digitization in the manufacturing and energy sector can lead to productivity improvements that exceed traditional productivity improvement

ranges by far [19]. Furthermore, the energy plant lifetime can be increased by 30% through the implementation of advanced digitization methods [19]. The sustainable digitization in the energy sector can be realized by the implementation of digitization methods in all process development stages of energy technologies. To implement digitization in the process development of energy technologies, a digital reflection of the physical facility, called virtual representation [20] needs to be developed during the process development life-cycle besides the physical facility itself. Fully evolved virtual representations in the end of the process development of energy technologies enable the realization of smart interconnected energy systems. Additionally, a large optimization potential through the early integration of virtual representations in the process development framework, called Frontloading, arise [21]. In Fig. 1, the cost reduction potential through Frontloading and learning in the process development of energy technologies are visualized. The cost reduction potentials are based on a comparison with the virtual product development regarding Frontloading [21–26] and several literature studies regarding learning in the rollout phase [27, 28].

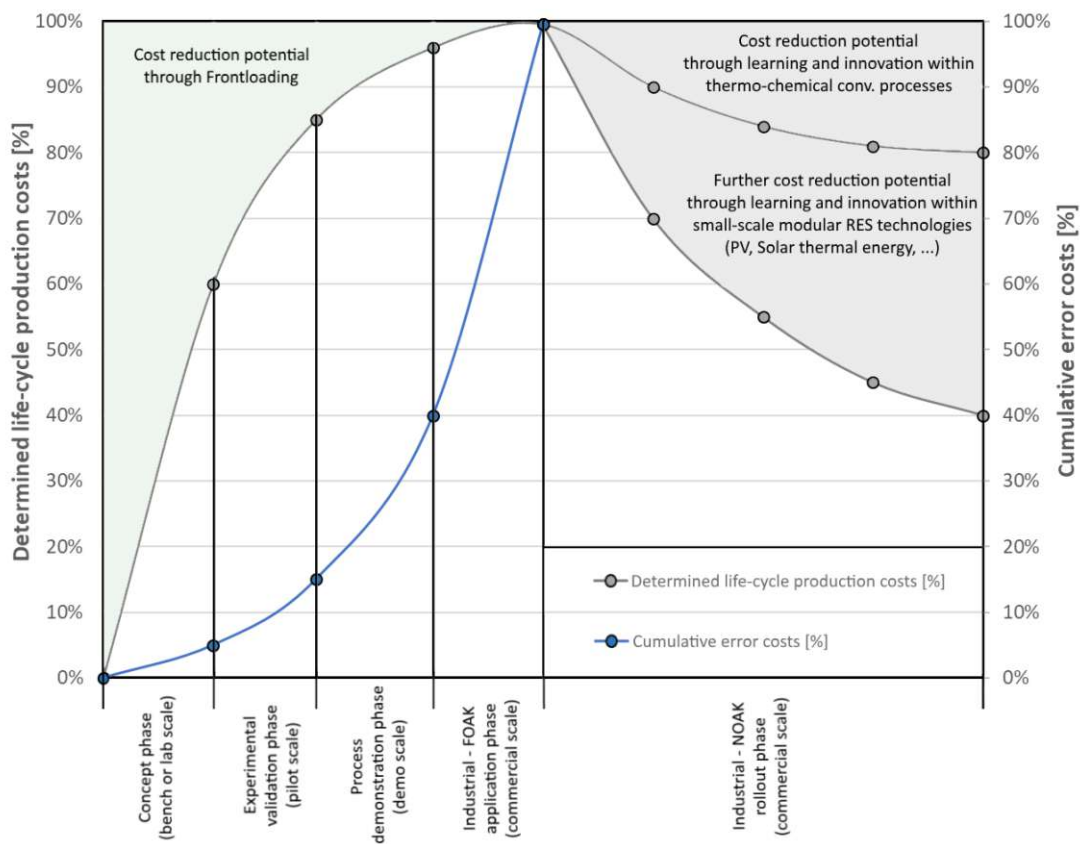


Fig. 1: Cost reduction potential through Frontloading and learning in the process development [29]

In the concept phase of the process development, the plant layout with all utilities and process units is fixed. Subsequently, 60% of the life-cycle production costs are determined within the concept phase [29]. Furthermore, cumulative error costs refer to the costs for a necessary change in the respective process development phase, which increase exponentially in the course of the process development. Therefore, the early integration and continuous evolution of virtual representations to optimize the energy technology along the process development life-cycle is essential.

1.1 Aim & Scope

To implement virtual representations in each stage of the process development life-cycle, a unified modelling framework for developing digital reflections of energy technologies has to be defined. Therefore, this doctoral thesis follows the idea to provide a unified modelling framework for the process development of energy technologies. In order to realize a unified modelling framework, possible virtual

representation properties and applications as well as the discussion of a modelling readiness level have to be investigated. Additionally, the most important sustainability indicators, which can be used for the optimization of energy technologies, have to be identified. Afterwards, several use-cases of energy technologies are investigated to apply the proposed methodology in different process development stages. Finally, several virtual representations are used to investigate appropriate energy system integration scenarios. In order to address all these ideas and topics, the following research questions are considered:

- *How can be a framework for the development of high-fidelity virtual representations within the area of process development in the energy sector defined?*
- *How should the modelling readiness level of a virtual representation be defined to realize the use of appropriate models and technologies in each stage of process development?*
- *How can virtual representations be used to find appropriate energy system integration scenarios?*

1.2 Methodology of the thesis

To answer the raised research questions, the doctoral thesis is based on six peer-reviewed journal publications (**Papers I to VI** in Fig. 2). After explaining the state of knowledge in the field of virtual representations, process development and the investigated energy technologies, a novel modelling framework especially for the process development environment (**Paper I**) is proposed. Furthermore, the investigated scientific publications comprise the development of virtual representation use-cases in different process development life-cycle phases and levels of integration (**Paper I, II, III and IV**) as well as feasibility studies for the integration of different energy technologies in decentralized and centralized energy systems (**Paper V and VI**). The results and methodologies of the peer-reviewed journal publications are supported and enlarged by several conference contributions and project reports.

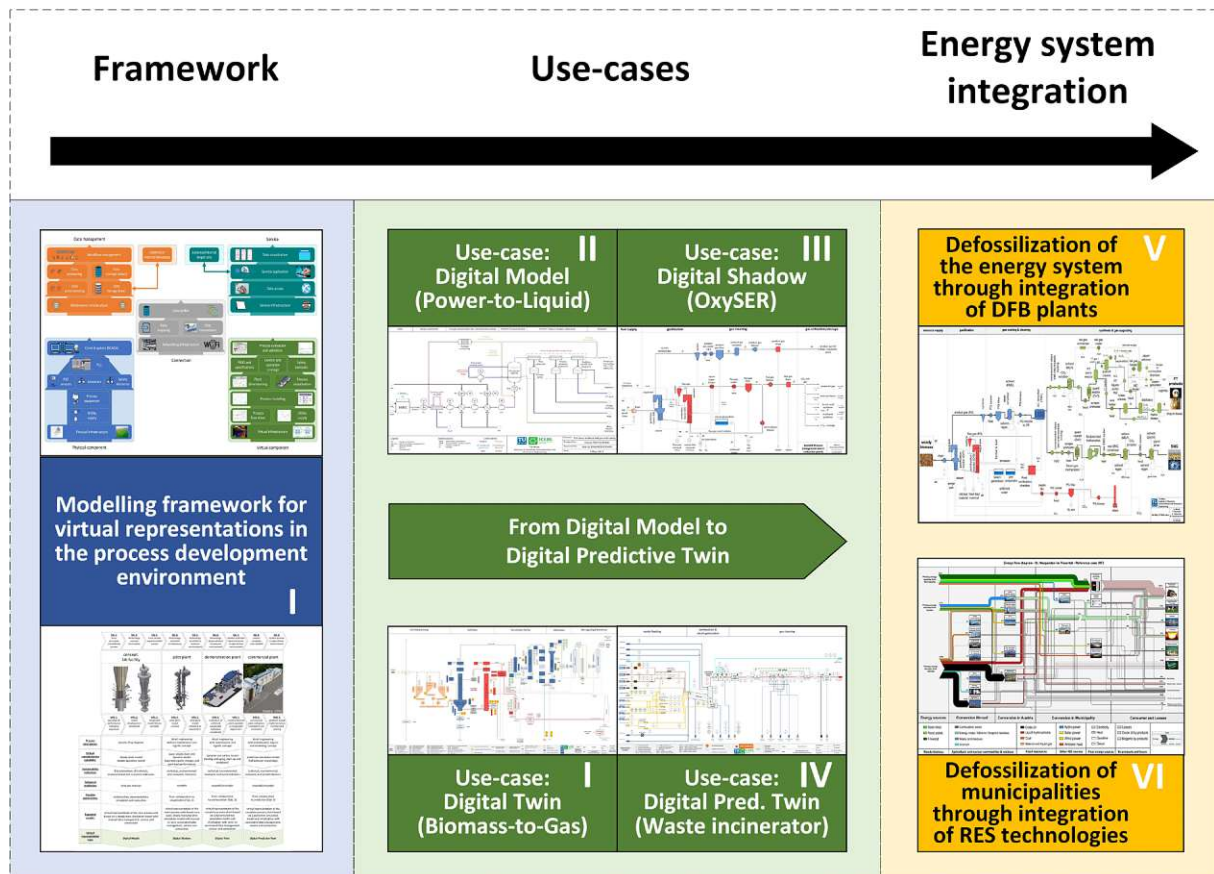


Fig. 2: Schematic methodology of the doctoral thesis (images visualized in chapter 5 and appendix)

The proposed methodology in **Paper I** is based on several years of domain experience and a comprehensive literature research about virtual representation frameworks in different industries. The introduced concept builds a novel modelling framework for virtual representations in the process development environment of energy technologies. Subsequently, four use-cases of virtual representation approaches in different development stages with different level of integrations have been investigated. The Digital Model of a Power-to-Liquid plant in **Paper II** supports the engineering of a pilot plant based on lab-scale experimental results and literature data. The Digital Shadow in **Paper III** helps to investigate the suitability and scale-up of the sorption enhanced reforming process in combination with oxyfuel combustion for the production of a below zero emission reducing gas for the iron and steel industry based on pilot-scale experiments. Additionally, two advanced use-cases of virtual representations have been investigated. In addition to explaining the methodology, **Paper I** also contain a use-case for a Digital Twin of a Biomass-to-Gas plant to automate the synthetic natural gas production process in order to find optimum operation points based on a dynamic simulation model. **Paper IV** shows a concept for a Digital Predictive Twin implemented in a hazardous waste rotary kiln incineration plant to optimize the waste management, plant operation and maintenance. Finally, **Papers V and VI** are based on feasibility studies for integrating energy technologies in the energy system supported by virtual representations. In **Paper V**, several feasibility studies for integrating dual fluidized bed plants in different energy sectors in Austria are conducted. **Paper VI** focuses on developing a novel energy modelling tool called ENECO₂Calc. A large data base with economic and ecologic footprints of energy technologies allows the user to undertake feasibility studies to find appropriate energy transition scenarios for any municipality in Austria.

2 Virtual representations in the energy sector

In this chapter, a literature review regarding virtual representations is conducted to summarize the state of the art of virtual representations in different industries. Subsequently, different virtual representation definitions are gathered to compare different industry views on this topic. Additionally, a general framework at a superordinate level is presented. Furthermore, a virtual representation architecture is visualized to show different hierarchy levels, plant life-cycle phases and different stakeholders who could be the virtual representation' users. Virtual representation properties and applications are collected to classify different use-cases and digital support tools. Finally, virtual representation challenges are discussed to point out difficulties within the development progress of virtual representations.

2.1 Definitions of virtual representations

A literature review of virtual representation definitions in literature is crucial for developing an appropriate modelling framework. In literature, lots of terms are used synonymously. The terms “Digital Twin”, “Digital Shadow”, “Digital Model”, “virtual representation” and “cyber-physical equivalence” are often used for general descriptions of digital reflections of physical objects independent on the field of application [20, 30]. Further phrases like “cyber-physical production system”, “product avatar” or “virtual testbed” are used for digital reflections of physical objects in specific disciplines [30]. The term “cyber-physical production system” is applied for the digitization of a manufacturing process, while the “virtual testbed” aims to describe product development applications [30]. The phrase “product avatar” is mainly connected with digital reflections of products along the whole product life-cycle [29, 30].

In this doctoral thesis, the term “virtual representation” is defined as the overall expression of virtual objects mirroring a physical facility [29]. Additionally, there are a lot of different definitions for virtual representations in the literature, summarized in Tab. 2. The first mention of a Digital Twin was given in 2002 by Grieves and Vickers [31]. Therein, the linkage between physical and virtual entity was highlighted. In many literature studies, the definition of NASA in 2012, is stated as the first actual definition of Digital Twins, wherein Digital Twins are realized through the integration of physical models to mirror the life of the physical facility [32]. Most definitions come from the manufacturing and product life-cycle management sector [33] and agree that virtual representations are based on a link between the virtual and physical object. There is also a broad consensus that sensor data from smart devices and online measurements serve as data input for simulation models. However, the definitions differ regarding the real-time capability, model fidelity and level of integration. Furthermore, the applications of virtual representations depend strongly on the considered industry sector. There are different applications ranging from the monitoring of the current and future states of the physical object to maintenance approaches. Additionally, no consensus exists about virtual representations' life-cycle perspective [34]. The level of integration by Kritzinger et al. [20] and the five mandatory virtual representation dimensions according to Tao et al. [33] will be explained in detail to enable further classification of virtual representations. [29]

Subsequently, the level of integration according to Kritzinger et al. [20] is introduced. Therein, the terms “Digital Model”, “Digital Shadow” and “Digital Twin” are connected with specific levels of integration to enable a classification of virtual representations. In 2021, the levels of integration were extended by Aheleroff et al. [35] by the “Digital Predictive Twin”, which represents the most integrated stage of virtual representations.

Tab. 2: Selection of virtual representation definitions in literature [29]

No.	Year	Definition of virtual representation	Key points	Field of application	Ref.
1	2002	"The digital twin is a digital informational construct of a physical system, created as an entity on its own and linked with the physical system."	Digital and physical system linked	Product life-cycle management	[31, 36]
2	2012	"A Digital Twin is an integrated multi-physics, multi-scale, probabilistic simulation of a vehicle or system that uses the best available physical models, sensor updates, fleet history, etc., to mirror the life of its corresponding flying twin."	Best available physical models	Aeronautics	[32, 37]
3	2012	"The digital twin consists of a virtual representation of a production system that is able to run on different simulation disciplines characterized by the synchronization between the virtual and real system, thanks to sensed data and connected smart devices, mathematical models and real-time data elaboration."	Different simulation disciplines and real-time data elaboration, enabling optimization of the system behavior within each life-cycle phase	Manufacturing	[37, 38]
4	2015	"Very realistic models of the process' current state and its behavior in interaction with the environment in the real world."	Realistic models to monitor the current state	Manufacturing	[37, 39]
5	2016	"Virtual substitutes of real-world objects consisting of virtual representations and communication capabilities making up smart objects acting as intelligent nodes inside the internet of things and services."	Virtual substitutes with communication capabilities	Robotics	[40]
6	2016	"The simulation of the physical object itself to predict future states of the system."	Prediction of future states of the system	Manufacturing	[41]
7	2018	"The digital twin is actually a living model of the physical asset or system, which continually adapts to operational changes based on the collected online data and information, and can forecast the future of the corresponding physical counterpart."	Living model with continual adaptation to operational changes	Aircraft maintenance	[42]
8	2018	"A digital twin is a digital representation of a physical item or assembly using integrated simulations and service data. The digital representation holds information from multiple sources across the product life cycle. This information is continuously updated and is visualized in a variety of ways to predict current and future conditions, in both design and operational environments, to enhance decision making."	Multiple sources across the life-cycle deliver information, enhance decision-making by predicting functions	Product life-cycle management	[43, 44]
9	2018	"A Digital Twin is a set of virtual information that fully describes a potential or actual physical production from the micro atomic level to the macro geometrical level."	Fully detailed description of a physical production process	Manufacturing	[44, 45]
10	2019	"A Digital Twin is a virtual instance of a physical system (twin) that is continually updated with the latter's performance, maintenance, and health status data throughout the physical system's life cycle."	Continually updated virtual instance along the whole life-cycle	Product life-cycle management	[44, 46]
11	2019	"DT is defined as a digital copy of a physical asset, collecting real-time data from the asset and deriving information not being measured directly in the hardware."	Collecting of real-time data	Product life-cycle management	[47, 48]
12	2019	"Digital twin can be regarded as a paradigm by means of which selected online measurements are dynamically assimilated into the simulation world, with the running simulation model guiding the real world adaptively in reverse."	Support instrument to guide physical facilities based on dynamic simulation models	Maritime industry	[48, 49]
13	2019	"A Digital Twin is a virtual representation that matches the physical attributes of a "real world" factory, production line, product, or component in real-time, through the use of sensors, cameras, and other data collection techniques. In other words, DT is a live model that is used to drive business outcomes, and can be implemented by manufacturing companies for multiple purposes like "DT of an entire facility", "DT of a production line process within a facility" or as "DT of a specific asset within a production line.""	Matching physical attributes of a factory, production line or component in real-time by the use of live-models	Manufacturing	[17, 50]
14	2019	"Themes related to the Digital Twin are the decoupling between physical and cyber entity, the presence and frequency of sensorial data flows, the use of computer simulation, the control of cyber over physical entity, the co-evolution of physical and cyber entity as well as the co-existence of physical and cyber entity."	Presence of sensorial data flows and co-evolution of physical and cyber entities	Manufacturing	[51]
15	2019	"A complete Digital Twin should include five dimensions: physical part, virtual part, connection, data, and service."	Five Digital Twin dimensions	Industry	[33]
16	2022	"A Digital Twin is a virtual representation that matches the physical attributes of a "real world" entity, through measured values and domain knowledge and features automated bidirectional communication with that entity."	Bidirectional data communication between physical and virtual facility	Manufacturing	[34]

In Fig. 3, the levels of integration are visualized. Therefore, the Digital Model defines a virtual representation with offline data-exchange between physical and virtual component [20, 29, 35]. The Digital Shadow stands for a virtual representation with one-directional real-time data communication either from the physical to the virtual component or vice versa. A Digital Twin represents virtual representations with a bi-directional real-time data communication between the physical and virtual component to realize automation applications. The Digital Predictive Twin defines virtual representations with predictive modelling and data communication capabilities to realize for example predictive maintenance applications. [20, 29, 35]

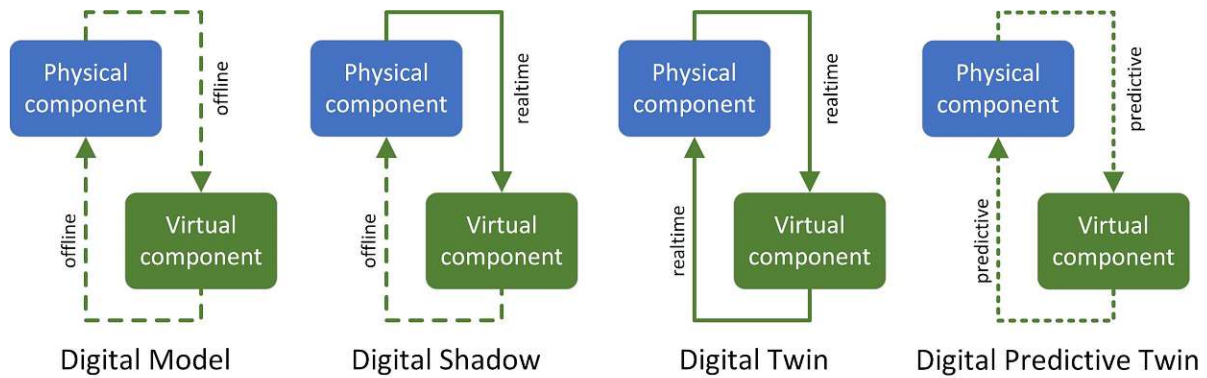


Fig. 3: Virtual representation integration levels of concerning data communication [29]
(Reprinted with permission from [35], Copyright 2021 Elsevier)

In addition to the level of integration of virtual representations, the five-dimension (5D) model from Tao et al. [33] is critical for the proposed methodology and is therefore explained subsequently. In Fig. 4, the 5D model is visualized. The previously discussed dimensions of the physical and virtual component are extended by the data management and service dimension as well as the connection, which represents the linkage of all other dimensions [29, 33]. Therefore, the 5D model approach defines that each virtual representation consists of a physical and virtual component, data management, service and connection dimension. In the context of the energy sector, the physical component refers to an investigated experimental or industrial facility. The virtual component comprises all process simulation and 3D-CAD models, flowsheets and specifications belonging to the investigated facility. The data management is responsible for processing and storage of all gathered data. In the service dimension the foreseen applications or services are realized. For example, decision-making processes and user-interfaces are placed in the service dimension. Several connections between the mentioned dimensions, enable the data communication and make up the fifth dimension. [29, 33]

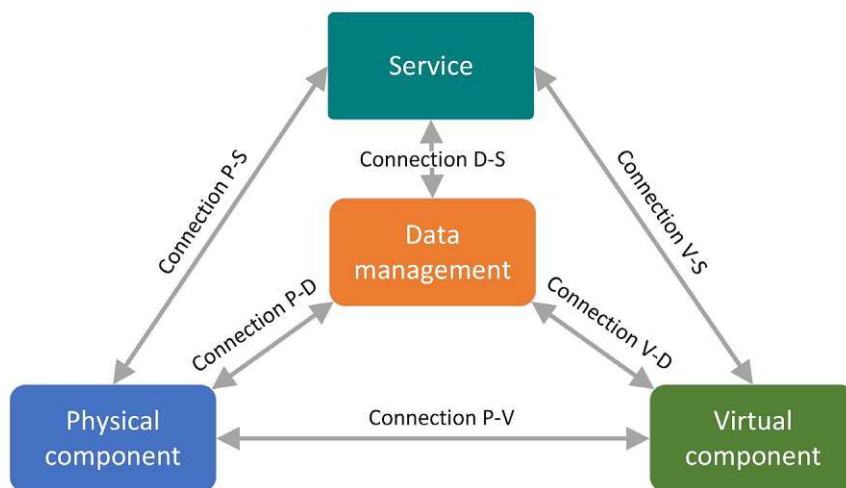


Fig. 4: 5D model for virtual representations concerning a holistic approach [29, 33]
(Reprinted with permission from [52], Copyright 2021 Elsevier)

Summing up, the raised definitions concerning various industry sectors are used to find an appropriate novel definition for the development of virtual representations in the process development of energy technologies. Subsequently, the classification according to the level of integration and the 5D model is used for the development of a novel modelling framework for the process development in the energy sector in chapter 5.

2.2 General superordinate framework of virtual representations

Besides the definition of virtual representations, it is important to discuss a general superordinate framework approach as a basis for the considerations of the novel modelling framework in the energy sector. In Fig. 5, a general superordinate virtual representation framework including all necessary modules is presented. Therein, it can be seen that a virtual representation is always based on measurement data from different sensors of the physical component. The raw measurement data is sent to a pre-processing module. Afterwards, the pre-processed data is integrated in a simulation module to evaluate and interpret the sensor data within a plant model. [29, 53]

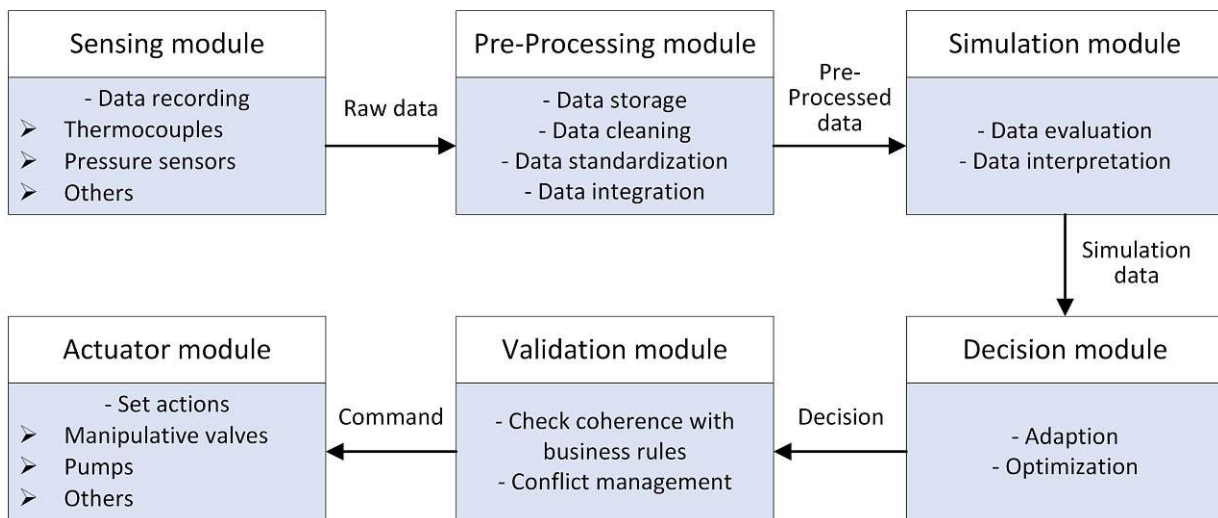


Fig. 5: Proposed modules within a general superordinate virtual representation framework [53]

The simulation results are used in the decision module to adapt and optimize several operation parameters in the physical facility. The decisions are sent to a validation module to validate the decision values according to business rules and plant constraints. After passing the validation module, the commands are sent to the actuators to set actions. [29, 53]

Furthermore, the proposed virtual representation modules can be realized in different virtual representation layers. In Fig. 6, the available virtual representation layers are visualized. Therein, it can be seen that the physical twins and related data acquisition and control instances are located in the field layer. The edge layer consists of the local computing power in terms of local servers and all user devices, which are used to interact with the physical twin via the virtual representation. All cloud-based storage, services and servers for cloud computing are provided in the cloud layer. The field, edge and cloud layer are connected via the network layer [54], where the data communication is realized. [55]

In the following chapters, possible applications in the energy sector are summarized. Furthermore, stakeholders and users of virtual representations are described within the reference architecture model to raise different energy plant hierarchy layers and life-cycle phases. Finally, the most important virtual representation properties are gathered and challenges in the development of virtual representations described.

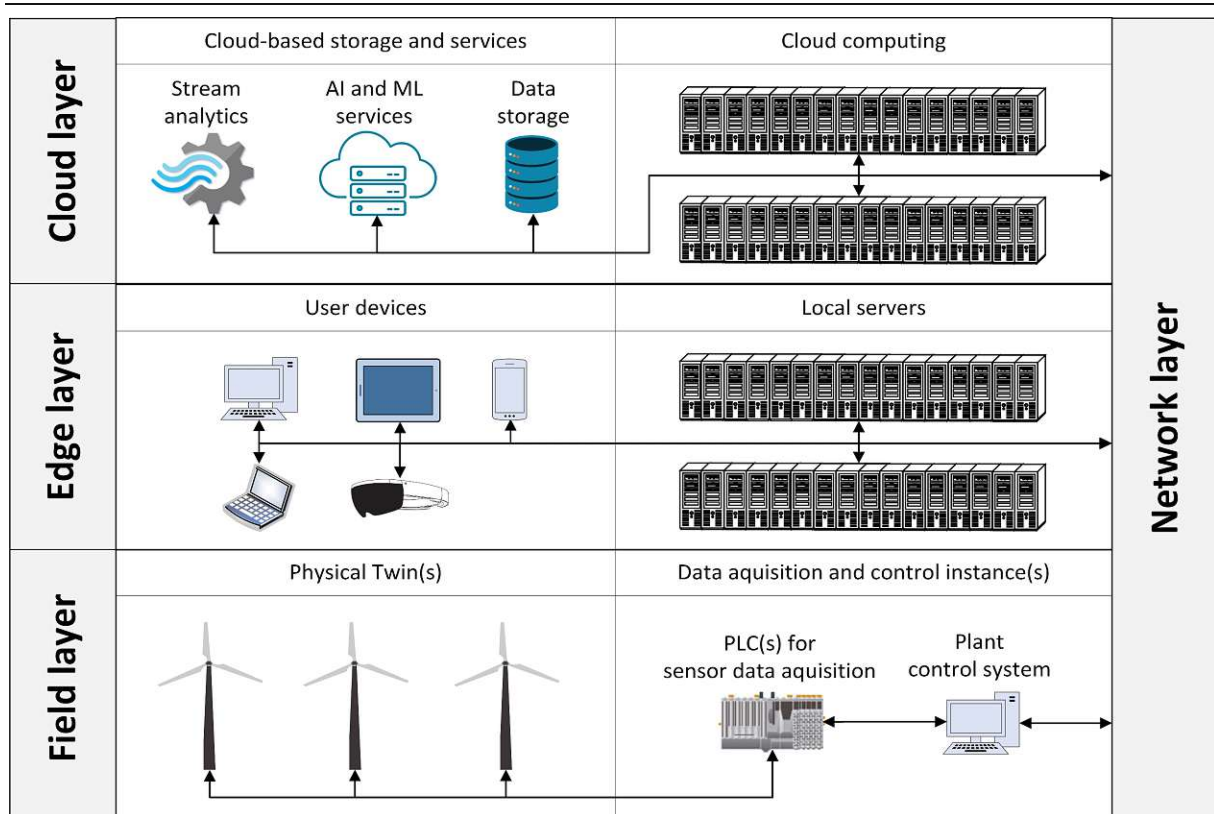


Fig. 6: Available virtual representation layers within a framework [55]
(own images or licensed from Adobe Stock)

2.3 Applications of virtual representations

For the development of virtual representations, it is essential to first define the foreseen applications. Therefore, it is important to gather applications of virtual representations in the energy sector. In Tab. 3, possible applications of virtual representations along the life-cycle of energy plants are listed. To cluster these applications, 9 subgroups were formed [29, 30]:

- **Collaboration** stands for cooperation and coordination activities to cross-link plant operators with internal and external stakeholders.
- **Documentation** applications gather all tasks with the goal to reach state-of-the-art process documentation along the whole plant life-cycle chain.
- **Simulation and Monitoring** tasks support the plant design and commissioning and observe the process performance by the use of state-of-the-art simulation models.
- **Evaluation and Verification** comprise all applications with the goal of information analysis, which helps to optimize the process from the design to the decommissioning phase by implementing sustainability indicators [29].
- The **Visualization** group summarizes all applications using a detailed 3D model as exemplary design or maintenance assistant.
- **Planning and Decision making** put together all virtual representation applications with the goal of scheduling, economic and ecologic dispatching as well as proactive action selection services.
- **Emulation** gathers all tasks which use nearly an exact duplication of the physical facility, by combining the simulation of the process behavior and the illustration of the plant geometry with the help of emulators like the flight training device for pilots.
- **Orchestration** stands for all applications which fulfill automation tasks from the design to the decommissioning phase.
- **Prediction** comprises all applications that help to align future tasks more accurately, ranging from market analysis to predicting the physical entities' plant lifetime and residual value.

Summing up, by the use of virtual representations a lot of application possibilities arise along the plant life-cycle. The raised application subgroups help to classify possible use-cases, whereby the requirements for the simulation model and thus the complexity of the virtual representation increase from collaboration to prediction. In any case, before developing virtual representations, foreseen applications must be defined in order to be able to align the properties of the virtual representations accordingly.

For specific applications in various industries, a reference is made to [20, 30, 33, 35–37, 53, 56–58]. Subsequently, the virtual representation architecture is raised to discuss beside the foreseen applications also possible stakeholders and users of virtual representations.

Tab. 3: Possible virtual representation applications in the energy sector along the plant life-cycle phases [29]

Virtual representation applications	Conceptual design	Engineering	Construction and Commissioning	Operation	Maintenance	Optimization	Decommissioning
Collaboration [17, 48, 59, 60]	cooperation with suppliers, experts and inter-divisional coordination		coordination of suppliers	coordination of logistics	coordination of supplier	collaboration with external experts	coordination of reuse and disposal
Documentation [30, 48, 59, 61]	process life-cycle management for up-to-date documentation						
Simulation and Monitoring [17, 37, 44, 59, 62]	assistant for constructive and technical process design and construction			real-time performance monitoring	condition monitoring	reconfiguration and reconditioning	design of reuse
Evaluation and Verification [17, 48, 57, 59]	holistic evaluation of process design and construction			quality control	fault diagnosis/anomaly detection	holistic optimization	evaluation of reuse and disposal
Visualization [30, 59]	collision check and merchandising		construction assistant	support process understanding	visualization of 3D model or servicing plan	-	merchandising for reuse
Planning and Decision Making [17, 37, 57, 59]	scheduling and support from design to commissioning			scheduling of operation and utility handling	proactive services	economic and ecologic dispatching	schedule for plant lifetime
Emulation [59, 61–63]	risk assessment		virtual commissioning	support and training of plant operators and maintenance engineers			virtual decommissioning
Orchestration [17, 36, 48, 59]	automation of process design and construction			process automation	automated maintenance services	advanced control strategies	-
Prediction [36, 48, 57, 59]	demand analysis and market prediction		stage of completion prediction	prediction of future performance	predictive maintenance	fault prediction of physical entities	prediction of the physical entities' plant lifetime

2.4 Virtual representation architecture

After the definition of foreseen applications, it is important to define possible users and stakeholders of the planned virtual representation. The reference architecture model in the scope of energy plants gives a holistic view on energy enterprises hierarchy layers and connected life-cycle perspectives of energy plants. Therefore, the development of virtual representations shall be based on a clear strategy, which energy plant hierarchy layers and life-cycle phases have to be addressed. [17, 29]

In Fig. 7, the reference architecture model in the scope of energy plants is visualized. The development of the reference architecture model for the energy sector is based on the reference architecture model for industry 4.0 (RAMI 4.0) [17, 64] and adapted versions [35, 59]. Therein, a holistic view on manufacturing enterprises should help to support digitization initiatives in the industry 4.0 context to point out a holistic framework for the development of future products and business models [35]. The adapted reference architecture model for the energy sector comprises the view on different energy plant hierarchy layers and life-cycle phases as well as virtual representation dimensions to show the variety of players, which could be addressed within the development and application of virtual representations.

The energy plant hierarchy layers, which are adapted from IEC 62264 [65], range from the process to the energy system level. The process level stands for the physical process equipment, where energy conversion takes place. In the field level, the decentral data acquisition through sensors and signals are realized. In the control level, programmable logic controller (PLC) pool and control subsystems of the field level. The overarching process control level, is characterized by the supervisory control and data acquisition (SCADA) system and the connected human-machine interface (HMI), where the monitoring and control of energy plants take place. In the operating level, the coordination and supervision of various energy plants within a company takes place, supported by the manufacturing execution system (MES) originating from the manufacturing industry [29]. The enterprise level is characterized by the enterprise resource planning (ERP) system, where the coordination of the main business processes within a company like staff, resource and budget planning takes place. For the interconnection of different energy provider, distributor and consumer, the energy system level with the grid infrastructure has to be addressed. [29, 59]

The life-cycle phases of energy plants range from the conceptual design to the decommissioning phase [59]. In the conceptual design phase, the general plant layout with the definition of all input and output streams is realized. The following basic and detail engineering phases are based on the conceptual design, wherein all documents and specifications for the procurement process are generated. The construction & commissioning phase ranges from the procurement of equipment to the installation and first operation of the energy plant to prove if the plant works and all contractually specified performance figures can be reached. In the operation phase, the plant operator runs the energy plant to produce the desired product. The maintenance phase stands for the service and replacement of sub-systems to ensure safe and stable operation. The optimization phase includes the holistic optimization of the energy plant to improve the plant operation regarding chosen performance indicators. In the last life-cycle phase, the decommissioning of the energy plant takes place after a certain lifetime. To summarize, the development of virtual representations should be based on a clear strategy, which energy plant life-cycle phases and hierarchy layers have to be addressed in which process development stage. Furthermore, these decisions influence the development framework of all virtual representation dimensions. [29, 59]

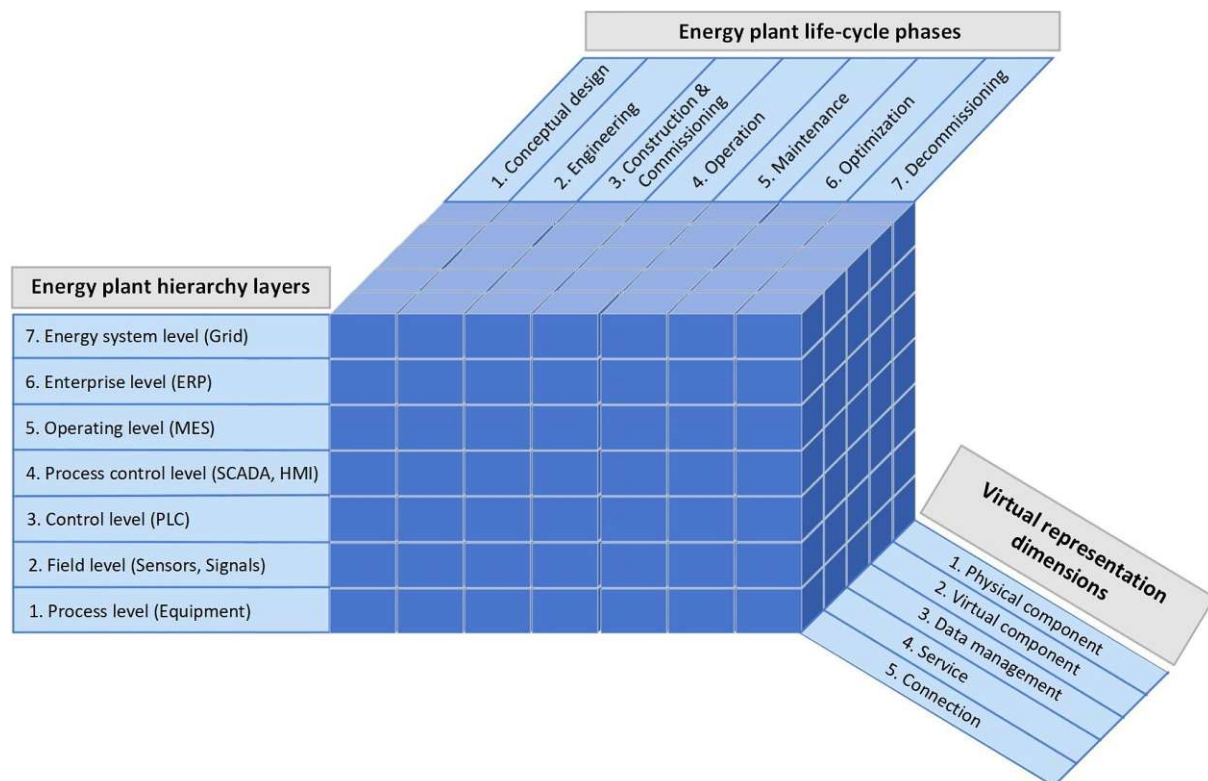


Fig. 7: Reference architecture model in the scope of energy plants [17, 35, 59, 64]

2.5 Properties of virtual representations

In addition to the definition of applications and stakeholders, it is essential to define appropriate virtual representation properties. Therefore, possible properties of virtual representations have to be discussed. For the development of a virtual representation modelling framework, it should be clearly defined which properties in the foreseen application have to be addressed. The Gemini principles give a first overall guideline, which properties a virtual representation have to fulfil [66]. In a nutshell, the Gemini principles are guiding that virtual representations have to be developed by considering the following three overarching objectives [66]:

- Virtual representations must have a clear **purpose**,
- virtual representations must be **trustworthy**,
- and virtual representations must **function** effectively.

For identifying the purpose, it is important to define which energy plant hierarchy layers and life-cycle phases have to be considered, as mentioned in the virtual representation architecture in chapter 2.4. Furthermore, the definition of foreseen applications of the virtual representation helps to clarify the purpose. Trustworthy and functional virtual representations can be developed by integrating high-fidelity models verified and validated by several domain experts. Further verification and validation sections should be always integrated in the modelling framework for cross-checking of the virtual representation results and decisions to ensure the functionality. [29, 66]

Besides the overarching guidelines given by the Gemini principles, further detailed virtual representation properties from literature are summarized in Tab. 4 [29]. The properties are classified in 16 property classes which are grouped according to the virtual representation dimension focus. Each property class is defined through three to four property levels, which can be used for the detailed description of a virtual representation.

First of all, there are four overall property classes defined, which describe superordinate properties of virtual representations. For example, the vertical integration indicates, the ability to deal with different energy plant hierarchy layers, as discussed in chapter 2.4. Therefore, it is quite important to define, whether the foreseen virtual representation should work on the equipment, plant, enterprise or the overarching energy system level [54]. The interoperability stands for the equivalence of different model representations, ranging from comparable over convertible to standardized models [67]. The comparability of different model approaches is a prerequisite for developing trustworthy virtual representations. The final expansion stage is the standardization of virtual representation building blocks to ensure an easy adaption of virtual representations due to different needs of various applications. The flexibility regarding integration or replacement of models is covered by the expansibility [67]. Finally, the reliability and resilience of the virtual representation can be determined by the functional safety level, which ranges from the systematic capability for detecting failures to the automated replacement of faulty building blocks [54]. Apart from the properties concerning the entire virtual representation, there are individual virtual representation properties for each dimension listed. [29]

The physical component, which represents the experimental facility or industrial plant, can be classified by the technological scale-up possibility, degree of automation and physical safety. The technological scale-up possibility enables the classification of processes regarding scalability of all sub-units [68]. The degree of automation indicates the ratio between manual and automated tasks executed during the plant operation and maintenance phase. The physical safety can be divided into primary, secondary and tertiary safety measures [69]. The safety measures range from primary safety measures, summarizing all measures for preventing hazardous operation condition, to tertiary safety measures, which limit the impact of incidents. [29, 69]

Tab. 4: Possible virtual representation properties in the energy sector [29]

Property classes	Focus	Property levels				Ref.
		Level 0:	Level 1:	Level 2:	Level 3:	
Vertical integration	Overall	Equipment level	Plant level	Enterprise level	Energy system level	[54, 67]
Interoperability		Comparable	Convertible	Standardized		[54, 67]
Expansibility		Fixed layout	Adaptable layout	Automated layout		[67]
Functional safety		Systematic capability	Implemented redundancies	Predictable failure analysis	Automated replacement	[54, 70]
Technological scale-up possibility	Physical component	Modular	Partly scalable	Fully scalable		[68, 71]
Degree of automation		Manual	Semi-automated	Fully automated		[72]
Physical safety		Tertiary safety measures	Secondary + Tertiary safety measures	Primary + Secondary + Tertiary safety measures		[69]
Virtual representation capability	Virtual component	Static	Quasistatic/ Dynamic	Ad-hoc	Predictive	[73, 74]
Virtual representation fidelity		Black box (macroscopic level)	Gray box (intermediate level)	White box (microscopic level)		[67, 74]
Virtual representation intelligence		Human triggered	Automated	Partial Autonomous	Autonomous (self-evolving)	[73, 74]
Connectivity mode	Data management and connection	Manual	Uni-directional	Bi-directional	Automatic	[73, 74]
Data integration level		Manual	Semi-automated	Fully automated		[60]
Update frequency		Yearly/Monthly	Weekly/Daily	Hourly/ minute by minute	Immediate real-time / event driven	[54, 73, 74]
Cybersecurity		Role-based access control	Discretionary access protection	Mandatory access control	Verified access control	[54, 75–77]
Human interaction	Service	Smart user devices	Virtual and Augmented Reality	Smart hybrid		[73, 74]
User focus		Single	Multiple without interaction of energy plant hierarchy layers	Multiple with fully interaction of energy plant hierarchy layers		[60]

The virtual representation capability, fidelity and intelligence constitute the virtual component property classes. The time-dependency of the used simulation models is described with the virtual representation capability [74]. Static and quasistatic virtual representation capabilities stand for simulation approaches with time-independent simulation models and input parameters. Dynamic approaches are based on time-dependent simulation models and input parameters. The difference between dynamic and quasistatic simulation models is that dynamic models consider changes in previous time steps by feeding time series of input data to calculate time series of output data while quasistatic models calculate each time step separately until a steady state is reached. The ad-hoc capability of virtual representations is defined by the use of current input parameters (live operational data) to enable real-time simulation. The ad-hoc model can either be based on quasistatic or dynamic behaviour models. The predictive modelling approach, enables look-ahead applications like predictive maintenance [74]. The virtual representation fidelity indicates the knowledge of the simulation model about the internal processes and structures such as geometry, thermodynamic, kinetic or control behaviour [67, 74]. As an example, a simulation model of a heat exchanger purely based on mass and energy balances can be defined as black box model. If fouling factors are added to simulate the poorer heat transfer due to deposits, this could be defined as

gray box model. The additional integration of geometric factors or flow properties to determine the exact heat transfer could be defined as white box model. Finally, the virtual representation intelligence covers the ability of automated decision making. [29, 74]

The following four virtual representation properties classify virtual representations in terms of the data management and connection dimension. The connectivity mode describes the data exchange level ranging from manual over uni- and bi-directional to automatic data exchange [73, 74]. The automatic data transmission stands for flexible communication pathways based on predefined rules, which could be the application of addressing different simulation models depending on operating states. The degree of automation of the data transmission can be classified with the data integration level [60]. The update frequency depends on the foreseen application and ranges from a yearly data frequency to a real-time or event driven data exchange [74]. The term “real-time” is seen very differently in various applications of virtual representations. In the field of robotics, real-time approaches have to interact within several milliseconds. In contrast, in the energy sector, very sluggish processes are usually observed, which means that second-by-second data transmission often is more than adequate. In the context of the update frequency, topics like latency, jitter, throughput and bandwidth have to be considered. More details can be found in [54]. Finally, the cybersecurity property should be addressed within the data management and connection dimensions to implement protection features against unauthorized access [77]. In addition to authorization and verification, the cybersecurity should also focus on the topic of cryptographic protection. [29, 54]

The virtual representation service dimension can be classified by two further properties. The human interaction describes the control possibilities for users exemplary via smart user devices or virtual and augmented reality glasses or a mix of both (smart hybrid) and the user focus implies the amount of users in different hierarchy layers. [29, 60, 74]

In summary, the presented properties for virtual representations give the possibility to define requirements for future applications or to classify and compare existing virtual representations. However, it should be explicitly mentioned that the order of the levels does not provide any value judgement on the quality of virtual representations, since every application has different requirements. Therefore, often lower property levels in various dimensions are sufficient.

2.6 Virtual representation challenges

For the development of suitable virtual representation frameworks, it is important to address beside the foreseen applications, stakeholders and properties, potential problems and challenges. Possible challenges have to already be discussed in the concept phase. The main challenges for the development of virtual representations in the energy sector can be summarized very well by referencing to Chen et al. [36], Singh et al. [61], Sharma et al. [78] and Juarez et al. [53]. Chen et al. summarized that most of the challenges can be classified as time-, safety- or mission-critical [36]:

Time-critical challenges:

- Checking of data resolution, quality and latency [36] → should be reconciled with the foreseen application
- Use of a stable high-fidelity two-way data connection [36, 78] → a reliable data connection is the most important aspect within the development of virtual representations – for critical applications, backup solutions should step in during outages

Safety-critical challenges:

- Decoupling of control system and virtual representation [36] → control system of plant should be controllable at any time, independent of virtual representation, to ensure manual intervention in case of failures

- Cybersecurity safety measures [36, 61, 78] → data privacy, confidentiality, transparency and ownership of data must be guaranteed at all times - additionally, clearly defined access controls must be in place at various hierarchy levels

Mission-critical challenges:

- Use of standardized data interfaces and communication protocols [36, 53, 61, 78] → The consolidation of heterogeneous software tools and equipment requires the use of standardized interfaces – use of standardized data interfaces enables the development of exchangeable modelling blocks – standardized virtual representation framework with exchangeable modelling blocks enables quick adaptation with regard to in-house changes of standards or software tools or the use of the models for other applications
- Use of simulation models which are robust and valid for a wide range of operation points and applications [36] → to cover a wider operating range, several models can also be used depending on the operating condition
- Parametrization of simulation models should be fast and user-friendly [36, 78] → quick intervention in different types of drifts (model, concept and data drift) must be possible – if changes are predictable or can be estimated, adaptive modelling techniques can also assist
- Periodic verification and recalibration of whole measurement equipment [29, 36] → virtual representations rely on trustworthy measurement data – therefore, continuous verification and recalibration of measurement equipment is indispensable to avoid sensor drifts
- Consideration of inconsistencies between physical and virtual system [36] → emerging deviations between model predictions and reality must be taken into account – compensation calculations based on the knowledge of measurement inaccuracies or disturbance values can help – if necessary simplified back-up models (e.g. black box models) are also conceivable
- Keep simulation models as simple as possible according to the desired application [36, 61] → model complexity must be in line with application to save computational costs – reduced order modelling can help

In the course of the development of virtual representation frameworks, the summarized challenges must be addressed in order to avoid operation breakdowns and thus high costs. After defining future applications, stakeholders and properties for the virtual representation and identifying potential challenges in advance, the next chapter will focus on process development.

3 Evaluation and Verification of process development

Many energy technologies have already been developed to commercial maturity, such as thermal combustion of biomass or waste, as well as solar PV and wind turbines. Nevertheless, there is still potential for optimization, especially through the interaction with virtual representations. However, in order to achieve climate neutrality in 2050, new renewable technologies must also be researched in order to drastically reduce greenhouse gases as quickly as possible.

For the assessment of the physical development progress of energy technologies, the Technology readiness level (TRL) has been introduced. In analogy, the Modelling readiness level (MRL) was proposed by Müller in the year 2022 [29, 79] for virtual representations. Additionally, sustainability indicators are summarized in this chapter to evaluate and compare different energy technologies along the process development. Furthermore, the sustainability indicators help to verify the optimization potentials by using virtual representations.

3.1 Technology vs. Modelling readiness level

The process development of energy technologies from concept to commercial scale is defined by the TRL, which was first introduced and used by NASA [80] for the development within the aerospace sector. The TRL scale comprises 9 levels which are shown on the top in Fig. 8. The first development steps of an energy technology are characterised by TRL 1, which means that the basic technological principles have been scientifically proven. Commercialization of energy technologies can be said to have succeeded when the system has been proven in the operational environment, which is characterized by TRL 9. Additionally, TRL 1-3 can be summarized as the concept and lab scale phase. Pilot plants are used within TRL 4-5. The following phase from TRL 6-7 is accompanied by a demonstration plant. Finally, TRL 8-9 are put together as the commercial scale phase. [29, 79]

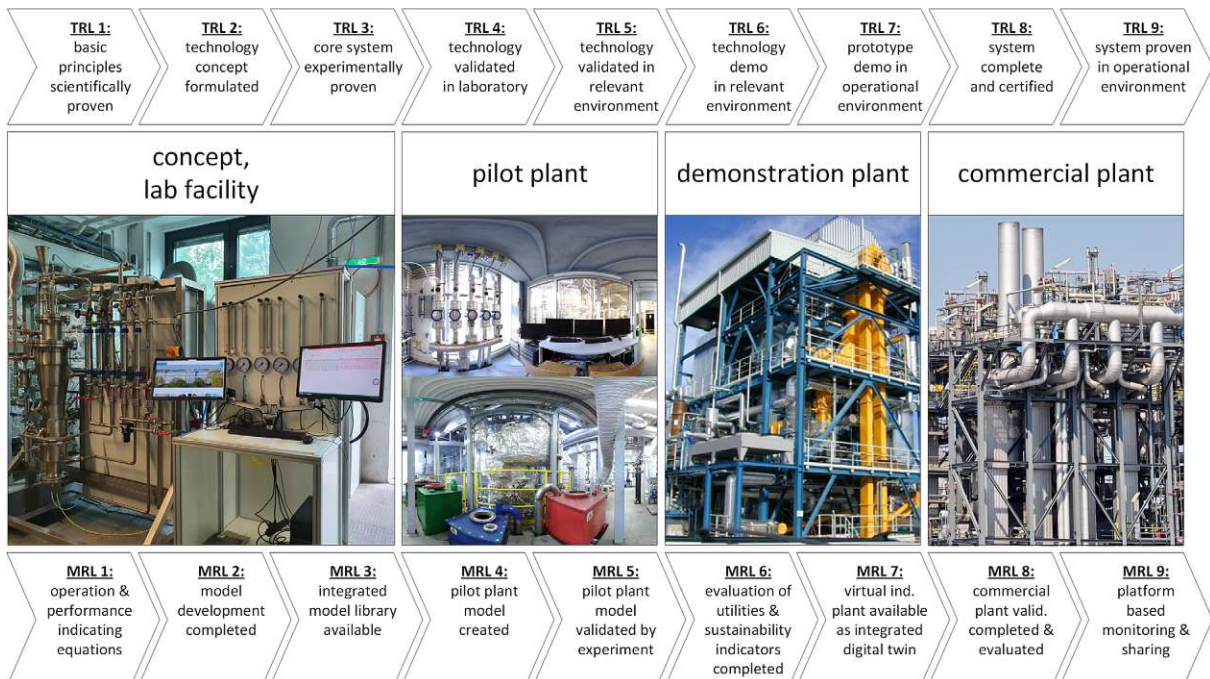


Fig. 8: Technology and modelling readiness level for the evaluation of the process development progress [29] (own images or licensed from Adobe Stock)

The virtual representation is characterized by the MRL, which also is visualized at the bottom of Fig. 8. In analogy to the TRL, the MRL also ranges from 1-9. Thus, the MRL proposes that within the concept and lab scale phase of MRL 1-3, the operation & performance indicating equations should be raised and

integrated in a simulation model. As a consequence, an integrated model library for the investigated energy technology is available and helps by the validation of test series within the lab scale facility. Subsequently, from MRL 4-5 the virtual representation should be adapted according to the pilot plant phase. In contrast to the lab facility, the pilot plant already comprises all main process units. In the lab facility, only the core process unit is typically investigated. Therefore, within MRL 4-5, the simulation model has to be enlarged by all main process units and validated with experimental data from pilot plant test runs. In the demonstration plant phase, the virtual representation has to reach MRL 6-7. Demonstration plants are characterized as a first prototype in an operational environment, which means that all production steps beginning from utility logistics up to product logistics are in place. Thus, for the first time the virtual representation can analyse the complete process chain through sustainability indicators based on experimental campaigns. Consequently, all the plant documentation in form of the 3D model and specification sheets as well as the accompanying simulation model are henceforth available as an integrated Digital Twin. In the final commercial plant phase from MRL 8-9, the existing plant documentation and simulation model are validated and evaluated with operational data from commercial plants over a longer period. As a result, the virtual representation is ready for the platform-based implementation, monitoring & sharing to ensure a knowledge transfer to all subsequent commercial plants. [29, 79]

For the best possible support within the development process of energy technologies, Müller proposed that the MRL should always be one level ahead to predict the future behaviour of energy technologies and therefore the virtual representation helps to design plants of the next development stage. [79]

3.2 Sustainability indicators in the energy sector

In addition to the TRL and MRL, the sustainability indicators help to evaluate the performance of energy technologies. Furthermore, a comparison of different energy technologies becomes possible and the optimization potential of energy technologies through the integration of virtual representations can be quantified.

In Tab. 5, selected sustainability indicators are summarized [29]. The sustainability indicators are divided into four groups. In the first group, all the technical indicators are gathered to describe the performance of a plant regarding conversion rates, efficiencies, lifetime and availability. [29]

The second group represents the environmental indicators, which are classified into the air, soil, ground and water conditions, natural resources, utility consumption and waste production. A detailed investigation of environmental indicators is only possible through life-cycle assessment (LCA). Further details regarding LCAs especially in terms of fundamentals, requirements, frameworks and guidelines can be found in DIN EN ISO 14040 [81], DIN EN ISO 14044 [82] and others e.g. [29].

In addition to the technical and environmental indicator group, the economic indicators are gathered. Therein, the levelized production costs (LCOP) compares the amount of product produced to the cost of investment, operation and maintenance over a given plant lifetime. Therefore, the LCOP helps to compare and evaluate different renewable energy technologies regarding economic viability. Additionally, the operating cash flow, the net present value, the payback time, the return on investment and the gross domestic or regional product are further economic indicators to evaluate the performance of energy technologies. [29]

The fourth group summarizes all social indicators. Therein, all parameters are collected that can quantify the direct impact on humans. Listed examples are the human toxicity or the job creation potential [29]. After explaining the basics of virtual representations and highlighting the specifics of process development, in the following chapter the investigated energy technologies are explained.

Tab. 5: Selected sustainability indicators for the evaluation of energy technologies [29]

Sustainability indicators		Unit	Description	Ref.	
Technical indicators	Conversion rate**	%	Measuring the performance of a reactor or plant by observing the converted amount of a specific compound during a reaction.	[71, 83]	
	Energetic efficiency	%	Measuring the performance of a technology by comparing the energy content of input and output streams.	[84]	
	Exergetic efficiency	%	Measuring the performance of a technology by considering the irreversibility of a process.	[85]	
	Plant lifetime	a	Measuring the usable period of a plant.	[84]	
	Plant availability	FLH/a	Measuring the degree of utilization per year of a reactor or plant by referring to an operation at nominal power.	[84, 86]	
Environmental indicators	Emissions to air	Global warming potential (e.g., CO ₂ , CH ₄ , N ₂ O, etc.)	kg CO ₂ -eq/FU*	Measuring the insulating effect of greenhouse gases in the atmosphere preventing the earth from losing heat gained from the sun.	[87–93]
		Acidification potential (e.g., NO _x , SO _x , etc.)	g SO ₂ -eq/FU*	Measuring emissions resulting in acid rain, which harms soil, water supplies, human and animal organisms, and the ecosystem.	[87, 88, 90–92]
		Ground air quality (particulates, photochemical oxidants)	kg PM ₁₀ -eq/FU* kg NMVOC/FU*	Measuring gaseous and solid emissions which affect the ground level atmosphere.	[87, 88, 90–92, 94]
		Ozone-depleting potential	kg R-11-eq/FU*	Measuring the depletion of the ozone layer in the atmosphere caused by the emission of e.g., chemical foaming and cleaning agents.	[87, 88, 90–92]
	Soil, ground and water conditions	Eutrophication	g PO ₄ ²⁻ -eq/FU*	Measuring concentrations of nitrates and phosphates, which can encourage excessive growth of algae and reduce oxygen levels within freshwater and marine water.	[88–92]
		Ecotoxicity	kg 1,4-DB-eq/FU*	Measuring the potential for biological, chemical or physical stressors within freshwater, marine or terrestrial ecosystems.	[90, 92]
		Water consumption	kg H ₂ O/FU*	Measuring the amount of consumed process water.	[87–90]
	Natural resources, utility consumption and waste production	Primary energy consumption - fossil	MJ/FU*	Measuring the total fossil energy demand of a process.	[93, 95]
		Primary energy consumption - renewable	MJ/FU*	Measuring the total renewable energy demand of a process.	[93, 95]
		Electricity consumption	kWh _{el} /FU*	Measuring the total electricity demand of a process.	[87, 93]
		Carbon utilization factor**	%	Measuring the amount of carbon converted from the fuel to the product within a process.	[83, 96, 97]
		Abiotic depletion	kg Sb-eq	Measuring the over-extraction of minerals, fossil fuels and other non-living, non-renewable materials which can lead to the exhaustion of natural resources.	[87, 88, 90]
		Wastewater amount	kg H ₂ O/FU*	Measuring the amount of produced wastewater.	[87]
Solid waste amount		kg ash/FU*	Measuring the amount of produced disposable waste.	[87]	
	Land use	m ² /FU*	Measuring the amount of land needed for the construction of a plant.	[87, 90]	
Economic indicators	Levelized production costs	EUR/FU*	Measuring the price that would need to be charged per functional unit to achieve a net present value of zero for an investment.	[28, 91, 98–100]	
	Operating cash flow	EUR/a	Measuring the profit/losses generated over a specific time period during regular operation.	[28, 98, 100, 101]	
	Net present value	EUR	Evaluates the technology investment by considering the time value of money.	[28, 98, 100, 101]	
	Payback time	a	Measuring the time required for return of the technology investment by revenues.	[28, 98, 102]	
	Return on investment	%	Measuring the return of an investment by comparing profit and investment.	[101]	
	Gross domestic/regional product (GDP/GRP)	EUR	Measuring the added value created through energy provision in a country (GDP) or considered region (GRP) within a certain period.	[87, 103]	
Social indicators	Human toxicity	kg 1,4-DB-eq/FU*	Measuring the quantity of substances emitted to the environment that harm humans.	[87, 89–92]	
	Job creation	-	Measuring the number of jobs created by the erection of a new plant.	[87, 103]	

* FU: functional unit
(quantifiable description of the product function that serves as a comparable reference basis for all calculations) [81, 82]

** specific parameter for carbon-based technologies

4 Fundamentals of investigated energy technologies

Within this doctoral thesis, several use-cases of virtual representations as digital support tools for energy technologies are investigated. In this chapter, the underlying fundamentals of these energy technologies are presented. In Fig. 9, the technology portfolio of this doctoral thesis is visualized. Therein, the investigated process routes are sketched:

- **Hazardous waste incineration**

Residuals and waste from industry and municipality can be converted via thermal combustion process to hot flue gas. The hot flue gas is cleaned in several gas cleaning steps and the flue gas heat is used within a waste heat recovery boiler (heat exchanger system) to produce superheated steam. The superheated steam is converted within a steam turbine to district heat and electricity. [104]

- **Biomass-to-Gas**

The Biomass-to-Gas (BtG) process is based on a fuel flexible dual fluidized bed (DFB) gasification process for the thermo-chemical conversion of biomass to product gas. In the fluidized bed gasification system, a variety of residuals and waste from industry and municipalities as well as nearly all other types of residuals and energy crops from agriculture and woody biomass can be used [105, 106]. The generated product gas passes through several gas cleaning and cooling steps to reach syngas quality. The following methanation step converts the clean product gas, which is called syngas, to raw synthetic natural gas (raw-SNG). In further gas upgrading steps, undesired gas components are removed to produce the final product, which is called synthetic natural gas (SNG). The resulting SNG fulfills the required gas quality and can be fed to the Austrian gas grid. [83]

- **Biomass-based production of reducing gas via OxySER process**

The OxySER process also uses the same DFB gasification system for the production of the product gas. The difference lies in the bed material used and the operating conditions. If limestone is used instead of olivine and the gasification temperature is decreased, a H₂-enriched product gas can be produced in the so-called sorption enhanced reforming (SER) process [98, 107]. The H₂-enriched product gas, is favorable for several synthesis processes or the production of H₂. The product gas is further cleaned, cooled and used in this setup as reducing gas for the iron and steel industry. The necessary heat for the gasification process is provided by a coupled combustion reactor, where pure oxygen is used instead of air as oxidation agent, which allows the production of nitrogen-free flue gas, which is called oxyfuel combustion. The produced flue gas mainly consists of CO₂ and can be used for carbon capture and utilization (CCU) applications or stored in underground deposits (CCS). [98, 107, 108]

- **Biomass-to-Liquid**

The Biomass-to-Liquid (BtL) process is in analogy to the BtG process based on the DFB gasification process with subsequent gas cleaning and cooling steps. Instead of a methanation process, the clean syngas is converted within a Fischer-Tropsch (FT) reactor into FT syncrude. The FT syncrude consists of FT waxes, FT diesel, FT naphtha and further short-chain hydrocarbons. The short-chain hydrocarbons together with the unconverted gas (mainly H₂, CO and CO₂), which is together called tail gas, is reformed and recirculated before the FT reactor. In further product upgrading steps, the FT waxes are hydrocracked to increase the yields of FT naphtha and FT diesel. The FT diesel fraction is further upgraded in a hydrotreater to fulfill the legal requirements for synthetic diesel. The by-product FT naphtha is further upgraded within a refinery. [109–113]

- **Power-to-Liquid**

The Power-to-Liquid (PtL) process is based on the electro-chemical conversion of carbon dioxide (CO₂) and water (H₂O) to syngas (co-electrolysis), which is in chemical terms similar to the syngas from the biomass gasification process. The CO₂ used in the PtL process can come from a variety of sources.

However, renewable CO₂ sources like biogas or biomass power plants are preferable. For the electro-chemical conversion, a co-electrolysis unit is used, which is able to simultaneously convert CO₂ and H₂O to hydrogen (H₂) and carbon monoxide (CO). Thereby the required H₂/CO ratio for the following FT synthesis process can be adjusted. The resulting FT syncrude is further upgraded within a refinery. [114, 115]

In the following subchapters, the fundamentals of the underlying key technologies for the investigated process routes are explained in further detail.

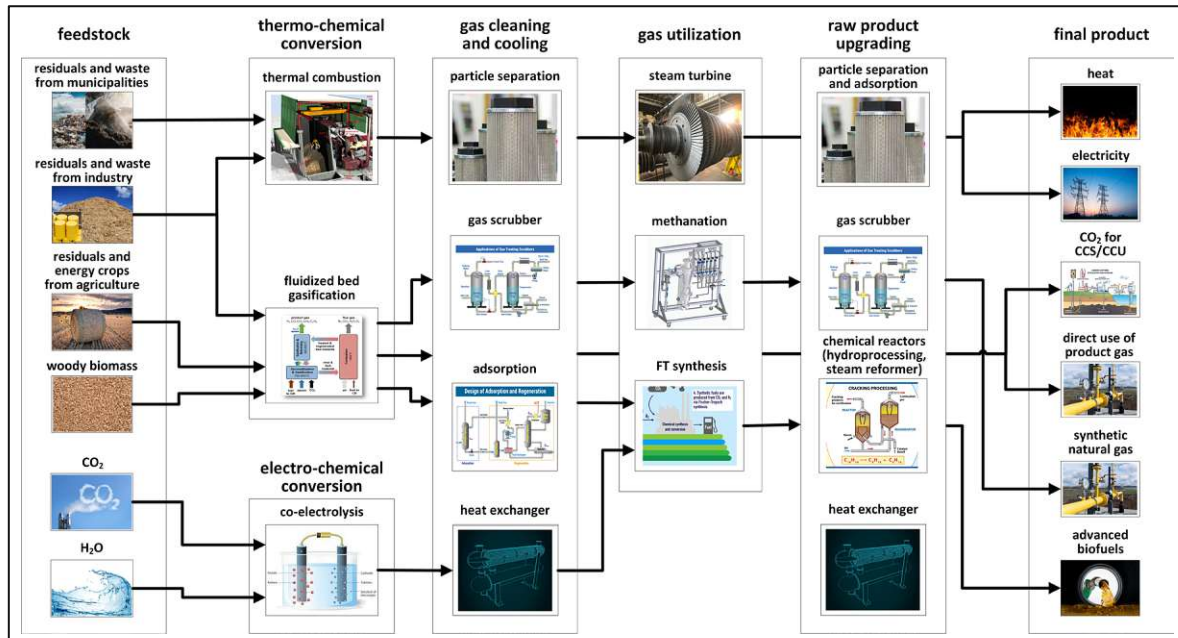


Fig. 9: Technology portfolio of doctoral thesis (own images or licensed from Adobe Stock)

4.1 Thermal combustion of hazardous waste

The overarching goal in thermal-combustion processes is to convert the chemical energy of the solid streams as efficiently as possible into heat. The combustion process passes through various stages, whereby the solid streams are first heated and the resulting conversion products are subsequently oxidized. In the first stage, the solid streams are endothermically dried and heated up to 200°C. Therein, the free and bound water in the cells is removed. In the following endothermic pyrolytic decomposition phase between 200-600°C, the organic macro molecules from the dry solid streams are broken up. As a consequence, molecule fragments in the form of volatile compounds are released. The emitted volatile compounds enclose the solid fuel and prevent contact with the surrounding gas atmosphere. Therefore, not the entire fuel is volatilized and char and ash are produced during the pyrolytic decomposition phase. If the thermo-chemical conversion process is interrupted at this point, it is referred to as pyrolysis [116]. After the pyrolytic decomposition phase, the endothermic gasification phase takes place between 600-1000°C. Here, the char is partly oxidized by a limited supply of air or oxygen. In the gasification reactions, the char is converted into a flammable gas, called product gas, that consist of compounds such as carbon monoxide (CO) and hydrogen (H₂). If the thermo-chemical conversion process is interrupted at this point, it is referred to as a gasification process. In the final oxidation phase, the intermediate products of the previous stages are completely oxidized. Therein, the energy content of the oxidized components is released in form of heat. Therefore, the oxidation phase is an exothermic process, which covers the heat demand for the previous thermo-chemical conversion stages. At the end of the oxidation phase, the occurring flue gas mainly consists of oxidation products carbon dioxide (CO₂) and water (H₂O). The discussed thermo-chemical conversion stages can take place under different operating conditions and gas atmospheres. Furthermore, the individual stages can also proceed spatially separated one after another. If all stages are passed through, the process is called thermal combustion. [98, 116]

In terms of thermal treatment of hazardous waste fractions, the thermal combustion helps to decrease the amount of deposited waste [117]. In case of thermal waste treatment, the thermo-chemical conversion process is based on atmospheric oxygen (air) [118, 119]. Hazardous waste streams can either be solids or liquids. The thermal conversion process of solid waste streams is initiated through heating, while the conversion of liquid waste streams is started by vaporization and exceeding the ignition temperature within the presence of a spark [104]. To reach complete combustion conditions, enough temperature, turbulence and residence time is required [119]. Furthermore, the amount of atmospheric oxygen fed to the combustion chamber is important. Too large amounts of excess air cause a decrease of the combustion temperature, which negatively effects the efficiency. On the other hand, lack of air results in incomplete combustion [104, 119]. Further details to fundamentals of thermal combustion can be found in [118–120].

In addition to the criteria for achieving complete combustion, it is necessary to select the correct reactor type depending on the fuel. In the field of hazardous waste incineration, rotary kilns are often used because of their flexibility. In the following, the basics of the rotary kiln are briefly described, since it is investigated in the current work for hazardous waste incineration. In Fig. 10, a 3D visualization of a hazardous rotary kiln incinerator can be seen. There are several feeding options located in the front wall. With hospital waste and the so-called direct barrels, two different kinds of barrels can be fed to the rotary kiln. Furthermore, bunker waste can be transferred from the waste bunker via a crane into the feed hopper and then conveyed into the rotary kiln. Additionally, a front wall burner is installed for the thermal combustion of waste oil and lances for the thermal treatment of solvent mixtures. Primary air is blown into the rotary kiln through the front wall together with the various waste streams. Subsequently, the released flue gas is post-combusted in a post-combustion chamber under the supply of enough secondary and tertiary air to ensure complete combustion. The wet deslagger at the bottom of the post-combustion chamber is responsible for the removal of ash and slag. Subsequently, the hot flue gas is used to produce superheated steam in the waste heat recovery boiler. Finally, the superheated steam is fed to a steam turbine for producing electricity and heat. The cooled flue gas is cleaned in several gas cleaning steps to fulfill all the legal emission guidelines. [104, 118]

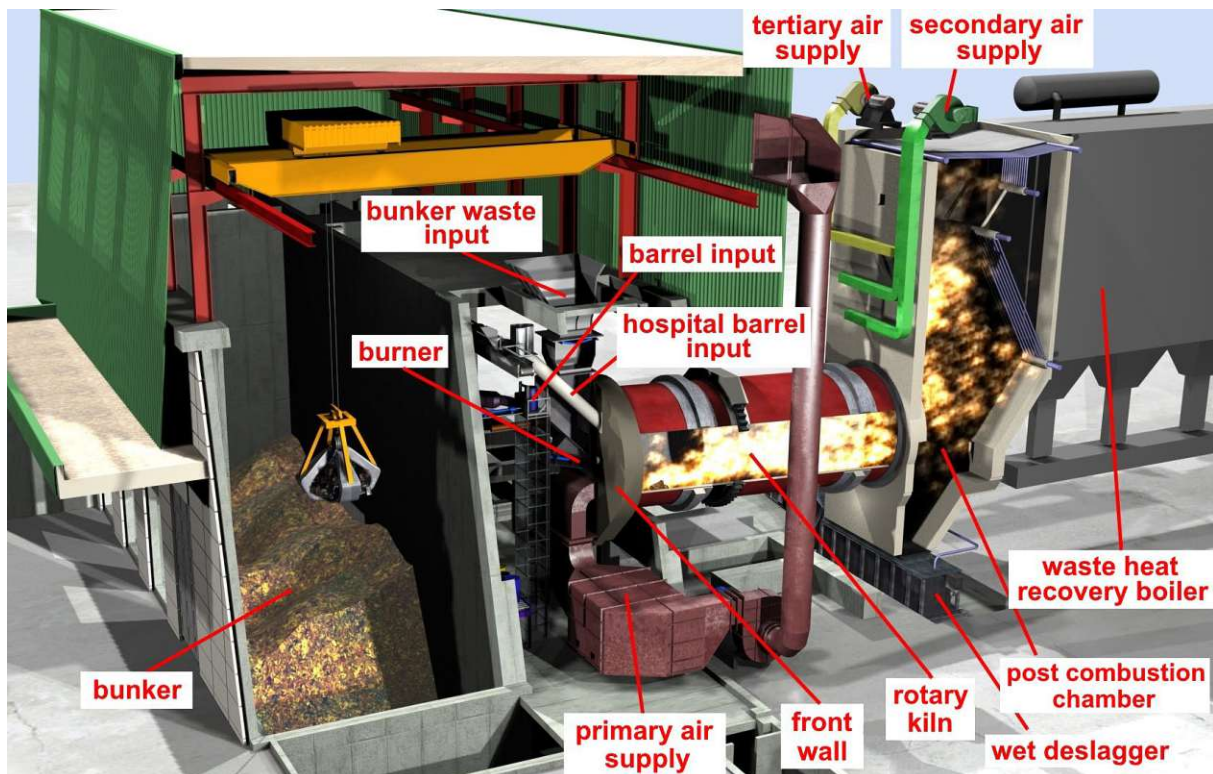


Fig. 10: 3D visualization of the hazardous waste incineration plant in Vienna at Simmeringer Haide [104]

4.2 Fluidized bed gasification of biomass and waste

In the previous chapter, the fundamentals of thermo-chemical conversion of biomass and waste were explained. The thermo-chemical conversion of biomass and waste can either be done directly via a complete oxidation as it is the case in the thermal combustion process or indirectly via intermediate stages to produce a secondary energy carrier. Gasification is an example of indirect thermo-chemical conversion, in which the biomass or waste is first heated and then converted into a combustible gas, called product gas, through several solid-gas and gas-gas reactions with an oxidizing agent. [98, 116]

Different concepts and technologies are available for gasification like the fixed-bed gasifier, fluidized bed gasifier and the entrained-flow gasifier. At TU Wien, the DFB gasification technology has been researched for several decades. Therefore, the gasification-based technologies in this thesis are all based on the DFB technology, which is discussed in more detail below [100, 105, 106]. In Fig. 11, the concept of DFB gasification is visualized. As can be seen, the technology is based on two fluidized bed reactors. In the gasification reactor, the drying and heating, pyrolytic decomposition and the gasification of biomass or waste take place in the presence of the gasification and fluidization agent steam at temperatures between 800-850°C. In the gasification reactor, product gas is released with the main components being hydrogen (H_2), carbon monoxide (CO), methane (CH_4) and carbon dioxide (CO_2). Further components are longer chain hydrocarbons like ethane (C_2H_6) and propane (C_3H_8), water (H_2O) as well as impurities like hydrogen sulfide (H_2S), ammonia (NH_3), hydrogen chloride (HCl), dust, char and tar. The product gas can be subsequently cooled and cleaned and further used for synthesis processes. The necessary heat for the endothermic gasification reactions is provided by the hot bed material, olivine, which is circulated between the two reactors. From the gasification reactor, the remaining char is transported together with the bed material to the combustion reactor. Therein, char is combusted under the presence of the oxidizing fluidization agent air at temperatures between 900-950°C. If required, additional fuel, like recirculated product gas, can be added to obtain the desired temperatures in the gasification reactor. Most biomass and waste types contain sufficient amounts of fixed carbon to provide the necessary amount of heat in the combustion reactor. In the combustion reactor, the bed material temperature is increased through the exothermic combustion reactions. Thus, the hot bed material can be transferred back to the gasification reactor to provide the necessary heat for the gasification process. In the combustion reactor, flue gas similar to a thermal combustion process is produced, which is also further cooled and cleaned. [105, 106, 116]

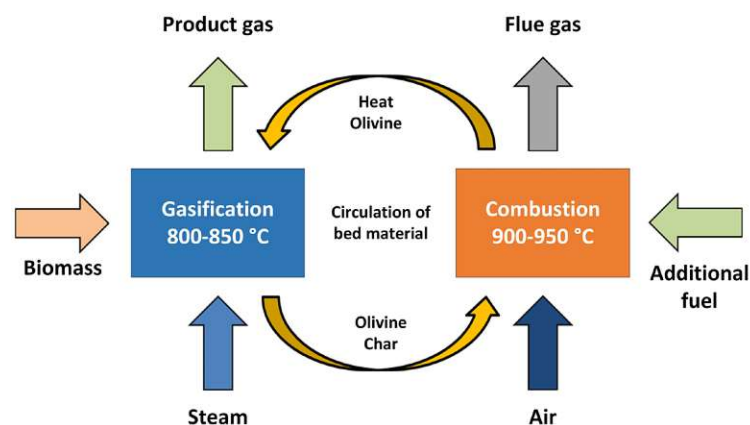


Fig. 11: Concept of dual fluidized bed gasification
(Reprinted with permission from [107], Copyright 2019 Elsevier)

The DFB gasification can be undertaken in different gasification modes. Different operation modes can be set by changing temperatures, bed material and fluidization agents in both reactors. In Fig. 12, the concept of sorption-enhanced reforming (SER) in combination with oxyfuel combustion (OxySER) is visualized as it is used in one of the use-cases in this thesis. In contrast to the classical DFB gasification,

limestone is used as bed material instead of olivine. Further, the gasification temperature is decreased to 600-700°C by cooling the bed material between both reactors. Additionally, the bed material limestone is not only used as a heat carrier but also as a CO₂ carrier. At lower gasification temperatures between 600-700°C, carbonation reactions take place. The calcium oxide (CaO) reacts with carbon dioxide (CO₂) in the gasification reactor to form calcium carbonate (CaCO₃), which is transported to the combustion reactor. At high temperatures of about 880-980°C in the combustion reactor, the calcination of limestone takes place by producing again CaO and releasing CO₂. The combustion reactor is additionally operated in oxyfuel mode, which means that instead of air as fluidization agent, pure oxygen is used to produce a nitrogen-free flue gas. For combustion temperature control, flue gas is recirculated and cooled to reduce the inlet oxygen concentration. In comparison with the conventional dual fluidized bed steam gasification process, in the SER mode a H₂-enriched product gas can be produced. Furthermore, selective CO₂ transport from the gasification to the combustion reactor and further to the flue gas is achieved. Additionally, the OxySER operation mode enables, the production of a nitrogen-free flue gas with high CO₂ concentrations above 90 vol.-%_{dry}. [98, 107, 108]

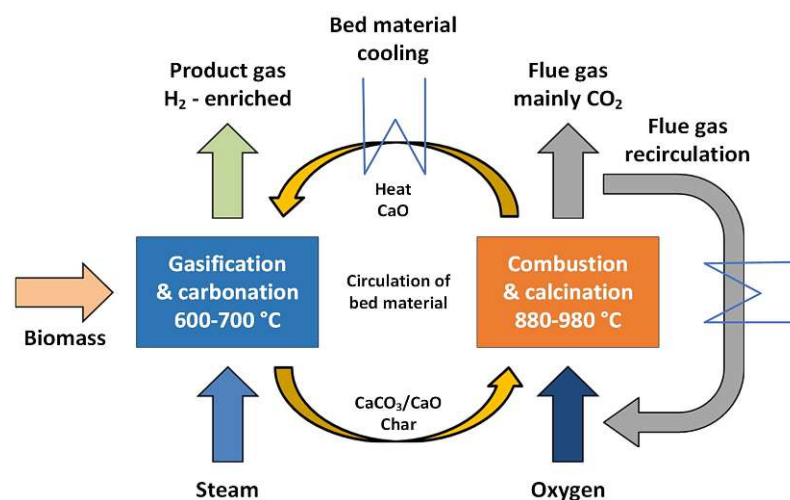


Fig. 12: Concept of sorption-enhanced reforming in combination with oxyfuel combustion (Reprinted with permission from [107], Copyright 2019 Elsevier)

4.3 Solid-oxide electrolyzer operating in co-electrolysis mode

Another option to produce syngas for synthesis processes is the electro-chemical conversion. Various electrolysis technologies are available, whereby a distinction is made between low-temperature and high-temperature electrolysis. Low-temperature electrolysis mostly works with temperatures below 100°C. The most common technologies are the alkaline water electrolysis and the proton exchange membrane electrolysis. In contrast, high-temperature electrolysis works with temperatures up to 1000°C. In Fig. 13, the differences between both electrolysis modes are visualized by the composition of the total energy demand as a function of the operating temperature. The total energy demand for electrolysis is nearly independent on the operating temperature and is composed of heat and electricity. While almost the entire energy requirement for low-temperature electrolysis must be provided by electricity, the energy requirement for high-temperature electrolyzers can be shifted to heat as the operating temperature increases. Shifting energy demand from electricity to heat can help if excess heat is available from surrounding processes. [115, 121]

For high-temperature electrolysis, the solid-oxide electrolyzer (SOEC) is particularly noteworthy. Electrolyzers of this type are operated at temperatures of 800-900°C and are based on catalyst systems with dispersed nickel in an yttria-stabilized zirconia framework [122]. Another advantage is that at higher temperatures, beside H₂O, CO₂ can also be converted within the electrolyzer unit, which is called co-electrolysis. In Fig. 14, the concept of a SOEC unit is visualized. Therein, it can be seen that through

the provision of electrons H_2O and CO_2 can be converted to H_2 and CO at the cathode. Additionally, the reverse water-gas-shift reaction is active to support the production of CO out of H_2 and CO_2 . According to Wang et al. [123] nearly the whole produced CO amount is attributable to the reverse water gas shift reaction. The oxygen ions released at the cathode are transported to the anode by the solid electrolyte. The oxygen ions are oxidized at the anode to gaseous O_2 . [115, 121, 123]

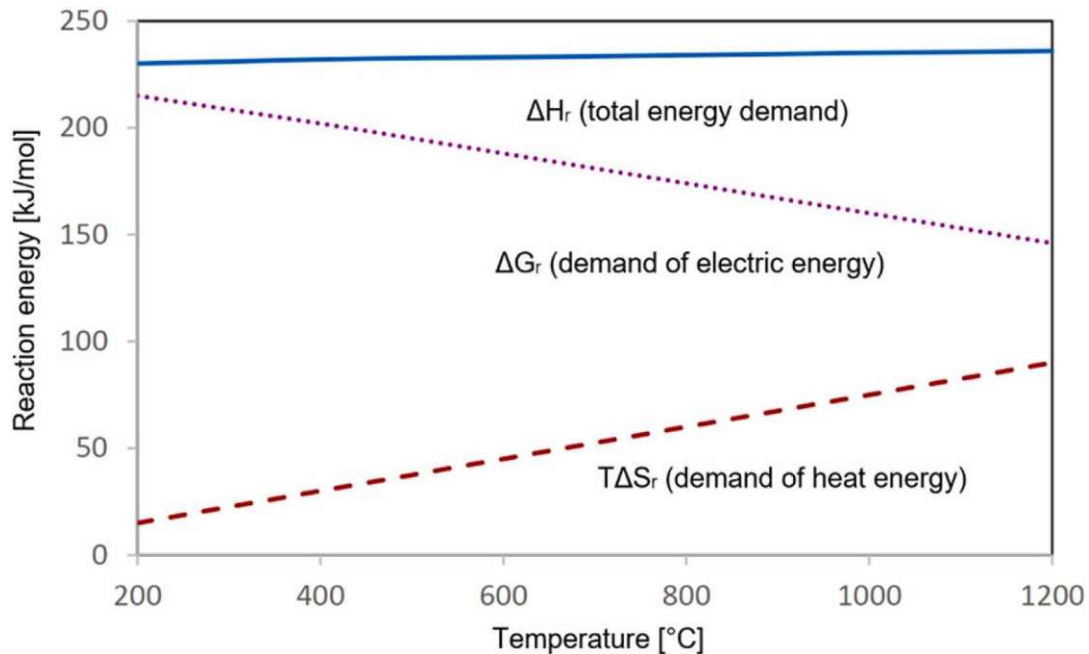


Fig. 13: Composition of total energy demand in electrolysis as a function of the operating temperature [115] (Reprinted with permission from [121], Copyright 2020 Elsevier)

The solid-oxide electrolyzer in co-electrolysis mode is able to produce syngas with the desired H_2/CO ratio for the subsequent synthesis process. The H_2/CO ratio from the produced syngas is mainly influenced by the ratio of feed mass flow rates of H_2O and CO_2 , whereas the affects according to the cell operating conditions are negligible. The total power demand of SOEC units is between 3.2-3.7 $\text{kWh}_{\text{el}}/\text{Nm}^3\text{H}_2$ depending on the literature source. [115, 124, 125]

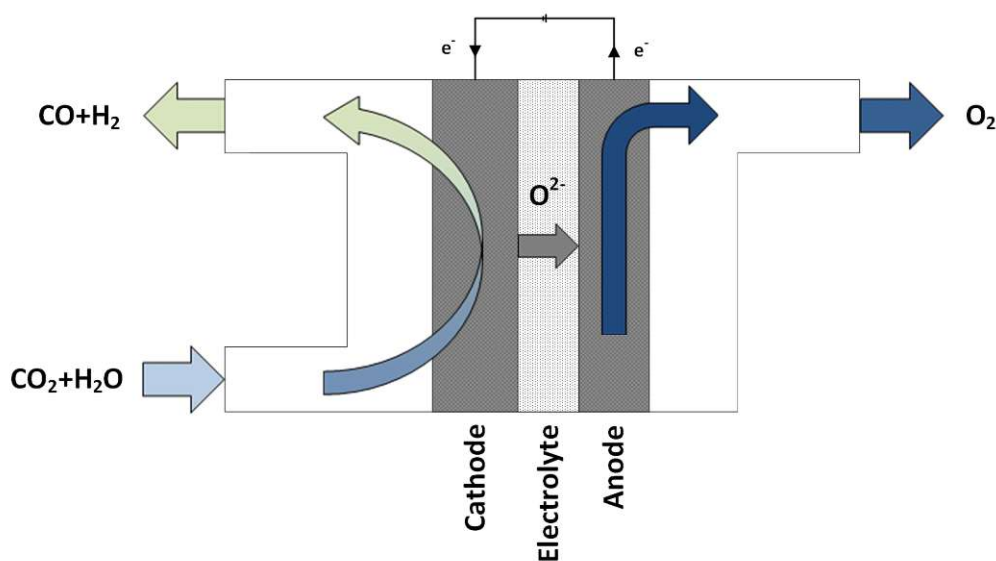


Fig. 14: Concept of a solid electrolysis cell on co-electrolysis mode [123, 126] (Reprinted with permission from [123], Copyright 2017 Elsevier)

4.4 Gas cleaning and cooling

The flue gas and product gas out of the different thermo-chemical conversion steps must be purified in several gas cleaning steps in order to be released to the environment in the case of flue gas or to be further processed in synthesis processes in case of product gas. Furthermore, purification and treatment of CO₂ from various renewable and fossil sources is also required, to meet the requirements for electro-chemical conversion. Additionally, heat exchangers are necessary to adapt temperature levels between different process units accurately.

Particle separation units are necessary for the separation of solid particles from the product or flue gas depending on the particle size, size distribution and number of particles. According to the different functions of particle separation, a distinction is made between cyclones, filtering separators and electrostatic precipitators. Further details to particle separation can be found in [116, 127–130].

In gas scrubbers, a scrubbing liquid, the so-called absorbent, is used to remove contaminations, the so-called absorptive, from gas streams. A wide variety of adsorbents are available to remove different kinds of absorptives. Further details to gas scrubbing can be found in [116, 127, 131].

In adsorption, gas molecules are physically bound to the surface of an adsorbent by means of van der Waals forces, dipole forces or chemical reactions. For the continuous operation of adsorption columns, an interplay between adsorption and desorption must take place in order to be able to separate the impurities from the adsorbent again and thus regenerate them. Further details to adsorption can be found in [116, 127, 132].

In nearly every energy plant, heat exchangers are necessary to adapt temperature levels between process units or for heat recovery. The selection of the most suitable heat exchanger type depends on the operating pressure and operating temperature, temperature difference between both mediums, corrosion, leakage and safety aspects, phase change, costs and space requirements. Further details regarding heat exchangers can be found in [127, 133].

4.5 Gas utilization

From thermal combustion, hot flue gas is produced, which is used for the production of superheated steam in a waste heat recovery boiler. The superheated steam is fed to a steam turbine for the production of heat and electricity. The cleaned syngas from the fluidized bed gasification process and the syngas after the electro-chemical conversion is suitable for different kinds of synthesis processes. The most important key figure in case of synthesis processes is the ratio between H₂ and CO. Different syngas compositions are advantageous depending on the synthesis application. The synthesis processes methanation and FT synthesis are described in more detail below. However, the syngas would also be suitable for other syntheses such as methanol synthesis.

4.5.1 Steam turbine

In the steam turbine, the superheated steam is expanded without heat exchange to the environment in order to produce heat and electricity. The incoming steam drives turbine blades, which drive the turbine shaft and generate electricity through a generator. The most simplified model for the description of steam power processes is the Clausius-Rankine process, where the following process steps are determined [116, 127, 134]:

- Isentropic expansion of steam in steam turbine
- Isobaric and isothermal liquefaction of steam in condenser
- Isentropic compression of water in feed water pump
- Isobaric heat exchange with the working fluid in the steam generator and superheater (waste heat recovery boiler)

The efficiency of steam turbines is determined by the temperature levels of the heat input and output. Thus, the efficiency can be influenced by an increase of the pressure and temperature level of the superheated steam, a decrease of the condenser pressure level, intermediate superheating of steam and regenerative feed water preheating. Steam turbines are built in radial and axial designs, whereby radial steam turbines are only used for smaller power ranges. [116, 127, 134]

4.5.2 Methanation

In the methanation process, the cleaned syngas is converted in a methanation reactor to mainly methane. For this process, a H_2/CO ratio of 3:1 is favorable. If enough hydrogen is available, CO_2 can also be converted to methane in addition to CO. The reactions that take place are strongly exothermic and occur in the presence of a catalyst. The most common type of catalyst is nickel-based. The reactions occur between 200-650°C and at pressure levels between 1-80 bar. Available reactor types are fixed-bed, fluidized bed or bubble column reactors. Due to the exothermic reactions, all reactor types are constructed to dissipate the reaction heat to protect the catalyst and to shift the reaction equilibrium to the product side. Fixed-bed reactors are usually designed with multiple stages in order to dissipate the reaction heat by intermediate cooling stages. In contrast, the fluidized bed methanation reactor design enables a simpler heat extraction and therefore a nearly isothermal operation. Furthermore, fewer methanation stages are necessary to achieve high methane contents. Experimental investigations by Bartik et al. [135, 136] showed that methane contents of > 70 vol.% can already be achieved with only one fluidized bed methanation stage for stoichiometric gas compositions. The resulting raw synthetic natural gas (SNG) needs to be upgraded after methanation to meet feed-in requirements [137]. In any case, the CO_2 , H_2O and possibly H_2 must be separated for this purpose. [83, 116, 127, 138]

4.5.3 Fischer-Tropsch Synthesis

The cleaned syngas can also be used for the production of FT products. For the FT synthesis, a H_2/CO ratio of 2 is favourable, which is lower compared to methanation processes. In FT synthesis, paraffines, olefins and oxygen compounds are produced, whereby mostly straight-chain hydrocarbons (alkane) are formed in different chain lengths. A large number of reactions take place simultaneously and the resulting FT product distribution is determined by the operating conditions and the catalyst used. Typically, iron-, nickel-, cobalt- or ruthenium-based catalysts are used for the FT synthesis. The reactions take place at temperatures between 200-350°C and a pressure range of 10-40 bar. Higher temperatures are favourable for the production of short-chain hydrocarbons. Higher pressure levels increase the conversion rates. Depending on the temperature level, the synthesis processes are divided into low temperature Fischer-Tropsch (LTFT) and high temperature Fischer-Tropsch (HTFT) processes. The easiest model for describing the FT product distribution is the Anderson-Schulz-Flory (ASF) distribution. The ASF model describes the FT product distribution by defining a chain growth probability, which is dependent on the operation parameters, the reactor type, the syngas quality and the catalyst. Typical chain growth probability values are in the range between 0.8 and 0.9. Low values favour the production of short-chain hydrocarbons and high values the production of long-chain hydrocarbons. In case of an average chain growth probability of 0.85, mostly naphtha (C_4-C_9) and diesel ($C_{10}-C_{19}$) are produced. Waxes (C_{20+}) and the light fraction (C_1-C_3) are produced only in smaller proportions. The produced light fraction is recirculated and reformed within a steam reformer to increase the conversion rates of the FT process. Naphtha is the raw product for the production of gasoline. Diesel can be used as Drop-in fuel [100, 139] in diesel engines after hydrotreating. Suitable reactor types for the FT synthesis are fixed-bed, fluidized bed, slurry and microchannel reactors, whereby microchannel reactors are a special form of fixed-bed reactors. [109, 110, 114, 116, 127]

4.6 Raw product upgrading

The raw products from the synthesis processes need to be upgraded to satisfy various criteria. To meet the feed-in requirements, the water from the raw-SNG still has to be removed using a condenser and a glycol scrubber. The CO₂ in the raw-SNG is removed using e.g. an amine scrubber. Gas scrubbers are already explained in chapter 4.4 and are not further discussed here. The FT products from the FT synthesis, are a mixture of the light fraction (C₁-C₃), naphtha (C₄-C₉), diesel (C₁₀-C₁₉) and waxes (C₂₀₊), which is called FT syncrude. First of all, the FT syncrude needs to be separated to obtain the individual fractions. This separation can be fulfilled by several types of distillation or separation units. Due to the different boiling points of the individual fractions, separation into the individual components can take place via heat supply [116, 140, 141]. The light fraction together with the unconverted gas, which is called tail gas, is recirculated and reformed to syngas within a steam reformer. Under high temperatures between 800-1100°C, the short-chain hydrocarbons are reformed with the addition of steam and heat [112, 116, 127, 141, 142]. The FT waxes are further processed within a hydrocracker, where the waxes are converted to shorter chain fractions like C₁-C₁₉. At pressures between 30-70 bar and temperatures between 300-400°C, and with the addition of hydrogen, the hydrocarbons are cracked [112, 116, 140, 141, 143-146]. The unconverted waxes can be recirculated. With the help of the hydrocracker, the yields of naphtha and diesel can be increased. After a further distillation unit, both diesel fractions are processed in a hydrotreater to fulfill all requirements for synthetic fuels according to DIN EN 15940 [139]. Therein, under the presence of a nickel-, cobalt- or molybdenum-based catalyst and hydrogen, alkene hydrogenation, hydrodeoxygenation and the reduction of aromatics takes place [112, 116, 141, 145-148]. The naphtha fraction is not further processed but can be sold as a crude product to the refinery, where it is upgraded to gasoline [112, 115, 135].

After the upgrading section, the main products are ready for use. The FT diesel fulfills all requirements for synthetic fuels according to DIN EN 15940 [139]. The FT naphtha is sold to the refinery as by-product. After processing, the SNG is also ready to be fed into the gas grid, as it meets all the requirements for the Austrian gas grid integration according to G B210 [137].

After explaining the fundamentals of virtual representations, process development, and the process concepts studied, the following chapter builds on this by proposing a framework for co-developing of virtual representations during process development to create synergies between the physical facility and the virtual representation. Afterwards, four use-cases for virtual representations in different process development stages are discussed to present the developed framework by means of applications. Finally, the developed virtual representations of different energy technologies are used to discuss market integration scenarios. In one scenario, the appropriate market is investigated from the perspective of the renewable technology and in a second scenario from the perspective of a municipality, to find out which energy technologies are best suited for achieving climate neutrality in 2050 based on local circumstances.

5 Framework for the development of virtual representations

Based on several years of domain experience and comprehensive literature research about the state of knowledge of virtual representations, this chapter proposes a novel framework for developing virtual representations in the energy sector. First of all, a Ten-point plan and an adapted definition for the development of virtual representations in the energy sector are mentioned. Furthermore, the physical and virtual process development are linked by combining the TRL and MRL presented in chapter 3. Finally, a novel modelling framework is visualized to enable a holistic model development along process development stages. All the content is based on the review paper [29] (**Paper I**).

5.1 Ten-point plan for the development of virtual representations

For the appropriate development of virtual representations in the energy sector, it is important to follow a sequence of design steps. Therefore, a **Ten-point plan** was developed to list the necessary design steps for the development of virtual representations:

1. Definition of planned virtual representation **applications**

First, the foreseen applications along the virtual representation life-cycle must be defined in order to align the development path. In chapter 2.3, possible applications in the energy sector are summarized.

2. Definition of foreseen virtual representation **stakeholders and users**

Based on the definition of the applications, the foreseen stakeholders and users, which are working with the digital support tool should be defined. In chapter 2.4, the virtual representation reference architecture model, gives a holistic view on possible actors and life-cycle stages of plants in the energy sector.

3. Derivation of necessary virtual representation **properties**

Based on the definition of planned applications and the connected stakeholders and users, appropriate virtual representation properties have to be defined to fulfill the foreseen applications. In chapter 2.5, several virtual representation properties for each dimension are summarized.

4. Risk assessment to list possible **hazards and challenges**

Afterwards, possible hazards and challenges have to be discussed within a risk assessment to take all risks into account in the subsequent framework development. In chapter 2.6, possible virtual representation challenges are collected.

5. Definition of **sustainability indicators** to set up the development goals

Before developing the overall virtual representation framework, it is essential to set up virtual representation development goals by defining sustainability indicators according to chapter 3.2.

6. Development of an appropriate **virtual representation framework** based on the 5D model

Next, the overall virtual representation framework can be defined based on the 5D model. Therein, all modelling blocks in each dimension must be selected according to the previously defined foreseen applications, stakeholders, properties, challenges and development goals. In chapter 5.4, a framework for the development of virtual representations in the energy sector is proposed.

7. **Development** of the individual **modelling blocks** for the physical, virtual, data management, service and connection dimension

As soon as the overall virtual representation framework is ready, the individual modelling blocks for the five virtual representation dimensions can be developed.

8. **Parameterization and testing** of the individual **modelling blocks** in the overall framework

Before integrating in the overall framework, each block has to be tested with historical offline plant data.

9. **Linking, parametrization and testing** of the overall **virtual representation**

After the individual tests, all modelling blocks can be inserted into the overall framework. Subsequently, the overall virtual representation can be parametrized and tested in the real operational environment.

10. Use, continuous improvement, as well as maintenance and servicing of virtual representation in the **operational environment**

After completion of all test runs, the virtual representation can be used in the operation environment for the foreseen applications. It has to be mentioned, that a continuous improvement and servicing of the virtual representation is essential to avoid model drifts over time.

5.2 **Novel definition for virtual representations in process development**

After discussing the necessary development steps within in the Ten-point plan, it is important to find a suitable definition for virtual representations in the process development of the energy sector. Many definitions from various industries are collected in chapter 2.1. Based on this, the following definition for virtual representations in the process development of energy technologies has been established:

Virtual representations in process development of energy technologies are digital reflections of physical facilities. The virtual component contains an abstracted model that is fitted as close as necessary to the physical component through the integration of measured values and domain knowledge [29].

Consequently, virtual representations in process development serve to secure the acquired knowledge along the process development chain. Furthermore, the virtual representation can be used to support a scale-up to the next larger physical unit during the individual process development stages and to preserve a digital reflection that is based on state-of-the-art knowledge. However, the virtual representation can not only be used to support engineering, but also in connection with the physical facility to help monitor and optimize plant operation and maintenance activities. In addition to the stated novel definition, the virtual representation should fulfil the following properties along the process development chain:

- **Parallel development of all five model dimensions** (physical component, virtual component, data management, service and connection) along the process development chain
- The same **defined development goals** in terms of sustainability indicators must be **monitored along the entire process development** chain
- The **virtual representation** should be **one development step ahead** of the physical plant
- The virtual representation should consist of **exchangeable modelling blocks** in order to be able to adapt the digital reflection as easily as possible depending on the application

In order to compare the development progress of the virtual representation with the physical facility, the following chapter links the TRL and MRL.

5.3 **Interaction of physical and virtual process development environment**

In Fig. 15, the TRL and MRL are connected with specific contents and results which should be achieved along the four development stages from concept and lab-scale over pilot and demonstration scale to commercial-scale. On the top, the TRL levels with the expected results, investigated process behaviour and realized infrastructure is visualized. Below, the MRL connected with the underlying process description, virtual representation properties as well as expected results are presented.

As mentioned before, the virtual representation should always be one step ahead of the physical plant. Therefore, in the first process development stage, a process flow diagram (PFD) is generated and an operating point typically for nominal power is simulated with a static simulation model using literature data. Based on these initial considerations, calculations of basic technical, economic and environmental

Framework for the development of virtual representations

sustainability indicators are carried out to verify feasibility and reasonability. The virtual representation helps with the collaboration, documentation, simulation and evaluation at this stage, based on the first plant specification and steady state simulation of the core process unit. The dimensions of data management, service and connection are still performed manually at this stage. The first simulations with the virtual representation allow the engineering and construction of the physical lab-scale facility, which consists of the core process unit. Subsequently, the physical facility is tested to find stable operation points within short-term test runs with the result to enable a first proof of concept of the investigated energy technology.





Expected results:	first calculations, proof of concept		mass & energy balances, design values for optimized operation point		detailed design values for continuous operation		detailed design values for competitive energy provision		
Investigated process behavior:	short-term (few hours), stable operation point		short-term (few days), operation point changes & part-load performance		long-term (few months), fouling and aging, start-up and shutdown		long-term (multiple years), full behavior knowledge		
Realised infrastructure:	core process unit		main process units without utility and product logistics		complete process chain with utility and product logistics		complete process chain with utility and product logistics		
Source TRL: [80]	TRL 1: basic principles scientifically proven	TRL 2: technology concept formulated	TRL 3: core system experimentally proven	TRL 4: technology validated in laboratory	TRL 5: technology validated in relevant environment	TRL 6: technology demo in relevant environment	TRL 7: prototype demo in operational environment	TRL 8: system complete and certified	TRL 9: system proven in operational environment
	concept, lab facility		pilot plant		demonstration plant		commercial plant		
									
Source MRL: [79]	MRL 1: operation & performance indicating equations	MRL 2: model development completed	MRL 3: integrated model library available	MRL 4: pilot plant model created	MRL 5: pilot plant model validated by experiment	MRL 6: evaluation of utilities & sust. indicators completed	MRL 7: virtual ind. plant available as integrated digital twin	MRL 8: commercial plant valid. completed & evaluated	MRL 9: platform based monitoring & sharing
Process description:	process flow diagram		detail engineering without maintenance and logistic concept		detail engineering with maintenance and logistic concept		detail engineering with maintenance, logistic & marketing concept		
Virtual representation capability:	steady state model (stable operation point)		quasistatic or dynamic model (operation point changes and part-load performance)		ad-hoc model (fouling and aging, start-up and shutdown)		predictive simulation model (full behavior knowledge)		
Sustainability indicators:	first estimations of technical, environmental and economic indicators		technical, environmental and economic indicators		technical, environm., economic and social indicators		technical, environm., economic and social indicators		
Temporal resolution:	once per test run		monthly		secondly/minutes		secondly/minutes		
Possible applications:	collaboration, documentation, simulation and evaluation		from collaboration to visualization (Tab. 3)		from collaboration to orchestration (Tab. 3)		from collaboration to prediction (Tab. 3)		
Expected results:	virtual representation of the core process unit based on a steady state simulation model with manual data management, service and connection		virtual representation of the main process units based on a quasistatic/dynamic simulation model with manual or semi-automated data management, service and connection		virtual representation of the complete process chain based on an dynamic/ad-hoc simulation model and virtualization with semi- or automated data management, service and connection		virtual representation of the complete process chain based on a predictive simulation model and virtualization with automated data management, service and connection		
Virtual representation type:	Digital Model		Digital Shadow		Digital Twin		Digital Predictive Twin		

Fig. 15: Technology and Modelling readiness level along the process development life-cycle of energy technologies [29, 79] (own images or licensed from Adobe Stock)

The first tests allow the validation of the simulation model in order to carry out the first scale-up step to the pilot plant. In the pilot-scale stage, the virtual representation is based on a quasistatic or dynamic simulation model to investigate operation point changes and part-load performances. Further application possibilities arise and the sustainability indicators can become more detailed. The quasistatic state or dynamic simulation model from the main process units is coupled with manual or semi-automated data management, service and connection dimensions. As a result, the first detail engineering of the energy technology becomes possible, which comprise mainly a piping and instrumentation diagram (P&ID), a process visualization with all connected specification sheets, a control and operation strategy as well as a safety and utility supply concept. Based on the documentation, a physical pilot-scale facility can be built, which consists of the main process units without product and utility logistics. The facility allows to investigate operation point changes and part-load performance. By integrating the measured values in the simulation model, validated mass and energy balances are produced, including detailed design values for an optimized operation point.

Should the pilot scale experiments prove successful, the virtual representation can be further developed to demo-scale, which is characterized by the investigation of the whole process chain including product and utility logistics. Therein, the simulation model should be based on ad-hoc model capabilities to analyse dynamic behaviours like fouling and aging as well as start-up and shutdown process in real-time. At this stage, the simulation model is coupled with a process virtualization and semi- or fully automated data management, service and connection to enable further applications. This results in optimized design values for the establishment of a demonstration plant for the investigation of long-term behaviour. In this physical demonstration facility, the long-term process behaviour can be analysed and lead after the validation with the simulation model to optimized design values for the continuous plant operation.

Finally, the virtual representation can be further developed to reach commercial-scale. Based on all previous test runs, a predictive simulation model can be developed to compile the full process behaviour knowledge. At this stage, a virtual representation based on a predictive simulation model and a detailed virtualization coupled with automated data management, service and connection is available, which allows to apply the virtual representation for all kind of applications from collaboration to prediction. The detailed investigation of various sustainability indicators enables the development of not only the detail engineering documents, but also a suitable marketing concept. As a result, commercial-scale plants can be planned and operated with the goal of an optimized competitive energy provision.

The virtual representation in each development stage can be named after the data integration level according to Kritzinger et al. [20] and Aheleroff et al. [35]. They can be referred to as Digital Model, Digital Shadow, Digital Twin and Digital Predictive Twin to symbolize the increasing model intelligence along the process development life-cycle.

5.4 Modelling framework in the energy process development environment

In order to know, which components make up a virtual representation and how to develop them in the course of process development, a novel framework is proposed in this chapter. In the development of virtual representations, the overarching goal is to develop frameworks that allow to link exchangeable modelling blocks. In Fig. 16, the novel virtual representation framework, which was first published in [29], is visualized.

The framework follows the 5D model from Tao et al. [33] as discussed in chapter 2.1. This shows that different unit operations must be developed in all five dimensions, which ideally can be used in a modular way. The framework is structured in such a way that infrastructure must be available in each dimension as a basis for the development of the individual units, which are built on the infrastructure using a bottom-up approach.

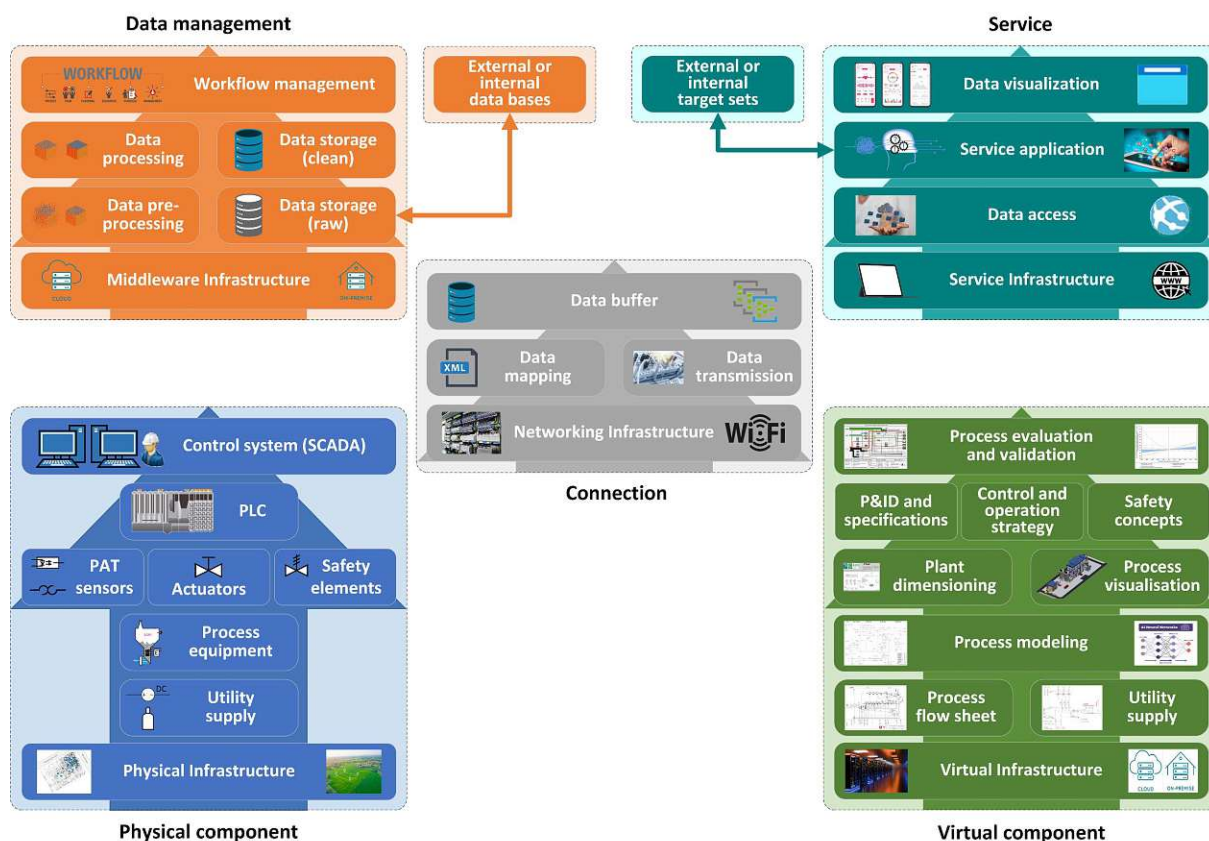


Fig. 16: 5D virtual representation framework in the process development environment [29]
(own images or licensed from Adobe Stock)

The physical component represents the physical facility ranging from lab- to commercial-scale. As physical infrastructure, e.g. an appropriate laboratory or plot of land is required. This allows the establishment of the physical facility consisting of the process equipment and the utility and product logistics. For monitoring and controlling the plant, process analytical technology (PAT) sensors, actuators and safety devices are necessary. The measuring and control devices are monitored and controlled via a programmable logical controller (PLC). Depending on the size of the plant, it is controlled by one or more PLCs via the control system.

The measurement data is subsequently transferred from the physical plant to the data management system. The data management is based on middleware infrastructure, which can be either on-premise or cloud-based. In large plants, data processing is usually performed in two stages. In the first stage, all raw data from the physical plant is stored locally and pre-processed to reduce the amount of transferred data. Subsequently, in a second stage, the pre-processed data is temporarily stored in a cloud-based storage and further processed to create appropriate data sets for various software tools. Additionally, data from internal or external data bases like laboratories can be integrated and processed together with the measurement data in the data management section. Finally, workflow management tools can be used to provide subsequent software tools and data bases with data sets in an automated way.

In the virtual component, the processed data sets are used in several software tools. Similar to the middleware the virtual infrastructure can either be on-premise or cloud-based. The underlying process flow sheet and utility supply documentation enables the simulation of the process according to the process layout in a suitable software tool. In the process simulation, first of all simulation units of each individual process unit are developed and stored in model libraries. The single process units can be modelled by the use of physics-based or semantic-based relations or a mix of both [48, 149]. The individual process simulation units are either connected in flowsheet- or script-based simulation environments. In addition to the model library, substance data bases are required for the definition of

process media. By using an appropriate solver, the underlying mathematical system of equations can be solved. The process simulation is directly connected and can interact with the 3D plant model via the plant dimensioning unit and the associated design equations. In correlation with the 3D process visualization, the P&ID, specifications, the control and operation strategy as well as safety concepts can be either developed or optimized. Finally, the process simulation results and the plant specifications can be used to evaluate and validate the energy technology by the use of sustainability indicators.

After the evaluation and verification of the simulation results in the virtual component, they are stored in the data management dimension and can be further used in the service dimension to execute the desired virtual representation applications, ranging from collaboration to process automation and prediction. Again, the service dimension requires a local or web-based service infrastructure. A multi-tier architecture is built on top of the service infrastructure. In the framework visualized in Fig. 16, the three-tier architecture [150] is used. Three-tier architectures are based on three layers consisting of the data access tier, the application tier and the data visualization or presentation tier. In the data access tier, simulation results or measurement data from the data management are requested and forwarded to the application tier. In this tier decisions are made, which can be referred to as service logic. With the help of internal or external target sets, such as the optimization of the process efficiency, specific data is visualized in the data visualization tier or control commands are directly sent back to the physical component. In the data visualization tier, users such as plant operators can interact with the virtual representation via smart user devices.

The connection dimension is responsible for the interaction of all the other previously described dimensions. Based on networking infrastructure, which can be made up of local networks like fieldbus systems, wireless and mobile networks or global networks like broadband internet [151], data transmission and data mapping protocols are used to enable data connection for the desired service. The distinction between data mapping and transmission can best be described by the seven-layer ISO OSI reference model [152], which can be seen as the universal standard for data communication. Therein, the data communication is divided into seven layers, whereby the first four layers are named as transport-oriented layers and are responsible for the data transmission. The layers five to seven can be summarized as application-oriented layers which are responsible for structuring the data, called data mapping [152]. An example of a widely used data transmission protocol would be TCP/IP via ethernet. Examples for data mapping protocols are FTP, HTTP, MQTT and OPC UA [48, 54, 152, 153]. Finally, a data buffer is often required to temporarily store or queue data sets before sending them to the desired application.

The underlying framework helps to develop virtual representations which are structured in exchangeable functional modelling blocks. At this point it should be mentioned that during the whole development process of virtual representations the data sovereignty, confidentiality and reliability must be guaranteed all the time independent on the used data interfaces and virtual representation layers.

In chapter 2.5, possible virtual representation properties were explained. To couple the process development with the properties of virtual representations, target requirements for virtual representation properties along the process development life-cycle are given. Therein, it can be seen that the process development stages from lab-scale to commercial-scale are coupled with the following virtual representation types:

- Concept and lab-scale stage → Digital Models
- Pilot plant stage → Digital Shadows
- Demonstration plant stage → Digital Twins
- Commercial plant stage → Digital Predictive Twins

Based on the virtual representation properties, presented in chapter 2.5, in Tab. 6 the defined target requirements for virtual representations along the process development of energy technologies are listed.

Tab. 6: Target requirements for virtual representation properties along the process development life-cycle [29]

Property classes and components	Focus	Concept, lab facility	Pilot plant	Demonstration plant	Commercial plant	
Vertical integration	Overall properties	Level 0: Equipment level	Level 1: Plant level		Level 2: Enterprise level	
Interoperability		Level 0: Comparable		Level 1: Convertible	Level 2: Standardized	
Expansibility		Level 0: Fixed layout	Level 1: Adaptable layout	Level 2: Automated layout		
Functional safety		Level 0: Systematic capability	Level 1: Implemented redundancies	Level 2: Predictable failure analysis	Level 3: Automated replacement	
Technological scale-up possibility	Physical component properties	Level 0: Modular	Level 1: Partly scalable	Level 2: Fully scalable		
Degree of automation		Level 0: Manual	Level 1: Semi-automated	Level 2: Fully automated		
Physical safety		Level 1: Secondary + Tertiary safety measures	Level 2: Primary + Secondary + Tertiary safety measures			
Virtual representation capability	Virtual component properties	Level 0: Static	Level 1: Quasistatic/ Dynamic	Level 2: Ad-hoc	Level 3: Predictive	
Virtual representation fidelity		Level 0: Black box (macroscopic level)	Level 1: Gray box (intermediate level)		Level 2: White box (microscopic level)	
Virtual representation intelligence		Level 0: Human triggered	Level 1: Automated	Level 2: Partial autonomous		
Connectivity mode	Data management and connection properties	Level 0: Manual	Level 1: Uni-directional	Level 2: Bi-directional		
Data integration level		Level 0: Manual	Level 1: Semi-automated	Level 2: Fully automated		
Update frequency		Level 0: Yearly/Monthly	Level 1: Weekly/Daily	Level 2: Hourly/every minute		
Cybersecurity		Level 0: Role-based access control	Level 1: Discretionary access protection	Level 2: Mandatory access control	Level 3: Verified access control	
Human interaction	Service properties	Level 0: Smart user devices				
User focus		Level 0: Single	Level 1: Multiple without interaction of energy plant hierarchy layers		Level 2: Multiple with fully interaction of energy plant hierarchy layers	
Virtual representation type		Digital Model (MRL 1-3)	Digital Shadow (MRL 4-5)	Digital Twin (MRL 6-7)	Digital Predictive Twin (MRL 8-9)	

The overview shows that virtual representations are to be further developed along the process development phases in all dimensions with the goal to enable a wide range of possible applications. However, the virtual representations must be designed in such a way that simplified modelling blocks can be used in each development phase in order to serve the entire range of possible applications at any time. To demonstrate the application of the novel framework, four use-cases in the different process development stages are presented in the following chapter.

6 Virtual representation use-cases within the energy sector

In the following chapter, the proposed framework explained in chapter 5 is applied in several use-cases. For each development stage from Digital Model to Digital Predictive Twin, an application was selected to demonstrate the usability of the novel framework. In Fig. 17, the four virtual representation use-cases presented in this thesis are visualized.

First of all, the development of a Power-to-Liquid (PtL) process is accompanied by a Digital Model, which helps by validating lab-scale experiments and scaling up the process to pilot scale. The Digital Model of the PtL process uses offline data to deliver validated mass and energy balances as a basis for the conceptual design of a 1 MW_{el} pilot plant in Graz (AUT) (**Paper II**) [114].

The second use-case deals with the further development of the sorption enhanced reforming (SER) process in combination with oxyfuel combustion (OxySER). The accompanying Digital Shadow is able to process measurement data from the 100 kW_{th} pilot plant at TU Wien continuously to visualize the process performance (**Paper III**) [98].

More advanced applications get possible with the Digital Twin of the third use-case. The Digital Twin for the Biomass-to-Gas (BtG) process enables the process automation of the 100 kW_{th} pilot plant at TU Wien. Therein, the measurement data is processed on a cloud platform and further transferred to a model predictive control (MPC) unit, where, based on the current process performance, changes of manipulated variables are sent to the control system directly to reach an optimized operation point. The simulation model of the MPC unit was also validated within a test run at the 1 MW_{th} demonstration plant from BEST in Vienna (AUT) to test the scale-up possibility of the used framework (**Paper I**) [29].

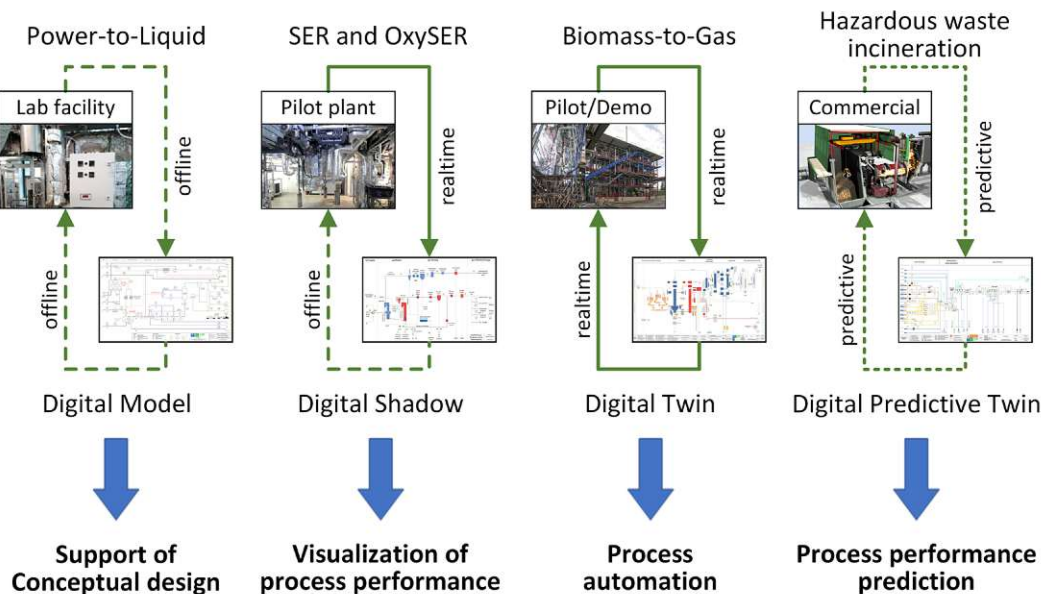


Fig. 17: Virtual representation use-cases presented in this PhD thesis
(Demo plant image Copyright BEST, Wolfgang Bledl)

Finally, the Digital Predictive Twin for a hazardous waste rotary kiln incineration plant is presented, which enables several applications. The underlying dynamic simulation model helps to determine the composition of different not entirely analysed hazardous waste fractions, by using process measurement data. As soon as the same type of waste fractions from the same supplier return, the virtual representation can be used to visualize and optimize the process performance by manipulating the order of hazardous waste fractions. If the waste management data base is coupled with the virtual representation, predictions can be made for the plant's performance presumed the waste fractions are incinerated in a specific order. As a result, not only the order of combustion but also the order of delivery can be influenced. Finally,

the Digital Predictive Twin can be used for the integration of predictive maintenance applications. For example, the condition monitoring of the furnace shell or waste heat recovery boiler become possible, allowing the operator to pre-emptively adjust the operation of the rotary kiln and estimate when the next maintenance is required (**Paper IV**) [104].

6.1 Digital Model of a Power-to-Liquid production plant

Synthetic fuels from the Power-to-Liquid process, better known as e-fuels, can definitely contribute to the reduction of greenhouse gases in the transport sector. Local, preferably biogenic, CO₂ sources can be used and converted together with water in a PtL process to e-fuels. The two main units are the solid oxide electrolyzer (SOEC) unit in co-electrolysis mode to produce syngas, and the Fischer-Tropsch slurry reactor to convert the syngas into FT syncrude. A detailed process flow diagram for the PtL process can be found in Fig. A1 in the appendix. Up to now, only lab facilities are available for the production of FT syncrude using this process route, which have been tested and validated over many experimental campaigns. To achieve pilot-scale stage, it is necessary to develop an overall plant design to maximize the plant efficiency and minimize the associated emissions and costs.

For this objective, a Digital Model was developed to support the engineering of a PtL plant. The pilot plant with a rated power of 1 MW_{el} is to be built in Graz on the site location of AVL List GmbH. More specifically, the Digital Model is intended to be used in the conceptual design phase of the pilot plant to test a wide variety of plant configurations with the goal to maximize the PtL efficiency. In Tab. 7, beside the desired applications, the stakeholders and users, challenges, and the investigated sustainability indicators of the virtual representation are also listed. Furthermore, the TRL and the MRL are discussed for the PtL process. The core systems SOEC and FT slurry reactor have been validated in a laboratory scale, but not coupled, which leads to a TRL of 3-4. The virtual representation within this use-case forms the basis for the planning and construction of a pilot plant with a nominal power of 1 MW_{el} based on validated experimental data from lab facilities. Consequently, the MRL can be set to 4 [114, 115]. All the following content regarding the PtL production plant is based on [114] (**Paper II**).

Tab. 7: General characteristics of the Digital Model

Applications (see chapter 2.3)	<ul style="list-style-type: none"> • Coordination with suppliers, experts and engineering partners (Collaboration in Conceptual design and Engineering phase) • Assistant for constructive and technical process design (Simulation in Conceptual design and Engineering phase) • Holistic evaluation of process design with the possibility to roll-out on a commercial scale (Evaluation and Verification in Conceptual design and Engineering phase)
Stakeholders & Users (see chapter 2.4)	<ul style="list-style-type: none"> • Process simulation experts, plant design engineering and manufacturing partners (Conceptual design, Engineering and Construction & Commissioning phase) • Plant operator (Engineering and Construction & Commissioning phase)
Challenges (see chapter 2.6)	<ul style="list-style-type: none"> • Use of standardized data interfaces and standardized experimental data (Mission-critical challenge) • Finding optimized operating points with PtL efficiencies >55% (Mission-critical challenge)
Sustainability indicators (see chapter 3.2)	<ul style="list-style-type: none"> • Power-to-Liquid efficiency (Technical indicator) $\eta_{PtL} = \frac{\sum_j \dot{m}_j * LHV_j}{P_{el,Total}}, j = [naphtha, middle\ distillate, wax]$ • CO conversion rate at system level (Technical indicator) $X_{CO} = \frac{\dot{n}_{CO,in} - \dot{n}_{CO,out}}{\dot{n}_{CO,in}}$
Technology Readiness Level (TRL) (see chapter 3.1)	<p>TRL 3-4 (Technology core systems separately validated in laboratory) → The core units SOEC in co-electrolysis mode and FT reactor are validated in laboratory separately → The validation of the whole process chain in relevant environment is outstanding</p>
Modelling Readiness Level (MRL) (see chapter 3.1)	<p>MRL 4 (Virtual representation of pilot plant available) → The virtual representation helps to find an optimized configuration for a pilot plant</p>

6.1.1 Framework of Digital Model

The framework of the Digital Model is discussed here to investigate different process configurations to support the conceptual design and engineering of a 1 MW_{el} (nominal power SOEC) pilot plant. In Fig. 18, the 5D modelling framework for the Digital Model of the PtL production plant is visualized. The PtL pilot plant is to be built in Graz at AVL List GmbH site. The following design data is handed over manually to the data management:

- Development of a modular scalable PtL pilot plant with a nominal power (SOEC) of 1 MW_{el}
- PtL efficiency of to be built pilot plant must exceed 55% (CO₂ from gas bottle)
- The pilot plant must be able to produce 500.000 litres of FT syncrude per year

Besides the design data, internal and external experimental data from different SOEC and FT lab units are gathered in the data management, which is based on an on-premise data server. Therein, especially the experimental data are processed and analysed to define appropriate process parameters for the PtL pilot plant. The processed data is stored and further handed over to the simulation model. The process simulation is based on the software IPSEpro 8.0 and is executed on a local user device. Therein, different process configurations and parameters are selected and simulated. In a process validation step, the simulation results are checked for plausibility and compared with each other. Subsequently, the model results are transferred to the service dimension also executed on the same local user device. The simulation results are stored in a model results data base to enable design decisions. By comparing the model results from the data base, experts from different fields and companies can discuss the advantages and disadvantages of the selected process configurations and parameters. Finally, the design decision leads to a frozen design which can be handed over to the basic engineering. All data communication in this framework is based on manual offline data transmission.

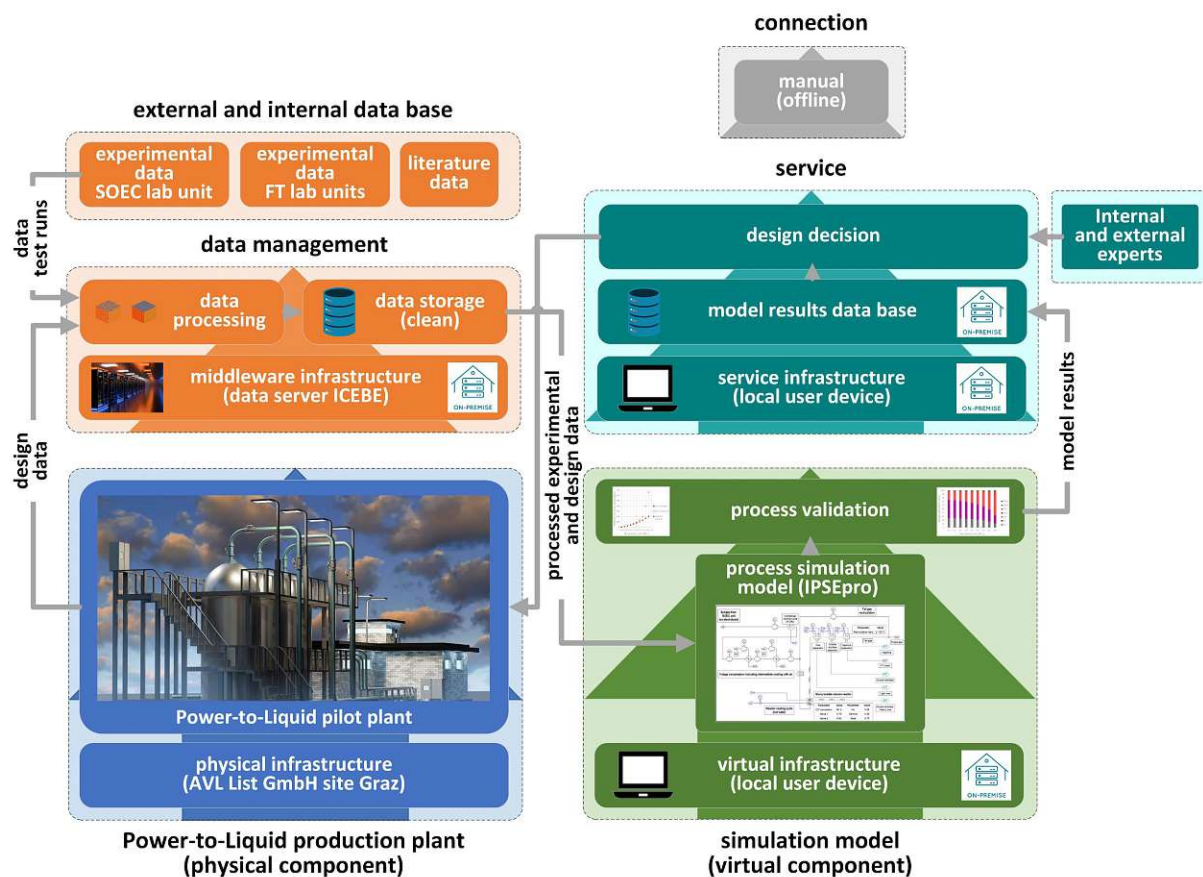


Fig. 18: 5D modelling framework of the virtual representation related to the PtL plant (own images or licensed from Adobe Stock)

6.1.2 Properties of Digital Model

The framework, presented in chapter 6.1.1 lead to the following virtual representation properties listed in Tab. 8. Most of the properties of the Digital Model can be defined at level 0 according to the minimum requirements for a Digital Model in the raised methodology (see chapter 5). The most important characteristic properties are vertical integration, the virtual representation capability and fidelity and the connectivity mode. The Digital Model covers the core process units, which leads to the equipment-based vertical integration level. Furthermore, the Digital Model is based on a steady-state simulation model in IPSEpro, based on a black box SOEC and gray box FT unit. Therefore, the overall system can be defined by the lowest capability and fidelity levels. The connectivity mode of the Digital Model can be defined as manual. All data transmission activities are carried out offline. In the following chapter the underlying process simulation model of the virtual component is explained.

Tab. 8: Digital Model properties for the PtL route

Property classes	Focus	Property level	Description
Vertical integration	Overall	Level 0: Equipment level	Only core process equipment units simulated.
Interoperability		Level 0: Comparable	Process simulation is executed in IPSEpro. The underlying model libraries are based on the equation-oriented language MDL, which is quite different to traditional program languages like C or C++. Resulting validated physical-based mass and energy balances are comparable with simulation results from other software tools but not convertible.
Expansibility		Level 1: Adaptable layout	The process simulation model is based on a model library. Therefore, the process layout can be adapted according to the desired configuration.
Functional safety		Level 0: Systematic capability	The mass and energy balances are validated after each simulation run to avoid systematic failure.
Technological scale-up possibility	Physical component	Level 0: Modular	The SOEC unit is only modularly scalable up to now. The FT unit is fully scalable. The selected overall system level is based on the lowest unit level.
Degree of automation		Level 1: Semi-automated	The PtL pilot plant should run continuously over several weeks. Therefore, a semi-automated operation mode is necessary.
Physical safety		Level 2: Primary + Secondary + Tertiary safety measures	The PtL pilot plant must be approved by the relevant authorities and the highest safety standards must be met.
Virtual representation capability	Virtual component	Level 0: Static	The virtual representation is based on a steady-state simulation model in IPSEpro.
Virtual representation fidelity		Level 0: Black box (macroscopic level)	The SOEC simulation model is only based on mass and energy balances (black box). The FT slurry reactor model is based on the extended ASF model to simulate the FT product distribution based on process parameters (gray box). The selected overall system level is based on the lowest unit level.
Virtual representation intelligence		Level 0: Human triggered	The simulation model is operated manually by defining suitable process configurations and parameters.
Connectivity mode	Data management and connection	Level 0: Manual	The virtual representation is based on offline experimental data from laboratory, design data and literature.
Data integration level		Level 0: Manual	
Update frequency		Level 0: Yearly/Monthly	The virtual representation aims to provide an average steady-state design point in the conceptual design phase.
Cybersecurity		Level 0: Role-based access control	The virtual representation is executed on an authorized local user devices.
Human interaction	Level 0: Smart user devices		
User focus	Service	Level 0: Single	The process simulation model is operated locally by only one developer.

6.1.3 Process simulation of Digital Model

The virtual component of the Digital Model is based on a steady-state process simulation model executed in the software IPSEpro 8.0, based on an equation-oriented modelling language called MDL. User-defined simulation models for each process unit were developed in the so-called model development kit based on mass and energy balances, which are subsequently interconnected in a flowsheet-based simulation environment. Furthermore, the SOEC model is based on the applicable stoichiometry of the chemical reactions for the conversion of H_2O to H_2 and CO_2 to CO . The FT slurry reactor model assumes that FT products are solely paraffins and the CO-conversion was assumed with 55%. Additionally, the extended ASF model, developed by Förtsch et al. [154] is used to estimate the FT product spectrum. The tail gas reformer is modelled as a Gibbs reactor. Furthermore, the stoichiometry of the chemical reactions for the conversion of CH_4 , C_2H_6 and C_3H_8 to CO and H_2 with defined conversion rates between 90-99% are used. Further details regarding the underlying simulation models can be found in [114, 115].

6.1.4 Results of Digital Model use-case

With the help of the virtual representation, optimum design parameters for the engineering of the PtL pilot plant can be determined. In the study, fixed operating conditions for SOEC and FT synthesis are assumed and the plant configuration options with respect to tail gas recirculation are investigated. In Fig. 19, the tail gas composition of the plant configurations with (left) and without (right) tail gas reforming are compared. It can be clearly seen that in the configuration without reforming, an exponential increase in CO_2 at higher recirculation rates occurs, which must be passed through the FT reactor and product separation. In Fig. 20 (left) the dependency of the tail gas volume flow on the recirculation ratio is visualized, where the exponential increase is also visible. Consequently, due to the more efficient use of tail gas in the case of the configuration with reforming together with high recirculation rates, the highest PtL efficiencies can be achieved, which is visualized in Fig. 20 (right).

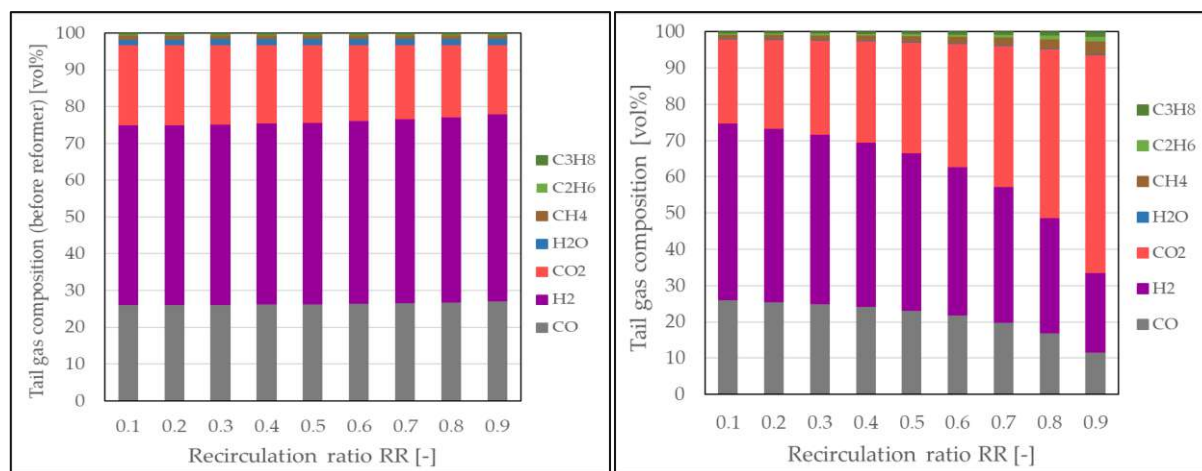


Fig. 19: Tail gas composition of plant configuration with (left) and without tail gas reforming (right) [114]

In Tab. 9, the resulting sustainability indicators for the investigated process configurations are listed. Therein, it can be seen that the plant configuration with tail gas recirculation and reforming delivers the best results. The desired performance parameters, as discussed in chapter 6.1.1, can only be achieved with the plant configuration with tail gas reforming by avoiding the accumulation of CO_2 in the tail gas. The PtL efficiency level $> 62\%$ and CO conversion rate level $> 96\%$ can be obtained and thus more than 550.000 litre of FT syncrude per year can be produced under consideration of high plant availability. However, the plant configuration with reforming requires a syngas from the SOEC with higher H_2/CO ratios. Furthermore, no additional purge gas in reforming mode is available for the steam production of the SOEC or external processes due to the internal consumption for the heat provision of the reforming process itself. The additional tail gas reforming process step also causes higher investment costs.

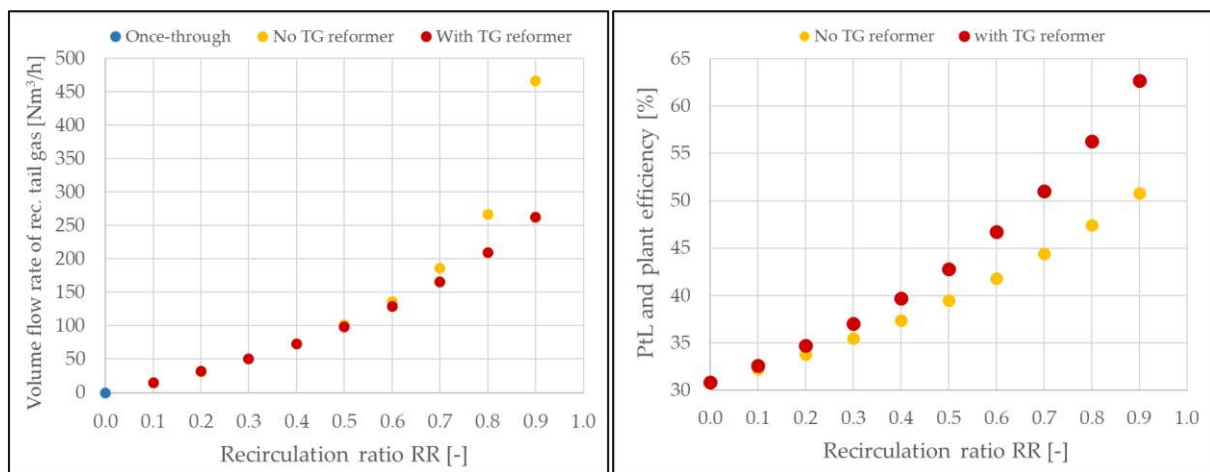


Fig. 20: Volume flow rate of tail gas (left) and Power-to-Liquid efficiency (right) both depending on the recirculation ratio and the plant configuration with and without tail gas reforming [114]

This results in design parameters for the investigated 1 MW_{el} pilot plant, which are visualized in Fig. 21. Based on a SOEC in co-electrolysis mode with a nominal power of 1 MW_{el} with an operating temperature of 850°C and ambient pressure level, about 343 Nm³/h of syngas with a H₂/CO ratio of 3.3 is produced. The reformed and recycled tail gas with a volume flow of 285 Nm³/h and a H₂/CO ratio of 1.2 is added to the syngas to reach the required H₂/CO ratio of 2. After a water removal step, a three-stage compression of the gas mixture to reach the required pressure level of 21 bar is conducted. Subsequently, the gas mixture is converted within the FT slurry reactor at a temperature level of 210 °C. The reaction heat is cooled by a hot water cooling cycle, which is not detailed further in the conception phase. The liquid FT product which is removed from the slurry continuously amounts to 18 kg/h and consists mostly of FT waxes. The gaseous FT product is separated in a multi-stage flash distillation. From the separation stage, 20.5 kg/h FT middle distillate, 13.7 kg/h FT naphtha and 5.6 kg/h FT waxes are gained. The tail gas is mostly recirculated (90%) to the tail gas reformer, where the short-chain hydrocarbons (C₁-C₃) are converted mostly to CO and H₂ while consuming H₂O. Furthermore, the rWGS reaction takes place to convert CO₂ to CO while consuming H₂. The necessary heat for the endothermic steam reforming reactions is provided by the combustion of a minor part (10%) of the tail gas.

Tab. 9: Resulting sustainability indicators for the investigated PtL process configurations [114]

Parameter (Sustainability indicator)	Unit	Once-Through without recirculation (RR = 0%)	Plant configuration without reformer (RR = 90%)	Plant configuration with reformer (RR = 90%)
Fischer-Tropsch products ¹	l _{FT} /a	~ 257 000	~ 426 000	~ 556 000
Power-to-Liquid efficiency	%	30.8	50.8	62.7
CO conversion rate at system level	%	55.0	92.4	96.5
Required H ₂ :CO ratio (SOEC)	-	2.0	2.1	3.3
Purge gas chemical energy	kW	365	102	- ²

¹ 7500 operating hours per year assumed
² purge gas needed for providing heat for tail gas reformer through combustion

For optimization of the provided design data, further studies regarding the CO₂ conversion within the SOEC and the FT reactor due to the use of rWGS active catalysts should be conducted. Furthermore, the tail gas reforming must be validated in experimental test series. In addition, a holistic optimization of the whole process route can only be undertaken by conducting experiments with different operating conditions in the SOEC and FT reactor. In that way, synergies, especially due to process heat integration, can be achieved, which can be implemented after the validation of pilot scale experiments. Finally, a techno-economic and ecological assessment is needed for commercial-scale plants. Further details to the PtL simulation results and first commercial-scale investigations can be found in [114, 115, 155, 156].

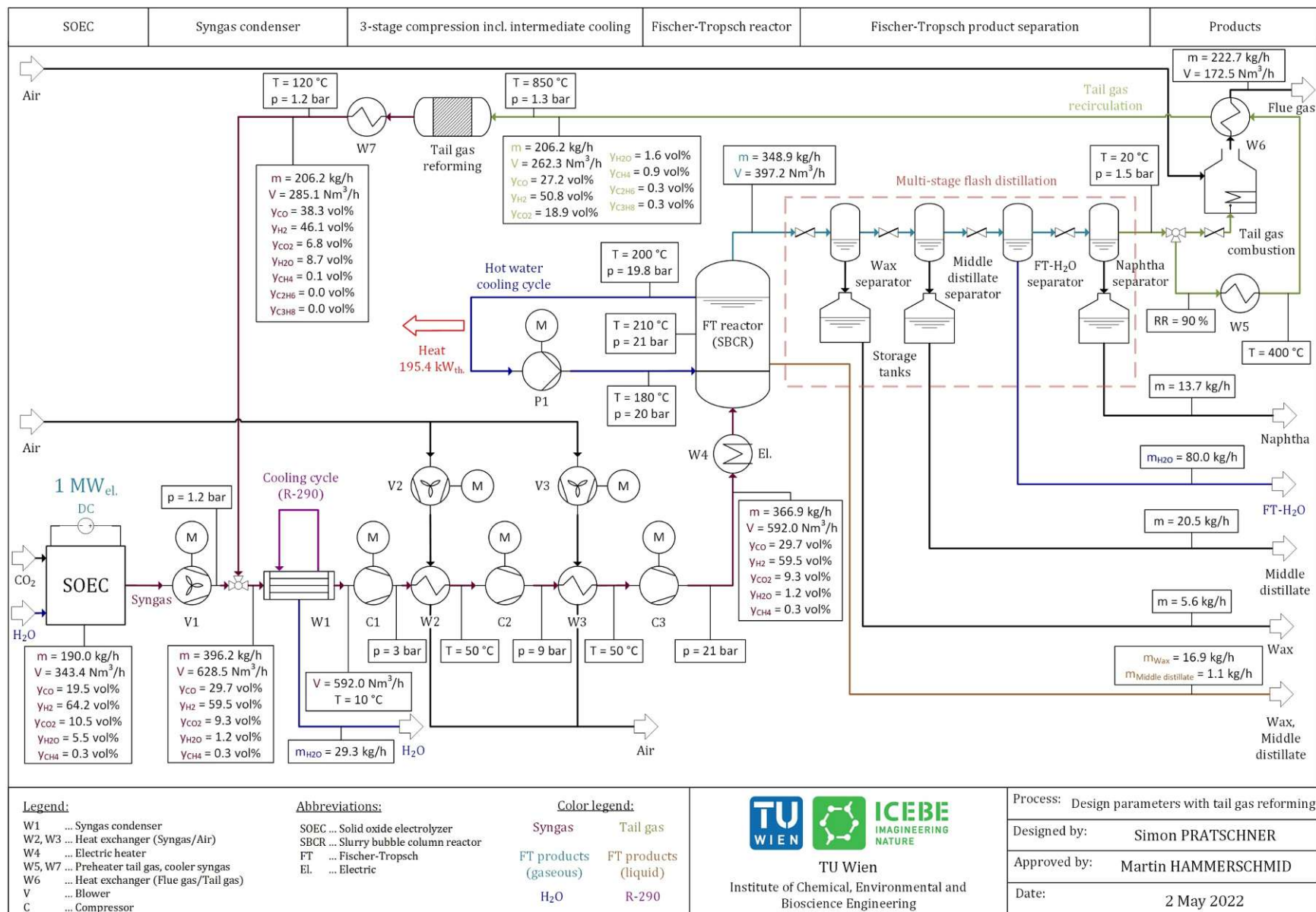


Fig. 21: Design parameters for the plant configuration with tail gas reforming within the 1 MW_{el} PtL pilot plant [114]

6.2 Digital Shadow of a zero-emission reducing gas production plant

The production of a biomass-based reducing gas for use in the raw iron production can be achieved with the sorption enhanced reforming (SER) process. By combining the SER process with oxyfuel combustion a zero-emission reducing gas can be produced utilizing the so-called OxySER process. In this process with subsequent gas cleaning steps, a suitable product gas for the use within the direct reduction process can be produced. In the OxySER process, pure oxygen is used instead of air, as a fluidization agent in the combustion reactor of the DFB gasification. Therefore, a nitrogen-free flue gas can be produced, which consists mainly of CO₂. If the CO₂ is further used in various industrial applications (carbon capture and utilization, CCU) or stored (carbon capture and storage, CCS), a below zero emission reducing gas can be produced. A detailed process flow diagram for the OxySER process can be found in Fig. A2 in the appendix. For the production of reducing gas with SER in a DFB gasification process, two pilot plants exist. In the 100 kW_{th} pilot plant at TU Wien several SER test runs were successfully carried out [98, 107]. In the 200 kW_{th} pilot plant at University of Stuttgart the SER and OxySER operation modes were successfully demonstrated [108].

In order to create a further scale up step towards a demonstration plant, large scale simulation studies are needed based on pilot plant experimental data to determine the environmental and economic footprint of biomass-based reducing gas production. In addition to the simulation studies, the Digital Shadow will also enable the coupling of the TU Wien pilot plant with the integrated simulation model to validate test runs continuously and to visualize sustainability indicators to find optimum operation points. In Tab. 10, general characteristics and goals of the Digital Shadow are listed. The applications range from process design investigations in the conceptual design and engineering phase to monitoring, visualization and validation of process parameters in the operation and optimization phase. Furthermore, stakeholders and users are defined, in this case process simulation experts and engineering partners for the investigation of the process design. Additionally, iron and steel industry experts are consulted to incorporate domain knowledge in the process design phase. Furthermore, plant operators from the pilot plant at TU Wien are consulted to adapt the intended visualizations to the necessities of the plant operation. The identified challenges are only mission-critical. The sustainability indicators show that within the Digital Shadow use-case, besides technical also economic and ecological parameters are considered. The technical indicators aim to achieve a product gas with the specified gas quality suitable for the iron and steel industry's direct reduction process. The economic and ecological indicators are selected to realize a comparison with other comparable technologies. The SER and OxySER process is already validated in pilot-scale, which leads to TRL of 4-5. The Digital Shadow includes validated experimental data from pilot plant experiments and helps to predict mass & energy balances, and economic and ecological footprints for large scale application. Therefore, the MRL can be set to 5-6. All the following content regarding the SER and OxySER production plant is based on [98] (**Paper III**).

Tab. 10: General characteristics of the Digital Shadow

<p>Applications (see chapter 2.3)</p>	<ul style="list-style-type: none"> Assistant for constructive and technical process design (Simulation in Conceptual design and Engineering phase) Automatic monitoring of process performance by visualization of sustainability indicators (Monitoring in Operation phase) Holistic evaluation and optimization of process design with the possibility to roll-out on a commercial scale (process parameters) (Evaluation and Verification in Engineering and Optimization phase)
<p>Stakeholders & Users (see chapter 2.4)</p>	<ul style="list-style-type: none"> Process simulation experts (Conceptual design and Engineering & Operation and Optimization phase) Plant design engineering partners (Conceptual design and Engineering phase) Iron and steel industry experts (Conceptual design and Engineering & Operation and Optimization phase) Plant operators of pilot plant TU Wien (Operation and Optimization phase)
<p>Challenges (see chapter 2.6)</p>	<ul style="list-style-type: none"> Use of standardized data interfaces (Mission-critical challenge) Standardization and harmonization of all available experimental data from various pilot plants (Mission-critical challenge) Finding optimized operating points with suitable reducing gas quality (Mission-critical challenge) Development of plant configurations with minimal production costs and CO₂ footprint (Mission-critical challenge)
<p>Sustainability indicators (see chapter 3.2)</p>	<ul style="list-style-type: none"> Gas quality (Technical indicator) $GQ = \frac{\% CO + \% H_2}{\% CO_2 + \% H_2O}$ CO₂ recovery rate (Technical indicator) $RR_{CO_2} = \frac{CO_2 \text{ volume flow flue gas}}{CO_2 \text{ volume flow total (FG + PG)}}$ Hydrogen / carbon monoxide ratio (Technical indicator) $H_2/CO = \frac{\% H_2}{\% CO}$ Relative net present value (Economic indicator) → compared with steam reforming of natural gas (reference option) $NPV_{rel} = [(R_{sec. prod.} - E)_0 - (R_{sec. prod.} - E)_{ref}] \cdot CDF - (I_0 - I_{ref.}) \quad , \quad CDF = \frac{(1+i)^n - 1}{i \cdot (1+i)^n}$ Levelized production costs (Economic indicator) $LCOP = \frac{I_0 + (E - R_{sec. prod.}) \cdot CDF}{M_{t,main prod.} \cdot CDF} \quad , \quad CDF = \frac{(1+i)^n - 1}{i \cdot (1+i)^n}$ Payback time analysis (Economic indicator) $A = P * \frac{i * (1+i)^{n_p}}{(1+i)^{n_p} - 1} \quad , \quad \text{payback time } n_p$ Global warming potential factor (Environmental indicator) $CO_{2e} = \frac{CO_{2e} \text{ emissions whole crude steel production process}}{\text{produced amount of crude steel}}$
<p>Technology Readiness Level (TRL) (see chapter 3.1)</p>	<p>TRL 4-5 (Main process units validated in pilot-scale) → The whole process chain from biomass feeding to product gas cleaning is tested in pilot-scale → The validation of the whole process chain in relevant environment is outstanding.</p>
<p>Modelling Readiness Level (MRL) (see chapter 3.1)</p>	<p>MRL 5-6 (Virtual representation of pilot plant available) → The virtual representation helps to find an optimized operation point in pilot scale and enable simulation studies for the investigation of the economic and ecological performance of the process.</p>

6.2.1 Framework of Digital Shadow

In Fig. 22, the 5D modelling framework for monitoring the biomass-based reducing gas production plant is visualized. Therein, it can be seen that the 100 kW_{th} DFB gasification pilot plant at TU Wien is the basis for the physical component. Raw sensor data from the control system or more precisely from the PLC is transmitted every minute via Modbus/TCP to a local edge device, where it is forwarded via MQTT to the IoT gateway of an Azure Cloud environment. The cloud-based data management processes and stores data to create suitable data sets for the following virtual component. The processed sensor data sets are transferred every minute via TCP/IP to a local edge device, where the simulation tool IPSEpro 8.0 is running. The model results are validated and handed over to the service dimension via TCP/IP. The service dimension application is based on local infrastructure and on-premise software and can be monitored on a local user device. The model results from the process simulation are continuously visualized on a MATLAB-based dashboard. New simulation results are added to the dashboard each minute, where the plant operators can monitor the process performance.

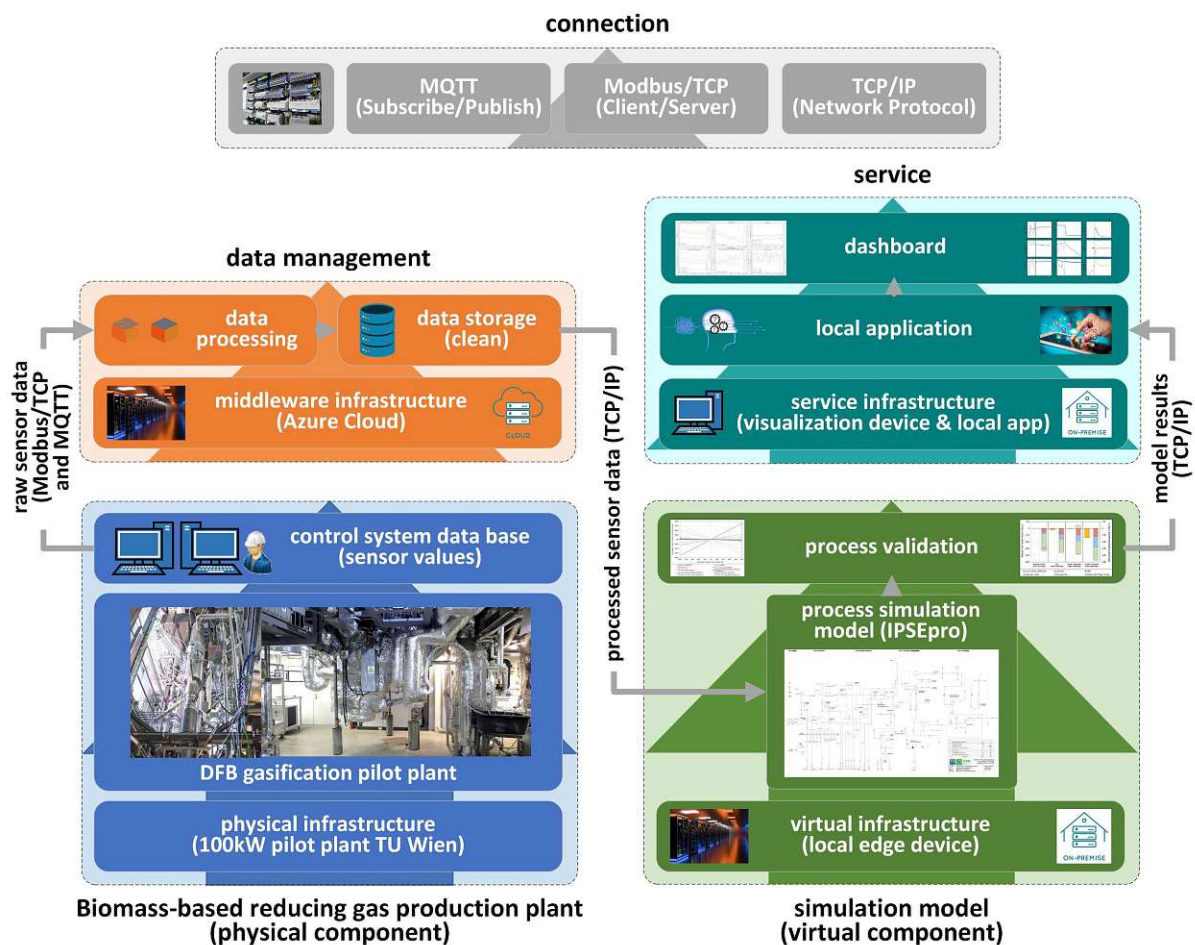


Fig. 22: 5D modelling framework of the virtual representation related to the SER and OxySER pilot plant (own images or licensed from Adobe Stock)

6.2.2 Properties of Digital Shadow

In Tab. 11, the properties of the investigated Digital Shadow use-case are listed. Therein it can be seen that through automated continuous validation of process performance, most properties can be defined as level 1. All the raised properties fulfil the required Digital Shadow property level according to the novel methodology. The Digital Shadow covers all main units of the process chain, which leads to the plant-based vertical integration level. Furthermore, a gray box quasistatic simulation model in ad-hoc mode is used to ensure the continuous process validation. The process performance is monitored continuously by running the process simulation every minute. Therefore, a uni-directional and semi-automated data transmission has been accomplished.

Tab. 11: Digital Shadow properties for the biomass-based reducing gas production plant

Property classes	Focus	Property level	Description
Vertical integration	Overall	Level 1: Plant level	Main units of process chain simulated.
Interoperability		Level 0: Comparable	Process simulation is executed in IPSEpro. The underlying model libraries are based on the equation-oriented language MDL, which is quite different to traditional program languages like C or C++. Resulting validated physical-based mass and energy balances are comparable with simulation results from other software tools but not convertible.
Expansibility		Level 1: Adaptable layout	The process simulation model is based on a model library. Therefore, the process layout can be adapted according to the desired configuration.
Functional safety		Level 1: Implemented redundancies	The mass and energy balances are validated after each simulation run to avoid systematic failure. In addition, to validating the simulation results, the measured value adjustments are displayed in the dashboard to provide the user with a further plausibility check.
Technological scale-up possibility	Physical component	Level 2: Fully scalable	The scalability of the DFB gasification unit was already demonstrated in several commercial-scale plants in different operation modes.
Degree of automation		Level 1: Semi-automated	The pilot plant is already operated for a few days at a time. Therefore, a semi-automated operation mode is implemented to support the plant operators.
Physical safety		Level 2: Primary + Secondary + Tertiary safety measures	The pilot plant has been approved by the relevant authorities and the highest safety standards must be met.
Virtual representation capability	Virtual component	Level 2: Ad-hoc (based on quasistatic model)	The virtual representation is based on the PSServer process module of IPSEpro. A quasistatic simulation model is executed every minute.
Virtual representation fidelity		Level 1: Gray box (intermediate level)	The DFB gasification (main process unit) is based on mass and energy balances. Furthermore, the equilibrium state of the rWGS reaction is calculated and the tar content in the product gas is determined via a correlation with the continuously measured methane content.
Virtual representation intelligence		Level 1: Automated	The simulation model calculates an operation point automatically every minute.
Connectivity mode	Data management and connection	Level 1: Uni-directional	The virtual representation is based on an automatic data flow (every minute) from the pilot plant to the data management. There, it is automatically processed and sent to the simulation model to validate the process performance continuously.
Data integration level		Level 2: Fully automated	
Update frequency		Level 2: Hourly/every minute	The virtual representation calculates the process performance every minute with a quasistatic simulation model in ad-hoc mode.
Cybersecurity		Level 1: Discretionary access protection	The data collection (control system), the data management (cloud) and the simulation environment (local edge device) are separated from each other in terms of system technology and separate access rights.
Human interaction	Service	Level 0: Smart user devices	The dashboard from the service dimension is visualized via a local MATLAB application on the local user device, where the operator can monitor the performance.
User focus		Level 1: Multiple without interaction of energy plant hierarchy layers	The dashboard from the service dimension can be viewed simultaneously by multiple operators and other stakeholders.

6.2.3 Process simulation of Digital Shadow

The virtual component of the Digital Shadow is based on a quasistatic process simulation model in ad-hoc mode executed in the software IPSEpro 8.0. Similar to the Digital Model use-case, user-defined MDL-based simulation models are interconnected in a flowsheet-based simulation environment. The validation mode is used to solve an overdetermined system of equations. This allows the measurement errors to be compensated by specifying the inaccuracies of different measurements. To enable the automated simulation, the PSServer module of IPSEpro is used, which provides a code-based interface to link the processed measurement data from the data management with the model parameters in IPSEpro. Furthermore, the simulation frequency can be defined. The process chain consists of the DFB gasification and further gas cooling and cleaning steps. All units are based on mass and energy balances. Furthermore, within the DFB gasification model [157] the equilibrium state of the rWGS reaction is calculated and the tar content in the product gas is determined via a correlation with the continuously measured methane content [158]. For further details about the model please refer to [98].

6.2.4 Results of Digital Shadow use-case

The Digital Shadow helps to investigate commercial-scale concepts and to monitor the process performance of the pilot plant at TU Wien to find optimized operation points. In Tab. 12, the input and output parameters for a 100 MW biomass-based reducing gas production plant in OxySER mode are listed. It can be seen that for the production of 100 MW reducing gas, 133 MW of wood chips are required. For the OxySER mode, about 11000 Nm³/h of oxygen are additionally required to capture about 36000 kg/h of CO₂ within the flue gas stream.

Tab. 12: Input and Output data of an OxySER plant with 100 MW reducing gas power [98]

Input			Output		
Parameter	Unit	Value	Parameter	Unit	Value
Fuel (wood chips wet)	MW	133	Reducing gas	MW	100
	kg/h	50400		Nm ³ /h	28800
Bed material inventory	kg	25000	Flue gas	Nm ³ /h	22800
Fresh bed material	kg/h	1770		kg/h	40200
Cooling capacity in % of fuel power	% (kW/kW _{th})	5 - 20	Carbon dioxide (for CCU)	kg/h	36100
Electricity consumption	kW	2800	Bed material	kg/h	1000
Oxygen	Nm ³ /h	11020	Ash and dust	kg/h	1050
Fresh water	kg/h	378			
Scrubber solvent (RME)	kg/h	200			

In Tab. 13, the sustainability indicators and main process parameters of the three investigated options are gathered. The required gas quality for the direct reduction process can be reached and a high H₂/CO ratio can be achieved. The required reduction gas can be produced at production costs between 10-15 €/GJ. The payback time shows the profitability compared to the natural gas-based direct reduction route. Thus, the resulted payback time of all three options are higher than the expected plant lifetime of 20 years. If the natural gas costs are doubled, which has already happened compared to the base year 2019, the calculated payback times of the biomass-based options are between 2-5 years.

In Fig. 23, the sensitivity analysis of the techno-economic analysis is visualized. Therein, the sensitivity of the relative net present value to changes of the underlying cost and revenue rates is investigated. The relative net present value describes the profitability of the biomass-based reducing gas production process compared to the state-of-the-art reducing gas production via steam reforming of fossil natural gas. The figure shows that the profitability of the biomass-based OxySER process compared to the steam reforming of natural gas is highly dependent on the wood price, natural gas price, CO₂ emission allowance price and the investment costs.

Tab. 13: Resulting sustainability indicators for the investigated SER and OxySER process configurations [98]

Parameter (Sustainability indicator)	Unit	Reducing gas production with wood-based SER (Option 1)	Reducing gas production with wood-based OxySER (existing ASU used and CCU applied) (Option 2)	Reducing gas production with wood-based OxySER (additional ASU used and no CCU applied) (Option 3)
Produced reducing gas	Nm ³ /h	28800	28800	28800
Captured and utilized CO ₂	kg/h	-	36100	-
Gas quality (reducing gas) (requirement: > 9)	-	9.8	9.8	9.8
CO ₂ recovery rate	%	-	> 95	-
Hydrogen / carbon monoxide ratio (requirement: > 0.5)	-	7.6	7.6	7.6
Levelized production costs	€/GJ _{reducing agent}	11.5	10.9	15.3
Payback time base year 2019 (natural gas costs 25 €/MWh)	a	∞	24	∞
Payback time base year 2021 (natural gas costs 50 €/MWh)	a	2	2	5
Global warming potential	t CO ₂ e/t _{CS}	0.28	< 0	0.28

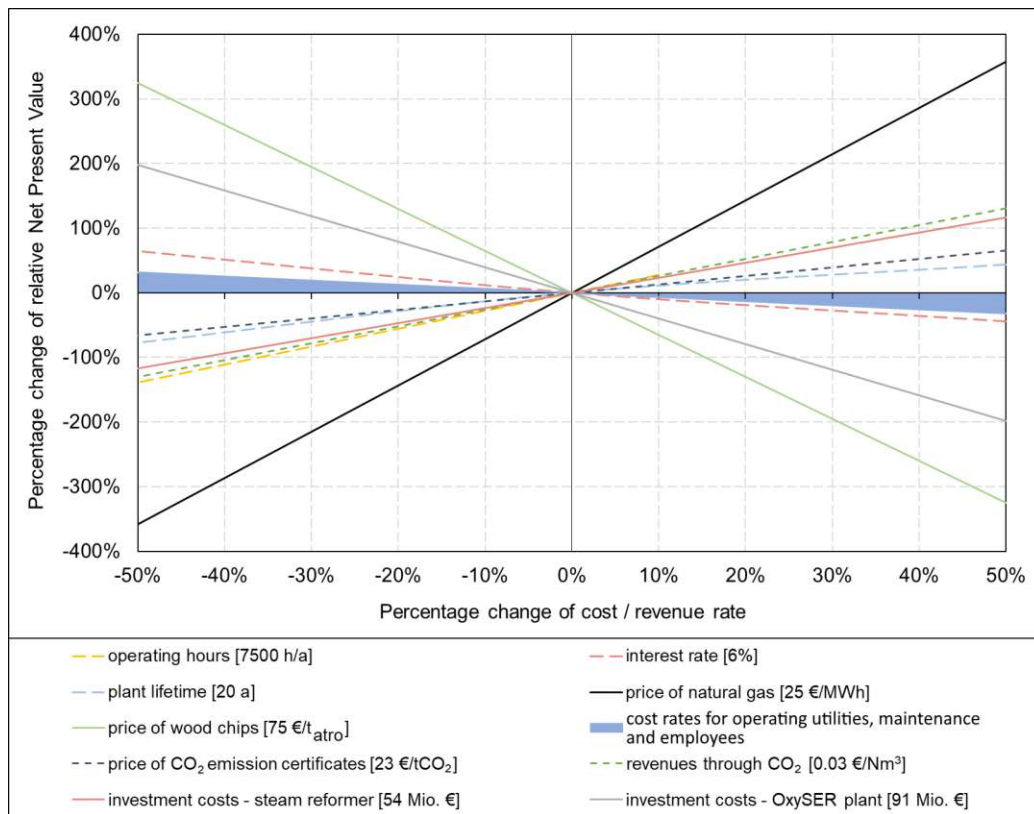


Fig. 23: Sensitivity analysis of the techno-economic analysis of different iron and steelmaking routes [98]

In Fig. 24, the economic and ecological footprint of different iron and steelmaking routes are compared. It can be seen that the state-of-the-art coal-based blast furnace process is the cheapest and most climate-damaging technology with about 5 €/GJ_{reducing agent} and 1.7 tCO₂e/t_{crude steel}. Approximately 50% of CO₂ emissions can be saved if steelmaking is replaced by natural gas- or hydrogen-based direct reduction instead of coal-based blast furnaces. The use of biomass-based reducing gas in direct reduction without CCU (Option 1 and 3) can save more than 80% of CO₂ emissions. If the captured CO₂ in OxySER mode is further utilized or stored (Option 2), a below zero emission reducing gas can be produced. The production costs of the biomass-based reducing gas are two to three times higher compared to the coal-based blast furnace process but in the same range as the natural gas-based direct reduction process.

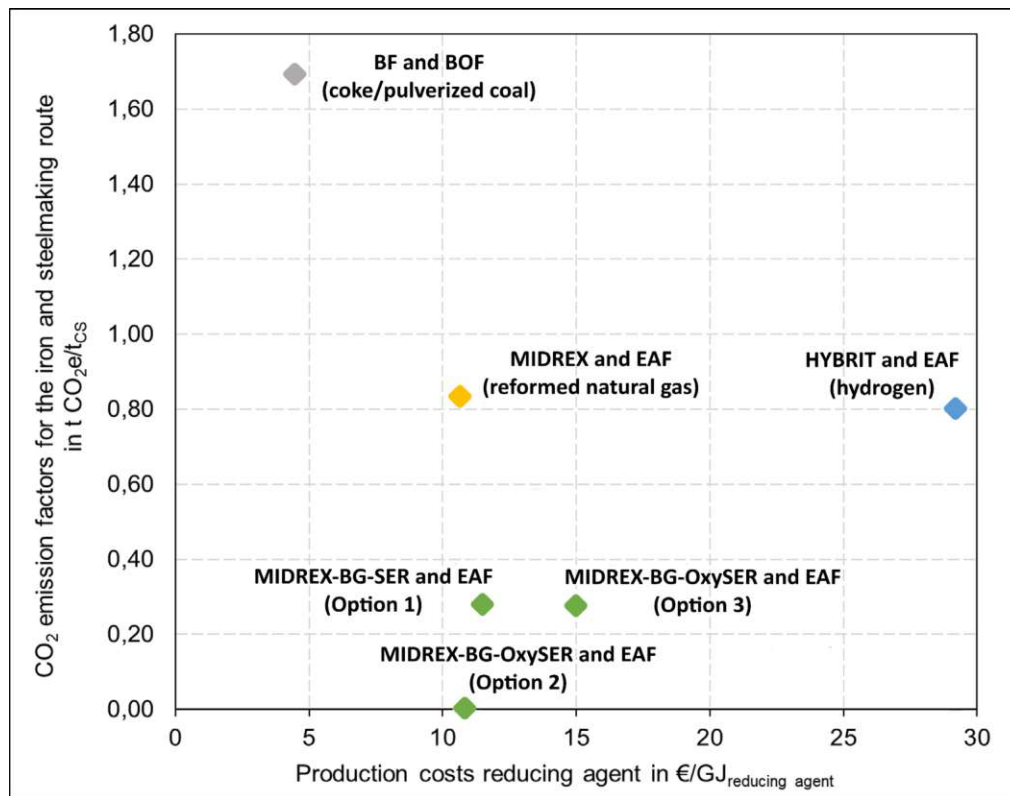


Fig. 24: Comparison of economic and ecological footprint of different iron and steelmaking routes [98]

Besides the simulation studies of commercial-scale plant concepts, the Digital Shadow is able to monitor the process performance of the 100 kW_{th} pilot plant at TU Wien. In Fig. 25, an exemplary dashboard from a conventional DFB steam gasification test run is shown. On the left side, the adjusted values, calculated by the process simulation, for the product and flue gas composition as well as the volume and mass flows of product and flue gas are visualized. On the right side, the proportional adjustments of various simulation results are shown in order to be able to check the reliability of the results. The process monitoring application of the 100 kW_{th} pilot plant at TU Wien can also be used for other operating modes like SER, but it can not be operated in OxySER mode due to the missing brickwork at the CR.

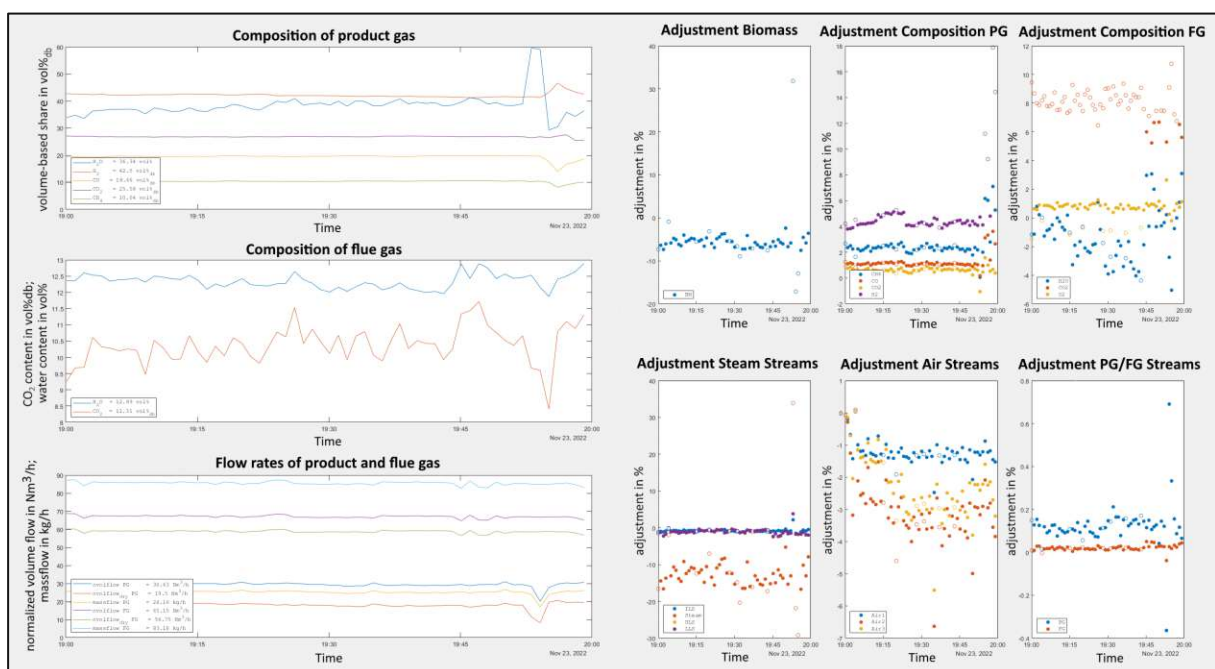


Fig. 25: MATLAB-based dashboard for monitoring the adjusted values for gas compositions & flow rates [158]

In Fig. 26, another dashboard for monitoring the process performance is visualized. Therein, several technical performance figures like efficiencies, the product gas yield and heat streams can be observed.

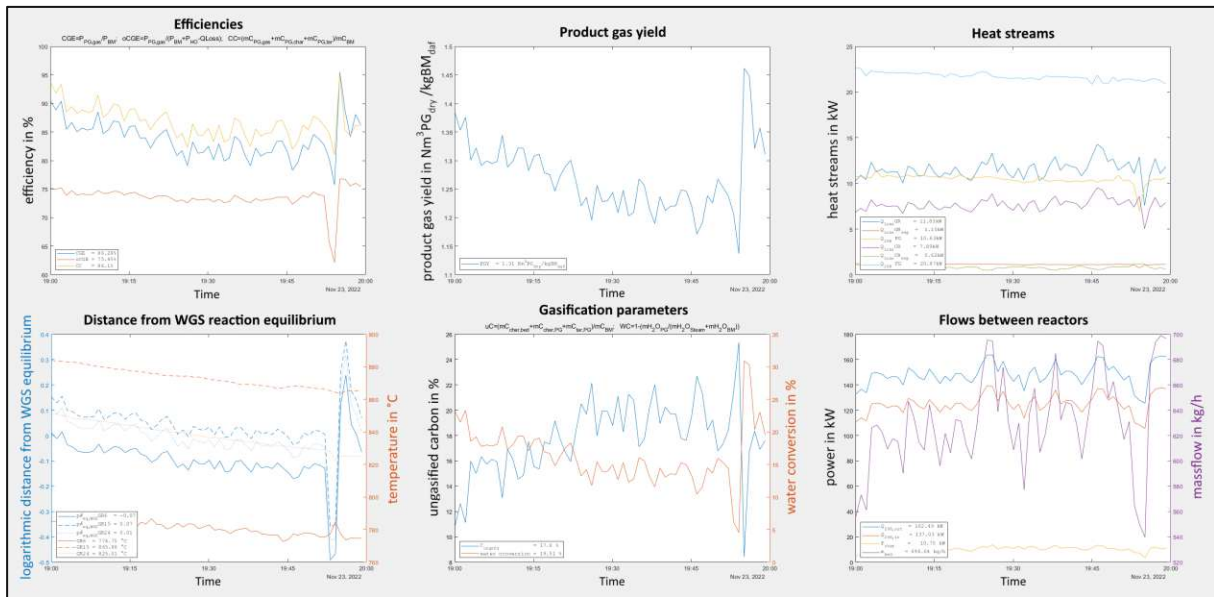


Fig. 26: MATLAB-based dashboard for monitoring the process performance [158]

The dashboards help plant operators to continuously assess the plant performance and to find optimized operating points. Further details about the simulation studies regarding the OxySER process can be found in [98].

6.3 Digital Twin of a Biomass-to-Gas production plant

The Digital Twin use-case is based on the Biomass-to-Gas process. Therein, biomass is converted to product gas within the DFB steam gasification process. The product gas is cleaned and cooled in several process steps before the clean product gas is converted further within a fluidized bed methanation process to raw-SNG. The raw-SNG consists mainly of methane, carbon dioxide, hydrogen and water. After a number of upgrading steps, SNG can be fed to the gas grid. A detailed process flow diagram for the Biomass-to-Gas process can be found in Fig. A3 in the appendix. The DFB gasification process has already been built at commercial-scale several times worldwide. The fluidized bed methanation process was first demonstrated at 1 MW_{SNG} scale in Güssing in 2009 [138]. At TU Wien a 100 kW_{th} DFB gasification pilot plant combined with a 10 kW_{th} fluidized bed methanation plant exists [135, 136].

In order to optimize the Biomass-to-Gas process before the final commercialization step, a Digital Twin was developed for the pilot plant at TU Wien. Apart from the possibilities listed in the Digital Shadow use-case, the Digital Twin enables a full process automation by coupling the physical facility with a flow-sheet based simulation model and a model predictive control (MPC) unit. Thus, the pilot plant can be operated automatically. Furthermore, optimized operation points can be reached with the digital assistant. In Tab. 14, general characteristics of the developed Digital Twin are listed. The applications are focused on the operation and optimization phase by monitoring and automation of the Biomass-to-Gas process. Due to the strong focus on operation, no engineering experts are needed. Therefore, the stakeholders are the plant operators and domain experts in several disciplines. Automation means that safety- and time-critical challenges have to be considered in addition to mission-critical ones. The sustainability indicators are focused on technical parameters. As the Biomass-to-Gas process was already demonstrated in Güssing, TRL 7 has been reached. Due to the automation of the pilot plant and the validation of the control concept with the 1 MW_{th} demonstration plant in Simmering, the MRL can also be declared as 7. All the following content regarding the BtG plant is based on [29] (**Paper I**).

Tab. 14: General characteristics of the Digital Twin

Applications (see chapter 2.3)	<ul style="list-style-type: none"> Automatic monitoring of process performance by visualization of sustainability indicators (Monitoring in Operation phase) Monitoring and optimization of product quality (Evaluation and Verification in Operation and Optimization phase) Condition monitoring and anomaly detection of process units (Monitoring and Evaluation in Maintenance phase) Process automation and optimization using advanced control strategies, which also allows to predict the future performance (Orchestration and Prediction in Operation and Optimization phase)
Stakeholders & Users (see chapter 2.4)	<ul style="list-style-type: none"> Process simulation experts (Operation and Optimization phase) Process control experts (Operation and Optimization phase) Data management and connection experts (Operation and Optimization phase) Plant operator of pilot plant at TU Wien (Operation and Optimization phase)
Challenges (see chapter 2.6)	<ul style="list-style-type: none"> Use of standardized data interfaces (Mission-critical challenge) Use of simulation models which are robust and valid for a wide range of operation points (Mission-critical challenge) Periodic verification and recalibration of measurement equipment (Mission-critical challenge) Decoupling of virtual representation's IT architecture from control system (Safety-critical challenge) Development of a stable high-fidelity two-way data connection by reaching sufficient data resolution, quality and latency (Time-critical challenge)
Sustainability indicators (see chapter 3.2)	<ul style="list-style-type: none"> Cold gas efficiency (Technical indicator) $\eta_{CG} = \frac{P_{PG} - (P_{CR,Fuel} - \dot{Q}_{loss,DFB} - P_{tar} - P_{char})}{P_{GR,Fuel}} * \frac{P_{RawSNG}}{P_{PG,syn} + P_{H2,ext}}$ Carbon utilization factor (Technical indicator) $\eta_C = \frac{\dot{m}_{C,PG}}{\dot{m}_{C,GR,Fuel}} * \frac{\dot{m}_{C,RawSNG}}{\dot{m}_{C,PG,syn}}$ Raw-SNG yield (Technical indicator) $SNGY = \frac{\dot{V}_{N,RawSNG}}{\dot{m}_{GR,Fuel} + \dot{m}_{H2,ext}}$
Technology Readiness Level (TRL) (see chapter 3.1)	TRL 7 (Whole process chain demonstrated in operational environment) → The whole process chain from biomass feeding to gas feed-in was already demonstrated at Güssing (AUT) in demo-scale → The long-term validation and roll-out of the process at commercial-scale is outstanding
Modelling Readiness Level (MRL) (see chapter 3.1)	MRL 7 (Integrated virtual representation of pilot and demo plant available) → The virtual representation helps to find an optimized operation point in pilot scale by process automation through advanced control strategies. The underlying model units of the virtual representation were also tested at demo-scale.

6.3.1 Framework of Digital Twin

In Fig. 27, the modelling framework of the Digital Twin use-case is visualized. Similar to the Digital Shadow use-case, the raw sensor data from the PLCs of the physical component are transmitted via Modbus TCP and MQTT to the Azure Cloud. The data processing steps are executed in the cloud. Afterwards, the processed sensor data is sent to the virtual component in two different intervals. The virtual component consists of an ad-hoc quasistatic simulation model in IPSEpro and a MATLAB-based model predictive control (MPC) unit. The simulation model in IPSEpro helps to validate the process operation by solving an overdetermined equation system just as in the Digital Shadow use-case and to determine not continuously analysed parameters like the water content of the product gas. This process validation step is executed once every minute. Therefore, the processed data sets from the data management are retrieved in the same time interval. The MPC is based on a holistic model and analyses the process in order to automatically perform manipulated variable changes to achieve predefined process goals. For that the MPC queries the processed data from the data management every 5 seconds,

together with additional results from the IPSEpro simulation to predict the future process performance nearly in real-time. The validated model results from IPSEpro are sent to a web application to visualize the most important process parameters and sustainability indicators. The validated model results are sent back to the PLCs of the pilot plant, in the form of requested changes in manipulated variables, to realize process automation. Additionally, the MPC's predictions and manipulated variable changes are visualized in MATLAB on a local user device. In the service dimension, the web application with a dashboard enables human interaction with the Digital Twin by allowing the operator to enter the target values and weightings for the manipulated variables.

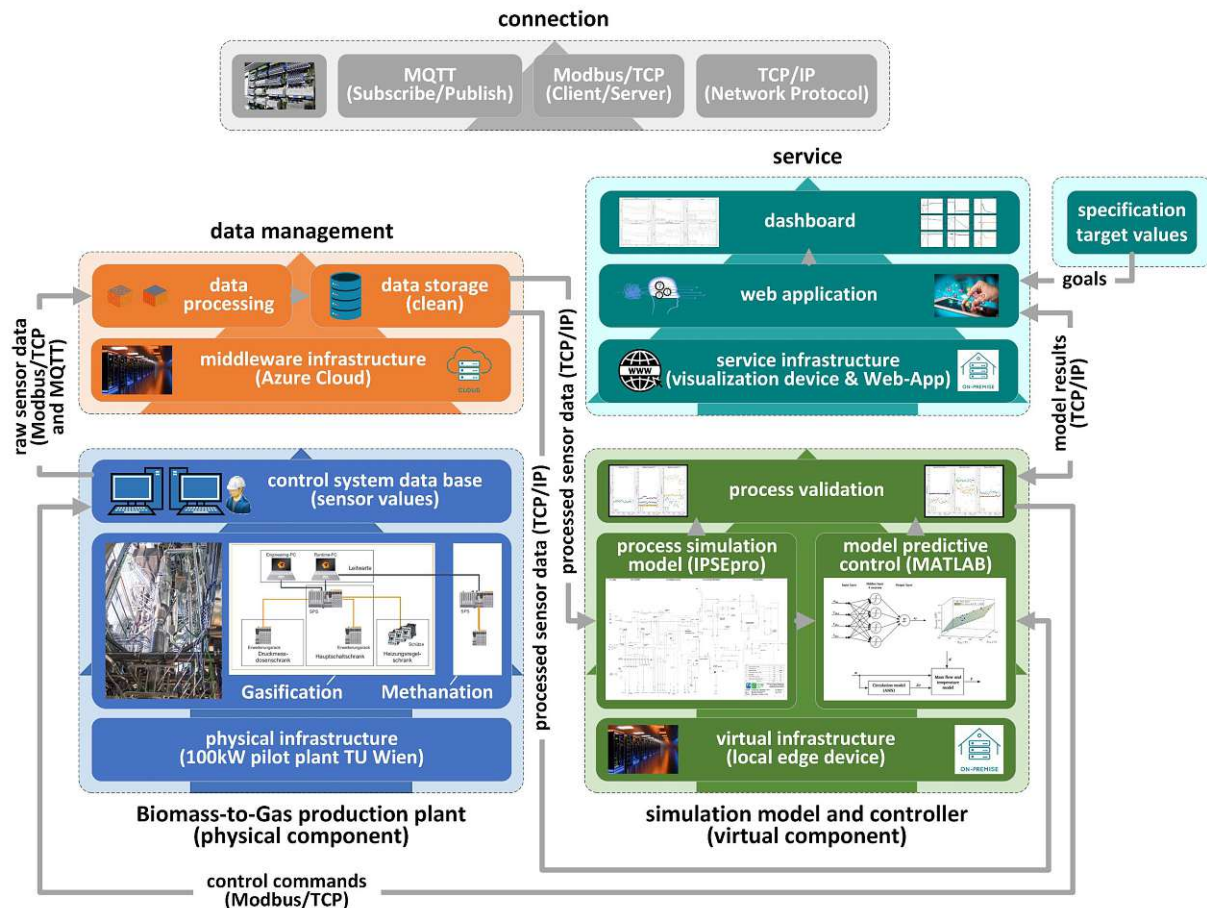


Fig. 27: 5D modelling framework of the virtual representation related to the Biomass-to-Gas pilot plant [29] (own images or licensed from Adobe Stock)

6.3.2 Properties of Digital Twin

The properties of the Digital Twin are listed in Tab. 15. Through the integration of the model predictive control unit and the bi-directional data communication many properties can be defined as level 2. Only the expansibility does not correspond to the required Digital Twin property level according to the novel methodology. The Digital Twin is integrated in the pilot plant at TU Wien. The underlying process models have been tested with experimental data from the 1 MW_{th} demonstration plant at Simmering (AUT). Therefore, the Digital Twin vertical integration level can be assigned to the plant level but the modular data management can be linked with other data bases to cover the enterprise level. The expansibility level is still at the adaptable layout level. To reach the required level of automated layout, the Digital Twin would additionally need to be able to respond to different plant configurations such as product gas recycling or different gas cleaning units. The gray box based predictive MPC and the ad-hoc IPSEpro simulation model enable a full automation of the pilot plant by a bi-directional data communication between the PLCs and the virtual component.

Tab. 15: Digital Twin properties for the Biomass-to-Gas production plant

Property classes	Focus	Property level	Description
Vertical integration	Overall	Level 1: Plant level	The virtual representation in this stage is based on the plant level. However, due to the modular design of the data management system, it is also possible to expand it to include other data bases e.g. from administration.
Interoperability		Level 1: Convertible	The process automation is mainly based on the MPC unit, which is developed and executed in MATLAB. The matrix-based MATLAB language is compatible and convertible to other traditional programming languages like C++, Java or Python.
Expansibility		Level 1: Adaptable layout	The process simulation models are based on model libraries. Therefore, the process layout can be adapted according to several plant configurations.
Functional safety		Level 2: Predictable failure analysis	The mass and energy balances are validated after each simulation run and compared to predefined constraints to avoid systematic failure. In addition, to validating the simulation results, the measured value adjustments are displayed in the dashboard to provide the user with a further plausibility check.
Technological scale-up possibility	Physical component	Level 2: Fully scalable	The scalability of the DFB gasification unit was already demonstrated in several commercial-scale plants in different operation modes. The methanation unit was already built in Güssing (AUT) in 1 MW _{SNG} scale.
Degree of automation		Level 2: Fully automated	The pilot plant was outfitted with automatic control valves. Therefore, a fully automated operation mode is available to support the plant operators.
Physical safety		Level 2: Primary + Secondary + Tertiary safety measures	The pilot plant has been approved by the relevant authorities and the highest safety standards must be met.
Virtual representation capability	Virtual component	Level 3: Predictive	The virtual representation is based on the PSServer process module of IPSEpro and the MPC unit based on MATLAB. Therefore, with the quasistatic IPSEpro model together with the predictive MPC unit, both in ad-hoc mode, a nearly real-time prediction of the future process performance can be realized.
Virtual representation fidelity		Level 1: Gray box (intermediate level)	The main process units DFB gasification and methanation are simulated based on mass and energy balances. In the MPC model, additional data-based correction terms are implemented and the methanation unit is based on a kinetic model approach. In the IPSEpro model, additionally the equilibrium state of the rWGS reaction is calculated and the tar content in the product gas is determined via a correlation with the continuously measured methane content.
Virtual representation intelligence		Level 2: Partial Autonomous	The simulation model calculates changes of manipulated variables every 5 seconds to reach desired predefined operation points as fast as possible.
Connectivity mode		Level 2: Bi-directional	The virtual representation enables a real-time closed-loop control of the pilot plant by calculating automatic changes of the manipulated variables every 5 seconds.
Data integration level	Level 2: Fully automated		
Update frequency	Level 3: Immediate real-time / event driven		
Cybersecurity	Data management and connection	Level 2: Mandatory access control	The data collection (control system), the data management (cloud) and the simulation environment (local edge device) are separated from each other in terms of system technology. Additionally, the web application is secured by an authentication system, which is coupled with the account system of TU Wien.
Human interaction	Service	Level 0: Smart user devices	The dashboard from the service dimension is visualized via a web-based application on the local visualization device, where the operator can monitor the performance and interact with the Digital Twin.
User focus		Level 1: Multiple without interaction of energy plant hierarchy layers	The web-based dashboard from the service dimension can be viewed and controlled simultaneously by multiple authorized operators and other stakeholders.

6.3.3 Process simulation of Digital Twin

The virtual component of the Digital Twin is based on two different model units. First, similar to the Digital Shadow use-case a quasistatic ad-hoc simulation model in IPSEpro 8.0 is used to validate the mass and energy balances by solving the overdetermined equation system. The MPC unit is based on dynamic simulation models which are able to request changes in manipulated variables to optimize the future process performance. The DFB MPC is based on two separated controllers. In the high-level MPC unit, the overall control inputs are processed to request the bed material circulation rate and the total needed air volume flow in the combustion reactor. The circulation MPC uses the estimation for the total air flow and the circulation rate to distribute the total amount of air to available air staging [159, 160]. The fluidized bed methanation unit is simulated via a dynamic kinetic-based model fitted with experimental data to describe the non-linear behaviour of the reactor. The reactor temperature is controlled by a PID controller [161]. In addition, it is planned to add a supervisory MPC to optimize the complete process chain in a holistic view [162]. Further details to the underlying simulation models can be found in [29, 159, 160, 162].

6.3.4 Results of Digital Twin use-case

The Digital Twin helps to automate the Biomass-to-Gas process of the 100 kW_{th} pilot plant at TU Wien. In Fig. 28, the validation of the underlying dynamic simulation model for the MPC of the DFB process can be seen. The operation points with blue background are used for the model training and the white background for model validation. It can be seen that the model can simulate the process behaviour very accurately for a wide range of fuel, oil, steam and air flow rates (manipulated variables).

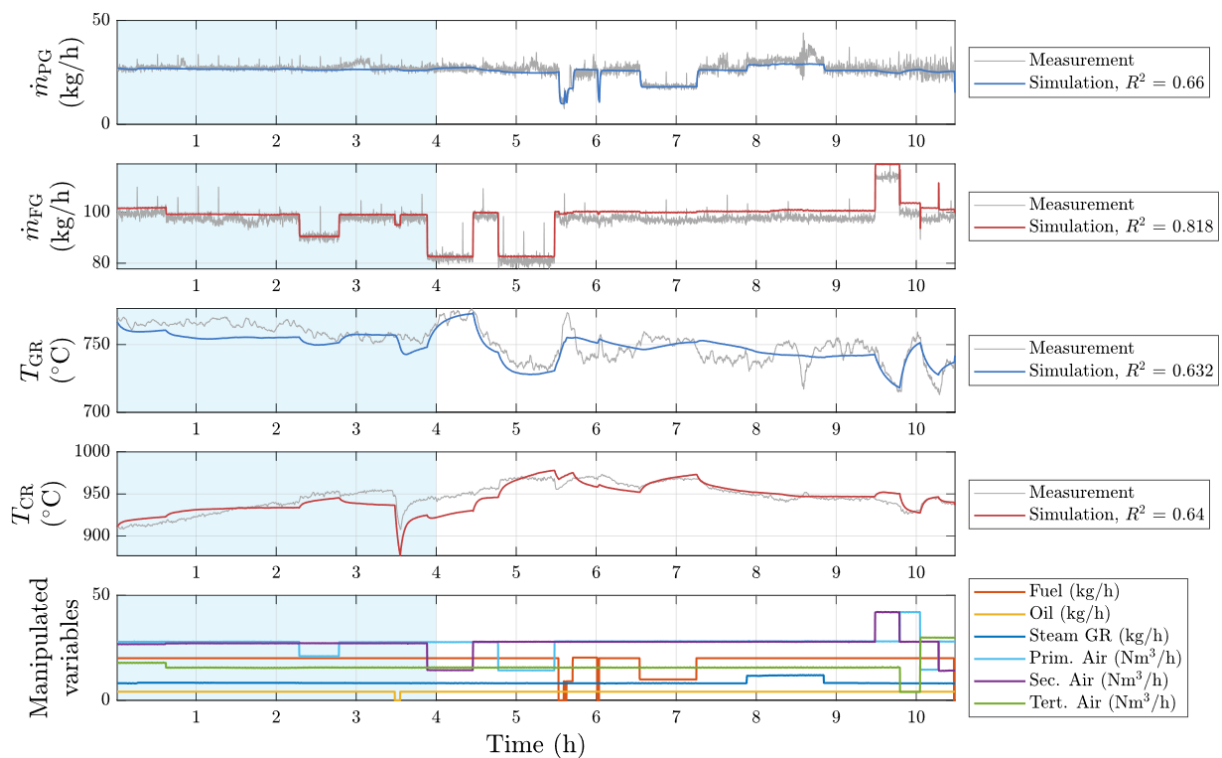


Fig. 28: Validation of the dynamic DFB model [159]

In Fig. 29, the web-based dashboards for the visualization of the simulation results from IPSEpro are shown. The web-based dashboard is a further development of the MATLAB-based dashboard from the Digital Shadow use-case and thus enables user access regardless of the user's location. The dashboard at the top shows the human interface for the specification of setpoints for important internal state variables. Furthermore, the technical sustainability indicators are visualized. The second dashboard at the bottom includes the visualization of further process parameters to monitor the gasification process.



Fig. 29: Dashboard of the IPSEpro simulation results with the MPC human interface and the sustainability indicators (top) and results for important process parameters (bottom)

Additionally, the MPC predictions are visualized in a local MATLAB-based dashboard which can be seen in Fig. 30. Therein, the controlled (left) and manipulated (right) variables are visualized. Each diagram is divided into the historical period with the comparison of estimation and measurement value (left of vertical line) and prediction period (right of vertical line). With the help of this dashboard, it is possible to observe which modifications of the manipulated variables (right) the MPC will perform and which expected changes this will cause in the controlled variables (left).

In summary, it can be concluded that automation was successfully demonstrated with the help of the Digital Twin. The 100 kW_{th} pilot plant at TU Wien could be operated in automatic mode and different operating point changes could be performed automatically over a whole day. Furthermore, a consolidation of all measured values could be performed with the result that the IPSEpro simulation model converges over a wide operating range and the model fits of the overdetermined solver are in a valid range. In addition, quantities that cannot be measured online, such as water and tar content, could be determined in real time with sufficient accuracy. A test run with the aim of optimizing the entire chain holistically with regard to technical, economic and ecological aspects is still pending. For further details on the underlying models and controllers please refer to [29, 158–162].

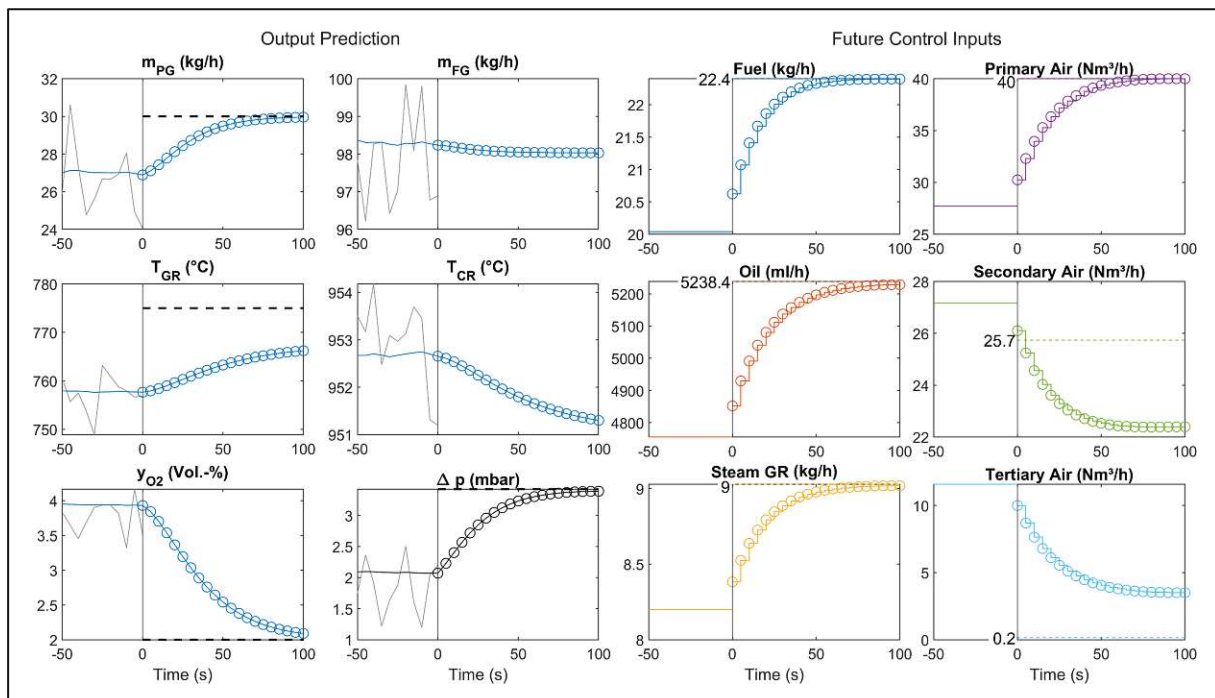


Fig. 30: Dashboard MPC predictions input and output parameters

6.4 Digital Predictive Twin of a hazardous waste incineration plant

The Digital Predictive Twin use-case is related to the hazardous waste incineration process. In a rotary kiln 8 different solid and liquid waste fractions are converted to a hot flue gas. The heat from the flue gas is used within a waste heat recovery boiler to produce superheated steam. Afterwards, the steam is used in a steam turbine to produce heat and power. A detailed flow diagram for the hazardous waste incineration process can be found in Fig. A4 in the appendix. In Vienna (AUT), a hazardous waste incineration plant exists with a capacity of about 100 000 tons of waste per year in two combustion lines, operated by Wien Energie GmbH. Since the partly toxic waste streams, cannot be fully analysed, plant operation is challenging. The batch-wise feeding of the different fuel feed lines together with the lack of knowledge about the combustion behaviour require a reactive process control of the plant to be able to react to the peak loads in the form of emissions and temperatures.

For the optimization of the hazardous waste incineration process, knowledge about the waste input streams has to be generated. The Digital Predictive Twin is able to determine the composition of not entirely analysed waste streams by using a dynamic simulation model. By creating a fuel analysis data base based on determined fuel compositions of these waste streams, the knowledge can be used for recurring fractions to optimize the waste management and process performance. In Tab. 16, the general characteristics of the Digital Predictive Twin are listed. As can be seen, the applications are focused on the monitoring and optimization of the waste management and process performance. Besides data management, simulation and control experts, plant operators and supervisors have to be considered in the development process. The challenges are similar to the Digital Twin use-case. The sustainability indicator in a hazardous waste incineration process are strongly focused on technical indicators with the overarching goal to maximize the plant availability. Hazardous waste incineration plants are commercially available, which leads to TRL 9. The accompanying virtual representation is evaluated and validated with commercial-scale operation data. Therefore, MRL 8 can be defined. In order to achieve MRL 9, the Digital Predictive Twin must be tested and validated in a long-term test under commercial conditions. All the following content regarding the hazardous waste incineration plant is based on [104] (Paper IV).

Tab. 16: General characteristics of the Digital Predictive Twin

Applications (see chapter 2.3)	<ul style="list-style-type: none"> Determination of waste compositions for fractions which have not been entirely analysed to create a fuel analysis data base to monitor the suppliers → basis for other service applications (Evaluation and Verification in Operation and Optimization phase) Monitoring and optimization of real-time process performance by adapting fuel feed sequence (exemplary barrel order) or operation conditions (Monitoring in Operation and Optimization phase) Condition monitoring and anomaly detection of process units – brickwork damage or fouling of waste heat recovery boiler (Monitoring and Evaluation in Maintenance phase) Process automation and optimization by manipulation of waste combustion order and waste delivery order (Orchestration and Prediction in Operation and Optimization phase)
Stakeholders & Users (see chapter 2.4)	<ul style="list-style-type: none"> Process simulation and control experts (Operation, Maintenance and Optimization phase) Data management experts (Operation, Maintenance and Optimization phase) Plant operator/supervisor and waste management supervisor - Wien Energie (Operation, Maintenance and Optimization phase)
Challenges (see chapter 2.6)	<ul style="list-style-type: none"> Use of standardized data interfaces (Mission-critical challenge) Use of simulation models which are valid for a wide range of operation points (Mission-critical challenge) Periodic verification and recalibration of measurement equipment (Mission-critical challenge) Decoupling of virtual representation's IT architecture from control system (Safety-critical challenge) Development of a stable high-fidelity two-way data connection by reaching sufficient data resolution, quality and latency (Time-critical challenge)
Sustainability indicators (see chapter 3.2)	<ul style="list-style-type: none"> Thermal fuel power (Technical indicator) $P_{th,total} = P_{bunker\ waste} + P_{barrels} + P_{shredded\ waste} + P_{pasty\ waste} + P_{hospital\ waste} + P_{waste\ water} + P_{waste\ oil} + P_{masterbatch} + P_{support\ fuel}$ Total energetic efficiency (Technical indicator) $\eta_{DRO} = \frac{P_{heat} + P_{elec.}}{P_{waste} + P_{support\ fuel}}$ Condition monitoring: thickness of brickwork (Technical indicator)
Technology Readiness Level (TRL) (see chapter 3.1)	TRL 9 (Hazardous waste incineration plants have been commercially available for decades)
Modelling Readiness Level (MRL) (see chapter 3.1)	MRL 8 (Commercial plant validation completed and evaluated) → The virtual representation helps to optimize the operation and maintenance at commercial scale if a fuel analysis data base of recurring waste fractions is established first.

6.4.1 Framework of Digital Predictive Twin

The development of the Digital Predictive Twin is based on the 5D modelling framework visualized in Fig. 31. Sensor data from the hazardous waste incineration plant control system is transmitted to the data management. In the data management, which is located on a local edge device, the sensor data, together with data from the laboratory, delivery and fuel classification data base, are processed using a Python script and stored. Appropriate data sets are sent to the simulation model located in the virtual component, which is also installed on the local edge device. The dynamic simulation model is developed in Python and is able to calculate time-dependent simulation results based on time-dependent inputs. In the process validation step, the time-dependent simulation results of the flue gas composition, flow rates, temperature and pressure profiles are compared with the respective measurement values. If the deviations between simulation results and measured values are below a certain tolerance, the results are considered valid and the estimated waste composition is accepted. In case of larger deviations, changes in the estimated waste composition are made on the basis of the results and a new simulation run is carried out. If a larger number of determined waste compositions were available, an additional machine learning (ML) algorithm could be trained and used in the virtual component to assist in estimating the waste composition based on the measured flue gas composition (dashed lines). The valid determined

waste compositions are stored in a fuel analysis data base located in the service dimension executed on a local edge device. The data base can be used to assess recurring waste streams better in terms of combustion behaviour. In the service application internal target sets are defined. These can be the maximization of the plant availability, the protection of the rotary kiln brickwork by operating the plant as smoothly as possible, or the minimization of peak loads by keeping the thermal fuel input homogenous. To achieve plant automation, it is necessary to report optimization targets for waste management back to the delivery data base and for plant operation back to the control system. The plant performance and stock levels are visualized on a local dashboard, to enable a holistic monitoring by plant operators and supervisors. The data transmission is currently based on manual operation but all the connections can be executed in real-time via Profibus.

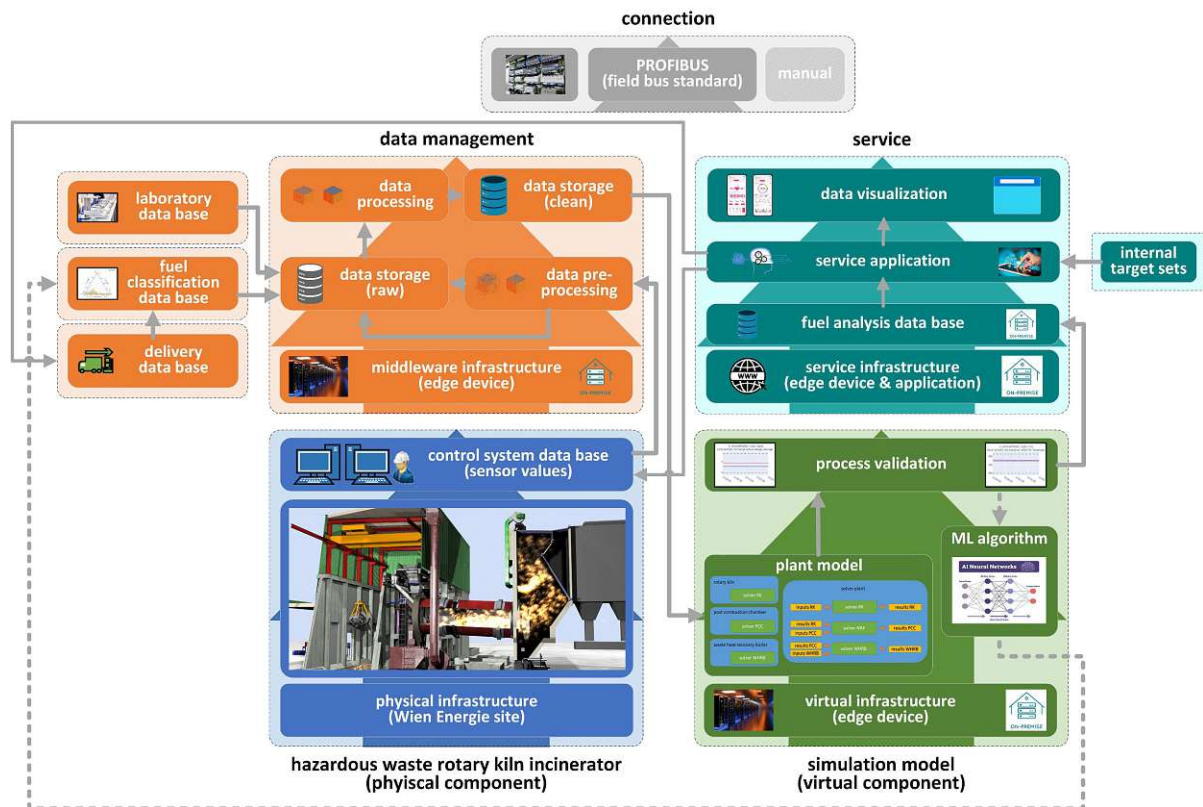


Fig. 31: 5D modelling framework of the virtual representation related to the hazardous waste incinerator [104] (own images or licensed from Adobe Stock)

6.4.2 Properties of Digital Predictive Twin

Similar to the other use-cases the properties of the Digital Predictive Twin are listed in Tab. 17. The virtual representation concept enables the prediction of the process performance by changing the order that the waste streams are incinerated. The integration and testing of the Digital Predictive Twin was undertaken in the operational commercial environment at Wien Energie site with a bi-directional data communication. Therefore, most of the properties can be defined as level 2 or 3, which is in line with the Digital Predictive Twin target requirements according to the novel methodology. The involvement of different company hierarchies leads to a vertical integration on enterprise level. The functional safety is at level 2, the predictable failure analysis. The automated replacement level could be achieved, for instance, by providing another independent black box model as a backup. The precautions against cybersecurity are rated at level 2. The Profibus connection already meets very high safety standards. The highest cybersecurity level 3 could be achieved by implementing another independent authentication or encryption system. The detailed dynamic simulation model based on Python results can be defined as a standardized white box modelling approach. Therefore, the underlying Digital Predictive Twin concept enables the prediction of the future process performance by changing the planned order of waste fraction incineration.

Tab. 17: Digital Predictive Twin properties for the hazardous waste incineration plant

Property classes	Focus	Property level	Description
Vertical integration	Overall	Level 2: Enterprise level	The virtual representation gathers data from the control system of the incineration plant, laboratory data and delivery data. The virtual representation enables the optimization of the complete waste supply chain.
Interoperability		Level 2: Standardized	The process automation is based on the dynamic simulation model based on Python, which is a widely used programming language.
Expansibility		Level 2: Automated layout	The process simulation models are based on model libraries. The simulation models are parametrized with experimental data sets from both incineration lines. Therefore, the model can be used for both process lines.
Functional safety		Level 2: Predictable failure analysis	The mass and energy balances are validated after each simulation run and compared to predefined constraints to avoid systematic failure.
Technological scale-up possibility	Physical component	Level 2: Fully scalable	The scalability of the hazardous waste incineration plant was already demonstrated in several commercial-scale plants worldwide.
Degree of automation		Level 2: Fully automated	In the commercial incinerator, a complete automation of the manipulated variables is implemented.
Physical safety		Level 2: Primary + Secondary + Tertiary safety measures	The commercial plant has been approved by the relevant authorities and the highest safety standards must be met.
Virtual representation capability	Virtual component	Level 3: Predictive	The virtual representation concept is based on a dynamic simulation model based on Python, which enables the prediction of the plant performance by changing the order of incinerated waste streams.
Virtual representation fidelity		Level 2: White box (microscopic level)	The simulation of the rotary kiln is based on a dynamic simulation model. The rotary kiln is vertically and horizontal discretized into several cells to simulate the transition from solid/liquid to gas phase along the incinerator and to consider the heat transfer to the environment. The waste heat recovery boiler is divided into two superheaters, an economizer and an evaporator. Furthermore, the steam drum and the fin walls are simulated via steady-state models.
Virtual representation intelligence		Level 2: Partial autonomous	The model concept includes the data connection with Profibus, which enables a real-time data transmission.
Connectivity mode	Data management and connection	Level 2: Bi-directional	The virtual representation concept enables a real-time closed-loop control of the commercial plant by the implemented Profibus data connection.
Data integration level		Level 2: Fully automated	
Update frequency		Level 3: Immediate real-time / event driven	
Cybersecurity		Level 2: Mandatory access control	The data collection (control system), the data management (local edge device) and the simulation environment (local edge device) are separated from each other in terms of system technology. Additionally, the service application is based on a local application, which can only be accessed by authorized employees.
Human interaction	Service	Level 0: Smart user devices	The dashboard from the service dimension is visualized via a local application executed via smart phones, tablets or other local user devices, where the operator can monitor the performance and interact with the Digital Predictive Twin.
User focus		Level 2: Multiple with interaction of energy plant hierarchy layers	The local dashboard from the service dimension can be viewed and controlled simultaneously by multiple authorized operators. Furthermore, plant supervisors and employees from the waste management can use the application to schedule waste deliveries.

6.4.3 Process simulation of Digital Predictive Twin

The process simulation model of the Digital Predictive Twin is based on an overarching plant model, which coordinates the sequential-based simulation approach. The plant simulation is based on a transient rotary kiln model and steady-state models for the post-combustion chamber and waste heat recovery boiler. First of all, in the transient rotary kiln model, the process sensor data for the waste and air inputs are introduced. The rotary kiln is axial discretized in a cylindrical grid with 13 sections. Besides the front wall as the first section, each meter of the rotary kiln makes up a further model section. Furthermore, the wall of each cylindrical section is further discretized in radial direction to consider heat transfer to the environment. In the first section, all lumpy waste fractions, barrels and pasty waste fractions are introduced as solid waste mix with a solid bed height decreasing along the rotary kiln in axial direction. In this way, material transfer in the rotary kiln can be simulated. The residence time is assumed to be constant due to a constant rotary kiln rotation speed. Additionally, heat transfer due to conduction, convection and radiation is considered. Moreover, mass transfer is integrated by calculating the drying, devolatilization, gasification and oxidation phase. Liquids are integrated in the front wall burner and directly converted to the gas phase. To integrate the reaction kinetics, global reactions are defined for each compound. After solving the mass and energy balances of each rotary kiln cell, the time-dependent results of the last cell are handed over to the steady-state post-combustion chamber, together with further measurement data regarding the waste water and secondary and tertiary air input. Therein, further gas-gas reactions take place. The inorganic ash components in the post-combustion chamber are assumed to be completely separated within the wet deslagger at the bottom of the chamber. The results of the hot flue gas after the post-combustion chamber are handed over to the steady-state model of the waste heat recovery boiler, together with further measurement data exemplary about the feed water. The waste heat recovery boiler model consists of several sub units. Therein, two evaporators, two superheaters, one injection cooler, one economiser and one steam drum are simulated in separate cells. In the waste heat recovery boiler, water is first heated up in the economiser, before it is pumped to the steam drum. The steam drum is connected with the two tube bundle evaporators as well as the fin wall, which is surrounding the waste heat recovery boiler, in natural circulation mode. The saturated steam from the steam drum is superheated in two stages before it is sent to the steam turbine. The time-dependent results of the waste heat recovery boiler model can be compared and validated afterwards with the processed measurement data of the flue gas composition, the gas and steam flow rates as well as temperature and pressure profiles. The difference of the simulated and measured values is calculated by the mean absolute percentage error (MAPE). The calculation of the MAPE is based on weighting of sensor values. The major gas components are weighted the highest, while the flue gas temperatures within the waste heat recovery boiler are weighted the lowest.

6.4.4 Results of Digital Predictive Twin use-case

The concept for the Digital Predictive Twin helps to optimize the process performance of the commercial hazardous waste incineration plant in Vienna. Several development steps are required to achieve the Digital Predictive Twin. First, a fuel analysis data base must be developed by analysing historical data sets to determine the waste composition of waste streams, which have not been analysed entirely. The determined waste composition and the related waste code and supplier are stored in the fuel analysis data base. Thus, verifying the delivered qualities of the waste streams is possible. In case of recurring fractions, the fuel analysis data base is used to optimize the hazardous waste incinerator.

Before the virtual representation can be used, the simulation model must be parameterized. For this purpose, three operating periods were selected in which only heating oil extra light was fired in the course of a holding mode. Due to the defined fuel composition, the set parameters in the simulation model could be adjusted until the MAPE was minimized for all three periods. Parameterization was completed after MAPE was below 12% for all three test runs. In Fig. 32, the comparison of the simulation results and the sensor values of one exemplary parametrization test run is visualized.

Comparing sensor values with solver results - HEL operation 2nd November 2021 - 09:30-12:00

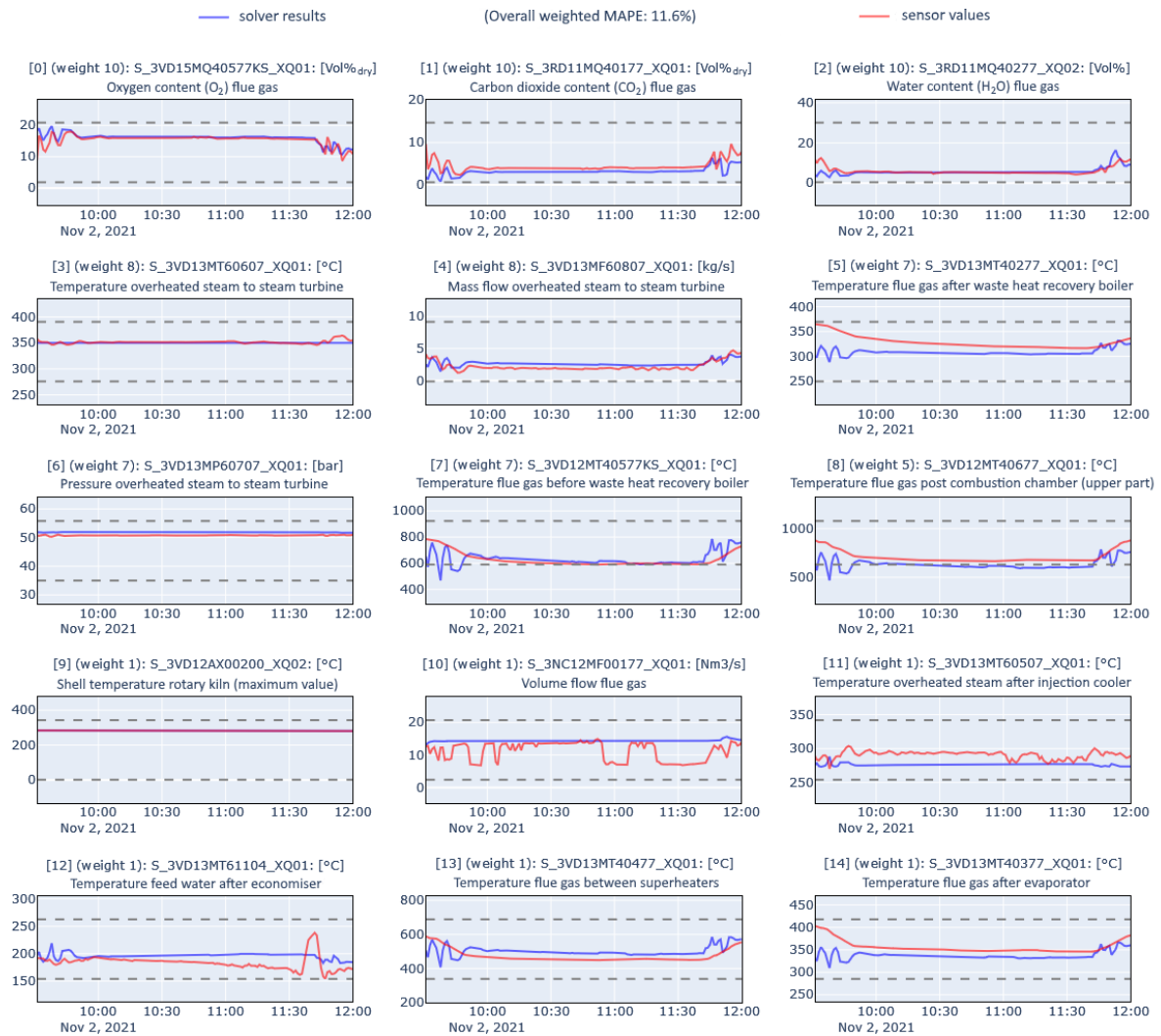


Fig. 32: Simulation and validation results for the model parametrization with a HEL test run [104]

After the parametrization of the simulation model, the possibility for the determination of the composition of waste streams, which were not entirely analysed, was demonstrated. To prove the feasibility of the concept, a period of operation with only hospital waste as fuel input was selected, which can be traced back to only one supplier and waste code (97101). For the mentioned waste code, three subcategories with diapers, wound dressings and cannulas are defined in the fuel classification data base. Subsequently, simulation runs were performed and compared with the three waste compositions of all three subcategories. In Fig. 33, the comparison of the simulation results and the sensor values for the test run with wound dressings is visualized. This subcategory delivered the best result with a MAPE of less than 16%.

Consequently, it can be concluded that the simulation model has been parameterized adequately and the functionality of the concept has been demonstrated. Furthermore, the virtual representation was installed on the Wien Energie site and connected with all required data bases and the control system via Profibus. As a result, the assistance system is ready for use from an infrastructural point of view for predictive real-time applications. However, in order to use the virtual representation in a sustainable manner, it is necessary to examine a large amount of historical measurement data and analyse additional waste compositions that are unknown. Additionally, the determined waste compositions should be verified by manual fuel analysis through a laboratory. In that way, the virtual representation helps to monitor compliance with the contracted waste qualities and composition.



Fig. 33: Simulation and validation results for the exemplary determination of the waste composition for a not analysed hospital waste fraction [163]

As soon as a comprehensive fuel data base is available, a wide range of further applications through the use of the virtual representation can be addressed, which can be categorized in operation, waste management and maintenance applications.

In order to show the broad operation application possibilities of the virtual representation, several dashboards were developed, which can be seen in Fig. 34 and Fig. 35. The dashboard in Fig. 34 (top) shows a possibility for the visualization of the historical and predicted thermal fuel power. The dashboard is designed to assist in meeting the overall goal of homogeneous operation of the hazardous waste incinerator. The dashboard in Fig. 34 (bottom) shows the stock levels of each waste input line to assist the scheduling of the future waste input under consideration of the available waste types. In the dashboards in Fig. 35, all waste input lines are visualized with their current thermal fuel power and indication if the mass flow and heating values are within given constraints. Moreover, the historical and predicted mass flow and lower heating value of each specific waste input line can be analysed. In summary, the virtual representations can help as support tool to monitor and automate the hazardous waste incinerator operation regarding stable and optimum operation conditions.

Furthermore, the virtual representation can be used for maintenance applications like the monitoring of the brickwork condition or the fouling of the waste heat recovery boiler. Due to the observation of the shell temperature of the rotary kiln or heat transfer within the waste heat recovery boiler, precise planning of downtimes and maintenance activities get possible.

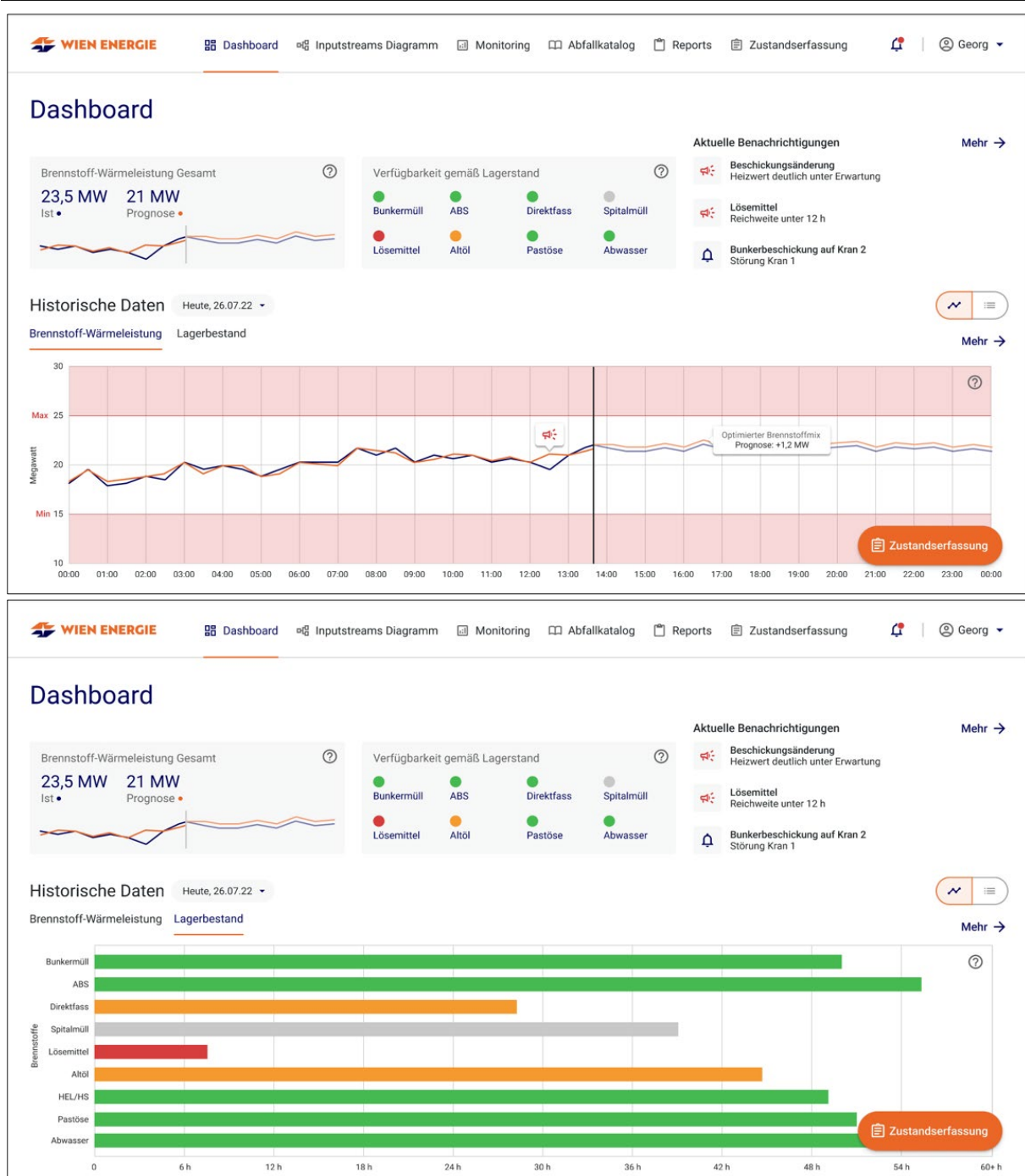


Fig. 34: Dashboards for the monitoring of the total historic and predicted thermal fuel power (top) and stock levels of each waste input line (bottom) [163]

In addition to virtual representation applications with focus on the operation and maintenance sector, it is also possible to intervene a step earlier, in waste management or at scheduling of waste deliveries. For example, the virtual representation can be used to optimize the barrel sequence regarding homogenous waste input to decrease temperature and emission peaks within the rotary kiln operation. Furthermore, the waste delivery plan could be coordinated to ensure that the waste qualities and quantities of the individual input streams are as well coordinated as possible at any time.

To demonstrate the optimization potential, it must be mentioned that the hazardous waste incinerator is currently operated at only 80% of nominal load to buffer peak loads. Due to the lack of knowledge about the waste composition, very high residual oxygen contents of 10-15 vol.-%_{dry} are often achieved in the flue gas for emission reasons. First investigations showed that, in addition to higher throughputs, the use of the virtual representation can contribute to an overall efficiency increase of more than 5% [104].

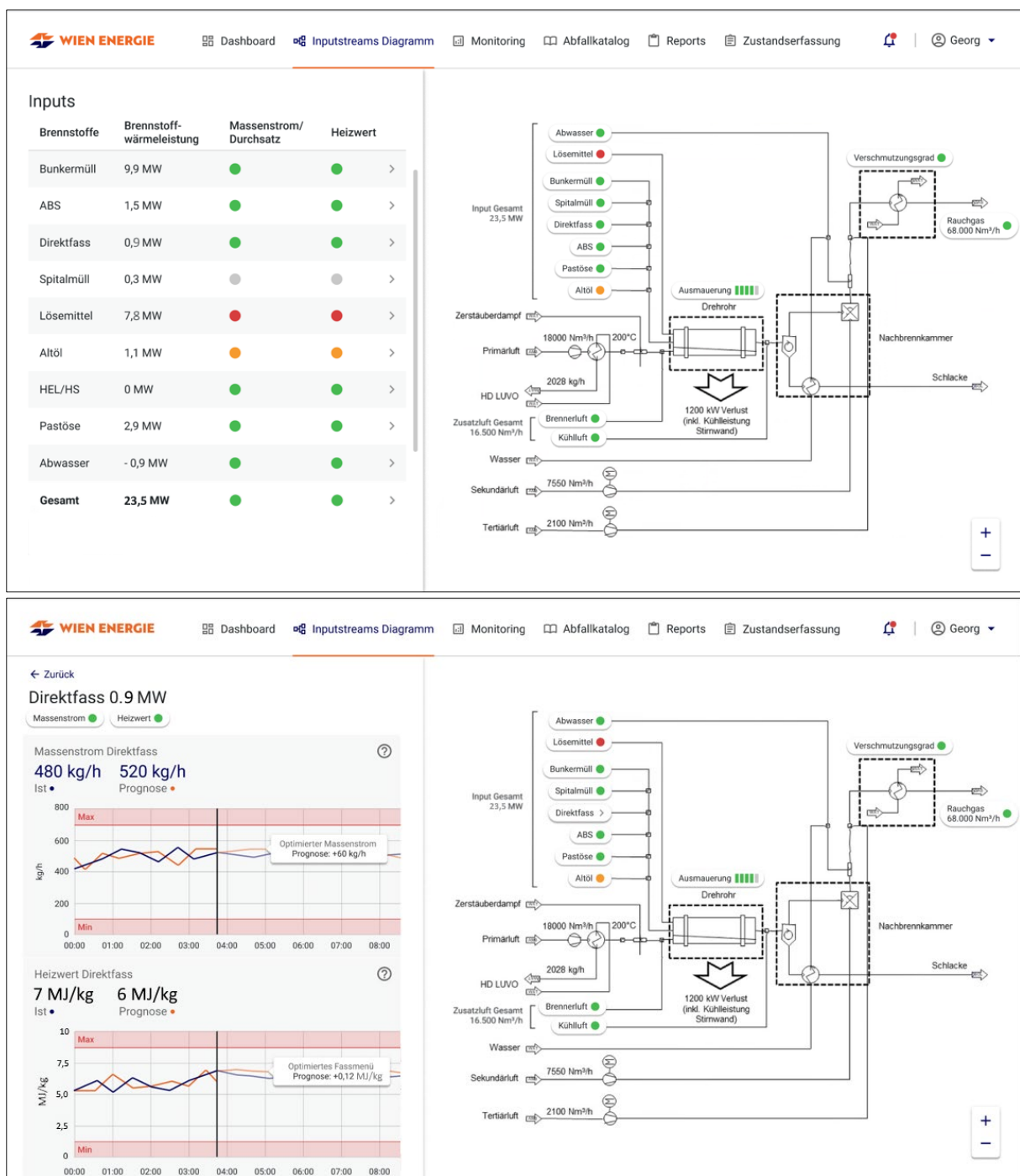


Fig. 35: Dashboards for the monitoring of the thermal fuel power of each waste input line (top) and the detailed historic and predicted mass flow and lower heating value of a specific waste input line (bottom) [163]

After presenting the four different use-cases, it can be concluded that the proposed modelling framework is broadly applicable to a wide range of energy technologies along all four process development stages. The next chapter will finally discuss how the developed virtual representations can be used to investigate energy system integration scenarios with respect to different industries or regions.

7 Energy system integration based on virtual representations

The virtual representations developed using the presented methodology can be used at any development stage to explore scenarios for energy system integration. As development and thus the MRL progresses, more detailed and thus more accurate mass and energy balances can be defined. As a consequence, the techno-economic, ecological and sociological analyses based on the mass and energy balances become more and more accurate. There are two basic options for developing energy system integration scenarios. As visualized in Fig. 36, either suitable sectors or regions can be investigated from the perspective of the developed energy technology, or suitable technologies can be explored from the perspective of a sector or region to meet a specific energy demand.

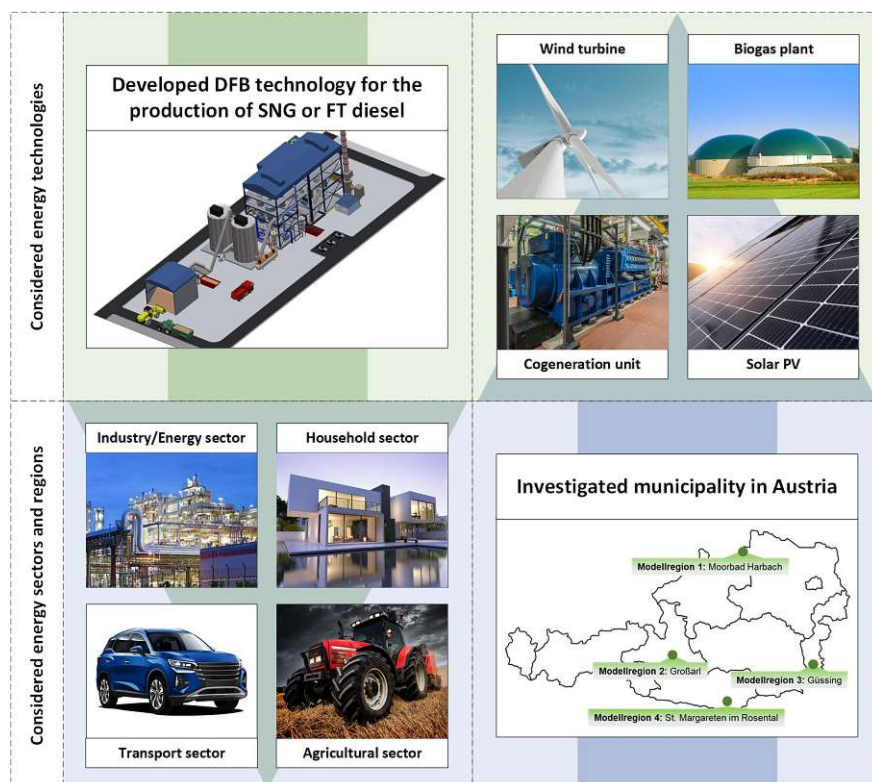


Fig. 36: Energy system integration possibilities for technologies based on virtual representations from the perspective of the developed energy technology (left), or from the perspective of a sector or region (right) (own images or licensed from Adobe Stock)

To demonstrate the two principal possibilities for examining energy system integration scenarios, two relevant studies are presented below in this chapter.

First of all, from the perspective of the Biomass-to-Gas and Biomass-to-Liquid technology, which are both based on DFB gasification, energy system integration studies in different sectors were conducted. Thus, techno-economic and environmental impacts through the integration of the considered technology in the respective sectors could be determined (**Paper V**) [112].

Furthermore, a tool called ENECO₂Calc was developed, which allows to calculate the final energy demand in form of electricity, heat and fuel for any municipality in Austria. Based on a large data base of established and promising energy technologies, defossilization strategies until 2050 can be studied to calculate their techno-economic and environmental impacts for the considered region (**Paper VI**) [164].

7.1 Defossilization of the energy system through integration of DFB plants

To demonstrate the potential for considering energy system integration scenarios from a technology perspective, the following chapter discusses integration scenarios for biomass-based SNG and FT diesel

production. First, the methodology of evaluating energy system integration scenarios is presented, followed by the results. All the following content regarding the techno-economic and ecologic assessment of Biomass-to-Gas and Biomass-to-Liquid process routes with the investigation of energy system integration scenarios is based on [112] (Paper V).

7.1.1 Methodology for the investigation of energy system integration scenarios

In this chapter, the techno-economic and ecological impact of the renewable products from the Biomass-to-Gas and Biomass-to-Liquid route are investigated. The Biomass-to-Gas route was already discussed within the Digital Twin use-case in chapter 6.3. In the Biomass-to-Liquid route the methanation step is substituted by the FT synthesis which was already discussed in the Digital Model use-case in chapter 6.1. A detailed process flow diagram can be found in Fig. A5 in the appendix. Both routes have reached demonstration scale. The process development for both technologies was accompanied by TU Wien and the findings of the experimental test runs were captured in a virtual representation. This knowledge can be used to investigate commercial-scale concepts and to develop energy system integration scenarios to find suitable roll-out strategies for both technologies. In Fig. 37, the methodology for the techno-economic and ecological assessment for the investigated scenarios is visualized.

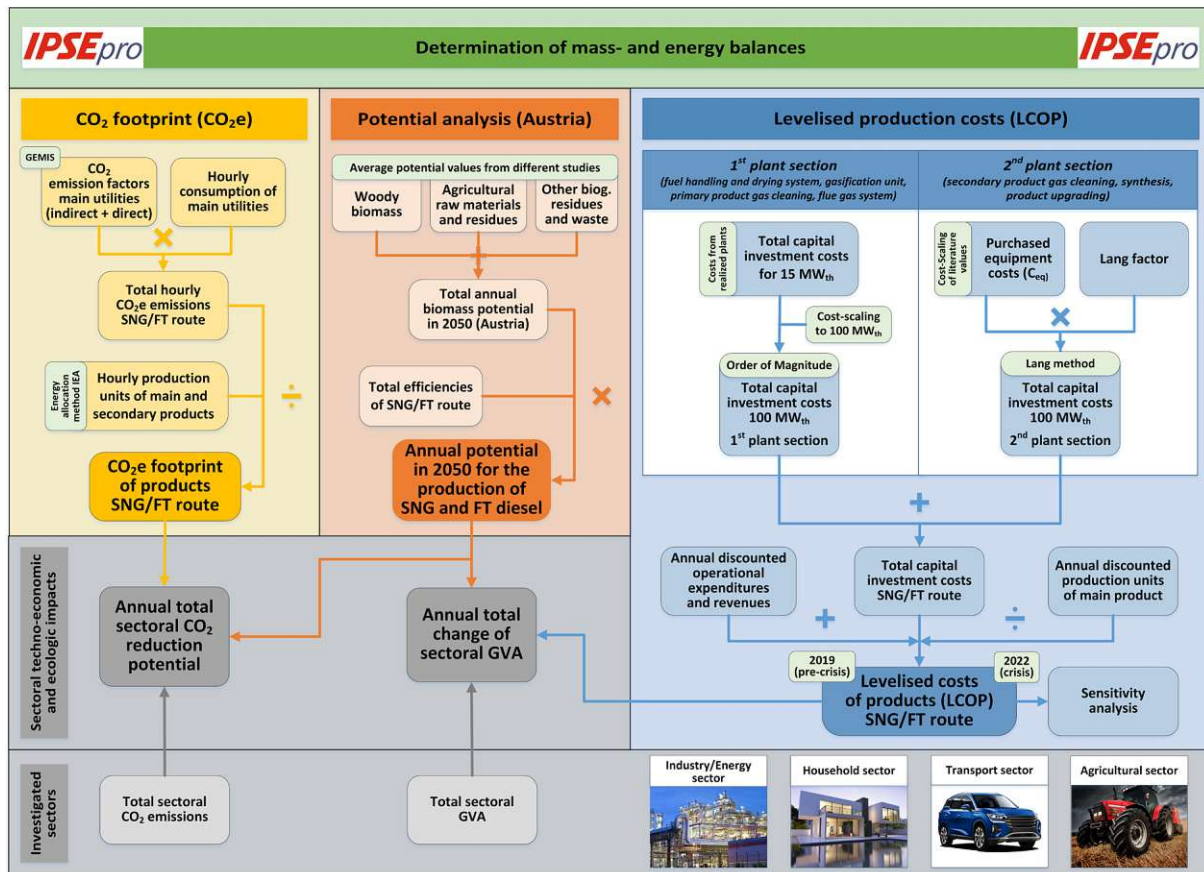


Fig. 37: Methodology for the investigation of energy system integration scenarios [112] (own images or licensed from Adobe Stock)

Based on the mass and energy balances of the virtual representation, the CO₂ footprint and the levelized production costs of both products were determined. Furthermore, several studies for biomass potentials in Austria were conducted to define additional biomass potentials in 2050. By comparing the CO₂ footprint of the renewable product with its fossil counterpart a CO₂ reduction potential can be defined. If the CO₂ reduction potential is compared with the sectoral energy demand and the total sectoral CO₂ emission, a total sectoral CO₂ reduction potential can be determined for each scenario. Similarly, the economic impact of the substitution scenarios can be calculated by comparing the sectoral surplus costs or savings with the sectoral gross value added (GVA). In the following, the techno-economic and

ecological impact for the integration of SNG in the energy sector, private and public sector and industry sector was investigated. Furthermore, a study regarding the integration of FT diesel in the private and public transport sector, heavy-duty traffic sector and heat and power sector was conducted.

7.1.2 Results of the techno-economic and ecological impact of integration scenarios

The virtual representation was used to perform process simulations for commercial plants on a 100 MW_{th} scale. This allowed all necessary input and output flows to be determined. From 100 MW_{th} woody biomass, either 65 MW SNG and 14.2 MW district heat or 36.6 MW FT products and 17.6 MW district heat can be produced.

Based on the mass and energy balances, the levelized production costs are determined. The production costs for biomass-based SNG are 70-91 €/MWh depending on whether pre-crisis (2019) or crisis times (2022) were considered. As can be seen in Fig. 38 (left), the determined production costs of SNG are in the range of household market prices for fossil natural gas in 2019 and in the range of industrial prices in 2022. Furthermore, a sensitivity analysis was conducted which can be seen in Fig. 38 (right). The results show that the biggest influence on the production costs are caused by the annual operating hours, the plant lifetime, the fuel costs, and the investment costs.

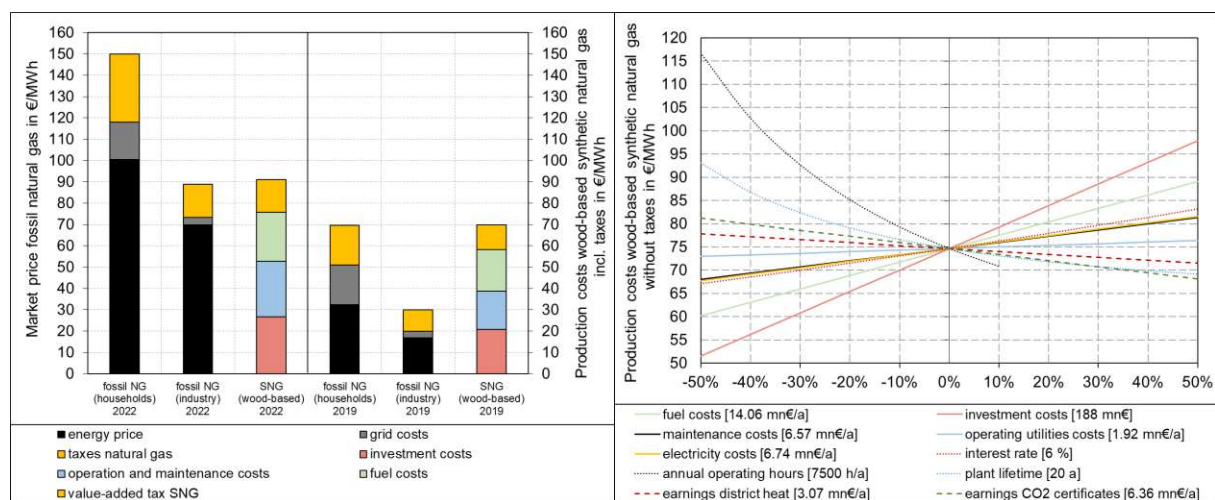


Fig. 38: Comparison of production costs of wood-based SNG with the market price of fossil counterparts (left) and sensitivity analysis of SNG production costs (right) [112]

The results for the levelized production costs of the biomass-based FT diesel are visualized in Fig. 39 (left), which are between 1.31-1.89 €/l depending on the considered reference year. The FT diesel production costs are in the range of the petrol station market prices for fossil diesel in both reference years. The results for the sensitivity analysis shown in Fig. 39 (right) are similar to the SNG route. If both production costs are compared on an energy basis, it can be seen that FT diesel with production costs of 137-198 €/MWh, costs about twice as much as SNG, costing 70-91 €/MWh. The higher price for FT diesel can be explained by the significantly higher investment costs for product upgrading, as well as the costs for hydrogen and higher electricity costs due to higher synthesis pressure.

The results for the CO₂ footprint of both routes are visualized in Fig. 40. The CO₂ footprints for biomass-based SNG (0.027 kg_{CO2e}/kWh_{SNG}) and for biomass-based FT diesel (0.269 kg_{CO2e}/l_{FT diesel}) are about 90% lower than their fossil counterparts. The most important factors influencing the calculation of the CO₂ footprint are biomass and RME as scrubber solvent. Hydrogen and electricity have no major impact on the CO₂ footprint, since the use of electricity from renewable sources was assumed.

Furthermore, a potential analysis was carried out to determine the annual additional biomass potential in 2050 compared to 2020. The potential analysis showed an additional biomass potential of 185 PJ/a in Austria in 2050, from which either 120 PJ/a of SNG or 67.5 PJ/a of FT diesel could be produced.

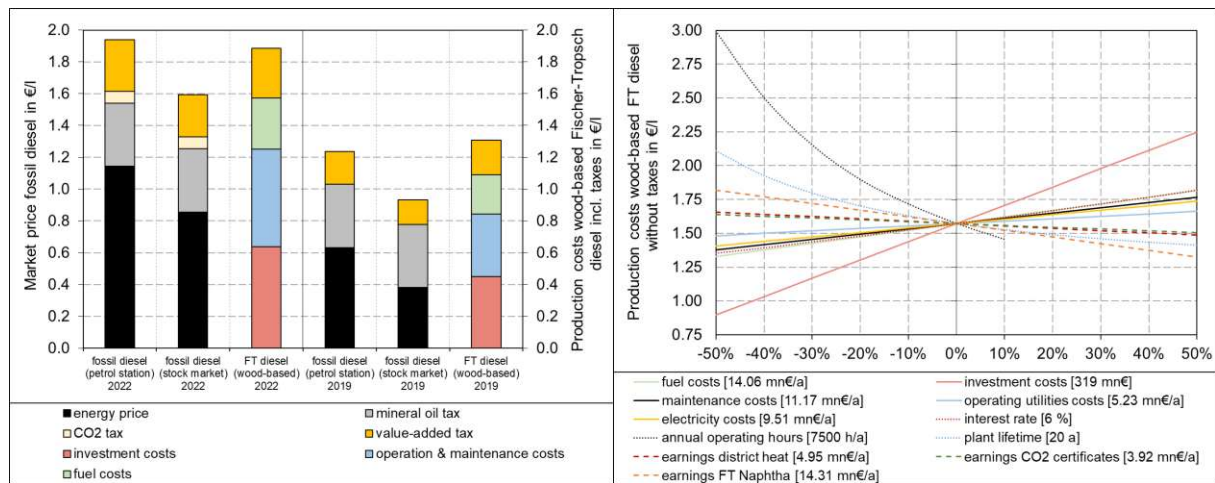


Fig. 39: Comparison of production costs of wood-based FT diesel with the market price of fossil counterparts (left) and sensitivity analysis of FT diesel production costs (right) [112]

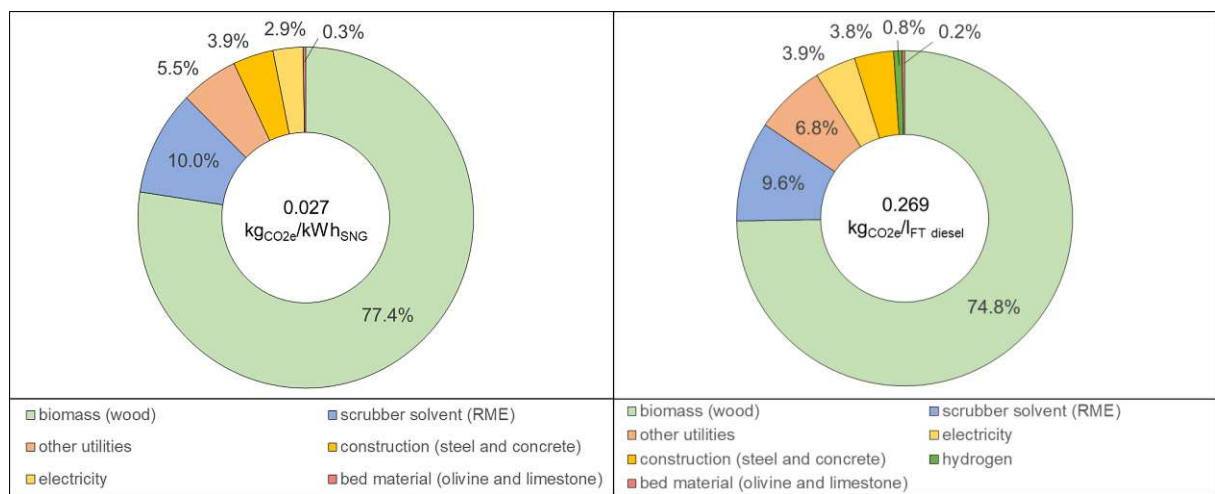


Fig. 40: Breakdown of the CO₂ footprint of wood-based SNG (left) and wood-based FT diesel (right) [112]

Based on the production costs, the CO₂ footprint and the determined biomass potential, energy system integration scenarios were developed which are listed in Tab. 18. For each scenario, the CO₂ reduction potential and impact on GVA are investigated, as well as possible alternatives to SNG and FT diesel in each sector discussed. Here, the color coding is intended to indicate, based on the traffic light colors, whether the introduction of biomass-based FT diesel or SNG has a noticeable positive impact (green), negligible impact (yellow), or negative impact (red) compared to the currently used fossil fuel. In the case of alternative technologies, the coloring targets whether there are many (red), few (yellow), or hardly (green) commercially available alternatives. Three suitable scenarios can be derived from this investigation. The use of SNG in gas power plants only for peak-load power coverage could be a good compromise between economic and ecological impact. In the industry sector, the use of SNG for the provision of high-temperature heat is a viable option, where no waste heat or heat pumps are available. Additionally, the use of FT diesel in the heavy-duty traffic sector represents an economically feasible option for the defossilization of inland navigation, railway, freight transport and agriculture and forestry. Further details about the underlying assumptions and simulation studies can be found in [112].

Tab. 18: Comparison of energy system integration scenarios of biomass-based SNG and FT diesel [112]

Implementation scenarios	Substituted natural gas or diesel demand in 2050	Additionally produced by-products	Sectoral CO ₂ reduction potential	Economic competitiveness (change of sectoral GVA)		Possible renewable alternatives
				2019	2022	
SNG use in energy sector	110 PJ/a	24 PJ/a district heat	89.1%	-12.4%	-0.5%	<u>Peak-load power coverage</u> (no comparable alternatives) <ul style="list-style-type: none"> increased interconnection to the European power grid additional storage facilities sector coupling
						<u>Provision of district heat</u> (possible limited alternatives available) <ul style="list-style-type: none"> heat pumps biomass heating plants solar thermal systems waste heat utilization hydrogen
SNG use in private and public sector (without mobility)	85 PJ/a	18.5 PJ/a district heat	70.6%	0%	8.6%	<u>Provision of decent heat</u> (good alternatives available – especially heat pumps and district heat) <ul style="list-style-type: none"> heat pumps solar thermal systems wood-fired boilers district heat
SNG use in industry	120 PJ/a	26.2 PJ/a district heat	30.3%	-2.0%	-0.1%	<u>Provision of high-temperature heat</u> (possible limited alternatives available) <ul style="list-style-type: none"> waste heat recovery hydrogen high-temperature heat pumps
FT diesel in private and public transport	61.5 PJ/a	38.4 PJ/a district heat and 29.6 PJ/a FT naphtha	40.2%	-0.2%	0.2%	<u>Alternative mobility options</u> (especially E-Mobility is a good commercially available alternative) <ul style="list-style-type: none"> battery electric vehicles fuel cell electric vehicles hydrogenated vegetable oil e-fuels
FT diesel in heavy-duty traffic	67.5 PJ/a	42.2 PJ/a district heat and 32.5 PJ/a FT naphtha	58.5%	-1,8%	-0.8%	<u>Alternative mobility options</u> (no commercially available alternatives) <ul style="list-style-type: none"> battery electric vehicles (limited) fuel cell electric vehicles hydrogenated vegetable oil e-fuels compressed natural gas vehicles
FT diesel in heat and power	9 PJ/a	5.5 PJ/a district heat and 4.2 PJ/a FT naphtha	2.6%	-0.1%	-0.1%	<u>Provision of high-temperature heat</u> (possible limited alternatives available) <ul style="list-style-type: none"> wood-fired boilers waste heat recovery hydrogen high-temperature heat pumps (limited usability)

7.2 Defossilization of municipalities through integration of RES technologies

In addition to the consideration from a technology perspective, an energy system integration consideration can also be carried out from the perspective of a sector or region. Therefore, the novel ENECO₂Calc tool is introduced which allows the determination of the final energy demand of a selected municipality in Austria. Furthermore, the CO₂ footprint and energy costs for the municipality can be determined and defossilization scenarios investigated. All the following content about the tool and the conducted investigations for the defossilization of a given municipality is based on [164] (**Paper VI**).

7.2.1 Methodology for investigation of defossilization scenarios of a selected municipality

In the context of this thesis, the tool ENECO₂Calc was developed, which is based on a variety of MS Excel spreadsheets. The tool consists of about 6500 relative and absolute predefined values based on studies and about 1000 user set values based on data from Statistik Austria to define the investigated municipality. The tool includes a data base of a variety of technologies with their sustainability

indicators determined by the use of virtual representations. In Fig. 41, the general methodology of ENECO₂Calc is visualized. First of all, the annual final energy demand in form of space heat, hot water, electricity and fuels can be determined, based on user-defined inputs about statistical data for a given municipality in Austria. Furthermore, the final energy demand and energy capacities are distributed according to given regional energy portfolios and are subsequently discretized month by month. The distributed and discretized final annual energy demand is multiplied by emissions and cost factors for the determination of an ecological and economic footprint in the sectors energy provision, energy distribution and infrastructure. After the determination of the current economic and ecological footprint, defossilization scenarios until 2050 can be investigated by adapting the future energy distributions. Finally, recommendations for the transformation of the regional energy system of the considered municipality can be given.

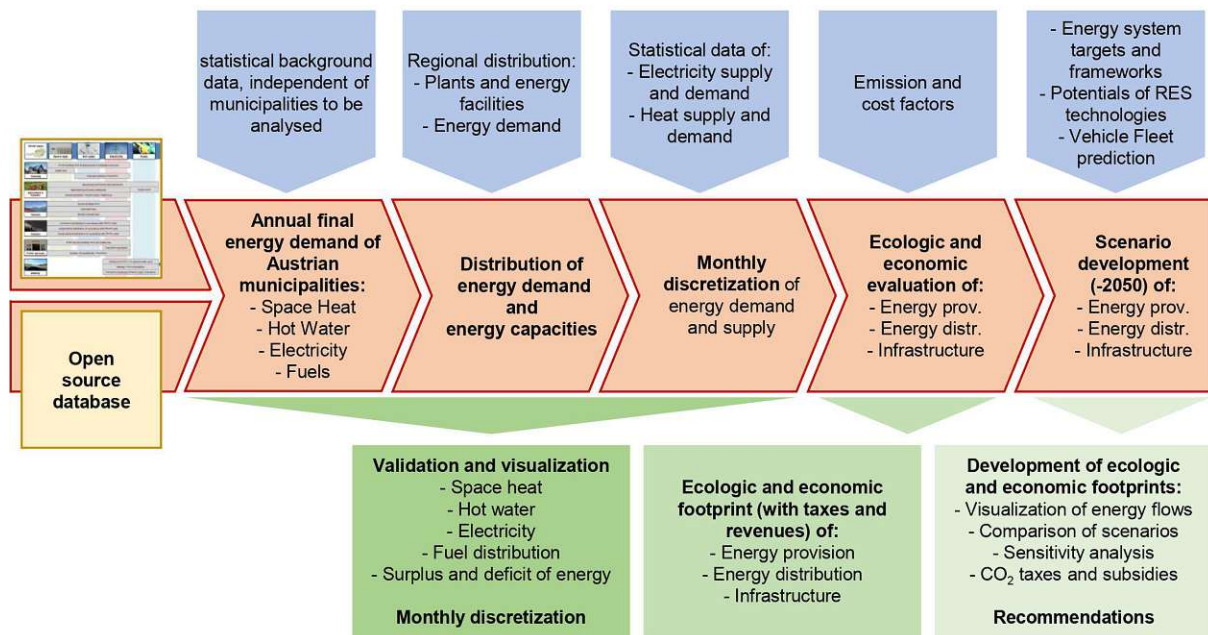


Fig. 41: Methodology of ENECO₂Calc [164]

To demonstrate the possibilities of the tool, the energy demand of the municipality St. Margareten im Rosental in Carinthia in Austria is calculated. Based on this, the current economic and ecological footprint is calculated and defossilization scenarios are developed. Therein, the Business-as-Usual (BAU), the Biomass-to-Mobility (BtM), the Biomass-to-Combined Heat and Power plants (BtCHP) and the Biomass-to-Gas (BtG) scenario are investigated. In the BAU scenario, the municipality's energy portfolio is not changed compared to the status quo. The BtM scenario is focused on synthetic fuels, through the central use of biomass for the production of FT diesel. In the BtCHP scenario, the regional biomass is used for the decentral production of electricity and heat in cogeneration units. In the BtG scenario, the biomass is used in commercial-scale Biomass-to-Gas plants for the production of SNG to defossilize the Austrian electricity mix. For detailed scenario assumptions a reference is made to [164].

7.2.2 Results of the techno-economic and ecological impact of defossilization scenarios

Subsequently the most important results for the investigation of defossilization scenarios for the municipality St. Margareten im Rosental are summarized. In Fig. 42, the final annual energy demand distribution for the year 2020 is visualized. It can be seen, that the total energy demand of St. Margareten im Rosental is mostly influenced by the space heat and electricity demand in the residential buildings sector as well as the diesel and gasoline demand in the mobility sector. For a more detailed energy demand analysis of the considered municipality, a reference is made to the detailed energy flow diagram in Fig. A6 in the appendix.

Based on the current annual final energy demand, defossilization scenarios for the year 2050 can be investigated. In Fig. 43, a comparison of the CO₂ footprints and the energy costs in the investigated scenarios is shown. Therein, it can be seen that through the realization of the BtG, BtCHP and BtM scenario between 80-90% of the CO₂ emission can be saved compared to the BAU scenario. The combination of heat pumps in the heat sector, biomass-based SNG in the electricity sector together with a strong focus on hydrogen-driven vehicles in the transport sector in the BtG scenario, leads to the lowest total emissions. At the same time, the energy costs are the highest compared to the other scenarios due to the higher heat production costs of heat pumps and the use of hydrogen in mobility. The lowest energy costs can be reached with the BtM scenario. Therein, a moderate use of heat pumps together with wood-fired boilers in the heat sector, solar PV in the electricity sector and a strong focus on synthetic fuels in the mobility sector is assumed. Above all, the comparatively lower investment costs for established diesel and gasoline vehicles contribute to the more favorable energy costs.

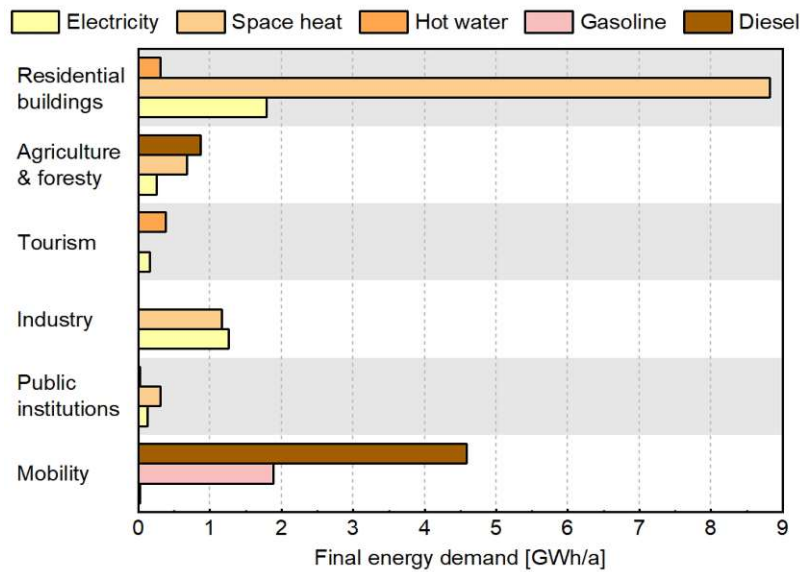


Fig. 42: Final energy demand distribution of St. Margareten im Rosental for the reference year 2020 [164]

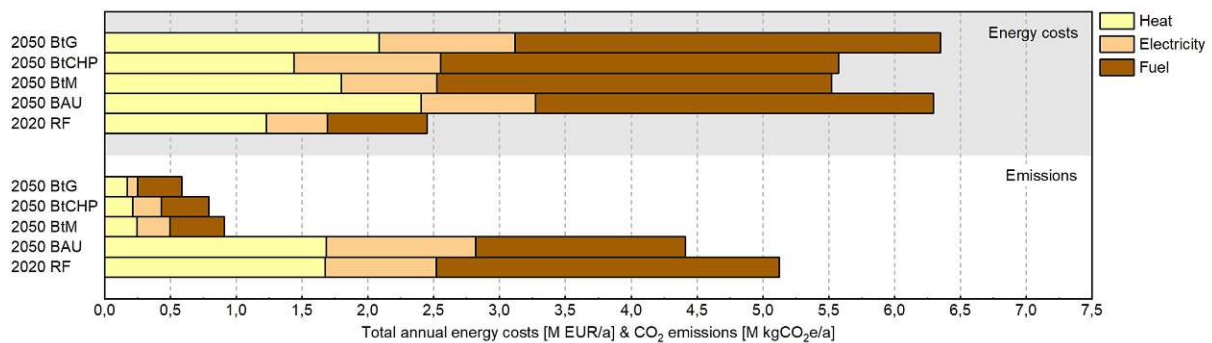


Fig. 43: Comparison of total annual CO₂e emissions and energy costs of the reference case (2020) with assumed scenarios (2050) [164]

The research showed that each scenario had strengths and weaknesses in each sector. The recommendation for the restructuring of the energy portfolio in St. Margareten im Rosental would therefore be a mixture of all three scenarios. Due to the large forest areas around St. Margareten, it is recommended for the heating sector to replace the existing coal and oil boilers with a mix of heat pumps and biomass boilers, either centralized or decentralized. In the electricity sector, biomass-based cogeneration units in a mix with solar PV would be favorable. Finally, in the mobility sector a mix of electrification in the private and public transport as well as synthetic fuels in the heavy-duty traffic sector could be the most promising approach. Further details on the investigations of the defossilization possibilities of the municipality of St. Margareten im Rosental can be found in [164].

8 Discussion of Results

In this chapter, the main findings of this thesis are summarized and discussed. Based on an extensive research on the fundamentals of virtual representations and the covered energy technologies as well as technology assessment possibilities, the following results were obtained:

Development of a novel modelling framework for the process development of energy technologies

The literature review on virtual representations showed that due to different requirements in various industries, no uniform methodology for the development of virtual representations is available to date [17, 33, 36, 48]. However, several frameworks for different field of applications exist in literature, which are listed in Tab. 19. Therein, the main contents of the frameworks are compared. All the exemplary listed frameworks are focused on manufacturing, product life-cycle management, pharmaceutical industry and robotics. No framework with focus on the energy sector exists. Most frameworks are based on the 5D model approach. Furthermore, the virtual component within the most frameworks comprises of a 3D-CAD and a process simulation model, whereby the latter is usually seen as a simulation of the production process steps which is often called model based systems engineering (MBSE) [39]. In chemical engineering like within the pharmaceutical or energy sector, process simulation models are addressed to investigate the process behaviour under different operating conditions. The definition of modelling blocks according to the 5D model approach was often conducted in the listed frameworks. In contrast, the definition of virtual representation properties and the categorization of various virtual representations according to the integration level was not executed in the majority of the frameworks. Furthermore, none of the frameworks contain an evolution strategy in the sense of process development.

Tab. 19: Overview of virtual representation frameworks in literature compared with the novel framework

No.	Year	Field of application	5D model approach (chapter 2.1)	Virtual component comprises of ...		Definition of modelling blocks	Virtual representation properties (chapter 2.5)	Virtual representation integration level (chapter 2.1)	Evolution strategy in development phase	Ref.
				3D CAD model	Process simulation model					
1	2015	Manufacturing	✗	✓	✓ (MBSE)	✗	✗	✗	✗	[39]
2	2018	Manufacturing	✓	✓	✓ (MBSE)	✗	✗	✗	✗	[57]
3	2020	Manufacturing	✓	✓	✓ (MBSE)	✓	✗	✗	✗	[165]
4	2020	Manufacturing	✓	✓	✓ (MBSE)	✓	✗	✗	✗	[166]
5	2021	Manufacturing	✓	✓	✓ (MBSE)	✓	✗	✓	✗	[53]
6	2017	Product life-cycle management	✗	✓	✓ (MBSE)	✗	✓	✗	✗	[67]
7	2018	Product life-cycle management	✓	✓	✓ (MBSE)	✓	✗	✗	✗	[45]
8	2019	Product life-cycle management	✓	✓	✓ (MBSE)	✗	✗	✓	✗	[46]
9	2020	Pharmaceutical industry	✓	✗	✓	✓	✗	✗	✗	[36]
10	2016	Robotics	✗	✓	✓ (MBSE)	✗	✗	✓	✗	[40]
novel framework		Energy sector	✓	✓	✓	✓	✓	✓	✓	-

Discussion of Results

In order to provide a suitable framework for the energy sector, in this work a novel framework for the development of virtual representations with focus on the process development environment of energy technologies has been proposed. The novel modelling framework combines all the features described above. Therefore, the framework is based on the 5D model approach and the virtual component comprises of a 3D-CAD and a process simulation model in the sense of chemical engineering. Moreover, all dimensions are defined through exchangeable modelling blocks and can be further described by appropriate virtual representation properties. Additionally, the framework uses the categorization of virtual representation integration levels to define an evolution strategy in the sense of process development. Finally, a novel definition for virtual representations in the energy sector was established. In Fig. 44, the overall evolution strategy of the framework is visualized. The main idea is based on the interaction of the physical and virtual process development environment by connecting the Technology with the Modelling Readiness Level. Thus, in addition to the physical process development from concept phase to commercial-scale phase, it is also necessary to co-develop the virtual representation according to the prescribed development goals.

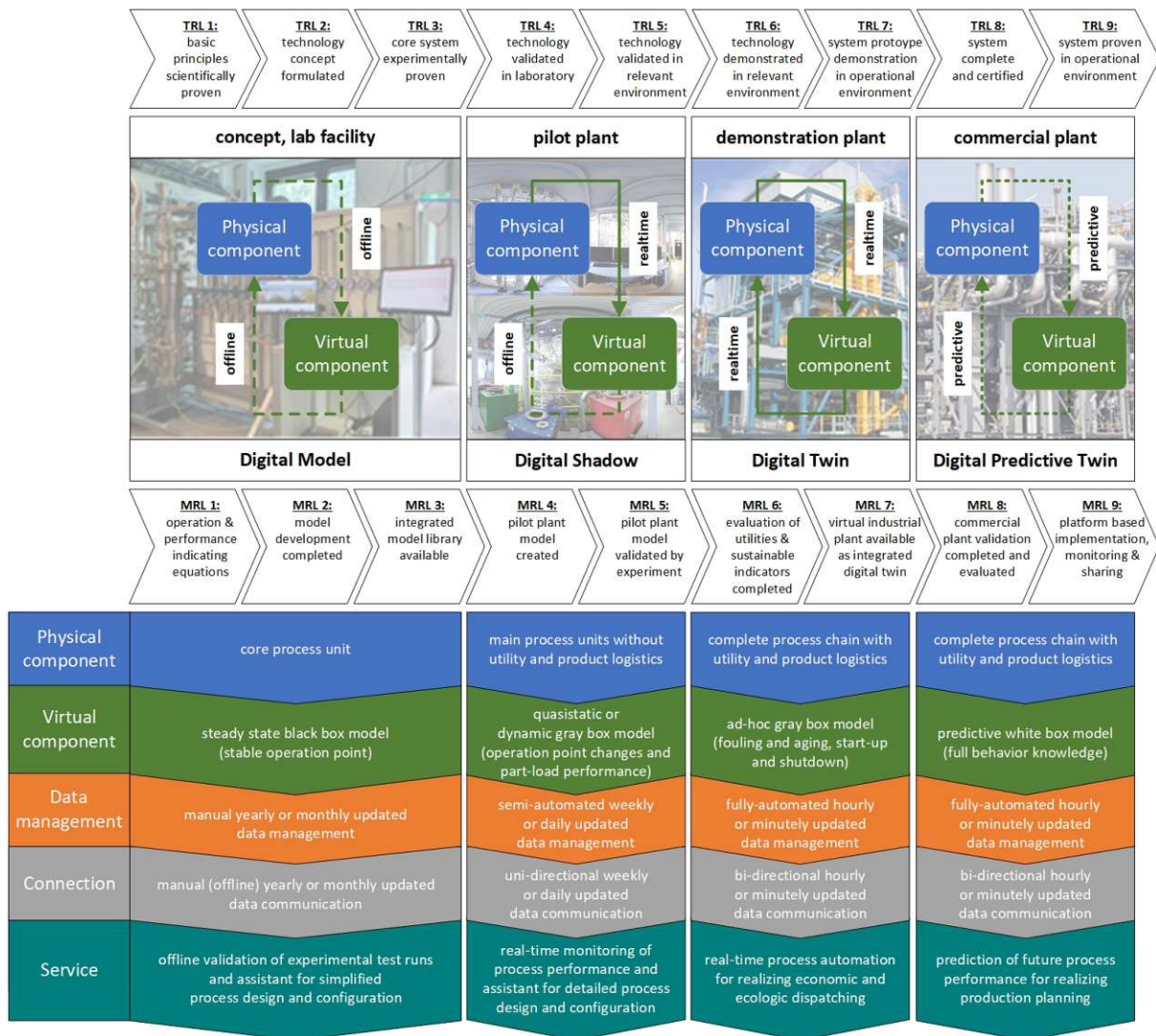


Fig. 44: Evolution strategy of the novel framework for developing of virtual representations in the energy sector

A set of quantifiable technical, environmental, economic and social indicators, referred to as sustainability indicators, were defined to identify development goals. Furthermore, the novel 5D modelling framework determines which exchangeable modelling blocks should be addressed and developed along the process development life-cycle. The overarching development goals of the five virtual representation dimensions physical component, virtual component, data management, connection and service are:

connection and service along the process development life-cycle are established. Moreover, required property levels for virtual representations in each process development phase have been defined to enable the widest possible application. Finally, the process development stages from concept to commercial-scale phase are accompanied by the virtual representation integration levels Digital Model to Digital Predictive Twin.

Application of the novel framework in different energy technology development stages

To test the applicability of the proposed novel framework, four applications have been elaborated at different process development stages. For that the 5D modelling framework was used to develop virtual representations with the required modelling blocks and properties according to the development stage. The following virtual representation use-cases from Digital Model to Digital Predictive Twin have been investigated:

- **Digital Model of a Power-to-Liquid production plant**

The Digital Model of a PtL plant is used to find a suitable conceptual plant design for a yet to be constructed pilot plant with a nominal power of 1 MW_{el}. Several publications on the simulation of different PtL process routes exist [113, 167–170]. However, the influence of different plant configurations for the optimization of a pilot plant layout and the interaction between SOEC in co-electrolysis mode and FT slurry reactor has not been investigated up to now. For that, a variety of plant configurations with different process parameters have been tested with the goal to maximize the PtL efficiency and the product yield. Based on a mixture of a black box and gray box-based steady-state process simulation model with offline data communication, a suitable plant configuration with appropriate process parameters could be determined through various simulation studies. For the construction of the pilot plant, the coupling of a SOEC in co-electrolysis mode with a FT slurry reactor is recommended. In addition, 90% of the tail gas is reformed in a steam reformer. The remaining 10% of the tail gas are burned in a combustor to provide the necessary heat for the steam reformer. With this plant configuration, the highest PtL efficiencies of >60% with simultaneous maximization of the product yield can be achieved.

- **Digital Shadow of a zero-emission reducing gas production plant**

The Digital Shadow of a biomass-based OxySER plant for the production of reducing gas for the Iron and Steel industry is developed to investigate the potential for large-scale production of biomass-based reducing gas. Furthermore, the real-time process monitoring through the visualization of sustainability indicators becomes possible. In literature, experimental investigations of SER [106, 107] and OxySER [108] as well as simplified commercial-scale concepts for the use of the H₂-enriched product gas in the Iron and Steel industry [171, 172] exist. However, none of the previously described works studies the suitability of the product gas to replace the reformed fossil natural gas for the direct reduction process in detail. Therefore, a gray box-based quasistatic process simulation model in ad-hoc mode with unidirectional data communication was developed, to enable the real-time monitoring of the SER process at the 100 kW_{th} pilot plant at TU Wien. Furthermore, a simulation study for the production of reducing gas with 100 MW power for the utilization in the direct reduction process was undertaken. As a result, biomass-based reducing gas with levelized production costs between 10-15 €/GJ, depending on the plant configuration, can be produced. More than 80% of CO₂ emissions can be saved if the biomass-based reducing gas direct reduction process is used instead of the coal-based blast furnace process. However, the production costs of the biomass-based reducing gas are two to three times higher compared to the coal-based blast furnace process.

- **Digital Twin of a Biomass-to-Gas production plant**

The Digital Twin of a BtG process is used to realize the full process automation of the 100 kW_{th} pilot plant at TU Wien. Experimental studies [135, 136, 138, 173] and techno-economic assessments [174] of BtG plants for the production of biomass-based SNG exist in literature. Furthermore, an advanced

control strategy for DFB plants was developed [175]. However, no holistic virtual representation for the optimization of the whole BtG process route exists. Therefore, a gray box-based quasistatic process simulation model in IPSEpro and a gray box-based model predictive controller in MATLAB with bi-directional real-time data communication were developed. With the help of the Digital Twin, full automation of the pilot plant at TU Wien was achieved. Over a full test day, the automation operation could be demonstrated and different operating points could be approached in an automated way. A further test run to optimize the process chain by maximizing sustainability indicators is still pending.

- **Digital Predictive Twin of a hazardous waste incineration plant**

Finally, a Digital Predictive Twin concept for the process optimization of the commercial-scale hazardous waste incineration plant in Vienna was developed. Model approaches for the web-based monitoring of incineration plants [176], the creation of batch-wise waste mixtures [177], the development of a soft sensor for prediction of temperature distribution in a rotary kiln [178], minimization of CO peak loads [179] and the development of tools for predictive maintenance [180] and design optimization [181] exist. All model approaches in literature rely on knowledge about the introduced waste streams. Therefore, a white box-based predictive process simulation model with bi-directional real-time data communication was developed. In addition to the control system measurement data, data from the delivery data base can also be processed in real-time. In that way, the Digital Predictive Twin allows the determination of not entirely analysed waste streams by analysing historical data. Once enough historical data has been analysed, the created fuel data base with the calculated waste compositions can be used to optimize the plant operation of the rotary kiln and subsequently the waste management, in case of recurring waste fractions. Better fuel knowledge can reduce peak loads in the form of temperature and emission peaks and in this way increase plant load. According to initial estimations, efficiency increases of more than 5% can be achieved. The virtual infrastructure at the Wien Energie site in Vienna was set up and the feasibility of determining unknown waste compositions was demonstrated. For the broad application of the Digital Predictive Twin a large amount of historical measurement data should be analysed to build up an extensive fuel data base. The resulting extensive fuel data base can then be used to actively improve the process performance.

Use of virtual representations for the investigation of energy system integration scenarios

The developed virtual representations can also be used during process development to explore energy system integration scenarios either from the perspective of the developed energy technology or from the perspective of a municipality. The following energy system integrations scenarios have been investigated:

- **Defossilization of the Austrian energy system by the integration of DFB plants**

The virtual representations of a Biomass-to-Liquid and Biomass-to-Gas process, both based on the DFB gasification technology, were used to investigate energy system integration scenarios from the perspective of the developed energy technology. In literature, techno-economic [174] and ecological [182, 183] assessments for both process routes exist. Nevertheless, none of them focuses on the use of both products in the Austrian energy system. Studies showed that a plant size of 100 MW thermal fuel power is an ideal trade-off between economy of scale and biomass procurement. Based on the techno-economic and ecological assessment of both product routes, specific energy system integration scenarios were developed. Consequently, the use of SNG in gas power plants for peak-load power coverage, the use of SNG for the provision of high-temperature heat in industry and the use of FT diesel in the heavy-duty traffic sector were selected as the most suitable applications for Austria.

- **Defossilization of Austrian municipalities by the integration of RES technologies**

Finally, the novel tool ENECO₂Calc was developed, which allows the investigation of defossilization scenarios from the perspective of an Austrian municipality. Numerous energy models with a wide range of different applications exist [184–188]. However, no municipality-based energy model for the

development of energy transition scenarios is available. ENECO₂Calc allows the determination of the current CO₂ footprint and energy costs of any Austrian municipality using consistent statistical data sets. Furthermore, the municipality's energy portfolio can be adapted to investigate defossilization scenarios until 2050. The novel energy modelling tool was tested by examining the Carinthian municipality St. Margareten im Rosental (AUT). Three energy transition scenarios were investigated and as a result a recommendation for the restructuring of the energy portfolio can be given.

In summary, this doctoral thesis focuses on the proposal of a novel framework for the development of virtual representations along the process development life-cycle of energy technologies. Furthermore, different virtual representation use-cases in different process development stages were investigated to test the applicability of the novel framework. Finally, energy system integration scenarios based on developed virtual representations were conducted.

9 Conclusion and Outlook

The climate crisis has shown the need for the development and optimization of climate-friendly and efficient energy technologies. The rapid and effective development of these technologies requires the use of virtual representations. The achieved research goals within this thesis and open research questions can be summarized as follows:

Achieved research goals

In literature, no uniform modelling framework for the development of virtual representations in the process development of energy technologies exist. Therefore, the achieved research goals within this thesis can be summarized by answering the research questions posed at the beginning.

How can be a framework for the development of high-fidelity virtual representations within the area of process development in the energy sector defined?

A novel framework for developing virtual representations of energy technologies with focus on the development environment was established and demonstrated in four different use-cases along the process development life-cycle. First of all, a Ten-point plan was developed to list the necessary design steps for the development of virtual representations. Based on the novel definition of virtual representations in the energy sector, a 5D modelling framework was raised to determine how the virtual representation should evolve along the process development life-cycle. Furthermore, the novel framework determines which exchangeable modelling blocks make up a virtual representation. In summary, the novel framework enables users to co-develop virtual representations of energy technologies according to the technology readiness level in order to realize a wide range of applications.

How should the modelling readiness level of a virtual representation be defined to realize the use of appropriate models and technologies in each stage of process development?

In addition to the 5D modelling framework, the Technology and Modelling Readiness Level are connected to couple the physical and virtual infrastructure development. Furthermore, 16 virtual representation property levels are defined to classify virtual representations. Moreover, required property levels for virtual representations in each process development phase have been specified to enable the widest possible application. In summary, the advancement from Digital Models in the concept and lab-scale phase to Digital Predictive Twins in the commercial-scale phase is the ultimate goal.

The usage of the novel 5D modelling framework along the whole process development life-cycle of an energy technology helps to evolve virtual representations according to the following overarching goals:

- Standardization of virtual representation development of energy technologies
- The early integration of virtual representations in the process development framework leads to a large development cost reduction potential
- Improvement of process performance and plant availability
- State-of-the-Art virtual representations enable technology learning in the roll-out phase
- State-of-the-Art virtual representations provide access to the documentation and simulation of new technologies for a wide range of plant engineers and manufacturers → The resulting market competition ensures a reduction in plant investment costs
- Realization of a smart interconnected energy system

How can virtual representations be used to find appropriate energy system integration scenarios?

Finally, the use of virtual representations for the investigation of energy system integration and defossilization scenarios was demonstrated. For that, energy system integration scenarios from the energy technology perspective based on the example of the Biomass-to-Gas and Biomass-to-Liquid processes were investigated to find the most suitable usage of SNG and FT diesel in the Austrian energy

system. Furthermore, a novel tool called ENECO₂Calc was developed to investigate energy transition scenarios from the perspective of any municipality in Austria. In summary, virtual representations developed according to this methodology can be used at any time to investigate energy system integration and defossilization scenarios for selected sectors or regions.

Future research goals

In order to further improve the proposed and tested methodology and to establish it in the process development of energy technologies, the following topics must be addressed in future research works:

- **Coupling of patent rights with the handover of virtual representations**

In order to take advantage of the full range of the listed benefits, the patent system needs to be revised. As a consequence, patent rights could be coupled with the complete handover of state-of-the-art virtual representations. This could, for example, enable the transfer of simulation and 3D models to various stakeholders to accelerate the design and construction of novel energy technologies. Furthermore, in the course of process development, the generated models can be used by external experts such as control or energy system engineers to develop advanced control strategies or energy system integration scenarios based on the state-of-the-art process models. Moreover, the plant owner can use the virtual representation to monitor and optimize the real-time process performance.

- **Establishment of an open-source strategy**

In contrast to changing the patent system, an open-source strategy could also help to accelerate the development of energy technologies. The Gaia-X project can be mentioned as a role model by trying to establish a trustworthy and cross-sectoral data exchange open for consumers and providers on a pan-European level. [189]

- **Applying the methodology along the entire development life-cycle of a single technology**

In this doctoral thesis, a standardized methodology for the development of energy technologies in the process development environment was defined. In order to be able to test the effectiveness and applicability of the established methodology in a holistic manner, the development of a virtual representation along the entire process development cycle of an energy technology should be accompanied by this methodology.

- **Further specification of virtual representation properties to modelling block level**

Furthermore, the established virtual representation properties can be further detailed and the individual evolution targets of the five virtual representation dimensions can be broken down to each individual exchangeable modelling block in each virtual representation dimension.

- **Standardization of data types and interfaces along the entire development life-cycle**

Moreover, approved standardized data types and interfaces could be defined along the process development cycle. In order to realize modelling blocks which can interact without restriction, it is necessary to develop standards for simulation models like the CAPE-OPEN interface standard. [190]

- **Testing of the methodology with 3D model applications**

Finally, it is important to note that the applications studied were all based on process simulation models. The integration of 3D models was not performed in this work. Therefore, in future research works, the methodology should be reviewed using applications that require the integration of a 3D model by realizing Building Information Modelling (BIM) to interlink the process simulation and 3D model. [191]

- **Integration of LCA software tools in 5D modelling framework**

Besides production costs and CO₂ footprints, various other sustainability indicators should be investigated in the context of life-cycle assessment in order to enable a holistic evaluation of energy technologies. Therefore, LCA software tools and databases should be integrated into the 5D modelling framework in order to realize comprehensive analyses.

List of Abbreviations

3D	three-dimensional
5D	five-dimensional
AI	artificial intelligence
ASF	Anderson-Schulz-Flory
ASU	air separation unit
AUT	Austria
BAU	Business-as-Usual scenario
BF	blast furnace
BG	biomass-based reduction gas
BIM	Building Information Modelling
BOF	basic oxygen steelmaking
BtCHP	Biomass-to-Combined Heat and Power plants scenario
BtG	Biomass-to-Gas (scenario)
BtL	Biomass-to-Liquid
BtM	Biomass-to-Mobility scenario
C & C++	traditional program languages
C ₁ -C ₃	Fischer-Tropsch product light fraction
C ₁ -C ₁₉	Fischer-Tropsch product mixture of light, naphtha and middle distillate fraction
C ₄ -C ₉	Fischer-Tropsch product naphtha fraction
C ₁₀ -C ₁₉	Fischer-Tropsch product middle distillate (diesel) fraction
C ₂₀₊	Fischer-Tropsch product wax fraction
CAD	computer aided design
CaO	calcium oxide
CCS	carbon capture and storage
CCU	carbon capture and utilization
CH ₄	methane
C ₂ H ₆	ethane
C ₃ H ₈	propane
C _x H _y	non condensable hydrocarbons
CO	carbon monoxide
CO ₂	carbon dioxide
CO _{2e}	carbon dioxide equivalent
CO ₂ -eq	carbon dioxide equivalent
CR	combustion reactor
CS	crude steel
DFB	dual fluidized bed
DT	Digital Twin
e ⁻	electrons
e-fuel	synthetic fuels based on renewable electricity and CO ₂ sources
EAF	electric arc furnace
ENECO ₂ Calc	energy modelling tool investigated in this doctoral thesis
ERP	enterprise resource planning
EU	European Union
EU ETS	European Union Emissions Trading System
FFG	Austrian Research Promotion Agency
FG	flue gas
Fig.	figure
FOAK	first of a kind
Fortran	traditional programming language

List of Abbreviations

FT	Fischer-Tropsch
FTP	file transfer protocol
FU	functional unit
Gaia-X	initiative to develop a federated secure data infrastructure for Europe
GDP	gross domestic product
GEMIS	software for life-cycle assessment
GR	gasification reactor
GRP	gross regional product
GVA	gross value added
H ₂	hydrogen
H ₂ O	water
H ₂ S	hydrogen sulfide
HCl	hydrogen chloride
HEL	heating oil extra light
HMI	human-machine interface
HTFT	high temperature Fischer-Tropsch
HTTP	hypertext transfer protocol
HYBRIT	Hydrogen Breakthrough Ironmaking Technology
ICEBE	Institute of Chemical, Environmental and Bioscience Engineering
IEA	International Energy Agency
IEC	International Electrotechnical Commission
IETS	industrial energy technologies and systems
IoT	Internet of Things
IPSEpro 8.0	software tool for process simulation (version 8.0)
ISO	International Organization for Standardization
Java	traditional programming language
LCA	life-cycle assessment
LCOP	levelized costs of products or levelized production costs
LTFT	low temperature Fischer-Tropsch
MAPE	mean absolute percentage error
MATLAB	matrix-based programming language
MBSE	model based systems engineering
MDL	model description language
MES	manufacturing execution system
MIDREX	direct reduction technology Iron and Steel Industry
ML	machine learning
Modbus	Client/Server communication protocol
MPC	model predictive controller
MRL	Modelling Readiness Level
MQTT	message queuing telemetry transport
N ₂	nitrogen
N ₂ O	nitrous oxide
NASA	National Aeronautics and Space Administration
NG	natural gas
NH ₃	ammonia
NOAK	nth of a kind
n.m.	not measured
NO _x	nitrous oxide (general form)
O ₂	oxygen
OPC UA	open platform communications unified architecture
org.	organic

List of Abbreviations

OSI	open systems interconnection
OxySER	sorption enhanced reforming in combination with oxyfuel combustion
P&ID	pipng and instrumentation diagram
PAT	process analytical technology
PFD	process flow diagram
PG	product gas
PID	proportional-integral-derivative
PLC	programmable logic controller
Profibus	standard for fieldbus communication
PSServer	Program module of IPSEpro for executing simulation flowsheets automatically
PtL	Power-to-Liquid
PV	photovoltaics
Python	traditional programming language
RAMI 4.0	reference architecture model for industry 4.0
raw-SNG	raw synthetic natural gas
RED	Renewable Energy Directive
Ref.	reference
RES	renewable energy sources
RF	Reference scenario
RME	rapeseed methyl ester
rWGS	reverse water-gas shift reaction
SCADA	supervisory control and data acquisition
SER	sorption enhanced reforming
SNG	synthetic natural gas
SOEC	solid oxide electrolyzer
SO ₂	sulfur dioxide
SO ₂ -eq	sulfur dioxide equivalent
SO _x	sulfur oxide (general form)
Tab.	table
TG	Fischer-Tropsch tail gas
TCP/IP	transmission control protocol/internet protocol
TRL	Technology Readiness Level

List of Symbols

$\%CO$	volumetric percent of carbon monoxide within reducing gas	[vol.-%]
$\%CO_2$	volumetric percent of carbon dioxide within reducing gas	[vol.-%]
$\%H_2$	volumetric percent of hydrogen within reducing gas	[vol.-%]
$\%H_2O$	volumetric percent of water within reducing gas	[vol.-%]
A	revenues minus the operation and maintenance costs	[€]
CDF	cumulative discount factor	[-]
C_{eq}	purchased equipment costs	[€]
CO_2e	global warming potential factor (carbon dioxide equivalent)	[t CO ₂ e/t _{CS}]
E	expenses	[€/a]
FLH/a	full load hours per year	[h/a]
FU	functional unit	[not fixed]
GQ	gas quality	[-]
H_2/CO	hydrogen to carbon monoxide ratio	[-]
i	interest rate	[%]
I_0	investment costs of considered process route	[€]
$I_{ref.}$	investment costs of reference option	[€]
LCOP	levelized production costs	[€/FU]
LHV _j	lower heating value of fraction j	[MJ/kg]
$\dot{m}_{C,GR,Fuel}$	mass flow of carbon within biomass-based fuel fed to gasification reactor	[kg/h]
$\dot{m}_{C,PG}$	mass flow of carbon within product gas without char and tar	[kg/h]
$\dot{m}_{C,PG,syn}$	mass flow of carbon within syngas	[kg/h]
$\dot{m}_{C,RawSNG}$	mass flow of carbon within raw synthetic natural gas	[kg/h]
\dot{m}_{FG}	mass flow of flue gas	[kg/h]
$\dot{m}_{GR,Fuel}$	mass flow of biomass-based fuel fed to gasification reactor	[kg/h]
$\dot{m}_{H_2,ext}$	mass flow of additional external hydrogen fed to methanation reactor	[kg/h]
\dot{m}_j	mass flow of fraction j	[kg/h]
\dot{m}_{PG}	mass flow of product gas	[kg/h]
$M_{t,main prod.}$	annual produced amount of main product	[MWh/a]
n	plant lifetime	[a]
n_p	payback time	[a]
$\dot{n}_{CO,in}$	molar flow of input fractions	[mol/h]
$\dot{n}_{CO,out}$	molar flow of output fractions	[mol/h]
NPV_{rel}	relative net present value	[€]
P	present worth capital costs	[€]
$P_{barrels}$	thermal fuel power of direct barrels fed to the rotary kiln	[MW _{th}]
$P_{bunker waste}$	thermal fuel power of bunker waste fed to the rotary kiln	[MW _{th}]
P_{char}	chemical power of char within product gas	[MW]
$P_{CR,Fuel}$	thermal fuel power of additional fuel fed to combustion reactor	[MW _{th}]
$P_{el.,Total}$	total electrical power consumption	[MW _{el}]
$P_{elec.}$	electrical power fed to electricity grid	[MW _{el}]
$P_{GR,Fuel}$	thermal fuel power of biomass fed to gasification reactor	[MW _{th}]
$P_{H_2,ext}$	additional external hydrogen power fed to the methanation reactor	[MW]
$P_{H_2,rec}$	recirculated hydrogen power fed to the methanation reactor	[MW]
P_{heat}	thermal power fed to district heating system	[MW _{th}]
$P_{hospital waste}$	thermal fuel power of hospital waste fed to the rotary kiln	[MW _{th}]
$P_{masterbatch}$	thermal fuel power of masterbatch (solvent mixture) fed to the rotary kiln	[MW _{th}]
$P_{pasty waste}$	thermal fuel power of pasty waste fed to the rotary kiln	[MW _{th}]

List of Symbols

P_{PG}	product gas power	[MW]
$P_{PG,rec}$	recycled product gas power	[MW]
P_{RawSNG}	raw synthetic natural gas power	[MW]
$P_{PG,syn}$	syngas power	[MW]
$P_{Shredded\ waste}$	thermal fuel power of shredded waste fed to the rotary kiln	[MW _{th}]
$P_{Support\ fuel}$	thermal fuel power of support fuel fed to the rotary kiln	[MW _{th}]
P_{tar}	chemical power of tars within product gas	[MW]
$P_{th,total}$	total amount of thermal fuel power fed to the rotary kiln	[MW _{th}]
P_{waste}	total thermal fuel power of all waste fractions fed to the rotary kiln	[MW _{th}]
$P_{waste\ oil}$	thermal fuel power of waste oil fed to the rotary kiln	[MW _{th}]
$P_{waste\ water}$	thermal fuel power of waste water fed to the rotary kiln	[MW _{th}]
$\dot{Q}_{loss,DFB}$	heating loss within the whole DFB system	[MW _{th}]
$R_{sec.\ prod.}$	revenues through secondary products	[€/a]
R^2	coefficient of determination	[-]
RR	recirculation ratio of Fischer-Tropsch tail gas	[%]
RR_{CO_2}	carbon dioxide recovery rate	[%]
$SNGY$	raw synthetic natural gas yield	[Nm ³ /kg]
T	temperature	[°C]
T_{CR}	temperature in combustion reactor	[°C]
T_{GR}	temperature in gasification reactor	[°C]
$\dot{V}_{N,RawSNG}$	standard volume flow of raw synthetic natural gas	[Nm ³ /h]
X_{CO}	carbon monoxide conversion rate at system level	[%]
ΔG_r	free Gibbs energy	[kJ/mol]
ΔH_r	reaction enthalpy	[kJ/mol]
ΔS_r	reaction entropy	[kJ/K/mol]
η_C	carbon utilization factor	[%]
η_{CG}	cold gas efficiency	[%]
η_{DRO}	total energetic efficiency of hazardous waste incineration plant	[%]
η_{FC}	fuel conversion rate	[%]
η_{PtL}	Power-to-Liquid efficiency	[%]
λ	air-fuel ratio	[-]

References

- [1] United Nations, 2005. Kyoto Protocol: Protokoll von Kyoto zum Rahmenübereinkommen der Vereinten Nationen über Klimaänderungen samt Anlagen. <https://www.ris.bka.gv.at/GeltendeFassung.wxe?Abfrage=Bundesnormen&Gesetzesnummer=20004173> (accessed 9 August 2023).
- [2] United Nations, 2015. The Paris Agreement – UNFCCC. https://unfccc.int/sites/default/files/english_paris_agreement.pdf (accessed 22 October 2021).
- [3] European Union, 2009. DIRECTIVE 2009/28/EC OF THE EUROPEAN PARLIAMENT AND OF THE COUNCIL of 23rd April 2009 on the promotion of the use of energy from renewable sources and amending and subsequently repealing Directives 2001/77/EC and 2003/30/EC. Official Journal of the European Union. <https://eur-lex.europa.eu/LexUriServ/LexUriServ.do?uri=OJ:L:2009:140:0016:0062:en:PDF> (accessed 09 August 2023).
- [4] European Union, 2018. DIRECTIVE (EU) 2018/2001 OF THE EUROPEAN PARLIAMENT AND OF THE COUNCIL of 11th December 2018 on the promotion of the use of energy from renewable sources, RED II. Official Journal of the European Union. <https://eur-lex.europa.eu/legal-content/DE/TXT/?qid=1575559881403&uri=CELEX:32018L2001> (accessed 12 May 2021).
- [5] European Union, 2019. The European Green Deal. https://commission.europa.eu/system/files/2019-12/european-green-deal-communication_de.pdf (accessed 02 July 2023).
- [6] European Union, 2021. REGULATION (EU) 2021/1119 OF THE EUROPEAN PARLIAMENT AND OF THE COUNCIL of 30th June 2021 establishing the framework for achieving climate neutrality and amending Regulations (EC) No 401/2009 and (EU) 2018/1999, European Climate Law. Official Journal of the European Union. <https://eur-lex.europa.eu/legal-content/EN/TXT/PDF/?uri=CELEX:32021R1119> (accessed 09 August 2023).
- [7] Suna, D., 2019. Studie Versorgungssicherheit & Flexibilität bei 100% erneuerbarem Strom in Österreich. 5. Praxis- und Wissensforum Fernwärme/Fernkälte, Austrian Institute of Technology. Vienna, Austria. https://www.ait.ac.at/fileadmin/mc/energy/downloads/News_and_Events/20190708_5FWK/A3_FernwaermeForum_Suna_20191119.pdf (accessed 9 August 2023).
- [8] Anderl, M., Bartel, A., Frei, E., Gugele, B., Gössl, M., Mayer, S., Heinfellner, H., Heller, C., Heuber, A., Köther, T., Krutzler, T., Kuschel, V., Lampert, C., Miess, M.G., Pazdernik, K., Perl, D., Poupá, S., Prutsch, A., Purzner, M., Rigler, E., Rockenschaub, K., Schieder, W., Schmid, C., Schmidt, G., Schnirzer, S., Schodl, B., Storch, A., Stranner, G., Svehla-Stix, S., Schwarzl, B., Schwaiger, E., Vogel, J., Weiss, P., Wiesenberger, H., Wieser, M., Zechmeister, A. 2022. Klimaschutzbericht 2022. Federal Environmental Agency, Vienna, Austria. <https://www.umweltbundesamt.at/fileadmin/site/publikationen/rep0816.pdf> (accessed 2 July 2023).
- [9] Federal Ministry for Sustainability and Tourism, 2019. Integrierter nationaler Energie- und Klimaplan für Österreich: Periode 2021-2030 gemäß Verordnung (EU) 2018/1999 des Europäischen Parlaments und des Rates über das Governance-System für die Energieunion und den Klimaschutz, Vienna, Austria. https://www.bmk.gv.at/themen/klima_umwelt/klimaschutz/nat_klimapolitik/energie_klimaplan.html (accessed 9 August 2023).
- [10] European Union, 2021. RICHTLINIE DES EUROPÄISCHEN PARLAMENTS UND DES RATES zur Änderung der Richtlinie (EU) 2018/2001 des Europäischen Parlaments und des Rates, der Verordnung (EU) 2018/1999 des Europäischen Parlaments und des Rates und der Richtlinie 98/70/EG des Europäischen Parlaments und des Rates im Hinblick auf die Förderung von Energie aus erneuerbaren Quellen und zur Aufhebung der Richtlinie (EU) 2015/652 des Rates. Proposal European Commission, https://eur-lex.europa.eu/resource.html?uri=cellar:dbb7eb9c-e575-11eb-a1a5-01aa75ed71a1.0013.02/DOC_1&format=PDF (accessed 9 July 2023).

References

- [11] European Union, 2012. RICHTLINIE 2012/27/EU DES EUROPÄISCHEN PARLAMENTS UND DES RATES zur Energieeffizienz, zur Änderung der Richtlinien 2009/125/EG und 2010/30/EU und zur Aufhebung der Richtlinien 2004/8/EG und 2006/32/EG. Energieeffizienzrichtlinie. Official Journal of the European Union. <https://eur-lex.europa.eu/LexUriServ/LexUriServ.do?uri=OJ:L:2012:315:0001:0056:DE:PDF> (accessed 9 August 2023)
- [12] Bundesrepublik Österreich, 2014. 72. Bundesgesetz, mit dem das Bundes-Energieeffizienzgesetz, das Bundesgesetz, mit dem der Betrieb von bestehenden hocheffizienten KWK-Anlagen über KWK-Punkte gesichert wird, und das Bundesgesetz, mit dem zusätzliche Mittel für Energieeffizienz bereitgestellt werden, erlassen sowie das Wärme- und Kälteleitungsausbaugesetz und das KWK-Gesetz geändert werden (Energieeffizienzpaket des Bundes): Bundes-Energieeffizienzgesetz (EEffG). Bundesgesetzblatt für die Republik Österreich. https://www.ris.bka.gv.at/Dokumente/BgblAuth/BGBLA_2014_I_72/BGBLA_2014_I_72.pdf (accessed 9 August 2023).
- [13] European Union, 2009. ENTSCHEIDUNG Nr. 406/2009/EG DES EUROPÄISCHEN PARLAMENTS UND DES RATES über die Anstrengungen der Mitgliedstaaten zur Reduktion ihrer Treibhausgasemissionen mit Blick auf die Erfüllung der Verpflichtungen der Gemeinschaft zur Reduktion der Treibhausgasemissionen bis 2020: Effort-Sharing Decision Nr. 406/2009/EG. Official Journal of the European Union. <https://eur-lex.europa.eu/LexUriServ/LexUriServ.do?uri=OJ:L:2009:140:0136:0148:DE:PDF> (accessed 9 August 2023).
- [14] Bundesrepublik Österreich, 2011. Bundesgesetz zur Einhaltung von Höchstmengen von Treibhausgasemissionen und zur Erarbeitung von wirksamen Maßnahmen zum Klimaschutz: Klimaschutzgesetz (KSG). <https://www.ris.bka.gv.at/GeltendeFassung.wxe?Abfrage=Bundesnormen&Gesetzesnummer=20007500> (accessed 13 September 2022).
- [15] European Union, 2009. RICHTLINIE 2009/29/EG DES EUROPÄISCHEN PARLAMENTS UND DES RATES zur Änderung der Richtlinie 2003/87/EG zwecks Verbesserung und Ausweitung des Gemeinschaftssystems für den Handel mit Treibhausgasemissionszertifikaten. Official Journal of the European Union. <https://eur-lex.europa.eu/LexUriServ/LexUriServ.do?uri=OJ:L:2009:140:0063:0087:de:PDF> (accessed 9 August 2023).
- [16] Bundesrepublik Österreich, 2011. Bundesgesetz über ein System für den Handel mit Treibhausgasemissionszertifikaten: Emissionszertifikategesetz 2011 (EZG 2011). <https://www.ris.bka.gv.at/eli/bgbl/I/2011/118> (accessed 9 August 2023).
- [17] Hofmann, R., Halmschlager, V., Knöttner, S., Leitner, B., Pernsteiner, D., Prendl, L., Sejkora, C., Steindl, G., Traupmann, A., 2020. Digitalization in Industry - an Austrian Perspective. TU Wien, Vienna.
- [18] O'Dwyer, E., Pan, I., Acha, S., Shah, N., 2019. Smart energy systems for sustainable smart cities: Current developments, trends and future directions. *Applied Energy* 237:581–597. <https://doi.org/10.1016/j.apenergy.2019.01.024>.
- [19] Borowski, P.F., 2021. Digitization, Digital Twins, Blockchain, and Industry 4.0 as Elements of Management Process in Enterprises in the Energy Sector. *Energies* 14(7):1885. <https://doi.org/10.3390/en14071885>.
- [20] Kritzinger, W., Karner, M., Traar, G., Henjes, J., Sihm, W., 2018. Digital Twin in manufacturing: A categorical literature review and classification. *IFAC-PapersOnLine* 51-11:1016–1022. <https://doi.org/10.1016/j.ifacol.2018.08.474>.
- [21] Grafinger, M., 2020. Virtuelle Produktentwicklung. Lecture notes LVA 307.414, TU Wien, Institute of Engineering Design and Product Development, Vienna.
- [22] Szeghő, K., Bercsey, T., 2007. Kosten- und Risikomanagement in der frühen Phase der Produktentwicklung. 18th Symposium „Design for X“, Technische und Wirtschaftswissenschaftliche Universität Budapest, Neunkirchen.

References

- [23] Ehrlenspiel, K., Kiewert, A., Lindemann, U., Mörtl, M., 2020. Kostengünstig Entwickeln und Konstruieren: Kostenmanagement bei der integrierten Produktentwicklung. 8. Auflage, Springer Vieweg, Berlin. <https://doi.org/10.1007/978-3-662-62591-0>.
- [24] Schulte, R., 2013. Rechnergestütztes Normteilemanagement als Beitrag zu einem optimierten Produktionsplanungsprozess in der Automobilindustrie. Dissertation, Helmut-Schmidt-Universität / Universität der Bundeswehr Hamburg, Fakultät für Maschinenbau, Hamburg.
- [25] Leistner, B. 2019. Fahrwerkentwicklung und produktionstechnische Integration ab der frühen Produktentstehungsphase. Wissenschaftliche Reihe Fahrzeugsystemdesign, Springer Vieweg, Wiesbaden. <https://doi.org/10.1007/978-3-658-26867-1>.
- [26] Weber, C., Husung, S., Cascini, G., Cantamessa, M., Marjanovic, D., Rotini, F., 2015. Product modularisation, product architecture, systems engineering, product service systems. 20th International Conference on Engineering Design (ICED15), Politecnico di Milano, Politecnico di Torino, Design Society, Proceedings vol. 7., Glasgow. ISBN 978-1-904670-70-4.
- [27] Maniatis, K., Landälv, I., Waldheim, L., van den Heuvel, E., Kalligeros, S., 2017. Final Report - Building up the Future: Sub Group on Advanced Biofuels - Sustainable Transport Forum, European Commission. Luxembourg. ISBN 978-92-79-69010-5.
- [28] Resch, G., Kranzl, L., Faninger, G., Geipel, J., 2020. Block 1: Introduction: energy & climate challenge and basics of economic assessment. VO Economic Perspectives of Renewable Energy Systems, Energy Economics Group (EEG), TU Wien, Vienna, Austria.
- [29] Hammerschmid, M., Rosenfeld, D.C., Bartik, A., Benedikt, F., Fuchs, J., Müller, S., 2023. Methodology for the Development of Virtual Representations within the Process Development Framework of Energy Plants: From Digital Model to Digital Predictive Twin-A Review. *Energies* 16:2641. <https://doi.org/10.3390/en16062641>.
- [30] Holler, M., Uebernickel, F., Brenner, W., 2016. Digital Twin Concepts in Manufacturing Industries - A Literature Review and Avenues for Further Research. Proceedings of the International Conference on Industrial Engineering 2016(8), Seoul.
- [31] Grieves, M., Vickers, J., 2016. Digital Twin: Mitigating Unpredictable, Undesirable Emergent Behavior in Complex Systems. In: *Transdisciplinary perspectives on complex systems*, Kahlen, F.-J., Flumerfelt, S., Alves, A. C., Springer, 85-113. https://doi.org/10.1007/978-3-319-38756-7_4.
- [32] Glaessgen, E. H., Stargel, D., 2012. The Digital Twin Paradigm for Future NASA and U.S. Air Force Vehicles. Proceedings 53rd AIAA/ASME/ASCE/AHS/ASC Structures, Structural Dynamics and Materials Conference 2012:1818. <https://doi.org/10.2514/6.2012-1818>.
- [33] Tao, F., Zhang, H., Liu, A., Nee, A.Y.C., 2019. Digital Twin in Industry: State-of-the-Art. *IEEE Transactions on Industrial Informatics* 15:2405–2415. <https://doi.org/10.1109/TII.2018.2873186>.
- [34] Birkelbach, F., Fluch, J., Jentsch, R., Kasper, L., Knapp, A., Knöttner, S., Kurz, T., Paczona, D., Schwarzmayr, P., Sharma, E., Tahir, A. J., Tugores, C. R., Zawodnik, V., 2022. Digital Twins - Terms & Definitions: TASK XVIII – Digitalization, Artificial Intelligence and related Technologies for Energy Efficiency and GHG Emissions Reduction in Industry. Institute of Energy Systems and Thermodynamics, TU Wien. Vienna, Austria.
- [35] Aheleroff, S., Xu, X., Zhong, R.Y., Lu, Y., 2021. Digital Twin as a Service (DTaaS) in Industry 4.0: An Architecture Reference Model. *Advanced Engineering Informatics* 47:101225. <https://doi.org/10.1016/j.aei.2020.101225>.
- [36] Chen, Y., Yang, O., Sampat, C., Bhalode, P., Ramachandran, R., Ierapetritou, M., 2020. Digital Twins in Pharmaceutical and Biopharmaceutical Manufacturing: A Literature Review. *Processes* 8:1088. <https://doi.org/10.3390/pr8091088>.
- [37] Negri, E., Fumagalli, L., Macchi, M., 2017. A review of the roles of Digital Twin in CPS-based production systems. *Procedia Manufacturing* 11:939–948. <https://doi.org/10.1016/j.promfg.2017.07.198>.

References

- [38] Garetti, M., Rosa, P., Terzi, S., 2012. Life Cycle Simulation for the design of Product–Service Systems. *Computers in Industry* 63:361–369. <https://doi.org/10.1016/j.compind.2012.02.007>.
- [39] Rosen, R., von Wichert, G., Lo, G., Bettenhausen, K. D., 2015. About The Importance of Autonomy and Digital Twins for the Future of Manufacturing. *IFAC-PapersOnLine* 48:567–572. <https://doi.org/10.1016/j.ifacol.2015.06.141>.
- [40] Schluse, M., Rossmann, J. 2016. From simulation to experimentable digital twins: Simulation-based development and operation of complex technical systems. *IEEE International Symposium on Systems Engineering (ISSE) 2016*:1–6. <http://doi.org/10.1109/SysEng.2016.7753162>.
- [41] Gabor, T., Belzner, L., Kiermeier, M., Beck, M. T., Neitz, A., 2016. A Simulation-Based Architecture for Smart Cyber-Physical Systems. *IEEE International Conference on Autonomic Computing (ICAC) 2016*:374–379. <https://doi.org/10.1109/ICAC.2016.29>.
- [42] Liu, Z., Meyendorf, N., Mrad, N., 2018. The role of data fusion in predictive maintenance using digital twin. *AIP Conference Proceedings* 1949:20023. <https://doi.org/10.1063/1.5031520>.
- [43] Vrabič, R., Erkoyuncu, J. A., Butala, P., Roy, R., 2018. Digital twins: Understanding the added value of integrated models for through-life engineering services. *Procedia Manufacturing* 16:139–146. <https://doi.org/10.1016/j.promfg.2018.10.167>.
- [44] Fuller, A., Fan, Z., Day, C., Barlow, C., 2020. Digital Twin: Enabling Technologies, Challenges and Open Research. *IEEE Access* 8:108952–108971. <https://doi.org/10.1109/ACCESS.2020.2998358>.
- [45] Zheng, Y., Yang, S., Cheng, H., 2018. An application framework of digital twin and its case study. *Journal of Ambient Intelligence and Humanized Computing*, vol. 10, 1141–1153. <https://doi.org/10.1007/s12652-018-0911-3>.
- [46] Madni, A. M., Madni, C. C., Lucero, S. D., 2019. Leveraging Digital Twin Technology in Model-Based Systems Engineering. *Systems*, vol. 7(1), 7. <https://doi.org/10.3390/systems7010007>.
- [47] Fotland, G., Haskins, C., Rølvåg, T., 2020. Trade study to select best alternative for cable and pulley simulation for cranes on offshore vessels. *Systems Engineering*, vol. 23(2), 177–188. <https://doi.org/10.1002/sys.21503>.
- [48] Liu, M., Fang, S., Dong, H., Xu, C., 2021. Review of digital twin about concepts, technologies, and industrial applications. *Journal of Manufacturing Systems* 58:346–361. <https://doi.org/10.1016/j.jmsy.2020.06.017>.
- [49] Wang, P., Yang, M., Peng, Y., Zhu, J., Ju, R., Yin, Q., 2019. Sensor Control in Anti-Submarine Warfare-A Digital Twin and Random Finite Sets Based Approach. *Entropy*, vol. 21(8), 767. <https://doi.org/10.3390/e21080767>.
- [50] Krumwiede, C., 2022. How Digital Twins are Completely Transforming Manufacturing. *LaptrinhX*. <https://laptrinhx.com/how-digital-twins-are-completely-transforming-manufacturing-3526002537/> (accessed 15 September 2022).
- [51] Srail, J., Settanni, E., Tsolakis, N., Aulakh, P., 2019. Supply Chain Digital Twins: Opportunities and Challenges Beyond the Hype. *23rd Cambridge International Manufacturing Symposium 2019*. <https://doi.org/10.17863/CAM.45897>.
- [52] Qi, Q., Tao, F., Hu, T., Anwer, N., Liu, A., Wei, Y., Wang, L., Nee, A.Y.C., 2021. Enabling technologies and tools for digital twin. *Journal of Manufacturing Systems* 58:3–21. <https://doi.org/10.1016/j.jmsy.2019.10.001>.
- [53] Juarez, M.G., Botti, V.J., Giret, A.S., 2021. Digital Twins: Review and Challenges. *Journal of Computing and Information Science in Engineering* 21. <https://doi.org/10.1115/1.4050244>.
- [54] Joshi, R., Didier, P., Jimenez, J., Carey, T., 2017. The Industrial Internet of Things Volume G5: Connectivity Framework, Technical Report IIC:PUB:G5:V1.01:PB:20180228. *Industrial Internet Consortium*. https://www.iiconsortium.org/pdf/IIC_PUB_G5_V1.0_PB_20170228.pdf (accessed 13 October 2022).

References

- [55] Booney, M., Wagg, D., Borgo, M. D., de Angelis, M., 2021. Digital Twin Operational Platform for Connectivity and Accessibility using Flask Python. Proceedings of the 24th International Conference on Model-Driven Engineering Languages and Systems: MODELS 2021. 237-241. Fukuoka, Japan. <https://doi.org/10.1109/MODELS-C53483.2021>.
- [56] Onile, A.E., Machlev, R., Petlenkov, E., Levron, Y., Belikov, J., 2021. Uses of the digital twins concept for energy services, intelligent recommendation systems, and demand side management: A review. Energy Reports 7:997–1015. <https://doi.org/10.1016/j.egy.2021.01.090>.
- [57] Qi, Q., Tao, F., 2018. Digital Twin and Big Data Towards Smart Manufacturing and Industry 4.0: 360 Degree Comparison. IEEE Access 6:3585–3593. <https://doi.org/10.1109/ACCESS.2018.2793265>.
- [58] Liu, Q., Liu, B., Wang, G., Zhang, C., 2019. A comparative study on digital twin models. AIP Conference Proceedings 2073, 020091-1–020091-6. <https://doi.org/10.1063/1.5090745>.
- [59] Güntner, G., Hoher, S., Eberle, M., Glachs, D., Kranzer, S., Schäfer, G., Schranz, C., 2020. Digital Twins im Anlagen-Lebenszyklus. Digitales Transferzentrum Salzburg, https://www.salzburgresearch.at/wp-content/uploads/2020/09/Digital_Twin_WP-final-1.pdf (accessed 13 October 2022).
- [60] Uhlenkamp, J.-F., Hribernik, K. A., Wellsandt, S., Thoben, K.-D., 2019. Digital Twin Applications: A first systemization of their dimensions. IEEE International Conference on Engineering, Technology and Innovation (ICE/ITMC) 2019:1-8. <https://doi.org/10.1109/ICE.2019.8792579>.
- [61] Singh, M., Fuenmayor, E., Hinchy, E.P., Qiao, Y., Murray, N., Devine, D., 2021. Digital Twin: Origin to Future. Applied System Innovation 4:36. <https://doi.org/10.3390/asi4020036>.
- [62] Jones, D., Snider, C., Nassehi, A., Yon, J., Hicks, B., 2020. Characterising the Digital Twin: A systematic literature review. CIRP Journal of Manufacturing Science and Technology 29:36–52. <https://doi.org/10.1016/j.cirpj.2020.02.002>.
- [63] Pires, F., Cachada, A., Barbosa, J., Moreira, A., Leitão, P., 2019. Digital Twin in Industry 4.0: Technologies, Applications and Challenges. IEEE 17th International Conference on Industrial Informatics (INDIN) 2019:721-726. <https://doi.org/10.1109/INDIN41052.2019.8972134>.
- [64] Schweichhart, K., 2016. Reference Architectural Model Industrie 4.0 (RAMI 4.0). Plattform Industrie 4.0. https://ec.europa.eu/futurium/en/system/files/ged/a2-schweichhart-reference_architectural_model_industrie_4.0_rami_4.0.pdf (accessed 9 August 2023).
- [65] International Electrotechnical Commission, 2020. IEC 62264: Enterprise-control system integration. <https://webstore.iec.ch/publication/59706> (accessed 13 October 2022).
- [66] Bolton, A., Blackwell, B., Dabson, I., Enzer, M., Evans, M., Fenemore, T., Harradence, F., Keaney, E., Kemp, A., Luck, A., Pawsey, N., Saville, S., Schooling, J., Sharp, M., Smith, T., Tennison, J., Whyte, J., Wilson, A., 2018. The Gemini Principles: Guiding values for the national digital twin and information management framework. Centre for Digital Built Britain, Cambridge. <https://doi.org/10.17863/CAM.32260>.
- [67] Schleich, B., Anwer, N., Mathieu, L., Wartzack, S., 2017. Shaping the digital twin for design and production engineering. CIRP Annals 66:141–144. <https://doi.org/10.1016/j.cirp.2017.04.040>.
- [68] Harmsen, J., 2019. Industrial process scale-up: A practical innovation guide from idea to commercial implementation, 2nd edition, Elsevier, Amsterdam. <https://doi.org/10.1016/C2018-0-00308-4>.
- [69] AUVA, 2017. Explosionsschutz – Sicherheitsinformation für Führungskräfte. Merkblatt, Vienna. <https://www.auva.at/cdscontent/load?contentid=10008.647857&version=1519986334> (accessed 13 October 2022).
- [70] International Electrotechnical Commission, 2011. IEC 61508: Functional safety of electrical/electronic/programmable electronic safety-related systems. <https://webstore.iec.ch/publication/5515> (accessed 13 October 2022).

References

- [71] Sinnott, R., Towler, G., 2020. Chemical engineering design. 6th edition. Coulson & Richardson's chemical engineering series. Butterworth-Heinemann an imprint of Elsevier, Kidlington, Oxford. ISBN: 9780081026007.
- [72] ROI-EFESO Management Consulting AG, 2021. Measurement and evaluation of the digitization maturity levels (IoT Scan) and roadmap. <https://www.roi-international.com/management-consulting/competences/increased-efficiency-through-digitisation-industry-40/digitization-maturity-levels> (accessed 30 December 2021).
- [73] Lamb, K., 2019. Principle-based digital twins: a scoping review. Centre for Digital Built Britain, Cambridge. <https://doi.org/10.17863/CAM.47094>.
- [74] Stark, R., Fresemann, C., Lindow, K., 2019. Development and operation of Digital Twins for technical systems and services. *CIRP Annals – Manufacturing Technology* 68:129–132. <https://doi.org/10.1016/j.cirp.2019.04.024>.
- [75] European Commission, 1992. Information Technology Security Evaluation Criteria (ITSEC) – Provisional harmonized criteria. Directorate-General for the Information Society and Media, Document COM(90) 314. Office for Official Publications of the European Communities. ISBN: 92-826-3004-8.
- [76] Department of Defense Computer Security Center, 1985. Department of Defense Trusted Computer System Evaluation Criteria: Orange Book. <https://csrc.nist.gov/csrc/media/publications/conference-paper/1998/10/08/proceedings-of-the-21st-nissc-998/documents/early-cs-papers/dod85.pdf> (accessed 13 October 2022).
- [77] Common Criteria Editorial Board, 2006. Common Criteria for Information Technology Security Evaluation. CCMB-2006-09-001. <https://www.commoncriteriaportal.org/files/ccfiles/CCPART1V3.1R1.pdf> (accessed 13 October 2022).
- [78] Sharma, A., Kosasih, E., Zhang, J., Brintrup, A., Calinescu, A., 2022. Digital Twins: State of the art theory and practice, challenges, and open research questions. *Journal of Industrial Information Integration* 30:100383. <https://doi.org/10.1016/j.jii.2022.100383>.
- [79] Müller, S., 2022. Energy Technology Development for Industrial Application: Modelling-based development of processes enabling reduced fossil carbon dioxide emissions by advanced digital methods. Habilitationsschrift, TU Wien, Institute of Chemical, Environmental and Bioscience Engineering, Vienna.
- [80] Héder, M., 2017. From NASA to EU: the evolution of the TRL scale in Public Sector Innovation. *The Innovation Journal: The Public Sector Innovation Journal* 22:3. https://www.innovation.cc/discussion-papers/2017_22_2_3_heder_nasa-to-eu-trl-scale.pdf (accessed 13 October 2022).
- [81] DIN e.V., 2021. DIN EN ISO 14040:2021-02, Umweltmanagement – Ökobilanz - Grundsätze und Rahmenbedingungen (ISO 14040:2006 + Amd 1:2020). Deutsche Fassung EN ISO 14040:2006 + A1:2020, Beuth Verlag. <https://dx.doi.org/10.31030/3179655>.
- [82] DIN e.V., 2021. DIN EN ISO 14044:2021-02, Umweltmanagement – Ökobilanz - Anforderungen und Anleitungen (ISO 14044:2006 + Amd 1:2017 + Amd 2:2020). Deutsche Fassung EN ISO 14044:2006 + A1:2018 + A2:2020, Beuth Verlag. <https://dx.doi.org/10.31030/3179656>.
- [83] Bartik, A., Benedikt, F., Lunzer, A., Walcher, C., Müller, S., Hofbauer, H., 2021. Thermodynamic investigation of SNG production based on dual fluidized bed gasification of biogenic residues. *Biomass Conversion and Biorefinery* 11:95–110. <https://doi.org/10.1007/s13399-020-00910-y>.
- [84] Hofbauer, H., 2018. Bewertung von Energiebereitstellungssystemen. Lecture notes LVA 159.830 Brennstoff- und Energietechnologie, TU Wien, Institute of Chemical, Environmental and Bioscience Engineering, Vienna.
- [85] Pröll, T., 2004. Potenziale der Wirbelschichtdampfvergasung fester Biomasse - Modellierung und Simulation auf Basis der Betriebserfahrungen am Biomassekraftwerk Güssing. Dissertation, TU Wien, Institute of Chemical, Environmental and Bioscience Engineering, Vienna.

References

- [86] Kost, C., Shammugam, S., Jülch, V., Nguyen, H.-T., Schlegl, T., 2018. Stromgestehungskosten erneuerbare Energien, Fraunhofer-Institut für solare Energiesysteme (ISE), Freiburg. https://www.ise.fraunhofer.de/content/dam/ise/de/documents/publications/studies/DE2018_ISE_Studie_Stromgestehungskosten_Erneuerbare_Energien.pdf (accessed 13 October 2022).
- [87] Bardos, R. P., Thomas, H. F., Smith, J. W. N., Harries, N. D., Evans, F., Boyle, R., Howard, T., Lewis, R., Thomas, A. O., Dent, V. L., Haslam, A., 2020. Sustainability assessment framework and indicators developed by SuRF-UK for land remediation option appraisal. *Remediation* 31:5–27. <https://doi.org/10.1002/rem.21668>.
- [88] TEPPFA, 2020, Life Cycle Assessment: Polypropylene (PP-r) pipe systems vs. copper environmental impact comparison. Technical report, Brussels. https://www.teppfa.eu/wp-content/uploads/LCA16_HC-Leaflet-PP-r-vs-Cu.pdf (accessed 13 October 2022).
- [89] Koch, D., Paul, M., Beisl, S., Friedl, A., Mihalyi, B., 2020. Life cycle assessment of a lignin nanoparticle biorefinery: Decision support for its process development. *Journal of Cleaner Production* 245:118760. <https://doi.org/10.1016/j.jclepro.2019.118760>.
- [90] Bauer, C., Hofer, J., Althaus, H.-J., Del Duce, A., Simons, A., 2015. The environmental performance of current and future passenger vehicles: Life cycle assessment based on a novel scenario analysis framework. *Applied Energy* 157:871–883. <https://doi.org/10.1016/j.apenergy.2015.01.019>.
- [91] Wulf, C., Kaltschmitt, M., 2018. Hydrogen Supply Chains for Mobility - Environmental and Economic Assessment. *Sustainability* 10:1699. <https://doi.org/10.3390/su10061699>.
- [92] Dreyer, L. C., Niemann, A. L., Hauschild, M. Z., 2003. Comparison of Three Different LCIA Methods: EDIP97, CML2001 and Eco-indicator 99. *International Journal of Life Cycle Assessment* 8:191–200. <https://doi.org/10.1007/BF02978471>.
- [93] Rosenfeld, D. C., Lindorfer, J., Fazeni-Fraisl, K., 2019. Comparison of advanced fuels - Which technology can win from the life cycle perspective?. *Journal of Cleaner Production* 238:117879. <https://doi.org/10.1016/j.jclepro.2019.117879>.
- [94] van Zelm, R., Preiss, P., van Goethem, T., Van Dingenen, R., Huijbregts, M., 2016. Regionalized life cycle impact assessment of air pollution on the global scale: Damage to human health and vegetation. *Atmospheric Environment* 134:129–137. <https://doi.org/10.1016/j.atmosenv.2016.03.044>.
- [95] Sphera, 2022. GaBi Software with Built-In Database (DB). Chicago. <https://gabi.sphera.com/austria/index/> (accessed 13 October 2022).
- [96] Mauerhofer, A. M., Müller, S., Bartik, A., Benedikt, F., Fuchs, J., Hammerschmid, M., Hofbauer, H., 2021. Conversion of CO₂ during the DFB biomass gasification process. *Biomass Conversion and Biorefinery* 11:15–27. <https://doi.org/10.1007/s13399-020-00822-x>.
- [97] Mauerhofer, A. M., 2020. Carbon Utilization by Application of CO₂ Gasification. Dissertation, TU Wien, Institute of Chemical, Environmental and Bioscience Engineering, Vienna.
- [98] Hammerschmid, M., Müller, S., Fuchs, J., Hofbauer, H., 2021. Evaluation of biomass-based production of below zero emission reducing gas for the iron and steel industry. *Biomass Conversion and Biorefinery* 11:169–187. <https://doi.org/10.1007/s13399-020-00939-z>.
- [99] Brown, D. R., 1994. Levelized production cost. An alternative form of discounted cash flow analysis. *Cost Engineering* 36/8. https://www.researchgate.net/publication/255933212_Levelized_production_cost_An_alternative_form_of_discounted_cash_flow_analysis/citations (accessed 13 October 2022).
- [100] Hofbauer, H., Mauerhofer, A., Benedikt, F., Hammerschmid, M., Bartik, A., Veress, M., Haas, R., Siebenhofer, M., Resch, G., 2020. Reallabor zur Herstellung von HolzdieSEL und Holzgas aus Biomasse und biogenen Reststoffen für die Land- und Forstwirtschaft. Technical report, TU Wien, Institute of Chemical, Environmental and Bioscience Engineering, Vienna. <https://dafne.at/projekte/ftsng-reallabor> (accessed 13 October 2022).

References

- [101] Brennan, D. J., 2020. Process industry economics: Principles, concepts and applications. 2nd edition, Elsevier, San Diego. ISBN: 9780128194669.
- [102] Piazzzi, S., Zhang, X., Patuzzi, F., Baratieri, M., 2020. Techno-economic assessment of turning gasification-based waste char into energy: A case study in South-Tyrol. *Waste Management* 105:550–559. <https://doi.org/10.1016/j.wasman.2020.02.038>.
- [103] Goers, S., Baresch, M., Tichler, R., Schneider, F., 2015. MOVE2 – Simulation model of the (Upper) Austrian economy with a special focus on energy including the socio-economic module MOVE2social: integration of income, age and gender. Technical Report, Energieinstitut an der Johannes-Kepler-Universität Linz. Linz. https://energieinstitut-linz.at/wp-content/uploads/2016/06/Macroeconomic-Simulation-Tool-MOVE2_MOVE2social_1.pdf (accessed 13 October 2022).
- [104] Hammerschmid, M., Aguiari, C., Kirnbauer, F., Zerobin, E., Brenner, M., Eisl, R., Nemeth, J., Buchberger, D., Ogris, G., Kolroser, R., Goia, A., Beyweiss, R., Kalch, K., Müller, S., Hofbauer, H., 2023. Thermal Twin 4.0: Digital Support Tool for Optimizing Hazardous Waste Rotary Kiln Incineration Plants. *Waste and Biomass Valorization* 2023. <https://doi.org/10.1007/s12649-022-02028-w>.
- [105] Benedikt, F., Schmid, J.C., Fuchs, J., Mauerhofer, A.M., Müller, S., Hofbauer, H., 2018. Fuel flexible gasification with an advanced 100 kW dual fluidized bed steam gasification pilot plant. *Energy* 164:329–343. <https://doi.org/10.1016/j.energy.2018.08.146>.
- [106] Schmid, J.C., Benedikt, F., Fuchs, J., Mauerhofer, A.M., Müller, S., Hofbauer, H., 2021. Syngas for biorefineries from thermochemical gasification of lignocellulosic fuels and residues—5 years' experience with an advanced dual fluidized bed gasifier design. *Biomass Conversion and Biorefinery* 11:2405–2442. <https://doi.org/10.1007/s13399-019-00486-2>.
- [107] Fuchs, J., Schmid, J.C., Müller, S., Hofbauer, H., 2019. Dual fluidized bed gasification of biomass with selective carbon dioxide removal and limestone as bed material: A review. *Renewable and Sustainable Energy Reviews* 107:212–231. <https://doi.org/10.1016/j.rser.2019.03.013>.
- [108] Schweitzer, D., Beirrow, M., Gredinger, A., Armbrust, N., Waizmann, G., Dieter, H., Scheffknecht, G., 2016. Pilot-Scale Demonstration of Oxy-SER steam Gasification: Production of Syngas with Pre-Combustion CO₂ Capture. *Energy Procedia* 86:56–68. <https://doi.org/10.1016/j.egypro.2016.01.007>.
- [109] Gruber, H., Groß, P., Rauch, R., Reichhold, A., Zweiler, R., Aichernig, C., Müller, S., Ataimisch, N., Hofbauer, H., 2019. Fischer-Tropsch products from biomass-derived syngas and renewable hydrogen. *Biomass Conversion and Biorefinery* 48:22. <https://doi.org/10.1007/s13399-019-00459-5>.
- [110] Gruber, H., 2020. Synthesis and Refining of Biomass-Derived Fischer-Tropsch Paraffin Waxes. PhD Thesis, TU Wien, Vienna, Austria.
- [111] Guilera, J., Díaz-López, J.A., Berenguer, A., Biset-Peiró, M., Andreu, T., 2022. Fischer-Tropsch synthesis: Towards a high-ly-selective catalyst by lanthanide promotion under relevant CO₂ syngas mixtures. *Applied Catalysis A: General* 629:118423. <https://doi.org/10.1016/j.apcata.2021.118423>.
- [112] Hammerschmid, M., Bartik, A., Benedikt, F., Veress, M., Pratschner, S., Müller, S., Hofbauer, H., 2023. Economic and ecological impacts on the integration of biomass-based SNG and FT diesel in the Austrian energy system. *Energies* 16:6097. <https://doi.org/10.3390/en16166097>.
- [113] Müller, S., Groß, P., Rauch, R., Zweiler, R., Aichernig, C., Fuchs, M., Hofbauer, H., 2018. Production of diesel from biomass and wind power – Energy storage by the use of the Fischer-Tropsch process. *Biomass Conversion and Biorefinery* 8:275–282. <https://doi.org/10.1007/s13399-017-0287-1>.
- [114] Pratschner, S., Hammerschmid, M., Müller, F.J., Müller, S., Winter, F., 2022. Simulation of a Pilot Scale Power-to-Liquid Plant Producing Synthetic Fuel and Wax by Combining Fischer-Tropsch Synthesis and SOEC. *Energies* 15:4134. <https://doi.org/10.3390/en15114134>.

- [115] Pratschner, S., Hammerschmid, M., Müller, S., Winter, F., 2023. Evaluation of CO₂ sources for Power-to-Liquid plants producing Fischer-Tropsch products. *Journal of CO₂ Utilization*, vol. 72, 102508. <https://doi.org/10.1016/j.jcou.2023.102508>.
- [116] Kaltschmitt, M., Hartmann, H., Hofbauer, H., 2016. *Energie aus Biomasse: Grundlagen, Techniken und Verfahren*, 3rd edition, Springer Vieweg, Berlin, Heidelberg. <https://doi.org/10.1007/978-3-662-47438-9>.
- [117] Schwarzböck, T., Rechberger, H., Cencic, O., Fellner, J., 2016. Anteil erneuerbarer Energien und klimarelevante CO₂-Emissionen aus der thermischen Verwertung von Abfällen in Österreich. *Österreichische Wasser- und Abfallwirtschaft*, vol. 68, 415–427. <https://doi.org/10.1007/s00506-016-0332-5>.
- [118] Richers, U., 1995. *Thermische Behandlung von Abfällen in Drehrohröfen - Eine Darstellung anhand der Literatur*. KIT Scientific reports 5548. Institut für Technische Chemie (ITC), Karlsruher Institut für Technologie (KIT), Karlsruhe. ISSN: 0947-8620.
- [119] Hofbauer, H., 2020. *Auslegung von Verbrennungsanlagen: Teil B - Verbrennungsrechnung und Auslegung von Brennräumen*. Lecture notes, Vienna.
- [120] Netz, H., 1991. *Handbuch Wärme: Erläuterungen, Beschreibungen, Definitionen, Richtlinien, Formeln, Tabellen, Diagramme und Abbildungen für alle Bereiche der Wärmetechnik*. 3rd ed., Gräfelfing/München, Resch Verlag. ISBN: 3878060696.
- [121] Ali, S., Sørensen, K., Nielsen, M. P., 2020. Modeling a novel combined solid oxide electrolysis cell (SOEC) - Biomass gasification renewable methanol production system. *Renewable Energy*, vol. 154, 1025–1034. <https://doi.org/10.1016/j.renene.2019.12.108>.
- [122] Shri Prakash, B., Senthil Kumar, S., Aruna, S. T., 2014. Properties and development of Ni/YSZ as an anode material in solid oxide fuel cell: A review. *Renewable and Sustainable Energy Reviews*. vol. 36, 149–179. <https://doi.org/10.1016/j.rser.2014.04.043>.
- [123] Wang, Y., Liu, T., Lei, L., Chen, F., 2017. High temperature solid oxide H₂O/CO₂ co-electrolysis for syngas production. *Fuel Processing Technology*, vol. 161, 248-258. <https://doi.org/10.1016/j.fuproc.2016.08.009>.
- [124] Schmidt, O., Gambhir, A., Staffell, I., Hawkes, A., Nelson, J., Few, S., 2017. Future cost and performance of water electrolysis: An expert elicitation study. *International Journal of Hydrogen Energy*, vol. 42(52), 30470-30492. <https://doi.org/10.1016/j.ijhydene.2017.10.045>.
- [125] Cinti, G., Discepoli, G., Bidini, G., Lanzini, A., Santarelli, M., 2016. Co-electrolysis of water and CO₂ in a solid oxide electrolyzer (SOE) stack. *International Journal of Energy Research*, vol. 40(2), 207-215. <https://doi.org/10.1002/er.3450>.
- [126] Fu, Q., Mabilat, C., Zahid, M., Brisse, A., Gautier, L., 2010. Syngas production via high-temperature steam/CO₂ co-electrolysis: an economic assessment. *Energy & Environmental Science*, vol. 3(10), 1382-1397. <https://doi.org/10.1039/C0EE00092B>.
- [127] Bakosch, C., 2021. *Automatisierung des Basic Engineering einer Produktgasaufbereitungsstrecke für die weitere Verwertung*. Master Thesis, Institut für Verfahrenstechnik, Umwelttechnik und technische Biowissenschaften, TU Wien. Vienna.
- [128] Schubert, H., 2002. *Handbuch der Mechanischen Verfahrenstechnik*. Wiley-VCH, Weinheim. ISBN: 978-3-527-30577-3.
- [129] Mauschwitz, G., 2018. *Staubabscheiden*. Lecture notes LVA 166.170, TU Wien, Institute of Chemical, Environmental and Bioscience Engineering, Vienna.
- [130] Intensiv Filter GmbH, 2020. *Know-How : Das große Intensiv-Filter Lexikon der Entstaubung*. Velbert-Langenberg. https://www.intensiv-filter.com/fileadmin/user_upload/downloads/Lexikon_der_Entstaubung_Intensiv-Filter.pdf (accessed 16 June 2023).
- [131] Bardolf, R., 2017. *Optimierung eines Produktgaswäschers bei der Biomassedampfvergasung im Zweibettwirbelschichtverfahren*. PhD Thesis, TU Wien, Vienna, Austria.

References

- [132] Schöny, G., Dietrich, F., Fuchs, J., Pröll, T., Hofbauer, H., 2017. A multi-stage fluidized bed system for continuous CO₂ capture by means of temperature swing adsorption - First results from bench scale experiments. *Powder Technology*, vol. 316, 519-527. <https://doi.org/10.1016/j.powtec.2016.11.066>.
- [133] Stephan, P., Kabelac, S., Kind, M., Mewes, D., Schaber, K., Wetzel, T.: *VDI-Wärmeatlas: Fachlicher Träger VDI-Gesellschaft Verfahrenstechnik und Chemieingenieurwesen*, 12th ed., Springer Vieweg, Berlin (2019).
- [134] Hofbauer, H., 2018. Konventionelle Stromerzeugung und Kraft/Wärme-Kopplung (Wärmekraftanlagen). Lecture notes LVA 159.830 Brennstoff- und Energietechnologie, TU Wien, Institute of Chemical, Environmental and Bioscience Engineering, Vienna.
- [135] Bartik, A., Benedikt, F., Fuchs, J., Hofbauer, H., Müller, S., 2023. Experimental investigation of hydrogen-intensified synthetic natural gas production via biomass gasification: a technical comparison of different production pathways. *Biomass Conversion and Biorefinery*. <https://doi.org/10.1007/s13399-023-04341-3>.
- [136] Bartik, A., Fuchs, J., Pacholik, G., Föttinger, K., Hofbauer, H., Müller, S., Benedikt, F., 2022. Experimental investigation on the methanation of hydrogen-rich syngas in a bubbling fluidized bed reactor utilizing an optimized catalyst. *Fuel Processing Technology* 237:107402. <https://doi.org/10.1016/j.fuproc.2022.107402>.
- [137] Österreichische Vereinigung für das Gas- und Wasserfach, 2021. Richtlinie G B210 - Gasbeschaffenheit: Gas quality. Vienna, Austria. https://shop.austrian-standards.at/action/default/public/details/697809/OEVGW_G_B210_2021_06 (accessed 2 July 2023).
- [138] Rehling, B., 2012. Development of the 1 MW Bio-SNG plant, evaluation on technological and economical aspects and upscaling considerations. PhD Thesis, TU Wien, Vienna, Austria.
- [139] Beuth Verlag, 2019. DIN EN 15940: Kraftstoffe - Paraffinischer Dieselkraftstoff aus Synthese oder Hydrierungsverfahren - Anforderungen und Prüfverfahren. Berlin, Germany. <https://www.beuth.de/de/norm/din-en-15940/309170058> (2 July 2023).
- [140] de Klerk, A., 2009. Can Fischer-Tropsch Syncrude Be Refined to On-Specification Diesel Fuel? *Energy Fuels* 23(9):4593–4604. <https://doi.org/10.1021/ef9005884>.
- [141] de Klerk, A., 2011. Fischer-Tropsch Refining. Wiley-VCH Verlag GmbH & Co. KGaA, Weinheim, Germany. ISBN: 9783527635603.
- [142] Schädel, B.T., Duisberg, M., Deutschmann, O., 2009. Steam reforming of methane, ethane, propane, butane, and natural gas over a rhodium-based catalyst. *Catalysis Today* 142:42–51. <https://doi.org/10.1016/j.cattod.2009.01.008>.
- [143] Kang, J., Ma, W., Keogh, R.A., Shafer, W.D., Jacobs, G., Davis, B.H., 2012. Hydrocracking and Hydroisomerization of n-Hexadecane, n-Octacosane and Fischer-Tropsch Wax Over a Pt/SiO₂-Al₂O₃ Catalyst. *Catalysis Letters* 142:1295–1305. <https://doi.org/10.1007/s10562-012-0910-5>.
- [144] Petersen, A.M., Chireshe, F., Okoro, O., Gorgens, J., van Dyk, J., 2021. Evaluating refinery configurations for deriving sustainable aviation fuel from ethanol or syncrude. *Fuel Processing Technology* 219:106879. <https://doi.org/10.1016/j.fuproc.2021.106879>.
- [145] Fahim, M.A., 2010. *Fundamentals of Petroleum Refining*. Elsevier Science & Technology, Oxford, England. ISBN: 978-0-444-52785-1.
- [146] Schablitzky, H. W., Lichtscheidl, J., Hutter, K., Hafner, C., Rauch, R., Hofbauer, H., 2011. Hydroprocessing of Fischer-Tropsch biowaxes to second-generation biofuels. *Biomass Conversion and Biorefinery*, vol. 1(1), 29-37. <https://doi.org/10.1007/s13399-010-0003-x>.
- [147] Busca, G., 2014. *Heterogeneous Catalytic Materials*. Elsevier, Amsterdam, Netherlands. ISBN: 978-0-444-59524-9.
- [148] Murali, C., Voolapalli, R.K., Ravichander, N., Gokak, D.T., Choudary, N.V., 2007. Trickle bed reactor model to simulate the performance of commercial diesel hydrotreating unit. *Fuel* 86:1176–1184. <https://doi.org/10.1016/j.fuel.2006.09.019>.

- [149] Pröll, T., 2020. Applied modelling in process engineering and energy technology. Lecture notes LVA 166.198, TU Wien, Institute of Chemical, Environmental and Bioscience Engineering, Vienna.
- [150] Helal, S., Hammer, J., Zhang, J., Khushraj, A., 2001. A three-tier architecture for ubiquitous data access. Proceedings ACS/IEEE International Conference on Computer Systems and Applications AICCSA 2001:177–180. <https://doi.org/10.1109/AICCSA.2001.933971>.
- [151] Heidrich, M., Luo, J. J., 2016. Industrial Internet of Things: Referenzarchitektur für die Kommunikation. Whitepaper, Fraunhofer-Institut für eingebettete Systeme und Kommunikationstechnik ESK, München. <https://www.iks.fraunhofer.de/content/dam/iks/documents/whitepaper-iiot.pdf> (accessed 13 October 2022).
- [152] Ala-Laurinaho, R., 2019. Sensor data transmission from a physical twin to a digital twin. Master Thesis, Aalto University, School of Engineering, Aalto. https://www.researchgate.net/publication/343474433_Sensor_Data_Transmission_from_a_Physical_Twin_to_a_Digital_Twin (accessed 13 October 2022).
- [153] Liu, Q., Chen, J., Liao, Y., Mueller, E., Jentsch, D., Boerner, F., She, M., 2015. An Application of Horizontal and Vertical Integration in Cyber-Physical Production Systems. Proceedings of the 2015 International Conference on Cyber-Enabled Distributed Computing and Knowledge Discovery 110–113. <https://doi.org/10.1109/CyberC.2015.22>.
- [154] Förtsch, D., Pabst, K., Groß-Hardt, E., 2015. The product distribution in Fischer-Tropsch synthesis: An extension of the ASF model to describe common deviations. Chemical Engineering Science 138:333–346. <https://doi.org/10.1016/j.ces.2015.07.005>.
- [155] Pratschner, S., Hammerschmid, M., Müller, S., Winter, F., 2023. CO₂ Footprint of Fischer-Tropsch Products produced by a Power-to-Liquid Plant. Proceedings 15th Mediterranean Congress of Chemical Engineering - MECCE 2023 at 30. May - 2. June 2023. Barcelona, Spain.
- [156] Pratschner, S., Hammerschmid, M., Müller, S., Winter, F., 2023. Converting CO₂ and H₂O into Fischer-Tropsch Products - A Techno-economic assessment. Proceedings 27th International Symposium for Chemical Reaction Engineering - ISCRE 27 at 11.-14. June 2023. Quebec City, Canada.
- [157] Pröll, T., Hofbauer, H., 2008. Development and Application of a Simulation Tool for Biomass Gasification Based Processes. International Journal of Chemical Reactor Engineering 6:A89. <https://doi.org/10.2202/1542-6580.1769>.
- [158] Jankovic, S., Hammerschmid, M., Müller, S., 2023. Design of a digital twin for a pilot plant for synthetic natural gas production. 7th Central European Biomass Conference - CEBC 2023, 18.-20. January 2023, Graz, Austria.
- [159] Stanger, L., Schirrer, A., Benedikt, F., Bartik, A., Jankovic, S., Müller, S., Kozek, M., 2023. Dynamic modeling of dual fluidized bed steam gasification for control design. Energy 265:126378. <https://doi.org/10.1016/j.energy.2022.126378>.
- [160] Stanger, L., Benedikt, F., Bartik, A., Jankovic, S., Hammerschmid, M., Müller, S., Schirrer, A., Jakubek, S., Kozek, M., 2023. Model predictive control of a dual fluidized bed gasification plant. Applied Energy, not published, currently under review (accessed 15 December 2023).
- [161] Grossgasteiger, L., 2022. Dynamic modeling and control of a fluidized bed methanation reactor. Master Thesis, Institut für Mechanik und Mechatronik, TU Wien. Vienna.
- [162] Jankovic, S., Hammerschmid, M., Stanger, L., Bartik, A., Benedikt, F., Müller, S., 2023. Implementation of a Digital Twin for a Pilot Plant for Synthetic Natural Gas Production from Biomass. 31st European Biomass Conference & Exhibition, Bologna, Italy, 05.-09.06.2023.
- [163] Hammerschmid, M., Kilian, M., Kirnbauer, F., Aguiari, C., Pachler, R., Zerobin, E., Brenner, M., Eisl, R., Nemeth, J., Buchberger, D., Strohmayer, N., Rezaeifar, Z., Fraundorfer, L., Matkovich, S., Ogris, G., Kolroser, R., Beyweiss, R., Kalch, K., Dittmer, V., Hopp, M., El Aeraky, S., Linder, P., Adam, L., Müller, S., Hofbauer, H., 2023. Final report Thermal Twin 4.0. Vienna.

- [164] Hammerschmid, M., Konrad, J., Werner, A., Popov, T., Müller, S., 2022. ENECO₂Calc—A Modeling Tool for the Investigation of Energy Transition Paths toward Climate Neutrality within Municipalities. *Energies* 15:7162. <https://doi.org/10.3390/en15197162>.
- [165] Bécue, A., Maia, E., Feeken, L., Borchers, P., Praça, I., 2020. A New Concept of Digital Twin Supporting Optimization and Resilience of Factories of the Future *Applied Sciences* 10(13): 4482. <https://doi.org/10.3390/app10134482>.
- [166] Lu, Y., Liu, C., Wang, K. I.-K., Huang, H., Xu, X., 2020. Digital Twin-driven smart manufacturing: Connotation, reference model, applications and research issues. *Robotics and Computer-Integrated Manufacturing* 61:101837. <https://doi.org/10.1016/j.rcim.2019.101837>.
- [167] Marchese, M., Giglio, E., Santarelli, M., Lanzini, A., 2020. Energy performance of Power-to-Liquid applications integrating biogas upgrading, reverse water gas shift, solid oxide electrolysis and Fischer-Tropsch technologies. *Energy Conversion and Management: X*, vol. 6. 100041. <https://doi.org/10.1016/j.ecmx.2020.100041>.
- [168] Gao, R., Zhang, C., Jun, K.-W., Kim, S. K., Park, H.-G., Zhao, T., Wang, L., Wan, H., Guan, G., 2021. Green liquid fuel and synthetic natural gas production via CO₂ hydrogenation combined with reverse water-gas-shift and Co-based Fischer-Tropsch synthesis. *Journal of CO₂ Utilization*, vol. 51. 101619. <https://doi.org/10.1016/j.jcou.2021.101619>.
- [169] Cinti, G., Baldinelli, A., Di Michele, A., Desideri, U., 2016. Integration of Solid Oxide Electrolyzer and Fischer-Tropsch: A sustainable pathway for synthetic fuel. *Applied Energy*, vol. 162, 308-320. <https://doi.org/10.1016/j.apenergy.2015.10.053>.
- [170] Becker, W. L., Braun, R. J., Penev, M., Melaina, M., 2012. Production of Fischer-Tropsch liquid fuels from high temperature solid oxide co-electrolysis units. *Energy*, vol. 47(1). 99-115. <https://doi.org/10.1016/j.energy.2012.08.047>.
- [171] Müller, S., 2013. Hydrogen from Biomass for Industry - Industrial Application of Hydrogen Production Based on Dual Fluid Gasification. PhD Thesis, TU Wien, Vienna, Austria.
- [172] Fuchs, J., 2021. Process characteristics of sorption enhanced reforming in an advanced gasification system. PhD Thesis, TU Wien, Vienna, Austria.
- [173] Thunman, H., Seemann, M., Berdugo Vilches, T., Maric, J., Pallares, D., Ström, H., Berndes, G., Knutsson, P., Larsson, A., Breitholtz, C., Santos, O., 2018. Advanced biofuel production via gasification - lessons learned from 200 man-years of research activity with Chalmers' research gasifier and the GoBiGas demonstration plant. *Energy Science and Engineering* 6:6–34. <https://doi.org/10.1002/ese3.188>.
- [174] Thunman, H., Gustavsson, C., Larsson, A., Gunnarsson, I., Tengberg, F., 2019. Economic assessment of advanced biofuel production via gasification using cost data from the GoBiGas plant. *Energy Science and Engineering* 7:217–229. <https://doi.org/10.1002/ese3.271>.
- [175] Nigitz, T., Gölles, M., Aichernig, C., Schneider, S., Hofbauer, H., Horn, M., 2020. Increased efficiency of dual fluidized bed plants via a novel control strategy. *Biomass and Bioenergy* 141:105688. <https://doi.org/10.1016/j.biombioe.2020.105688>.
- [176] Lei, Z., Zhou, H., Hu, W., Liu, G.-P., Guan, S., Feng, X., 2022. Toward a Web-Based Digital Twin Thermal Power Plant. *IEEE Trans. Ind. Inf.*, vol. 18, 1716–1725. <https://doi.org/10.1109/TII.2021.3086149>.
- [177] Wajda, A., Brociek, R., Pleszczyński, M., 2022. Optimization of Energy Recovery from Hazardous Waste in a Waste Incineration Plant with the Use of an Application. *Processes*, vol. 10, 462. <https://doi.org/10.3390/pr10030462>.
- [178] Xu, J., Fu, D., Shao, L., Zhang, X., Liu, G., 2021. A Soft Sensor Modeling of Cement Rotary Kiln Temperature Field Based on Model-Driven and Data-Driven Methods. *IEEE Sensors Journal*, vol. 21, 27632–27639. <https://doi.org/10.1109/JSEN.2021.3116937>.

References

- [179] Nolte, M., 2015. Betriebs- und modelltechnische Untersuchungen zur Verbesserung des Gasphasenausbrandes bei der instationären Gebindeverbrennung in einer Rückstandsverbrennungsanlage. PhD Thesis. Institut für Technische Chemie (ITC), Karlsruher Institut für Technologie (KIT), Karlsruhe, Germany.
- [180] Guillin-Estrada, W.D., Albuja, R., Davila, I.B., Rueda, B.S., Corredor, L., Gonzalez-Quiroga, A., Maury, H., 2022. Transient operation effects on the thermal and mechanical response of a large-scale rotary kiln. *Results in Engineering*, vol. 14, 100396. <https://doi.org/10.1016/j.rineng.2022.100396>.
- [181] Pirttiniemi, J., 2021. Development of design process of rotary kiln. Diploma thesis. LUT University, Lappeenranta, Finland.
- [182] Neuling, U., Kaltschmitt, M., 2018. Techno-economic and environmental analysis of aviation biofuels. *Fuel Processing Technology* 171:54–69. <https://doi.org/10.1016/j.fuproc.2017.09.022>.
- [183] Jungmeier, G., Canella, L., Pucker-Singer, J., Beermann, M., 2019. Geschätzte Treibhausgasemissionen und Primärenergieverbrauch in der Lebenszyklusanalyse von Pkw-basierten Verkehrssystemen, Graz, Austria.
- [184] Abart-Heriszt, L., Erker, S., Stoeglehner, G., 2019. The Energy Mosaic Austria - A Nationwide Energy and Greenhouse Gas Inventory on Municipal Level as Action Field of Integrated Spatial and Energy Planning. *Energies* 12:3065. <https://doi.org/10.3390/en12163065>.
- [185] Hall, L. M. H., Buckley, A. R., 2016. A review of energy systems models in the UK: Prevalent usage and categorisation. *Applied Energy* 169:607–628. <https://doi.org/10.1016/j.apenergy.2016.02.044>.
- [186] Lopion, P., Markewitz, P., Robinius, M., Stolten, D., 2018. A review of current challenges and trends in energy systems modeling. *Renewable and Sustainable Energy Reviews* 96:156–166. <https://doi.org/10.1016/j.rser.2018.07.045>.
- [187] Pfenninger, S., Hawkes, A., Keirstead, J., 2014. Energy systems modeling for twenty-first century energy challenges. *Renewable and Sustainable Energy Reviews* 33:74–86. <https://doi.org/10.1016/j.rser.2014.02.003>.
- [188] Pfenninger, S., Hirth, L., Schlecht, I., Schmid, E., Wiese, F., Brown, T., Davis, C., Gidden, M., Heinrichs, H., Heuberger, C., Hilpert, S., Krien, U., Matke, C., Nebel, A., Morrison, R., Müller, B., Pleßmann, G., Reeg, M., Richstein, J. C., Shivakumar, A., Staffell, I., Tröndle, T., Wingenbach, C., 2018. Opening the black box of energy modelling: Strategies and lessons learned. *Energy Strategy Reviews* 19:63-71. <https://doi.org/10.1016/j.esr.2017.12.002>.
- [189] Kraemer, P., Niebel, C., Reiberg, A., 2023. Gaia-X und Geschäftsmodelle: Typen und Beispiele: White Paper 1/2023. Gaia-X Hub Germany, München, Germany. <https://gaia-x-hub.de/wp-content/uploads/2023/02/Whitepaper-Gaia-X-Geschaeftsmodelle.pdf> (accessed 9 August 2023).
- [190] van Baten, J., Pons, M., 2014. CAPE-OPEN: Interoperability in Industrial Flowsheet Simulation Software. *Chemie Ingenieur Technik* 86: 1052-1064. <https://doi.org/10.1002/cite.201400009>.
- [191] Gao, H., Koch, C., Wu, Y., 2019. Building information modelling based building energy modelling: A review. *Applied Energy* 238:320–343. <https://doi.org/10.1016/j.apenergy.2019.01.032>.

Appendix

Process and energy flow diagrams

- Process flow diagram of Power-to-Liquid process (Digital Model use-case)
- Process flow diagram of OxySER process (Digital Shadow use-case)
- Process flow diagram of Biomass-to-Gas process (Digital Twin use-case)
- Process flow diagram of hazardous waste incineration plant (Digital Predictive Twin use-case)
- Process flow diagram of the 100 MW_{th} biomass-based FT and SNG routes (Investigation of energy system integration scenarios from energy technology perspective)
- Energy flow diagram of present annual energy demand of St. Margareten im Rosental (Investigation of defossilization scenarios from municipality perspective)

Publications relevant for this doctoral thesis

- Paper I: Novel modelling framework for the development of virtual representations in the process development and Digital Twin use-case of a Biomass-to-Gas production plant
- Paper II: Digital Model use-case of a Power-to-Liquid production plant
- Paper III: Digital Shadow of a zero-emission reducing gas production plant
- Paper IV: Digital Predictive Twin of a hazardous waste incineration plant
- Paper V: Defossilization of the Austrian energy system by the integration of DFB plants
- Paper VI: Defossilization of Austrian municipalities by the integration of RES technologies

Curriculum Vitae Martin Hammerschmid

Appendix

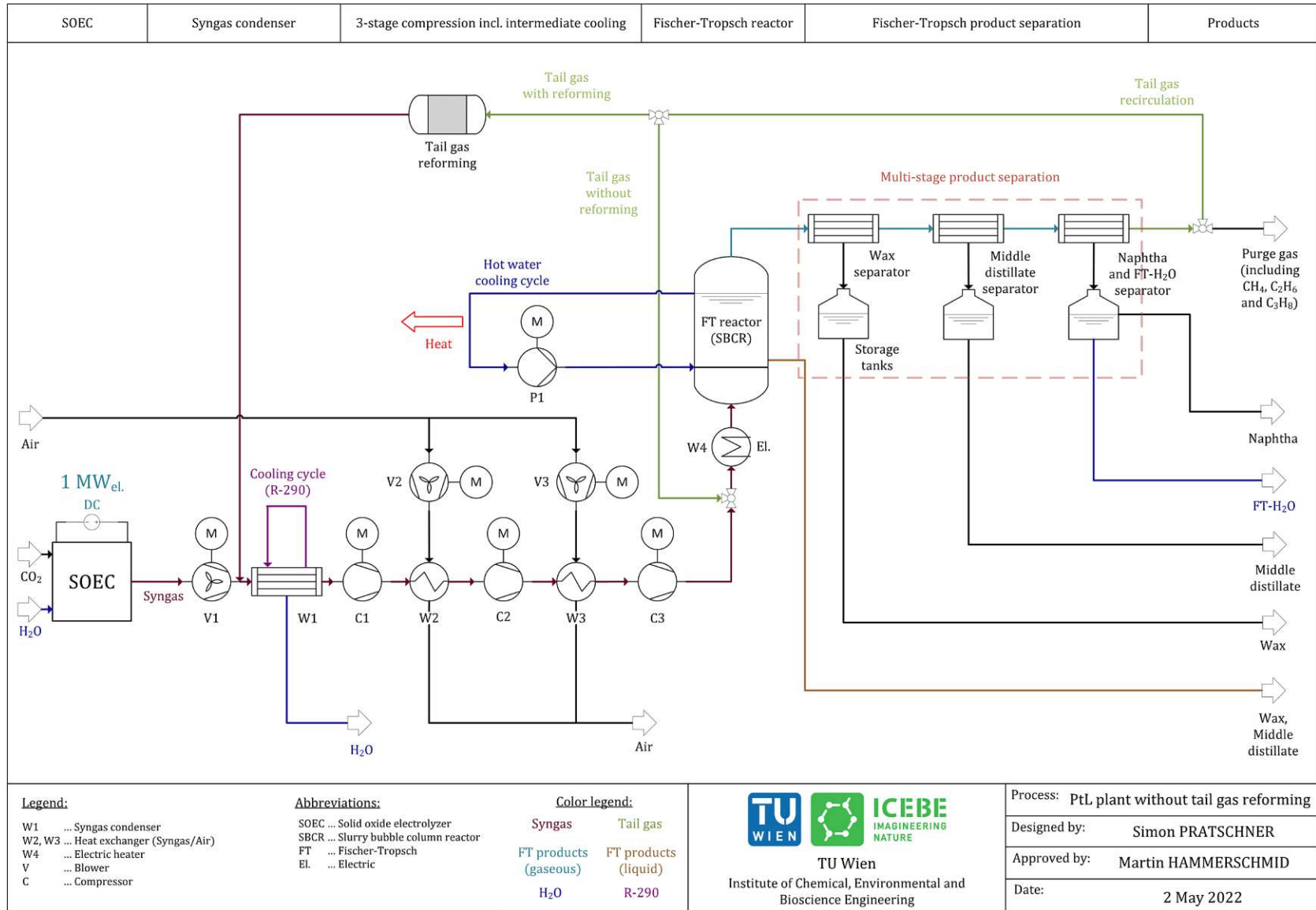


Fig. A1: Process flow diagram of Power-to-Liquid process [114]

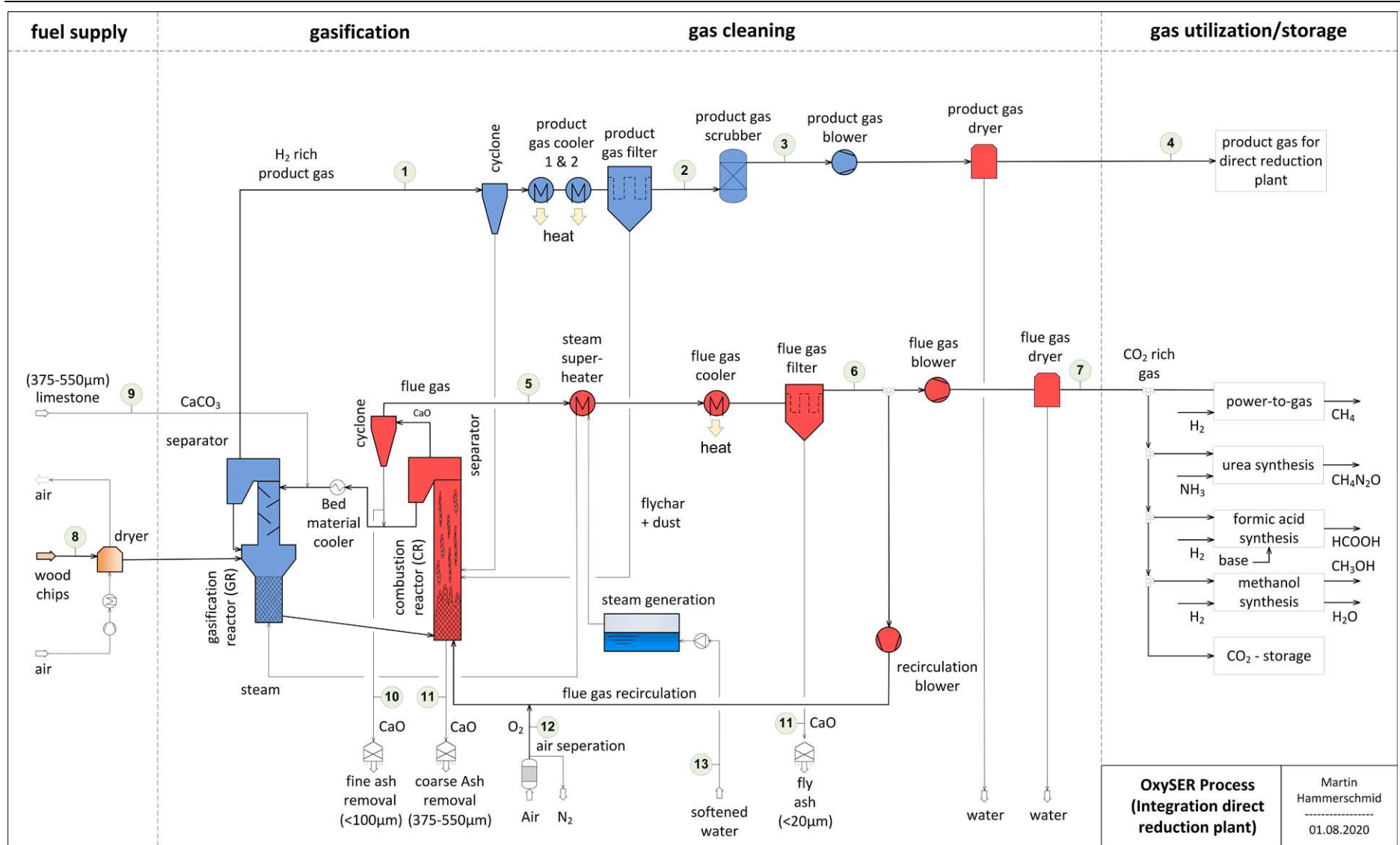


Fig. A2: Process flow diagram of OxySER process for the integration in the direct iron ore reduction plant [98]

Appendix

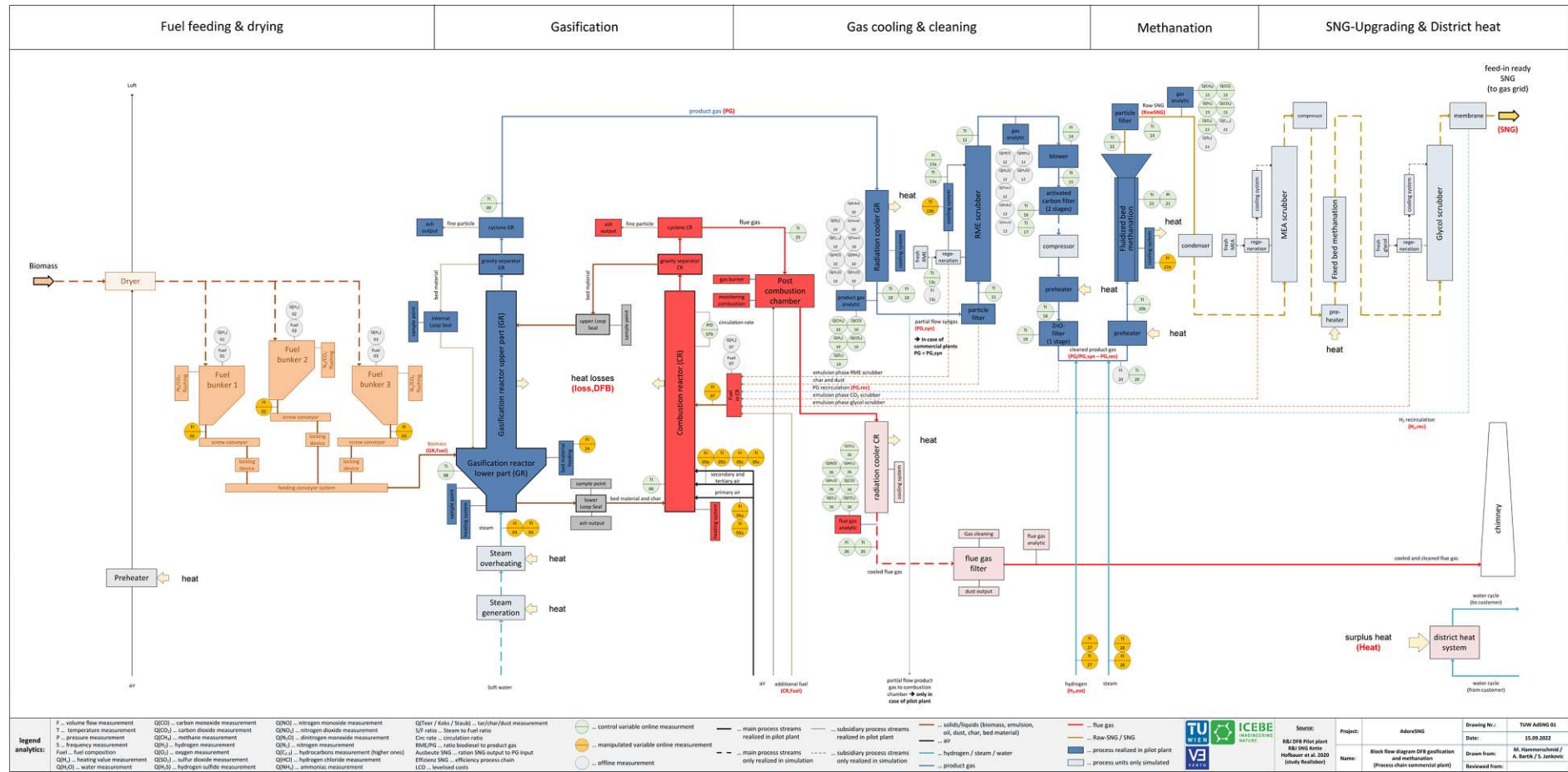


Fig. A3: Process flow diagram of Biomass-to-Gas process with visualization of realized process equipment in pilot plant (filled) and only simulated equipment (shaded)

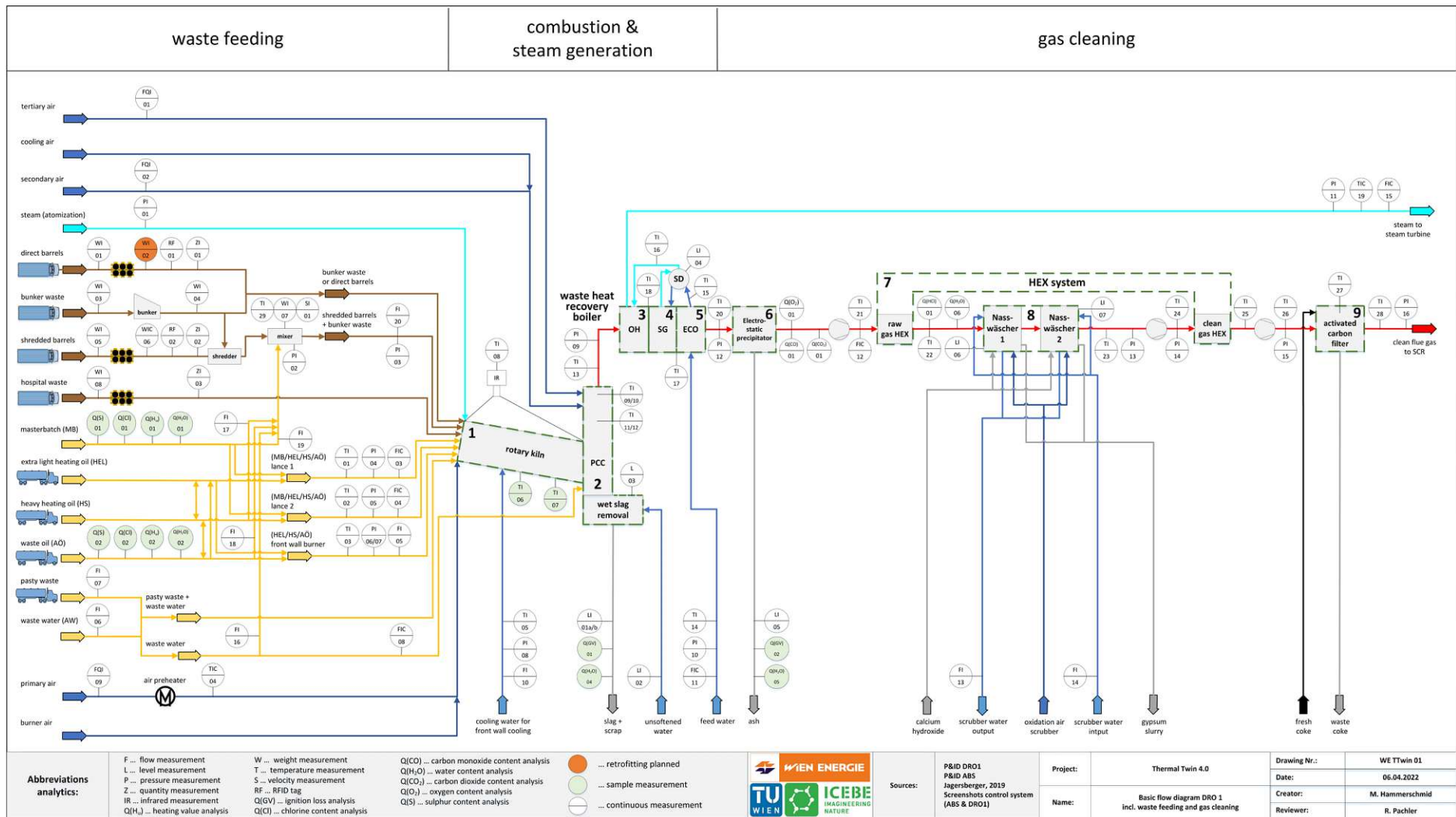


Fig. A4: Process flow diagram of the hazardous waste incineration plant in Vienna at Simmeringer Haide [104]

Appendix

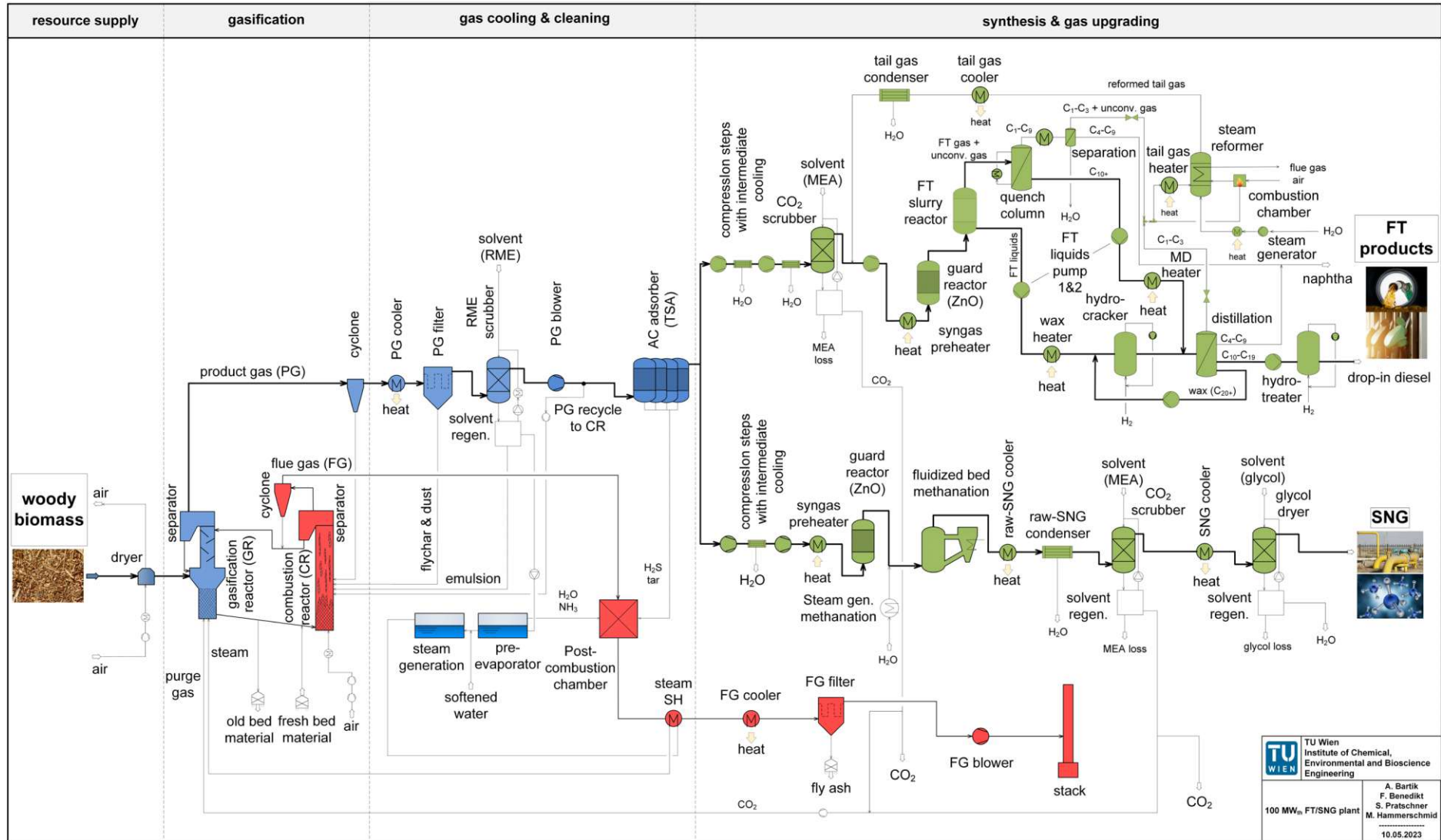


Fig. A5: Process flow diagram of the 100 MW_{th} FT and SNG routes (note: FT and SNG production are standalone routes but are displayed together in this picture) [112]

Appendix

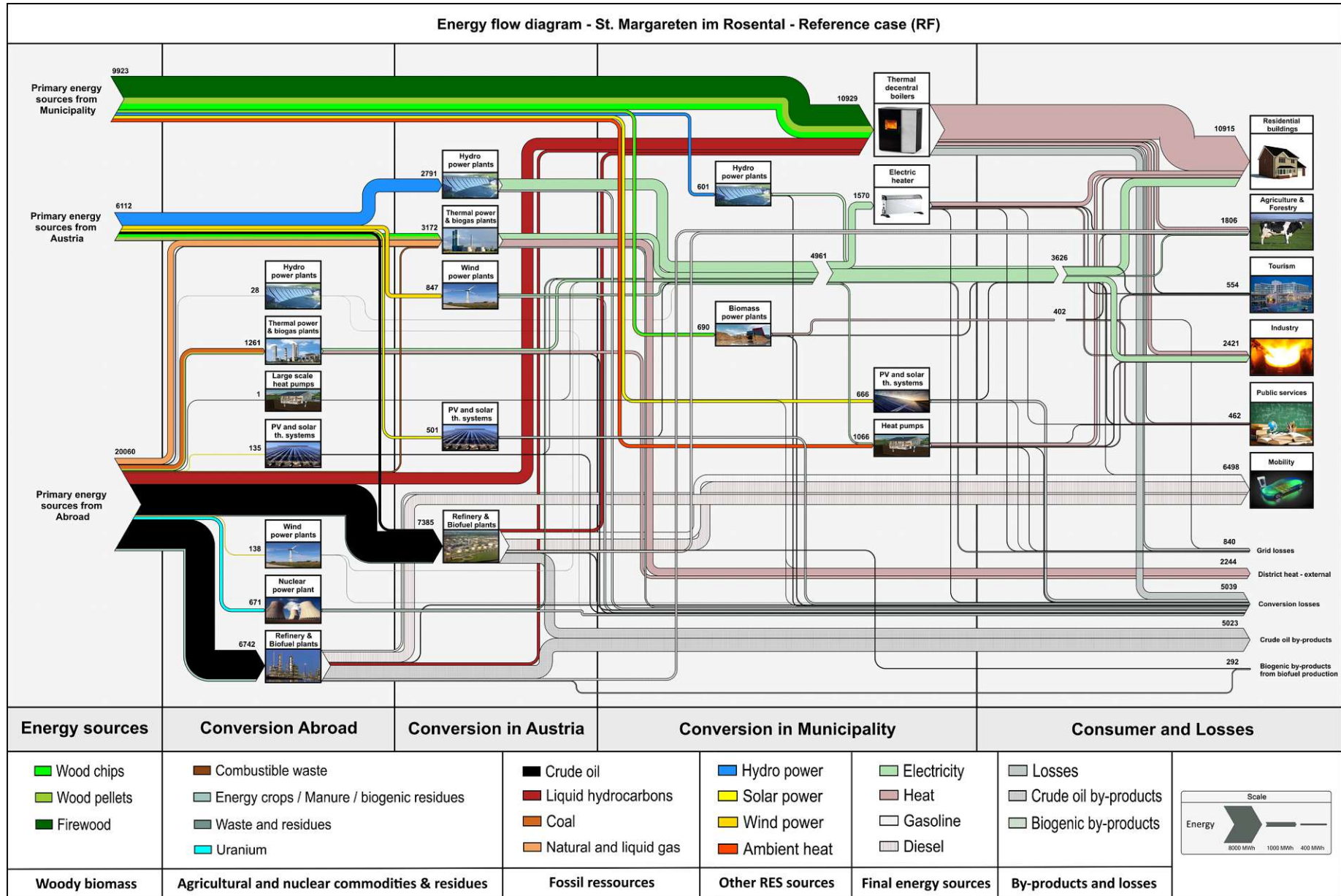


Fig. A6: Energy flow diagram of present annual energy demand of St. Margareten im Rosental based on the reference year 2020 [164]

Paper I

Methodology for the Development of Virtual Representations within the Process Development Framework of Energy Plants: From Digital Model to Digital Predictive Twin - A Review


Hammerschmid, M., Rosenfeld, D.C., Bartik, A., Benedikt, F.,
Fuchs, J., Müller, S.

Energies, 2023, 16(6), 2641, SI Digital Twin Technology in Energy
and Environmental Sector

<https://doi.org/10.3390/en16062641>

Review

Methodology for the Development of Virtual Representations within the Process Development Framework of Energy Plants: From Digital Model to Digital Predictive Twin—A Review

Martin Hammerschmid , Daniel Cenk Rosenfeld , Alexander Bartik , Florian Benedikt, Josef Fuchs and Stefan Müller

Institute of Chemical, Environmental and Bioscience Engineering, TU WIEN, Getreidemarkt 9/166, 1060 Vienna, Austria

* Correspondence: martin.hammerschmid@tuwien.ac.at

Abstract: Digital reflections of physical energy plants can help support and optimize energy technologies within their lifecycle. So far, no framework for the evolution of virtual representations throughout the process development lifecycle exists. Based on various concepts of virtual representations in different industries, this review paper focuses on developing a novel virtual representation framework for the process development environment within the energy sector. The proposed methodology enables the continuous evolution of virtual representations along the process development lifecycle. A novel definition for virtual representations in the process development environment is developed. Additionally, the most important virtual representation challenges, properties, and applications for developing a widely applicable framework are summarized. The essential sustainability indicators for the energy sector are listed to standardize the process evaluation throughout the process development lifecycle. The virtual representation and physical facility development can be synchronized by introducing a novel model readiness level. All these thoughts are covered through the novel virtual representation framework. Finally, the digital twin of a Bio-SNG production route is presented, to show the benefits of the methodology through a use case. This methodology helps to accelerate and monitor energy technology developments through the early implementation of virtual representations.

Keywords: virtual representation; digital twin; process simulation; sustainability; process development



Citation: Hammerschmid, M.; Rosenfeld, D.C.; Bartik, A.; Benedikt, F.; Fuchs, J.; Müller, S. Methodology for the Development of Virtual Representations within the Process Development Framework of Energy Plants: From Digital Model to Digital Predictive Twin—A Review. *Energies* **2023**, *16*, 2641. <https://doi.org/10.3390/en16062641>

Academic Editors: Gui Lu, Dewen Yuan, Han Hu and Xuhui Meng

Received: 19 January 2023
Revised: 1 March 2023
Accepted: 6 March 2023
Published: 10 March 2023



Copyright: © 2023 by the authors. Licensee MDPI, Basel, Switzerland. This article is an open access article distributed under the terms and conditions of the Creative Commons Attribution (CC BY) license (<https://creativecommons.org/licenses/by/4.0/>).

1. Introduction

Digitization plays an essential role in everyday life. A continuous digital transformation can be observed since the early 1990s, especially in the economy and research sectors [1]. Thus, novel business models have emerged, and the vast potential for efficiency has increased as savings on energy, emissions, and cost in the manufacturing and energy sector have arisen [2]. Regarding the energy transition in the European Union, the climate goals should be reached by following the climate and energy framework 2030 [3], which will be executed by the Renewable Energy Directive (RED II) [4]. Therein, it is formulated that climate neutrality should be reached by rapidly reducing greenhouse gas emissions by integrating renewable energy carriers into the energy sector. Furthermore, the main targets are improving energy efficiency and reducing final energy consumption. Digitization can help support the energy transition process by speeding up the development of innovative renewable processes and optimizing energy efficiency. To enable a smart interconnected energy system [2,5], a horizontal and vertical cross-linking of energy producers, distributors and consumers has to be realized [6]. Borowski et al. [7] mentioned that digitization in the manufacturing and energy sector can lead to cost improvements of more than 25% compared to conventional productivity improvements [7]. Furthermore, digitization can increase the lifetime of energy plants by up to 30% [7]. Additionally, due to the increasing

number of volatile energy technologies in the energy system, the supply security could be improved by advanced digital methods [2].

To achieve the proposed goals of climate neutrality by 2050 in the European Union, the development of novel environmentally friendly and innovative technologies must proceed quickly. The limited time leads to market competition within the renewable energy sector. On the one hand, the competition increases the efforts to develop novel technologies. On the other hand, the scale-up of novel, innovative energy technologies is often executed too early. Consequently, energy technologies that are not fully developed are scaled to the commercial and industrial scales without describing the full behavior of energy technologies with simulation models [8]. Since the physical plant is often better developed than the virtual representation, the same issues occur repeatedly. The solution to this problem can be the early evolution and implementation of virtual representations [9] within the process development, called frontloading [10]. Similar to virtual product development [10], early integration of virtual representations can help to save considerable time and money in the development process [10]. Furthermore, the virtual representations help to define ideal scale-up dates by determining and tracking milestones in the process development path. Figure 1 represents the cost reduction potential through frontloading and learning during process development. Therein, the theory of the increasing fixed production costs along the process development and the theory of learning and innovation in the technology rollout phase is combined [11]. By analogy with product development, it can be seen that about 65% of the production costs are defined in the conception phase [10,12]. Therefore, most of the energy production costs are determined within the conception phase by determining the input streams and process units. The early integration of virtual representations helps to compare different cost-effective process configurations [10]. Furthermore, development progress can be evaluated and validated by implementing virtual representations.

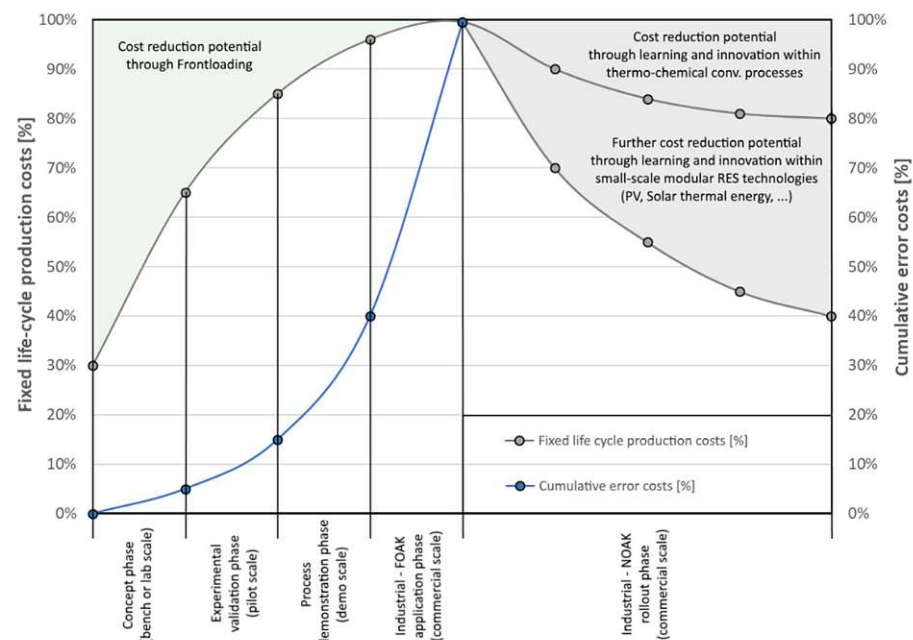


Figure 1. Cost reduction potential through frontloading and learning during process development [10–17].

In contrast to product development, developed processes are erected in lower quantities. Because the same process units are often used in different applications, advanced modeling techniques can help to lead the way towards a novel, cost-effective, renewable technology. Besides the acceleration of the development progress, virtual representations can also help to optimize the whole lifecycle of an energy plant from the early conception until the disposal phase [18]. Finally, the learning and innovation within the rollout

phase of novel energy technologies can be supported by virtual representations through state-of-the-art knowledge transfer.

To exploit this cost reduction potential in the energy sector, methodologies, frameworks, and standards must be introduced to harmonize the heterogeneous technology landscape [2]. Integrating standardized frameworks and methodologies within the process development sector can help to accelerate the development of novel environmentally friendly technologies.

So far, no framework for the evolution of virtual representations throughout the process development lifecycle exists. Therefore, this paper first reviews the existing literature in the area of frameworks, methodologies, properties, applications, and definitions for the development of digital twins in different industries. In Table 1, the review methodology is summarized. To improve the reliability and variety of the review process, three different databases were searched. Consequently, more than 130 papers were selected for the evaluation process. Within the evaluation process, the relevance of every paper was assessed by screening the title, abstract, introduction and conclusion. From the selected papers, more than half were excluded due to applications from non-comparable industries or misleading use of the terms “virtual representation” or “digital twin”. Finally, a total of 53 papers were included in this review paper.

Table 1. Methodology of screening papers.

Databases	ScienceDirect, Scopus, and Google Scholar
Article Type	Scientific articles published in peer-reviewed journals or conferences, white papers, and books
Search Strings	“digital twin”, “digital shadow”, “digital model”, “virtual representation”, “product avatar”, “cyber-physical equivalence”, “cyber-physical production system”, “virtual testbed”
Search Period	From January 2015 to June 2022
Screening Procedure	The relevance of the articles examined was determined by reviewing the title, abstract, introduction, and conclusion.
Exclusion Criteria	Several publications were excluded for the following reasons: <ul style="list-style-type: none"> ➤ Investigated industry is very different from the energy sector; ➤ Investigated application was misleadingly named as a digital twin or virtual representation.
Classification Scheme	The selected publications were divided into five groups: <ul style="list-style-type: none"> ➤ Frameworks and methodologies of virtual representations; ➤ Review articles about virtual representations; ➤ Definitions of virtual representations; ➤ Simulation models, emulation and Artificial Intelligence; ➤ Data communication.

Summing up the literature review, there are many ongoing investigations in the field of virtual representations around the world. Most of the screened methods and concepts focused on the manufacturing sector. As mentioned in several studies, no unified modeling framework for virtual representations exists [2,19–21]. One of the reasons for this lack of concepts and frameworks is the heterogeneous landscape in terms of data communication and software tools [2,20]. In this context, there are many different requirements in several industries. Further, the digitization in the industry is strongly influenced by the considered sector [20]. In the energy industry, few digital twins have been developed. However, there is a high demand for digital twins, especially in dispatch optimization problems and operational control [19]. There is also significant potential in the virtual verification and monitoring of plants. In the energy sector, virtual representations are mainly used as a support instrument for the engineering process [20]. However, none of the mentioned studies deal with designing a new technology from scratch [20].

To enable the wide use of virtual representations in all phases of the energy plant lifecycle, a unified modeling framework for developing energy technologies has to be introduced. The interaction between the physical facility and the virtual model should be defined within every stage of process development. Furthermore, the scale-up of energy technologies could be supported by accompanying virtual representations to monitor development goals within each process development stage. The development of virtual representations is often costly and challenging due to the mismatch between the physical process and the models. A unified framework helps to determine the required granularity, accuracy, and complexity in every process development phase [22,23], which leads to appropriate models. These models could preserve the process knowledge of experts and scientists during the development cycle of novel energy technologies. In addition to the virtual representation of the physical process in the simulation model, data availability and quality [2] have to evolve during the process development path. Therefore, the need for smart sensors and advanced data communication tools [2] arises. Furthermore, the topic of data security [19] has become more and more important within the development cycle. Finally, a unified modeling framework helps to support the multidisciplinary approach of process development to generate state-of-the-art virtual representations of energy technologies with particular regard to multicriteria optimization to support the way towards climate neutrality.

The present review paper discusses the idea of providing a unified modeling framework in process development within the energy sector. Process development should be accompanied by high-fidelity virtual representations to optimize and accelerate the development progress. Therefore, the monitoring of the process development progress should be reached by introducing a model readiness level, which implies that the development progress of the physical energy plant and the virtual model are in line. Finally, the focus should be on the multicriteria optimization of energy technologies concerning sustainability in each process development stage. For the elaboration of this novel framework, the present review paper contains the following parts:

- The summary of existing concepts of virtual representations;
- The comparison of different definitions of virtual representations;
- The collection of possible applications, challenges and properties of virtual representations in the energy sector;
- The ascertainment of sustainable development goals and sustainability indicators concerning process development;
- The definition of process development stages with the introduction of the modeling readiness level;
- The development of a unified modeling framework for the optimized development of novel energy technologies with a particular focus on the interaction between the physical facility and the virtual model.

2. Concept and Methodology

For the conception of a process development framework based on the integration of virtual representations, some fundamental topics must be discussed. First of all, a summary of existing concepts and definitions of virtual representations in different fields of applications are investigated. Furthermore, energy plant lifecycle phases and hierarchy layers are discussed to obtain an overall picture of possible stakeholders of virtual representations in the energy sector. The properties, challenges and applications of virtual representations build the basis for possible usage settings. To obtain an overall picture of the technology's impact on the environment, sustainability indicators for the process development are summarized. Additionally, the technology scale-up levels and levels of process engineering are explained. Finally, the novel modeling readiness level is introduced as the basis for the following development framework.

2.1. Existing Concepts and Methodologies of Virtual Representations

In the last decade, numerous researchers and international institutions created reviews regarding the development and application of virtual representations of physical objects. First, Kritzinger et al. [9] mentioned that there is no common understanding of the term “digital twin” in manufacturing. Therefore, Kritzinger et al. [9] and Aheleroff et al. [24] introduced a definition according to the level of integration. This means that a virtual representation of a physical object can be classified as a digital model, digital shadow, digital twin, or digital predictive twin. Furthermore, Qi et al. [25] and Tao et al. [19] reviewed big data and digital twin approaches, focusing on manufacturing, product design, health management, and some energy-related sectors. Additionally, five digital twin dimensions were introduced [19]. The review papers from Liu et al. [20,26] are also strongly connected to the manufacturing industry. The literature review from Chen et al. [21] is focused on pharmaceutical and biopharmaceutical manufacturing. Further review works about the concepts and potential of digital twins in the industry can be found in [22,23,27–31].

In addition to literature reviews, several frameworks, methodologies, and concepts for digital twins have been published in the last decade. Most of the architecture models and frameworks in the literature are focused on the manufacturing sector. For example, Moreno et al. [32] proposed a concept for the manufacturing sector based on the example of a punching machine. Qi and Tao [25] and Lu et al. [33] introduced concepts for smart manufacturing which are focused on a big data approach. Experimental digital twins are created by combining virtual testbeds and digital twins, according to Schluse et al. [34,35] and Dahmen et al. [36]. The main idea is to establish digital twins as the core part of the development process and build all other parts around them [34]. Uhlemann et al. [37] and Trabesinger et al. [38] introduced concepts for generating cyber-physical production systems based on the optimization of the data acquisition approach. A novel architecture for large-scale digital twin platforms with a focus on flexible data-centered communication for the use in reliable advanced driver assistance systems was developed by Yun et al. [39]. Further information about the concepts and methodologies of digital twins can be found in [40–47].

The conducted research regarding concepts and methodologies for virtual representations in different industries represents the basis for the elaboration of a novel methodology for the development of virtual representations in process development.

2.2. Definitions of Virtual Representations

The first step towards a process development framework for the integration of virtual representations is the definition of the term “virtual representation” itself. In this paper, the term “virtual representation” refers to the overall expression of virtual objects mirroring a physical process using advanced digital methods. In the literature, the terms “digital twin”, “digital shadow”, and “digital model”, as well as “virtual representations”, are often used synonymously [9]. Furthermore, phrases such as “product avatar”, “cyber-physical equivalence”, “cyber-physical production system” and “virtual testbeds” are used in the literature for defining virtual representations in specific applications [28].

The first introduction of the term “digital twin” as a virtual representation was given by Grieves in 2003 [48] in the context of product lifecycle management (PLM). In the last two centuries, many definitions have evolved in different applications. Consequently, no unique definition for virtual representations has been reached yet [9,22,27]. One main reason could be the broad spectrum of virtual representation applications, making it difficult to find a unified definition. In Table 2, selected definitions from the literature are summarized to obtain an overview of the broad range of descriptions.

Table 2. Selection of virtual representation definitions in the literature.

No.	Year	Definition of Virtual Representation	Key Points	Field of Application	Ref.
1	2003	“The digital twin is a digital informational construct of a physical system, created as an entity on its own and linked with the physical system.”	Digital and physical system linked	Product lifecycle management	[21,48]
2	2012	“A Digital Twin is an integrated multi-physics, multi-scale, probabilistic simulation of a vehicle or system that uses the best available physical models, sensor updates, fleet history, etc., to mirror the life of its corresponding flying twin.”	Best available physical models	Aeronautics	[27,49]
3	2012	“The digital twin consists of a virtual representation of a production system that is able to run on different simulation disciplines that is characterized by the synchronization between the virtual and real system, thanks to sensed data and connected smart devices, mathematical models and real time data elaboration. The topical role within Industry 4.0 manufacturing systems is to exploit these features to forecast and optimize the behavior of the production system at each life cycle phase in real time.”	Different simulation disciplines, connected smart devices and real-time data elaboration, enabling forecasting and optimization of the system behavior within each lifecycle phase	Manufacturing	[27,50]
4	2015	“Very realistic models of the process current state and its behavior in interaction with the environment in the real world”	Realistic models to monitor the current state	Manufacturing	[27,51]
5	2016	“Virtual substitutes of real-world objects consisting of virtual representations and communication capabilities making up smart objects acting as intelligent nodes inside the internet of things and services”	Virtual substitutes with communication capabilities	Robotics	[34]
6	2016	“The simulation of the physical object itself to predict future states of the system.”	Prediction of future states of the system	Manufacturing	[52]
7	2018	“The digital twin is actually a living model of the physical asset or system, which continually adapts to operational changes based on the collected online data and information, and can forecast the future of the corresponding physical counterpart.”	Living model with continual adaptation to operational changes	Aircraft maintenance	[53]
8	2018	“A digital twin is a digital representation of a physical item or assembly using integrated simulations and service data. The digital representation holds information from multiple sources across the product life cycle. This information is continuously updated and is visualized in a variety of ways to predict current and future conditions, in both design and operational environments, to enhance decision making.”	Multiple sources across the lifecycle deliver information, enhancing decision-making by predicting functions	Product lifecycle management	[54]
9	2019	“Themes related to the Digital Twin are the decoupling between physical and cyber entity, the presence and frequency of sensorial data flows, the use of computer simulation, the control of cyber over physical entity, the co-evolution of physical and cyber entity as well as the co-existence of physical and cyber entity.”	Presence of sensorial data flows and co-evolution of physical and cyber entities	Manufacturing	[55]
10	2019	“A complete Digital Twin should include five dimensions: physical part, virtual part, connection, data, and service.”	Five digital twin dimensions	Industry	[19]

Based on the summary of the selected definitions, it could be concluded that there is a broad consensus that a virtual representation is a digital reflection of a physical object. Additionally, the virtual representation is coupled with its physical counterpart and is an abstracted model description of the physical object. However, there are several inconsistencies in virtual representation characteristics in the literature. For example, there are different opinions about the data exchange, the real-time capability, the lifecycle perspective, and the fidelity level of the virtual representations.

For classifying virtual representations according to the data exchange between virtual and physical facility, the level of integration is discussed. Kritzinger et al., introduced the level of integration to differentiate virtual representations according to their data communication [9]. Figure 2 shows the integration levels of virtual representations. Therein, it can be seen that the digital model is characterized by two-way offline data communication between the physical and virtual components. The digital shadow is defined by one-way offline and one-way real-time communication between the two components. In the literature [9,24], the digital shadow is exclusively characterized by real-time data communication from the physical to the virtual component. Since there are also applications with a one-way real-time communication in the other direction, the term “digital shadow” is also valid for this approach. Digital twins are characterized by two-way real-time data communication between the physical and the virtual components [9]. Aheleroff et al. [24] extended the definition from Kritzinger et al. [9] using a predictive model approach, which is motivated by the work of Tuegel et al. [56]. The term “digital predictive twin” is introduced, which defines virtual representations with integrated predictive models.

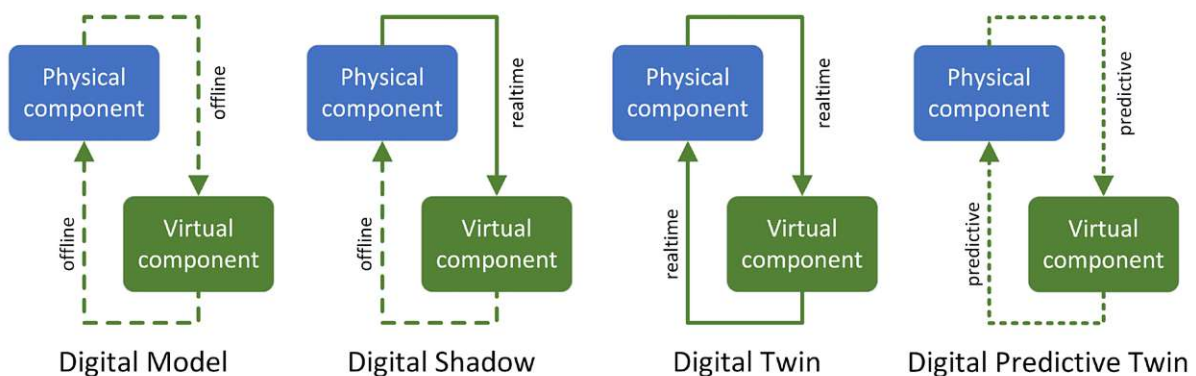


Figure 2. Virtual representation of integration levels concerning data communication. (Reprinted with permission from [24]. Copyright 2021 Elsevier).

In addition to the summarized definitions and levels of integration of virtual representations, the five-dimensional model, according to Tao et al. [19], is essential. As shown in Figure 3, the 5D model defines five mandatory parts for a complete virtual representation. The 5D model approach consists of physical and virtual components, data management, service, and connections. The physical component is the experimental or industrial facility to be investigated. The virtual component refers to all virtual models, flowsheets, and specifications, which serve as a basis for all virtual representation applications. The data management is responsible for the processing and storage of data. Within the service part, the investigated application is realized. The four mentioned parts are linked by connections responsible for the data transmission.

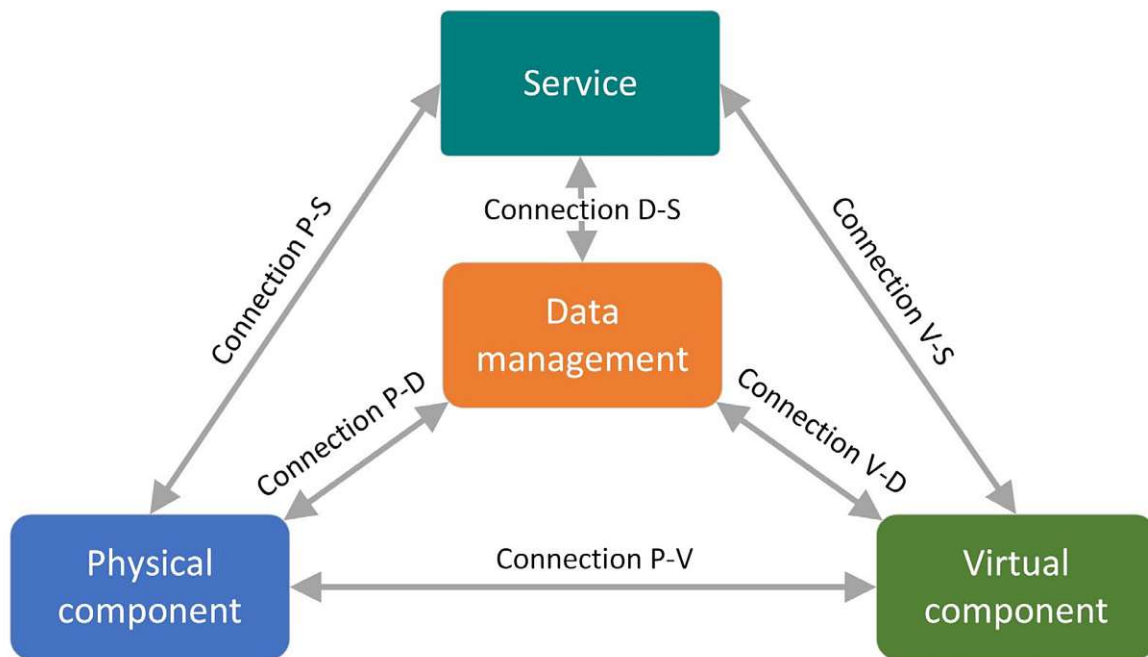


Figure 3. 5D model for virtual representations concerning a holistic approach. (Reprinted with permission from [57]. Copyright 2021 Elsevier).

Based on the summarized definitions in the literature, the level of integration approach, and the 5D model approach, a novel definition of virtual representations of energy technologies in the process development environment can be given:

Virtual representations in process development of energy technologies are digital reflections of physical facilities. The virtual component contains an abstracted model that is fitted as close as necessary to the physical component through the integration of measured values and domain knowledge.

Based on this definition, which emphasizes that the level of integration and model abstraction can differ in each process development and lifecycle phase, it is essential to develop a virtual representation by analogy with the physical facility with a clear overall development and engineering strategy [34]. This holistic approach requires the consideration of energy plant hierarchy levels [2] and energy plant lifecycle phases [54,58–60]. In the case of process development, the lifecycle perspective can be seen from two perspectives. On the one hand, the lifecycle perspective concerning the physical facility ranges from the design over the operation phase to the decommissioning phase [60]. On the other hand, the process development lifecycle perspective ranges from the lab-scale to the industrial-scale facility [61]. Each energy plant lifecycle phase is passed through in every process development phase, from lab to commercial scale. Therefore, the virtual representation architecture has to become more and more elaborate within process development. As well as the lifecycle perspective, the energy plant hierarchy layers have to be addressed to align the virtual representation framework with the foreseen user group. The energy plant hierarchy levels, according to IEC 62264 [62], range from the process level over the process control level to the enterprise level, and can be extended by the overarching energy system level. To conclude, the consideration of the lifecycle perspectives of energy plants and the energy plant hierarchy layers help to visualize the variety of players, which could be addressed within the development of a virtual representation. In addition to the discussion of the variety of virtual representation users, the planned applications and the associated properties, are discussed in the next section.

2.3. Applications, Challenges and Properties of Virtual Representations in the Energy Sector

There are many different applications in the process development framework in the energy sector [63] for the use of virtual representations. These applications are all confronted with different implementation types regarding energy plant hierarchy levels and lifecycle perspectives, as mentioned in Section 2.2. Furthermore, it is important to define virtual representation properties for developing a virtual representation framework. First, the Gemini principles [64] build a superordinate framework, which provides high-level guidelines for developing virtual representations regarding purpose, trust, and function. More detailed virtual representation properties can be defined based on these guidelines and principles.

Subsequently, the vast number of application possibilities within the energy sector must be discussed. Many literature reviews have summarized the possible applications of virtual representations in the industry in different fields [2,19–22,25–28,42,58,65,66]. Table 3 gives an overview of the possible virtual representation applications along the plant lifecycle phases, which are already discussed in Section 2.2.

Table 3. Possible virtual representation applications along the plant lifecycle phases.

Virtual Representation Applications	Conceptual Design and Engineering	Construction and Commissioning	Operation	Maintenance	Optimization	Decommissioning	Ref.
Collaboration	cooperation with suppliers, experts and inter-divisional coordination	coordination supplier	coordination logistics	coordination of spare parts supply and supplier	collaboration with external experts	coordination reuse and disposal	[2,20,58,65]
Documentation	process lifecycle management for the state-of-the-art documentation						[20,28,30,58]
Simulation and Monitoring	assistant for constructive and technical process design and construction		real-time performance	condition monitoring	reconfiguration and reconditioning	design of reuse	[2,22,27,58,66]
Evaluation and Verification	holistic evaluation of process design and construction		quality control	fault diagnosis/anomaly detection	holistic optimization	evaluation of reuse and disposal	[2,20,25,58]
Visualization	collision check and merchandising	construction assistant	support process understanding	visualization of 3D model or servicing plan	visualization of sustainability indicators	merchandising for reuse	[28,58]
Planning and Decision making	scheduling and support from design to commissioning		scheduling of operation and utility handling	proactive services	economic and ecologic dispatching	schedule for plant lifetime	[2,25,27,58]
Emulation	risk assessment	virtual commissioning	support and training of plant operators and maintenance engineers			virtual decommissioning	[22,30,42,58]
Orchestration	automation of process design and construction		process automation	automated maintenance services	advanced control strategies	-	[2,20,21,58]
Prediction	demand analysis and market prediction	stage of completion prediction	future performance	predictive maintenance	fault prediction of physical entities	prediction of a lifetime and residual value of physical entities	[20,21,25,58]

The given list of applications is incomplete and gives only an overview of the vast possibilities that arise with the development of virtual representations. The application possibilities can be categorized into nine groups, ranging from collaboration to prediction. Collaboration means the possibility of co-operation with different internal and external partners as well as the co-ordination possibilities arising from the virtual representation. The documentation aims to deliver state-of-the-art documentation of the energy plant throughout the whole lifecycle, often named “process lifecycle management”. The simulation and monitoring applications observe the process performance and support the design and commissioning. Several examples for simulation and monitoring applications can be found in [67–72]. The evaluation and verification stand for the information analysis, which helps to optimize the process from the design to the decommissioning phase by implementing sustainability indicators. The sustainability indicators are explained in detail in

Section 2.4. The visualization group stands for the use of a detailed 3D model, for example, as a design or maintenance assistant. Visualizing the sustainability indicators within the virtual representation can assist the plant operator in optimizing the process performance. The applications within the planning and decision-making group offer the possibilities that arise due to the implementation of virtual representations in terms of scheduling, economic and ecologic dispatching, and proactive action selection services. Emulation means nearly an exact duplication of the physical facility, consisting of the process behavior covered in the simulation and a detailed 3D model. Orchestration refers to the virtual control and automation tasks, which the implementation of a virtual representation could fulfill. Finally, the prediction services can range from market analysis to predicting the physical entities' plant lifetime and residual value.

In summary, there are many possibilities for the use of virtual representations in energy plants. Before developing a virtual representation framework, it is essential to define which applications in which energy plant lifecycle stage should be addressed. In addition to defining the applications, it is important to define which properties the virtual representation should fulfill to realize the foreseen applications. Beforehand, it is important to outline the challenges and problems which should be addressed during the evolution of virtual representation frameworks. As mentioned by Chen et al. [21], most challenges can be classified as time-, safety- or mission-critical. To enable stable real-time data communication between the physical and virtual components, it is important to decouple the control system from the virtual representation, which means that at any time the plant can be controlled manually via the control system. Additionally, cybersecurity safety measures against malicious attacks should be addressed. The data resolution, quality, and latency should be carefully checked and synchronized with the foreseen application. Furthermore, the heterogeneity of equipment for measuring components and control systems complicates the evolution of a standardized framework. Therefore, the use of standardized interfaces should be forced to realize exchangeable modeling blocks. The simulation models used should be robust and valid for a wide range of operations and applications to enable standardization. For advanced applications, hybrid or purely data-based models which have been parameterized for a specific application are often required. Consequently, a fast and user-friendly parametrization to other use cases should be enabled. Furthermore, a periodic recalibration of the simulation model must be considered to avoid model drifts. Finally, it should be pointed out that the results of virtual representations are all based on measurement values. Therefore, the continuous verification and recalibration of measurement equipment is indispensable. All these summarized challenges should be carefully addressed during the development of a virtual representation framework. The following discussion of virtual representation properties can assist with the development of an appropriate framework depending on the application [21].

In Table 4, an overview of possible virtual representation properties is listed. Therein, several property classes are defined to classify virtual representation approaches. The first property group has an overall focus. For example, the scalability indicates the implementation possibility of virtual representations within different energy plant hierarchy layers [73]. The interoperability specifies the equivalence between different model representations, which means the modeling tools are comparable, convertible or standardized [74]. The expansibility points out the flexibility of the used modeling techniques regarding the integration or replacement of models [74]. Finally, the functional safety represents the reliability and resilience of the virtual representation framework [73].

Table 4. Virtual representation properties in the energy sector.

Property Classes	Focus	Property Levels				Ref.
		Level 0:	Level 1:	Level 2:	Level 3:	
Scalability	Overall	Equipment level	Plant level	Enterprise level	Energy system level	[73,74]
Interoperability		Comparable	Convertible	Standardized		[73,74]
Expansibility		Fixed layout	Adaptable layout	Automated layout		[74]
Functional safety		Systematic capability	Implemented redundancies	Predictable failure analysis	Automated replacement	[73,75]
Technological scale-up possibility	Physical component	Modular	Partly scalable	Fully scalable		[76,77]
Degree of automation		Manual	Semi-automated	Fully automated		[78]
Physical safety		Primary safety measures	Secondary safety measures	Tertiary safety measures		[79]
Virtual representation capability	Virtual component	Static/Quasistatic	Dynamic	Ad hoc	Predictive	[45,63]
Virtual representation fidelity		Black box	Gray box	White box		[45,74]
Virtual representation intelligence		Human triggered	Automated	Partial Autonomous	Autonomous (self-evolving)	[45,63]
Connectivity mode		Manual	Unidirectional	Bidirectional	Automatic	[45,63]
Data integration level	Data management and connection	Manual	Semi-automated	Fully automated		[65]
Update frequency		Yearly/Monthly	Weekly/Daily	Hourly/every minute	Immediate real-time/event driven	[45,63,73]
Cybersecurity		Role-based access control	Discretionary access protection	Mandatory access control	Verified access control	[73,80–82]
Human interaction	Service	Smart devices	Virtual and Augmented Reality	Smart hybrid		[45,63]
User focus		Single	Multiple without interaction of energy plant hierarchy layers	Multiple with fully interaction of energy plant hierarchy layers		[65]

Furthermore, there are some individual properties listed for each virtual representation dimension. The physical component is classified by the technological scale-up possibility, the degree of automation, and the physical safety. For example, the technological scale-up possibility describes if all parts of the energy plant can be fully or partly scaled-up or if only a modular construction can manipulate the capacity. For example, the electrolysis of water is often not fully scalable due to technical limitations. The physical safety describes measures for preventing mechanical, electrical, chemical, biological, or explosion hazards and can be divided into primary, secondary, and tertiary safety measures [79]. Primary safety measures help to prevent hazard operation zones. Secondary safety measures include further precautions, e.g., the prevention of ignition sources, if hazard zones cannot be prevented. Tertiary safety measures describe structural hazard protection measures to limit the impact of incidents.

Additionally, there are several property classes for specifying the virtual component. The virtual representation capability implies the time dependency of the used models [45]. The fidelity stands for the degree of accuracy of the virtual component compared to the physical component [74]. Finally, the virtual representation intelligence indicates the ability of automatic decision-making, which ranges from human-triggered abilities over automated, rule-based approaches to autonomous full cognitive-acting approaches [45].

Moreover, data management and connection-focused property classes are mentioned. Therein, the connectivity mode refers to the integrated data exchange paths between the physical and the virtual component [45,65]. The data integration level represents the degree of automation of the data communication between the physical and virtual components [65]. The necessary update frequency of the virtual model depends on the application and ranges from weekly to real-time approaches [45]. Within the update frequency, the topics of latency,

jitter, throughput, and bandwidth are important to note [73]. The cybersecurity property class represents the integrated protection features within the virtual representation against unauthorized access [80]. Besides the authorization and verification topic, cryptographic protection should also be considered [73].

The virtual representations deliver services which can be classified by human interaction and user focus. The human interaction implies the communication possibilities of the user with virtual representation [45]. The user focus indicates the extent to which users deal with the virtual representation service [65]. The applications depend on different property levels of virtual representations, as discussed in Table 4, and deal with different plant hierarchy levels, as discussed in Section 2.2. Therefore, by developing virtual representations, it is essential to focus on the applications that must be addressed. Depending on the foreseen application, different property levels of virtual representations have to be implemented and different plant hierarchy levels considered. In developing novel energy technologies, it is crucial to develop the accompanying virtual representation so that as many applications along the energy plant lifecycle can be addressed. For the validation and evaluation of the virtual representation performance and the considered energy plant, it is essential to define key performance indicators (KPIs). These KPIs are even more important within the process development as a means of forming a holistic, optimized, sustainable energy process. Therefore, the KPIs are also named “sustainability indicators”.

2.4. Sustainability Indicators in the Energy Sector

Defining performance indicators is crucial for the development and optimization of energy processes. It is essential to link the performance indicators with sustainability to establish novel energy technologies and enable the energy transition towards climate neutrality. Therefore, the following performance indicators are called sustainability indicators. Successful development of novel energy technologies also implies compliance with legal, environmental, economic, and social requirements. Therefore, a multicriteria optimization of energy technologies regarding different aspects has to be fulfilled. The definition of sustainability can first be linked with the sustainable development goals (SDGs) [83]. They all highlight the global need for the sustainable development of the ecological, economic, and social environment. In terms of energy production, nearly all SDGs are relevant. Furthermore, the EU taxonomy [84] should be mentioned. This regulation provides a classification system, establishing a list of environmentally sustainable economic activities [84] exemplary in climate change mitigation. However, the EU taxonomy is controversial, because there is no common understanding of sustainability, especially in the energy sector.

Table 5 introduces the most important sustainability indicators for the energy sector to enable a method of quantifying sustainability. The sustainability indicators are classified into technical, environmental, economic, and social indicators according to [85]. Technical indicators are energetic and exergetic efficiency, which differ in considering the irreversibility of a process or lack thereof, when monitoring the performance of a process or plant. For carbon-based technologies, different conversion rates are also relevant to enable more detailed investigations. The plant lifetime and availability are essential indicators of supply reliability and economic aspects. The environmental indicators are classified into air, soil, ground, and water conditions, natural resources, utility consumption, and waste production. In terms of environmental indicators, it is essential to mention the lifecycle assessment methodology (LCA) to analyze environmental impacts. For detailed information regarding the fundamentals, requirements, frameworks, and guidelines of LCAs, refer to DIN EN ISO 14040 [86] and 14044 [87]. The assessment of environmental impacts is complex. However, developing and optimizing energy technologies regarding environmental requirements is important to enabling the energy transition towards climate neutrality. Besides technical and environmental indicators, economic indicators should be observed to enable affordable energy. The levelized production costs, which cover investment, fuel, operation, and maintenance costs over a lifetime, help to compare energy technologies with each other or the market value. The operating cash flow stands for

the liquidity of a plant operator. To compare different investment scenarios or analyze specific investments in the energy sector, the net present value, payback time, and return on investment are all suitable indicators. The gross domestic and regional value is the value added created through energy production in a country or region within a certain period. For quantifying social impacts caused by energy production, the human toxicity potential and the job creation indicator can be named, for example.

Table 5. Selected sustainability indicators for the evaluation of energy technologies.

Sustainability Indicators		Unit	Description	Ref.	
Technical indicators	Conversion rate **	%	Measuring the performance of a reactor or plant by observing the converted amount of a specific chemical compound during a reaction.	[76,88]	
	Energetic efficiency	%	Measuring the performance of a technology by comparing the energy content of input and output streams.	[89]	
	Exergetic efficiency	%	Measuring the performance of a technology by considering the irreversibility of a process.	[90]	
	Plant lifetime	a	Measuring the usability period of a plant.	[89]	
	Plant availability	FLH/a	Measuring the degree of utilization per year of a reactor or plant by referring to an operation at nominal power.	[89,91]	
Environmental indicators	Emissions to air	Global warming potential (e.g., CO ₂ , CH ₄ , N ₂ O, etc.)	kg CO ₂ -eq/FU *	Measuring the insulating effect of greenhouse gases in the atmosphere preventing the earth from losing heat gained from the sun.	[85,92–97]
		Acidification potential (e.g., NO _x , SO _x , etc.)	g SO ₂ -eq/FU *	Measuring emissions resulting in acid rain, which harms soil, water supplies, human and animal organisms, and the ecosystem.	[85,92,94–96]
		Ground air quality (particulates, photochemical oxidants)	kg PM ₁₀ -eq/FU * kg NMVOC/FU *	Measuring gaseous and solid emissions which affect the ground level atmosphere.	[85,92,94–96,98]
		Ozone-depleting potential	kg R-11-eq/FU *	Measuring the depletion of the ozone layer in the atmosphere caused by the emission of, e.g., chemical foaming and cleaning agents.	[85,92,94–96]
	Soil, ground and water conditions	Eutrophication	g PO ₄ ²⁻ -eq/FU *	Measuring concentrations of nitrates and phosphates, which can encourage excessive growth of algae and reduce oxygen levels within freshwater and marine water.	[92–96]
		Ecotoxicity	kg1,4-DB-eq/FU *	Measuring the potential for biological, chemical or physical stressors within freshwater, marine, or terrestrial ecosystems.	[94,96]
		Water consumption	kg H ₂ O/FU *	Measuring the amount of water consumed within a process.	[85,93,94]
	Natural resources, utility consumption and waste production	Primary energy consumption—fossil	MJ/FU *	Measuring the total fossil energy demand of a process.	[97,99]
		Primary energy consumption—renewable	MJ/FU *	Measuring the total renewable energy demand of a process.	[97,99]
		Electricity consumption	kWh _{el} /FU *	Measuring the total electricity demand of a process.	[85,97]
		Carbon utilization factor **	%	Measuring the amount of carbon converted from the fuel to the product within a process.	[88,100,101]
		Abiotic depletion	kg Sb-eq	Measuring the over-extraction of minerals, fossil fuels and other non-living, non-renewable materials which can lead to the exhaustion of natural resources.	[85,92,94]
		Wastewater amount	kg H ₂ O/FU *	Measuring the amount of wastewater produced within a process.	[85]
Solid waste amount (disposal) **		kg ash/FU *	Measuring the amount of disposable waste produced within a process.	[85]	
Land use	m ² /FU *	Measuring the amount of land needed for the construction of a plant.	[85,94]		

Table 5. Cont.

	Sustainability Indicators	Unit	Description	Ref.
Economic indicators	Levelized production costs	EUR/FU *	Measuring the price that would be charged per functional unit to achieve a net present value of zero for an investment.	[17,71,95,102,103]
	Operating cash flow	EUR/a	Measuring the profit/losses generated over a specific time period during regular operation.	[17,71,102,104]
	Net present value	EUR	Evaluates the technology investment by considering the time value of money.	[17,71,102,104]
	Payback time	a	Measuring the time required for return of the technology investment by revenues.	[17,71,105]
	Return on investment	%	Measuring the return of an investment by comparing profit and investment.	[104]
	Gross domestic/regional product (GDP/GRP)	EUR	Measuring the added value created through energy production in a country (GDP) or considered region (GRP) within a certain period.	[85,106]
Social indicators	Human toxicity	kg1,4-DB-eq/FU *	Measuring the quantity of substances emitted to the environment that harm humans.	[85,93–96]
	Job creation	-	Measuring the number of jobs created by the erection of a new plant.	[85,106]

* FU: functional unit (quantifiable description of the product function that serves as a comparable reference basis for all calculations) [86,87,107]. ** specific parameter for carbon-based technologies.

It should be noted that the overview of sustainability indicators in Table 5 introduces only selected quantifiable parameters. Of course, there are many more existing sustainability indicators. It is self-explanatory that not all of the presented sustainability indicators are applicable to all energy technologies. Depending on technology and location, these parameters also differ in importance and weighting. However, it should be clear that sustainable energy technologies can only be developed by considering a broad range of sustainability dimensions. Finally, the sustainable development and optimization of energy technologies shall always consider legal regulations, for example, emission and immission limits, or grid feed-in requirements. The definition of sustainability indicators forms the basis for quantifying development and optimization.

In summary, to develop a virtual representation framework in the process development environment, it is essential to define virtual representation applications and properties throughout the process development lifecycle. Furthermore, sustainability indicators have to be selected to ensure the evaluation and validation of the development's progress towards development goals. The following section introduces the novel model readiness level to link the sustainability indicators and virtual representation applications and properties with the process development lifecycle stages.

2.5. Introduction of the Modeling Readiness Level

Besides the technology performance evaluation via sustainability indicators, the definition of process development stages is essential for developing novel energy technologies. Therefore, the technology readiness level (TRL), which was first introduced by NASA [108], represents an important indicator for defining and monitoring the development progress. The TRL is also widely used within several national and international funding programs, such as EU Horizon 2020 [108], to classify research projects. In Figure 4, TRLs with the appropriate realized infrastructure, investigated process behavior, and the expected results within each process development lifecycle are visualized. Refer to [77,109] for further information on the TRL and related topics. To achieve the expected results in each process development stage, it is important to monitor and accompany the process development lifecycle with virtual representations. The virtual representation should combine all findings from the experimental test runs in each process development stage. To enable a successful framework for virtual representations, the definition of a modeling readiness level is important.

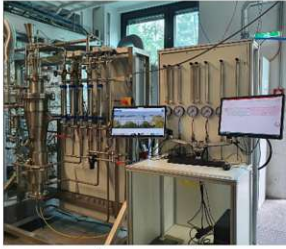



Expected results:	first calculations, proof of concept	mass & energy balances, detailed design values for optimized operation point	detailed design values for continuous operation	detailed design values for competitive energy production
Investigated process behavior:	short-term (few hours), stable operation point	short-term (few days), operation point changes and part-load performance	long-term (few months), fouling and aging, start-up and shutdown	long-term (multiple years), full behavior knowledge
Realised infrastructure:	core process unit	main process units without utility and product logistics	complete process chain with utility and product logistics	complete process chain with utility and product logistics
	TRL 1: basic principles scientifically proven	TRL 2: technology concept formulated	TRL 3: core system experimentally proven	TRL 4: technology validated in laboratory
		TRL 5: technology validated in relevant environment	TRL 6: technology demonstrated in relevant environment	TRL 7: system prototype demonstration in operational environment
			TRL 8: system complete and certified	TRL 9: system proven in operational environment
	concept, lab facility	pilot plant	demonstration plant	commercial plant
				
	MRL 1: operation & performance indicating equations	MRL 2: model development completed	MRL 3: integrated model library available	MRL 4: pilot plant model created
		MRL 5: pilot plant model validated by experiment	MRL 6: evaluation of utilities & sustainable indicators completed	MRL 7: virtual industrial plant available as integrated digital twin
			MRL 8: commercial plant validation completed and evaluated	MRL 9: platform based implementation, monitoring & sharing
Process description:	process flow diagram	detail engineering without maintenance and logistic concept	detail engineering with maintenance and logistic concept	detail engineering with maintenance, logistic and marketing concept
Virtual representation capability:	steady state model (stable operation point)	quasi steady state and dynamic model (operation point changes and part-load performance)	dynamic and ad-hoc model (fouling and aging, start-up and shutdown)	predictive simulation model (full behavior knowledge)
Sustainability indicators:	first estimations of technical, environmental and economic indicators	technical, environmental and economic indicators	technical, environmental, economic and social indicators	technical, environmental, economic and social indicators
Temporal resolution:	once per test run	monthly	secondly/minutes	secondly/minutes
Possible applications:	collaboration, documentation, simulation and evaluation	from collaboration to visualization (Tab. 3)	from collaboration to orchestration (Tab. 3)	from collaboration to prediction (Tab. 3)
Expected results:	virtual representation of the core process unit based on a steady state simulation model with manual data management, service and connection	virtual representation of the main process units based on a quasi steady state/dynamic simulation model with manual or semi-automated data management, service and connection	virtual representation of the complete process chain based on a dynamic/ad-hoc simulation model and virtualization with semi- or automated data management, service and connection	virtual representation of the complete process chain based on a predictive simulation model and virtualization with automated data management, service and connection
Virtual representation type:	Digital Model	Digital Shadow	Digital Twin	Digital Predictive Twin

Figure 4. Modeling readiness level along the process development lifecycle of energy technologies [109–111].

After 10 years of investigation, Müller S. proposed the modeling readiness level (MRL) [109], by analogy with the TRL for the physical facility, to evaluate the development progress of virtual representations. Therefore, the virtual representation should evolve together with the physical experimental or commercial facility. Subsequently, the virtual representation capability, intelligence, and fidelity must increase throughout the process development lifecycle based on observations carried out within experimental test rigs. The mentioned key observations within each process development stage in terms of process behavior, operation mode, considered infrastructure, and expected results are listed in Figure 4. The MRL serves as a support instrument for tracking the development of virtual representations and should always be one step ahead of the TRL to enable forward planning.

In Figure 4, the MRL throughout the process development lifecycle of energy technologies is discussed. By analogy with the TRL, the same process development lifecycle

stages are followed. In the concept and lab facility stage, TRLs 1–3 describe the way towards an experimentally proven core system. By analogy with the virtual representation in this process development stage, MRLs 1–3 are defined and range from the definition of operation and performance indication equations to the development of an integrated model library. During this first development stage, the temporal resolution is oriented towards the validation of the batch lab facility once per test run. The outcome shall be a virtual representation of the core process unit based on a steady-state simulation model with manual data management, service, and connection. For monitoring the sustainability and performance of the process in this development stage, first estimations of technical, environmental, and economic indicators based on the steady-state model are mandatory. Possible applications in this first stage for the virtual representation can be collaboration, documentation, simulation, or evaluation tasks as introduced in Table 3. Furthermore, the virtual representation types from digital model to digital predictive twin are linked with the process development lifecycle stages. In the concept and lab facility stage, all properties are connected to the virtual representation type of a digital model. The following pilot plant stage is covered by TRLs 4–5, validating the technology from laboratory to the real environment. Corresponding to the TRLs 4–5, the MRLs 4–5 define the creation and validation of a pilot plant model based on the main process units. Expected results in this stage are a virtual representation of the main process units based on a quasi-steady-state and dynamic simulation model with manual or semi-automated data management, service, and connection. The quasi-steady-state simulation model can observe and compare different operation points to find an optimum. Additionally, the dynamic model can display operation point changes and part-load observations to first consider monthly time-dependent operation behaviors caused by deviations of the input streams. The process performance analysis in this stage is based on the quasi-steady-state simulation model executed by reliable technical, environmental, and economic investigations. The virtual representation type in this stage is called “digital shadow”, and it enables applications in collaboration, documentation, simulation, evaluation, and verification and visualization. The demonstration plant stage is covered by TRLs 6–7: the technology and system prototype demonstration in a relevant and operational environment. Simultaneously, the demonstration plant phase is accompanied by MRLs 6–7. Demonstration plants are characterized by the realization of the complete process chain, including utility and product logistics for the first time. Therefore, the complete evaluation of all utility streams and sustainability indicators becomes possible at MRL 6. Besides the technical, environmental, and economic indicators, social indicators can be analyzed due to the definition of a location. MRL 7 describes the completion of the 3D and simulation model consisting of all subunits of the whole process chain, including utility and product logistics. Therefore, the expected result in the demonstration plant stage is a virtual representation of the complete process chain based on a dynamic and ad hoc simulation model and virtualization with semi-automated or automated data management, service, and connection. The dynamic simulation model can analyze long-term process behaviors such as fouling and aging as well as start-up and shutdown scenarios. The ad hoc simulation model enables the real-time observation of the physical process. The virtual representation in this stage is named the “digital twin”, and it enables most of the mentioned application fields according to Table 3, from collaboration to orchestration. The final commercial plant stage is characterized by TRLs 8–9, ranging from the complete and certified system to an approved market-ready competitive energy production plant in an operational environment. The corresponding MRL 8 describes the validation and evaluation of the virtual representation models by commercial energy plant facilities. Finally, MRL 9 is defined by the platform-based implementation, monitoring, and sharing of the virtual representation to enable a fast market penetration. The expected virtual representation in the final development stage includes the complete process chain based on a predictive simulation model and virtualization with automated data management, service, and connection. The expected results imply that the virtual representation, called

the digital predictive twin, can deal with all kinds of short-term and long-term behaviors to enable applications from collaboration to prediction (see Table 3).

The definition of the MRL paves the way to introducing a virtual representation framework, which should help to develop appropriate models in each process development stage.

3. Virtual Representation Framework in the Process Development Environment

Subsequently, a virtual representation framework in the context of the process development environment is defined to provide a guideline for creating and developing appropriate virtual representations throughout the process development lifecycle. First of all, it should be mentioned that each virtual representation concept focuses on sovereignty, confidentiality, and reliability [109]. Furthermore, the virtual representation framework shall be based on standardized replaceable modules, called block modeling, to develop widely applicable virtual representations [66]. In Section 1, different framework approaches related to different fields of applications are summarized. These frameworks differ according to entities and properties as well as the architecture regarding information and network level. Different network architectures imply, for example, different data processing approaches. Therefore, defining an appropriate, generally accepted virtual representation framework is complex. For the development of a widely applicable virtual representation framework in the energy sector, the subsequently introduced framework addresses the development of virtual representations throughout the process development lifecycle.

The following 5D virtual representation framework is based on the 5D model as mentioned in Section 2.2. In Figure 5, the proposed 5D framework for developing virtual representations in the process development environment is visualized. Therein, it can be seen that every virtual representation consists of five dimensions. Every dimension is based on several subunits. The arrows in the background symbolize the order of the subunits.

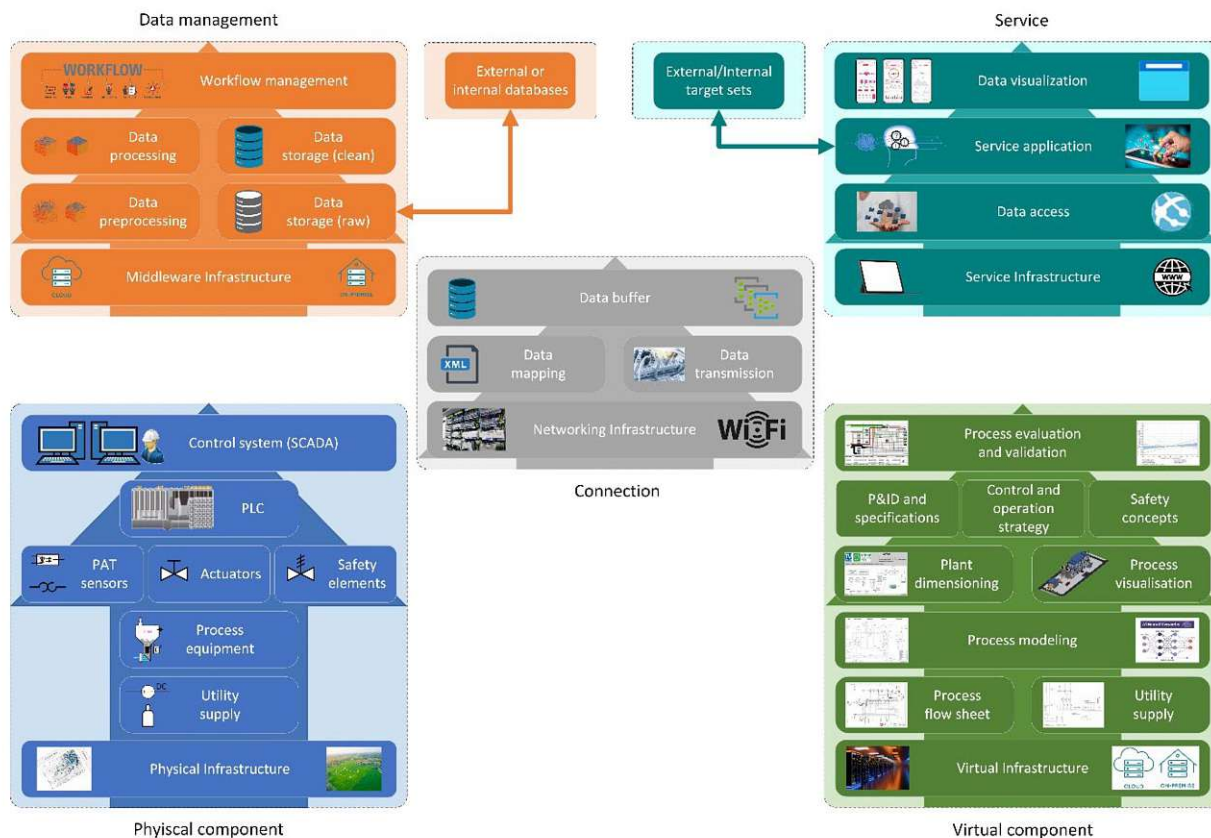


Figure 5. 5D virtual representation framework in the process development environment.

The physical component consists of the energy plant and the required physical infrastructure. This infrastructure includes the construction site and necessary utility supplies such as electricity, heat, or other process media. The most important part of the physical component is the process equipment, which is made up of the core energy production or conversion process units. Process analytical technology (PAT) sensors monitor the energy plant. PAT sensors comprise a wide range of analytical tasks, including thermocouples, pressure sensors, gas composition analytics, and orifice flowmeters for volume flow or other measurement applications. Actuators control the energy plant, for example, by manipulating valves. Safety elements are essential to prevent accidents and raise employee physical safety. To gather all the measuring and control signals from PAT sensors, actuators, and safety elements, one or more programmable logic controllers (PLCs) are used. The PLCs also form the interface between sensors, actuators, safety elements and the supervisory control and data acquisition system (SCADA). The data communication with other virtual representation dimensions can be realized by an interface to the SCADA system or directly from the PLCs.

The data management dimension is responsible for data handling. On the one hand, the data management is responsible for storing and processing the sensor data from the physical component out of the PLCs or SCADA system to feed the virtual component with appropriate datasets. On the other hand, data management also serves as an interface between the virtual component and service dimension to store and process modeling results. The data management dimension requires middleware infrastructure, which can be provided on premises via an edge device or cloud applications. The requirements of the middleware infrastructure are more or less driven by the desired services, the associated processing time, and the number of datasets. Data processing and data storage are often realized in two stages. Therefore, if the raw datasets from the physical component are large, the data preprocessing step is often set up on premises to realize a local filter to reduce the data size by condensing the datasets. The filtered datasets are stored in raw data storage, also often on premises, before the filtered data are transmitted to the cloud for a second processing step and to store the clean data properly. However, all these steps can also be realized exclusively on premises or within a cloud architecture. Additionally to the raw data from the physical component, further data from external databases such as analysis results from the laboratory can be merged with the filtered sensor values in the first storage stage. The last step within the data management dimension is workflow management. Workflow management systems are applied to arrange and streamline business processes [112]. Workflow management systems are mandatory in the case of complex workflow architecture.

Subsequently, the processed data from the data management are used in the virtual component to carry out the calculation, simulation, visualization, and specification tasks. All these subtasks are based on the virtual infrastructure, which can be analogous with the middleware infrastructure either on premises or based on cloud architecture or a mixture of both. In the first step, the process flowsheet and the utility supply build up the process layout, including all subunits and process media. The following process modeling is the core unit of the virtual component. Therein, physical-based or semantic data-based models describe the process behavior based on the defined process layout and media. In terms of physical modeling approaches, for example, mass and energy balances, kinetic approaches or computational fluid dynamics help to define input and output process flows as well as more detailed reaction and fluid dynamic behaviors [113]. Semantic modeling comprises all data-based approaches concerning machine learning, deep learning, ontology modeling approaches, and many more [20]. In terms of an engineering approach, the process simulation results serve as the input for plant dimensioning to define and optimize the geometry of all subprocess units. The following process visualization enables the illustration of the whole system. It should be mentioned that the engineering process is iterative. In terms of virtual representation applications, the process visualization (3D model) together with the process model can be seen as the core units to realize high-

fidelity results and an immersive experience. On the basis of the 3D model, the piping and instrumentation diagram (P&ID), specifications, the control and operation strategy and safety concepts can be prepared. Refer to [76] for further details of engineering workflows and documents. Finally, the designed and optimized process should be validated based on sensitivity analysis, plausibility checks and domain knowledge. The process evaluation on the basis of the sustainability indicators helps assess the considered process and compare it with the best available competing technologies.

The service dimension is required to execute desired applications, ranging from data visualization for monitoring to process automation. By analogy with all the other dimensions, the service infrastructure delivers the architecture for developing the desired service. These can be local or web-based services hosted on premises or on cloud-based infrastructure. Provided services are physically separated within a multitier architecture. The most well-known framework for services is the three-tier architecture [114]. The three-tier architecture consists of a data access tier, the application tier and the data visualization or presentation tier. Within the data access layer, data from the data management and virtual component dimension are retrieved and processed to the service application layer. The service application layer builds up the logic of the service, where decisions and control take place. This can either be caused by internal or external target sets, which can be triggered through users or predefined functional units. The data visualization is the presentation layer, where services can be accessed through an appropriate user interface.

Finally, the connection layer represents the interface between the other dimensions. The data connection is based on networking infrastructure. The required networking infrastructure is driven by the desired service and can be, on the one hand, local networks such as fieldbus systems, wireless networks, or mobile networks [115]. On the other hand, global infrastructure such as the broadband internet via ethernet can be used [115]. The data connection is divided into data mapping and data transmission. The seven-layer ISO OSI reference model [116] describes the universal standard for data communication. Therein, each layer is required for particular tasks. The data transmission summarizes all transport-oriented layers from the physical to the transport layer [116]. The application-oriented layers are summarized as data mapping subunits, where the data structure is determined. For example, TCP IP data transport via ethernet protocol can be assigned to the data transmission [6]. Well-known data mapping protocols include FTP, HTTP, MQTT, and OPC UA [6,73]. The data buffer is responsible for intermediate storage or queuing data packets to supply the application with appropriate datasets.

The five dimensions of physical and virtual components, data management, service, and connection together form the 5D virtual representation framework in the process development environment. It should be mentioned that data sovereignty, confidentiality, and reliability are the overarching goals. The framework is formed by interchangeable functional blocks based on standardized models, protocols, and guidelines. Additionally, the overall MRL level classified into the process development phases concept and lab facility, pilot plant, demonstration plant and the commercial plant can be linked with the five dimensions of virtual representations and the overall virtual representation properties. Table 6 gives an overview of mandatory dimension properties and overall virtual representation properties along the process development lifecycle. Therefore, each virtual representation dimension and subunit must evolve within each process development stage. Regarding the physical component, the physical infrastructure has to be extended from the core process unit in the concept and lab facility stage to the complete process chain in the commercial plant development stage. The decentral utility supply at the beginning of the development lifecycle must be replaced by fully integrated utility supply logistics at the end of the process development. The SCADA system shall be evolved from an automation system in the lab facility to a fully integrated process control system in the commercial plant. The virtual component steady-state simulation models have to be replaced stage-wise towards a fully predictive simulation model supplemented by virtualization of the complete process chain. The data management, service, and connection dimensions

start with manual processes in the concept and lab facility stage towards fully automated processes in the commercial plant.

Table 6. Overall virtual representation properties within the 5D model approach.

Property Classes and Components	Focus	Concept, Lab Facility	Pilot Plant	Demonstration Plant	Commercial Plant
Scalability	Overall properties	Level 0: Equipment level	Level 1: Plant level	Level 2: Enterprise level	Level 3: Energy system level
Interoperability		Level 0: Comparable		Level 1: Convertible	Level 2: Standardized
Expansibility		Level 0: Fixed layout	Level 1: Adaptable layout	Level 2: Automated layout	
Functional safety		Level 0: Systematic capability	Level 1: Implemented redundancies	Level 2: Predictable failure analysis	Level 3: Automated replacement
Physical component	Virtual representation dimensions (5D)	Core process unit with decentral utility supply and automation system	Main process units with decentral utility supply and process control system	Complete process chain with central utility supply, product use and process control system	Complete process chain with fully integrated utility supply, product logistics and process control system
Virtual component		Steady-state simulation model of core process unit available	Quasi-steady-state simulation model of main process units available	Dynamic simulation model and virtualization of complete process chain available	Predictive simulation model and virtualization of complete process chain available
Data management		Manual data processing and storage approaches	Manual or semi-automated data processing and storage approaches	Semi- or automated data processing and storage approaches	Automated data processing and storage approaches with integrated workflow management
Service		Manual service application	Manual or semi-automated service application	Semi- or automated service application	Automated service application
Connection		Manual data communication	Manual or semi-automated data communication	Semi- or fully automated data communication	Automated data communication
Virtual representation type		Digital Model (MRL 1–3)	Digital Shadow (MRL 4–5)	Digital Twin (MRL 6–7)	Digital Predictive Twin (MRL 8–9)

Table 6 shows that the overall properties, as discussed in Section 2.3, namely scalability, interoperability, expansibility, and functional safety, are also linked with the MRL and development stages. The scalability indicates the possibility of evolution of virtual representations regarding the use within different energy plant hierarchy layers [73]. The virtual representation scalability in the concept and lab facility is on the equipment level because only the core process unit is available. The scalability reaches the energy system level in the commercial plant stage to connect the virtual representation with external stakeholders such as grid operators or suppliers. The virtual representation interoperability evolves towards standardized units, which means that all functional blocks are based on standard-

ized models to enable cross-linking with other virtual representation environments. The expansibility refers to the flexibility of the used functional blocks to realize flexible layouts regarding replacing subunits or changes in the process streamline. Finally, functional safety should be evolved from systematic fault detection to the automated replacement of defective subunits.

The linkage of virtual representation properties with the MRL can also be enlarged to the dimension level, as outlined in Table 4. Not all proposed properties are mandatory for the desired services in the considered development stage. However, the virtual representation framework has to evolve to cover the proposed properties and requirements in each process development stage to ensure maximum freedom regarding possible services. In summary, each dimension has to evolve throughout the process development lifecycle. The physical component has to evolve from a core process unit in the concept and lab scale phase to a fully developed complete process chain in the commercial plant phase. Besides the development of the process equipment and utility supply, the physical safety and degree of automation has to evolve, and the possibility for scaling up must be approved along the process development lifecycle. The virtual component has to evolve from a steady-state simulation model to a predictive simulation model and virtualization of the energy technology to preserve the full knowledge of behavior. Consequently, the virtual representation capability, fidelity, and intelligence has to evolve. For realizing virtual representations for commercial plants, the manual data processing, storage, and communication approaches in the data management and connection dimension has to be replaced continuously by automated approaches throughout the lifecycle. The evolution of the data management and connection dimension can be evaluated by the virtual representation properties' connectivity mode, data integration level, update frequency, and cybersecurity. The foreseen services along the process development lifecycle will change. Therefore, the service dimension has to evolve as well.

Ultimately, a biomass-to-gas production route is utilized to explain the benefits of the virtual representation framework. The described technology is based on a dual fluidized bed gasification unit to convert biomass into product gas. Afterward, this product gas is cleaned in several steps to reach syngas quality. Within the methanation unit, the syngas is converted into raw Bio-SNG. After some upgrading steps, the Bio-SNG fulfills all requirements and can be fed into the gas grid system. The 1 MW Bio-SNG plant in Güssing, commissioned in 2008, represents the world's first synthetic natural gas production unit based on woody biomass at a demo scale [117]. In 2009, the Bio-SNG process was demonstrated successfully at a scale of 1 MW in Güssing [117]. The gasification unit in Güssing was operated for more than 10 years and had reached over 7500 operation hours by 2012. Based on this achievement, a 20 MW Bio-SNG plant in Gothenburg was planned, erected and operated. However, the 20 MW Bio-SNG demonstration plant could not reproduce the high number of operating hours in the gasification unit [102,118,119]. Several shutdowns occurred due to problems with the biomass feeding system, cooler clogging, and oscillating syngas quality [119]. Subsequently, this leads to the question of why the learned lessons from Güssing could not be transferred to Gothenburg. There could be several reasons, such as different utilities or other technical aspects. Furthermore, changing engineering companies might lead to a loss of domain knowledge.

All these problems can be improved by applying the raised 5D virtual representation framework. The quasi-steady-state simulation model from Güssing [117] was not suitable for condensing all lessons learned in a virtual model. Therefore, it is essential that the MRL is always one step ahead of the TRL to enable forward planning and anticipate future behavior. Furthermore, the virtual representation should always be able to process and reproduce gained knowledge from test runs. This would help to avoid recurring technology issues. To tackle the described issues, the research project ADORe-SNG [120] has been initiated to develop a virtual representation of the Bio-SNG route at a pilot scale. A digital predictive twin was developed to optimize the pilot-scale Bio-SNG production route. In

Figure 6, the virtual representation framework for the digital twin use case of the Bio-SNG production route is visualized.

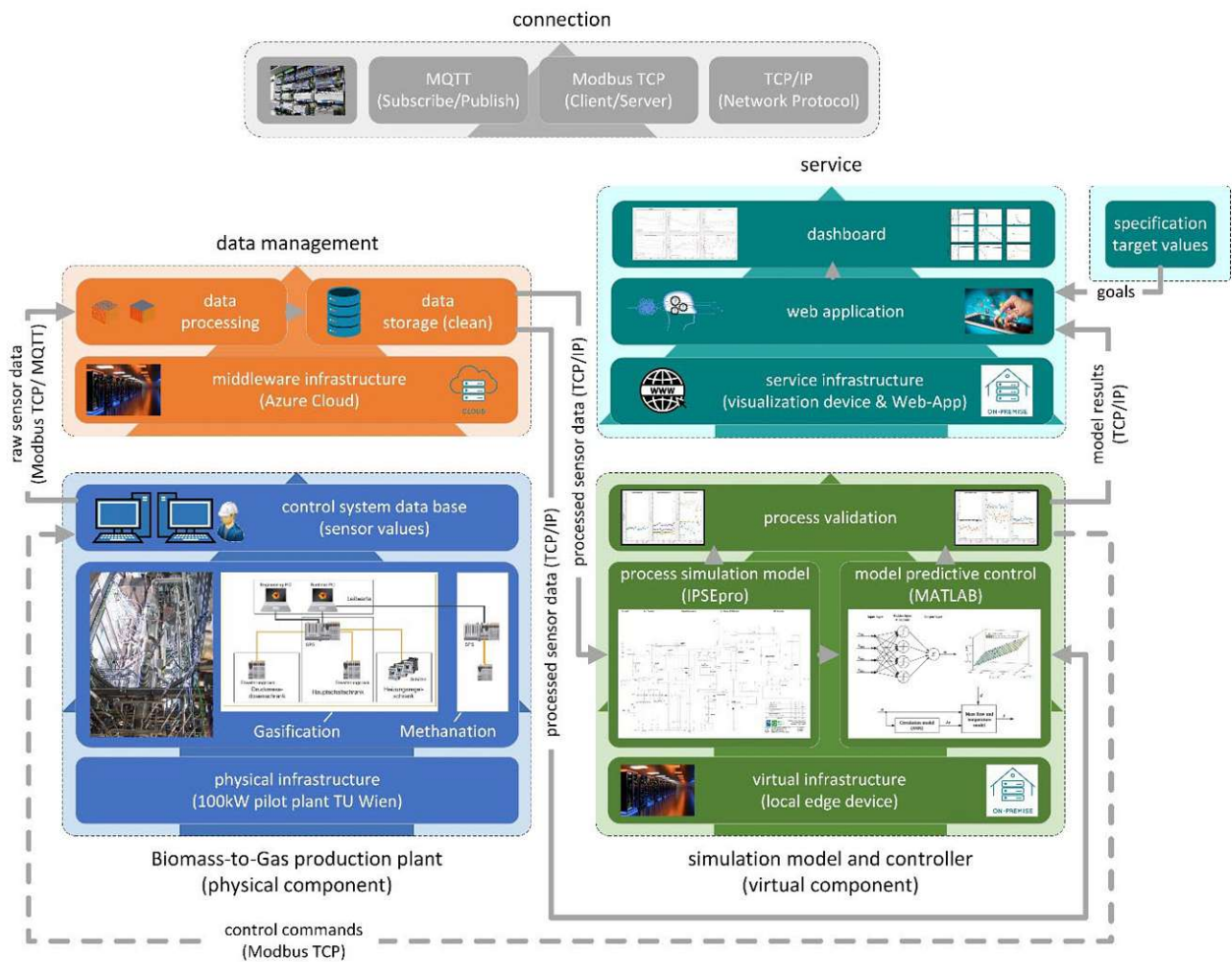


Figure 6. 5D virtual representation framework Bio-SNG route adapted from [121–123].

Within this project, a digital twin was implemented for the operation optimization of the 100 kW Bio-SNG pilot plant from TU Wien. The pilot plant is monitored and controlled via the APROL control system, which represents the top layer of the physical component. The raw sensor data are sent in real-time from the control system to the cloud-based data management. Afterwards, the real-time processed sensor data are sent every minute to the process simulation model in IPSEpro 8.0 and every five seconds to the model predictive control unit in MATLAB R2021b. The process simulation model helps to determine the present state of the process by the use of an overdetermined quasi-steady-state model. Furthermore, the consolidation of all measurement values as well as the determination of non-measurable variables is possible. The model predictive control unit helps to predict the plant's behavior as a function of the manipulated variables by the use of a gray-box-based dynamic model. With the help of the model predictive control unit, a full automation of the plant can be reached. The results from the process simulation model are used in the model predictive control unit to parametrize the dynamic model every minute. The results from the process simulation model and the model predictive control unit are validated in the final step from the virtual component dimension. Then, the model results are handed over to the service dimension, where finally a web application is used for the real-time data visualization. The results from the process simulation model are mostly sustainability indicators such as process efficiencies and yields. The results from the model predictive

control unit are predictions for several manipulated variables to reach user-defined target values, which can be also defined within the web-application by the operator. Finally, the validated results from the model predictive control unit in the form of modifications of manipulated variables are returned to the control system to realize a fully automated closed-loop system [121–123].

The digital twin for the pilot plant of the Bio-SNG production route is already implemented and operational with real-time data. Moreover, an optimized operation point could be reached and held by the controller. Long-term operation of the digital twin is planned soon. The results from comparable control concepts showed that the fuel consumption could be reduced by 5%, while the product gas amount remained constant [124]. Furthermore, the number of operators can be reduced due the process automation.

Finally, the developed virtual representation framework can accompany further engineering and demonstration processes at a larger scale to gain better knowledge about process behavior and to gather this domain knowledge within the virtual representation. Based on these investigations, the concept should be validated at a 1 MW demonstration scale dual fluidized bed gasification plant in Vienna in Simmering. Further, a Bio-SNG plant in Güssing [125] and a 5 MW demonstration plant in Austria [102] are in the planning stage.

4. Conclusion and Outlook

The scope of this publication was the development of a virtual representation framework in the process development environment. The progress of process development can be monitored by introducing the novel modeling readiness level. Therefore, the modeling readiness level serves as a support for tracking the development of virtual representations and should always be one step ahead of the technology readiness level to enable forward planning.

Each virtual representation consists of five dimensions and should be based on the state-of-the-art models, which evolve along the process development lifecycle. The virtual representation framework is based on a novel definition, which implies that every virtual representation, independent of the process development and lifecycle phase, should fulfill the following statements:

- The virtual representation is a digital reflection of the physical facility;
- The virtual component contains an abstracted model that is fitted as close as necessary to the physical component through the integration of measured values and domain knowledge;
- The level of integration and model abstraction can differ in each stage, depending on the application.

The energy plant lifecycle perspectives and energy plant hierarchy layers are raised to obtain an overall picture of the different players and phases during a process development cycle. Virtual representation applications are summarized to show the variety of services that can be enabled due to the evolution of a virtual representation. Subsequently, possible virtual representation applications should always be defined to ensure a suitable framework. Challenges for the implementation of virtual representations are discussed to guide the development of frameworks. Additionally, properties of virtual representations are defined to address the evolutionary possibilities in each virtual representation dimension. Furthermore, the most common sustainability indicators are collected to enable a harmonized process evaluation through the integration of development goals in each lifecycle phase. The novel model readiness level is introduced to couple the virtual representation's evolution with the physical facility's process development. Therefore, the knowledge gained due to experimental test runs is preserved in the virtual component. Following the raised virtual representation framework, the final technology readiness level, which implies the proof of concept in a commercial environment, can only be reached if full knowledge of the behavior can be predicted with the accompanying virtual representation. Finally, the virtual representation framework determines the possible subunits for each dimension

in the scope of the process development framework. The five virtual representation dimensions are also linked throughout the process development lifecycle phases with the modeling readiness level and accompanying overall properties.

Summing up, the presented virtual representation framework in the scope of the process development environment enables the standardization of the virtual representation development along the process development lifecycle. Therefore, the knowledge gained from the experimental test runs is preserved, the process development is always based on state-of-the-art models and the scale-up is not executed too early.

However, future research should focus on the validation of the novel virtual representation framework. Therefore, several process development cases of different energy technologies should be accompanied by the proposed methodology. Furthermore, it is essential to note that, independent of the virtual representation evolution stage, the sovereignty, confidentiality, and reliability of the monitored energy technology are prioritized. Finally, the virtual representation framework should be built on standardized, exchangeable block models in each dimension to enable fast adaptations depending on the addressed application. To conclude, the introduced virtual representation framework helps to enable smart interconnected energy systems. This is reached by accompanying the whole process development lifecycle with a suitable virtual representation from the beginning.

Author Contributions: Conceptualization, M.H., D.C.R., A.B., F.B. and S.M.; methodology, M.H., D.C.R., A.B., F.B., J.F. and S.M.; validation, M.H., A.B., F.B., J.F. and S.M.; investigation, M.H., D.C.R., A.B. and F.B.; resources, M.H., D.C.R., A.B. and F.B.; writing—original draft preparation, M.H., D.C.R. and A.B.; writing—review and editing, F.B., J.F. and S.M.; visualization, M.H., A.B. and F.B.; supervision, S.M.; project administration, F.B. and S.M.; funding acquisition, F.B. and S.M. All authors have read and agreed to the published version of the manuscript.

Funding: The present work contains results of the project ADORe-SNG (881135), which is being conducted within the “Energieforschung” research program funded by the Austrian Climate and Energy Fund and processed by the Austrian Research Promotion Agency (FFG). The authors acknowledge TU Wien Bibliothek for financial support through its Open Access Funding Programme.

Data Availability Statement: Selected data that support the findings of this study are available from the corresponding author, M. Hammerschmid, upon reasonable request. Furthermore, it has to be mentioned that the review was not registered, and no review protocol was prepared.

Conflicts of Interest: The authors declare no conflict of interest.

Abbreviations

3D	three-dimensional
5D	five-dimensional
Bio-SNG	biomass-based synthetic natural gas produced via gasification and methanation
CH ₄	methane
CO ₂	carbon dioxide
CO ₂ -eq	carbon dioxide equivalent
DT	digital twin
EU	European Union
FTP	file transfer protocol
GDP	gross domestic product
GRP	gross regional product
ISO	International Organization for Standardization
H ₂ O	water
Horizon 2020	framework program funding research, technological development and innovation
HTTP	hypertext transfer protocol
KPI	key performance indicators

LCA	lifecycle assessment
MRL	modeling readiness level
MQTT	message queuing telemetry transport
N ₂ O	nitrous oxide
NASA	National Aeronautics and Space Administration
NO _x	nitrous oxide (general form)
OPC UA	open platform communications unified architecture
OSI	open systems interconnection
P&ID	pipng and instrumentation diagram
PAT	process analytical technology
PLC	programmable logic controller
PLM	product lifecycle management
RED II	Renewable Energy Directive
Ref.	reference
SCADA	supervisory control and data acquisition
SDG	sustainable development goals
SO ₂	sulfur dioxide
SO ₂ -eq	sulfur dioxide equivalent
SO _x	sulfur oxide (general form)
TCP IP	transmission control protocol/internet protocol
TRL	technology readiness level
Symbols	
%	percent
a	number of years
FLH/a	full load hours per year
FU	functional unit
g PO ₄ ²⁻ -eq	grams of phosphate equivalent
g SO ₂ -eq	grams of sulfur dioxide equivalent
kg 1,4-DB-eq	kilograms of dichlorobenzene equivalent
kg CO ₂ -eq	kilograms of carbon dioxide equivalent
kg H ₂ O	kilograms of water
kg NMVOC	kilograms of non-methane volatile organic compounds
kg PM ₁₀ -eq	kilograms of particulate matter equivalent with a particle size smaller than 10 μm
kg R-11-eq	kilograms of trichlorofluoromethane equivalent
kg Sb-eq	kilograms of antimony equivalents
kWh _{el}	kilowatt hours of electrical energy
m ²	square meter
MJ	megajoule
MW	megawatt

References

- Mertens, P.; Barbian, D.; Baier, S. *Digitalisierung und Industrie 4.0—Eine Relativierung*; Springer: Wiesbaden, Germany, 2017. [CrossRef]
- Hofmann, R.; Halmschlager, V.; Knöttner, S.; Leitner, B.; Pernsteiner, D.; Prendl, L.; Sejkora, C.; Steindl, G.; Traupmann, A. *Digitalization in Industry—An Austrian Perspective*; TU Wien: Vienna, Austria, 2020.
- European Union. 2030 Climate and Energy Policy Framework. Brussels, Belgium. 2014. Available online: https://climate.ec.europa.eu/eu-action/climate-strategies-targets/2030-climate-energy-framework_en (accessed on 12 October 2022).
- European Union. Directive (EU) 2018/2001 of the European Parliament and of the Council of 11 December 2018 on the Promotion of the Use of Energy from Renewable Sources, RED II. Official Journal of the European Union. 2018. Available online: <https://eur-lex.europa.eu/legal-content/DE/TXT/PDF/?uri=CELEX:32018L2001&from=EN> (accessed on 12 October 2022).
- O'Dwyer, E.; Pan, I.; Acha, S.; Shah, N. Smart energy systems for sustainable smart cities: Current developments, trends and future directions. *Appl. Energy* **2019**, *237*, 581–597. [CrossRef]
- Liu, Q.; Chen, J.; Liao, Y.; Mueller, E.; Jentsch, D.; Boerner, F.; She, M. An Application of Horizontal and Vertical Integration in Cyber-Physical Production Systems. In Proceedings of the 2015 International Conference on Cyber-Enabled Distributed Computing and Knowledge Discovery, Xi'an, China, 17–19 September 2015; pp. 110–113. [CrossRef]
- Borowski, P.F. Digitization, Digital Twins, Blockchain, and Industry 4.0 as Elements of Management Process in Enterprises in the Energy Sector. *Energies* **2021**, *14*, 1885. [CrossRef]

8. Bentolila, M.; Alshanski, I.; Novoa, R.; Gilon, C. Optimization of Chemical Processes by the Hydrodynamic Simulation Method (HSM). *ChemEngineering* **2018**, *2*, 21. [\[CrossRef\]](#)
9. Kritzing, W.; Karner, M.; Traar, G.; Henjes, J.; Sih, W. Digital Twin in manufacturing: A categorical literature review and classification. *IFAC PapersOnLine* **2018**, *51*, 1016–1022. [\[CrossRef\]](#)
10. Grafinger, M. *Virtuelle Produktentwicklung: Lecture Notes LVA 307.414*; TU Wien, Institute of Engineering Design and Product Development: Vienna, Austria, 2020.
11. Maniatis, K.; Landäl, I.; Waldheim, L.; van den Heuvel, E.; Kalligeros, S. *Building Up the Future—Cost of Biofuel: Subgroup on Advanced Biofuels—Sustainable Transport Forum*; European Commission: Brussels, Belgium, 2017. [\[CrossRef\]](#)
12. Szeghó, K.; Bercsey, T. Kosten- und Risikomanagement in der frühen Phase der Produktentwicklung. In Proceedings of the 18th Symposium „Design for X“, Neukirchen/Erlangen, Germany, 11–12 October 2007.
13. Ehrlenspiel, K.; Kiewert, A.; Lindemann, U.; Mörtl, M. *Kostengünstig Entwickeln und Konstruieren: Kostenmanagement bei der Integrierten Produktentwicklung. Auflage*; Springer: Berlin, Germany, 2020. [\[CrossRef\]](#)
14. Schulte, R. Rechnergestütztes Normteilemanagement als Beitrag zu Einem Optimierten Produktionsplanungsprozess in der Automobilindustrie. Ph.D. Thesis, Fakultät für Maschinenbau, Helmut-Schmidt-Universität/Universität der Bundeswehr Hamburg, Hamburg, Germany, 2013.
15. Leistner, B. Fahrwerkentwicklung und Produktionstechnische Integration ab der Frühen Produktentstehungsphase. In *Wissenschaftliche Reihe Fahrzeugsystemdesign*; Springer: Wiesbaden, Germany, 2019. [\[CrossRef\]](#)
16. Weber, C.; Husung, S.; Cascini, G.; Cantamessa, M.; Marjanovic, D.; Rotini, F. Product Modularisation, Product Architecture, Systems Engineering, Product Service Systems. In Proceedings of the 20th International Conference on Engineering Design (ICED15), Politecnico di Milano, Politecnico di Torino, Design Society, Milan, Italy, 27–30 July 2015; ISBN 978-1-904670-70-4.
17. Resch, G.; Kranzl, L.; Faninger, G.; Geipel, J. *Block 1: Introduction: Energy & Climate Challenge and Basics of Economic Assessment. Lecture Notes Economic Perspectives of Renewable Energy Systems*; TU Wien, Institute of Energy Systems and Electrical Drives: Vienna, Austria, 2020.
18. Chau, C.K.; Leung, T.M.; Ng, W.Y. A review on Life Cycle Assessment, Life Cycle Energy Assessment and Life Cycle Carbon Emissions Assessment on buildings. *Appl. Energy* **2015**, *143*, 395–413. [\[CrossRef\]](#)
19. Tao, F.; Zhang, H.; Liu, A.; Nee, A.Y.C. Digital Twin in Industry: State-of-the-Art. *IEEE Trans. Ind. Inform.* **2018**, *15*, 2405–2415. [\[CrossRef\]](#)
20. Liu, M.; Fang, S.; Dong, H.; Xu, C. Review of digital twin about concepts, technologies, and industrial applications. *J. Manuf. Syst.* **2021**, *58*, 346–361. [\[CrossRef\]](#)
21. Chen, Y.; Yang, O.; Sampat, C.; Bhalode, P.; Ramachandran, R.; Ierapetritou, M. Digital Twins in Pharmaceutical and Biopharmaceutical Manufacturing: A Literature Review. *Processes* **2020**, *8*, 1088. [\[CrossRef\]](#)
22. Jones, D.; Snider, C.; Nassehi, A.; Yon, J.; Hicks, B. Characterising the Digital Twin: A systematic literature review. *CIRP J. Manuf. Sci. Technol.* **2020**, *29*, 36–52. [\[CrossRef\]](#)
23. Onile, A.E.; Machlev, R.; Petlenkov, E.; Levron, Y.; Belikov, J. Uses of the digital twins concept for energy services, intelligent recommendation systems, and demand side management: A review. *Energy Rep.* **2021**, *7*, 997–1015. [\[CrossRef\]](#)
24. Aheleroff, S.; Xu, X.; Zhong, R.Y.; Lu, Y. Digital Twin as a Service (DTaaS) in Industry 4.0: An Architecture Reference Model. *Adv. Eng. Inform.* **2021**, *47*, 101225. [\[CrossRef\]](#)
25. Qi, Q.; Tao, F. Digital Twin and Big Data Towards Smart Manufacturing and Industry 4.0: 360 Degree Comparison. *IEEE Access* **2018**, *6*, 3585–3593. [\[CrossRef\]](#)
26. Liu, Q.; Liu, B.; Wang, G.; Zhang, C. A comparative study on digital twin models. *AIP Conf. Proc.* **2019**, *2073*, 020091. [\[CrossRef\]](#)
27. Negri, E.; Fumagalli, L.; Macchi, M. A Review of the Roles of Digital Twin in CPS-based Production Systems. *Procedia Manuf.* **2017**, *11*, 939–948. [\[CrossRef\]](#)
28. Holler, M.; Uebernickel, F.; Brenner, W. Digital Twin Concepts in Manufacturing Industries—A Literature Review and Avenues for Further Research. In Proceedings of the International Conference on Industrial Engineering, Seoul, Republic of Korea, 10–12 October 2016.
29. Sharma, A.; Kosasih, E.; Zhang, J.; Brintrup, A.; Calinescu, A. Digital Twins: State of the art theory and practice, challenges, and open research questions. *J. Ind. Inf. Integr.* **2022**, *30*, 383. [\[CrossRef\]](#)
30. Singh, M.; Fuenmayor, E.; Hinchy, E.P.; Qiao, Y.; Murray, N.; Devine, D. Digital Twin: Origin to Future. *Appl. Syst. Innov.* **2021**, *4*, 36. [\[CrossRef\]](#)
31. Juarez, M.G.J.; Botti, V.J.; Giret, A.S. Digital Twins: Review and Challenges. *J. Comput. Inf. Sci. Eng.* **2021**, *21*, 030802. [\[CrossRef\]](#)
32. Moreno, A.; Velez, G.; Ardanza, A.; Barandiaran, I.; de Infante, R.; Chopitea, R. Virtualisation process of a sheet metal punching machine within the Industry 4.0 vision. *Int. J. Interact. Des. Manuf.* **2017**, *11*, 365–373. [\[CrossRef\]](#)
33. Lu, Y.; Liu, C.; Kevin, I.; Wang, K.; Huang, H.; Xu, X. Digital Twin-driven smart manufacturing: Connotation, reference model, applications and research issues. *Robot. Comput. Integr. Manuf.* **2020**, *61*, 101837. [\[CrossRef\]](#)
34. Schluse, M.; Rossmann, J. From Simulation to Experimentable Digital Twins: Simulation-Based Development and Operation of Complex Technical Systems. In Proceedings of the 2016 IEEE International Symposium on Systems Engineering (ISSE), Edinburgh, UK, 3–5 October 2016; pp. 1–6. [\[CrossRef\]](#)
35. Schluse, M.; Priggemeyer, M.; Atorf, L.; Rossmann, J. Experimentable Digital Twins—Streamlining Simulation-Based Systems Engineering for Industry 4. *IEEE Trans. Ind. Inform.* **2018**, *14*, 1722–1731. [\[CrossRef\]](#)

36. Dahmen, U.; Rossmann, J. Experimentable Digital Twins for a Modeling and Simulation-Based Engineering Approach. In Proceedings of the 2018 IEEE International Systems Engineering Symposium (ISSE), Rome, Italy, 1–3 October 2018; pp. 1–8. [\[CrossRef\]](#)
37. Uhlemann, T.H.-J.; Lehmann, C.; Steinhilper, R. The Digital Twin: Realizing the Cyber-Physical Production System for Industry 4. In Proceedings of the 24th CIRP Conference on Life Cycle Engineering, Kamakura, Japan, 8–10 March 2017; Volume 61, pp. 335–340. [\[CrossRef\]](#)
38. Trabesinger, S.; Pichler, R.; Schall, D.; Gfrerer, R. Connectivity as a prior challenge in establishing CPPS on basis of heterogeneous IT-software environments. *Procedia Manuf.* **2019**, *31*, 370–376. [\[CrossRef\]](#)
39. Yun, S.; Park, J.-H.; Kim, W.-T. Data-Centric Middleware Based Digital Twin Platform for Dependable Cyber-Physical Systems. In Proceedings of the 2017 Ninth International Conference on Ubiquitous and Future Networks (ICUFN), Milan, Italy, 4–7 July 2017; pp. 922–926.
40. Smarslok, B.; Culler, A.; Mahadevan, S. Error Quantification and Confidence Assessment of Aerothermal Model Predictions for Hypersonic Aircraft. In Proceedings of the 53rd AIAA/ASME/ASCE/AHS/ASC Structures, Structural Dynamics and Materials Conference, Honolulu, Hawaii, 23–26 April 2012; p. 1817. [\[CrossRef\]](#)
41. TU Wien. Pilotfabrik der TU Wien—Industrie 4.0. 2022. Available online: <https://www.pilotfabrik.at/> (accessed on 13 October 2022).
42. Pires, F.; Cachada, A.; Barbosa, J.; Moreira, A.P.; Leitao, P. Digital Twin in Industry 4.0: Technologies, Applications and Challenges. In Proceedings of the IEEE 17th International Conference on Industrial Informatics (INDIN), Helsinki, Finland, 22–25 July 2019; pp. 721–726. [\[CrossRef\]](#)
43. Sierla, S.; Azangoo, M.; Fay, A.; Vyatkin, V.; Papakonstantinou, N. Integrating 2D and 3D Digital Plant Information Towards Automatic Generation of Digital Twins. In Proceedings of the 2020 IEEE 29th International Symposium on Industrial Electronics, Delft, The Netherlands, 17–19 June 2020; pp. 460–467. [\[CrossRef\]](#)
44. Stark, R.; Damerau, T. Digital Twin. In *CIRP Encyclopedia of Production Engineering*; Springer: Berlin/Heidelberg, Germany, 2020. [\[CrossRef\]](#)
45. Stark, R.; Fresemann, C.; Lindow, K. Development and operation of Digital Twins for technical systems and services. *CIRP Ann.* **2019**, *68*, 129–132. [\[CrossRef\]](#)
46. Herwig, C.; Pörtner, R.; Möller, J. Digital twins: Applications to the Design and Optimization of Bioprocesses. In *Advances in Biochemical Engineering, Biotechnology*; Springer: Berlin/Heidelberg, Germany, 2021; Volume 177, ISBN 13:978-3030716554.
47. Herwig, C.; Pörtner, R.; Möller, J. Tools and Concepts for Smart Biomanufacturing. In *Advances in Biochemical Engineering, Biotechnology*; Springer: Berlin/Heidelberg, Germany, 2021; Volume 176, ISBN 13:978-3030716592.
48. Grieves, M. Digital Twin: Manufacturing Excellence through Virtual Factory Replication. White Paper. 2015. Available online: <https://www.3ds.com/fileadmin/PRODUCTS-SERVICES/DELMIA/PDF/Whitepaper/DELMIA-APRISO-Digital-Twin-Whitepaper.pdf> (accessed on 13 October 2022).
49. Glaessgen, E.; Stargel, D. The Digital Twin Paradigm for Future NASA and U.S. Air Force Vehicles. In Proceedings of the 53rd AIAA/ASME/ASCE/AHS/ASC Structures, Structural Dynamics and Materials Conference, Honolulu, HI, USA, 23–26 April 2012. [\[CrossRef\]](#)
50. Garetti, M.; Rosa, P.; Terzi, S. Life Cycle Simulation for the design of Product–Service Systems. *Comput. Ind.* **2012**, *63*, 361–369. [\[CrossRef\]](#)
51. Rosen, R.; von Wichert, G.; Lo, G.; Bettenhausen, K.D. About The Importance of Autonomy and Digital Twins for the Future of Manufacturing. *IFAC PapersOnLine* **2015**, *48*, 567–572. [\[CrossRef\]](#)
52. Gabor, T.; Belzner, L.; Kiermeier, M.; Beck, M.T.; Neitz, A. A Simulation-Based Architecture for Smart Cyber-Physical Systems. In Proceedings of the 2016 IEEE International Conference on Autonomic Computing (ICAC), Wuerzburg, Germany, 17–22 July 2016; pp. 374–379. [\[CrossRef\]](#)
53. Liu, Z.; Meyendorf, N.; Mrad, N. The role of data fusion in predictive maintenance using digital twin. *AIP Conf. Proc.* **2018**, *1949*, 020023. [\[CrossRef\]](#)
54. Vrabič, R.; Erkoyuncu, J.A.; Butala, P.; Roy, R. Digital twins: Understanding the added value of integrated models for through-life engineering services. *Procedia Manuf.* **2018**, *16*, 139–146. [\[CrossRef\]](#)
55. Srai, J.; Settanni, E.; Tsolakis, N.; Aulakh, P. Supply Chain Digital Twins: Opportunities and Challenges Beyond the Hype. In Proceedings of the 23rd Cambridge International Manufacturing Symposium 2019, Cambridge, UK, 26–27 September 2019. [\[CrossRef\]](#)
56. Tuegel, E.; Ingraffea, A.R.; Eason, T.G.; Spottswood, S.M. Reengineering Aircraft Structural Life Prediction Using a Digital Twin. *Int. J. Aerosp. Eng.* **2011**, *2011*, 154798. [\[CrossRef\]](#)
57. Qi, Q.; Tao, F.; Hu, T.; Anwer, N.; Liu, A.; Wei, Y.; Wang, L.; Nee, A. Enabling technologies and tools for digital twin. *J. Manuf. Syst.* **2019**, *58*, 3–21. [\[CrossRef\]](#)
58. Güntner, G.; Hoher, S.; Eberle, M.; Glachs, D.; Kranzer, S.; Schäfer, G.; Schranz, C. Digital Twins im Anlagen-Lebenszyklus. Digitales Transferzentrum Salzburg. 2020. Available online: https://www.salzburgresearch.at/wp-content/uploads/2020/09/Digital_Twin_WP-final-1.pdf (accessed on 13 October 2022).

59. Boschert, S.; Heinrich, C.; Rosen, R. Next Generation Digital Twin. In Proceedings of the 12th International Symposium on Tools and Methods of Competitive Engineering (TMCE), Las Palmas de Gran Canaria, Spain, 7–11 May 2018; pp. 209–218, ISBN 978-94-6186-910-4.
60. Boschert, S.; Rosen, R. Digital Twin—The Simulation Aspect. In *Mechatronic Futures*; Hehenberger, P., Bradley, D., Eds.; Springer International Publishing: Cham, Switzerland, 2016; pp. 59–74. [CrossRef]
61. Müller, S.; Schmid, J.C.; Hofbauer, H. Holzgas—Wärme, Strom, Gas und Treibstoffe aus Biomasse. In *Energie, Versorgung, Sicherheit*; Pfemeter, C., Liptay, P., Eds.; Österreichischer Biomasse-Verband: Vienna, Austria, 2017; pp. 59–61. Available online: <http://hdl.handle.net/20.500.12708/29656> (accessed on 13 October 2022).
62. International Electrotechnical Commission. IEC 62264: Enterprise-Control System Integration. 2020. Available online: <https://webstore.iec.ch/publication/59706> (accessed on 13 October 2022).
63. Lamb, K. *Principle-Based Digital Twins: A Scoping Review*; Centre for Digital Built Britain: Cambridge, UK, 2019. [CrossRef]
64. Bolton, A.; Blackwell, B.; Dabson, I.; Enzer, M.; Evans, M.; Fenemore, T.; Harradence, F.; Keaney, E.; Kemp, A.; Luck, A.; et al. *The Gemini Principles: Guiding Values for the National Digital Twin and Information Management Framework*; University of Cambridge: Cambridge, UK, 2018; p. 15. [CrossRef]
65. Uhlenkamp, J.-F.; Hribernik, K.A.; Wellsandt, S.; Thoben, K.-D. Digital Twin Applications: A First Systemization of Their Dimensions. In Proceedings of the IEEE International Conference on Engineering, Technology and Innovation (ICE/ITMC), Valbonne Sophia-Antipolis, France, 17–19 June 2019; pp. 1–8. [CrossRef]
66. Fuller, A.; Fan, Z.; Day, C.; Barlow, C. Digital Twin: Enabling Technologies, Challenges and Open Research. *IEEE Access* **2020**, *8*, 108952–108971. [CrossRef]
67. Müller, S.; Fuchs, J.; Schmid, J.; Benedikt, F.; Hofbauer, H. Experimental development of sorption enhanced reforming by the use of an advanced gasification test plant. *Int. J. Hydrogen Energy* **2017**, *42*, 29694–29707. [CrossRef]
68. Müller, S.; Groß, P.; Rauch, R.; Zweiler, R.; Aichernig, C.; Fuchs, M.; Hofbauer, H. Production of diesel from biomass and wind power—Energy storage by the use of the Fischer-Tropsch process. *Biomass Convers. Biorefinery* **2017**, *8*, 275–282. [CrossRef]
69. Pratschner, S.; Hammerschmid, M.; Müller, F.J.; Müller, S.; Winter, F. Simulation of a Pilot Scale Power-to-Liquid Plant Producing Synthetic Fuel and Wax by Combining Fischer-Tropsch Synthesis and SOEC. *Energies* **2022**, *15*, 4134. [CrossRef]
70. Lunzer, A.; Kraft, S.; Müller, S.; Hofbauer, H. CPFD simulation of a dual fluidized bed cold flow model. *Biomass- Convers. Biorefinery* **2021**, *11*, 189–203. [CrossRef]
71. Hammerschmid, M.; Müller, S.; Fuchs, J.; Hofbauer, H. Evaluation of biomass-based production of below zero emission reducing gas for the iron and steel industry. *Biomass Convers. Biorefinery* **2021**, *11*, 169–187. [CrossRef]
72. Müller, S.; Theiss, L.; Fleiß, B.; Hammerschmid, M.; Fuchs, J.; Penthor, S.; Rosenfeld, D.C.; Lehner, M.; Hofbauer, H. Dual fluidized bed based technologies for carbon dioxide reduction—Example hot metal production. *Biomass Convers. Biorefinery* **2021**, *11*, 159–168. [CrossRef]
73. Joshi, R.; Didier, P.; Jimenez, J.; Carey, T. The Industrial Internet of Things Volume G5: Connectivity Framework, Technical Report IIC:PUB:G5:V1.01:PB. Industrial Internet Consortium. 2017. Available online: https://www.iiconsortium.org/pdf/IIC_PUB_G5_V1.0_PB_20170228.pdf (accessed on 13 October 2022).
74. Schleich, B.; Anwer, N.; Mathieu, L.; Wartzack, S. Shaping the digital twin for design and production engineering. *CIRP Ann.* **2017**, *66*, 141–144. [CrossRef]
75. International Electrotechnical Commission. IEC 61508: Functional Safety of Electrical/Electronic/Programmable Electronic Safety-Related Systems. Available online: <https://webstore.iec.ch/publication/5515> (accessed on 13 October 2022).
76. Sinnott, R.; Towler, G. *Chemical Engineering Design*, 6th ed.; Coulson & Richardson's Chemical Engineering Series; Butterworth-Heinemann: Oxford, UK, 2020; ISBN 9780081026007.
77. Harmsen, J. *Industrial Process Scale-Up: A Practical Innovation Guide from Idea to Commercial Implementation*, 2nd ed.; Elsevier: Amsterdam, The Netherlands, 2019. [CrossRef]
78. ROI-EFESO. Management Consulting AG, Measurement and Evaluation of the Digitization Maturity Levels (IoT Scan) and Roadmap. 2021. Available online: <https://www.roi-international.com/management-consulting/competences/increased-efficiency-through-digitisation-industry-40/digitization-maturity-levels> (accessed on 30 December 2021).
79. AUVA. Explosionsschutz—Sicherheitsinformation für Führungskräfte. Merkblatt, Vienna. 2017. Available online: <https://www.auva.at/cdscontent/load?contentid=10008.647857&version=1519986334> (accessed on 13 October 2022).
80. Common Criteria Editorial Board. Common Criteria for Information Technology Security Evaluation. CCMB-2006-09-001. 2006. Available online: <https://www.commoncriteriaportal.org/files/ccfiles/CCPART1V3.1R1.pdf> (accessed on 13 October 2022).
81. European Commission. *Information Technology Security Evaluation Criteria (ITSEC)—Provisional Harmonized Criteria*; Directorate-General for the Information Society and Media, Document COM(90) Office for Official Publications of the European Communities: Brussels, Belgium, 1992; ISBN 92-826-3004-8.
82. Department of Defense Computer Security Center. Department of Defense Trusted Computer System Evaluation Criteria. Orange Book. 1985. Available online: <https://csrc.nist.gov/csrc/media/publications/conference-paper/1998/10/08/proceedings-of-the-21st-nissc-1998/documents/early-cs-papers/dod85.pdf> (accessed on 13 October 2022).
83. Global Compact Network Austria. Sustainable Development Goals—SDGs. 2016. Available online: <https://globalcompact.at/sustainable-development-goals> (accessed on 13 October 2022).

84. European Commission. Regulation (EU) 2020/852 of the European Parliament and of the Council of 18 June 2020 on the Establishment of a Framework to Facilitate Sustainable Investment, and Amending Regulation (EU) 2019/2088. Official Journal of the European Union. 2020. Available online: <https://eur-lex.europa.eu/eli/reg/2020/852/oj> (accessed on 13 October 2022).
85. Bardos, R.P.; Thomas, H.F.; Smith, J.W.N.; Harries, N.D.; Evans, F.; Boyle, R.; Howard, T.; Lewis, R.; Thomas, A.O.; Dent, V.L.; et al. Sustainability assessment framework and indicators developed by SuRF-UK for land remediation option appraisal. *Remediat. J.* **2020**, *31*, 5–27. [[CrossRef](#)]
86. DIN EN ISO 14040:2021-02; Umweltmanagement_Ökobilanz_-Grundsätze und Rahmenbedingungen (ISO_14040:2006_+ Amd_1:2020); Deutsche Fassung EN_ISO_14040:2006_+ A1:2020. Beuth Verlag GmbH: Berlin, Germany, 2021. [[CrossRef](#)]
87. DIN EN ISO 14044:2021-02; Umweltmanagement_Ökobilanz_-Anforderungen und Anleitungen (ISO_14044:2006_+ Amd_1:2017_+ Amd_2:2020); Deutsche Fassung EN_ISO_14044:2006_+ A1:2018_+ A2:2020. Beuth Verlag GmbH: Berlin, Germany, 2021. [[CrossRef](#)]
88. Bartik, A.; Benedikt, F.; Lunzer, A.; Walcher, C.; Müller, S.; Hofbauer, H. Thermodynamic investigation of SNG production based on dual fluidized bed gasification of biogenic residues. *Biomass Convers. Biorefinery* **2020**, *11*, 95–110. [[CrossRef](#)]
89. Hofbauer, H. *Bewertung von Energiebereitstellungssystemen*; Lecture Notes LVA 159.830 Brennstoff- und Energie-Technologie; TU Wien, Institute of Chemical, Environmental and Bioscience Engineering: Vienna, Austria, 2018.
90. Pröll, T. Potenziale der Wirbelschichtdampfvergasung fester Biomasse—Modellierung und Simulation auf Basis der Betriebserfahrungen am Biomassekraftwerk Güssing. Ph.D. Thesis, TU Wien, Institute of Chemical, Environmental and Bioscience Engineering, Vienna, Austria, 2004.
91. Kost, C.; Shammugam, S.; Jülch, V.; Nguyen, H.-T.; Schlegl, T. Stromgestehungskosten Erneuerbare Energien, Fraunhofer-Institut für solare Energiesysteme (ISE), Freiburg. 2018. Available online: https://www.ise.fraunhofer.de/content/dam/ise/de/documents/publications/studies/DE2018_ISE_Studie_Stromgestehungskosten_Erneuerbare_Energien.pdf (accessed on 13 October 2022).
92. TEPPFA. Life Cycle Assessment: Polypropylene (PP-r) Pipe Systems vs. Copper Environmental Impact Comparison. Technical Report, Brussels. 2020. Available online: https://www.teppfa.eu/wp-content/uploads/LCA16_HC-Leaflet-PP-r-vs-Cu.pdf (accessed on 13 October 2022).
93. Koch, D.; Paul, M.; Beisl, S.; Friedl, A.; Mihalyi, B. Life cycle assessment of a lignin nanoparticle biorefinery: Decision support for its process development. *J. Clean. Prod.* **2020**, *245*, 118760. [[CrossRef](#)]
94. Bauer, C.; Hofer, J.; Althaus, H.-J.; Del Duce, A.; Simons, A. The environmental performance of current and future passenger vehicles: Life cycle assessment based on a novel scenario analysis framework. *Appl. Energy* **2015**, *157*, 871–883. [[CrossRef](#)]
95. Wulf, C.; Kaltschmitt, M. Hydrogen Supply Chains for Mobility—Environmental and Economic Assessment. *Sustainability* **2018**, *10*, 1699. [[CrossRef](#)]
96. Dreyer, L.C.; Niemann, A.L.; Hauschild, M.Z. Comparison of Three Different LCIA Methods: EDIP97, CML2001 and Eco-indicator. *Int. J. Life Cycle Assess.* **2003**, *8*, 191–200. [[CrossRef](#)]
97. Rosenfeld, D.C.; Lindorfer, J.; Fazen-Fraisal, K. Comparison of advanced fuels—Which technology can win from the life cycle perspective? *J. Clean. Prod.* **2019**, *238*, 117879. [[CrossRef](#)]
98. Van Zelm, R.; Preiss, P.; van Goethem, T.; Van Dingenen, R.; Huijbregts, M. Regionalized life cycle impact assessment of air pollution on the global scale: Damage to human health and vegetation. *Atmospheric Environ.* **2016**, *134*, 129–137. [[CrossRef](#)]
99. Sphera. GaBi Software with Built-In Database (DB). Chicago. 2022. Available online: <https://gabi.sphera.com/austria/index/> (accessed on 13 October 2022).
100. Mauerhofer, A.M. Carbon Utilization by Application of CO₂ Gasification. Ph.D. Thesis, TU Wien, Institute of Chemical, Environmental and Bioscience Engineering, Vienna, Austria, 2020.
101. Mauerhofer, A.M.; Müller, S.; Bartik, A.; Benedikt, F.; Fuchs, J.; Hammerschmid, M.; Hofbauer, H. Conversion of CO₂ during the DFB biomass gasification process. *Biomass Convers. Biorefinery* **2021**, *11*, 15–27. [[CrossRef](#)]
102. Hofbauer, H.; Mauerhofer, A.; Benedikt, F.; Hammerschmid, M.; Bartik, A.; Veress, M.; Haas, R.; Siebenhofer, M.; Resch, G. *Reallabor zur Herstellung von Holzdiezel und Holzgas aus Biomasse und biogenen Reststoffen für die Land- und Forstwirtschaft*; Technical Report; TU Wien, Institute of Chemical, Environmental and Bioscience Engineering: Vienna, Austria, 2020. Available online: <https://dafne.at/projekte/ftsng-reallabor> (accessed on 13 October 2022).
103. Brown, D.R. Levelized Production Cost. An Alternative Form of Discounted Cash Flow Analysis. *Cost Eng.* **1994**, *36*, 13. Available online: https://www.researchgate.net/publication/255933212_Levelized_production_cost_An_alternative_form_of_discounted_cash_flow_analysis/citations (accessed on 13 October 2022).
104. Brennan, D.J. *Process Industry Economics: Principles, Concepts and Applications*, 2nd ed.; Elsevier: San Diego, CA, USA, 2020; ISBN 9780128194669.
105. Piazza, S.; Zhang, X.; Patuzzi, F.; Baratieri, M. Techno-economic assessment of turning gasification-based waste char into energy: A case study in South-Tyrol. *Waste Manag.* **2020**, *105*, 550–559. [[CrossRef](#)]
106. Goers, S.; Baresch, M.; Tichler, R.; Schneider, F. MOVE2—Simulation Model of the (Upper) Austrian Economy with a Special Focus on Energy Including the Socio-Economic Module MOVE2social: Integration of Income, Age and Gender; Technical Report; Energieinstitut an der Johannes-Kepler-Universität Linz: Linz, Austria, 2015. Available online: https://energieinstitut-linz.at/wp-content/uploads/2016/06/Macroeconometric-Simulation-Tool-MOVE2_MOVE2social_1.pdf (accessed on 13 October 2022).

107. Arzoumanidis, I.; D'Eusanio, M.; Raggi, A.; Petti, L. Functional Unit Definition Criteria in Life Cycle Assessment and Social Life Cycle Assessment: A Discussion. In *Perspectives on Social LCA: Contributions from the 6th International Conference*; Traverso, M., Petti, L., Zamagni, A., Eds.; Springer: Berlin, Germany, 2019; pp. 1–10. [CrossRef]
108. Héder, M. From NASA to EU: The evolution of the TRL scale in Public Sector Innovation. *Innov. J.* **2017**, *22*, 3. Available online: https://www.innovation.cc/discussion-papers/2017_22_2_3_heder_nasa-to-eu-trl-scale.pdf (accessed on 13 October 2022).
109. Müller, S. *Energy Technology Development for Industrial Application: Modelling-Based Development of Processes Enabling Reduced Fossil Carbon Dioxide Emissions by Advanced Digital Methods*; Habilitationsschrift; TU Wien, Institute of Chemical, Environmental and Bioscience Engineering: Vienna, Austria, 2022.
110. Bartik, A.; Fuchs, J.; Müller, S.; Hofbauer, H. Development of an Internally Circulating Fluidized Bed for Catalytic Methanation of Syngas. In *Proceedings of the 16th Minisymposium Verfahrenstechnik and 7th Partikelforum 2020*; Jordan, C., Ed.; TU Wien, Institute of Chemical, Environmental and Bioscience Engineering: Vienna, Austria, 2020. [CrossRef]
111. Diem, R. Design, Construction and Startup of an Advanced 100 kW Dual Fluidized Bed System for Thermal Gasification. Ph.D. Thesis, TU Wien, Institute of Chemical, Environmental and Bioscience Engineering, Vienna, Austria, 2015.
112. Mohan, C.; Alonso, G.; Gunthoer, R.; Mohan, K.; Reinwald, B. An Overview of the Exotica Research Project on Workflow MANAGEMENT Systems. 1995. Available online: <https://www.semanticscholar.org/paper/An-Overview-of-the-Exotica-Research-Project-on-Mohan-Alonso/78df876ac42a772b52686353f8bb89b58244d444> (accessed on 13 October 2022).
113. Pröll, T. *Applied Modelling in Process Engineering and Energy Technology*; Lecture Notes LVA 166.198; TU Wien, Institute of Chemical, Environmental and Bioscience Engineering: Vienna, Austria, 2020.
114. Helal, S.; Hammer, J.; Zhang, J.; Khushraj, A. A Three-Tier Architecture for Ubiquitous Data Access. In *Proceedings of the ACS/IEEE International Conference on Computer Systems and Applications, Beirut, Lebanon, 25–29 June 2002*. [CrossRef]
115. Heidrich, M.; Luo, J.J. *Industrial Internet of Things: Referenzarchitektur für die Kommunikation*; Whitepaper; Fraunhofer-Institut für Eingebettete Systeme und Kommunikationstechnik ESK: Munich, Germany, 2016. Available online: <https://www.iks.fraunhofer.de/content/dam/iks/documents/whitepaper-iiot.pdf> (accessed on 13 October 2022).
116. Ala-Laurinaho, R. Sensor Data Transmission from a Physical Twin to a Digital Twin. Master Thesis, School of Engineering, Aalto University, Aalto, Finland, 2019. Available online: https://www.researchgate.net/publication/343474433_Sensor_Data_Transmission_from_a_Physical_Twin_to_a_Digital_Twin (accessed on 13 October 2022).
117. Rehling, B. Development of the 1 MW Bio-SNG Plant, Evaluation on Technological and Economical Aspects and Upscaling Considerations. Ph.D. Thesis, TU Wien, Institute of Chemical, Environmental and Bioscience Engineering, Vienna, Austria, 2012.
118. Bakosch, C. Automatisierung des Basic Engineering einer Produktgasaufbereitungsstrecke für die Weitere Verwertung. Master Thesis, TU Wien, Institute of Chemical, Environmental and Bioscience Engineering, Vienna, Austria, 2021.
119. Thunman, H.; Seemann, M.; Vilches, T.B.; Maric, J.; Pallares, D.; Ström, H.; Berndes, G.; Knutsson, P.; Larsson, A.; Breitholtz, C.; et al. Advanced biofuel production via gasification—Lessons learned from 200 man-years of research activity with Chalmers' research gasifier and the GoBiGas demonstration plant. *Energy Sci. Eng.* **2018**, *6*, 6–34. [CrossRef]
120. FFG. ADORe-SNG: Comprehensive Automation, Digitalisation & Optimization of Renewable & Sustainable SNG-Production. 2021. Available online: <https://projekte.ffg.at/projekt/3862075> (accessed on 13 October 2022).
121. Stanger, L.; Schirrer, A.; Benedikt, F.; Bartik, A.; Jankovic, S.; Müller, S.; Kozek, M. Dynamic modeling of dual fluidized bed steam gasification for control design. *Energy* **2023**, *265*, 126378. [CrossRef]
122. Jankovic, S.; Hammerschmid, M.; Stanger, L.; Bartik, A.; Benedikt, F.; Müller, S. Design of a Digital Twin for a Pilot Plant for Synthetic Natural Gas Production. In *Proceedings of the 7th Central European Biomass Conference (CEBC), Graz, Austria, 18–20 January 2023*.
123. Hammerschmid, M.; Aguiari, C.; Kirnbauer, F.; Zerobin, E.; Brenner, M.; Eisl, R.; Nemeth, J.; Buchberger, D.; Ogris, G.; Kolroser, R.; et al. Thermal Twin 4.0: Digital Support Tool for Optimizing Hazardous Waste Rotary Kiln Incineration Plants. *Waste Biomass Valorization* **2023**, 1–22. [CrossRef]
124. Nigitz, T.; Gölles, M.; Aichernig, C.; Schneider, S.; Hofbauer, H.; Horn, M. Increased efficiency of dual fluidized bed plants via a novel control strategy. *Biomass Bioenergy* **2020**, *141*, 105688. [CrossRef]
125. Center for Future Energy Technologies, Pilotanlage für Wasserstoff aus Holz. 2022. Available online: <https://www.cfet-strem.com/pilotanlage> (accessed on 13 October 2022).

Disclaimer/Publisher's Note: The statements, opinions and data contained in all publications are solely those of the individual author(s) and contributor(s) and not of MDPI and/or the editor(s). MDPI and/or the editor(s) disclaim responsibility for any injury to people or property resulting from any ideas, methods, instructions or products referred to in the content.

Paper II

Simulation of a Pilot Scale Power-to-Liquid Plant Producing Synthetic Fuel and Wax by Combining Fischer–Tropsch Synthesis and SOEC

Pratschner, S., Hammerschmid, M., Müller, F.J., Müller, S., Winter, F.

Energies, 2022, 15(11), 4134

<https://doi.org/10.3390/en15114134>

Article

Simulation of a Pilot Scale Power-to-Liquid Plant Producing Synthetic Fuel and Wax by Combining Fischer–Tropsch Synthesis and SOEC

Simon Pratschner , Martin Hammerschmid , Florian J. Müller , Stefan Müller  and Franz Winter 

Institute of Chemical, Environmental and Bioscience Engineering, TU Wien, Getreidemarkt 9/166, 1060 Vienna, Austria; martin.hammerschmid@tuwien.ac.at (M.H.); florian.johann.mueller@tuwien.ac.at (F.J.M.); stefan.mueller@tuwien.ac.at (S.M.); franz.winter@tuwien.ac.at (F.W.)

* Correspondence: simon.pratschner@tuwien.ac.at

Abstract: Power-to-Liquid (PtL) plants can viably implement carbon capture and utilization technologies in Europe. In addition, local CO₂ sources can be valorized to substitute oil and gas imports. This work's aim was to determine the PtL efficiency obtained by combining a solid oxide electrolyzer (SOEC) and Fischer–Tropsch synthesis. In addition, a recommended plant configuration to produce synthetic fuel and wax at pilot scale is established. The presented process configurations with and without a tail gas reformer were modeled and analyzed using IPSEpro as simulation software. A maximum mass flow rate of naphtha, middle distillate and wax of 57.8 kg/h can be realized by using a SOEC unit operated in co-electrolysis mode, with a rated power of 1 MW_{el}. A maximum PtL efficiency of 50.8% was found for the process configuration without a tail gas reformer. Implementing a tail gas reformer resulted in a maximum PtL efficiency of 62.7%. Hence, the reforming of tail gas is highly beneficial for the PtL plant's productivity and efficiency. Nevertheless, a process configuration based on the recirculation of tail gas without a reformer is recommended as a feasible solution to manage the transition from laboratory scale to industrial applications.

Keywords: Power-to-Liquid; carbon capture and utilization; synthetic fuel and wax; Fischer–Tropsch; SOEC; co-electrolysis of CO₂ and H₂O; tail gas reforming; pilot scale



Citation: Pratschner, S.; Hammerschmid, M.; Müller, F.J.; Müller, S.; Winter, F. Simulation of a Pilot Scale Power-to-Liquid Plant Producing Synthetic Fuel and Wax by Combining Fischer–Tropsch Synthesis and SOEC. *Energies* **2022**, *15*, 4134. <https://doi.org/10.3390/en15114134>

Academic Editor: Francesco Frusteri

Received: 4 May 2022

Accepted: 28 May 2022

Published: 4 June 2022

Publisher's Note: MDPI stays neutral with regard to jurisdictional claims in published maps and institutional affiliations.



Copyright: © 2022 by the authors. Licensee MDPI, Basel, Switzerland. This article is an open access article distributed under the terms and conditions of the Creative Commons Attribution (CC BY) license (<https://creativecommons.org/licenses/by/4.0/>).

1. Introduction

Despite increased media interest in the consequences of the climate crisis, the global mean CO₂ level in the atmosphere is still rising by about 2.5 ppm per year and reached a value of 414 ppm in October 2021, an increase of 2.4 ppm compared to October 2020 [1,2]. In 2020, about 83% of the global primary energy demand was still derived from fossil sources [3]. An increase in the EU27 transportation sector's greenhouse gas (GHG) emissions of 33% compared to 1990 highlights the urgency of a sustainable reformation to reach the goal of being climate-neutral in 2050, whereas other sectors managed to reduce their GHG emissions by 32%. Transportation is responsible for about 29% of the EU27's total GHG emissions: 15% of the total GHG emissions are produced by passenger cars and vans, 5% by trucks and buses and 4% respectively by aviation and marine navigation [4,5]. A comprehensive overview of several technologies and scenarios to tackle the mobility sector's weak performance concerning GHG emissions can be found in [6].

Besides battery electric vehicles, plug-in hybrid technologies and biofuels, synthetic fuels pose an attractive transitional solution for individual mobility and have the potential to replace conventional fossil fuels in applications requiring high energy density—i.e., aviation, marine navigation and off-road vehicles, e.g., construction, agricultural or forestry vehicles—on a long-term basis [7]. In summary, the implementation of synthetic fuels includes the following advantages:

- High energy density;

- Applicability for existing technologies;
- Suitability for heavy-duty applications;
- Quick deployment, since no infrastructural adaptations are required.

An overview of current Power-to-X (PtX) projects throughout Europe was given by Wulf et al. in [8]. In June 2020, 220 PtX research and demonstration projects were realized, finished or planned in Europe. Some of the mentioned plants were not commissioned at release and have not been constructed as of April 2022. Germany, Spain and the UK have the highest shares of PtX plants in Europe. Power-to-Gas (PtG) plants obtained the highest share of 94%. Power-to-H₂ applications had a share of 67%, whereas Power-to-Methane plants had a share of 27%. The production of methanol and other technologies, i.e., the production of DME or Fischer–Tropsch products, accounted for 3%. Low-temperature electrolysis technologies, i.e., alkaline electrolyzers and proton exchange membrane electrolyzers (PEMEC), were by far the preferred technology for H₂ production, as shown by their share being larger than 90%, whereas high-temperature solid oxide electrolyzers (SOEC) were applied in less than 10% of the analyzed projects.

An overview concerning completed and ongoing Power-to-Liquid projects based on the synthesis of methanol or Fischer–Tropsch products is given in Table 1.

Finding a way to commercialize liquid fuels produced by lignocellulosic feedstocks or CO₂ streams in combination with renewable H₂ is one goal of [9] within the “Advancefuel” project, which is analyzing several conversion technologies to produce fuels such as methanol, DME, gasoline and diesel. An alternative route for the production of Fischer–Tropsch products based on syngas generated via biomass gasification, i.e., Biomass-to-Liquid, is presented in [10]. The upcycling of waste, e.g., municipal waste, sewage sludge or residues from the pulp and paper industry to renewable fuel and wax via dual-fluidized bed gasification and Fischer–Tropsch synthesis is planned to be realized within the “Waste2Value” project conducted in Vienna, Austria [11]. A concept for a PtL plant based on the synthesis of methanol in combination with a biomass heating plant and a conventional alkaline electrolyzer was analyzed in [12]. Besides the produced methanol, heat was transferred to a district heating network provided by a fluidized bed combustor operating in air or oxyfuel mode.

Table 1. Overview of completed and ongoing Power-to-Liquid projects.

Name	Location	CO ₂ Source	Power Source	Electrolyzer	Synthesis	m _{Products} ¹	Source
Haru Oni	Magellanes, CHL	DAC	Wind power	PEM	Methanol	- ²	[13]
George Olah Plant	Svartsengi, IS	Geothermal	Geothermal	Alkaline	Methanol	4000 t/a	[14]
MefCO ₂	Niederaussem, GER	Coal plant	Surplus el.	PEM	Methanol	365 t/a	[15]
Norsk e-fuel	Mosjoen, NOR	DAC	Wind power	SOEC	Fischer–Tropsch	12.5 t/a	[16]
- ²	Werlte, GER	Biogas + DAC	Renewable	- ²	Fischer–Tropsch	350 t/a	[17]
- ²	Frankfurt, GER	Biogas plant	- ²	- ²	Fischer–Tropsch	3500 t/a	[18]

¹ According to the stated source. ² Information not available.

Fischer–Tropsch synthesis has been researched and optimized for several decades, and hence is well established at an industrial scale. De Klerk provided an extensive overview of the process itself and industrial plants in [19]. Martinelli et al. gave a comprehensive examination of the Fischer–Tropsch process in combination with SOEC or biomass gasification as syngas production technologies [20]. Detailed information about the impacts of process conditions—temperature, pressure, space velocity, H₂:CO ratio, etc.—can be found in [21–26]. Refining Fischer–Tropsch syncrude to on-specification diesel fuel is far from trivial, since several technological aspects need to be synchronized with national diesel fuel standards to comply with required intervals for parameters, i.e., the cetane number, density and viscosity [27]. Lately, Fischer–Tropsch waxes have received increasing attention due to their low amounts of aromatic and sulfurous compounds, hence having high potential as feedstock for the cosmetic industry [28].

Choosing the appropriate reactor design for PtL plants at a pilot scale is crucial. Fluidized bed reactor systems, either stationary or circulating, are applied for high-temperature

Fischer–Tropsch (HTFT) synthesis processes [29] but are not considered in this work, since the system aims at maximizing the middle distillate and wax fractions. In general, three reactor types can be considered for low-temperature Fischer–Tropsch (LTFT) applications, i.e., slurry bubble column reactors (SBCR), fixed bed multitubular reactors (FBMR) and microstructured reactors. The advantages and disadvantages of SBCR and FBMR reactors can be found in [29–31]. Detailed information regarding existing reactors at an industrial scale is stated in [19]. The current status of microstructured reactors and an analysis concerning the effect of process parameters can be found in [32,33].

Previous work concerning the simulation of Power-to-Liquid plants via Fischer–Tropsch synthesis is summarized in Table 2. The syngas was either provided by a solid-oxide electrolyzer operating in co-electrolysis mode, a low-temperature electrolyzer in combination with a reverse water-gas shift (rWGS) reactor, or biomass gasification. The simulation of the Fischer–Tropsch synthesis was based on a Co-based catalyst with different approaches concerning the chemistry inside the reactor, i.e., the standard Anderson–Schulz–Flory (ASF) distribution, kinetic modeling and basic reaction stoichiometry. In general, the chosen values concerning the chain growth probability were around 0.9 to maximize the yield of long-chain hydrocarbons. Most of the authors assumed rather optimistic CO conversions of higher than 70%. The recirculation of tail gas (TG) to the inlet of the SOEC unit or rWGS reactor was considered in the majority of the listed works. Another option is to realize a short recycle configuration to the Fischer–Tropsch reactor’s inlet.

Table 2. Overview of previous works on the simulation of Power-to-Liquid plants based on Fischer–Tropsch synthesis.

Syngas Production	Fischer–Tropsch Model	Catalyst	Chain Growth Probability α	CO Conversion	Tail Gas Recirculation	Source
SOEC/rWGS	Standard ASF + kinetic model	Co-based	- ¹	70% (per pass)	Inlet SOEC/ inlet rWGS	[34]
SOEC	Standard ASF	Co-based	0.94	87% (per pass)	Inlet SOEC	[35]
rWGS	Standard ASF	Co-based	- ¹	100% (plant)	Inlet rWGS/ inlet FT reactor	[36]
SOEC	Standard ASF + kinetic model	Co-based	0.90	80% (per pass)	No recirculation	[37]
SOEC	- ¹	Co-based	0.90	80% (per pass)	Inlet SOEC/ inlet FT reactor	[38]
rWGS	Reaction stoichiometry	Co-based	- ¹	- ¹	Inlet rWGS	[39]
Biomass gasification ²	Standard ASF	Co-based	0.89–0.93	40% (per pass)	No recirculation	[40]

¹ Not specified. ² Combining process simulation and experimental validation.

The main aim of this work was to answer the question of which Power-to-Liquid efficiencies can be realized by pilot scale plants combining an SOEC unit with Fischer–Tropsch synthesis. In addition, an ideal plant configuration for the production of synthetic liquid fuels and wax at a pilot scale is provided as a result of the presented work. In comparison to the comparable research stated in Table 2, the underlying work shifts the focus toward the Fischer–Tropsch process itself by applying the extended ASF distribution model and analyzing the recirculation of tail gas prior to the Fischer–Tropsch reactor instead of the SOEC. Furthermore, a process route including a tail gas reformer to convert short-chain hydrocarbons and CO₂ to syngas is analyzed.

2. Materials and Methods

The presented work is based on the results obtained by the process simulation of two design configurations for a PtL plant producing Fischer–Tropsch products. IPSEpro (version 8), stationary equation-orientated simulation software based on the numerical solving of equation systems via the Newton–Raphson method, was applied to develop the underlying model consisting of the following subprocesses:

- Co-electrolysis of CO₂ and H₂O with a subsequent syngas condenser;
- Using a blower to overcome the pressure drop caused by the syngas condenser;

- Three-staged syngas compression with intermediate cooling by ambient air;
- Fischer–Tropsch reaction;
- Product separation;
- Tail gas recirculation and tail gas reforming;
- Tail gas combustion.

An overview of a process configuration of a PtL plant at the pilot scale without a tail gas reformer is given in Figure 1. Syngas provided by the SOEC unit is transferred to the condenser by a blower to overcome its pressure drop. After water separation, the syngas is compressed to the Fischer–Tropsch reactor’s pressure level via a three-stage compression step with intermediate cooling by ambient air. The SOEC’s syngas and the recirculated tail gas are mixed before being transferred into the reactor. A hot water cooling cycle ensures the removal of the reaction heat. A share of the produced middle distillate and wax leave the reactor as a liquid. The rest of the Fischer–Tropsch products, water and unconverted gases are drained as gases and transferred to the subsequent product separation unit. Within this process configuration, the separation of wax, middle distillate, naphtha and water is realized by three heat exchangers based on water as a cooling agent. Subsequently, a share of the tail gas stream is recirculated in front of the Fischer–Tropsch reactor, whereas the remaining tail gas leaves the system as purge gas.

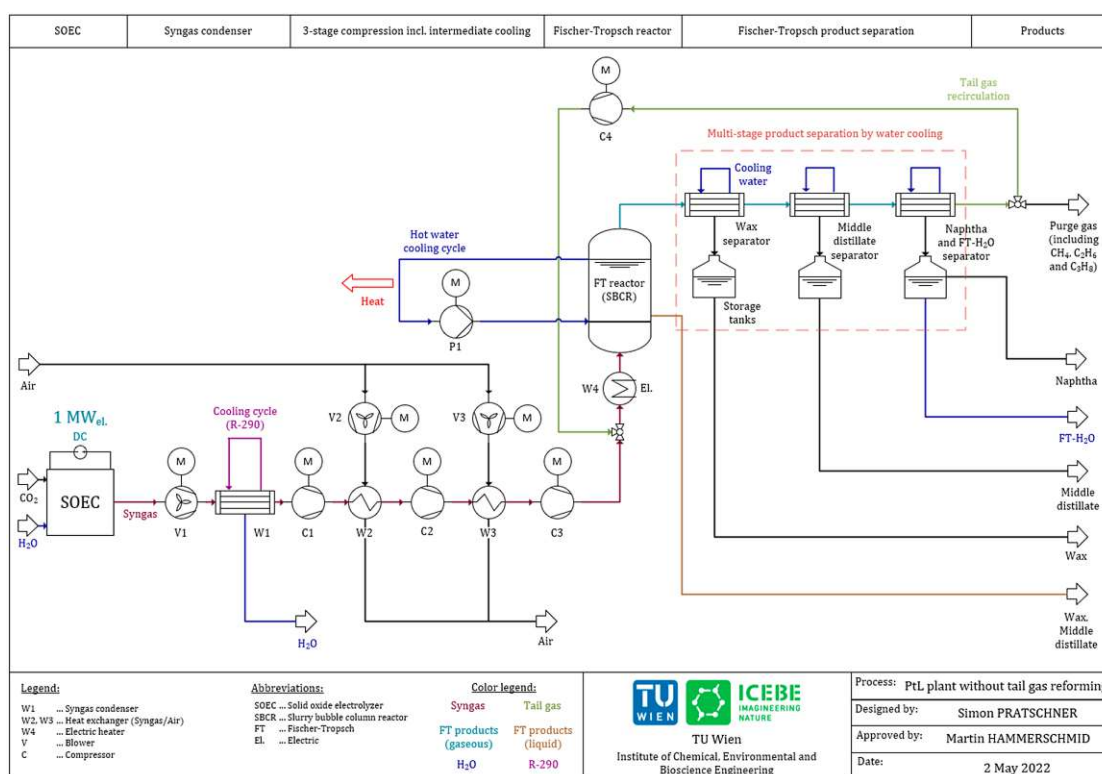


Figure 1. Scheme of the Power-to-Liquid plant without tail gas reforming.

The proposed process route that includes a tail gas reformer is displayed in Figure 2, showing the following differences from Figure 1:

- The recirculated tail gas is inserted in front of the syngas condenser;
- The product separation is realized by a multi-stage flash distillation;
- Purge gas is combusted to heat the recirculated tail gas;
- A tail gas reformer ensures the conversion of CO₂ and hydrocarbons inside the recirculated tail gas stream.

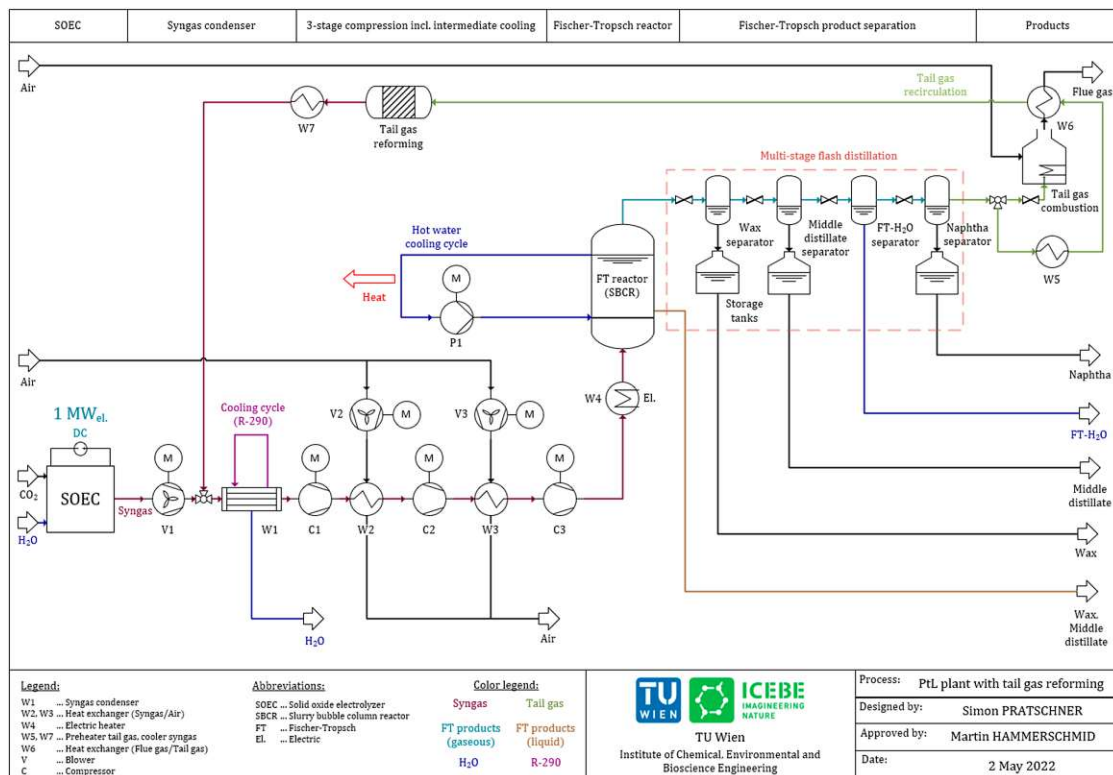


Figure 2. Scheme of the Power-to-Liquid plant with tail gas reforming.

The implementations of the presented flowcharts in IPSEpro are shown in Figure 3 for the process configuration without a tail gas reformer and in Figure 4 for the one including a tail gas reformer.

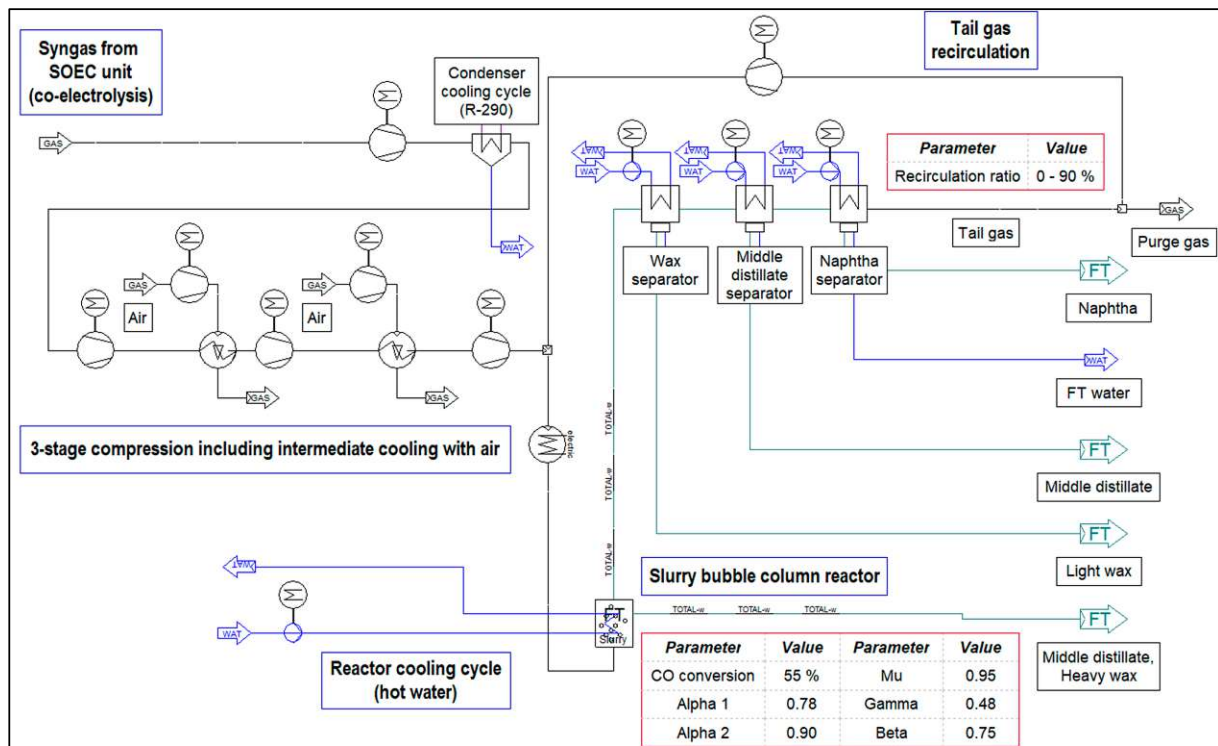


Figure 3. Implementation in IPSEpro—process configuration without tail gas reforming.

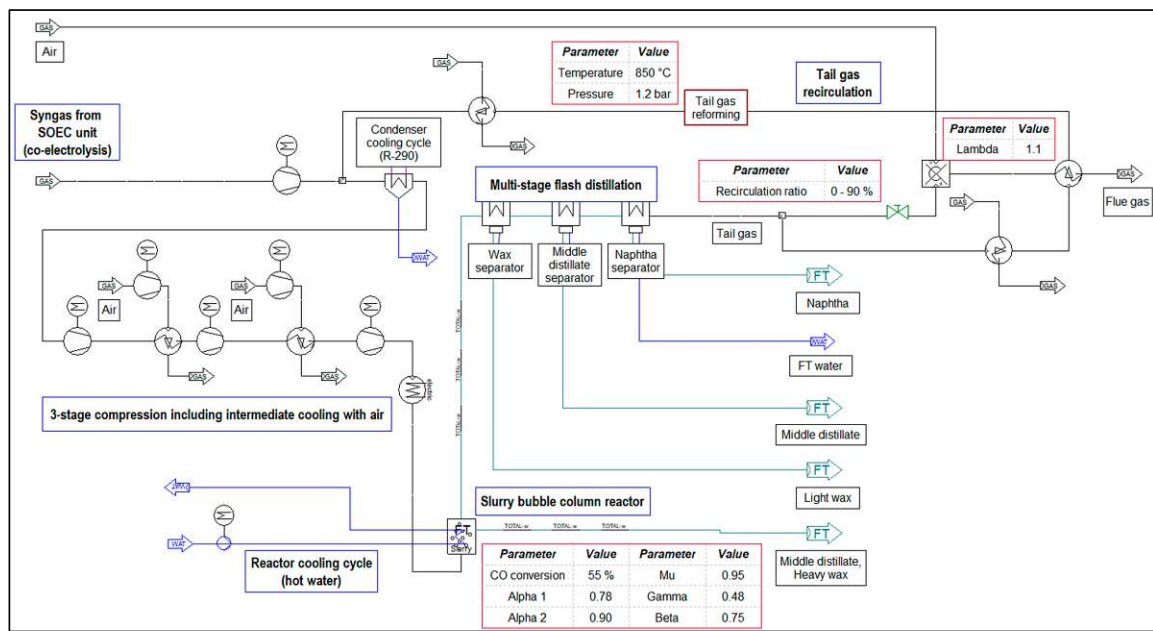


Figure 4. Implementation in IPSEpro—process configuration including tail gas reforming.

Table 3 provides a list of the parameters chosen for the process simulation. Detailed explanations of the subprocesses are given within the following subsections.

Table 3. Important parameters of the process simulation.

Parameter	Symbol	Value	Unit	Source
SOEC and syngas				
SOEC power input	P_{SOEC}	1	MW_{el}	Chosen design
Syngas mass flow rate	m_{Syngas}	190	kg/h	Calculation [41]
Temperature syngas	T_{Syngas}	120	$^{\circ}C$	Assumption
Volume share of CO	y_{CO}	27.9 ¹	vol%	[34]
Volume share of H ₂	y_{H_2}	55.8 ¹	vol%	[34]
Volume share of H ₂ O	y_{H_2O}	5.5 ²	vol%	[34]
Volume share of CO ₂	y_{CO_2}	10.5 ²	vol%	[34]
Volume share of CH ₄	y_{CH_4}	0.3 ²	vol%	[34]
Temperature condenser OUT	$T_{Con.}$	10	$^{\circ}C$	Assumption
Syngas compression and intermediate cooling				
Pressure condenser OUT	$P_{Con.}$	1	bar	Assumption
Pressure C1	P_{C1}	3	bar	[42]
Pressure C2	P_{C2}	8	bar	[42]
Pressure C3	P_{C3}	21	bar	[42]
Temperature W2 and W3	$T_{W2,W3}$	50	$^{\circ}C$	Assumption
Fischer–Tropsch synthesis				
Temperature FT reactor	T_{FT}	210	$^{\circ}C$	[19]
Pressure FT reactor	P_{FT}	21	bar	[19]
CO conversion FT reactor	$X_{CO,Reactor}$	55	%	[43,44]
rWGS activity FT reactor	$X_{rWGS,Reactor}$	0	%	[19]
Chain growth probability	α_1	0.78	-	Based on [43]
Chain growth probability	α_2	0.90	-	Based on [43]
Factor to merge α_1 and α_2	μ	0.95	-	Based on [43]
Readsorption factor	γ	0.48	-	Based on [43]
Termination factor	β	0.75	-	Based on [43]
Tail gas recirculation and reforming				
Recirculation ratio	RR	0–90	%	Chosen design
Temperature reformer	$T_{Reformer}$	850	$^{\circ}C$	Chosen design
Pressure reformer	$P_{Reformer}$	1.2	bar	Chosen design
Tail gas combustion				
Air ratio	λ	1.1	-	Assumption
Temperature flue gas	$T_{Flue\ gas}$	1100	$^{\circ}C$	Assumption
Product fractions				
Methane	C_1			Number of carbon atoms
Ethane and propane	C_2-C_3			Number of carbon atoms
Naphtha	C_4-C_9			Number of carbon atoms
Middle distillate	$C_{10}-C_{19}$			Number of carbon atoms
Wax	C_{20+}			Number of carbon atoms

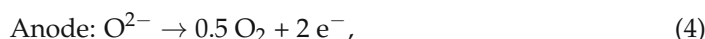
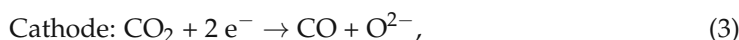
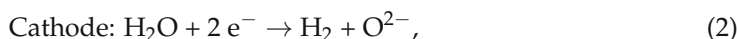
¹ Varied to maintain $H_2:CO_{FT} = 2.2$ constant.

2.1. SOEC (Co-Electrolysis) and Condenser

Thermodynamically, the required enthalpy for water splitting is provided by electrical and thermal energy, as can be seen in Equation (1). An increase in the thermal energy provided to the cell decreases the required input of electricity [45].

$$\Delta_r H = \Delta_r G + T \cdot \Delta_r S, \quad (1)$$

Due to this behavior, the application of high-temperature electrolysis technologies, i.e., SOEC, has the potential to significantly improve the efficiency of PtL plants when combined with strongly exothermal chemical synthesis processes [46]. Since conventional syngas consisting of CO and H₂ is required for Fischer–Tropsch processes applying a Co-based catalyst, we chose to have the electrolysis unit operate under co-electrolysis conditions, converting CO₂ and H₂O to CO and H₂, at atmospheric pressure and a temperature of 850 °C. Detailed information about state-of-the-art materials used for electrodes and the electrolyte in high-temperature electrolysis cells can be found in [47]. Equations (2)–(4) show the underlying chemical reactions of a high-temperature electrolyzer in co-electrolysis mode [34].



According to literature, an assumed mass flow rate of 190 kg/h of syngas is provided by the SOEC unit, operating at $T_{\text{SOEC}} = 850$ °C and $p_{\text{SOEC}} = 1$ bar, consuming 1 MW_{el.} of electric power. The amount of H₂ inside the syngas stream and the required amount of H₂ for the formation of CO via the rWGS reaction correspond to an energy demand of 3.37 kWh/Nm³ H₂ according to [41], for the syngas' base case composition listed in Table 3 [34], and an efficiency of 80%. The volume fractions of CO and H₂ can be varied by adapting the share of H₂O at the SOEC unit's inlet to adjust the required H₂:CO ratio for process routes that include the recirculation of tail gas [34]. The data listed in Table 3 imply a reactant utilization rate of around 80% [38].

A blower after the SOEC unit ensures overcoming the pressure difference of 0.2 bar caused by the condenser, applying C₃H₈, i.e., R-290, as a cooling medium.

2.2. Syngas Compression with Intermediate Cooling

Syngas leaves the SOEC unit at atmospheric pressure, and hence needs to be compressed to the synthesis pressure of $p_{\text{FT}} = 21$ bar. In addition, the recirculated syngas needs to be re-pressurized after being separated via multi-stage flash distillation [48] for the process route that includes tail gas reforming. The compressors' efficiencies were assumed as $\eta_{\text{Compr.,s}} = \eta_{\text{Compr.,m}} = 0.9$, whereas the electric motors' efficiencies were chosen as $\eta_{\text{Motor,m}} = 0.99$ and $\eta_{\text{Motor,el}} = 0.96$.

2.3. Fischer–Tropsch Synthesis

The applied Fischer–Tropsch model is based on an LTFT process in an SBCR using a Co-based catalyst, operating at a temperature of $T_{\text{FT}} = 210$ °C and a pressure of $p_{\text{FT}} = 21$ bar. At industrial scale, Fischer–Tropsch catalysts are either based on cobalt, obtaining higher activity, fewer by-products and longer lifetimes; or iron, which is cheaper and shows activity in the rWGS reaction. Important properties are the possible hydrogenating nature of the applied material, which will result in a higher share of non-saturated hydrocarbons, and the selectivity for by-products, which can be manipulated by the addition of alkali metals as promoters [20,30]. Additional information regarding the production of Fischer–Tropsch catalysts can be found in [49].

It is assumed that the formed Fischer–Tropsch products are solely paraffins, as shown in Equation (5).



2.3.1. Extended ASF Distribution

The extended ASF (eASF) model, as proposed by Förtsch et al., was used to find the product spectrum of the synthesized hydrocarbons [50], since the standard ASF distribution does not consider three primary deviations from real applications:

- Underestimation of the formation of CH_4 ;
- Overestimation of the formation of C_2H_6 ;
- Deviation of the chain growth probability α for long-chain hydrocarbons, C_{13+} .

The following parameters and equations were introduced by Förtsch et al. to minimize the deviation from real applications:

- α_1 : Chain growth probability for hydrocarbons ranging from C_1 to C_7 ;
- α_2 : Chain growth probability for hydrocarbons with C_{13+} ;
- μ : Factor for merging α_1 and α_2 ;
- γ : Termination factor to depict the higher selectivity for CH_4 ;
- β : Readsorption factor to depict the lower selectivity for C_2H_6 .

The molar fractions of CH_4 , C_2H_6 and $\text{C}_{n>2}$ can be determined by Equations (6)–(8), respectively [50].

$$x_{\text{CH}_4} = (1 - \mu) \cdot [1 - \alpha_1 \cdot (1 - \gamma)] + \mu \cdot (1 - \alpha_2), \quad (6)$$

$$x_{\text{C}_2\text{H}_6} = (1 - \mu) \cdot (1 - \alpha_1) \cdot \alpha_1 \cdot \frac{1 - \beta}{1 - \beta \cdot (1 - \alpha_1)} \cdot (1 - \gamma) + \mu \cdot (1 - \alpha_2) \cdot \alpha_2, \quad (7)$$

$$x_{\text{C}_n\text{H}_{2n+2}} = (1 - \mu) \cdot (1 - \alpha_1) \cdot \alpha_1^{(n-1)} \cdot \frac{1 - \gamma}{1 - \beta \cdot (1 - \alpha_1)} \cdot \mu \cdot (1 - \alpha_2) \cdot \alpha_2^{(n-1)}, \quad (8)$$

The Co-based catalyst's assumed eASF parameters, as listed in Table 3, were based on the findings of Guilera et al. [43].

2.3.2. Reactor Cooling

Since Fischer–Tropsch synthesis is a highly exothermic process (see Equation (5)), the reaction heat needs to be transferred out of the reactor to avoid hot spots which might result in alternating the product selectivity and catalyst deactivation due to sintering processes. Industrial reactors are preferably cooled by the evaporation of boiling water at a certain pressure level, i.e., boiling water reactors. However, this reactor type requires a rather sophisticated design which might not be feasible for pilot scale applications; thus, a cooling design circulating pressurized hot water was chosen for the modeled Fischer–Tropsch reactor.

2.3.3. Chemical Conversion

A CO conversion of $X_{\text{CO,Reactor}} = 55\%$ was assumed for the Fischer–Tropsch reactor according to [43,44]. As stated previously, Co-based Fischer–Tropsch catalysts are not active for the rWGS reaction, and hence $X_{\text{rWGS,Reactor}}$ was set to 0%.

2.4. Products and Product Separation

2.4.1. Fischer–Tropsch Products

As stated in Section 2.3, besides water only alkanes are considered as Fischer–Tropsch products. Table 3 shows the chosen division of product fractions based on the molecule's number of carbon atoms.

2.4.2. Product Separation without Tail Gas Reforming

The separation of products without tail gas reforming is realized by a series of separators being cooled with pressurized water, as can be seen in Figure 1. To minimize the required power to repressurize the tail gas to $p_{FT} = 21$ bar, the pressure level after the product separation step should be as high as possible while separating H_2O and condensable hydrocarbons. Light waxes and the middle distillate fraction can be drained as liquids within a first separation step, whereas H_2O , naphtha, methane, ethane and propane remain gaseous.

2.4.3. Product Separation with Tail Gas Reforming

Since the reforming of tail gas is favored at low-pressure levels, as explained in Section 2.6, the separation of products can be realized by serial flash distillation, as depicted in Figure 2. Light waxes, the middle distillate, the naphtha fraction and H_2O , are gradually separated by depressurizing the gas mixture to a pressure level of $p_{Reformer} = 1.2$ bar, including an excess of 0.2 bar to overcome downstream heat exchanger units.

2.5. Tail Gas Recirculation

The recirculation of tail gas is a profound method with which to increase the overall conversion of CO for chemical plants based on syngas as a precursor, going hand in hand with an increase in the synthesized products and hence the plant's PtL efficiency. The recirculation ratio RR is defined as the mass flow rate of recirculated tail gas divided by the total mass flow rate of tail gas (Equation (9)). To avoid the accumulation of CO_2 and CH_4 in the recirculated tail gas, a share of the stream needs to be drained from the system as purge gas. For the process configuration including tail gas reforming, the purge gas is combusted to heat the recirculated tail gas to the reformer's operating temperature of 850 °C.

$$RR = \frac{m_{Tail\ gas,Rec.}}{m_{Tail\ gas,Total}}, \quad (9)$$

2.5.1. Process Configuration without Tail Gas Reforming

Since the separation of products is realized under synthesis pressure, only one additional compressor is required to compensate for the separator's pressure drops, and the recirculated tail gas can be inserted before the Fischer–Tropsch reactor, as shown in Figure 1.

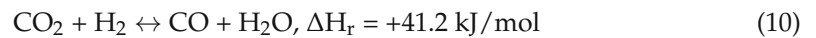
2.5.2. Process Configuration with Tail Gas Reforming

As illustrated in Figure 2, the purge gas is combusted to heat the recirculated tail gas to the reformer's temperature of $T_{Reformer} = 850$ °C. Before the reformer, a water injector can be installed to add an extra degree of freedom to manipulate the chemical reactions inside the tail gas reformer. An additional heat exchanger after the reformer is required to cool the gas stream before it is inserted prior to the syngas condenser, removing non-converted water of the co-electrolysis process and excess water leaving the reformer. It is recommended to utilize the transferred heat for preheating and evaporating the SOEC's water input. A maximum value of $RR_{max.} = 0.9$ was defined to ensure the heating of recirculated tail gas to the reformer's temperature level. In addition, the limitation of RR to 0.9 secures the comparability of process configurations with and without a tail gas reformer.

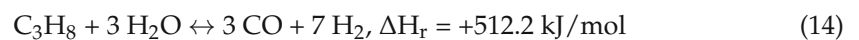
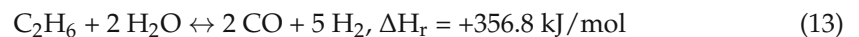
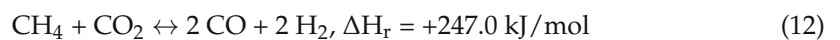
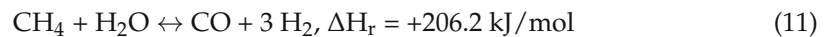
2.6. Tail Gas Reforming

The tail gas reformer was modeled as a Gibbs reactor with the "Equilib" model of FactSage version 8.1, reforming the tail gas in accordance with the chemical equilibrium at a temperature of $T_{Reformer} = 850$ °C and a pressure of $p_{Reformer} = 1.2$ bar. A sufficient residence time inside the reactor was assumed to ensure the realization of chemical equilib-

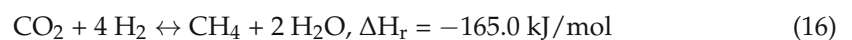
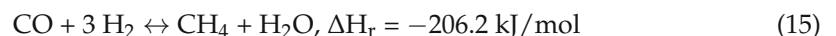
rium. The following chemical reactions were assumed to have the highest impact on the reformer's performance.



The rWGS reaction (Equation (10)) has its chemical equilibrium at a temperature of around 800–850 °C, as sufficient conversion rates exist at temperatures surpassing 800 °C and are not affected by a change in pressure. The addition of H₂ favors the conversion of CO₂, whereas H₂O inside the feed stream mitigates the CO₂ conversion [51].



Equations (11)–(14) show the underlying chemical reactions of the steam reforming of methane, ethane and propane. To boost the conversion of short-chain hydrocarbons, the addition of H₂O into the tail gas stream was considered but was not realized in the process simulation, since the H₂O demand of Equations (11)–(14) can be fully covered by the formed H₂O due to the rWGS reaction (Equation (10)). After the principle of Le Chatelier, the reforming of short-chain hydrocarbons by steam is enhanced with a high temperatures, low pressure and high share of water inside the stream [19].



The methanation via CO (15) and CO₂ (16) hydrogenation should be avoided, since CH₄ is a product of the Fischer–Tropsch synthesis, and hence reduces the Fischer–Tropsch reactor's productivity. After Le Chatelier, the formation of CH₄ can be reduced by a low pressure level inside the reformer and the addition of steam at the reactor's inlet [52].

In summary, to maximize the conversion of CO₂ and short-chain hydrocarbons, the tail gas reformer should be operated at a high temperature and low pressure. The addition of H₂ would favor the conversion of CO₂ according to the rWGS reaction (Equation (10)). However, this would conclude in high shares of short-chain hydrocarbons after the reformer (Equations (15) and (16)), and was hence not included. A high share of steam inside the tail gas stream lowers the conversion of CO₂ but is essential to reform hydrocarbons according to Equations (11), (13) and (14).

2.7. Power-to-Liquid Efficiency and Plant Efficiency

The Power-to-Liquid efficiency η_{PtL} is defined as the chemical energy stored in products divided by the system's total electric power input. Two different efficiency rates were defined to be able to directly compare process routes with and without tail gas reforming: Firstly, the PtL efficiency excluding methane, ethane and propane (17); and secondly, the plant efficiency including methane, ethane and propane (18).

$$\eta_{\text{PtL}} = \frac{\sum_j m_j \cdot \text{LHV}_j}{P_{\text{el.,Total}}}, j = [\text{naphtha, middle distillate, wax}] \quad (17)$$

$$\eta_{\text{Plant}} = \frac{\sum_k m_k \cdot \text{LHV}_k}{P_{\text{el.,Total}}}, k = [\text{CH}_4, \text{C}_2\text{H}_6, \text{C}_3\text{H}_8, \text{naphtha, middle distillate, wax}] \quad (18)$$

2.8. Utilization of Purge Gas

To avoid the accumulation of CO₂ and short-chain hydrocarbons, i.e., methane, ethane and propane, a share of the tail gas needs to be drained from the system as purge gas.

Either this gas stream can be used for downstream synthesis processes, or the stream's chemical energy can be utilized to evaporate H₂O or heat the recirculated tail gas when using a tail gas reformer.

3. Results

3.1. Recommended Design Parameters for a Pilot Scale Power-to-Liquid Plant

The recommended design parameters for the provided configurations of a Power-to-Liquid plant with and without a tail gas reformer, as illustrated in Figures 1 and 2, are presented within this section. The shown mass flow rates, volume flow rates, temperature levels, pressure levels and stream compositions are based on the parameters listed in Table 3 and a recirculation ratio of tail gas of RR = 90%. Figure 5 shows the obtained design parameters for the process configuration without a tail gas reformer.

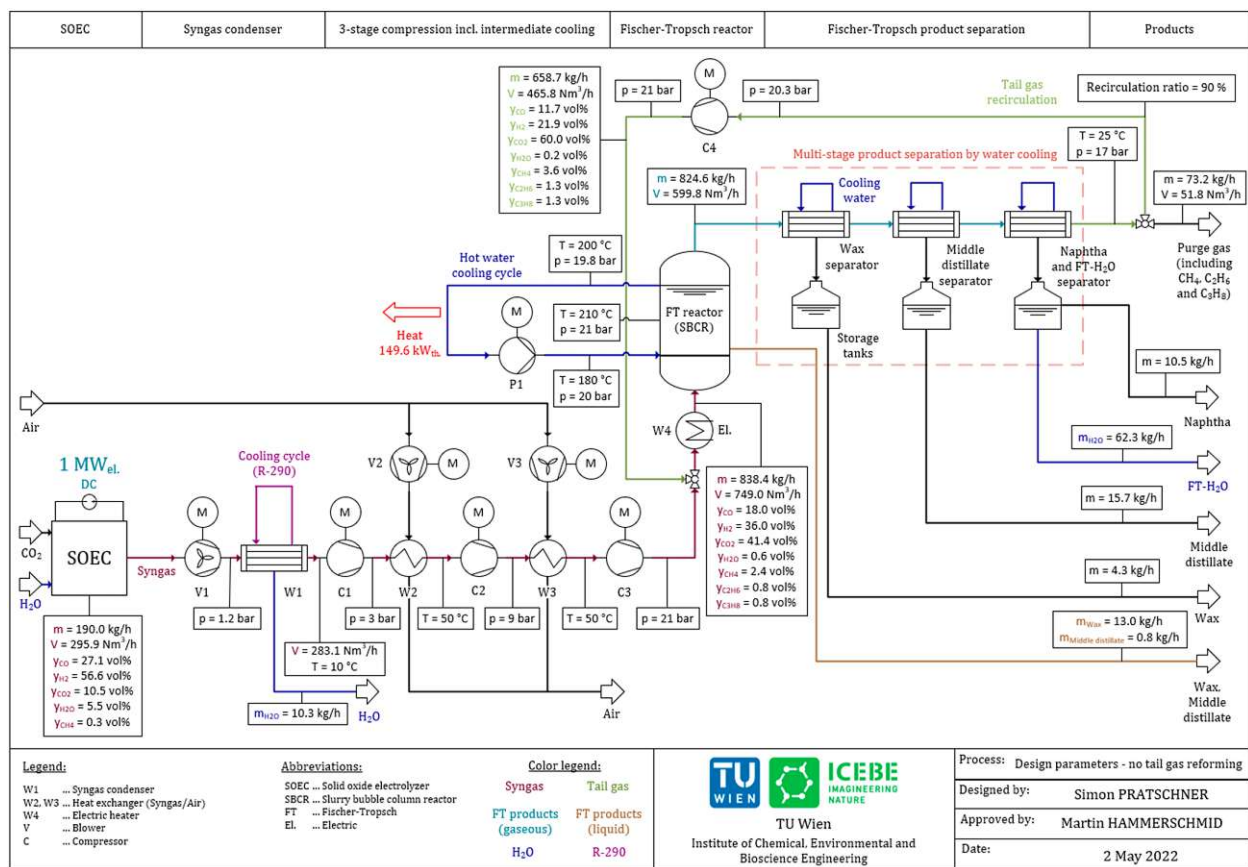


Figure 5. Design parameters of the plant configuration without tail gas reforming.

Figure 6 shows the recommended design parameters of a pilot scale Power-to-Liquid plant for the process configuration including a tail gas reformer based on the parameters listed in Table 3 and a recirculation ratio of RR = 90%.

The plant's parameters, e.g., Power-to-Liquid efficiency, Fischer-Tropsch products and CO conversion, are analyzed within the following sections.

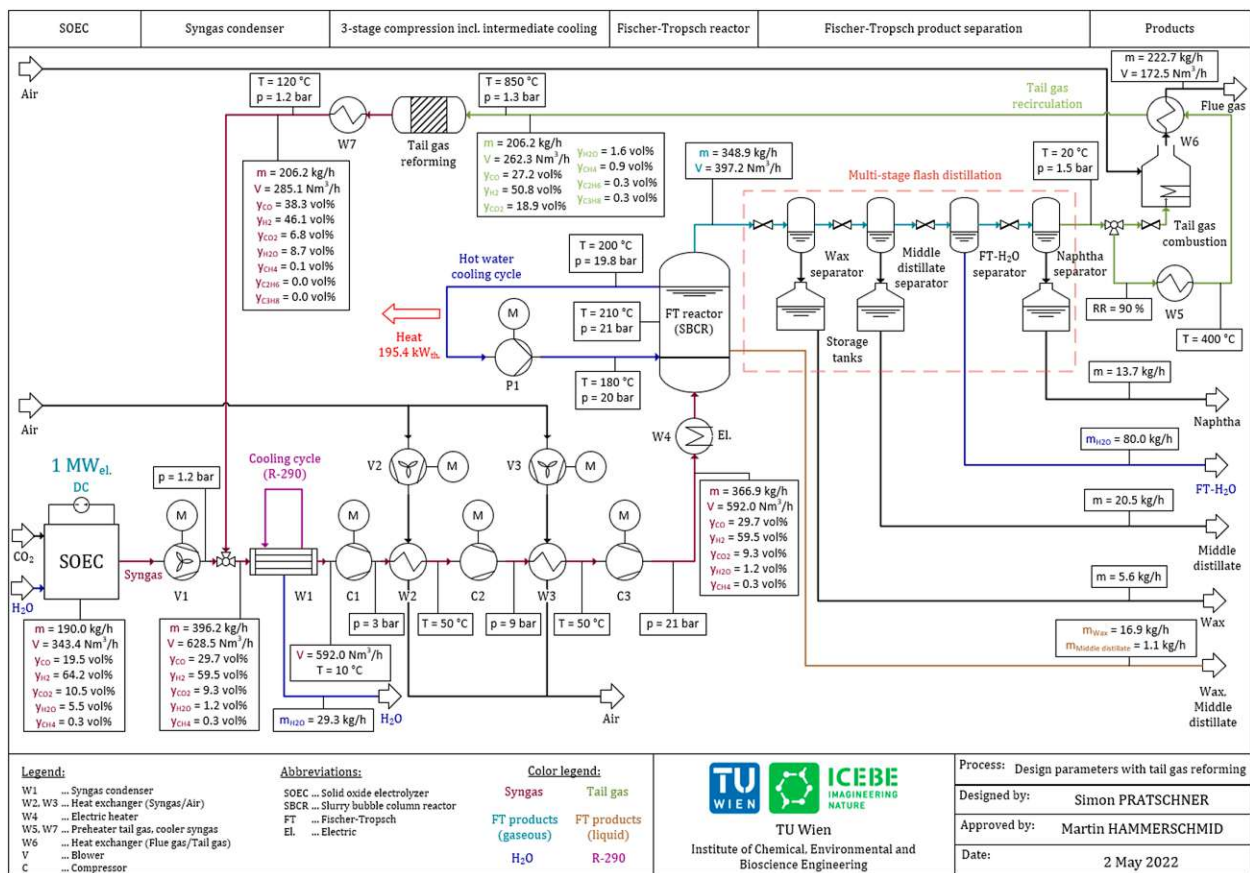


Figure 6. Design parameters of the plant configuration including tail gas reforming.

3.2. Fischer–Tropsch Synthesis—Products and Reaction Heat

The mass flow rates and distributions of the produced hydrocarbons, the produced Fischer–Tropsch water and the reaction heat are analyzed in this section. According to Table 3, the product fractions are divided into methane, ethane, propane, naphtha, middle distillate and wax. Table 4 summarizes the findings concerning the mass flow rates of Fischer–Tropsch products and the released reaction heat for process configurations with or without a tail gas reformer. The once-through configuration can be seen as a basic scenario with no recirculation of tail gas. As expected, high values of the recirculation ratio led to a significant rise in the obtained product streams. Without a tail gas reformer, a maximum mass flow rate of 47.8 kg/h could be realized. The integration of a tail gas reformer resulted in a maximum achievable product stream of 57.8 kg/h. However, this came at the price of combusting the purge gas, making it unavailable for potential downstream applications.

Table 4. Fischer–Tropsch products and reaction heat for various process configurations.

Fischer–Tropsch Products [kg/h]	Process Configuration (Recirculation Ratio of Tail Gas)		
	Once-Through (RR = 0%)	No Reformer (RR = 90%)	With Reformer (RR = 90%)
CH ₄	1.1 ¹	1.3 ¹	– ²
Ethane and propane	1.3 ¹	2.2 ¹	– ²
Naphtha	6.3	10.5	13.7
Middle distillate	10.0	16.5	21.5
Wax	10.4	17.3	22.6
Σ Fischer–Tropsch products	29.1	47.8	57.8
Fischer–Tropsch H ₂ O	36.5	62.3	80.0
Reaction heat [kW _{th}]	90.3	149.6	195.4

¹ Entrained inside the purge gas stream. ² Purge gas is combusted to heat the tail gas before the reformer.

Figure 7 depicts the rise in hydrocarbons obtained with an increase in the recirculation ratio. In general, the mass flow rates of products rise exponentially with an increase in RR but show a significantly higher slope when including a tail gas reformer. As mentioned before, the purge gas needs to be combusted to heat the recirculated tail gas before the reformer. Hence, no methane, ethane or propane can be obtained when applying a tail gas reformer.

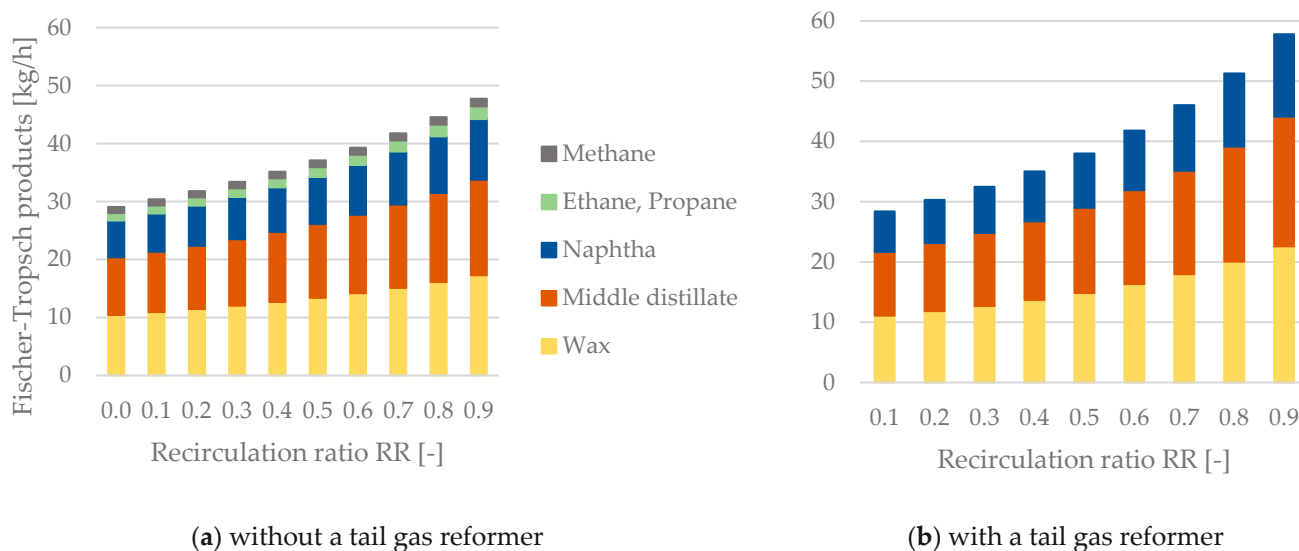


Figure 7. Fischer-Tropsch products as a function of the recirculation ratio RR—(a) process configuration without a tail gas reformer, (b) process configuration with a tail gas reformer.

3.3. $H_2:CO$ Ratio of the SOEC (Co-Electrolysis) Unit

As explained in Section 2.1, the SOEC unit controls the reactor's $H_2:CO$ ratio at $H_2:CO_{FT} = 2$ by adjusting its $H_2:CO$ ratio. For process routes excluding tail gas reforming, $H_2:CO_{SOEC}$ does only change from 2.00 (RR = 0.0) to 2.09 (RR = 0.9), whereas $H_2:CO_{SOEC}$ increases to a value of 3.30 (RR = 0.9) when implementing the reforming of tail gas. A graphical display for $H_2:CO_{SOEC}$ as a function of RR is plotted in Figure 8.

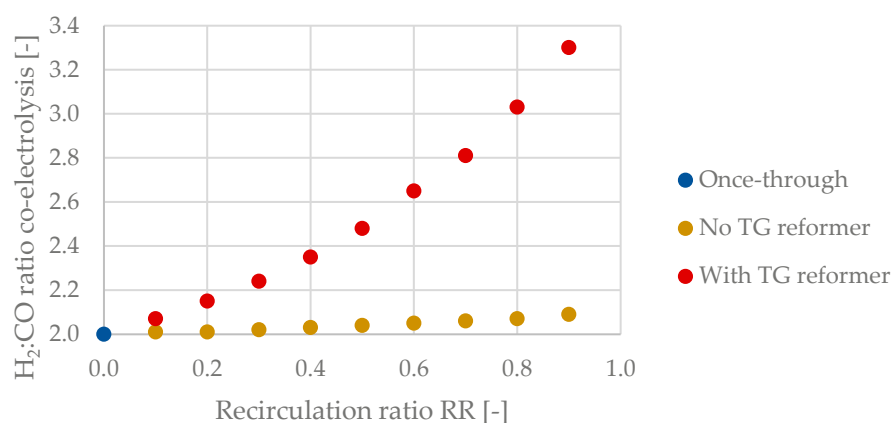


Figure 8. $H_2:CO$ ratio of the SOEC (co-electrolysis) unit with and without a tail gas reformer.

3.4. Tail Gas

Analyzing the mass flow and volume flow rates, along with the composition of the recirculated tail gas stream, is critical to answering the posed questions and will be elaborated in detail in this section.

3.4.1. Mass Flow and Volume Flow Rates of recirculated Tail Gas

Figure 9 highlights the significant difference in the recirculated tail gas streams when comparing process configurations with and without tail gas reforming. The difference between the mass flow rates is negligible for $RR < 0.5$. However, the amounts of recirculated tail gas diverge rapidly as the recirculation ratio surpasses a value of 0.5. A maximum difference of 452.5 kg/h can be seen for a recirculation ratio of 0.9. This rapid growth for configuration B can be explained by the accumulation of CO_2 inside the tail gas stream, as elaborated in Section 3.4.2. The differences appear to be less critical when analyzing the volume flow rates of recirculated tail gas with diverging values for recirculation ratios of 0.7 and higher.

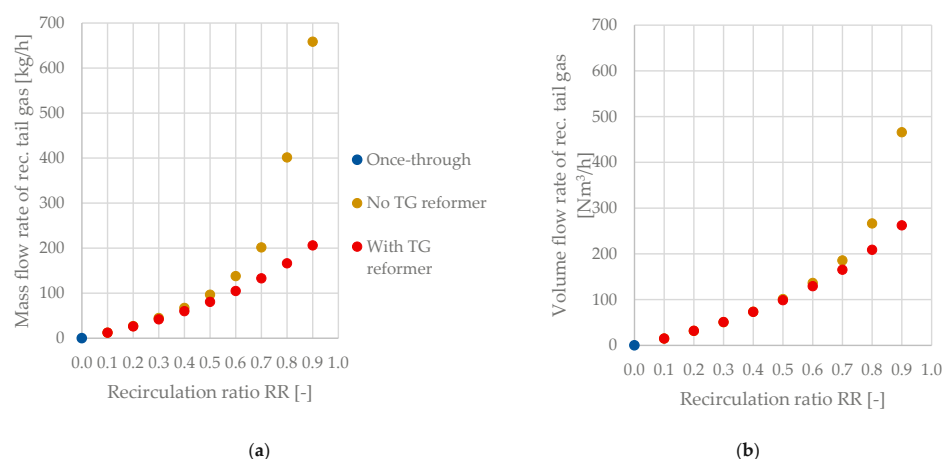


Figure 9. Recirculated tail gas as a function of the recirculation ratio RR and the process configuration—(a) mass flow rate, (b) volume flow rate.

3.4.2. Composition of Tail Gas and Tail Gas Reforming

The tail gas leaving the product separation step consists of the following compounds:

- Non-reacted reactants, i.e., CO and H_2 ;
- Inert gases, i.e., CO_2 ;
- Non-condensed products, i.e., CH_4 , ethane, propane and Fischer–Tropsch H_2O .

The tail gas compositions for the respective process configuration and recirculation ratio are stated in Table 5. Implementing a tail gas reformer reduces the shares of CO_2 , CH_4 , ethane and propane inside the tail gas stream significantly. A disadvantage is the increased percentage of water due to the reverse water–gas shift reaction.

Table 5. Tail gas composition for process configurations with and without a tail gas reformer.

Parameter	Symbol	Unit	Process Configuration (Recirculation Ratio of Tail Gas)			
			Once-Through (RR = 0%)	No Reformer (RR = 90%)	Reformer IN (RR = 90%)	Reformer OUT (RR = 90%)
CO	y_{CO}	vol%	26.0	11.7	27.2	38.4
H_2	y_{H_2}	vol%	48.7	21.9	50.8	45.2
CO_2	y_{CO_2}	vol%	21.7	60.1	18.9	7.2
H_2O	y_{H_2O}	vol%	2.0	0.2	1.6	9.1
CH_4	y_{CH_4}	vol%	1.0	3.6	0.9	0.1
Ethane	$y_{C_2H_6}$	vol%	0.3	1.3	0.3	0.0
Propane	$y_{C_3H_8}$	vol%	0.3	1.2	0.3	0.0

The tail gas composition of the process route without a reformer as a function of the recirculation ratio is plotted in Figure 10. A significant rise in the share of CO_2 can be seen after surpassing a recirculation ratio of 0.6. Non-condensable products, i.e., CH_4 , ethane and propane, also accumulate in the tail gas stream but are less crucial than CO_2 . The maximum share of $y_{CO_2} = 60.1$ vol% inside the system can be seen at $RR = 0.9$.

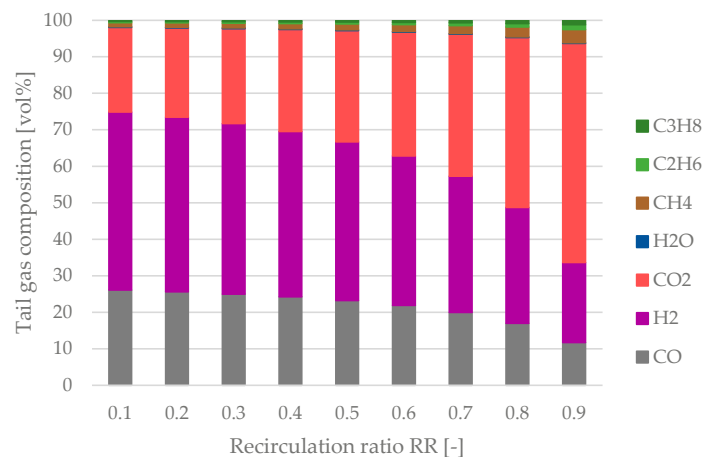


Figure 10. Tail gas composition as a function of the recirculation ratio RR for the process configuration without a tail gas reformer.

The tail gas composition at the reformer's inlet and outlet is plotted in Figure 11. A relative constant regime before and after the reactor can be noted. The share of CO at the reformer's inlet remains almost constant, whereas the share of H₂ increases slightly with a rise in the recirculation ratio. Small shares of gaseous hydrocarbons can be seen at the reactor's inlet, which are almost entirely converted to H₂ and CO inside the reformer. A significant increase concerning the share of H₂O after the reformer occurs. Hence, the insertion of additional steam before the tail gas reformer is not beneficial. A sufficient amount of H₂O is formed by the rWGS reaction inside the reformer (Equation (10)) to cover the H₂O demand for the reforming of gaseous hydrocarbons.

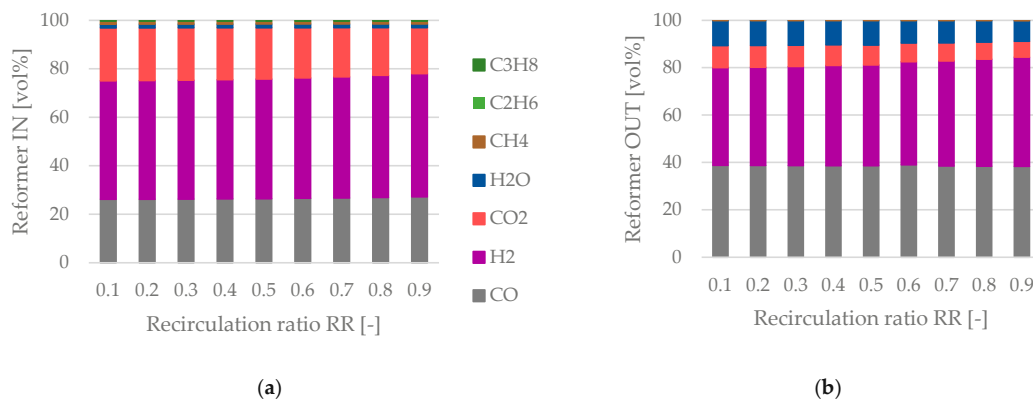


Figure 11. Tail gas reforming—(a) tail gas composition at the reformer's inlet, (b) tail gas composition at the reformer's outlet as a function of the recirculation ratio.

3.5. Purge Gas

The combustion of purge gas is not necessary for process configurations without a tail gas reformer. Hence, the mass flow rate of purge gas and the stream's chemical energy are important factors for designing potential downstream processes.

Figure 12 shows the mass flow rate of purge gas being drained from the system (Figure 12a) and the purge gas stream's chemical energy (Figure 12b) as a function of the recirculation ratio RR. The mass flow rate of purge gas ranges from 116.6 to 73.2 kg/h. The stream's chemical energy decreases disproportionately from 365.3 to 102.1 kW due to the stream's increasing share of CO₂ for an increase in the amount of recirculated tail gas.

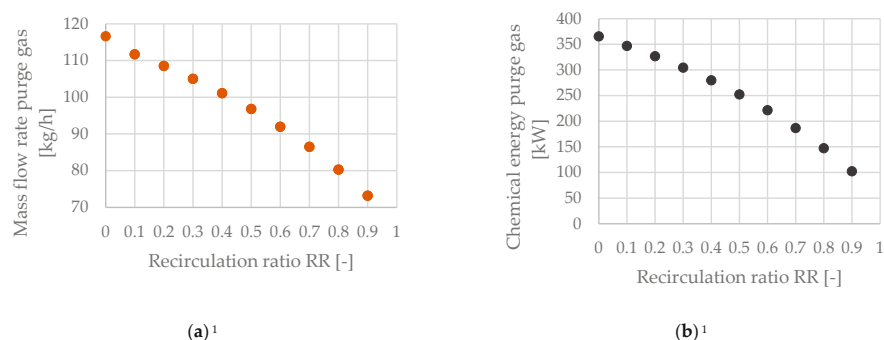


Figure 12. Purge gas stream for the configuration without a tail gas reformer—(a) mass flow rate as a function of the recirculation ratio, (b) chemical energy as a function of the recirculation ratio. ¹ No purge gas stream occurs for the process route that includes a tail gas reformer.

3.6. Power Demand of Auxiliary Equipment

The PtL plant's auxiliary power demand includes all devices except the SOEC unit, i.e., compressors, blowers, the syngas condenser and pumps. Since the SOEC's power input was set as constant, 1 MW_{el.}, the electricity demand of auxiliary devices defines the plant's PtL efficiency, in combination with the product's chemical energy. The following process steps require electricity:

- Syngas compression;
- Syngas condensing;
- Syngas intermediate cooling;
- Tail gas recirculation;
- Pumping for the reactor cooling cycle and the separation of products.

Figure 13 shows a comparison of the auxiliary equipment's power demand between plant configurations without (Figure 13a) and with (Figure 13b) a tail gas reformer. The syngas compression accounts for the highest share, whereas the power demand of pumps is negligible. If no tail gas reformer is integrated, the recirculation ratio has almost no effect on the power demand. An exponential increase can be seen when analyzing the process configuration including a tail gas reformer. Reasons for this behavior are the recirculation of tail gas to the condenser's inlet and the depressurization via a multi-stage flash distillation to increase the conversion of CO₂ and hydrocarbons inside the reformer.

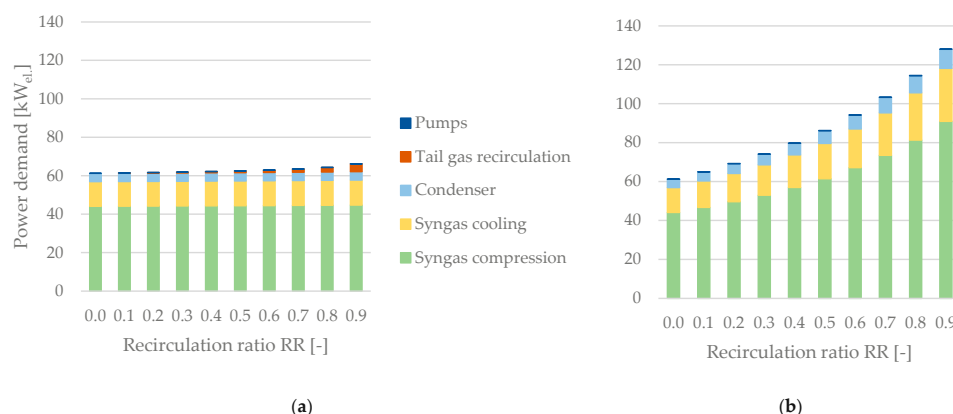


Figure 13. Power demand of auxiliary equipment excluding the SOEC unit as a function of the recirculation ratio—(a) without a tail gas reformer, (b) with a tail gas reformer.

3.7. Power-to-Liquid Efficiency and Plant Efficiency

As described in Section 2.7, the PtL efficiency η_{PtL} is defined as the rate of the products' chemical energy generation, excluding CH₄ and LPG and the total electricity input into the system (Equation (17)). To enhance comparability between process configurations with

and without a tail gas reformer, an additional indicator, the plant efficiency η_{Plant} , has been introduced (Equation (18)).

Table 6 sums up the Power-to-Liquid efficiency and plant efficiency of the analyzed process configurations. A significant increase in η_{PtL} can be realized by raising the recirculation ratio RR with a maximum value of 62.7% when implementing a tail gas reformer.

Table 6. Power-to-Liquid efficiency and plant efficiency for the chosen process configurations.

Parameter	Symbol	Unit	Process Configuration (Recirculation Ratio of Tail Gas)		
			Once-Through (RR = 0%)	No Reformer (RR = 90%)	With Reformer (RR = 90%)
Power-to-Liquid efficiency ¹	η_{PtL}	%	30.8	50.8	62.7
Plant efficiency ²	η_{Plant}	%	33.8	55.2	62.7
Total power demand	P_{Total}	kW_{el}	1061.3	1066.3	1128.1

¹ Excluding CH_4 , ethane and propane inside the purge gas stream. ² Including CH_4 , ethane and propane inside the purge gas stream.

The exponential development of η_{PtL} and η_{Plant} as a function of the recirculation ratio is plotted in Figure 14.

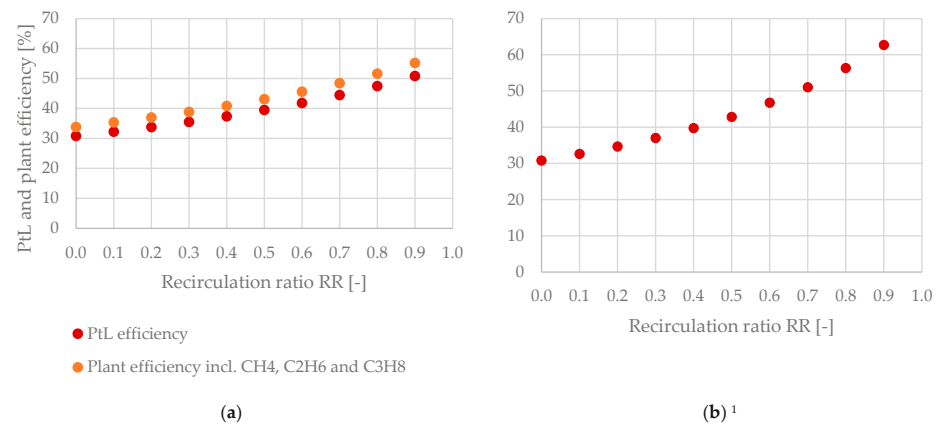


Figure 14. Power-to-Liquid efficiency and plant efficiency as a function of the recirculation ratio—(a) without tail gas reforming, (b) with tail gas reforming. ¹ η_{PtL} and η_{Plant} are equal due to the combustion of the purge gas stream.

3.8. CO Conversion of the Power-to-Liquid Plant

The growth of $X_{\text{CO,Plant}}$ is exponential for the process configuration without a reformer and linear when implementing a tail gas reformer, as depicted in Figure 15. This behavior can be explained by the significant change of the tail gas composition without a reformer, whereas the composition of tail gas is almost constant at the reformer's outlet, as stated in Section 3.4.2. The maximum values obtained were 92.4% with no tail gas reformer and 96.5% when implementing a reformer.

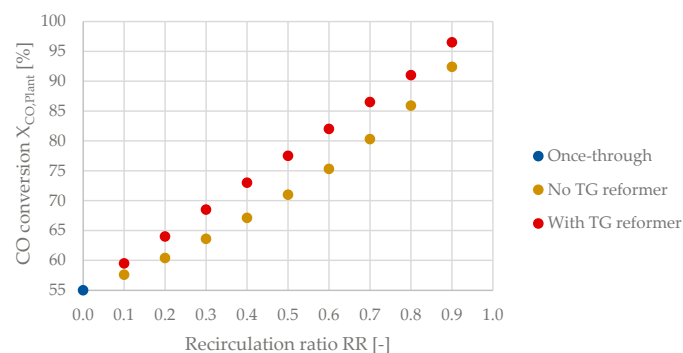


Figure 15. CO conversion at a system level as a function of the recirculation ratio.

4. Discussion

The underlying work highlights the importance of tail gas recirculation to achieve feasible Power-to-Liquid efficiencies. A maximum value of 62.7% could be realized by adding a tail gas reformer to the recirculation line compared to only 30.8% via a once-through configuration. A significant accumulation of CO₂ inside the system of up to 60.1 vol% was observed without a tail gas reforming step, limiting the performance of process configurations without a tail gas reformer to a maximum Power-to-Liquid efficiency of 50.8%. A possible option to solve this problem is to increase the SOEC's CO₂ conversion. In addition, the application of a Fe-based Fischer–Tropsch catalyst might be a viable option due to its activity in the rWGS reaction.

Becker et al. determined a system efficiency of 51% for a plant including the subsequent processing of the Fischer–Tropsch syncrude to gasoline and diesel [37]. Cinti et al. included the recirculation of tail gas to the SOEC (operating in co-electrolysis mode) unit's inlet in combination with a Fischer–Tropsch reactor, and obtained a PtL efficiency of 57% [35]. Maximum PtL efficiencies of 54.2% (air mode) and 51.9% (oxyfuel mode) were obtained for a PtL plant valorizing biogenic CO₂ derived from the combustion of woodchips to methanol by [12]. PtL efficiencies of up to 63% are possible for systems including a high-temperature electrolyzer valorizing CO₂ originating from a highly concentrated source, e.g., a biogas upgrading plant, according to [46]. Hence, this work's maximum Power-to-Liquid efficiency of 62.7% seems reasonable, since the CO₂ capture unit's power demand was not considered.

Table 7 sums up the advantages and disadvantages of process configurations with and without a tail gas reformer. The plant's key performance indicators, i.e., the Power-to-Liquid efficiency and the mass flow rates of produced hydrocarbons, benefit significantly from implementing a tail gas reformer. However, to keep the system's complexity at a feasible level for the swift deployment of pilot scale PtL plants, a configuration without an additional tail gas reformer is a viable option.

Table 7. Performances and feasibility of pilot scale plants producing synthetic fuels and wax with and without implementing a tail gas reformer.

Parameter	Process Configuration	
	Without Tail Gas Reformer	With Tail Gas Reformer
PtL efficiency η_{PtL}	–	+
Fischer–Tropsch products	–	+
Technical expenditure	+	– ¹
Costs	+	– ¹
Deployment speed	+	–
Utilization of purge gas	+	– ²

¹ Additional reactor and catalyst are required for tail gas reforming. ² Purge gas is combusted to heat the tail gas before the reformer.

PtL plants at pilot scale can potentially be combined with decentralized wind turbines or solar power plants to avoid rising electricity prices, making renewable fuels and wax economically competitive to products derived from increasingly expensive fossil resources.

This work aimed to shift the focus towards the Fischer–Tropsch synthesis by applying the extended ASF distribution and internal tail gas recirculation to the Fischer–Tropsch reactor's inlet. Hence, we added value to previous studies, which mainly used the standard ASF distribution and rather idealized assumptions concerning the Fischer–Tropsch synthesis. In addition, two process configurations, i.e., with and without a tail gas reformer, were analyzed to provide a recommendation concerning the ideal plant configuration for the quick deployment of Power-to-Liquid plants at a pilot scale.

5. Conclusions

The presented work was conducted to answer the question of which Power-to-Liquid efficiencies can be realized by pilot scale plants combining a SOEC unit with Fischer–

Tropsch synthesis. In addition, a recommended plant configuration for the production of synthetic fuels and wax at a pilot scale was provided.

Table 8 sums up this work's central findings by comparing the key performance indicators obtained by the respective process configuration.

Table 8. Obtained key performance indicators of the Power-to-Liquid plant for the respective process configurations with and without a tail gas reformer.

Parameter	Symbol	Unit	Process Configuration (Recirculation Ratio of Tail Gas)		
			Once-Through (RR = 0%)	No Reformer (RR = 90%)	With Reformer (RR = 90%)
Power-to-Liquid efficiency	η_{PtL}	%	30.8	50.8	62.7
Fischer–Tropsch products ¹	m_{FT}	kg/h	26.7	44.3	57.8
CO conversion of the plant	$X_{\text{CO,Plant}}$	%	55.0	92.4	96.5
Required H ₂ :CO ratio (SOEC)	H ₂ :CO _{SOEC}	-	2.00	2.09	3.30
Total power demand ²	P_{el}	kW _{el.}	1061.3	1066.3	1128.1
Purge gas chemical energy	$U_{\text{Purge gas}}$	kW	365.3	102.1	- ³

¹ Excluding CH₄, ethane and propane inside the purge gas stream. ² Power demand of the SOEC is 1000 kW_{el.}

³ Purge gas is combusted to heat the tail gas before the reformer.

A more sophisticated model concerning the SOEC should be developed and applied for future research to evaluate the presented results. Furthermore, the synergy between the SOEC unit and the Fischer–Tropsch reactor needs to be analyzed from an engineering perspective for various modes of operation. Designing the tail gas reforming process in detail has significant potential to improve the concept's feasibility at an industrial scale. Another possibility for improvement is the validation and extension of the presented Fischer–Tropsch model by conducting laboratory-scale experiments including several catalysts based on cobalt or iron. Process heat integration is a crucial way to secure the presented concept's feasibility but was not within this work's scope. Hence, future research should focus on implementing state-of-the-art heat integration methods, e.g., pinch analysis and multi-criteria analysis. In addition, a cost estimate of the respective process routes needs to be conducted to persuade possible investors to fund Power-to-Liquid plants producing synthetic fuel and wax. Conducting a techno-economic assessment is essential to transfer PtL plants to the next level, and thus should be prioritized in future research projects.

Author Contributions: Conceptualization, S.P., S.M. and F.W.; methodology, S.P. and M.H.; software, S.P. and M.H.; validation, S.P., M.H. and F.J.M.; investigation, S.P.; resources, M.H. and S.M.; data curation, S.P. and M.H.; writing—original draft preparation, S.P.; writing—review and editing, S.P., F.W.; visualization, S.P., M.H. and F.J.M.; supervision, S.M. and F.W.; project administration, S.M.; All authors have read and agreed to the published version of the manuscript.

Funding: The underlying work has received funding from the Mobility of the Future program—a research, technology and innovation funding program of the Federal Ministry of Climate Action, Environment, Energy, Mobility, Innovation and Technology, Republic of Austria. The Austrian Research Promotion Agency (FFG) has been authorized for the program management of the project “IFE—Innovation Flüssige Energie” (project #884340). In addition, the authors would like to thank TU Wien Bibliothek for covering the APC through its Open Access Funding Program.

Data Availability Statement: For further information regarding data presented in this article, please contact the corresponding author.

Acknowledgments: The authors would like to acknowledge the “IFE—Innovation Flüssige Energie” consortia, the doctoral college CO₂Refinery at TU Wien and the open access funding by TU Wien.

Conflicts of Interest: The authors declare no conflict of interest.

Abbreviations

ASF	Anderson–Schulz–Flory distribution
C	Compressor
CCU	Carbon capture and utilization
DAC	Direct air capture
DME	Dimethyl ether
eASF	Extended Anderson-Schulz-Flory distribution
FBMR	Fixed bed multitubular reactor
FT	Fischer–Tropsch
GHG	Greenhouse gas
HTFT	High-temperature Fischer–Tropsch synthesis
LTFT	Low-temperature Fischer–Tropsch synthesis
PEMEC	Proton exchange membrane electrolysis cell
rWGS	Reverse water-gas shift
SBCR	Slurry bubble column reactor
SOEC	Solid oxide electrolysis cell
Syngas	Synthesis gas provided by the SOEC unit
TG	Tail gas
PtX	Power-to-X
PtG	Power-to-Gas
PtL	Power-to-Liquid
V	Blower
W	Heat exchanger

Nomenclature

<i>LHV</i>	Lower heating value [MJ/kg]
<i>m</i>	Mass flow rate [kg/h]
<i>P</i>	Power [kW_{el}]
<i>p</i>	Pressure [bar]
<i>RR</i>	Recirculation ratio [-,%]
<i>T</i>	Temperature [K, °C]
<i>U</i>	Chemical energy [kW]
X_{CO}	CO conversion [%]
<i>x</i>	Molar fraction [-]
<i>y</i>	Volume fraction [vol%]
α_1	Dominant chain growth probability for C_1 to C_7 (eASF) [-]
α_2	Dominant chain growth probability for C_{13+} (eASF) [-]
β	Readsorption factor—selectivity for C_2H_6 (eASF) [-]
γ	Termination factor—selectivity for CH_4 (eASF) [-]
η	Efficiency [%]
λ	Air ratio [-]
μ	Factor to merge α_1 and α_2 (eASF) [-]
$\Delta_r G$	Gibbs free energy of a chemical reaction [kJ/mol]
$\Delta_r H$	Reaction enthalpy [kJ/mol]
$\Delta_r S$	Reaction entropy [kJ/(mol·K)]
<i>m.</i>	Mechanical
<i>el.</i>	Electric
<i>th.</i>	Thermal
<i>max.</i>	Maximum
<i>s</i>	Isentropic
<i>Compr.</i>	Compressor/compression
<i>Con.</i>	Condenser
<i>Rec.</i>	Recirculation/recirculated

References

1. Trends in Atmospheric Carbon Dioxide—Annual Mean Global Carbon Dioxide Growth Rates. Available online: https://gml.noaa.gov/ccgg/trends/gl_gr.html (accessed on 7 January 2022).
2. Trends in Atmospheric Carbon Dioxide—Global Monthly Mean CO₂. Available online: <https://gml.noaa.gov/ccgg/trends/global.html> (accessed on 7 January 2022).
3. BP p.l.c. Statistical Review of World Energy—70th Edition. 2021. Available online: <https://www.bp.com/content/dam/bp/business-sites/en/global/corporate/pdfs/energy-economics/statistical-review/bp-stats-review-2021-full-report.pdf> (accessed on 7 January 2022).
4. Buysse, C.; Miller, J. Transport Could Burn up the EU's Entire Carbon Budget. Available online: <https://theicct.org/blog/staff/eu-carbon-budget-apr2021> (accessed on 7 January 2022).
5. Josh A European Green Deal. Striving to Be the First Climate-Neutral Continent. Available online: https://ec.europa.eu/info/strategy/priorities-2019-2024/european-green-deal_en (accessed on 7 January 2022).
6. Austrian Automobile, Motorcycle and Touring Club. Expertenbericht Mobilität und Klimaschutz 2030. Available online: <https://www.oeamtc.at/club/oeamtc-expertenbericht-mobilitaet-klimaschutz-2030-25873728#:~:text=%22Alles%20in%20alles%20werden%20die,betont%20%C3%96AMTC%2DDirektor%20Oliver%20Schmerold> (accessed on 17 March 2022).
7. E-FUEL—The Renewable Fuel. Available online: <https://www.sunfire.de/en/e-fuel> (accessed on 7 January 2022).
8. Wulf, C.; Zapp, P.; Schreiber, A. Review of Power-to-X Demonstration Projects in Europe. *Front. Energy Res.* **2020**, *8*, 191. [CrossRef]
9. Karka, P.; Johnsson, F.; Papadokonstantakis, S. Perspectives for Greening European Fossil-Fuel Infrastructures Through Use of Biomass: The Case of Liquid Biofuels Based on Lignocellulosic Resources. *Front. Energy Res.* **2021**, *9*, 636782. [CrossRef]
10. Mailaram, S.; Kumar, P.; Kunamalla, A.; Saklecha, P.; Maity, S.K. Biomass, Biorefinery, and Biofuels. In *Sustainable Fuel Technologies Handbook*; Elsevier: Amsterdam, The Netherlands, 2021; pp. 51–87. ISBN 978-0-12-822989-7.
11. Green Fuel from Residual Waste. Available online: <https://smartcity.wien.gv.at/en/waste2value/> (accessed on 24 May 2022).
12. Pratschner, S.; Skopec, P.; Hrdlicka, J.; Winter, F. Power-to-Green Methanol via CO₂ Hydrogenation—A Concept Study Including Oxyfuel Fluidized Bed Combustion of Biomass. *Energies* **2021**, *14*, 4638. [CrossRef]
13. Siemens Energy. Haru Oni: A New Age of Discovery. Available online: <https://www.siemens-energy.com/global/en/news/magazine/2021/haru-oni.html> (accessed on 7 January 2022).
14. Marlin, D.S.; Sarron, E.; Sigurbjörnsson, Ó. Process Advantages of Direct CO₂ to Methanol Synthesis. *Front. Chem.* **2018**, *6*. [CrossRef]
15. Bowker, M. Methanol Synthesis from CO₂ Hydrogenation. *ChemCatChem* **2019**, *11*, 4238–4246. [CrossRef] [PubMed]
16. Norsk E-Fuel. Supplying Your Renewable Fuel. Unlimited. On the Road to Climate Neutral Transportation. Available online: <https://www.norsk-e-fuel.com/en/> (accessed on 7 January 2022).
17. Fisch, I. Sustainable E-Fuels for Aviation. Available online: <https://ineratec.de/en/e-fuels-for-aviation/> (accessed on 7 January 2022).
18. Industrial Power-to-Liquid Pioneer Plant in Germany 2022. INERATEC. Available online: <https://ineratec.de/en/power-to-liquid-pioneer-plant-2022/> (accessed on 17 March 2022).
19. de Klerk, A. *Fischer-Tropsch Refining*, 1st ed.; Wiley-VCH: Weinheim, Germany, 2011; ISBN 978-3-527-63560-3.
20. Martinelli, M.; Gnanamani, M.K.; LeViness, S.; Jacobs, G.; Shafer, W.D. An Overview of Fischer-Tropsch Synthesis: X_tL Processes, Catalysts and Reactors. *Appl. Catal. A Gen.* **2020**, *608*, 117740. [CrossRef]
21. Badoga, S.; Gnanamani, M.K.; Martinelli, M.; Sparks, D.E.; Ma, W. Effect of Start-up Solvent on the Performance of Co Catalyst for Fischer-Tropsch Synthesis in Stirred-Tank Reactor. *Fuel* **2020**, *272*, 117707. [CrossRef]
22. Visconti, C.G.; Lietti, L.; Tronconi, E.; Rossini, S. Kinetics of Low-Temperature Fischer-Tropsch Synthesis on Cobalt Catalysts: Are Both Slurry Autoclave and Tubular Packed-Bed Reactors Adequate to Collect Relevant Data at Lab-Scale? *Can. J. Chem. Eng.* **2016**, *94*, 685–695. [CrossRef]
23. Todic, B.; Nowicki, L.; Nikacevic, N.; Bukur, D.B. Fischer–Tropsch Synthesis Product Selectivity over an Industrial Iron-Based Catalyst: Effect of Process Conditions. *Catal. Today* **2016**, *261*, 28–39. [CrossRef]
24. Peña, D.; Griboval-Constant, A.; Lecocq, V.; Diehl, F.; Khodakov, A.Y. Influence of Operating Conditions in a Continuously Stirred Tank Reactor on the Formation of Carbon Species on Alumina Supported Cobalt Fischer–Tropsch Catalysts. *Catal. Today* **2013**, *215*, 43–51. [CrossRef]
25. Chambrey, S.; Fongarland, P.; Karaca, H.; Piché, S.; Griboval-Constant, A.; Schweich, D.; Luck, F.; Savin, S.; Khodakov, A.Y. Fischer–Tropsch Synthesis in Milli-Fixed Bed Reactor: Comparison with Centimetric Fixed Bed and Slurry Stirred Tank Reactors. *Catal. Today* **2011**, *171*, 201–206. [CrossRef]
26. de Klerk, A. Can Fischer–Tropsch Syncrude Be Refined to On-Specification Diesel Fuel? *Energy Fuels* **2009**, *23*, 4593–4604. [CrossRef]
27. Gruber, H.; Groß, P.; Rauch, R.; Reichhold, A.; Zweiler, R.; Aichernig, C.; Müller, S.; Ataimisch, N.; Hofbauer, H. Fischer-Tropsch Products from Biomass-Derived Syngas and Renewable Hydrogen. *Biomass Conv. Bioref.* **2021**, *11*, 2281–2292. [CrossRef]
28. Bekker, M.; Louw, N.R.; Jansen Van Rensburg, V.J.; Potgieter, J. The Benefits of Fischer-Tropsch Waxes in Synthetic Petroleum Jelly. *Int. J. Cosmet. Sci.* **2013**, *35*, 99–104. [CrossRef]
29. Guettel, R.; Kunz, U.; Turek, T. Reactors for Fischer-Tropsch Synthesis. *Chem. Eng. Technol.* **2008**, *31*, 746–754. [CrossRef]

30. Maitlis, P.M.; de Klerk, A. (Eds.) *Greener Fischer-Tropsch Processes for Fuels and Feedstocks*; Wiley-VCH: Weinheim, Germany, 2013; ISBN 978-3-527-32945-8.
31. Makhura, E.; Rakereng, J.; Rapoo, O.; Danha, G. Effect of the Operation Parameters on the Fischer Tropsch Synthesis Process Using Different Reactors. *Procedia Manuf.* **2019**, *35*, 349–355. [CrossRef]
32. Pfeifer, P.; Schmidt, S.; Betzner, F.; Kollmann, M.; Loewert, M.; Böltken, T.; Piermartini, P. Scale-up of Microstructured Fischer-Tropsch Reactors—Status and Perspectives. *Curr. Opin. Chem. Eng.* **2022**, *36*, 100776. [CrossRef]
33. Yang, J.; Boullousa, E.; Myrstad, R.; Venik, H.; Pfeifer, P.; Holmen, A. Fischer-Tropsch Synthesis on Co-Based Catalysts in a Microchannel Reactor—Effect of Temperature and Pressure on Selectivity and Stability. In *Fischer-Tropsch Synthesis, Catalysts and Catalysis*; CRC Press: Boca Raton, FL, USA, 2016; Chapter 12; pp. 223–251. ISBN 978-1-4665-5529-7.
34. Marchese, M.; Giglio, E.; Santarelli, M.; Lanzini, A. Energy Performance of Power-to-Liquid Applications Integrating Biogas Upgrading, Reverse Water Gas Shift, Solid Oxide Electrolysis and Fischer-Tropsch Technologies. *Energy Convers. Manag.* **2020**, *6*, 100041. [CrossRef]
35. Cinti, G.; Baldinelli, A.; Di Michele, A.; Desideri, U. Integration of Solid Oxide Electrolyzer and Fischer-Tropsch: A Sustainable Pathway for Synthetic Fuel. *Appl. Energy* **2016**, *162*, 308–320. [CrossRef]
36. König, D.H.; Freiberg, M.; Dietrich, R.-U.; Wörner, A. Techno-Economic Study of the Storage of Fluctuating Renewable Energy in Liquid Hydrocarbons. *Fuel* **2015**, *159*, 289–297. [CrossRef]
37. Becker, W.L.; Braun, R.J.; Penev, M.; Melaina, M. Production of Fischer-Tropsch Liquid Fuels from High Temperature Solid Oxide Co-Electrolysis Units. *Energy* **2012**, *47*, 99–115. [CrossRef]
38. Herz, G.; Reichelt, E.; Jahn, M. Techno-Economic Analysis of a Co-Electrolysis-Based Synthesis Process for the Production of Hydrocarbons. *Appl. Energy* **2018**, *215*, 309–320. [CrossRef]
39. Gao, R.; Zhang, C.; Jun, K.-W.; Kim, S.K.; Park, H.-G.; Zhao, T.; Wang, L.; Wan, H.; Guan, G. Green Liquid Fuel and Synthetic Natural Gas Production via CO₂ Hydrogenation Combined with Reverse Water-Gas-Shift and Co-based Fischer-Tropsch Synthesis. *J. CO₂ Util.* **2021**, *51*, 101619. [CrossRef]
40. Müller, S.; Groß, P.; Rauch, R.; Zweiler, R.; Aichernig, C.; Fuchs, M.; Hofbauer, H. Production of Diesel from Biomass and Wind Power—Energy Storage by the Use of the Fischer-Tropsch Process. *Biomass Conv. Bioref.* **2018**, *8*, 275–282. [CrossRef]
41. HELMETH—High Temperature Electrolysis Cell (SOEC). Available online: <http://www.helmeth.eu/index.php/technologies/high-temperature-electrolysis-cell-soec> (accessed on 22 February 2022).
42. Avallone, E.A.; Baumeister, T.; Sadegh, A.M. *Marks' Standard Handbook for Mechanical Engineers*; McGraw-Hill: New York, NY, USA, 2007; Chapter 14; ISBN 978-1-60119-653-8.
43. Guiler, J.; Díaz-López, J.A.; Berenguer, A.; Biset-Peiró, M.; Andreu, T. Fischer-Tropsch Synthesis: Towards a Highly-Selective Catalyst by Lanthanide Promotion under Relevant CO₂ Syngas Mixtures. *Appl. Catal. A Gen.* **2022**, *629*, 118423. [CrossRef]
44. Sauciuc, A.; Abosteif, Z.; Weber, G.; Potetz, A.; Rauch, R.; Hofbauer, H.; Schaub, G.; Dumitrescu, L. Influence of Operating Conditions on the Performance of Biomass-Based Fischer-Tropsch Synthesis. *Biomass Conv. Bioref.* **2012**, *2*, 253–263. [CrossRef]
45. Coutanceau, C.; Baranton, S.; Audichon, T. Hydrogen Production from Water Electrolysis. In *Hydrogen Electrochemical Production*; Elsevier: Amsterdam, The Netherlands, 2018; pp. 17–62. ISBN 978-0-12-811250-2.
46. Schmidt, P.; Weindorf, W. *Power-to-Liquids: Potential and Perspectives for the Future Supply of Renewable Aviation Fuel 2016*; German Environment Agency: Dessau-Roßlau, Germany, 2016; ISSN 2363-829X. Available online: https://www.umweltbundesamt.de/sites/default/files/medien/377/publikationen/161005_uba_hintergrund_ptl_barrierefrei.pdf (accessed on 17 March 2022).
47. Hauch, A.; Brodersen, K.; Chen, M.; Mogensen, M.B. Ni/YSZ Electrodes Structures Optimized for Increased Electrolysis Performance and Durability. *Solid State Ion.* **2016**, *293*, 27–36. [CrossRef]
48. Sattler, K. *Thermische Trennverfahren: Grundlagen, Auslegung, Apparate*; Wiley-VCH: Weinheim, Germany, 2007; Chapter 2; pp. 116–117. ISBN 978-3-527-30243-7.
49. Zhai, P.; Sun, G.; Zhu, Q.; Ma, D. Fischer-Tropsch Synthesis Nanostructured Catalysts: Understanding Structural Characteristics and Catalytic Reaction. *Nanotechnol. Rev.* **2013**, *2*, 547–576. [CrossRef]
50. Förtsch, D.; Pabst, K.; Groß-Hardt, E. The Product Distribution in Fischer-Tropsch Synthesis: An Extension of the ASF Model to Describe Common Deviations. *Chem. Eng. Sci.* **2015**, *138*, 333–346. [CrossRef]
51. Sengupta, S.; Jha, A.; Shende, P.; Maskara, R.; Das, A.K. Catalytic Performance of Co and Ni Doped Fe-Based Catalysts for the Hydrogenation of CO₂ to CO via Reverse Water-Gas Shift Reaction. *J. Environ. Chem. Eng.* **2019**, *7*, 102911. [CrossRef]
52. de Miranda, P.E.V. (Ed.) *Science and Engineering of Hydrogen-Based Energy Technologies: Hydrogen Production and Practical Applications in Energy Generation*; Academic Press Is an Imprint of Elsevier: London, UK; San Diego, CA, USA, 2019; ISBN 978-0-12-814251-6.

Paper III

Evaluation of biomass-based production of below zero emission reducing gas for the iron and steel industry

Hammerschmid, M., Müller, S., Fuchs, J., Hofbauer, H.

Biomass Conversion and Biorefinery, 2020, 11, 169-187

<https://doi.org/10.1007/s13399-020-00939-z>



Evaluation of biomass-based production of below zero emission reducing gas for the iron and steel industry

Martin Hammerschmid¹ · Stefan Müller¹ · Josef Fuchs¹ · Hermann Hofbauer¹

Received: 3 April 2020 / Revised: 1 August 2020 / Accepted: 4 August 2020 / Published online: 9 September 2020
© The Author(s) 2020

Abstract

The present paper focuses on the production of a below zero emission reducing gas for use in raw iron production. The biomass-based concept of sorption-enhanced reforming combined with oxyfuel combustion constitutes an additional opportunity for selective separation of CO₂. First experimental results from the test plant at TU Wien (100 kW) have been implemented. Based on these results, it could be demonstrated that the biomass-based product gas fulfills all requirements for the use in direct reduction plants and a concept for the commercial-scale use was developed. Additionally, the profitability of the below zero emission reducing gas concept within a techno-economic assessment is investigated. The results of the techno-economic assessment show that the production of biomass-based reducing gas can compete with the conventional natural gas route, if the required oxygen is delivered by an existing air separation unit and the utilization of the separated CO₂ is possible. The production costs of the biomass-based reducing gas are in the range of natural gas-based reducing gas and twice as high as the production of fossil coke in a coke oven plant. The CO₂ footprint of a direct reduction plant fed with biomass-based reducing gas is more than 80% lower compared with the conventional blast furnace route and could be even more if carbon capture and utilization is applied. Therefore, the biomass-based production of reducing gas could definitely make a reasonable contribution to a reduction of fossil CO₂ emissions within the iron and steel sector in Austria.

Keywords Iron and steel · Low-carbon steelmaking · Direct reduction · Biomass · Sorption-enhanced reforming · Oxyfuel combustion

1 Introduction

Today the iron and steel industry in EU-28 is responsible for 200 million tons of carbon dioxide [1] which amounts to a share of 5% of the total carbon dioxide equivalent (CO₂e) [2] emissions [3]. These numbers show that especially the transformation of heavy load industries like the iron and steel industry towards low-carbon technologies will be challenging. In Austria the iron and steel industry also contributes to a significant share concerning greenhouse gas emissions. In 2017, 8.1 million tons of crude steel were produced in Austria [4], which are responsible for around 16% of the total greenhouse gas emissions [5]. Technological development

has enabled to improve the energy efficiency and to reduce CO₂ emissions in this sector. However, the principles of steelmaking have not changed fundamentally over the years. In 2017, over 91% of the Austrian crude steel was produced within oxygen-blown converters, which were fed with hot metal from blast furnaces. The remaining share was produced within electric arc furnaces [4]. According to the EU Roadmap 2050 [6], the CO₂ emissions within the iron and steel industry must be reduced by around 85%. To accomplish this major goal, a complete conversion towards low-carbon steelmaking technologies has to be done.

Numerous researchers and international institutions investigate alternative low-carbon steelmaking routes. Especially, the ULCOS program [7, 8] has evaluated the CO₂ reduction potential of over 80 existing and potential technologies. Several investigations are working on further optimization of fossil fuel-based state-of-the-art processes like the coke and pulverized coal-based-integrated blast furnace route [9–11]. All this optimization steps to reduce the consumption of fossil fuels are limited [12]. For reaching the previous described

✉ Martin Hammerschmid
martin.hammerschmid@tuwien.ac.at

¹ Institute of Chemical Engineering, Environmental and Bioscience Engineering, TU WIEN, Getreidemarkt 9/166, 1060 Vienna, Austria

climate goals within the iron and steel sector, a fundamental change of steelmaking is necessary. The ULCOS program [7, 8] identified four technologies with CO₂ emission reduction potentials of more than 50%. The technologies within this program, which are based on carbon capture and storage (CCS) or utilization (CCU), are the top-gas recycling within the blast furnace (BF-TGR-CCS/U), a novel bath-smelting technology (HISARNA-CCS/U) [13, 14], and a novel direct reduction process (ULCORED-CCS/U). Only the novel ULCOLYSIS [15] process, which is characterized by melting iron ore through electric direct reduction, is not based on CCS or CCU. In addition to the research activities in Europe, the COURSE50 program in Japan, POSCO in Korea, AISI in the USA, and the Australian program are some international examples for investigations regarding CO₂ reduction in the iron and steel industry [16]. The COURSE50 program [8, 16, 17] is focused on H₂-based reducing agents in blast furnace (BF) for decreasing the fossil coke consumption and technologies for capturing, separating, and recovering CO₂ from the BF gas. POSCO [8, 16, 18] in Korea is working on the adaptation of CCS and CCU to smelting reduction processes, like the FINEX and COREX process. Furthermore, POSCO is researching in bio-slag utilization, pre-reduction and heat recovery of hot sinter, CO₂ absorption using ammonia scrubber, hydrogen production out of coke-oven gas (COG), and iron ore reduction using hydrogen-enriched syngas. AISI [8, 16] is working on the molten oxide electrolysis, which is similar to the ULCOLYSIS concept and iron making by hydrogen flash smelting. The research programs regarding breakthrough iron and steelmaking technologies in Brazil, Canada, and Australia [19] are all strongly focused on biomass-based iron and steel production routes for replacing fossil coal and coke by use of biomass-derived chars as substitutes [8, 16, 20].

Summing up, there are a lot of investigations going on around the world to reduce the CO₂ footprint of the iron and steel industry.

The most of the previous described concepts apply CCS or CCU to reach a CO₂ reduction potential over 50% in comparison to the conventional integrated BF route. Nevertheless, the implementation of CCS requires a fundamental investigation due to storage sites and long-term response of the environment. Beside the CCS or CCU-based approaches, the replacement of fossil fuel-based reducing agents by biomass-based substitutes or the use of hydrogen as reducing agent are promising approaches for reaching the climate targets within the iron and steel sector. Furthermore, some electric direct reduction processes like ULCOWIN, MOE, and ULCOLYSIS are under investigation. One possible CO₂ reduction path could also be the rise of the share of steel production through electric arc furnaces. Therefore, enough high-quality scrap must be available.

With respect to the estimates regarding biomass potential in the next decades [20, 21], in Austria beside the rise of the

share of steel production through scrap-based electric arc furnaces, another possible synergetic transition option seems to be the replacement of the integrated blast furnace route with the direct reduction of iron ore based on biomass-based reducing gas. The Austrian steel manufacturing and processing group, voestalpine AG, is already operating one of the biggest direct reduction plants, based on the MIDREX concept and reformed natural gas as reducing agent in Texas [22]. This approach would combine the gained expertise within the field of direct reduction with the Austria-developed concept of dual fluidized bed steam gasification [23]. Within the present work, a biomass-based production of biogenic reducing gas through dual fluidized bed steam gasification, which allows the replacement of steam reformed natural gas, is investigated. At this stage, it remains unclear if the investigated process is competitive with respect to other production routes for the supply of reducing gas for iron ore reduction.

So far, following question has not been answered sufficiently:

How can the production of biomass-based reducing gas via dual fluidized bed steam gasification enable a reasonable contribution to a reduction of fossil CO₂ emissions within the iron and steel sector?

The following paper describes the results of the investigated process enabling the production of a below zero emission reducing gas by applying the biomass-based dual fluidized bed steam gasification technology in combination with carbon capture and utilization. The investigations are based on experimental results combined with simulation work. The present paper discusses:

- The *comparison of different iron- and steelmaking routes regarding their CO₂ footprint*
- The *proposed process concept* for the production of biomass-based reducing gas
- *Experimental and simulation results* achieved
- The results of a *techno-economic assessment*

2 Concept and methodology

With regard to the techno-economic assessment of the selective separation of CO₂ technology OxySER, a plant concept for the integration in a direct reduction process has been developed. Beforehand, a short overview and comparison of primary and secondary iron and steelmaking routes regarding their CO₂ footprints will be given. Furthermore, the application of dual fluidized bed steam gasification with respect to the combination of sorption-enhanced reforming and oxyfuel combustion will be explained.

2.1 Comparison of iron and steelmaking routes regarding their CO₂ footprint

Two main steelmaking processes can be distinguished. The primary steelmaking route converts virgin iron ores into crude steel (CS). Secondary steelmaking is characterized by the recycling of iron and steel scrap in an electric arc furnace [8, 24]. Table 1 gives an overview of chosen iron and steelmaking routes and the comparison regarding CO₂ footprint. First of all, the primary steelmaking integrated blast furnace (BF) route, which is predominant in Austria. Thereby, steel production takes place at an integrated steel plant, where iron ores are reduced into hot metal through the use of reduction agents such as coke or coal. Afterwards, the hot metal is converted into steel by oxygen injection in a basic oxygen furnace (BOF). As result of the high energy demand of 11.4 GJ/t_{CS} on fossil reducing agents, the CO₂ footprint of the BF-BOF route is with 1.694 t CO₂e/t_{CS} very high [25]. Furthermore, the secondary steelmaking electric arc furnace (EAF) route is used in Austria. Therein, the major feedstock is ferrous scrap, which is melted mainly through the use of electricity. However, increasing the share of EAF steel is constrained by the availability of scrap, and the quality requirements for steel grades have to meet [8]. The smelting reduction route belongs also to the state-of-the-art iron and steelmaking routes. Within this route, iron ores are heated and pre-reduced by the off-gas coming from the smelter-gasifier. The pre-reduction step could be realized in a shaft kiln (COREX) or a fluidized bed reactor (FINEX). Pre-reduced iron ores are then melted in the smelter-gasifier. The smelter-gasifier uses oxygen and coal as a reducing agent. Afterwards, the hot metal is also fed to the BOF for steelmaking. Another possibility of steelmaking is the primary direct reduction (DR) route. MIDREX is one of the used direct reduction technologies. It is characterized by the reduction of iron ores into solid direct reduced iron (DRI) within a shaft kiln. The direct reduction technologies could also work within a fluidized bed reactor. Examples include the FINMET and CIRORED process [38]. The direct reduction is driven by the fed of a reducing gas. Currently, the commercial used reducing gas is based on the reforming of natural gas. For extended information regarding the fundamentals of iron and steelmaking routes, a reference is made to [8, 24, 39].

Beside the previous described state-of-the-art iron and steelmaking routes, some innovative developments and investigations are compared with the conventional routes regarding their energy demand, CO₂ footprint, merit, and demerit in Table 1. Therein, the integrated blast furnace route (BF and BOF) which is predominant in Austria is set as reference regarding CO₂ emissions. Recycling of the blast furnace top-gas in combination with CCS or CCU (BF-TGR-CCS/U and BOF) or the replacement of fossil coal by biogenic substitutes reduces the fossil reducing agent demand and decrease the

CO₂ footprint of integrated blast furnace routes up to 50% [7, 16, 26, 30, 31].

The replacement of the BF by smelting reduction processes like the COREX or FINEX process would raise slightly the CO₂ footprint due to the high consumption of fossil coal. An ecologically favorable operation of smelting reduction processes only could be realized by the use of CCS or CCU [8, 16, 18]. The use of a smelting reduction technology based on bath-smelting (HISARNA-CCS/U and EAF) in combination with CCS would reduce the CO₂ emissions up to 80% [7, 16].

Direct reduction plants enable a big CO₂ emission saving potential in comparison with the integrated BF route due to the present used reformed natural gas as reducing agent. Reformed natural gas consists to a large extent of hydrogen, which results in lower CO₂ emissions due to the oxidation of hydrogen to steam within the reduction process [12]. The replacement of the integrated BF route by the state-of-the-art MIDREX plant, which is based on the reduction of iron ore within a shaft kiln by the use of reformed natural gas, would decrease the CO₂ emissions by 50% in comparison with the reference route [12, 32, 33]. The economic viability of direct reduction-based routes, which are based on reformed natural gas, strongly depend on the natural gas price which is in Europe much higher than in North America [33]. Within the ULCOS project, a novel direct reduction process (ULCORED-CCS/U) based on partial oxidized natural gas is investigated [7, 8]. By the reduction of the required amount of natural gas and the application of CCS or CCU, the CO₂ emissions could be decreased up to 65% compared with the reference route. The dual fluidized bed steam gasification process, based on the bed material limestone, which is called sorption-enhanced reforming (SER), produces a biomass-based hydrogen-rich gas, which allows the replacement of the steam reforming unit for reforming of natural gas. The application of SER to produce a biomass-based reducing gas for the MIDREX process (MIDREX-BG-SER) reduces the CO₂ footprint compared with the integrated BF route up to 80%. The combination of SER with oxyfuel combustion (OxySER) enables an in situ CO₂ sorption within the reducing gas production process. Beside the production of biomass-based reducing gas, a CCU or CCS ready CO₂ stream is released. Therefore, a below zero emission reducing gas due to the application of CCU or CCS is generated. Another direct reduction breakthrough technology could be the HYBRIT process, which is based on the reducing agent hydrogen, produced by electrolysis [16, 26, 34, 35]. Therefore, the emissions within the HYBRIT process are mostly caused by the CO₂ footprint of the electricity mix. With regard to the Austrian electricity mix, with a CO₂ footprint of 0.218 kg CO₂e/kWh_{el} [36], a CO₂ emission saving potential up to 50% could be reached with the HYBRIT process.

Table 1 Overview of different iron and steelmaking routes including their energy demands and CO₂ emissions [16]

Iron and steelmaking route ¹	Description of the technology	Reducing agent	Total energy demand [GJ/t _{cs}]	Energy demand reducing agent [GJ/t _{cs}]	N et power demand [GJ/t _{cs}]	CO ₂ emissions ² [t CO ₂ e/t _{cs}]	Savings potential ² [%CO ₂ e]	Advantages	Disadvantages	Literature
Integrated Blast Furnace route										
BF and BOF	Fossil reducing agents (coke and pulverized coal) are used as reducing agents; mixture of sinter, pellets, and additives are fed to the BF	Coke/coal	19.2	15.3	0.6	1.694	–	Production of HM in existing BF for steelmaking is the most cost-efficient technology to-day	State of the art BFs are operated near their theoretical minimum energy limit, further CO ₂ reductions are difficult	[25–27]
BF-TGR-CCS/U and BOF	Upgraded and recirculated BF gas is used as reducing agent, parts of pulverized coal and top-charged coke are replaced, CCS can be used for further CO ₂ reduction	Coke/coal/recirculated BF gas	20.0	11.6	1.4	0.813	– 52%	Top-gas recycling captures CO ₂ and enables CCS, Reduction of fossil reducing agent demand	Higher total energy demand because of additional energy demand for carbon capture, higher net energy demand due to the lack of power recovery from BF gas	[7, 15, 26, 28, 29]
BF-Bio-Char and BOF	Charcoal replaces fossil coal by 100% in the BF	Coke/charcoal	19.2	15.3	0.6	1.220	– 28%	Replacement of fossil coal by charcoal could be quite straightforward	Charcoal is more expensive than fossil coal, handling, transportation and storage is more difficult compared with fossil coal	[16, 26, 30, 31]
Smelting reduction route										
COREX and BOF	Combination of pre-reduction in a shaft kiln and smelter-gasifier	Coal	17.7	15.9	0.6	1.975	+ 17%	No need for coke oven plant	Restrictions for non-coking coal quality, customer for export gas necessary for economic viability	[12, 16, 26]
FINEX and BOF	Combination of pre-reduction in a fluidized bed reactor and smelter-gasifier	coal	–	–	–	1.910	+ 13%	No need for coke oven plant, pelletizing, sintering or agglomeration of iron-bearing materials	Technology not wide-spread	[12, 16]
HISARNA-CCS/U and EAF	Bath-smelting technology which combines coal	Coal	18.0	15.0	2.5	0.330	– 81%	No need for coke oven and	Technology at demonstration stage,	[7, 16]

Table 1 (continued)

Iron and steelmaking route ¹	Description of the technology	Reducing agent	Total energy demand [GJ/t _{cs}]	Energy demand reducing agent [GJ/t _{cs}]	N et power demand [GJ/t _{cs}]	CO ₂ emissions ² [t CO ₂ e/ t _{cs}]	Savings potential ² [%CO ₂ e]	Advantages	Disadvantages	Literature
Direct reduction route MIDREX and EAF	pre-heating and partial pyrolysis in a reactor, a smelter vessel is used for final ore reduction and a melting cyclone for ore smelting	Reformed natural gas	16.6	10.0	2.8	0.835	-51%	sinter/pellet plant. Use of non-coking coal qualities. Economic viable even at small size	more net power demand because of EAF and CCS	[12, 32, 33]
ULCORED-CCS/U and EAF	DRI production based on shaft furnace with reformed natural gas as reducing agent. Based on lump/pellet ore.	Partial oxidized natural gas	-	-	-	0.600	-65%	Reduction of natural gas consumption helps to reduce OPEX	OPEX strongly depend on natural gas price, which is very different around the world Requires pure oxygen instead of air. Technology at demonstration stage	[7, 8]
MIDREX-BG-SER and EAF	Reformed natural gas is replaced by biomass-based reducing gas produced by dual fluidized bed steam gasification	Biomass-based reducing gas	16.6	10.0	2.8	0.280*	-83%	Replacement of reformed natural gas by biomass-based reducing gas could be quite straightforward	OPEX strongly depend on biomass price	Captured within this paper
MIDREX-BG-OxySER-CCS/U and EAF	Reformed natural gas is replaced by biomass-based reducing gas produced by dual fluidized bed steam gasification and in situ CO ₂ capture and utilization	Biomass-based reducing gas	-	10.0	-	Below zero**	More than 100% reduction	Replacement of reformed natural gas by biomass-based reducing gas could be quite straightforward	OPEX strongly depend on biomass price. CCS or CCU approach requires pure oxygen instead of air as fluidization agent in the fluidized bed system	Captured within this paper
HYBRIT and EAF	Hydrogen produced with water electrolysis is used as reducing agent	Hydrogen	14.7	6.8	12.6	0.800	-53%	CO ₂ emissions very low if renewable energy sources	Hydrogen production is quite expensive with current technologies and	[16, 26, 34, 35]

Table 1 (continued)

Iron and steelmaking route ¹	Description of the technology	Reducing agent	Total energy demand [GJ/t _{cs}]	Energy demand reducing agent [GJ/t _{cs}]	Net power demand [GJ/t _{cs}]	CO ₂ emissions ² [t CO ₂ e/t _{cs}]	Savings potential ² [%CO ₂ e]	Advantages	Disadvantages	Literature
	within a direct reduction plant							are used. Almost zero direct emissions from production	requires a lot of electrical energy. Technology at demonstration stage	
Secondary steelmaking route										
EAF	Instead of DRI, scrap is used as iron source	Electricity	3.3	-	2.1	0.190	-89%	DRI production is replaced by recycling of ferrous scrap. Almost zero direct emissions from production	Increasing the share of EAF steel is constrained by the availability of high quality scrap	[12, 26]
Other steelmaking routes										
ULCOLYSIS	Melting iron ore at 1600 °C by using electric direct reduction	Electricity	15.0	-	13.0	0.800	-53%	CO ₂ emissions very low if renewable energy sources are used. Almost zero direct emissions from production	Technology at lab scale. High net power demand	[7, 16]

¹ Energy values and CO₂ emissions includes material preparation, ironmaking, steelmaking, and casting/based on 80% hot metal or DRI and 20% scrap except from secondary steelmaking route: 100% scrap in EAF

² CO₂ emission factor for grid/calculation model: 0.218 kg CO₂e/kWh_{el} (Austrian electricity mix)/saving potential in comparison with BF and BOF route as reference [36]

* Assumptions: energy values are the same as within the MIDREX route, and the CO₂ emissions are calculated by the difference between the emissions from the MIDREX route based on natural gas and the caused emissions only through natural gas as reducing gas [37]

** Assumptions: energy values are the same as within the MIDREX route with CCS [7] and the CO₂ emissions are below zero because of the combination from the use of a biomass-based feedstock with CCS or CCU

Further possibilities are the rise of the share of steel production through scrap-based electric arc furnaces. This steel-making route enables CO₂ reduction potentials up to 90%, because of the replacement from ironmaking processes with scrap. The EAF-based routes are strongly depended on the availability of high-quality scrap [12, 26]. Furthermore, some novel electric direct reduction processes, like the ULCOLYSIS project, are under investigation [7, 16]. Similar to the HYBRIT process, the electric direct reduction processes are strongly depended on the CO₂ footprint of the national electricity mix, because of the high-net power demands.

Several technologies provide the possibility of additional carbon-emission reduction by sequestration of CO₂. The use of post-combustion capture technologies, like pressure swing adsorption or amine scrubber, is the possibility for the sequestration of CO₂ within iron and steelmaking routes [40]. Within the OxySER process, through the in situ CO₂ sorption, a CCU or CCS ready CO₂ stream is produced. Further explanations regarding CO₂ sequestration can be found in [41–43]. The selective separated and purified CO₂ could be used in further process steps as raw material, *carbon capture and utilization*, or stored in underground deposits, *carbon capture and storage* [43, 44].

Today around 230 million tons of carbon dioxide per year are globally utilized materially. One hundred thirty million tons are used in urea manufacturing and 80 million tons for enhanced oil recovery [45]. With the assumption that hydrogen for the ammoniac production is produced by water electrolysis, which is beside CO₂ the primary energy source for urea production, external CO₂ is necessary for the urea synthesis. In Linz, near to one of the main sites for iron and steel production, a urea synthesis plant with a production rate of around 400,000 t per year of urea is located [46]. Therein, around 300,000 t CO₂ per year are required for the production of the given amount of urea [46]. Further utilization possibilities could be CO₂-derived fuels, like methanol or FT-synthesis and power to gas. Furthermore, the utilization within CO₂-derived chemicals beside urea, like formic acid synthesis, or CO₂-derived building materials, like the production of concrete, could be promising alternatives [45].

Beside the CCU technologies, CO₂ can also be stored in underground deposits. CCS is banned in Austria except research projects up to a storage volume of 100,000 t of CO₂ [44]. For further information regarding CCU and CCS, a reference is made to [40, 45, 47–49].

Since biomass releases the same amount of CO₂ as it aggregates during its growth, the utilization of biogenic fuels can contribute significantly to a reduction of CO₂ emissions. Therefore, the main focus of the paper lies on the production of a below zero emission reducing gas by the use of oxyfuel combustion in combination with sorption-enhanced reforming. This technology for the selective separation of

CO₂ uses as fluidization agent a mix of pure oxygen and recirculated flue gas. Therefore, the nitrogen from the air is excluded from the combustion system [42].

2.2 Combination of oxyfuel combustion and sorption-enhanced reforming

A promising option for the selective separation of CO₂ from biomass and the generation of a hydrogen-rich product gas at the same time is the sorption-enhanced reforming process in combination with oxyfuel combustion (OxySER). The sorption-enhanced reforming (SER) is based on the dual fluidized bed steam gasification process. The main carbon-related (gas-solid) and gas-gas reactions are shown in Table 2. Test runs at the 100 kW pilot plant at TU Wien showed calculated overall cold gas efficiencies of around 70% [51, 52]. Detailed information regarding the dual fluidized bed steam gasification process can be found in literature [37, 51–54].

The combination of oxyfuel combustion and sorption-enhanced reforming combines the advantages of both technologies. Figure 1 represents the concept of the combined technology [44]. First of all, biomass, residues, or waste materials are introduced in the gasification reactor. Limestone is used as bed material which serves as transport medium for heat but also as carrier for CO₂ from the gasification reactor (GR) to the combustion reactor (CR) by adjusting the temperature levels in the reactors correctly. Within the OxySER process, steam serves as fluidization and gasification agent in the GR. Therein, several endothermic gasification reactions take place in a temperature range between 600 and 700 °C [37]. Residual char is transferred with the bed material from the GR to the CR. Due to the combination of SER with oxyfuel combustion, pure oxygen instead of air is used as fluidization agent in the CR, which is operated within a temperature range between 900 and 950 °C. By combustion of residual char in the CR, heat is released. This suitable temperature profiles in the GR and CR ensure that the bed material (limestone) is first calcined to calcium oxide (CaO) at high temperatures in the CR (13). Then the CaO is carbonized in the GR with the carbon dioxide from the product gas (12). Thus, in this cyclic process, a transport of CO₂ from the product gas to the flue gas appears [52]. The use of steam in the gasification reactor and the water gas shift reaction (8) in combination with in situ CO₂ sorption via the bed material system CaO/CaCO₃ enables the production of a nitrogen-free and hydrogen-enriched product gas [37, 56]. Due to the combination of SER with oxyfuel combustion, in addition to the nitrogen-free and hydrogen-enriched product gas, a CO₂-enriched flue gas is generated caused by the use of pure oxygen as fluidization agent in the CR instead of air [57].

The CO₂ equilibrium partial pressure in the CaO/CaCO₃ system and the associated operation conditions for the

gasification and combustion can be found in [52]. By the use of renewable fuels and a continuous selective separation and storage or utilization of CO₂, an improved CO₂ balance can be achieved [44, 57].

Table 3 represents a comparison between the product and flue gas compositions of conventional gasification, SER, and OxySER. The results are based on test runs with the 100 kW pilot plant at TU Wien and the 200 kW pilot plant at University of Stuttgart [37, 57]. As mentioned above, the carbon dioxide content of the product gas could be reduced through the SER method. Furthermore, the hydrogen content is higher in comparison with conventional gasification. The possibility of adjusting the H₂/CO ratio over a wide range makes the SER process very flexible according to product gas applications [52]. The catalytic activity of limestone enables a reduction of tar at the same time [37, 44, 58]. The comparison between the SER and OxySER process illustrates that a CO₂-enriched flue gas in the OxySER test rig in Stuttgart was obtained [57]. In Table 4 the proximate and ultimate analyses of used wood pellets for gasification test runs with the 100 kW pilot plant at TU Wien are listed.

However, OxySER implies the following advantages in comparison to the conventional gasification:

- Selective CO₂ transport to flue gas
- Decrease of tar content in product gas
- High CO₂ content in flue gas > 90 vol.-%_{dry} [57]
- Smaller flue gas stream because of flue gas recirculation
- Nitrogen free flue gas

These assumptions according to experimental results serve as a basis for the conception of an industrial application.

2.3 Integrated OxySER concept for the production of below zero emission reducing gas

The OxySER plant concept for integration in a direct reduction plant is illustrated in Fig. 2. The plant concept is designed for a product gas power of 100 MW. For the production of 100 MW product gas, 50,400 kg/h of wood chips with a water content of 40 wt.-% are required [37]. The wood chips are treated in a biomass dryer. Afterwards the biomass is fed in the gasification reactor. The bed material inventory (limestone) of the system contains 25,000 kg. In the gasification reactor, a H₂-enriched product gas with a temperature of 680 °C is produced. Subsequently, the dust particles are removed from the product gas by a cyclone. Besides ash, these dust particles contain still carbon. This is the reason why the particles are recirculated to the combustion reactor. Afterwards, the product gas is cooled down to 180 °C. The released heat can be used for preheating of the biomass dryer air [44]. Furthermore, the product gas filter separates further fine dust particles from the product gas stream and conveys

them back to the combustion reactor. After that, tar is separated in a scrubber, and water is condensed. Biodiesel (RME) is used as solvent. The product gas exits the scrubber with a temperature of 40 °C. Afterwards, it is compressed in a blower, before it is dried to a water content of 1.5% and fed to the compression and preheating of the direct reduction plant. The CO₂-enriched flue gas leaves the combustion reactor with a temperature of 900 °C. The flue gas is cooled down to 180 °C by the steam superheater and a flue gas cooler. Steam is heated up to 450 °C in a countercurrent heat exchanger. Fly ash is removed out of the system by a flue gas filter. A partial flow from the flue gas is recirculated and mixed with pure oxygen. Pure oxygen is produced by an air separation unit. The remaining flue gas stream is compressed in the flue gas blower, and water is condensed in a flue gas dryer. The cleaned CO₂-rich gas can be used in different CCU processes, like urea or methanol synthesis [44].

The integration approach offers the advantage to use existing equipment, like the air separation unit from the steel-making facility. Furthermore, the generated product gas can be used directly in the direct reduction plant, as reducing gas [44]. For this application, a compression up to approx. 2.5 bar and preheating of the product gas up to 900 °C are necessary.

2.4 Simulation of mass and energy balances with IPSEpro

The calculation of mass and energy balances for different operation points with the stationary equation-orientated flow sheet simulation software IPSEpro enables the validation of process data. All data which cannot be measured during experimental test runs can be determined by the calculation of closed mass and energy balances. These equations are solved by the numerical Newton-Raphson Algorithm [59, 60]. Therefore, no models regarding kinetic or fluid dynamic approaches are considered. The used simulation models within the software IPSEpro are based on model libraries, which were developed at TU Wien over many years [61]. All experimental results from the pilot plant at TU Wien, presented within this publication, were validated with IPSEpro. Uncertainties are given by the accuracy of measurement data which relies on used analysis methods. The measurement accuracy of the ultimate and proximate analysis is listed in Table 4. The validation percentage error of the gasification model is covered by the range of values which are listed in Table 3. For further information regarding IPSEpro, a reference is made to [61, 62]. Due to the validation of the results from the pilot plant at University of Stuttgart, a reference is made to [57].

The simulation results for the OxySER concept for the production of below zero emission reducing gas presented in Section 2.3 are based on scale up of the experimental results of the pilot plants. The simulation model of the dual fluidized

Table 2 Important gas-solid and gas-gas reactions during thermochemical fuel conversion [50]

Important heterogeneous reactions (gas-solid)			
Oxidation of carbon	$C + O_2 \rightarrow CO_2$	Highly exothermic	(1)
Partial oxidation of carbon	$C + \frac{1}{2} O_2 \rightarrow CO$	Exothermic	(2)
Heterogeneous water-gas shift reaction	$C + H_2O \rightarrow CO + H_2$	Endothermic	(3)
Boudouard reaction	$C + CO_2 \rightarrow 2 CO$	Endothermic	(4)
Hydrogenation of carbon	$C + 2 H_2 \rightarrow CH_4$	Slightly exothermic	(5)
Generalized steam gasification of solid fuel (bulk reaction)	$C_x H_y O_z + (x-z)H_2O \rightarrow x CO + (x-z + \frac{y}{2})H_2$	Endothermic	(6)
Important homogeneous reactions (gas-gas)			
Oxidation of hydrogen	$2 H_2 + O_2 \rightarrow 2 H_2O$	Highly exothermic	(7)
Homogeneous water-gas shift reaction	$CO + H_2O \rightarrow CO_2 + H_2$	Slightly exothermic	(8)
Methanation	$CO + 3 H_2 \rightarrow CH_4 + H_2O$	Exothermic	(9)
Generalized steam reforming of hydrocarbons	$C_x H_y + x H_2O \rightarrow x CO + (x + \frac{y}{2})H_2$	Endothermic	(10)
Generalized dry reforming of hydrocarbons	$C_x H_y + x CO_2 \rightarrow 2x CO + \frac{y}{2} H_2$	Endothermic	(11)
Important reactions of active bed material (limestone) for SER			
Carbonation	$CaO + CO_2 \rightarrow CaCO_3$	Exothermic	(12)
Calcination	$CaCO_3 \rightarrow CaO + CO_2$	Endothermic	(13)

bed steam gasification system is based on an exergy study of T. Pröll [63].

2.5 Techno-economic assessment with net present value calculation

The techno-economic assessment regarding the net present value (NPV) calculation serves as decision-making tool for the valuation of upcoming investments. The NPV is a function of the investment and operating costs. The operating costs are multiplied by the cumulative present value factor, which includes the interest rate and the plant lifetime. Therefore, the NPV calculation helps to compare expected payments in the future with current payments. Further information can be found in [54, 64]. Cost rates have been updated to the year 2019 by using data from a chemical engineering plant cost index (CEPCI) database [65]. For the calculation of the investment costs, the cost-scaling method was used [66].

The techno-economic analysis is based on the following *business case* that an operator of a direct reduced iron plant would like to build a new reducing gas supply unit driven by a biogenic feedstock. The goal to produce 100 MW reducing gas should be achieved with regard to CO₂ emissions. The reference option (option 0) is the production of reducing gas by steam reforming of natural gas. Furthermore, three biogenic alternative options (options 1–3) are compared with the reference option:

- *Option 0* (reference case): Production of 100 MW reducing gas through steam reforming of natural gas
- *Option 1*: Production of 100 MW reducing gas through gasification of wood chips by SER
- *Option 2*: Production of 100 MW reducing gas through gasification of wood chips by an integrated OxySER plant
- *Option 3*: Production of 100 MW reducing gas through gasification of wood chips by a greenfield OxySER plant

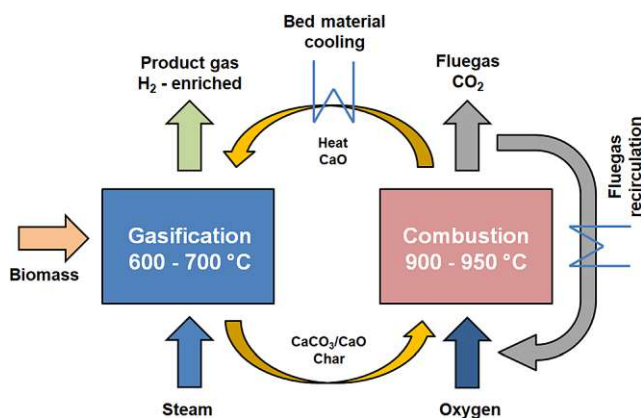


Fig. 1 Concept of OxySER [55]

The SER process in option 1 requires no pure oxygen, consequently no ASU for operation. However, the flue gas of the SER process cannot be exploited in further utilization steps because of the high nitrogen content in the flue gas. The alternative option 2 is based on the SER process in combination with oxyfuel combustion implemented in an existing iron and steel plant facility. The process heat is used for preheating of the reducing gas. The required oxygen is delivered from an existing ASU within the iron and steel plant facility. Furthermore, the OxySER process is based on the assumption that the CO₂ is sold as product for utilization to a urea synthesis plant. Option 3 is based on the OxySER process without the benefits from option 2.

Table 3 Comparison product and flue gas composition of conventional gasification, SER, and OxySER [37, 57]

Parameter	Unit	Conventional gasification (100 kW)	Gasification by SER (100 kW)	Gasification by SER (200 kW)	Gasification by OxySER (200 kW)
Plant location		TU Wien	TU Wien	University Stuttgart	University Stuttgart
Reference		[37]	[37]	[57]	[57]
Fuel		Wood pellets	Wood pellets	Wood pellets	Wood pellets
Bed material		Olivine	Limestone	Limestone	Limestone
Particle size	mm	0.4–0.6	0.5–1.3	0.3–0.7	0.3–0.7
Product gas composition					
Water (H ₂ O)	vol.-%	30–45	50–65	50	50
Hydrogen (H ₂)	vol.-% _{dry}	36–42	55–75	69–72	70
Carbon monoxide (CO)	vol.-% _{dry}	19–24	4–11	8–11	8
Carbon dioxide (CO ₂)	vol.-% _{dry}	20–25	6–20	5–7	8
Methane (CH ₄)	vol.-% _{dry}	9–12	8–14	11–12	11
Non cond. hydrocarbons (C _x H _y)	vol.-% _{dry}	2.3–3.2	1.5–3.8	2–3	3
Dust particles	g/Nm ³	10–20	20–50	n.m.	n.m.
Tar	g/Nm ³	4–8	0.3–0.9	14	6
Flue gas composition					
Water (H ₂ O)	vol.-%	n.m.	n.m.	14	30
Oxygen (O ₂)	vol.-% _{dry}	n.m.	n.m.	7	9
Nitrogen (N ₂)	vol.-% _{dry}	n.m.	n.m.	46	-
Carbon dioxide (CO ₂)	vol.-% _{dry}	n.m.	n.m.	47	91

n.m., not measured

This means that, in option 3, the costs for pure oxygen are higher in consideration to the use of a greenfield ASU. Furthermore, no earnings through CO₂ utilization are considered.

Furthermore, a payback analysis has been done by solving the following equation, where A are the savings minus the operation and maintenance costs, P is the present worth capital costs, and IR is the interest rate. The variable n represents the number of years to return the investment in comparison with the reference case [67].

$$A = P * \frac{IR * (1 + IR)^n}{(1 + IR)^n - 1}$$

3 Results and discussion

Based on experiences of the pilot plant from the TU Wien and the University of Stuttgart, combined with the previously

Table 4 Proximate and ultimate analyses of used wood pellets for gasification test runs [51]

Parameter	Unit	Meas. accuracy (%)	Wood pellets (100 kW)
Water content (H ₂ O)	wt.-%	± 4.3	7.2
Ash content (550 °C)	wt.-% _{dry}	± 9.2	0.2
Carbon (C)	wt.-% _{daf}	± 1.0	50.8
Hydrogen (H)	wt.-% _{daf}	± 5.0	5.9
Nitrogen (N)	wt.-% _{daf}	± 5.0	0.2
Sulfur (S)	wt.-% _{daf}	± 7.5	0.005
Chlorine (Cl)	wt.-% _{daf}	± 7.5	0.005
Oxygen (O)*	wt.-% _{daf}	-	43.1
Volatile matter	wt.-% _{daf}	± 0.45	85.6
Lower heating value, moist	MJ/kg	± 1.0	17.4

* Calculated by difference to 100 wt.-%_{daf}

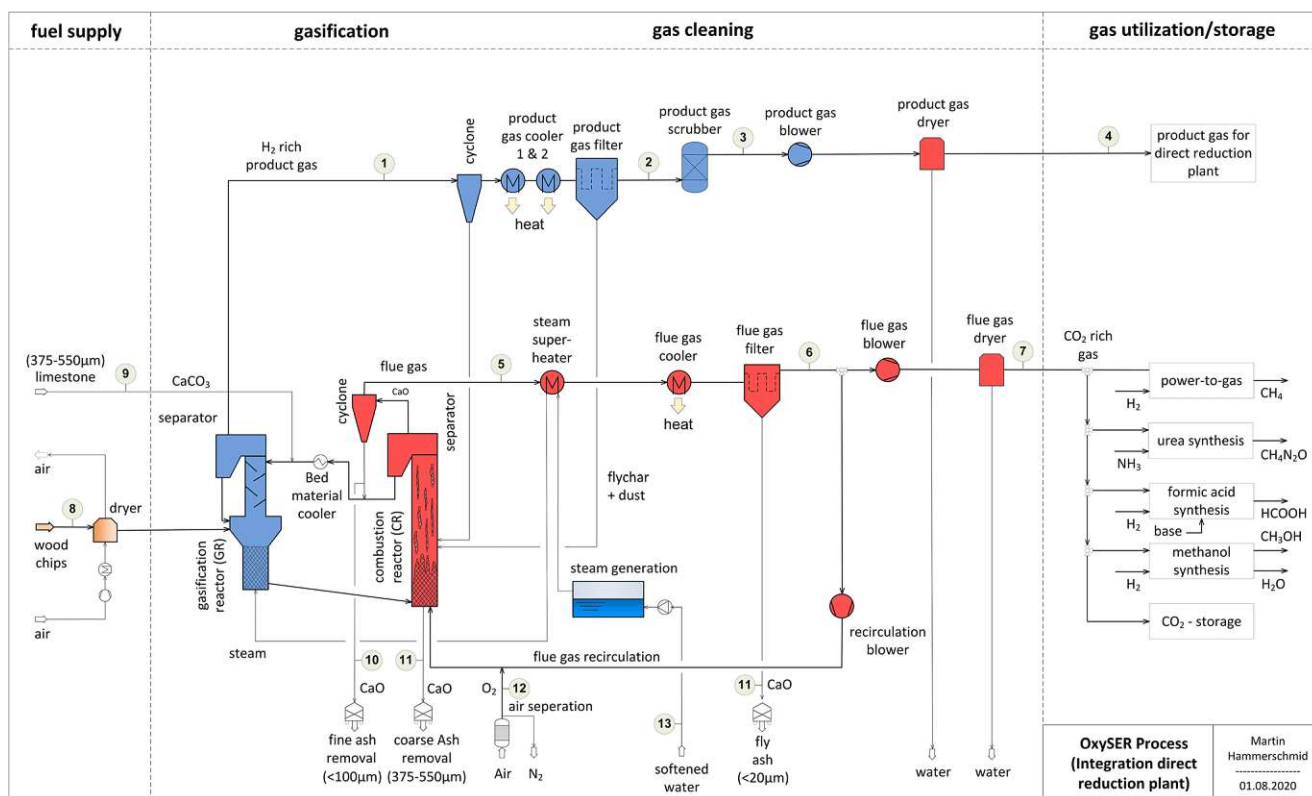


Fig. 2 OxySER plant concept with 100-MW product gas power for the production of reducing gas as feedstock for a direct reduction plant

described concept, mass and energy balances for the OxySER plant concept for integration in a direct reduction plant were calculated. Furthermore, mass and energy balances are the basis for a techno-economic assessment. In Table 5 the most important streamline data of chosen flow streams, marked in Fig. 2, are shown. Table 6 and Table 7 represent the input and output data and operating parameters of an OxySER plant.

Table 6 shows the input and output flows of an OxySER plant with 100 MW product gas energy. It can be seen that 50,400 kg/h of wood chips and 11,020 Nm³/h of pure oxygen are required for the generation of 28,800 Nm³/h product gas. The product gas is used as reducing gas in the direct reduction route. Furthermore, 36,100 kg/h of CO₂ can be recovered for further utilization. The costs for final disposal of 1050 kg/h of ash and dust have been taken into account.

In Table 8, the main requirements on the product gas for the utilization in the direct reduction plant are listed. The comparison illustrates that the generated below zero emission product gas out of the OxySER plant meets, except from the temperature and pressure, all the requirements. The concept is based on the assumption that the reducing gas is compressed and preheated before it is fed to the direct reduction plant. Therefore, the required temperature and pressure are reached after compression and preheating of the product gas.

The techno-economic assessment relies on the results of the IPSEpro simulation. Table 9 represents the fuel prices for chosen fuel types and cost rates for utilities. It is thus

evident that the European natural gas price with 25 €/MWh is more expensive than in other continents. Exemplary, the costs for one employee per year are assumed to 70,000 €/a, and the expected plant lifetime of an OxySER plant is 20 years.

Table 10 represents the investment cost rates for the NPV calculation. The presented investment costs are based on total capital investment costs of realized fluidized bed steam gasification plants driven as combined heat and power plants reduced by the costs through the gas engine. Furthermore, this investment costs are updated by CEPCI and scaled with the cost-scaling method. For the integrated OxySER plant, the assumption was made that the oxygen from the air separation unit (ASU) of the iron and steel plant is used. For the green-field OxySER plant, the whole investment costs for an ASU were added.

The techno-economic analysis is based on the Section 2.5 that described *business case*, wherein an operator of a direct reduced iron plant would like to build a new reducing gas supply unit driven by a biogenic feedstock. The NPV calculation, which is shown in Table 11, serves as decision-making tool. The goal to produce 100 MW reducing gas should be achieved with regard to CO₂ emissions. The reference option (option 0) is the production of reducing gas by steam reforming of natural gas. Furthermore, three biogenic alternative options (options 1–3), which are described in Section 2.5, are compared with the reference option.

Table 5 Streamline data of the OxySER concept according to Fig. 2

Parameter	Unit	Product gas streams				Flue gas streams		
		Product gas after GR (1)	Product gas after filter (2)	Product gas after scrubber (3)	Reducing gas for DR (4)	Flue gas after CR (5)	Flue gas after filter (6)	Flue gas to CCU (7)
Streamline in Fig. 2	–							
Pressure	Bara	Ambient	Ambient	Ambient	Ambient	Ambient	Ambient	Ambient
Temperature	°C	675	150	40	60	950	160	160
Mass flow rate	kg/h	26,000	25,500	16,000	15,800	93,200	92,600	36,100
Volume flow rate	Nm ³ /h	40,500	40,000	28,800	28,400	53,000	52,500	20,500
Water content	wt.-%	35.0	35.0	8.0	1.5	15.0	15.0	5.0
Hydrogen (H ₂)	vol.-% _{dry}	69.2	69.2	69.2	69.2	0	0	0
Carbon monoxide (CO)	vol.-% _{dry}	9.1	9.1	9.1	9.1	2.8	2.8	2.8
Carbon dioxide (CO ₂)	vol.-% _{dry}	6.5	6.5	6.5	6.5	91.2	91.2	91.2
Methane (CH ₄)	vol.-% _{dry}	11.0	11.0	11.0	11.0	0	0	0
Non cond. Hydrocarbons (C _x H _y)	vol.-% _{dry}	2.4	2.4	2.4	2.4	0	0	0
Oxygen (O ₂)	vol.-% _{dry}	0.1	0.1	0.1	0.1	6.0	6.0	6.0
Nitrogen (N ₂)	vol.-% _{dry}	1.7	1.7	1.7	1.7	0	0	0
Dust particle	g/Nm ³	10	0.025	0	0	20	0	0
Tar content*	g/Nm ³	4	0.5	0.025	0.025	0	0	0

*Tar is considered in the simulation model as naphthalene (main component in the DFB product gas) [51]

Table 11 represents the net present value calculation for the production of 100 MW reducing gas. Therein, the fuel energy per year, the investment costs including interest and fuel costs per year are listed. Beside the fuel costs, Table 11 shows also all other consumption-related costs. Costs for CO₂ emission certificates are paid only for the use of fossil fuels (reference case). The relative NPV represents the profitability of alternative production routes in comparison with the reference case and the payback period for return of investment. The NPV of all alternative options

(1–3) shows negative values. This means that the operation of SER and OxySER with wood chips based on the expected plant lifetime of 20 years is less profitable than the reference option. The techno-economic comparison between SER and OxySER shows that in option 2, the earnings through carbon dioxide are higher than the oxygen costs. In option 3, no earnings through CO₂ utilization and no benefits regarding oxygen costs have been considered. Therefore, an extremely negative NPV in option 3 is the result. The payback analysis shows that only option 2

Table 6 Input and Output data of an OxySER plant with 100 MW product gas energy

Input					Output				
Parameter	Streamline in Fig. 2	Unit	Value	Ref.	Parameter	Streamline in Fig. 2	Unit	Value	Ref.
Bed material inventory	-	kg	25,000	[37]	Product gas	(3)	Nm ³ /h	28,800	IPSE
Fuel (wood chips)	(8)	kg/h	50,400	[37]	Flue gas	(8)	Nm ³ /h	53,000	IPSE
Fresh bed material	(9)	kg/h	1770	[37, 64]	Ash and dust	(11)	kg/h	1050	[37]
Cooling capacity in % of fuel power	-	%	5–20	[68]	Bed material	(10)	kg/h	1000	[44]
Electricity consumption	-	kW	2800	[37]	Carbon dioxide (for CCU)	(7)	kg/h	36,100	[37]
Oxygen	(12)	Nm ³ /h	11,020	[37]					
Fresh water	(13)	kg/h	378	[37]					
Scrubber solvent (RME)	-	kg/h	200	[37]					
Flushing gas	-	Nm ³ /h	500	[37]					

Table 7 Operating parameters of an OxySER plant with 100 MW product gas energy

Parameter	Unit	Value	Ref.
Lower heating value, moist (wood chips)	MJ/kg	9.53	[37]
Water content (wood chips)	wt.-%	40	[37]
Combustion temperature	°C	900–950	[69]
Gasification temperature	°C	625–680	[69]
Particle size (bed material)	µm	375–550	Asm.
Coarse ash	µm	375–550	Asm.
Fine ash	µm	< 100	Asm.
Very fine ash	µm	< 20	Asm.
Water content (PG to DR)	vol.-%	1.50	IPSE
CO ₂ recovery rate*	%	>95	IPSE

$$*CO_2 = \frac{CO_2 \text{ volume flow flue gas}}{CO_2 \text{ volume flow total (FG+PG)}}$$

could return the investment regarding the expected interest rate in comparison with the reference case. However, the payback time of 24 years is very long and would not be profitable. Option 1 and option 3 could not return the investment in comparison to the reference case.

Furthermore, the reducing gas production costs of the four different routes were calculated. As can be seen from Table 11, the production costs (LCOP) of the reference case are with 39.0 €/MWh as the lowest followed by the integrated OxySER process with 39.4 €/MWh. Figure 3 represents the discounted expenses and revenues, divided in the main cost categories. It can be seen that the fuel costs are the main cost driver in the process. The techno-economic comparison points out that the production costs of a below zero emission reducing gas could only be in the range of steam-reformed natural gas, if generated CO₂ can be utilized and the pure oxygen is delivered by an integrated ASU. Otherwise, the production of biomass-based reducing gas via the SER process is preferable. A further reduction of the production costs of the biomass-based reducing gas could be reached by the use of cheaper fuels.

Table 8 Requirements on product gas for the utilization in the direct reduction plant [22, 70]

Parameter	Unit	Requirement reducing gas	Value product gas
Temperature	°C	> 900	60
Pressure	bara	2–4	1.05
H ₂ /CO ratio	-	0.5 - ∞	7.6
Gas quality*	-	> 9	9.8
Methane	vol.-%	> 3.5	11.0
Sulfur (H ₂ S)	ppm	< 100	< 20
Soot	mg/Nm ³	< 100	-

$$*Gas \text{ quality} = (\%CO + \%H_2) / (\%CO_2 + \%H_2O) [70]$$

Additionally, a sensitivity analysis of the NPV calculation has been created. The results for the sensitivity analysis based on the NPV of option 2 are shown in Fig. 4. The sensitivity analysis shows that the fuel prices of natural gas and wood chips are the most sensitive cost rates. The fuel cost rates depend very much on the plant location. Furthermore, the NPV in this techno-economic comparison is also sensitive to the investment costs of the reducing agent production route, the revenues through CCU, the price of CO₂ emission certificates, the plant lifetime, the operating hours, and the interest rate. The revenues through CCU depend on the availability of consumers. The sensitivity to operating hours and plant life time reaffirms high importance to a high plant availability during the whole plant life cycle. Cost rates for operating utilities, maintenance, and employees are less sensible to the results.

Finally, a comparison of the production costs of the biomass-based reducing gas with other reducing agents like reformed natural gas, hydrogen, or coke has been done. The comparison in Fig. 5 shows that the production of biomass-based reducing gas via OxySER (option 2) and SER is more than twice as expensive as the production of coke in a coking plant, but it is in the same range than the production of reducing gas via steam reforming of natural gas. All fuel costs are based on European price levels. Especially, the natural gas price strongly depends on the plant site. For example, the natural gas price in Europe is four to five times higher than in North America [33]. This is the reason why most of the existing direct reduction plants are built in oil-rich countries [33]. The production of hydrogen using water electrolysis is currently economically not competitive. On the ecologic point of view, the use of biomass-based reducing gas without CCU decrease the CO₂ emissions of the whole process chain for the production of crude steel down to 0.28 t CO₂e/t_{CS}. This amounts to a reduction of CO₂ emissions in comparison with the integrated BF-BOF route by more than 80%. Further on, the use of CCU within an OxySER plant could create a CO₂ sink, since biomass releases the same amount of CO₂ as it aggregates during its growth.

With regard to 8.1 million tons of crude steel production in Austria, in the year 2017 [4], and an estimated woody biomass potential of around 50 PJ in the year 2030 [21], 13 biomass-based reducing gas plants (OxySER or SER) with a reducing gas power of 100 MW could be implemented. This would result in the production of around 35 Mio. GJ of biomass-based reducing gas for the direct reduction process, which is sufficient for the production of 3.5 Mio. tons of crude steel. One of the biomass-based reducing gas plants could be operated via the OxySER process with regard to the CCU potential from the nearby urea synthesis plant of 300,000 t CO₂ per year [46]. Further CCU potential could be arise through the production of CO₂-derived fuels or chemicals [41].

Table 9 Cost rates for utilities and NPV calculation

Utility cost rate	Unit	Value	Ref.	NPV cost rate	Unit	Value	Ref.
Wood chips (Austria)	€/MWh	15.7	[71]	Maintenance costs per year	%/a	2.00	[54]
Natural gas (Austria)	€/MWh	25.0	[72]	Insurance, administration, and tax per year	%/a	1.50	[73]
Electricity	€/kWh _{el}	0.04	[64]	Number of employees (integration)	-	3	[64]
Limestone	€/t	35	[64]	Number of employees (greenfield)	-	7	[44, 64]
Nitrogen	€/Nm ³	0.003	[64]	Expected plant life time	a	20	[73]
Fresh water	€/t	0.02	[64]	Annual operating hours	h/a	7500	[64]
Solvent (RME)	€/t	960	[64]	Interest rate (IR)	%	6	[74]
Oxygen (air separator available)	€/Nm ³	0.022*	[44]	Costs of one employee per year	€/a	70,000*	[64]
Oxygen (greenfield)	€/Nm ³	0.075*	[37]				
Emission allowances certificate	€/t _{CO2}	23	[75]				
Costs for ash disposal	€/t	90	CHP Güssing				
CO ₂ expenses	€/Nm ³	0.03	[76]				

4 Conclusion and outlook

The scope of this publication was the investigation of a concept for the production of a below zero emission reducing gas for the use in a direct reduction plant and whether it has a reasonable contribution to a reduction of fossil CO₂ emissions within the iron and steel sector in Austria. The gasification via SER allows the in situ CO₂ sorption via the bed material system CaO/CaCO₃. Therefore, a selective transport of carbon dioxide from the product gas to the flue gas stream is reached. The use of a mix of pure oxygen and recirculated flue gas as fluidization agent in the CR results in a nearly pure CO₂ flue gas stream. Through the in situ CO₂ sorption, CO₂ recovery rates up to 95% can be reached. The CO₂ could be used for further synthesis processes like, e.g., the urea synthesis. Therefore, a below zero emission reducing gas could be produced.

The experimental and simulation results show that the produced below zero emission OxySER product gas meets all requirements for the use in a direct reduction plant. The use of the biomass-based reducing gas out of the SER process within a MIDREX plant would decrease the emitted CO₂ emission by 83% in comparison to the blast furnace route. The use of a below zero emission reducing gas out of the OxySER process by the use of CCU would create a CO₂ sink. The results of the techno-economic assessment show that the production of reducing gas via sorption-enhanced reforming in combination with oxyfuel combustion can compete with the natural gas route, if the required pure oxygen is delivered by an available ASU and if CCU is possible. Otherwise, the SER process is more profitable. Furthermore, the sensitivity analysis of the cost rates exhibited that the fuel and investment costs are strongly dependent on the profitability of the OxySER plant and in consequence the direct reduction plant.

Table 10 Investment costs for NPV calculation

Parameter	Unit	Value	Ref.
Investment costs SER plant (total capital investment costs)*	Mio. €	85	[37] adapted by CEPCI
Investment costs integrated OxySER plant (SER plus maintenance ASU)**	Mio. €	91	[37, 66] adapted by CEPCI
Investment costs greenfield OxySER plant (SER plus total investment costs ASU)***	Mio. €	115	[37, 66] adapted by CEPCI
Investment costs Steam Reformer natural gas	Mio. €	54	[77] adapted by CEPCI

*Investment costs are based on scaled total capital investment costs of realized dual fluidized bed steam gasification plants driven as combined heat and power plants reduced by the costs of the gas engine/investment costs updated with CEPCI [37]

**Investment costs are based on costs SER plant raised by a third of the ASU maintenance costs (2% of the investment costs per year with an expected lifetime of 20 years)/assumption: 50% of ASU is used for OxySER plant and 50% for iron and steel plant

***ASU investment costs: approx. 30 Mio. € [66] adapted by CEPCI

Table 11 Net present value calculation for the production of 100 MW reducing gas

Parameter	Unit	Steam Reforming (100% natural gas)	SER (100% wood chips)	Integration OxySER (100% wood chips)	Greenfield OxySER (100% wood chips)
		Option 0	Option 1	Option 2	Option 3
Boundary conditions					
Reducing gas for direct reduction	MW	100	100	100	100
Natural gas consumption	MWh/a	750 000			
Wood chips consumption	MWh/a		997 500	997 500	997 500
Investment costs incl. interest	€	54 000 000	85 000 000	91 000 000	115 000 000
Expenses					
Fuel costs natural gas	€/a	18 750 000			
Fuel costs wood chips	€/a		17 010 000	17 010 000	17 010 000
CO ₂ emission certificates	€/a	3 450 000			
Maintenance, insurance, etc.	€/a	1 890 000	2 975 000	3 185 000	4 025 000
Employee costs	€/a	70 000	210 000	210 000	490 000
Auxiliaries	€/a	356 000	1 916 000	1 916 000	1 916 000
Electricity costs	€/a		835 500	835 500	835 500
Ash disposal costs	€/a		709 000	709 000	709 000
Oxygen costs	€/a			1 818 000	6 198 500
Sum of expenses per year	€/a	24 516 000	23 655 500	25 683 500	31 184 000
Earnings					
Earnings CO ₂ utilization	€/a			4 102 000	
Sum of earnings per year	€/a			4 102 000	
Net present value calculation					
Expenses - Earnings	€/a	24 516 000	23 655 500	21 581 500	31 184 000
Additional investment costs (P) (compared to reference option)	€	0	31 000 000	37 000 000	61 000 000
Operating expenses savings (A)	€/a	0	860 500	2 934 500	- 6 668 000
Relative Net Present Value	€	0	- 21 128 000	- 3 340 000	- 137 500 000
Payback analysis (Return of investment period compared to reference case)					
Payback time (n)*	a	-	∞	24	∞
Production costs reducing gas (LCOP)					
Production costs reducing gas (LCOP)**	€/MWh	39.0	41.4	39.4	54.9
	€/GJ	10.8	11.5	10.9	15.3
* Payback analysis: $A = P * \frac{IR * (1+IR)^n}{(1+IR)^n - 1}$ [67]					
** LCOP = $\frac{\text{Sum of discounted (expenses-earnings)}}{\text{Discounted Delivered reducing gas}} = \frac{\epsilon}{MWh} = \frac{\epsilon}{GJ}$ [78, 79]					

Fig. 3 Relative net present value

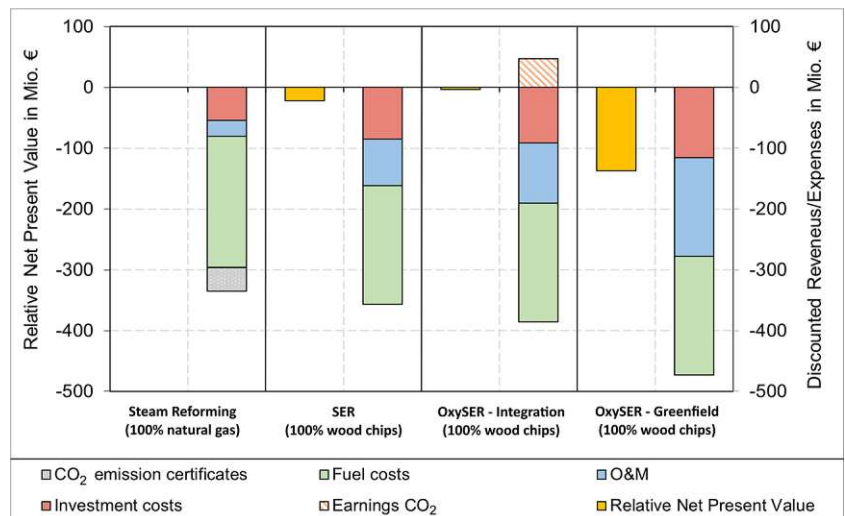
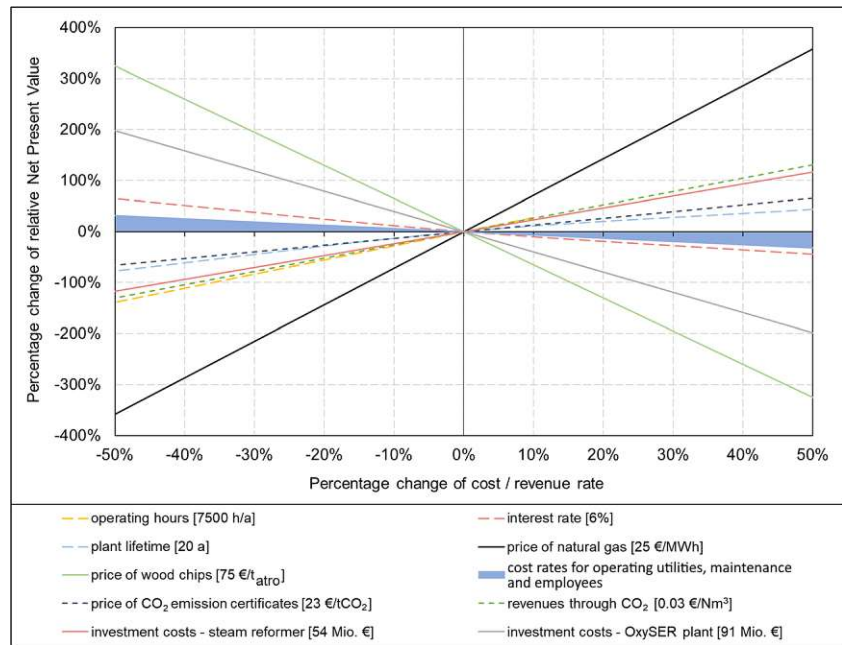


Fig. 4 Sensitivity analysis of the NPV calculation

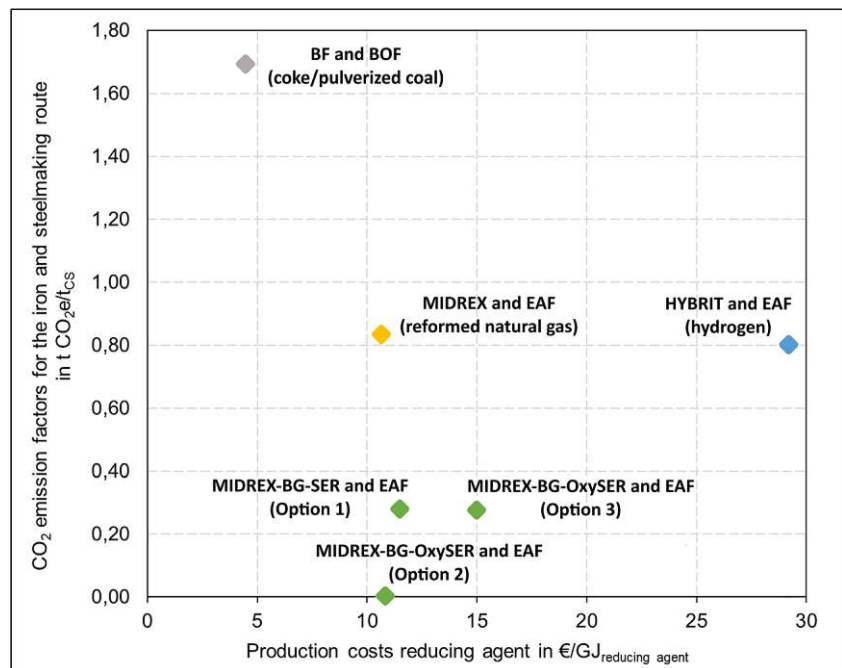


The production costs of the biomass-based reducing gas are more than twice as high as the fossil coke, which is used mainly in the blast furnace route.

Summing up, the presented integrated concept and the calculated results enable valuable data for further design of the proposed concept. Beforehand a demonstration at a significant scale is recommended. Further on, the implementation of the energy flows from an iron and steel plant within the simulation model could improve the current model regarding to efficiency. The profitability of the direct reduction with a biomass-

based reducing gas or natural gas is strongly dependent on the availability of sufficient fuel. With regard to the woody biomass potentials in Austria in the year 2030, the production of 3.5 Mio. tons of crude steel by the use of biomass-based reducing gas could be reached. Due to the substitution of the integrated BF and BOF route by the MIDREX-BG-SER and EAF route, the reduction of 6.8 Mio. tons of CO₂e could be reached. This amount would decrease the CO₂ emissions within the iron and steel sector in Austria by 50%. Concluding, the production of biomass-based reducing gas

Fig. 5 Economic and ecologic comparison of different Iron and Steelmaking routes [12, 20, 25, 34, 80]



could definitely help to contribute on the way to defossilization of the iron and steelmaking industry in Austria.

Funding Open access funding provided by TU Wien (TUW). The present work contains results of the project ERBA II which is being conducted within the “Energieforschung” research program funded by the Austrian Climate and Energy Fund and processed by the Austrian Research Promotion Agency (FFG). The work has been accomplished in cooperation with voestalpine Stahl GmbH and voestalpine Stahl Donawitz GmbH.

Data availability The data that support the findings of this study are available from the corresponding author, M. Hammerschmid, upon reasonable request.

Compliance with ethical standards

Conflicts of interest The authors declare that they have no conflict of interest.

Code availability Not applicable.

Abbreviations AISI, American Iron and Steel Institute; Asm., assumption; ASU, air separation unit; BF, blast furnace; BG, biomass-based reducing gas; BOF, basic oxygen furnace; C, carbon; CaCO₃, calcium carbonate; CaO, calcium oxide; CCS, carbon capture and storage; CCS/U, carbon capture and storage or utilization; CCU, carbon capture and utilization; CEPCI, chemical engineering plant cost index; CH₃OH, methanol; CH₄, methane; CH₄N₂O, urea; CHP, combined heat and power; CIRCORED, novel direct reduction technology; CO, carbon monoxide; CO₂, carbon dioxide; CO₂e, carbon dioxide equivalent; COG, coke oven gas; COREX, smelting reduction technology; COURSE50, CO₂ ultimate reduction steelmaking process by innovative technology for cool Earth 50 located in Japan; CR, combustion reactor; CS, crude steel; C_xH_y, non condensable hydrocarbons; DR, direct reduction; DRI, direct reduced iron; dry, dry basis; EAF, electric arc furnace; EU-28, member states of the European Union (until January 2020); FG, flue gas; FINEX, smelting reduction technology; FINMET, direct reduction technology; GR, gasification reactor; H₂, hydrogen; H₂O, water; H₂S, hydrogen sulfide; HCOOH, formic acid; HISARNA, novel bath-smelting technology; HM, hot metal; HYBRIT, Hydrogen Breakthrough Ironmaking Technology; IPSEpro, software tool for process simulation; LCOP, leveled costs of products; MIDREX, state-of-the-art direct reduction technology; MOE, molten oxide electrolysis; N₂, nitrogen; NH₃, ammonia; NPV, net present value; O₂, oxygen; OPEX, operational expenditure; OxySER, sorption-enhanced reforming in comb. with oxyfuel combustion; PG, product gas; POSCO, iron and steelmaking company located in Korea; Ref., reference; RME, rapeseed methyl ester; SER, sorption-enhanced reforming; t_{CS}, tons of crude steel; TGR, top-gas recycling; ULCOLYSIS, novel electric direct reduction technology; ULCORED, novel direct reduction technology; ULCOS, ultra-low CO₂ steelmaking; ULCOWIN, novel electric direct reduction technology; vol.-%, volumetric percent wet; vol.-%_{dry}, volumetric percent dry; wt.-%, weight percent wet; wt.-%_{daf}, weight percent dry and ash free; wt.-%_{dry}, weight percent dry

Symbols %CO, volume percent of carbon monoxide within reducing gas; %CO₂, volume percent of carbon dioxide within reducing gas; %H₂, volume percent of hydrogen within reducing gas; %H₂O, volume percent of water within reducing gas; A, savings minus the operation and

maintenance costs; *IR*, interest rate; *n*, payback period; *P*, present worth capital costs

Open Access This article is licensed under a Creative Commons Attribution 4.0 International License, which permits use, sharing, adaptation, distribution and reproduction in any medium or format, as long as you give appropriate credit to the original author(s) and the source, provide a link to the Creative Commons licence, and indicate if changes were made. The images or other third party material in this article are included in the article's Creative Commons licence, unless indicated otherwise in a credit line to the material. If material is not included in the article's Creative Commons licence and your intended use is not permitted by statutory regulation or exceeds the permitted use, you will need to obtain permission directly from the copyright holder. To view a copy of this licence, visit <http://creativecommons.org/licenses/by/4.0/>.

References

- Borkent B, De Beer J (2016) Carbon costs for the steel sector in Europe post-2020-impact assessment of the proposed ETS revision. Utrecht
- Metz B, Davidson O, Meyer L, Bosch P, Dave R (2007) Climate change 2007 - mitigation. Cambridge University Press, Cambridge, United Kingdom and New York, USA
- Eurostat (2017) Greenhouse gas emissions by source sector. Statistical office of the European Union. <https://ec.europa.eu/eurostat/data/database>. Accessed 25 Mar 2020
- World Steel Association (2018) Steel statistical yearbook 2018. Brussels
- Zechmeister A, Anderl M, Geiger K, et al (2019) Klimaschutzbericht 2019 - Analyse der Treibhausgas-Emissionen bis 2017. Wien
- Anderl M, Burgstaller J, Gugele B, et al (2018) Klimaschutzbericht 2018. Wien
- Quader MA, Ahmed S, Dawal SZ, Nukman Y (2016) Present needs, recent progress and future trends of energy-efficient ultra-low carbon dioxide (CO₂) steelmaking (ULCOS) program. *Renew Sust Energ Rev* 55:537–549. <https://doi.org/10.1016/j.rser.2015.10.101>
- Eder W, Moffat G (2013) A steel roadmap for a low carbon Europe 2050. Brussels
- Wang H, Sheng C, Lu X (2017) Knowledge-based control and optimization of blast furnace gas system in steel industry. *IEEE Access* 5:25034–25045. <https://doi.org/10.1109/ACCESS.2017.2763630>
- Shen X, Chen L, Xia S, Xie Z, Qin X (2018) Burdening proportion and new energy-saving technologies analysis and optimization for iron and steel production system. *Cleaner Production* 172:2153–2166. <https://doi.org/10.1016/j.jclepro.2017.11.204>
- Sato M, Takahashi K, Nouchi T, Ariyama T (2015) Prediction of next-generation ironmaking process based on oxygen blast furnace suitable for CO₂ mitigation and energy flexibility. *ISIJ Int* 55:2105–2114
- Rammer B, Millner R, Boehm C (2017) Comparing the CO₂ emissions of different steelmaking routes. *BHM Berg- und Hüttenmännische Monatshefte* 162:7–13. <https://doi.org/10.1007/s00501-016-0561-8>
- Zhang H, Wang G, Wang J, Xue Q (2019) Recent development of energy-saving technologies in ironmaking industry. *IOP Conf Series Earth Environ Sci* 233:052016. <https://doi.org/10.1088/1755-1315/233/5/052016>

14. Buergler T, Kofler I (2016) Direct reduction technology as a flexible tool to reduce the CO₂ intensity of Iron and steelmaking. *BHM Berg- und Hüttenmännische Monatshefte* 162:14–19. <https://doi.org/10.1007/s00501-016-0567-2>
15. Junjie Y (2018) Progress and future of breakthrough low-carbon steelmaking technology (ULCOS) of EU Technologies in Global Steel Industry. 3:15–22. <https://doi.org/10.11648/j.ijmpem.20180302.11>
16. Suopajarvi H, Umeki K, Mousa E, Hedayati A, Romar H, Kempainen A, Wang C, Phounglamcheik A, Tuomikoski S, Norberg N, Andefors A, Öhman M, Lassi U, Fabritius T (2018) Use of biomass in integrated steelmaking – status quo, future needs and comparison to other low-CO₂ steel production technologies. *Appl Energy* 213:384–407. <https://doi.org/10.1016/j.apenergy.2018.01.060>
17. Tonomura S, Kikuchi N, Ishiwata N, Tomisaki S (2016) Concept and current state of CO₂ ultimate reduction in the steelmaking process (COURSE50) aimed at sustainability in the Japanese steel industry. *J Sustain Metall* 2:191–199. <https://doi.org/10.1007/s40831-016-0066-4>
18. Zhao J, Zuo H, Wang Y, Wang J, Xue Q (2020) Review of green and low-carbon ironmaking technology. *Ironmak Steelmak* 47: 296–306. <https://doi.org/10.1080/03019233.2019.1639029>
19. Jahanshahi S, Mathieson JG, Reimink H (2016) Low emission steelmaking. *Sustain Metall* 2:185–190. <https://doi.org/10.1007/s40831-016-0065-5>
20. Mandova H, Leduc S, Wang C, Wetterlund E, Patrizio P, Gale W, Kraxner F (2018) Possibilities for CO₂ emission reduction using biomass in European integrated steel plants. *Biomass Bioenergy* 115:231–243
21. Titschenbacher F, Pfemeter C (2019) Basisdaten 2019 - Bioenergie. Graz
22. Lorraine L (2019) Direct from MIDREX - 3rd quarter 2019. North Carolina
23. Hofbauer H (2013) Biomass gasification for electricity and fuels, Large Scale. *Renew Energy Syst*:459–478. <https://doi.org/10.1007/978-1-4614-5820-3>
24. Wörtler M, Schuler F, Voigt N, et al (2013) Steel's contribution to a low-carbon Europe 2050. Boston Consulting Group. Steel Institute VDEh. Boston
25. Prammer J, Schubert M (2019) Umwelteklärung Voestalpine 2019. Voestalpine AG. Linz
26. Otto A, Robinius M, Grube T, Schiebahn S, Praktijn A, Stolten D (2017) Power-to-steel: reducing CO₂ through the integration of renewable energy and hydrogen into the German steel industry. *Energies* 10:451. <https://doi.org/10.3390/en10040451>
27. Worrell E, Price L, Neelis M, et al (2008) World best practice energy intensity values for selected industrial sectors. Ernest Orlando Lawrence Berkeley National Laboratory LBNL-62806
28. Liu L, Jiang Z, Zhang X, Lu Y, He J, Wang J, Zhang X (2018) Effects of top gas recycling on in-furnace status, productivity, and energy consumption of oxygen blast furnace. *Energy* 163:144–150. <https://doi.org/10.1016/j.energy.2018.08.114>
29. Hooey L, Tobiesen A, Johns J, Santos S (2013) Techno-economic study of an integrated steelworks equipped with oxygen blast furnace and CO₂ capture. *Energy Procedia* 37:7139–7151. <https://doi.org/10.1016/j.egypro.2013.06.651>
30. Suopajarvi H, Kempainen A, Haapakangas J, Fabritius T (2017) Extensive review of the opportunities to use biomass-based fuels in iron and steelmaking processes. *Cleaner Production* 148:–734. <https://doi.org/10.1016/j.jclepro.2017.02.029>
31. Wang C, Mellin P, Lövgren J, Nilsson L, Yang W, Salman H, Hultgren A, Larsson M (2015) Biomass as blast furnace injectant - considering availability, pretreatment and deployment in the Swedish steel industry. *Energy Convers Manag* 102:217–226. <https://doi.org/10.1016/j.enconman.2015.04.013>
32. Kopfle JT, Mcclelland JM, Metius GE (2008) Green(er) steelmaking with the Midrex direct reduction process. MIDREX Technologies
33. Ravenscroft C (2017) Direct from MIDREX - 2nd quarter 2017. MIDREX Technologies. North Carolina
34. SSAB (2017) HYBRIT - fossil-free-steel. Summary of findings from pre-feasibility study 2016–2017. Sweden
35. Hölling M, Weng M, Gellert S (2018) Bewertung der Herstellung von Eisenschwamm unter Verwendung von Wasserstoff. Hamburg
36. Corradi O, Hinkle T, Collignon M, et al (2020) Electricity map - CO₂ Emissionen. Tomorrow. <https://www.electricitymap.org/?countryCode=AT&page=country>. Accessed 26 Mar 2020
37. Müller S (2013) Hydrogen from biomass for industry-industrial application of hydrogen production based on dual fluid gasification. Dissertation. TU Wien
38. Spreitzer D, Schenk J (2019) Reduction of iron oxides with hydrogen - a review. *Montanuniversität Leoben Steel Res Online* 1900108:1900108. <https://doi.org/10.1002/srin.201900108>
39. VDEh (2020) Hot metal and crude steel production. *Stahl Online*. <https://www.vdeh.de/en/technology/steelmaking/>. Accessed 25 Jun 2020
40. Ramírez-Santos ÁA, Castel C, Favre E (2018) A review of gas separation technologies within emission reduction programs in the iron and steel sector: current application and development perspectives. *Sep Purif Technol* 194:425–442. <https://doi.org/10.1016/j.seppur.2017.11.063>
41. Markewitz P, Zhao L, Robinius M (2017) Technologiebericht 2.3 CO₂-Abscheidung und Speicherung (CCS). Wuppertal, Karlsruhe, Saarbrücken
42. Tondl G (2013) Oxyfuel Verbrennung von Klärschlamm. Institute of Chemical, Environmental and Bioscience Engineering. Dissertation. Wien
43. Kuckshinrichs W, Markewitz P, Linssen J, et al (2010) Weltweite Innovationen bei der Entwicklung von CCS-Technologien und Möglichkeiten der Nutzung und des Recyclings von CO₂. Forschungszentrum Jülich. ISBN 978-3-89336-617-0. Berlin
44. Hammerschmid M (2016) Evaluierung von sorption enhanced reforming in Kombination mit Oxyfuel-combustion für die Abscheidung von CO₂. Bachelor Thesis. TU Wien
45. Berghout N, McCulloch S (2019) Putting CO₂ to use. Technology Report. International Energy Agency. France
46. Oktawiec D (2009) Erarbeitung eines Konzeptes zur Einhaltung der neu zu erwartenden Abwassergrenzwerte für die Harnstoff- und Melaminanlagen. Master Thesis. Montanuniversität Leoben
47. Leeson D, Mac Dowell N, Shah N, Petit C, Fennell PS (2017) A techno-economic analysis and systematic review of carbon capture and storage (CCS) applied to the iron and steel, cement, oil refining and pulp and paper industries, as well as other high purity sources. *Int J Greenh Gas Control* 61:71–84. <https://doi.org/10.1016/j.ijggc.2017.03.020>
48. Koch T, Scheelhaase T, Jonas N, et al (2016) Evaluation zur Nutzung von Kohlendioxid (CO₂) als Rohstoff in der Emscher-Lippe-Region - Erstellung einer Potentialanalyse. Hamburg
49. Werpy T, Petersen G (2004) Top value added chemicals from biomass. *US Dep Energy* 1:76. <https://doi.org/10.2172/926125>
50. Schmid JC (2014) Development of a novel dual fluidized bed gasification system. Dissertation TU Wien
51. Schmid JC, Benedikt F, Fuchs J, et al (2019) Syngas for biorefineries from thermochemical gasification of lignocellulosic fuels and residues - 5 years' experience with an advanced dual fluidized bed gasifier design. *Biomass Conversion and Biorefinery*. TU Wien
52. Fuchs J, Schmid JC, Müller S, Hofbauer H (2019) Dual fluidized bed gasification of biomass with selective carbon dioxide removal and limestone as bed material: a review. *Renew Sust Energy Rev* 107:212–231. <https://doi.org/10.1016/j.rser.2019.03.013>

53. Schmid JC, Kolbitsch M, Fuchs J, et al (2016) Steam gasification of exhausted olive pomace with a dual fluidized bed pilot plant at TU Wien. Technical Report. TU Wien
54. Hammerschmid M (2019) Entwicklung eines virtuellen Planungsraums anhand des Basic Engineering einer Zweibettwirbelschichtanlage. Diploma Thesis. TU Wien
55. Fuchs J, Wagner K, Kuba M, et al (2017) Thermische Vergasung minderwertiger Reststoffe zur Produktion von Wertstoffen und Energie. Blickpunkt Forschung. Vienna
56. Koppatz S (2008) In-situ Produktgaskonditionierung durch selektive CO₂-Abscheidung bei Wirbelschicht- Dampfvergasung von Biomasse: Machbarkeitsnachweis im industriellen Maßstab. Diploma Thesis. TU Wien
57. Schweitzer D, Beirou M, Gredinger A, Armbrust N, Waizmann G, Dieter H, Scheffknecht G (2016) Pilot-scale demonstration of oxy-SER steam gasification: production of syngas with pre-combustion CO₂ capture. Energy Procedia 86:56–68. <https://doi.org/10.1016/j.egypro.2016.01.007>
58. Soukup G (2009) Der AER-Prozess, Weiterentwicklung in einer Technikumsanlage und Demonstration an einer Großanlage. Dissertation. TU Wien
59. SimTech Simulation Technology (2011) IPSEpro process simulator - model development kit (manual). Graz
60. SimTech Simulation Technology (2011) IPSEpro process simulator - process simulation environment (manual). Graz
61. Pröll T, Hofbauer H (2008) development and application of a simulation tool for biomass gasification based processes. Int J Chem React Eng 6:A89. <https://doi.org/10.2202/1542-6580.1769>
62. Müller S, Fuchs J, Schmid JC, Benedikt F, Hofbauer H (2017) Experimental development of sorption enhanced reforming by the use of an advanced gasification test plant. Int J Hydrog Energy 42: 29694–29707. <https://doi.org/10.1016/j.ijhydene.2017.10.119>
63. Pröll T (2004) Potenziale der Wirbelschichtdampfvergasung fester Biomasse – Modellierung und Simulation auf Basis der Betriebserfahrungen am Biomassekraftwerk Güssing. Dissertation. Technische Universität Wien
64. Schmid JC (2016) Technoökonomische Fallstudien als Entscheidungsunterstützung für das strategische Management. Masterarbeit. Fachhochschule Burgenland
65. Lozowski D (2020) Chemical Engineering Plant Cost Index. <https://www.chemengonline.com/pci>. Accessed 25 May 2020
66. Neuling U, Kaltschmitt M (2018) Techno-economic and environmental analysis of aviation biofuels. Fuel Process Technol 171:54–69. <https://doi.org/10.1016/j.fuproc.2017.09.022>
67. Piazza S, Zhang X, Patuzzi F, Baratieri M (2020) Techno-economic assessment of turning gasification-based waste char into energy: a case study in South-Tyrol. Waste Manag 105:550–559. <https://doi.org/10.1016/j.wasman.2020.02.038>
68. Jentsch R (2015) Modellierung des SER-Prozesses in einem neuen Zweibettwirbelschicht-Dampfvergaser-System. Diplomarbeit. TU Wien
69. Fuchs J, Schmid JC, Benedikt F, Müller S, Hofbauer H, Stocker H, Kieberger N, Bürgler T (2018) The impact of bed material cycle rate on in-situ CO₂ removal for sorption enhanced reforming of different fuel types. Energy 162:35–44. <https://doi.org/10.1016/j.energy.2018.07.199>
70. Cheeley R (1999) Gasification and the MIDREX® direct reduction process. In: AISTech - Iron and Steel Technology Conference Proceedings. San Francisco, pp. 633–639
71. Horvath E (2019) Holzmarktbericht Jänner-Dezember 2019. LK Österreich. Wien
72. E-Control (2020) Preisentwicklungen Strom und Erdgas. <https://www.e-control.at/statistik/gas/marktstatistik/preisentwicklung>. Accessed 27 Mar 2020
73. Thrän D, Pfeiffer D (2013) Methodenhandbuch - Stoffstromorientierte Bilanzierung der Klimagaseffekte, Ed. 4. Energetische Biomassenutzung. BMU. Leipzig
74. Damodaran A (2019) Cost of equity and capital. http://people.stern.nyu.edu/adamodar/New_Home_Page/dataarchived.html#discrate. Accessed 6 Jan 2020
75. EEX (2019) European Emission Allowances (EUA). <https://www.eex.com/en/market-data/emission-allowances/spot-market/european-emission-allowances#!/2016/05/26>. Accessed 4 Jul 2019
76. Zimmermann AW, Wunderlich J, Müller L, Buchner GA, Marxen A, Michailos S, Armstrong K, Naims H, McCord S, Styring P, Sick V, Schomäcker R (2020) Techno-economic assessment guidelines for CO₂ utilization. Front Energy Res 8:5. <https://doi.org/10.3389/fenrg.2020.00005>
77. Körner A, Tam C, Bennett S (2015) Technology roadmap - hydrogen and fuel cells. IEA. Paris
78. Kost C, Shammugam S, Jülch V, et al (2018) Stromgestehungskosten Erneuerbare Energien. Fraunhofer Institut. Freiburg
79. Konstantin P (2017) Praxisbuch Energiewirtschaft: Energieumwandlung, -transport und -beschaffung, Übertragungsnetzausbau und Kernenergieausstieg, 4. Auflage
80. Godula-Jopek A, Stolten D (2015) Hydrogen production by electrolysis, 1st ed. Wiley-VCH, Weinheim

Publisher's Note Springer Nature remains neutral with regard to jurisdictional claims in published maps and institutional affiliations.

Paper IV

Thermal Twin 4.0: Digital Support Tool for Optimizing Hazardous Waste Rotary Kiln Incineration Plants

Hammerschmid, M., Aguiari, C., Kirnbauer, F., Zerobin, E., Brenner, M.,
Eisl, R., Nemeth, J., Buchberger, D., Ogris, G., Kolroser, R., Goia, A.,
Beyweiss, R., Kalch, K., Müller, S., Hofbauer, H.

Waste and Biomass Valorization, 2023, 14, 2745-2766

<https://doi.org/10.1007/s12649-022-02028-w>



Thermal Twin 4.0: Digital Support Tool for Optimizing Hazardous Waste Rotary Kiln Incineration Plants

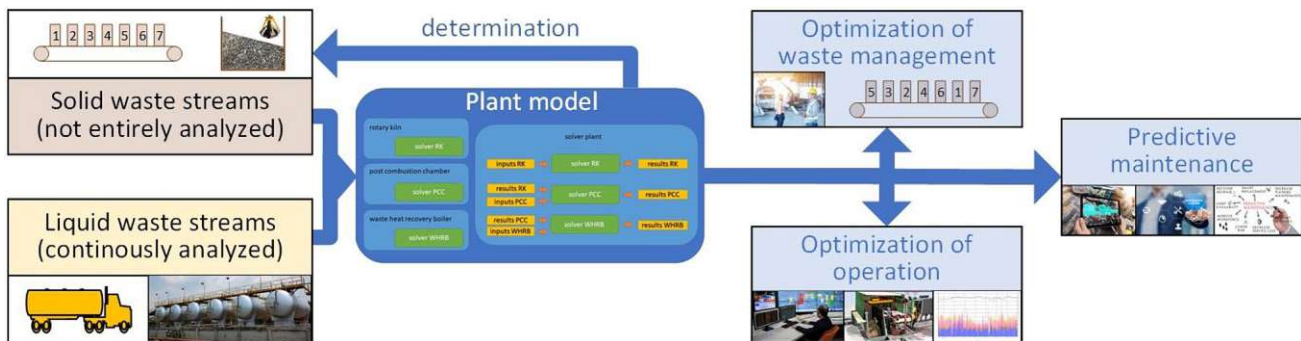
M. Hammerschmid¹ · C. Aguiari² · F. Kirnbauer² · E. Zerobin² · M. Brenner² · R. Eisl³ · J. Nemeth³ · D. Buchberger³ · G. Ogris⁴ · R. Kolroser⁴ · A. Goia⁴ · R. Beyweiss⁴ · K. Kalch⁴ · S. Müller¹ · H. Hofbauer¹

Received: 8 July 2022 / Accepted: 21 December 2022 / Published online: 9 January 2023
© The Author(s) 2023

Abstract

The present paper focuses on developing a novel virtual representation framework for optimizing standalone hazardous waste rotary kiln incineration plants. A digital support tool can be provided to optimize the plant's waste management, operation, and maintenance by combining thermochemical-based simulation models with a fuel classification system. First of all, the virtual representation can be used to determine the waste composition of not entirely analyzed waste streams. Furthermore, the determined waste compositions of historically fed waste streams can be used to enable further advanced applications. The determined waste compositions are linked with the appropriate waste code and supplier, which first enables the monitoring of the delivered waste streams. In the case of recurring fractions, the virtual representation can be used to optimize the barrel sequence to reach homogenous waste inputs. Additionally, the plant operation can be optimized regarding stable operation conditions due to the knowledge about waste compositions of recurring fractions. The parametrization results fit very well with the comparable sensor values. Therefore, the novel virtual representation of the hazardous waste incineration plant could definitely make a reasonable contribution to optimize the efficiency of thermal waste treatment within the hazardous waste sector in Austria and Europe.

Graphical Abstract



Keywords Rotary kiln · Digital twin · Hazardous waste incineration · Virtual representation · Waste classification · Simulation

Abbreviations

3D Three-dimensional
5D Five dimensions
C Carbon

$C_xH_yO_z$ Volatiles
 CH_4 Methane
Cl Chlorine
CO Carbon monoxide
 CO_2 Carbon dioxide
ECO Economiser
EV Evaporator

✉ M. Hammerschmid
martin.hammerschmid@tuwien.ac.at

Extended author information available on the last page of the article

H ₂	Hydrogen
H ₂ O	Water/steam
HCl	Hydrogen chloride
HEL	Heating oil extra light
HEX	Heat exchanger system
HHV	Higher heating value
HS	Heavy heating oil
JSON	Data exchange format
m.-%	Mass percent wet
m.-% _{daf}	Mass percent dry and ash free
MAPE	Mean absolute percentage error
MB	Masterbatch (solvent mixture)
N	Nitrogen
NumPy	Python library
O ₂	Oxygen
Pandas	Python library
PCC	Post combustion chamber
PROFIBUS	Field bus communication standard
PW	Pasty waste
Python	Programming language
RK	Rotary kiln
S	Sulfur
SO ₂	Sulfur dioxide
SD	Steam drum
SH	Superheater
vol.-%	Volume percent wet
vol.-% _{dry}	Volume percent dry
WHRB	Waste heat recovery boiler
WO	Waste oil
WW	Waste water
Δ _R H ₀	Enthalpy of reaction at standard conditions

Statement of Novelty

All digital support tools published in the field of waste incineration plants rely on knowledge about the composition of the introduced waste streams. Therefore, a novel virtual representation framework is presented, enabling the determination of not entirely analyzed solid waste streams. Furthermore, in terms of recurring waste fractions, this knowledge can be used to optimize the operation, waste management, and maintenance of hazardous waste rotary kiln incineration plants. The central part of the virtual representation is the plant model, consisting of a transient rotary kiln model and steady-state models of the post-combustion chamber and waste heat recovery boiler. The plant model validation was achieved due to the integration of test datasets from the hazardous waste incineration plant in Vienna.

Introduction

At least since the Paris climate agreement [1] the energy transition path towards climate neutrality has been accepted worldwide and has to be considered in each sector. Thermal waste treatment deals with well-established technologies for sanitizing waste streams and reducing the final waste load for disposal in landfills [2]. Therefore, thermal waste treatment will be essential in converting non-recyclable waste streams into valuable products in a climate-neutral world. In Austria, the waste sector is responsible for 2.9% of the national greenhouse gas emissions, whereby about half of these emissions are caused by thermal waste treatment plants [3]. The energy transition process shall be reached mainly with high shares of renewable energy carriers and energy efficiency improvements [4]. In terms of energy efficiency, digitization enables significant productivity improvement rates by implementing advanced digital methods [5]. A significant optimization potential regarding efficiency increase and emission reduction arises in the thermal waste treatment sector. Due to inhomogeneous waste streams, the operation of waste incineration plants is challenging. Significantly, batch-wise barrel combustion leads to peak loads in terms of temperature and emissions [6]. Therefore, the operation of waste incineration plants is always a balance between low-emission and efficient operation. *Digital modeling tools* can help to *optimize waste incinerators*.

Numerous researchers and international institutions investigate thermal waste incineration plants' different modeling and optimization approaches. Exemplary, Lei et al. developed a web-based digital twin of a thermal power plant to monitor and control the facility [7]. Kabugo et al. [8] proposed a methodology to monitor and predict the heating value and temperature of the flue gas stream of a waste treatment plant. The waste treatment plant in Mannheim was optimized by implementing a combustion performance control through fuzzy logic [9, 10]. Additionally, several technology-related modeling and optimization approaches to this more general thermal waste treatment optimization concepts exist. Several types of incinerators exist for thermal waste treatment, which can be classified by their application fields [11]. Waste incinerators with mechanical grates are mainly used to treat household waste [11]. In terms of household waste incinerators, Zhuang et al. [12] investigated a numerical simulation method of municipal solid waste incinerators to realize a digital twin system. Due to the uniform temperature distribution, fluidized bed incinerators are primarily built to burn sewage sludge and municipal solid waste [11]. Rotary kilns are very flexible in terms of different types of waste streams. Therefore, rotary kilns are widely used for the incineration

of hazardous waste [11]. For the optimization of rotary kilns, many models have been developed. Liu and Specht [13] investigated the residence time behavior of hazardous waste fractions in rotary kilns. The heat and mass transfer of rotary kilns were researched, for example, by Chen et al. [14] and Silcox and Perching [15]. Further research work can be classified as thermal conversion investigations in oxygen-rich [16, 17] and oxygen-free [18] atmospheres, as well as other topics [9, 19].

Additionally, hazardous waste incineration plants should be divided into co-incineration plants and standalone incineration plants. Co-incineration plants like rotary kilns within cement plants are characterized by the treatment of mainly well-known waste streams. In contrast, standalone hazardous waste incineration plants face various hazardous input streams [20]. In the research field of co-incineration plants, Yao et al. [21] proposed a concept for modeling the thermal efficiency of a cement clinker calcination system. Furthermore, Zhang et al. [22, 23] investigated a co-incineration system by a numerical simulation to predict mixed waste streams' granular motion and combustion interactions within a rotary kiln. Finally, Xu et al. [24] established a soft sensor that can predict the temperature distribution within the rotary kiln by combining computational fluid dynamics and multilayer perceptrons. Many digital modeling tools exist within the context of standalone hazardous waste incineration plants. Guillin-Estrada et al. [25] published a tool for predicting mechanical failures in predictive maintenance. Pirttiniemi [26] investigated a novel methodology to support the rotary kilns' design process. Furthermore, several thermochemical-based simulation models have been published to optimize the performance of rotary kiln incinerators [27–29]. Additionally, Wajda et al. [20] developed a digital tool for creating batch-wise waste mixtures to optimize the operation of rotary kilns. Nolte introduced an intelligent control system for minimizing the CO emission peak loads within hazardous waste incineration plants [6].

To summarize, there are a lot of investigations published in the fields of hazardous waste incineration plants. However, all these *optimization approaches rely on knowledge about the composition and properties of the introduced waste streams*. Since many hazardous waste fractions cannot be analyzed [27], there is a need for an advanced digital support tool. Therefore, a *novel virtual representation of a hazardous waste rotary kiln incineration plant is first introduced in this work*. Combining transient and steady-state thermochemical-based simulation models with a machine learning algorithm enables the *determination of historical hazardous waste feed streams*. The determination of multiple historical hazardous waste feed streams allows the creation of a fuel analysis data base, which is the basis for optimizing the performance of each standalone hazardous waste incineration plant due to using the data base knowledge in terms

of recurring fractions. The present paper describes the novel digital support tool, which is based on the virtual representation methodology. Furthermore, the virtual representation will be applied and validated within Vienna's hazardous waste incineration plant at Simmeringer Haide. Thus, the paper discusses the following sections:

- Definition of virtual representations within the energy sector
- State of the art of hazardous waste rotary kiln incineration
- Methodology of the thermochemical-based plant simulation model
- Methodology of data processing for waste input streams
- Test series for parametrization and application of the plant simulation model
- Methodology for the overall virtual representation framework
- Simulation results for parametrization test series
- Applications for optimizing the hazardous waste incineration based on the virtual representation

The methodology and simulation results of the novel virtual representation for the hazardous waste incineration plant are based on the funded research project Thermal Twin 4.0 [30]. The holistic virtual representation framework for the determination of waste stream compositions and further applications for the optimization of the hazardous waste incineration plant is reached by *interdisciplinary collaboration* between experts in the research fields of chemical engineering, energy systems, and thermodynamics as well as informatics.

Concept and Methodology

The overall concept and methodology of the virtual representation framework of the hazardous waste incineration plant are based on the broad definition of virtual representations within the energy sector. Furthermore, the state-of-the-art hazardous waste rotary kiln incinerators, the leveraging thermochemical-based plant simulation model, and the data processing approaches are the building blocks for the overall virtual representation framework. Finally, investigated test series with the hazardous waste incineration plant of Wien Energie in Vienna at Simmeringer Haide are explained to parametrize and validate the plant simulation model.

Definition of Virtual Representations in the Energy Sector

First, to develop a virtual representation framework, it is essential to discuss the definition of virtual

representations in the energy sector. The term “virtual representation” can be used as the overall expression of virtual objects mirroring a physical process [31]. In literature, there are several terms like “digital model”, “digital shadow”, “digital twin” and “digital predictive twin” used synonymously for virtual representations [31, 32]. Kritzinger et al. [32] and Aheleroff et al. [33] classified these terms according to the data integration level. In Fig. 1, the virtual representation classification *levels of data integration* are visualized. Therefore, the digital model represents a virtual representation with only manual data communication between physical and virtual components [32]. Digital shadows are based on uni-directional and digital twins on a bi-directional real-time data communication [32]. The highest data integration level can be reached within digital predictive twins, where the virtual models and the data communication can predict future operation conditions [33].

Additionally, to the virtual representation definition concerning the data integration level, Tao et al. [34] published the *5D model*, which defines that each digital twin shall be *based on five dimensions*. Within this work, the 5D model is used for any kind of virtual representation independent on the data integration level. The five dimensions are the physical and virtual component, data management, service, and the connections in-between [31, 34].

Subsequently, the state of the art of hazardous waste rotary kiln incineration plants, the considered waste incineration plant in Vienna at Simmeringer Haide, and the developed thermochemical-based simulation models and data processing steps are discussed. The definition of virtual representations in terms of data integration level and dimensions forms the foundation for the following virtual representation framework in the implementation section.

Hazardous Waste Rotary Kiln Incineration

The thermal treatment of hazardous waste fractions is conducted to eliminate harmful substances and compounds and minimize the amount of deposited waste, which reduces the related greenhouse gas emissions [35]. The thermal conversion of waste streams is based on exothermic oxidation reactions of the waste with atmospheric oxygen [11, 36]. Combustible waste streams consist mainly of carbon, hydrogen, oxygen, sulfur, nitrogen, and chlorine, which are building up together the ultimate analysis. Furthermore, the amount of ash and water is building up together with the fixed carbon and volatile compounds the proximate analysis. The thermal conversion of solid waste streams is initiated through heating. In contrast, the combustion of liquid and gaseous waste streams is started by exceeding the ignition temperature with the presence of a spark. Furthermore, for complete combustion, enough temperature, enough turbulence for a thoroughly mixed fuel with air, as well as sufficient residence time is needed [36]. Therefore, the mix of fuel and air is essential to reach complete combustion. Excess air means a decrease in the combustion temperature, resulting in incomplete oxidation or efficiency decrease. Lack of air also results in incomplete combustion. In addition to the combustion air input, oxygen is provided through the fuel itself, which decreases the required oxygen amount from the combustion air. Further details about combustion and reactor types can be found in [11, 36, 37].

The present work focuses on integrating a virtual representation in the hazardous waste rotary kiln incineration plant from Wien Energie in Vienna at Simmeringer Haide. Therefore, a 3D visualization of the considered plant in Fig. 2 and a basic flow diagram in Fig. 3 are shown. Therein it can be seen that the rotary kiln is the central combustion unit. The waste feeding to the rotary kiln is realized through several input lines in the front wall of the rotary kiln. As shown in Fig. 3, four solid waste streams are fed to

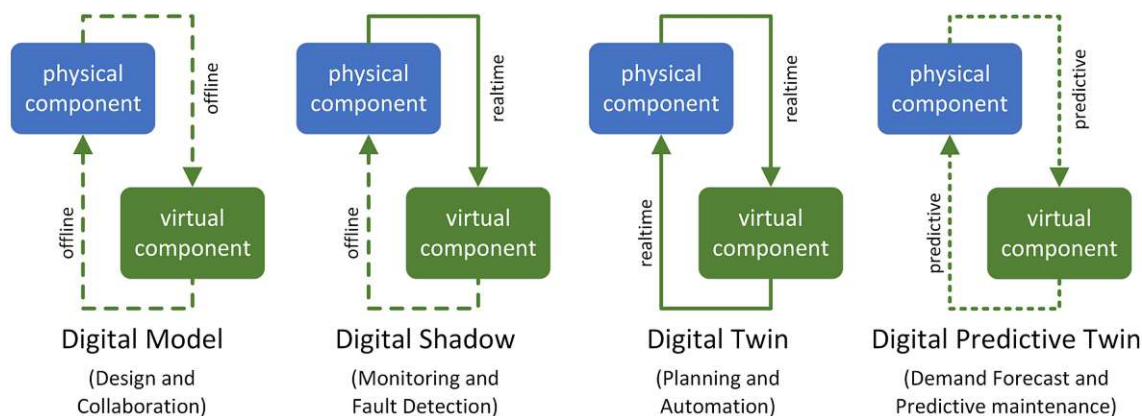


Fig. 1 Virtual representation stages concerning the data integration level [31–33]



Fig. 2 3D visualization of the hazardous waste rotary kiln incinerator in Vienna at Simmeringer Haide [38]

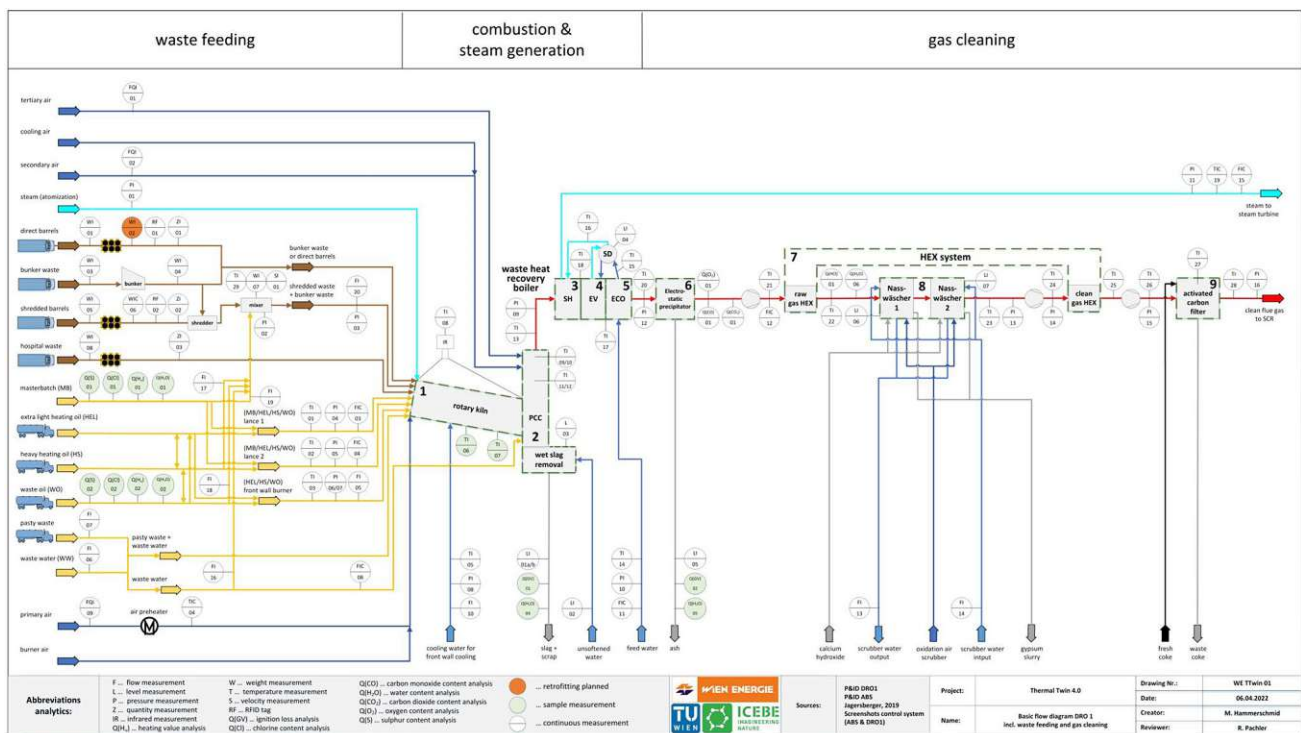


Fig. 3 Basic flow diagram of hazardous waste rotary kiln incinerator in Vienna at Simmeringer Haide

the rotary kiln, which are direct and shredded barrels, bunker, and hospital waste. Bunker waste and direct barrels are fed through the same front wall input. The shredded barrels are mixed with parts of the bunker waste, which are mainly screenings from the sewage treatment plant. Additionally,

four liquid and pasty input lines are installed. Two lances are feeding mainly masterbatch (MB) fractions, which are solvent mixtures as well as extra light heating oil (HEL), heavy heating oil (HS), and waste oil (WO) during heating-up. The front wall burner mainly processes WO and again

HEL for the heat-up procedure. Furthermore, a pasty lance is installed, wherein a mix of pasty waste and waste water is fed. These waste streams are burned with primary air in the rotary kiln and the post-combustion chamber (PCC) at 900–1400 °C [11]. In the PCC, secondary air is introduced to provide oxygen for combustion. Tertiary air and additional waste water are also mainly introduced to control the combustion temperature. Afterwards, the hot flue gas heat is used in the waste heat recovery boiler (WHRB) to produce superheated steam for the steam turbine to produce electricity and district heat. The WHRB consists of two superheaters (SH), two evaporators (EV), one economiser (ECO), the steam drum (SD), and the coated fin wall, which is also part of the evaporator system. Finally, the flue gas is cleaned with an electrostatic precipitator, two scrubber units, and an activated carbon filter. The heat exchanger system (HEX) is installed to use the flue gas heat before the scrubber system to heat-up the flue gas after the scrubber system to reach the required temperature for the following activated carbon bed. After the last coarse cleaning step, the flue gas is introduced to the overall fine gas cleaning steps starting with a selective catalytic reduction unit. The fine gas cleaning units at the Wien Energie site are used to clean all flue gas streams out of different combustion lines.

The operation of a hazardous waste rotary kiln incineration plant is *very challenging*. One of the main challenges arises from batch-wise waste feeding, which results in peak load emissions of mainly carbon monoxide and soot [6]. Besides the batch-wise feeding of barrels and bunker waste, it is also *essential to introduce a balanced mix of waste streams in the rotary kiln*, which is more or less constant over time regarding the heating value. The solid fractions are not entirely analyzed regarding waste composition and heating value. As a consequence, it is challenging to realize constant operation conditions. Therefore, the rotary kiln's standard operation and the WHRB must be far from the design point. Typically, an average steam production load of around 80% from the design point of the WHRB is pursued to allow reserve capacity to cope with the peak loads due to batch-wise feeding of inhomogeneous waste streams [27].

Concluding, the operation of the hazardous waste incineration plant is more reactive than proactive in tackling the challenging operating conditions due to inhomogeneous waste input and composition. To solve this problem, the *virtual representation of the hazardous waste incineration plant is developed to determine the not entirely analyzed waste fractions*. Furthermore, the knowledge about the composition and heating value of recurring waste streams is used to optimize the rotary kiln operation. Subsequently, the virtual representation main building blocks with the thermochemical-based modeling approach and the executed data processing steps are explained.

Thermochemical-Based Plant Model of the Hazardous Waste Incineration Plant

A thermochemical-based simulation model was developed to enable the determination of not entirely analyzed waste fractions. The simulation model is written in Python and is built up of transient and steady-state models. As shown in Fig. 3, the whole hazardous waste rotary kiln incineration plant is divided into nine sub-units. The rotary kiln (sub-unit 1) and the PCC (sub-unit 2) form the combustion process. Afterwards, within the WHRB (sub-units 3–5), the flue gas heat produces superheated steam as input for the steam turbine. After steam generation, the flue gas is introduced to the gas cleaning section (sub-units 6–9). The simulation model does not cover the gas cleaning section to optimize the calculation time. The overall simulation model is based on a sequential modeling approach. Subsequently, the thermochemical-based simulation models of the implemented sub-units rotary kiln, PCC, and WHRB are explained.

In Fig. 4, the thermochemical-based modeling approaches of the rotary kiln according to [39] and the model of the PCC are visualized. Therein, it can be seen that the rotary kiln is implemented in the overall plant model as a *thermochemical-based transient model*. Therefore, the rotary kiln is discretized through a one-dimensional cylindrical grid divided into a predefined number of uniform sections in the axial direction. The rotary kiln is divided into 1 m sections in the axial direction for this approach. The wall of each axial section is further discretized in the radial direction to model the heat losses to the environment. Additionally, the front wall is discretized in the axial direction to implement the front wall cooling. The waste fractions are introduced in the first rotary kiln section (cell 1). The lumpy waste fractions with bunker and shredded waste are treated as solid phases with decreasing bed height along with the rotary kiln, according to [40, 41]. The direct barrels and hospital waste fractions can be treated as discrete barrel elements by considering that the barrels are firstly heated up before the liquid and solid fractions inside are converted to gas species. In the present work, the barrel fractions of direct barrels and hospital waste are treated as solid phases to simplify the model. Additionally, the pasty waste fraction is mixed with waste water and can be fed into the rotary kiln over an additional lance. However, the pasty waste fraction is treated as solid fraction due to the similar physical behavior. Therefore, the bunker waste, shredded waste, direct barrels, hospital waste, and pasty waste fractions are treated as solids and simplified introduced as a solid mixture into the rotary kiln for this approach. The front wall burner converts the liquid oil model, mostly WO, to a gas model within the first cell. Therefore, the flame length is set to 1 m to end within the first section. The MB fractions, fed through two lances together with atomized steam, are treated as liquid phases,

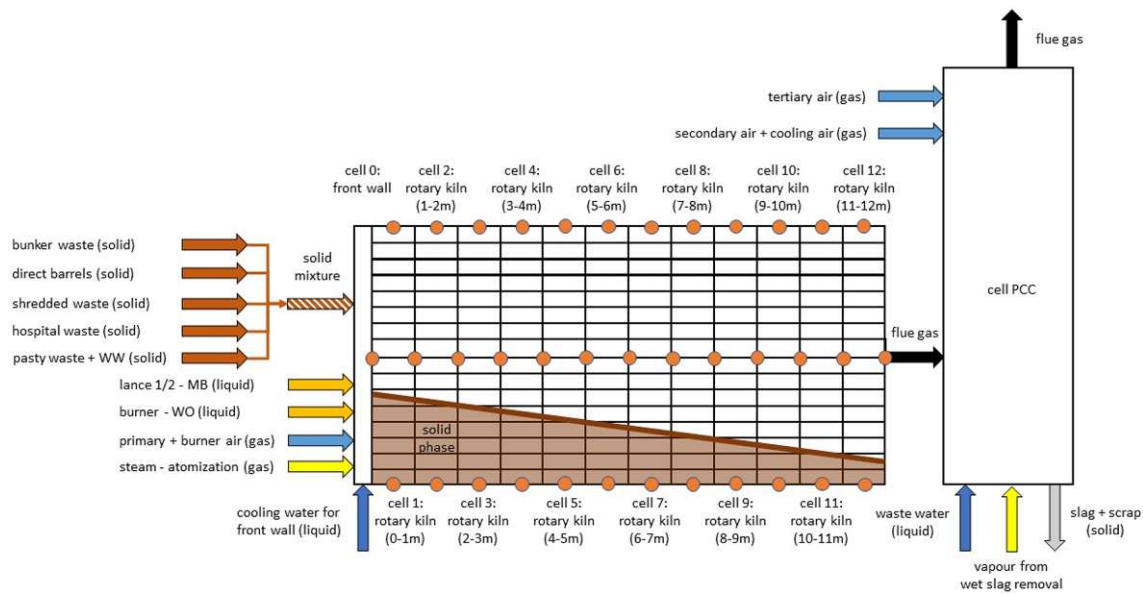


Fig. 4 Modeling approaches of the rotary kiln and post-combustion chamber

which are assumed to fully react over a defined spray length, where the gaseous reaction products are added as sources to the gas phase and the solid products (e.g., ash) to the solid bed phase. Additionally, primary and front wall burner air are added as gas models to deliver the necessary oxygen for the combustion reaction. The ash fraction, which is part of the solid and liquid model, is assumed to be inert and is transported with the solid bed phase to the PCC, where it is entirely removed through the wet deslagger. The ash fraction is modeled as fixed inert composition with SiO₂ as main component. Therefore, the influences of heavy metals and salts due to fouling are modeled by fixed values and influences due to emission peaks are neglected. The residence time of the solids within each cell could be implemented through a mean residence time dependent on the geometry, volume flow, and the rotary kiln speed according to [13]. For this approach, the residence time of the solids, which is

dependent on the solid phase bed height, is assumed to be constant due to a constant rotary kiln speed. A reference is made to [39] for further information on material transport.

In addition to the material transport, heat transfer is integrated into the simulation model [42]. In the rotary kiln the following heat transfer mechanisms are considered:

- heat conduction through the wall depending on the brickwork,
- thermal convection between gas/solid, gas/wall and wall/solid,
- and thermal radiation between wall/solid, gas/solid, and gas/wall.

Finally, the mass transfer within the rotary kiln is defined. Therefore, the solid fraction passes through the drying, devolatilization, gasification, and oxidation phase

Table 1 Considered combustion reactions in the transient rotary kiln model [6, 44]

Important heterogeneous reactions (solid–gas)			
Partial oxidation of carbon	$C + \frac{1}{2}O_2 \rightarrow CO$	$\Delta_R H_0 = -110.5\text{kJ/mol}$	(1)
Complete oxidation of carbon	$C + O_2 \rightarrow CO_2$	$\Delta_R H_0 = -393.5\text{kJ/mol}$	(2)
Important homogeneous reactions (gas–gas)			
Oxidation of carbon monoxide	$CO + \frac{1}{2}O_2 \rightarrow CO_2$	$\Delta_R H_0 = -283.0\text{kJ/mol}$	(3)
Oxidation of hydrogen	$2H_2 + O_2 \rightarrow 2H_2O$	$\Delta_R H_0 = -241.8\text{kJ/mol}$	(4)
Oxidation of methane	$CH_4 + 2O_2 \rightarrow CO_2 + 2H_2O$	$\Delta_R H_0 = -802.6\text{kJ/mol}$	(5)
Oxidation of volatiles	$C_xH_yO_z + \left(x + \frac{1}{4}y - \frac{1}{2}z\right)O_2 \rightarrow uCO_2 + \frac{1}{2}yH_2O$	$\Delta_R H_0 \ll 0\text{kJ/mol}$	(6)
Oxidation of sulfur	$S + O_2 \rightarrow SO_2$	$\Delta_R H_0 = -574.0\text{kJ/mol}$	(7)
Hydrogenation of chlorine	$Cl + \frac{1}{2}H_2 \rightarrow HCl$	$\Delta_R H_0 = -213.6\text{kJ/mol}$	(8)

[43]. The liquid fractions are evaporated, and the gas fractions are oxidized according to the available oxygen. Nitrogen is assumed to be inert. Furthermore, global reactions are defined to consider the reaction kinetics. The considered reactions, except the evaporation of water, are summarized in Table 1.

Further details regarding combustion reactions in rotary kilns can be found in [6, 36, 39]. Ash melting phases are not considered within the transient model of the rotary kiln. Concluding, the transient gas and solid mass and species, as well as the coupled energy balance of gas, solid, and the inner wall cell balances, are solved iteratively for the whole kiln. After each iteration, the radial energy balance of the outer kiln mantle wall cells and the axial energy balance of the outer front wall cells are solved. The boundary conditions are updated for each time step. Hence, transient changes in fuel feed are included. The boundary conditions within each cell enable the transient approach, which hands over the energy state to the following cell. This approach ensures the transient behavior because the rotary kiln model is aware of the mass and energy balances of the previous periods. Therefore, a continuous fuel feed can be balanced. After the time step calculation of the kiln, the gas and solid results at the kiln outlet boundary are handed over to the *steady-state model of the PCC*, where the gas is further oxidized by the secondary and tertiary air inlet stream. The secondary air is increased by a fixed cooling air, discovered by an extensive false air measurement campaign [38]. In the PCC also, waste water is introduced, which is evaporated

immediately. In addition to the gas model, also the ash is handed over from the rotary kiln to the PCC, which is entirely removed from the system by the wet deslagger in the form of slag and scrap. Therefore, the PCC model simplifies that no ash is transported with the gas phase to the WHRB. Furthermore, water from the wet deslagger is evaporated in the PCC and transferred to the gas model in the form of vapour. To determine the evaporated water from the wet deslagger, a fixed ratio dependent on the solid input stream is introduced. To summarize, the PCC consists of gas–gas reactions and water evaporation from the waste water lance and the wet deslagger.

After the PCC, the resulting flue gas is introduced in the *steady-state model of the WHRB*. The steady-state model approach for the PCC and WHRB is chosen to decrease the calculation time of the simulation model. Compared to the rotary kiln combustion processes, the reaction time of the gas–gas reactions in the PCC and the heat exchange in the WHRB are much faster. Therefore, the steady-state approach also delivers reasonable solutions. The WHRB, visualized in Fig. 5, consists of two tube bundle evaporators, two superheaters, the injection cooler, the economiser, and the steam drum. Additionally, the WHRB is coated with a fin wall, which is not visualized in Fig. 5. In the fin wall, water evaporation occurs in the same way as within both evaporators. Firstly, the hot flue gas is introduced to the first natural circulation evaporator for steam generation. Afterwards, the flue gas is used for steam superheating in a two-step process. The remaining flue gas heat is used for steam generation within a

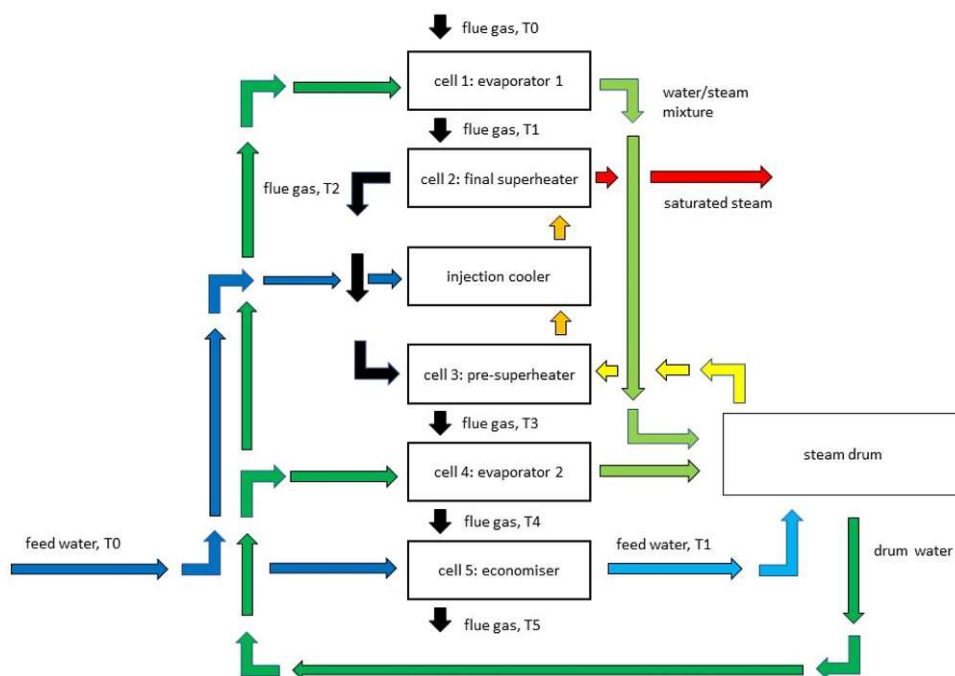


Fig. 5 Modeling approach of waste heat recovery boiler

second natural circulation evaporator and in the economiser to preheat the feed water. The preheated feed water is fed to the steam drum, which is connected with the two natural circulation tube bundle evaporators and the fin wall. The evaporator units return a water-steam mixture to the steam drum, where the mixture is separated. Saturated steam is fed to the pre-superheater, wherein it gets overheated in the first step. Finally, the superheated steam is cooled down via injection cooler before introducing it into the final superheating step. The overheated steam is converted within a steam turbine to electricity and heat. In the steady-state model of the WHRB, the following heat transfer processes are considered according to [42]:

- heat conduction through the tube bundles and the fin wall,
- thermal forced convection between gas/fin wall, gas/tube bundles, steam/tube bundles, and water/tube bundles,
- thermal free convection between water-steam mixture/fin wall and water-steam mixture/tube bundles,
- and thermal radiation between gas/fin wall and gas/tube bundles.

The heat loss from the steam drum and fin wall to the environment is neglected in the WHRB model. The fin wall is divided into five sections related to the number of sub-units in the WHRB (see Fig. 5). Therefore, the evaporation and heat transfer from the fin wall is partly considered in each unit. For solving the steady-state model of the WHRB, the mass- and energy balances are solved through a sequential approach. Firstly, the mass- and energy balances of the evaporator 1 are solved. Afterwards, the following cells final superheater, pre-superheater, evaporator 2, and economiser are solved. This results in an iterative approach to implement the characteristics of natural circulation. For this reason, the

produced amount and steam temperature in the superheaters influence the flue gas temperature and vice-versa.

Finally, the transient rotary kiln model and the steady-state model of the PCC and WHRB have to be connected. Therefore, the *plant model*, shown in Fig. 6, delivers the *sequential approach for solving the thermochemical-based hazardous waste incineration model*. The plant model is fed with input data for a given time interval. For this approach, a minute timestep is chosen. First, the solver must be initialized, wherein materials, reactions, and other properties like spray and flame length are defined. Furthermore, the sub-units have to be created to form the plant model. Subsequently, the plant model starts after initializing the transient rotary kiln solver, which is solved for every timestep. Afterwards, the rotary kiln solver results are handed over to the PCC solver, where the mass- and energy balances are solved with new input values for the PCC. Finally, the results of the PCC, together with new inputs, are fed to the WHRB to solve the final mass- and energy balance for steam production. Each mass- and energy balance delivers itself a unique solution. Due to the linkage of a vast number of mass- and energy balances, an iterative solution must be applied. Therefore, the mathematical solution of the plant model's mass- and energy balances is found by applying the linear algebra function of the NumPy library [45–47] based on Python. Each solver runs as long the stop criterion is not reached. Therefore, a predefined number of iteration steps are executed, or the iteration changes are less than a predefined value.

The described thermochemical-based plant model enables the calculation and validation of operation conditions. Before running the plant model, several data processing steps must be executed to feed the solver with appropriate values.

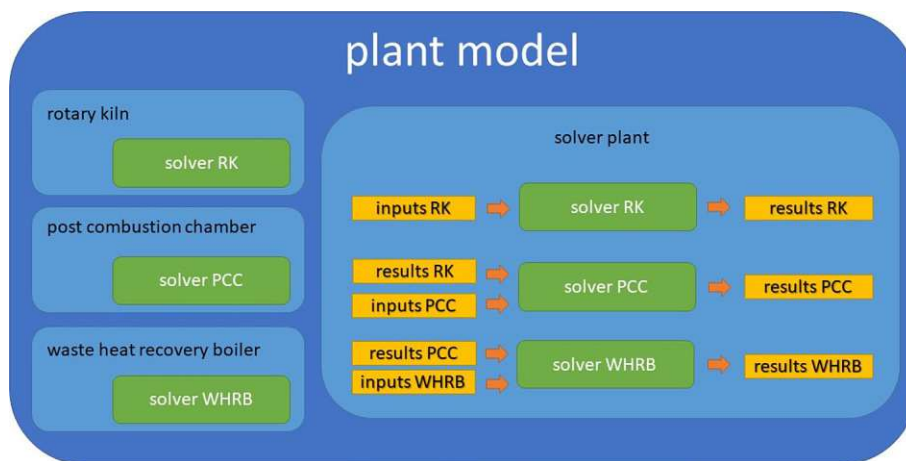


Fig. 6 Sequential thermochemical-based plant model

Data Processing Approaches of the Hazardous Waste Incineration Plant

In the previous chapter, the thermochemical-based plant model is described. In addition to the thermochemical-based model assumptions, the data sources and the related data processing have to be discussed. Several data bases need to provide appropriate data sets to enable a smooth operation of the plant model. Data inputs of online measured sensor values from the control system data base provide information about flow rates, temperature and pressure profiles, gas analytics, and much more. Offline measured laboratory analysis values from the laboratory data base provide information about fuel, ash, and slag compositions. Additionally, delivery data from the delivery data base provide information about the delivered waste stream, which consists of the supplier information, waste code, quantity, and storage location. *All mentioned data inputs must be preprocessed and further processed to convert them to appropriate data sets for the plant model.* Furthermore, a fuel classification model is introduced to connect waste codes according to [48] with a novel waste code classification.

All data processing steps are based on Python. The pandas [49] and NumPy [46] libraries are used for data preprocessing and processing all input values for the solver. The raw data sets are based mainly on sensor data, which detects only changes in sensor values. Therefore, the data sets must be preprocessed to deliver uniform periodic datasets. Due to the slow reaction behavior of the plant, minutely time steps are chosen. Data gaps are closed through a forward filling process. The preprocessed datasets are the basis for the following data processing steps:

1. selection of a time period,
2. generation of material inputs for all waste streams,
 - a. determination of a waste composition mixture for all solid fractions,
 - b. determination of a waste composition for each liquid and pasty fraction,
3. generation of material inputs for air streams,
4. generation of data for other individual sensors,
5. generation of JSON solver input files based on all generated data.

In Fig. 7, the waste stream input determination methodology is visualized. Therein, it can be seen that the delivered liquid and pasty waste streams are mainly mixed to reach homogenous fuel compositions. HEL and HS are only used within the burner and lances for heat-up and holding modes. The mass and volume flow of the liquid and pasty waste streams are determined via processed

sensor values from the control system data base. The waste compositions of the pasty and liquid waste streams are mostly set values. In Table 2, the assumed values for ultimate and proximate analyses are listed. The ultimate analysis values and the water content are based on laboratory values [27] and standard values [36]. Except for the water content, the proximate analysis values are based on own assumptions, which refer to approximate values from other liquid fuel compositions [50, 51]. The waste water fraction is approximated with pure water. The masterbatch waste composition is mainly based on daily laboratory analysis values. Not entirely analyzed ultimate analysis values from MB are based on a determination via the offline analyzed higher heating value (HHV) and the formula of Boie [36]. Finally, the liquid waste inputs via burner and lances and the pasty waste and waste water mix via the pasty lance are handed over to the rotary kiln solver. The waste water lance input in the PCC is also provided as a liquid fuel to the PCC solver.

The solid waste stream inputs are mostly not entirely analyzed. The developed virtual representation shall be able to close this gap. The applied methodology for handling solid waste inputs can be seen in Fig. 7. Therefore, the bunker waste deliveries are directly fed to the bunker after passing the truck scale and are assumed as a homogenous daily mix. The mass flow of the bunker waste is determined via the weight from the crane scale over a specific period. Direct barrels are converted via the barrel chute in the rotary kiln as a whole. The daily order of direct barrels is determined, which are fed via a conveyor belt. The mass flow for the direct barrel input is determined via barrel counter over period and barrel weight. The shredded waste is introduced over a separate input line in the rotary kiln. Harmless barrels are shredded and mixed with bunker waste and small amounts of liquid fuels. The liquid fuels are neglected because of the low quantities. The added bunker waste is mostly screenings. For this reason, the added bunker waste is assumed as screenings with a share of 12.5 m.%. The assumed ultimate and proximate analyses for the screenings are listed in Table 2. For determining the hospital waste input, the deliveries entry information and the pusher sensor data for counting the barrels are used. Finally, the solid fuel input in the rotary kiln solver is determined by mixing the four solid input lines. The compositions of the solid input lines bunker waste, direct barrels, shredded waste, and hospital waste are mostly non-analyzed. Therefore, a novel fuel classification model has been developed.

The *fuel classification model is based on a vast fuel data base*. More than 200 samples of proximate and ultimate analysis are listed for regularly used acids, caustics, oils, biogenic and fossil residues, chemicals, solvents, and plastics. The development of the fuel data base is based on the chemical compositions of two available fuel data bases

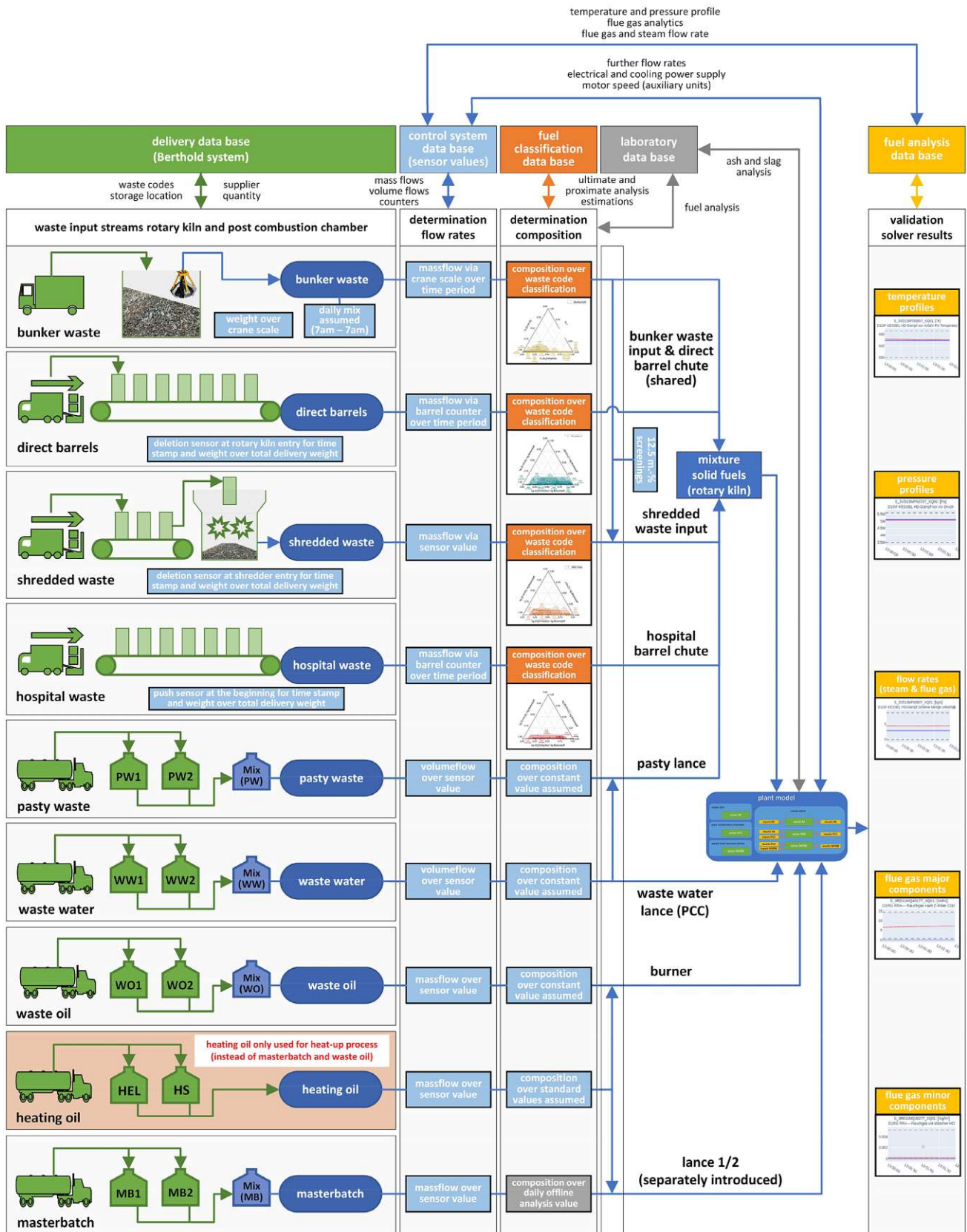


Fig. 7 Data processing steps within the hazardous waste incineration plant

Die approbierte gedruckte Originalversion dieser Dissertation ist an der TU Wien Bibliothek verfügbar. The approved original version of this doctoral thesis is available in print at TU Wien Bibliothek.

Table 2 Assumed ultimate and proximate analysis values for waste streams

Liquid and pasty waste streams	Ultimate analysis					Proximate analysis					Refs
	C [m.-% _{daf}]	H [m.-% _{daf}]	N [m.-% _{daf}]	S [m.-% _{daf}]	Cl [m.-% _{daf}]	O [m.-% _{daf}]	H ₂ O [m.-%]	Fixed C [m.-%]	Volatiles [m.-%]	Ash [m.-%]	
Waste oil (WO)	84.0	15.5	0.2	0.3	0	0	8.3	0.9	90.8	0	[27]
Extra light heating oil (HEL)	86.5	13.0	0.2	0.1	0	0.2	0	0.5	99.5	0	[36]
Heavy heating oil (HS)	84.5	11.5	0.5	2.5	0	1.0	0	0.5	99.5	0	[36]
Pasty waste (PW)	61.9	10.5	0	0	0	27.6	68.5	0.6	30.9	0	[27]
Waste water (WW)	0	0	0	0	0	0	100	0	0	0	–
Masterbatch (MB) ^a	40–85	4–14	5 (fixed)	Daily analyzed	Daily analyzed	0–14	Daily analyzed	1 (dry)	98 (dry)	1 (dry)	–
Screenings (bunker waste)	44.9	6.19	0.3	0.1	0.01	48.5	50.0	1.0	40.9	8.1	–

^aMB daily analyzed (HHV, S, Cl)—the other ultimate analysis values are calculated daily out of LHV by using the formula of Boie [36] and further constraints (value ranges assumed according to historical laboratory analysis values), LHV is calculated in relation to the daily analyzed HHV according to [36]

[50, 51], and internal laboratory data from Wien Energie. Subsequently, the sample data base *builds up proximate and ultimate analysis value ranges* based on 3–5 characteristic sample points. According to [48], the fuel classification model comprises the most frequently used waste codes within the input lines: bunker waste, direct barrels, shredded and hospital waste. The classification model consists of 29 bunker, 25 direct barrel, 14 shredded, and 6 hospital waste codes. The fuel classification is visualized in ternary plots (see Fig. 8), which represent a combination of ultimate and proximate analysis ranges for each waste code in each solid waste input line. The general methodology of the ternary plots highlights high calorific waste streams in the left and low calorific waste streams in the right bottom corner.

The fuel classification model data base builds the foundation for approximating compositions for the introduced solid waste streams. Within the data processing approach, ultimate and proximate analysis values for each solid waste stream are chosen, built up by a combination of the underlying subclasses for each waste code. The determined compositions for the solid waste input streams complete the required data inputs for the plant model.

To summarize, the plant model in Fig. 7 is fed with processed volume and mass flows from sensor values based on the control system data base. Furthermore, daily analyzed laboratory data for masterbatch and predefined compositions for the other liquid and pasty waste streams are introduced to the plant model. Moreover, the determined fuel compositions of the solid waste streams out of the fuel classification model, together with the waste code and supplier information out of the delivery data base enable the solid waste characterization for the following plant model. The plant model is fed with several liquid streams and the solid fuel mixture, determined through the individual waste streams. Additionally, ash and slag analysis from the laboratory data base and further sensor values from the control system data base complete the input values for the plant model. Finally, the plant model delivers minutely time-dependent results for temperature and pressure profiles, flow rates as well as major and minor flue gas components. The *periodic results are compared with sensor values* from the control system data base. For this reason, the *mean absolute percentage error (MAPE) as metrics* is calculated. If the metrics surpass a certain predefined tolerance, the fuel composition values of the solid waste streams based on the fuel classification model are modified and again fed to the plant model until the results of the plant model fit well with the sensor values.

Test Series of the Hazardous Waste Incineration Plant

The virtual representation has to be parametrized before it can be used to determine not entirely analyzed waste

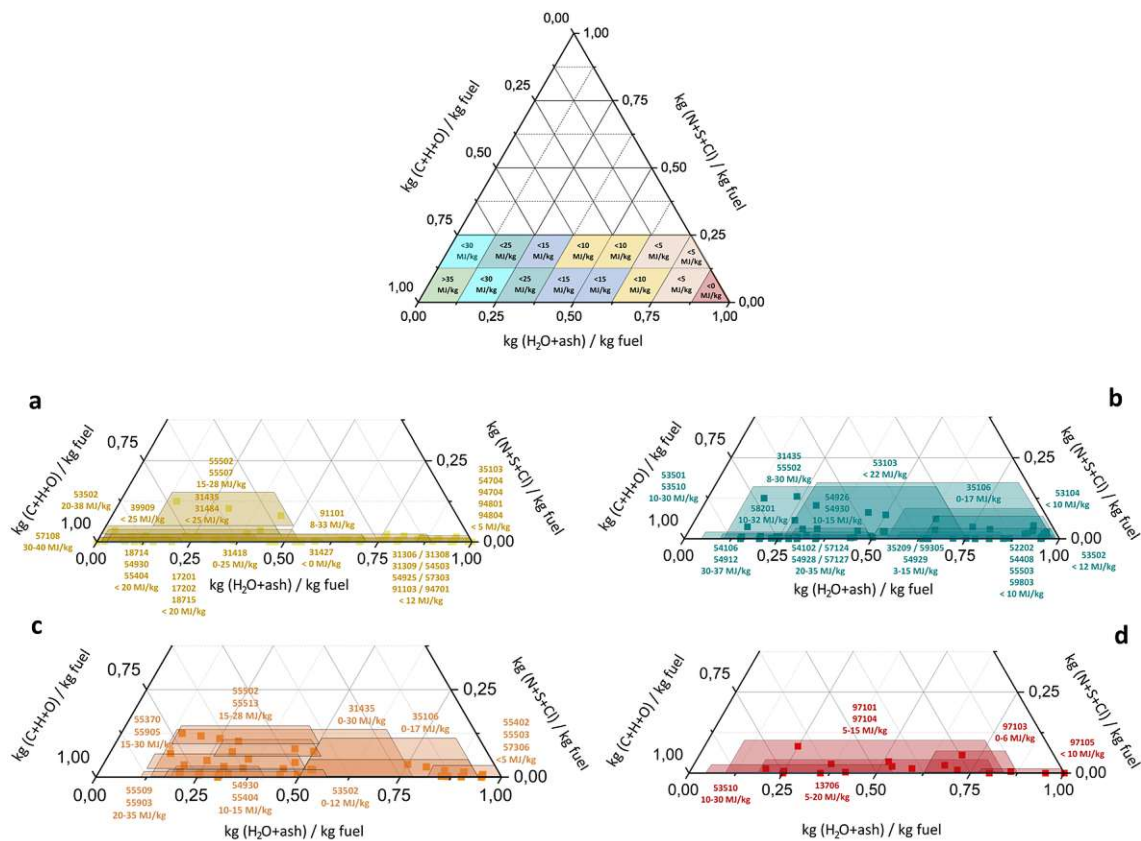


Fig. 8 Fuel classification visualization from the general methodology (top), bunker waste (a), direct barrels (b), shredded waste (c) and hospital waste (d)

fractions, as mentioned within the first implementation step. Therefore, a series of test runs were executed in April, October, and November 2021. The simulation order for parametrization of the plant model and the following determination of not entirely analyzed waste fractions is visualized in Table 3. Therein, it can be seen that the plant model is parametrized with data points where only one solid waste input stream was fed. Within the parametrization step, all the set values in the plant model are adjusted until the results are consistent with the sensor values from the control system data base. Afterwards, the virtual representation is used to determine not entirely analyzed solid waste fractions. First of all, test run periods with only bunker and hospital waste are introduced. Subsequently, data points with bunker waste and direct barrels and further data points with more and more waste input streams are considered. Liquid and pasty waste streams, except HEL for heat-up and holding mode operation, are not listed in Table 3 for simplification. The pasty input line is usually in operation as long as there is pasty waste in the storage. The waste water input line in the PCC is always in operation and helps with temperature regulation. Furthermore, the burner and one of both lances are

also always in operation. To summarize, the test series from 2021 is the basis for the parametrization described in the following chapter. Determining not entirely analyzed waste streams will be the next step after the parametrization and is not executed within this work.

Implementation of the Virtual Representation in the Hazardous Waste Incineration Plant

Finally, the implementation of the virtual representation is based on the described concepts and methods from the previous chapters. Therefore, the raised definition of virtual representations provides the requirements for the developed framework. Therein, the described thermochemical-based plant model and the data processing steps are the main building blocks within the overall virtual representation framework, which is subsequently presented. Afterwards, the simulation results for the parametrization test series are explained. The parametrized plant model enables the determination of not entirely analyzed waste streams to create a fuel analysis data base. In the end, possible future

Table 3 Simulation order regarding test series 2021 for parametrization of the plant model and determination of not entirely analyzed waste streams

Test series 2021 simulation order	Waste input streams (X = in operation / (X) partly in operation)				
	Bunker waste	Direct barrels	Shredded waste	Hospital waste	HEL (lances + burner)
Parametrization Plant model					
2nd Nov. 09:30–12:00					X
9th Nov. 13:00–15:00					X
23rd Nov. 12:50–15:00					X
Determination of not entirely analyzed waste input streams					
16th Nov. 14:30–17:00				X	
10th Nov. 17:50–22:20	X				
14th Nov. 09:30–13:20	X				
14th Nov. 14:30–19:15	X				
15th Nov. 09:05–19:25	X				
8th Nov. 10:00 – 9th Nov. 08:00	X			X	
19th Nov. 14:20–17:20	X			X	
10th Nov. 07:10–17:50	X			X	
25th Nov. 18:35–22:05	X			X	
27th Nov. 12:40–16:20	X			X	
24th Nov. 08:50 – 25th Nov. 05:00	X	X			
25th Nov. 23:50 – 26th Nov. 08:35	X	X			
26th Nov. 12:00 – 27th Nov. 02:40	X	X			
27th Nov. 03:35–12:15	X	X			
27th Nov. 16:40 – 28th Nov. 12:35	X	X			
17th Nov. 10:30 – 19th Nov. 14:20	X	X		X	
20th Nov. 09:10 – 23rd Nov. 12:10	X	X		X	
29th Oct. 14:30 – 31st Oct. 10:00	X	X	X	X	
17th April 10:00 – 19th April 04:00	X	X	X	X	
19th April 04:00 – 23rd April 16:00	X	X	X	X	
26th Oct. 00:00 – 29th Oct. 08:00	X	X	(X)	X	

applications of the virtual representation, which are based on the fuel analysis data base are discussed.

Overall Virtual Representation Framework for the digitization of the Hazardous Waste Incineration

The overall virtual representation framework is dependent on the foreseen application. Therefore, an implementation concept is introduced, which can be seen as a four-stage process according to the data integration level of Kritzinger et al. [32] and Aheleroff et al. [33]:

1. **Digital Model:** Determination of not entirely analyzed historically fed waste streams to create a fuel analysis data base

2. **Digital Shadow:** Implementation and use of fuel analysis data base for the optimization of the plant performance
3. **Digital Twin:** Automation or semi-automation of hazardous waste rotary kiln incineration plant operation
4. **Digital Predictive Twin:** Forward planning of hazardous waste rotary kiln incineration plant operation

To enable the determination of not entirely analyzed waste fractions, the parametrization of the plant model, which is explained in the following chapter needs to be fulfilled. Only the parametrization of the plant model, which is the basis for all the following implementation levels, is realized in this work. In the first implementation level (*digital model*), all the data communication is done manually to create a fuel analysis data base based on the results of the virtual representation simulation approach. Nevertheless, the following overall virtual representation framework includes

implementation steps two and three, which are the *digital shadow* and the *digital twin*. The digital shadow can use the knowledge about recurring fractions from the fuel analysis data base out of the first implementation step to improve the plant performance due to optimizing, for example the order of waste inputs or the air inlet. The digital twin is based on bi-directional data communication, enabling the automation or semi-automation of the plant operation or waste management. Finally, the *digital predictive twin* enables the forward planning of the plant operation or waste management.

An overall virtual representation framework has to be established to enable the application of the virtual representation within all the mentioned data integration levels from the implementation concept. Furthermore, the framework follows the methodology for developing virtual representations within the process development framework of energy plants, presented by Hammerschmid et al. [31]. *The overall methodology combines the aforementioned thermochemical-based plant model and data processing approaches to form a novel virtual representation framework for the digitization of the hazardous waste rotary kiln incineration*, shown in Fig. 9. Therein, the hazardous waste rotary kiln incinerator at the Wien Energie site in Vienna at Simmeringer Haide builds up the *physical component*. The control system data base represents the interface to the data management.

Therefore, all the online measured sensor values are handed over to the data management. The *data management*, which is the middleware, is located on a local edge device and based on Python’s Pandas library [49]. Within a two-step process, the sensor values and values from other data bases are processed to prepare appropriate datasets for the thermochemical-based plant model. The sensor values are always recorded if there is any change. Therefore, the sensor values must be filtered and forward filled in the data preprocessing step to create appropriate datasets for the raw data storage. The delivery data base, which includes the waste codes, suppliers, and the delivery quantity, introduces this information to the raw data storage via the fuel classification data base. All the waste code proximate and ultimate analysis sub classes are stored therein. Thus, the waste information from the delivery data base allows the selection of an appropriate ultimate and proximate analysis from the fuel classification data base, which is determined over a random combination of predefined subclasses within any waste code. The fuel analysis determination process can be supervised manually. Subsequently, the determined fuel compositions are introduced together with the offline analysis data from the masterbatch out of the laboratory data base to the raw storage data. Afterward, the collected data sets are further processed to mix fuels and create appropriate data inputs for the

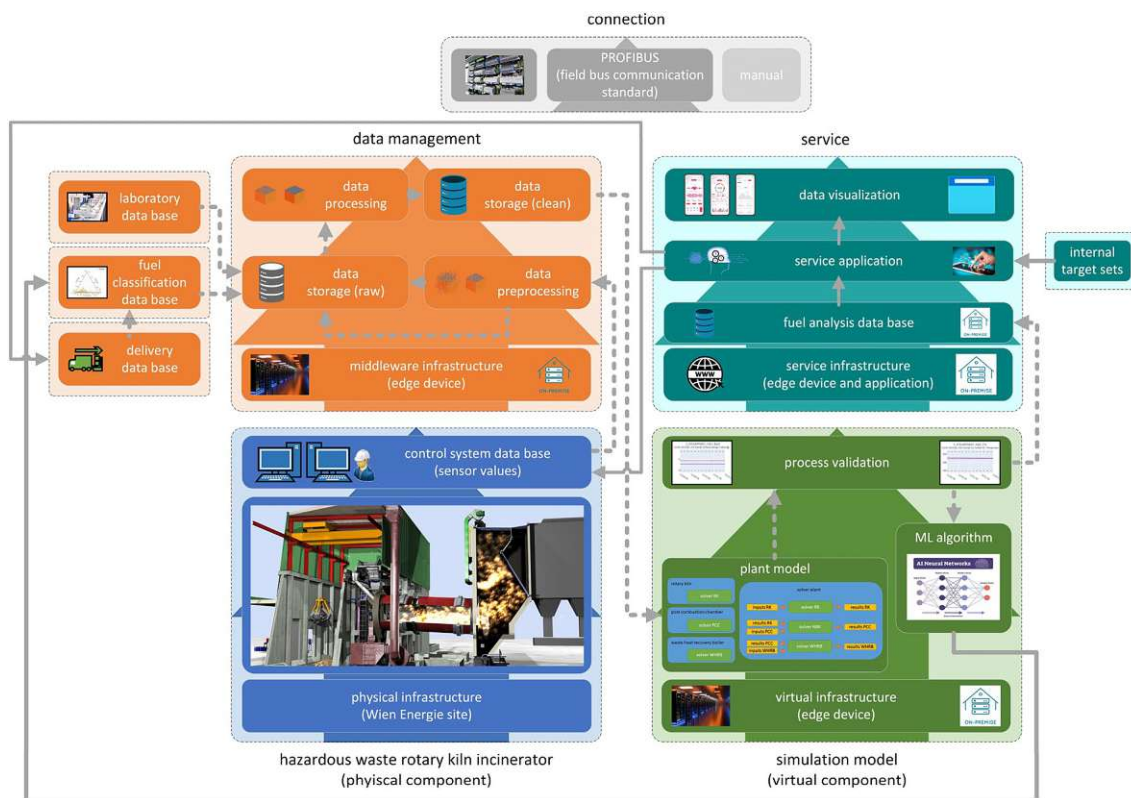


Fig. 9 Overall virtual representation framework for the digitization of the hazardous waste rotary kiln incinerator

Die approbierte gedruckte Originalversion dieser Dissertation ist an der TU Wien Bibliothek verfügbar. The approved original version of this doctoral thesis is available in print at TU Wien Bibliothek.

simulation model. The processed datasets are stored in a further data storage to enable a data buffer before introducing the data sets in the thermochemical-based plant simulation model. Furthermore, the aforementioned implementation stages have to be considered. The first implementation stage (digital model) is determining the ultimate and proximate analysis of historically fed waste streams. The following stages use this knowledge within a fuel analysis data base to enable further applications like the optimization of the plant performance. Within the digital model approach, the virtual component includes the thermochemical-based plant model and the process validation step. In the following implementation steps, the virtual component will be extended by a machine learning (ML) algorithm. These models are operated on the same local edge device as the data management approaches. The plant model is fed with the data sets from the data management, and the results are validated with several sensor values. If the comparison values are close enough to the results from the plant model, the validated data set is fed to the service dimension's fuel analysis data base. Suppose the comparison values do not pass the validation step, the fuel classification data base chooses another combination of subclasses for the fuel analysis, and the plant model is fed with new data sets. If enough waste streams are determined and stored in the fuel analysis data base, these data sets can be used to train the ML algorithm for advanced implementation stages. The trained ML algorithm can be used to replace the random selection of an ultimate and proximate analysis within the fuel classification data base to simplify the data management.

The *service dimension* also depends strongly on the foreseen implementation stage. The determination of not entirely analyzed waste inputs within the digital model stage is based on a local edge device with a fuel analysis data base, wherein the valid data sets are stored. Suppose the fuel analysis data base should be further used to optimize the process performance of the hazardous waste rotary kiln incineration plant, the service dimension has to be expanded by at least two further layers. Within the often used three-tier architecture [52], the data access layer, which is the fuel analysis data base is expanded by the service application, which represents the logic layer, and the data visualization, which can be seen as the presentation layer [52]. The service application can be local or web-based. To support the plant operation and waste management, web-based applications could be favorable to create a platform-independent solution. In the service application layer, the knowledge about recurring waste fractions from the fuel analysis data base can be used to optimize waste management or plant operating procedures. Therefore, exemplary knowledge about liquid waste fractions enables the determination of target values for the solid waste mix in terms of mass flow and fuel analysis, which are also fed to the service application layer. The data visualization

layer presents the proposed actions for optimizing the plant performance or the order of waste inputs within the waste management. The data visualization layer is the web-based frontend where the stakeholders can interact with the application. The *connection dimension* is responsible for data communication. Within the digital model implementation stage, only manual communication workflows are realized to determine the not entirely analyzed solid waste streams, which results in a fuel analysis data base. In Fig. 9, all the manual data communication from the physical component to the fuel analysis data base in the service dimension are illustrated by dashed lines. For further advanced applications in the digital shadow and digital twin implementation stage, the data communication will be realized with PROFIBUS, a field bus communication standard [53]. In the following digital shadow implementation stage, characterized by a unidirectional data communication, all the manual data flows are replaced by PROFIBUS. Furthermore, the data communication will be extended by a data transfer from the ML algorithm to the fuel classification data base and the data transfer within the service dimension from the fuel analysis data base to the data visualization. In the digital twin implementation stage, the results of the plant model are fed to the service dimension. In the service application layer, which represents the logic, control commands will be sent automatically to the control system data base to optimize the plant performance. Further control commands can be sent to the delivery data base to optimize waste management. Further information regarding data communication can be found in [54].

Based on this overall virtual representation framework, first test series were executed to parametrize and validate the plant model. Finally, future applications of the virtual representation framework are discussed.

Parametrization of Plant Model

Before the virtual representation can be used to determine not entirely analyzed waste streams, the plant model's parametrization must be executed. Based on the test series in Table 3, three datasets with HEL as fuel input were chosen to parametrize the plant model. Due to the well-known HEL input during heat-up and holding modes, these test runs are suitable for the parametrization process. The overall virtual representation framework from Fig. 9 was applied for the parametrization. Therefore, the sensor values from the control system data base within the test run periods from Table 3, together with the well-known HEL composition from the fuel classification data base are processed within the data management and further introduced to the plant model. The plant model results are checked within the process validation stage. If the sensor values from the flow

rates, pressure, and temperature profiles from the flue gas and overheated steam, as well as the flue gas major components, deviate too much from the plant model results, the set values within the plant model were adjusted. The following set values within the plant model were adjusted:

- fixed air inputs in the rotary kiln and the PCC, which were detected during a wrong air measurement campaign [38],
- fixed amount of water which will be evaporated in the wet deslagger,
- decrease of the heat transfer within the WHRB due to fouling,

- fixed amount of heat loss in the post combustion chamber.

The MAPE has been chosen as a metric to quantify the deviation between sensor values and plant model results. Furthermore, it has to be noted that the calculation of the overall MAPE is based on a weighting of the sensor values. For example, the major gas components are weighted with the highest and the flue gas temperatures within the WHRB with the lowest factor. The deviation between the minor gas component results with the sensor values are neglected within the parametrization step. The reason is the assumption of complete combustion in the plant model, which leads

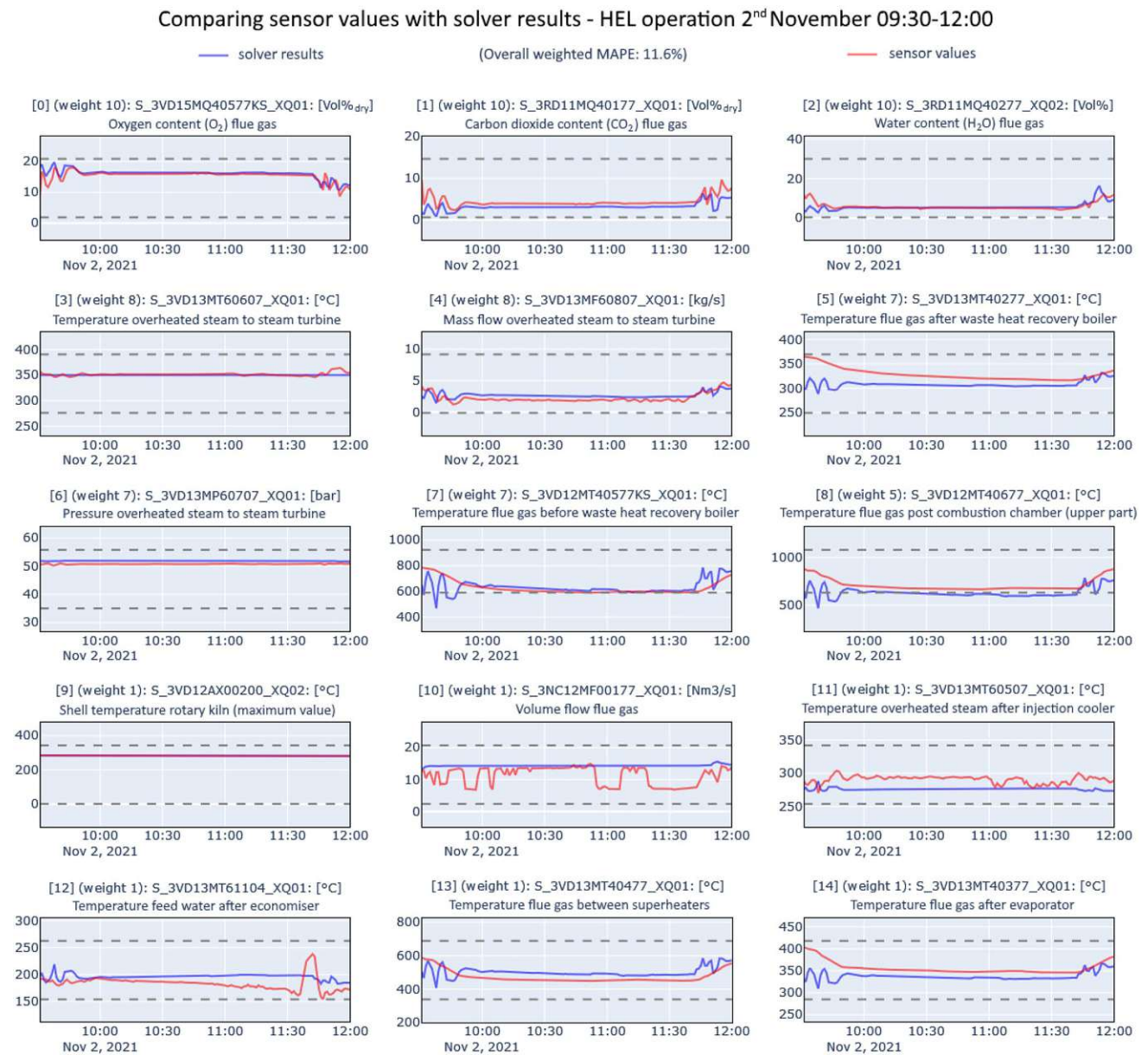


Fig. 10 Simulation and validation results from the test run of Nov. 2nd with HEL input

to zero CO emissions. The HCl content is neglected in the parametrization step due to the assumption of chlorine-free HEL, which also leads to zero HCl emissions. The parametrization of the plant model and the relating adjustments of the aforementioned set values were executed as long the MAPE was for all three chosen test runs (see Table 3) smaller than 12%. In Fig. 10, the simulation and validation results of the test run from Nov 2nd are exemplarily visualized to show the excellent correlation within the parametrization. The visualized test run period is based on a holding mode with HEL as fuel input. In the beginning of the chosen test run period, a deviation between sensor and solver results especially for the temperature values can be seen. The consistent decrease of the temperature sensor values in the beginning can be explained by a transient response from full-load operation to holding mode with HEL. The assumed ultimate and proximate analysis values for HEL can be found in Table 2. The fluctuations of the volume flow sensor value of the flue gas can be explained by disturbances of the measuring orifice.

Afterwards, the *plant model can be seen as parametrized and is ready to determine not entirely analyzed waste inputs*. Subsequently, the test series from Table 3 will be processed to investigate the first test runs with only one not entirely analyzed waste input stream. Then, the test runs with various not entirely analyzed waste inputs can be conducted. Finally, the future applications of the virtual representation are discussed, which are enabled due to the parametrization of the plant model.

Future Applications of the Virtual Representation

The parametrization of the plant model enables the broad use of the virtual representation to *optimize the waste management, operation, and maintenance* of the hazardous waste rotary kiln incineration plant. In Table 4, the possible *future service applications* of the virtual representation are listed. Therein, it can be seen that the possible service applications are ordered according to the data integration level. Suppose the virtual representation is used as a digital model, meaning only manual data communication between the virtual and physical dimensions takes place. In that case, the creation of the fuel analysis data base can be realized, which is the basis for all the following services. The digital shadow is characterized as one-directional data communication and can be used to optimize the waste input order and plan the waste delivery. Furthermore, the kiln operation can be monitored and optimized regarding stable operation conditions. In terms of maintenance, the digital shadow can monitor the plant components and plan downtimes. The digital twin enables bi-directional data communication. Therefore, the automated optimization of the waste management or plant operation is possible due to automated feedback from the

virtual to the physical plant. The final data integration level of the digital predictive twin helps to provide a support tool for the waste management, plant operator, or maintenance staff to predict future stocks, operation conditions, or downtimes. Finally, the digital predictive twin can be used to train plant operators. However, the list of service applications is not exhaustive, and other service applications can also be investigated.

Conclusion and Outlook

The scope of this publication was the investigation of a framework to realize a virtual representation for the digitization of a hazardous waste incineration plant. Based on the state-of-the-art 5D model and data integration level, a novel virtual representation framework for the use within a standalone hazardous waste rotary kiln incineration plant was investigated. The virtual representation framework consists of the physical plant, which communicates with the data management via the control system data base. The sensor values out of the control system data base together with further values from other data bases will be processed to create appropriate datasets for the following plant model. The determination of the waste composition of the solid waste streams is supported by the novel fuel classification data base, which returns proximate and ultimate analysis value ranges based on the delivered waste code. The data inputs are fed with minutely-based datasets to the thermochemical-based plant model to calculate the flow rates, temperature, and pressure profiles of the flue gas and overheated steam. Furthermore, the major and minor flue gas components can be determined. The plant model results are compared with the accompanying sensor values within a validation step. This virtual representation framework enables the determination of not entirely analyzed waste input streams to monitor waste deliveries. Furthermore, this information can be used in terms of recurring fractions to optimize waste management and plant operation due to the better knowledge of waste inputs.

The thermochemical-based plant model was validated with test runs based on well-known waste inputs. Therefore, three test runs from November 2021 within the hazardous waste rotary kiln incineration plant at Simmeringer Haide in Vienna with HEL input were used to parametrize and validate the plant model. Within these test runs, the waste input is well-defined, and thus the set parameters within the plant model could be adjusted to reach a good approximation to the sensor values. The parametrization of the plant model and the relating adjustments of the aforementioned set values were executed as long the MAPE was for all three chosen test runs smaller than 12%. The parametrized plant model enables the application of the

Table 4 Future service applications of the virtual representation

Data integration level	Possible future service applications of virtual representation	
	Waste management	Maintenance
Digital model	Creation of fuel analysis data base → basis for all other service applications (Monitoring of waste composition of delivered waste streams)	Monitoring of brickwork damage → Correlation between brickwork and shell temperature of rotary kiln due to the heat transfer enables predictive maintenance → Precise planning of downtimes and maintenance activities possible
Digital shadow	Optimization of barrel sequence regarding homogeneous waste input (shredded, hospital, and direct barrels) → Local or web-based application for waste management to guide the forklift drivers → Decrease of temperature and emission peaks within the rotary kiln operation Optimization of waste delivery order to enable balanced waste inputs → Local or web-based application for waste management to coordinate the suppliers	Monitoring of fouling within waste heat recovery boiler → Observation of heat transfer within WHRB → Precise planning of downtimes and maintenance activities possible Fault diagnosis and anomaly detection of defective plant components
Digital twin	Automated optimization of barrel sequence regarding homogeneous waste input (shredded, hospital, and direct barrels) Automated optimization of waste delivery order to enable balanced waste inputs Support tool to simulate predictive stocks to enable a balanced waste delivery plan	Automated restriction of plant operation to delay the downtime due to fouling or brickwork damage Automated planning of maintenance work with external partners
Digital predictive twin	Support tool to simulate predictive operation conditions dependent on planned waste input and plant settings → Local or web-based application for the plant operator to collaborate with waste management or plant supervisors and external experts → It can be used for operational planning or within operational problems Simulation tool to train plant operators for the prediction of possible operation conditions dependent on planned waste input and plant settings	Planning of downtimes with regard to the availability of other plants from the energy provider → Economic and ecologic dispatching

virtual representation for the determination of not entirely analyzed solid waste streams. Thereby, the solid waste compositions are adjusted according to the ultimate and proximate analysis value ranges out of the fuel classification data base as long as the plant model results are near to the sensor values. Various determined solid waste streams are building up the fuel analysis data base, which is the basis for further virtual representation applications. If the determined solid waste streams recur, the knowledge can be used to optimize the waste management, operation, and maintenance of the hazardous waste rotary kiln incineration plant. The possible applications range from digital model services with offline data communication to digital predictive twin services with automatic data communication coupled with predictive simulation models. First of all, the creation of a fuel analysis data base by the determination of not entirely analyzed waste streams is crucial to enable further advanced applications. To obtain trustworthy results, a long-term test run is important to validate the determined waste stream compositions with offline laboratory analysis. In this way, the assumptions regarding bunker, shredder and barrel storage can be approved. The storage management together with set values regarding the wrong air amounts, fouling and heat losses are the key influencing factors in the virtual representation. For achieving digital control, it is essential to ensure reliable measurements. For this reason, periodic control measurement campaigns with accompanying calibration are very important.

Summing up, the presented parametrized virtual representation framework is the basis for the determination of not entirely analyzed solid waste streams and further applications to optimize the performance of the waste management, operation, and maintenance within a fully digitized hazardous waste rotary kiln incineration plant. To validate the whole virtual representation framework, the determination of not entirely analyzed waste input streams should be accompanied by a comprehensive fuel analysis test series to enable a proof of concept. The thermochemical-based plant model can be enlarged by more detailed reaction mechanisms or fluid dynamic modeling approaches. Further improvements to the plant model can be realized by implementing a mechanism to integrate the aging of brickworks within the rotary kiln. The comprehensive implementation of heat losses to the environment within all the sub-units can also be marked as a possible optimization step. Implementing the flue gas cleaning units and combining the thermochemical-based plant model with 3D models could enable further service applications, especially in the maintenance sector. However, the presented virtual representation framework for a fully digitized hazardous waste incineration plant could

help contribute to a high-efficiency thermal conversion of hazardous waste. First investigations showed that through the implementation of the novel framework within the hazardous waste incineration plant in Vienna at Simmeringer Haide, an *overall efficiency increase of more than 5% can be reached*. After a long-term test run of the virtual representation in the foreseen hazardous waste incineration plant, the tool can be transferred to other identical hazardous waste rotary kiln incinerators. Furthermore, the virtual representation can be parametrized to other rotary kiln incineration plants for example within the cement and paper industry. Through the modular structure of the virtual representation, the tool can be also used for other types of incinerators after adapting the simulation and data acquisition models.

Acknowledgements The present work contains results of the project Thermal Twin 4.0, which is being conducted within the “Produktion in der Stadt 2019” research program funded by the Vienna Business Agency. The authors acknowledge TU Wien Bibliothek for financial support through its Open Access Funding Programme.

Author Contributions All authors contributed to the study conception and design. The fuel classification model was provided by MH, SM and HH (TU Wien). The thermochemical-based simulation model was developed by DB, JN and RE (Enrag GmbH). The data processing was developed by AG, RB, KK, RK and GO (Cloudflight Austria GmbH). Material preparation and data collection of test series as well as preparation of design data for the hazardous waste incineration plant were performed by CA, FK, EZ and MB (Wien Energie GmbH). The first draft of the manuscript was written by MH (TU Wien) and all authors commented on previous versions of the manuscript. All authors read and approved the final manuscript.

Funding Open access funding provided by TU Wien (TUW). The present work contains results of the project Thermal Twin 4.0 which is being conducted within the “Produktion in der Stadt 2019” research program funded by the Vienna Business Agency.

Data Availability The data that support the findings of this study are available from the corresponding author, M. Hammerschmid, upon reasonable request.

Declarations

Competing interests The authors have no relevant financial or non-financial interests to disclose.

Open Access This article is licensed under a Creative Commons Attribution 4.0 International License, which permits use, sharing, adaptation, distribution and reproduction in any medium or format, as long as you give appropriate credit to the original author(s) and the source, provide a link to the Creative Commons licence, and indicate if changes were made. The images or other third party material in this article are included in the article's Creative Commons licence, unless indicated otherwise in a credit line to the material. If material is not included in the article's Creative Commons licence and your intended use is not permitted by statutory regulation or exceeds the permitted use, you will need to obtain permission directly from the copyright holder. To view a copy of this licence, visit <http://creativecommons.org/licenses/by/4.0/>.

References

- United Nations: Paris agreement 2015. <https://unfccc.int/process-and-meetings/the-paris-agreement/the-paris-agreement>. Accessed 12 Apr 2022
- Österreichischer Wasser- und Abfallwirtschaftsverband (ÖWAV): ÖWAV-ExpertInnenpapier - Der Stellenwert der thermischen Abfallverwertung in der Kreislaufwirtschaft am Beispiel Österreich. ÖWAV-Arbeitsausschuss, Thermische Behandlung“ Wien (2020)
- Zechmeister, A., Anderl, M., Bartel, A., Geiger, K., Gugele, B., Gössl, M., Haider, S., Heinfellner, H., Heller, C., Köther, T., Krutzler, T., Kuschel, V., Lampert, C., Neier, H., Pazdernik, K., Perl, D., Poupá, S., Prutsch, A., Purzner, M., Rigler, E., Schieder, W., Schmid, C., Schmidt, G., Schodl, B., Storch, A., Stranner, G., Schwarzl, B., Schwaiger, E., Vogel, J., Weiss, P., Wiesenberger, H., Wieser, M.: Klimaschutzbericht 2021. Umweltbundesamt Österreich, Wien (2021)
- European Union: Renewable Energy Directive (RED II) - Directive (EU) 2018/2001 of the European Parliament and of the Council. Official Journal of the European Union of 11 December 2018 on the promotion of the use of energy from renewable sources. https://eur-lex.europa.eu/legal-content/EN/TXT/?uri=uriserv:OJ.L_.2018.328.01.0082.01.ENG&toc=OJ:L:2018:328:TOC. Accessed 22 June 2022
- Borowski, P.F.: Digitization, digital twins, blockchain, and industry 4.0 as elements of management process in enterprises in the energy sector. *Energies* **14**, 1885 (2021). <https://doi.org/10.3390/en14071885>
- Nolte, M.: Betriebs- und modelltechnische Untersuchungen zur Verbesserung des Gasphasenausbrandes bei der instationären Gebindeverbrennung in einer Rückstandsverbrennungsanlage. Dissertation. Institut für Technische Chemie (ITC), Karlsruher Institut für Technologie (KIT), Karlsruhe (2015)
- Lei, Z., Zhou, H., Hu, W., Liu, G.-P., Guan, S., Feng, X.: Toward a web-based digital twin thermal power plant. *IEEE Trans. Ind. Inf.* **18**, 1716–1725 (2022). <https://doi.org/10.1109/TII.2021.3086149>
- Kabugo, J.C., Jämsä-Jounela, S.-L., Schiemann, R., Binder, C.: Industry 4.0 based process data analytics platform: a waste-to-energy plant case study. *Int. J. Electr. PowerEnergy Syst.* **115**, 105508 (2020). <https://doi.org/10.1016/j.ijepes.2019.105508>
- Richers, U.: Beitrag der Abfallverbrennung zur Energieversorgung in Deutschland. KIT Scientific reports 7746. Institut für Technologiefolgenabschätzung und Systemanalyse (ITAS), Karlsruher Institut für Technologie (KIT), Karlsruhe (2018)
- Albert, F.W.: Fuzzy logic and its application in waste-to-energy-plants - Success with a control system based on "fuzzy control". VGB Kraftwerkstechnik (1998)
- Richers, U.: Thermische Behandlung von Abfällen in Drehrohröfen - Eine Darstellung anhand der Literatur. KIT Scientific reports 5548. Institut für Technische Chemie (ITC), Karlsruher Institut für Technologie (KIT), Karlsruhe (1995)
- Zhuang, J., Tang, J., Aljerf, L.: Comprehensive review on mechanism analysis and numerical simulation of municipal solid waste incineration process based on mechanical grate. *Fuel* **320**, 123826 (2022). <https://doi.org/10.1016/j.fuel.2022.123826>
- Liu, X.Y., Specht, E.: Mean residence time and hold-up of solids in rotary kilns. *Chem. Eng. Sci.* **61**, 5176–5181 (2006). <https://doi.org/10.1016/j.ces.2006.03.054>
- Chen, K.S., Tu, J.T., Chang, Y.R.: Simulation of steady-state heat and mass transfer in a rotary kiln incinerator. *Hazard. Waste Hazard. Mater.* **10**, 397–411 (1993). <https://doi.org/10.1089/hwm.1993.10.397>
- Silcox, G.D., Perching, D.W.: The effects of rotary kiln operating conditions and design on burden heating rates as determined by a mathematical model of rotary kiln heat transfer. *J. Air Waste Manag. Assoc.* **40**, 337–344 (1990). <https://doi.org/10.1080/10473289.1990.10466691>
- Bürkle, S.: Reaktionskinetische Charakterisierung abfalltypischer Stoffe und deren Verbrennung in einem Drehrohröfen unter Sauerstoffanreicherung. Dissertation. Institut für Katalyseforschung und -technik (IKFT). Karlsruher Institut für Technologie (KIT), Karlsruhe (1998)
- Müller-Roosen, M.: Untersuchungen zur Hochtemperaturabfallverbrennung mit Sauerstoffanreicherung. Dissertation. RWTH Aachen University, Aachen (1997)
- Gehrman, H.-J.: Mathematische Modellierung und experimentelle Untersuchungen zur Pyrolyse von Abfällen in Drehrohrsystemen. Dissertation. Bauhaus-Universität Weimar, Weimar (2006)
- Wendt, J.O.L., Linak, W.P., Lemieux, P.M.: Prediction of transient behavior during batch incineration of liquid wastes in rotary kilns. *Hazard. Waste Hazard. Mater.* **7**, 41–54 (1990). <https://doi.org/10.1089/hwm.1990.7.41>
- Wajda, A., Brociek, R., Pleszczyński, M.: Optimization of energy recovery from hazardous waste in a waste incineration plant with the use of an application. *Processes* **10**, 462 (2022). <https://doi.org/10.3390/pr10030462>
- Yao, Y., Ding, S., Chen, Y.: Modeling of the thermal efficiency of a whole cement clinker calcination system and its application on a 5000 MT/D production line. *Energies* **13**, 5257 (2020). <https://doi.org/10.3390/en13205257>
- Zhang, B., He, J., Hu, C., Chen, W.: Experimental and numerical simulation study on co-incineration of solid and liquid wastes for green production of pesticides. *Processes* **7**, 649 (2019). <https://doi.org/10.3390/pr7100649>
- Zhang, S., Wang, F.: Effect of interactions during co-combustion of organic hazardous wastes on thermal characteristics, kinetics, and pollutant emissions. *J. Hazard. Mater.* **423**, 127209 (2022). <https://doi.org/10.1016/j.jhazmat.2021.127209>
- Xu, J., Fu, D., Shao, L., Zhang, X., Liu, G.: A soft sensor modeling of cement rotary kiln temperature field based on model-driven and data-driven methods. *IEEE Sens. J.* **21**, 27632–27639 (2021). <https://doi.org/10.1109/JSEN.2021.3116937>
- Guillin-Estrada, W.D., Albuja, R., Davila, I.B., Rueda, B.S., Corredor, L., Gonzalez-Quiroga, A., Maury, H.: Transient operation effects on the thermal and mechanical response of a large-scale rotary kiln. *Results Eng.* **14**, 100396 (2022). <https://doi.org/10.1016/j.rineng.2022.100396>
- Pirttiniemi, J.: Development of design process of rotary kiln. Diploma thesis. LUT University, Lappeenranta (2021)
- Jagersberger, L.: Analyse und Modellierung eines Drehrohröfen-Prozesses zur Verbrennung von Sonderabfällen. Master thesis. Montanuniversität Leoben, Leoben (2019)
- Bujak, J.: Determination of the optimal area of waste incineration in a rotary kiln using a simulation model. *Waste Manag.* **42**, 148–158 (2015). <https://doi.org/10.1016/j.wasman.2015.04.034>
- Behmanesh, N., Manousiouthakis, V.I., Allen, D.T.: Optimizing the throughput of hazardous waste incinerators. *AIChE J.* **36**, 1707–1714 (1990). <https://doi.org/10.1002/aic.690361111>
- TU Wien: Thermal Twin 4.0. https://www.vt.tuwien.ac.at/brennstoff_und_energiesystemtechnik/industrieanlagendesign_und_anwendung_digitaler_methoden/projekte/thermal_twin_40/?L=504. Accessed 16 Apr 2022
- Hammerschmid, M., Rosenfeld, D.C., Bartik, A., Benedikt, F., Müller, S.: From digital model to digital predictive twin - methodology for the development of virtual representations within the process development framework of energy plants. TU Wien, Vienna (2022)

32. Kritzinger, W., Karner, M., Traar, G., Henjes, J., Sihn, W.: Digital Twin in manufacturing: a categorical literature review and classification. *IFAC-PapersOnLine* **51**, 1016–1022 (2018). <https://doi.org/10.1016/j.ifacol.2018.08.474>
33. Ahleroff, S., Xu, X., Zhong, R.Y., Lu, Y.: Digital twin as a service (DTaaS) in industry 4.0: an architecture reference model. *Adv. Eng. Inform.* **47**, 101225 (2021). <https://doi.org/10.1016/j.aei.2020.101225>
34. Tao, F., Zhang, H., Liu, A., Nee, A.Y.C.: Digital twin in industry: state-of-the-art. *IEEE Trans. Ind. Inf.* **15**, 2405–2415 (2019). <https://doi.org/10.1109/TII.2018.2873186>
35. Schwarzböck, T., Rechberger, H., Cencic, O., Fellner, J.: Anteil erneuerbarer Energien und klimarelevante CO₂-Emissionen aus der thermischen Verwertung von Abfällen in Österreich. *Österr Wasser- und Abfallw* **68**, 415–427 (2016). <https://doi.org/10.1007/s00506-016-0332-5>
36. Hofbauer, H.: Auslegung von Verbrennungsanlagen: Teil B - Verbrennungsrechnung und Auslegung von Brennräumen. Lecture notes, Vienna (2020)
37. Netz, H.: Handbuch Wärme: Erläuterungen, Beschreibungen, Definitionen, Richtlinien, Formeln, Tabellen, Diagramme und Abbildungen für alle Bereiche der Wärmetechnik, 3rd edn. Resch Verlag, Gräfelfing/München (1991)
38. Aguiari, C.J.: "Bericht Lufteintrag DRO: Sondermüllverbrennungsanlage - Simmeringer Haide. internal report. Wien Energie, Vienna (2022)
39. Ginsberg, T.: Dynamische Modellierung von Drehrohröfen. Dissertation. RWTH Aachen University, Aachen (2011)
40. Grote, K.-H., Feldhusen, G.: *Dubbel: Taschenbuch für den Maschinenbau*, 24th edn. Springer Vieweg, Berlin-Heidelberg (2014)
41. Liu, X.Y., Zhang, J., Specht, E., Shi, Y.C., Herz, F.: Analytical solution for the axial solid transport in rotary kilns. *Chem. Eng. Sci.* **64**, 428–431 (2009). <https://doi.org/10.1016/j.ces.2008.10.024>
42. Stephan, P., Kabelac, S., Kind, M., Mewes, D., Schaber, K., Wetzel, T.: *VDI-Wärmeatlas: Fachlicher Träger VDI-Gesellschaft Verfahrenstechnik und Chemieingenieurwesen*, 12th edn. Springer Vieweg, Berlin (2019)
43. Kaltschmitt, M., Hartmann, H., Hofbauer, H.: *Energie aus Biomasse: Grundlagen, Techniken und Verfahren*, 3rd edn. Springer Vieweg, Berlin-Heidelberg (2016)
44. Hammerschmid, M., Müller, S., Fuchs, J., Hofbauer, H.: Evaluation of biomass-based production of below zero emission reducing gas for the iron and steel industry. *Biomass Convers. Bioref.* **11**, 169–187 (2021). <https://doi.org/10.1007/s13399-020-00939-z>
45. NumPy Developers: *Linear algebra (numpy.linalg) - NumPy v1.22 Manual*. <https://numpy.org/doc/stable/reference/routines.linalg.html#module-numpy.linalg>. Accessed 3 May 2022
46. Oliphant, T.E.: *Guide to NumPy*. <https://ecs.wgtn.ac.nz/foswiki/pub/Support/ManualPagesAndDocumentation/numpybook.pdf>. Accessed 23 June 2022
47. Strang, G.: *Linear Algebra and Its Applications*, 2nd edn. Academic Press, Orlando (1980)
48. Bundesministerium für Klimaschutz, Umwelt, Energie, Mobilität, Innovation und Technologie: *Abfallverzeichnisverordnung 2020*. <https://www.ris.bka.gv.at/GeltendeFassung.wxe?Abfrage=Bundesnormen&Gesetzesnummer=20011285&FassungVom=2022-05-05>. Accessed 23 June 2022
49. Betancourt, R., Chen, S.: *Python for SAS Users: A SAS-Oriented Introduction to Python*. Apress, New York (2019)
50. Grzymek, A.: *Research information system for a smart lab use case scaling up of bio-fuel plant models: fuel analysis database - test laboratory for combustion systems TU Wien*. Master thesis, Institute for Chemical, Environmental and Bioscience Engineering, TU Wien, Vienna (2022)
51. TNO Biobased and Circular Technologies: *Phyllis 2 - Database for (treated) biomass, algae, feedstocks for biogas production and biochar*. <https://phyllis.nl/>. Accessed 23 June 2022
52. Helal, S., Hammer, J., Zhang, J., Khushraj, A.: *A three-tier architecture for ubiquitous data access*. In: *Proceedings ACS/IEEE International Conference on Computer Systems and Applications*, pp. 177–180. Beirut (2001)
53. CENELEC: *Industrielle Kommunikationsnetze - Feldbusse: Teil 1: Überblick und Leitfaden zu den Normen der Reihen IEC 61158 und IEC 61784, IEC 61158-1:2019*. DKE, VDE Verlag, Web <https://www.dke.de/de/normen-standards/dokument?id=7138085&type=dke%7Cdokument>. Accessed 23 June 2022
54. Joshi, R., Didier, P., Jimenez, J., Carey, T.: *The Industrial Internet of Things Volume G5: Connectivity Framework*. Boston (2017)

Publisher's Note Springer Nature remains neutral with regard to jurisdictional claims in published maps and institutional affiliations.

Authors and Affiliations

M. Hammerschmid¹ · C. Aguiari² · F. Kirnbauer² · E. Zerobin² · M. Brenner² · R. Eisl³ · J. Nemeth³ · D. Buchberger³ · G. Ogris⁴ · R. Kolroser⁴ · A. Goia⁴ · R. Beyweiss⁴ · K. Kalch⁴ · S. Müller¹ · H. Hofbauer¹

¹ Institute of Chemical, Environmental and Bioscience Engineering, TU WIEN, Getreidemarkt 9/166, 1060 Vienna, Austria

² Wien Energie GmbH, 11. Haidequerstraße 7, 1110 Vienna, Austria

³ Enrag GmbH, Industriestraße 18, 4800 Attnang-Puchheim, Austria

⁴ Cloudflight Austria GmbH, Huemerstraße 23, 4020 Linz, Austria

Paper V

Economic and ecological impacts on the integration of biomass-based SNG and FT diesel in the Austrian energy system

Hammerschmid, M., Bartik, A., Benedikt, F., Veress, M., Pratschner, S.,
Müller, S., Hofbauer, H.

Energies, 2023, 16(16), 6097

<https://doi.org/10.3390/en16166097>

Article

Economic and Ecological Impacts on the Integration of Biomass-Based SNG and FT Diesel in the Austrian Energy System

Martin Hammerschmid ^{*}, Alexander Bartik , Florian Benedikt, Marton Veress, Simon Pratschner , Stefan Müller  and Hermann Hofbauer 

Institute of Chemical, Environmental and Bioscience Engineering, TU Wien, Getreidemarkt 9/166, 1060 Vienna, Austria

* Correspondence: martin.hammerschmid@tuwien.ac.at

Abstract: The production of sustainable, biomass-based synthetic natural gas (SNG) and Fischer-Tropsch (FT) diesel can contribute significantly to climate neutrality. This work aims to determine the commercial-scale production costs and CO₂ footprint of biomass-based SNG and FT diesel to find suitable integration scenarios for both products in the Austrian energy system. Based on the simulation results, either 65 MW SNG and 14.2 MW district heat, or 36.6 MW FT diesel, 17.6 MW FT naphtha, and 22.8 MW district heat can be produced from 100 MW biomass. The production costs with taxes for wood-based SNG are 70–91 EUR /MWh and for FT diesel they are 1.31–1.89 EUR /L, depending on whether pre-crisis or crisis times are considered, which are in the range of fossil market prices. The CO₂ footprint of both products is 90% lower than that of their fossil counterparts. Finally, suitable integration scenarios for SNG and FT diesel in the Austrian energy system were determined. For SNG, use within the energy sector for covering electricity peak loads or use in the industry sector for providing high-temperature heat were identified as the most promising scenarios. In the case of FT diesel, its use in the heavy-duty traffic sector seems most suitable.

Keywords: gasification; methanation; Fischer-Tropsch; simulation; techno-economic assessment; CO₂ footprint



Citation: Hammerschmid, M.; Bartik, A.; Benedikt, F.; Veress, M.; Pratschner, S.; Müller, S.; Hofbauer, H. Economic and Ecological Impacts on the Integration of Biomass-Based SNG and FT Diesel in the Austrian Energy System. *Energies* **2023**, *16*, 6097. <https://doi.org/10.3390/en16166097>

Academic Editors: Elem Patricia Alves Rocha, Clara Mendoza Martinez and Esa Kari Vakkilainen

Received: 4 July 2023

Revised: 7 August 2023

Accepted: 14 August 2023

Published: 21 August 2023



Copyright: © 2023 by the authors. Licensee MDPI, Basel, Switzerland. This article is an open access article distributed under the terms and conditions of the Creative Commons Attribution (CC BY) license (<https://creativecommons.org/licenses/by/4.0/>).

1. Introduction

The increasingly visible climate change around the world requires sustainable solutions. The European Green Deal [1] aims to set the path to Europe's climate neutrality by 2050. Currently, only approximately 20% of Europe's gross final energy consumption is covered by renewable energy sources (RES). In Austria, even more ambitious targets are being set for climate neutrality by 2040. Considering the RES share of 36.5% based on Austria's gross final energy consumption, sustainable solutions in the whole energy system must be found quickly. The most considerable proportion of greenhouse gas emissions are caused by generating electricity, heat, cold, and fuels using fossil feedstocks like natural gas, coal, and mineral oil [2].

In addition to already proven renewable technologies, such as solar PV, wind power, hydropower, and heat pumps using environmental heat, bioenergy can contribute significantly to achieving climate neutrality. The most significant advantage of bioenergy is that there is great potential, especially in Austria, to produce the required energy sources, such as electricity, heat, and fuels, with domestic raw materials. The use of lignocellulosic biomass in the heat and power sector has already been proven for decades. Furthermore, oil crops have been used to produce biodiesel for many years. Sugar and starch crops are used within fermentation plants to produce bioethanol. Additionally, sugar and starch crops can be fed together with biodegradable municipal solid waste to anaerobic digestion plants to generate heat, power, and biomethane. Gasification technologies play a crucial role in

expanding the range of bioenergy products [3]. At TU Wien, dual fluidized bed (DFB) gasification technology has been investigated for decades. It has been proven that this technology is suitable for use with a wide range of raw materials. Almost all lignocellulosic biomass and significant parts of biogenic residues can be converted to high-quality product gas, mainly consisting of hydrogen, carbon monoxide, carbon dioxide, and methane. After purification of the produced gas, it can be converted into high-value products such as hydrogen, synthetic fuels, synthetic natural gas, or platform chemicals in addition to electricity and heat production in a gas engine or gas turbine [4].

In 2002, the first demo plant based on DFB gasification technology for the production of heat and power based on woody biomass went into operation in Güssing (AT), with a thermal fuel power of 8 MW_{th}. In the following 15 years, more than 100,000 h of operation were achieved. This successful demonstration resulted in the construction of further commercial plants on a scale of 3.8 to 15.5 MW_{th} in Oberwart (AT), Villach (AT), Senden (DE), Nongbua (TH), and Wajima (JP) in the last two decades. Many plants have been forced to shut down recently due to high production costs for heat and electricity using high-quality wood chips. As a result, research work in recent years has been focusing on using lower-grade feedstocks [5] and producing higher-grade synthesis products such as synthetic natural gas (SNG) [6] or Fischer–Tropsch (FT) diesel. In 2009, the world's first fluidized bed methanation pilot plant, with a SNG power of 1 MW_{SNG}, was integrated into the existing DFB plant in Güssing. The largest DFB plant to date, with a scale of 33 MW_{th}, was commissioned in Gothenburg (SE) in the frame of the GoBiGas project in 2013 [7]. In the GoBiGas project, the product gas was used to produce 20 MW SNG in a fixed-bed methanation synthesis process. In 2022, a DFB plant using lower-grade feedstocks with a scale of 1 MW_{th} was commissioned in Vienna (AT) at a waste processing location. Additionally, the product gas in Vienna can be converted in a FT slurry reactor to FT products [8–10]. Due to the large number of DFB facilities, nearly 200,000 industrial operating hours could be collected, demonstrating the DFB gasification process. Therefore, the DFB gasification process itself has already reached the commercial scale. The DFB demo plant in Vienna helps to test and investigate the use of lower-grade feedstocks in an industrial operational environment, thereby increasing the technological readiness level. From a scientific and technical point of view, fixed-bed methanation has been successfully demonstrated in Gothenburg. However, the Gothenburg plant was forced to shut down for economic reasons. Alternatively, fluidized bed methanation can be used for SNG production with the advantage that, instead of a multi-stage fixed bed methanation, only a single-stage fluidized bed methanation unit is required for the production of the desired raw-SNG. To commercialize fluidized bed SNG and FT diesel production based on product gas from DFB gasification, a further demo plant in an operational environment, covering the process from biomass supply until product use, is required to check the findings of the pilot plants in long-term test runs [11].

Based on a study from TU Wien [11], the Austrian Government decided to fund the establishment of a 5 MW_{th} demonstration plant for the biomass-based production of SNG and FT diesel. With the help of this demo plant, the remaining knowledge gaps in terms of long-term behavior should be closed. The findings should be used to promote the commercialization of DFB technology in connection with SNG and FT diesel production in Austria. Numerous researchers have investigated the technical feasibility of the primary process units of the assessed process routes. The technical feasibility of the DFB gasification process with different feedstocks, bed materials, and gasification temperatures has been investigated intensively at the pilot scale [4,5,12]. Additionally, it was demonstrated at the pilot scale that DFB gasification, coupled with oxyfuel combustion, can capture an almost pure CO₂ stream in the flue gas in addition to a high-quality product gas [13–15]. Furthermore, intensive development work has already been carried out concerning the layout and design of DFB plants [16]. Moreover, the large-scale demonstration of DFB plants [7] and studies on their implementation in existing industries [17] have been executed. Furthermore, the necessary gas cleaning steps following the gasification process have been

successfully demonstrated [18,19]. The experimental validation and demonstration of the methanation unit [6,20–22] and FT synthesis [23–27] have also been conducted.

Summing up, the technical feasibility of the production of biomass-based SNG and FT diesel has been proven. After the first operation phase with the 5 MW_{th} demo plant, the remaining knowledge gaps can be clarified, and commercialization can start. Assessments for similar process routes regarding the production costs [28,29] and the CO₂ footprint [29,30] have been conducted and presented in the literature. However, neither a techno-economic nor an environmental analysis have been performed yet based on, from the current view, optimized commercial-scale concepts with the goal of reaching the status of drop-in fuels according to the Austrian gas grid feed-in guidelines [31] and synthetic fuel standards [32]. This analysis is urgently needed to determine a suitable integration strategy for the two products in the Austrian energy system. Furthermore, the investigation of energy system integration scenarios allows us to study socio-economic impacts such as sectoral competitiveness.

For this reason, this paper investigates commercial-scale concepts for producing wood-based SNG and FT diesel at a thermal fuel power of 100 MW for integration in the Austrian energy system. In detail, the paper discusses the following sections:

- Potential analysis of biogenic feedstock suitable for DFB gasification in Austria;
- Modelling of commercial scale concepts for the production of biomass-based SNG and FT diesel;
- Techno-economic and ecological assessment of both routes;
- Development of integration scenarios for biomass-based SNG and FT diesel in the Austrian energy system.

Based on the developed commercial scale concepts, the mass and energy balances of both process routes are calculated. The simulation results are the basis for determining the production costs and CO₂ footprints. To consider the economic impact of the crises arising from the Ukrainian war and COVID-19 on the Austrian energy market, the techno-economic analyses are based on the reference years 2019 (pre-crisis level) and 2022 (crisis level). With the help of the production costs, the CO₂ footprint, and the Austrian biomass potential, the substitution possibilities, the influence on the sectoral greenhouse gas emissions, and the sectoral gross value added can be calculated. Finally, suitable integration scenarios can be proposed for using biomass-based SNG and FT diesel in the Austrian energy system. Concluding, based on existing literature, the paper provides a novel comprehensive techno-economic and ecological assessment of the commercial-scale production of biomass-based SNG and FT diesel with the aim of reaching the status of drop-in fuels according to the Austrian gas grid feed-in guidelines and synthetic fuel standards. Thus, the techno-economic and ecological impact on various Austrian energy sectors can be calculated by substituting fossil natural gas and diesel with biomass-based SNG and FT diesel.

2. Materials and Methods

In the following section, all applied methods are discussed. The biomass potential analysis builds the basis for defossilization capacities in the Austrian energy system. Furthermore, commercial scale concepts are presented to provide information approximately assumptions within the process simulation. Additionally, the methodologies for the techno-economic and ecological assessment are explained. Finally, scenarios for integrating biomass-based SNG and FT diesel into the Austrian energy system are discussed.

2.1. Potential Analysis of Biogenic Feedstock

For the discussion of the integration possibilities of DFB plants into the Austrian energy system, it is necessary to determine the biomass potential for such plants in Austria. The evaluation of the biomass potential until 2050 is based on studies from the Austrian biomass association [33], the feasibility study “Reallabor” [11], and studies from Dißauer et al. [34] and Hammerschmid et al. [35]. A fluidized bed gasifier is able to process various raw and residual materials since fluidized beds have proven to be robust and fuel-flexible

for the thermo-chemical conversion of various feedstocks [4,5,11]. The following defined biomass potentials refer to the year 2050 and can be understood as reduced technical potentials [35,36]. The reduced technical potential in 2050 can be seen as the additional amount of biomass made available by political and social changes and efforts without endangering sustainable agriculture and forestry. Table 1 lists the technical biomass potential from different literature studies. The value for woody biomass ranges between 50–126 PJ/a, including forest biomass, bark, and sawmill by-products. Thus, a reduced technical potential of 75 PJ/a is assumed in this study. A range of 100–200 PJ/a can be determined for the technical biomass potential of agricultural raw materials and residues, which comprise short-rotation wood, straw, beet leaves, corncobs, grapevine pruning, and miscanthus within this study. The available values of the mentioned studies are partly based on very ambitious expansion targets for short-rotation wood and miscanthus. Furthermore, ambitious targets for the energetic utilization of straw were adopted. To ensure sustainable agriculture, a lower reduced technical potential of 80 PJ/a is assumed for the present study. Furthermore, the technical biomass potential of other biogenic residues and waste are investigated, including waste wood, sewage sludge, manure, and biogenic rejects from several industries. The mentioned studies list an additional technical biomass potential of 10–67 PJ/a, which corresponds to a reduced technical biomass potential of 30 PJ/a.

Table 1. Analysis of reduced technical biomass potential in 2050.

Property Classes and Components	Additional Technical Biomass Potential 2050 (Study Dißauer et al. [34])	Additional Technical Biomass Potential 2050 (Study Biomass Association [33])	Additional Technical Biomass Potential 2050 Scenario “High” and “Biomasse Max” (Study Kranzl et al. [37])	Additional Reduced Technical Biomass Potential 2050 (Present Study)
Woody biomass	126 PJ/a	50 PJ/a	110 PJ/a	75 PJ/a
Agricultural raw materials and residues	126 PJ/a	200 PJ/a	100 PJ/a	80 PJ/a
Other biogenic residues and waste	67 PJ/a	50 PJ/a	10 PJ/a	30 PJ/a

In total, an additional reduced technical biomass potential of 185 PJ/a is defined within this potential analysis based on literature values. Additionally, the potential analysis in [11] showed that a plant size of 100 MW_{th} builds up a good compromise between low specific investment costs due to economy of scale and sustainable biomass procurement. At this point, it must be mentioned again that, in any case, attention must be paid to sustainable agricultural and forestry management.

2.2. Commercial Scale SNG and FT Production Concepts

The underlying commercial-scale process concepts of the FT diesel and SNG routes are presented as a basis for the techno-economic and ecological assessment and scenarios for technology roll-out. The conceptual design of the biomass-based FT diesel and SNG route described in this chapter is based on experience through the operation of laboratory, pilot, and demonstration plants. Furthermore, commercial DFB plants were scientifically monitored. The scalability of all the investigated individual process units has already been demonstrated in other applications, at least on a demonstration scale.

Figure 1 depicts the proposed process routes for producing SNG and FT products from woody biomass on a 100 MW_{th} scale. The process flowsheet is divided into four main sections: resource supply, gasification, gas cooling, cleaning, and synthesis, and gas upgrading. Both process routes only differ in the synthesis and gas upgrading steps, depending on the desired product. Otherwise, the same process layout can be utilized,

which reduces the engineering efforts for both routes. Note that the process routes are meant as standalone SNG or FT production routes and are only displayed together to save space and showcase their similarity. Furthermore, only the main process units are shown in the simplified process flow diagram (PFD). Heat displacement and regeneration steps are omitted for better legibility. Process simulation of this flow sheet was performed with the process simulation software IPSEpro 8.0. The process simulation is based on wood chips as the fuel. The assumed biomass composition can be found in the Supplementary Materials. Furthermore, no variations were considered with regard to fuel. However, experiments have shown that the main components of the resulting product gas hardly change, but the impurities vary strongly due to the fuel variation [5]. Consequently, more impurities in the product gas would require a more extensive product gas cleaning section. Moreover, research is still needed for the large-scale use of low-grade fuels such as sewage sludge in DFB gasification. Therefore, the developed plant concept only applies to woody biomass. A detailed list of the assumptions and process parameters used for the simulation is shown in the Supplementary Materials.

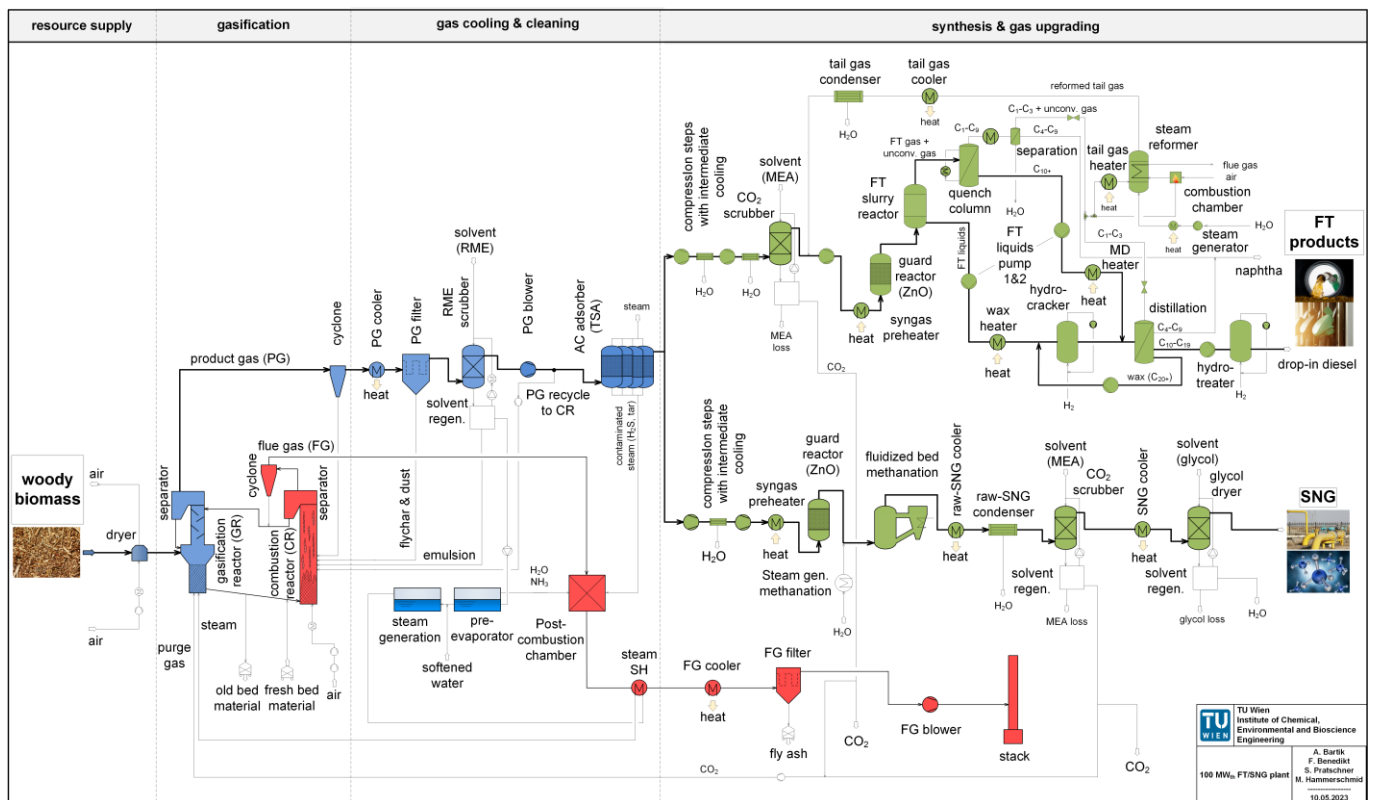


Figure 1. Simplified process flow diagram of the 100 MW_{th} FT and SNG routes (note: FT and SNG production are standalone routes but are displayed together in this picture).

The resource supply section consists of the on-site fuel handling and storage, as well as a dryer to reduce the moisture content of the fuel to an optimal and constant level for gasification, which is approximately 20%. In this study, the considered fuel is woody biomass (cf. Section 2.1).

The heat required for drying is supplied internally through heat displacement. The gasification section at approximately 820 °C is based on the advanced DFB steam gasification technology, utilizing a mixture of olivine and limestone as a bed material (80/20 wt.%) in contrast to the classical, industrially proven DFB steam gasification. The product gas, which mainly consists of H₂, CO, CO₂, CH₄, and H₂O, leaves the gasification reactor and is cooled to 180 °C in heat exchangers (PG cooler). In the coarse gas cleaning section, dust is removed in a baghouse filter (PG filter) and tars are separated in a biodiesel scrubber

at 40 °C based on the solvent rapeseed methyl ester (RME). Additionally, water vapor condenses in the biodiesel scrubber and enables the separation of water-soluble substances from the product gas, like ammonia (NH_3). The tar-rich RME and the condensed water are directed into a phase separator (solvent regen). Here, the liquid separates into a clear RME phase, an emulsion phase, and a water phase. The clear RME phase is recirculated to the scrubber, while the water phase is evaporated, superheated, and reused as a gasification agent in the gasification reactor. In this way, the freshwater consumption of the DFB system is reduced. The emulsion phase consists of a mixture of RME, absorbed tars, and water, and is utilized as additional fuel in the combustion reactor. Downstream of the biodiesel scrubber, part of the product gas is recirculated to the combustion reactor to provide the necessary heat for gasification. This way, there is no need for an external fuel supply to the combustion reactor during the process. In the fine gas cleaning section, all remaining impurities that harm the catalysts during the synthesis processes and are unwanted in the final product are removed. Activated carbon filters (AC filters) remove light aromatic compounds such as benzene, toluene, or naphthalene, as well as sulfur compounds such as hydrogen sulfide (H_2S). The activated carbon filters are operated through temperature swing adsorption (TSA), and the regeneration is carried out with steam at 250 °C [38]. The contaminated steam is disposed of in the post-combustion chamber. At this point, the requirements of the FT and SNG processes, and, therefore, the process chains, start to differ.

For the SNG route, the product gas is compressed to 10 bar in a two-stage inter-cooled compressor and preheated to 250 °C. ZnO acts as a protection layer against sulfur breakthrough. The conversion of syngas to raw-SNG takes place in a cooled fluidized bed methanation reactor at 320 °C in the presence of a nickel catalyst. A thermodynamic equilibrium model is used for this stage. After heat recovery, a condenser separates water from the raw SNG, and the gas enters an amine scrubber for CO_2 removal. The condensed water is fully reused within the process, e.g., for steam regeneration of the activated carbon or for steam addition upstream of the methanation reactor. In the last step, the gas is dried in a glycol scrubber and transferred to the natural gas grid following the specifications of the Austrian gas grid (ÖVGW G B210 [31]).

The product gas is compressed in three stages to 21 bar for the FT route. After the second compression step, CO_2 is removed in an amine scrubber at 10 bar, and recycled tail gas from the steam reformer is added to the product gas stream. Similar to the SNG route, the syngas is preheated, passes a ZnO guard bed and enters a FT slurry reactor at 230 °C. For the simulation of the FT reactor, the extended Anderson–Schulz–Flory distribution from Förtsch et al. [39], with modeling parameters according to Pratschner et al. [40], and a single-pass CO conversion of 50% are assumed. Liquid FT products are withdrawn from the slurry reactor and pumped into a hydrocracker. The hydrocracker converts long-chain FT products with hydrogen on a platinum catalyst to shorter molecules and thus increases the output of the desired diesel fraction. A consecutive distillation separates the product from the hydrocracker into different molecular weight fractions. Gaseous molecules ($\text{C}_1\text{--C}_3$) are directed to the steam reformer, and $\text{C}_4\text{--C}_9$ molecules are sold as a naphtha fraction to a refinery. Long-chain waxes (C_{20+}) are recycled to the hydrocracker and converted to low-boiling hydrocarbons ($\text{C}_1\text{--C}_{19}$). The properties of the desired diesel fraction ($\text{C}_{10}\text{--C}_{19}$) are further adjusted in a hydrotreater, allowing the production of drop-in diesel fuel with similar properties to its fossil counterpart, according to DIN EN 15940 [32]. The gaseous phase leaving the FT slurry reactor consists of molecules with different chain-lengths and unconverted syngas. Thus, a quench column condenses C_{10+} hydrocarbons pumped to the fractional distillation. A further condensation step separates a naphtha fraction from the remaining gas. $\text{C}_1\text{--C}_3$ molecules and unconverted syngas are brought to a steam reformer to reclaim CO and H_2 . The necessary heat for the steam reformer is provided through the combustion of a partial flow (15%) of the gas itself. The reformed tail gas is then reintroduced to the process upstream of the FT slurry reactor for further conversion.

Furthermore, CO_2 and district heat are generated as side products from these processes. Additionally, for the FT route, a naphtha fraction can be sold to the refinery. CO_2 is a main

component in the product gas and is separated in amine scrubbers with an assumed purity of 95%. After upgrading, the CO₂ is sold and creates additional revenues. District heat is a result of the thermal nature of the involved processes. Heat sources and sinks are matched in this study so that no external heat supply is required. Nevertheless, heat at temperature levels above 100 °C remains, which can be utilized as district heat and create additional revenues. The processes also generate water at various steps along the process chains (e.g., RME scrubber, condensation steps, etc.), which is assumed to be internally reused for steam production (e.g., gasification agent, regeneration of activated carbon, etc.). Because of the water and hydrogen content of the biomass, typically more water is produced than consumed. Therefore, wastewater disposal costs are included for the effluent streams. However, a potentially necessary water upgrading for the internally recycled water is neglected. For the DFB gasification process itself, the internal use of steam as a gasification agent from the condensed water phase from the RME scrubber, with pre-evaporation to remove unwanted impurities via the post-combustion chamber, is industrially proven.

2.3. Techno-Economic and Ecological Assessment

The techno-economic and ecological assessment is performed based on the process simulation of the biomass-based SNG and FT diesel route. The techno-economic investigation follows the net present value method, which analyzes a pending investment by discounting future payments and revenues to the present. The levelized costs of products (LCOP) in terms of synthetic natural gas and FT diesel are calculated according to Equation (1). Thus, the LCOP are influenced by the total capital investment costs of the plant (I_0), the annual expenditures (E), the annual revenues of secondary products ($R_{sec. prod.}$), and the annual quantity of the produced main product ($M_{t, main prod.}$). The discounting of the revenues, expenditures, and the annual quantity of the produced main product is considered using the cumulative discount factor (CDF) according to Equation (2), which is a function of the interest rate (i) and the plant lifetime (n) [41–44]. The total capital investment costs of the biomass-based SNG and FT diesel route with a 100 MW_{th} thermal fuel power scale are based on the visualized methodology in Figure 2. For the techno-economic assessment, the process route is divided into two sections. The first plant section, from the biomass feeding system until the primary product gas cleaning, has been built already several times worldwide at a commercial scale with a plant size from 8–32 MW_{th} [11]. According to the order of magnitude method [11,45], the inflation-adjusted total capital investment costs of the plants in Güssing, Oberwart, and Senden are used to determine the total capital investment costs of an average DFB plant with a thermal fuel power of 15 MW_{th}. The final total capital investment costs for a 100 MW_{th} scale for the first plant section are calculated using the cost-scaling method [11] according to Equation (3). The total capital investment costs of the second plant section are calculated via the cost-scaling of inflation-adjusted literature values according to Equation (3). The purchased equipment costs are multiplied by a Lang factor of 4.87 for solid-fluid-processing plants, according to Peters et al. [46], to consider all additional costs like instrumentation and control, piping, or electrical equipment. The expenditures and revenues are calculated based on simulation results and cost rates for all operating utilities. Two base years for calculating the LCOP for SNG and synthetic FT diesel are selected, namely 2019 and 2022. The year 2019 provides an investigation concerning the pre-crisis level. The increased energy prices after COVID-19 and the Ukraine war are reflected by the base year 2022. For the SNG process route, the expenditures are compensated by the revenues from the sale of district heat and captured CO₂. In the FT process route, naphtha is produced as a by-product in addition to CO₂ and district heat. Additionally, the resulting LCOP values are based on a plant lifetime of 20 years. Further details on calculating the total capital investment costs and the considered cost rates and assumptions for the techno-economic assessment are summarized in the Supplementary Materials.

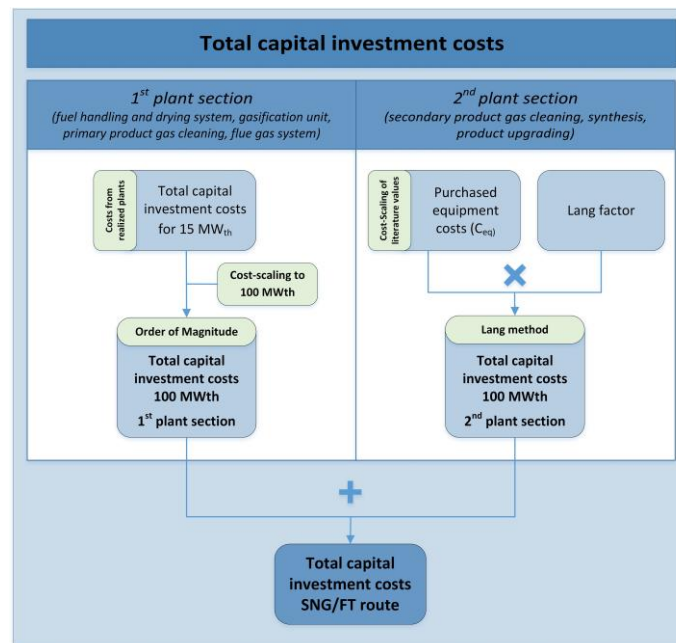


Figure 2. Methodology for the calculation of total capital investment costs [11,45].

The resulting *LCOPs* for both routes are compared with the market prices of their fossil equivalents and *LCOPs* of alternative renewable routes. Finally, a sensitivity analysis is conducted to analyze the influences of assumed cost rates on the resulting *LCOP* values. For further details on the determination of the *LCOP*, a reference is made to [46]

$$LCOP = \frac{I_0 + (E - R_{sec.prod.}) \cdot CDF}{M_{t,main prod.} \cdot CDF} \quad (1)$$

$$CDF = \frac{(1+i)^n - 1}{i \cdot (1+i)^n} \quad (2)$$

$$C_{eq,design} = C_{eq,base} * \left(\frac{S_{design}}{S_{base}} \right)^r * Z * \left(\frac{CEPCI_{base year}}{CEPCI_{2019/2022}} \right) \quad (3)$$

Additionally, an ecological assessment of both process routes is conducted to analyze the CO₂ footprint of the produced synthetic products. The process balance boundaries are defined by a Well-to-Tank approach [47,48]. The calculation of greenhouse gas emissions is based on the unit CO₂ equivalents (CO₂e) in order to achieve a standardization of the climate impact of different greenhouse gases. Therefore, the CO₂ footprint of both process routes is determined by calculating the direct and indirect greenhouse gas emissions of the main utilities, including the built-in steel and concrete, via ecological factors. The ecological factors are mainly based on databases from the Federal Environmental Agency of Austria [49], Germany [50], and the database of the software tool GEMIS 5.0 [51]. For the ecological factor of the consumed electricity, it is assumed that green electricity is used [49]. In accordance with the IEA [49], the energy allocation method was applied to allocate the resulting absolute CO₂e emissions to the primary and secondary products. The functional unit for the techno-economic and ecological assessment is MWh_{SNG} for the SNG route and l_{Diesel} for the FT route. At this point, it must be mentioned that for a holistic life cycle assessment of the two biomass-based products, many other ecological factors such as acidification potential, eutrophication, and land use have to be considered in addition to the CO₂ footprint. Further details on calculating the ecological footprint are summarized in the Supplementary Materials.

2.4. Scenarios for Integrating Biomass-Based SNG and FT Diesel in the Austrian Energy System

The techno-economic and ecological assessment of the 100 MW biomass-based SNG and FT route form the basis for discussing the scenarios for integrating biomass-based SNG and FT diesel into the Austrian energy system. The techno-economic assessment explained in Section 2.3 is based on woody biomass. Other feedstocks like energy crops, straw, or sewage sludge are mostly cheaper than woody biomass. However, the more complex gas cleaning process in the case of non-woody biomass also induces higher investment and operating costs. Furthermore, the ecological assessment is also based on woody biomass. The use of different feedstocks influences the resulting CO₂ footprint. Nevertheless, for the following scenarios, the whole biomass potential from the potential analysis is considered, assuming that the production costs and CO₂ footprint of SNG and FT diesel remain constant independent of the feedstock. In total, six scenarios for integrating drop-in FT diesel or SNG into the Austrian energy system are discussed. The underlying demand for natural gas and diesel is based on 2021 [2,52]. Below, the scenarios considered are explained, showing the broad integration possibilities of the two products.

(a) SNG use in the energy sector

The first scenario is based on the use of SNG in the energy sector for defossilization of existing heat, combined heat and power, and power plants. Due to the increasing share of fluctuating renewable energy sources in the Austrian power grid, further flexibility options have to be installed to ensure the security of supply. On the one hand, this can be achieved through the increased interconnection to the European power grid with corresponding national grid reinforcement and grid expansion projects, as well as the installation of additional storage facilities [53]. On the other hand, existing gas-fired power plants could be retained for peak load coverage and still be defossilized with SNG. Additionally, gas-fired heat plants based on biomass-based SNG can decrease the CO₂ footprint of existing district heating systems directly. Within this scenario, the natural gas consumption from the energy sector is completely substituted with biomass-based SNG based on industry prices. The defossilization potential assumes that the natural gas consumption in the energy sector remains constant until 2050.

(b) SNG use in the private and public sector (without mobility)

In the second scenario, the use of SNG in the private and public sector is considered, which means that existing gas boilers in private households, public and private services, and aggregates in the agriculture and forestry sector are retained and driven by biomass-based SNG. Of course, renewable heat supply in the private sector can also be achieved via other technologies, such as heat pumps or solar thermal, but the necessary high inlet temperatures in old apartments, as they are found in Vienna, can only be achieved satisfactorily by district heat or wood-fired boilers [54]. Therefore, the defossilization of existing gas infrastructure in the public and private sector using biomass-based SNG can also contribute to a sustainable energy system. The following techno-economic assessment in this scenario is based on household prices. The defossilization potential assumes that the natural gas consumption in this sector remains constant until 2050.

(c) SNG use in the industry

The third scenario for integrating biomass-based SNG in the Austrian energy system is integration in the manufacturing sector. Natural gas in burners is used in different sectors like the chemical, pulp and paper, cement, or steel industries to provide high-temperature heat for several production processes. Integrating biomass-based SNG in the industry would be an easy way to provide the necessary high-temperature heat without any changes in the current utilized process chains [55]. Furthermore, the material use of natural gas in the industry sector could be easily substituted with biomass-based SNG. The techno-economic assessment in this scenario is based on industry prices. The defossilization potential assumes that the natural gas consumption in the industry sector remains constant until 2050.

(d) FT diesel in private and public transport

Therein, the use of biomass-based FT diesel as drop-in fuel in conventional diesel cars and buses is considered. For evaluating the defossilization potential, it is assumed, according to [35], that the number of diesel cars and the associated diesel demand will be reduced by half until 2050. The number of diesel buses will remain constant until 2050. The techno-economic assessment in this scenario is based on petrol station market prices for private consumers.

(e) FT diesel in heavy-duty traffic

The fifth scenario is based on integrating biomass-based FT diesel in the heavy-duty traffic sector. In this sector, freight transport with light and heavy commercial vehicles (LCV and HCV) and the diesel demand in agriculture and forestry is considered. Furthermore, the diesel demand for inland navigation and railway is discussed. For calculating the defossilization potential in this scenario, it is assumed that the number of LCVs will be reduced, simultaneously with the number of cars, by half until 2050 [35]. The number of diesel-driven HCVs, tractors, ships, and trains will remain constant until 2050 [35]. For the techno-economic assessment, the mean value of the petrol station market price for private consumers and the stock market diesel price is considered.

(f) FT diesel in heat and power

Finally, the sixth scenario includes the integration of FT diesel in the heat and power sector. Therein, the diesel demand in the manufacturing and the public and private sectors is considered. Similar to the use of SNG in industry, FT diesel can provide high-temperature heat. The diesel demand in the public and private service sectors can be mainly attributed to, e.g., emergency diesel aggregates in hospitals and other critical infrastructure. The diesel demand in the manufacturing sector is assumed to remain constant until 2050, whereas a reduction by half is assumed for the public and private sector due to a substitution with other renewable technologies [35]. The techno-economic assessment is based on the stock market diesel price.

These six scenarios are further investigated and compared to discuss the techno-economic and ecological impact of each integration possibility. Therefore, the natural gas and diesel demand in 2050 is estimated in all sectors and compared with the SNG and FT diesel potential. Furthermore, the CO₂ reduction potential ($CO_2e_{red,sector i}$) through the substitution of natural gas with SNG or fossil diesel with FT diesel is investigated in each scenario (see Equation (4)). For this, the annual amount of sectoral used gas or diesel ($E_{gas/diesel,sector i}$) is multiplied by the difference in CO₂ footprints between the renewable biomass-based product and its fossil counterpart (FP) and divided by the absolute annual CO₂ emissions in the respective sector ($CO_2e_{tot,sector i}$). Finally, the techno-economic comparison between the SNG and FT diesel production costs with the market prices (MP) of the fossil counterpart shows the economic competitiveness (EC) of both products (see Equation (5)). The comparison of the total additional costs or savings per year with the gross value added (GVA) shows the economic impact in the respective sector. The GVA is calculated from the gross production values achieved, reduced by all advance outlays. Simplified, GVA could be described as a company's revenue minus expenses for all kinds of utilities. The resulting GVA is ultimately shared among all the stakeholders involved, namely the employees, the company owners, and the state. Consequently, the EC determines the percentage by which the sectoral GVA or, in approximation, the profit changes as a result of switching to biomass-based SNG or FT diesel.

$$CO_2e_{red,sector i} = \frac{E_{gas/diesel,sector i} * (FP_{fos.gas/diesel} - FP_{SNG/FTdiesel})}{CO_2e_{tot,sector i}} \quad (4)$$

$$EC_{sector i} = \frac{E_{gas/diesel,sector i} * (MP_{fos.gas/diesel} - LCOP_{SNG/FTdiesel})}{GVA_{total,sector i}} \quad (5)$$

Finally, alternative options for using SNG and FT diesel are discussed, which can contribute to a sustainable energy system in the individual sectors. Consequently, in addition to a quantitative comparison of the individual scenarios based on techno-economic and ecological footprints, a qualitative comparison of possible alternatives can be used to find the most suitable application for SNG and FT diesel.

3. Results and Discussion

In this chapter, all results are visualized and discussed. First of all, the input and output streams of both commercial scale routes for producing wood-based SNG and FT diesel with a thermal fuel power input of 100 MW_{th} are determined. Then, the techno-economic and ecological competitiveness of each route, regarding leveled production costs and CO₂ footprints, is assessed. Finally, the integration of biomass-based SNG and FT diesel in several sectors of the Austrian energy system is discussed.

3.1. Input- and Output Streams of Commercial SNG and FT Production Plants

In Section 2.2, the commercial scale concepts for both investigated routes were presented. Based on these concepts, the process simulation results in terms of input and output streams for both routes are presented in this chapter. In Table 2, the input and output streams for the production of wood-based SNG based on 100 MW_{th} scale are summarized. Thus, it can be concluded that approximately 65 MW of SNG can be generated from 100 MW_{th} woody biomass. In addition, approximately 14.2 MW of district heat and 6150 Nm³/h of CO₂ for storage or utilization can be recovered.

Table 2. Input and output streams for producing wood-based SNG related to a thermal fuel power of 100 MW.

Input Stream	Plant Input		Value	Output Stream	Plant Output	
	Unit	Value			Unit	Value
Biomass (wood)	kg/h	33,250	Synthetic natural gas	Nm ³ /h	6840	
	kW _{before drying}	94,360		kW	64,960	
	kW _{after drying}	100,000		District heat	kW	14,170
Fresh bed material (80% olivine and 20% limestone)	kg/h	150	Captured CO ₂ for storage or utilization	Nm ³ /h	6150	
Fresh scrubber solvent (rapeseed methyl ester)	kg/h	110	Ash and dust	kg/h	350	
Fresh amine (monoethanolamine)	kg/h	18.4	Waste water	kg/h	320	
Fresh glycol	kg/h	0.1				
Electricity	kW	4340				

Table 3 shows the input and output streams for the production of wood-based FT diesel based on a 100 MW_{th} scale. Therein, it can be seen that through the gasification of woody biomass with subsequent gas cleaning, FT synthesis, and FT upgrading, approximately 36.6 MW of drop-in FT diesel can be produced. Additionally, 22.8 MW district heat, 17.6 MW FT naphtha, and 3790 Nm³/h of CO₂ can be recovered.

In comparison, the SNG process yields a higher energetic efficiency than the FT process. About 79% of the chemical energy from the woody biomass can be transferred to SNG and district heat, whereas 77% is found in FT diesel, naphtha, and district heat. Furthermore, more CO₂ needs to be captured in the SNG process due to a higher CO₂ capture rate and less carbon in the product per molecule of CH₄ compared to FT products. Thus, more amine is also needed for the scrubber. In the FT process route, more electricity is required to reach higher synthesis pressure levels. Additionally, hydrogen is needed to upgrade FT products in the hydrocracker and hydrotreater. The presented simulation results are the basis for the calculation of the techno-economic and ecological results.

Table 3. Input and output streams for producing wood-based FT diesel related to thermal fuel power of 100 MW.

Input Stream	Plant Input		Plant Output		
	Unit	Value	Output Stream	Unit	Value
Biomass (wood)	kg/h	33,250	FT diesel	L/h	3850
	kW _{before drying}	94,360		kW	36,563
	kW _{after drying}	100,000		L/h	2000
Fresh bed material (80% olivine and 20% limestone)	kg/h	150	FT naphtha	kW	17,561
Fresh scrubber solvent (rapeseed methyl ester)	kg/h	110	District heat	kW	22,823
Fresh amine (monoethanolamine)	kg/h	11.5	Captured CO ₂ for storage or utilization	Nm ³ /h	3790
Hydrogen (for hydrocracking and hydrotreating)	kg/h	26.3	Ash and dust	kg/h	350
Electricity	kW	6120	Waste water	kg/h	2635

3.2. Techno-Economic Results of Commercial SNG and FT Production Plants

Based on the simulation results, a techno-economic assessment determines the levelized production costs for both commercial-scale routes. The underlying methodology for determining the production costs for wood-based SNG and FT diesel is explained in Section 2.3.

Figure 3 visualizes the production costs of wood-based SNG for the 100 MW_{th} scale. They are compared with the household and industry market prices of fossil natural gas based on the pre-crisis year 2019 and crisis year 2022. The production costs for SNG consist of approximately one-third each, namely, of fuel, operation and maintenance, and investment costs. For the base year 2019, the production costs of SNG, including taxes, are around 70 EUR /MWh. For 2022, the production costs rose to approximately 91 EUR /MWh. The increase in production costs is attributable to all three previously mentioned cost drivers. While the investment costs increased by 37% and the fuel costs by 27%, the most significant price increase, with 57%, was seen for operation and maintenance (O&M) costs. This is due to the doubling of the industrial electricity price from 2019 to 2022. However, the price increases were partially compensated by the rising purchase prices for district heat and CO₂. Meanwhile, market prices for fossil natural gas doubled in the household sector and tripled in the industrial sector during the period under consideration. Consequently, production costs of wood-based SNG are at household market price levels in 2019 and at industrial market price levels in 2022 compared to fossil natural gas.

In Figure 4 (left), the determined production costs excluding taxes for wood-based SNG for 2019 are compared with those for alternatives based on renewable energy sources (RES), according to Terlouw et al. [56] and Götz et al. [57]. These alternatives comprise e-fuels based on renewable electricity and CO₂ from biogenic sources and biomethane based on manure and corn silage. The comparison shows that the production costs for biomethane are 20–55% higher than the SNG production costs based on woody biomass in the 100 MW scale. The e-fuels' production costs are 175% higher than the production costs for wood-based SNG. In this comparison, the plant scale for biomethane is considerably lower, which is unfavorable regarding the economy of scale, and biomethane plants are not being built much larger. In the case of e-fuels, the high production costs can be attributed primarily to the high dependency on the underlying electricity price, which is the main price driver.

In Figure 4 (right), the sensitivity analysis of the SNG production costs based on the year 2022 is visualized. The most significant influence on SNG production costs is caused by the annual operating hours, the plant lifetime, the fuel costs, and the investment costs. Consequently, high plant availability and lifetime, and minimization of investment and fuel costs must be realized to keep production costs low. Furthermore, a moderate influence on SNG production costs is induced by interest rate, electricity price, maintenance, insurance

and administration costs, and earnings through captured CO₂ and district heat. Other operating utility costs have little to no impact on SNG production costs.

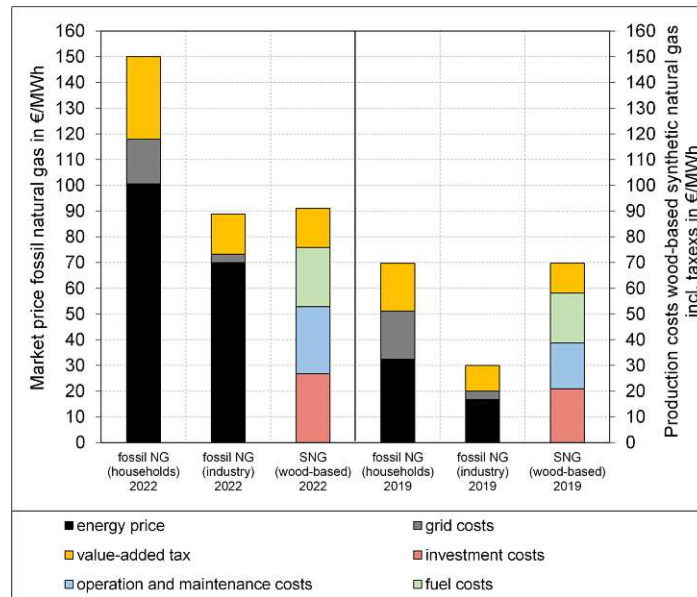


Figure 3. Comparison of production costs of wood-based SNG with the market price of fossil counterparts based on the years 2019 and 2022.

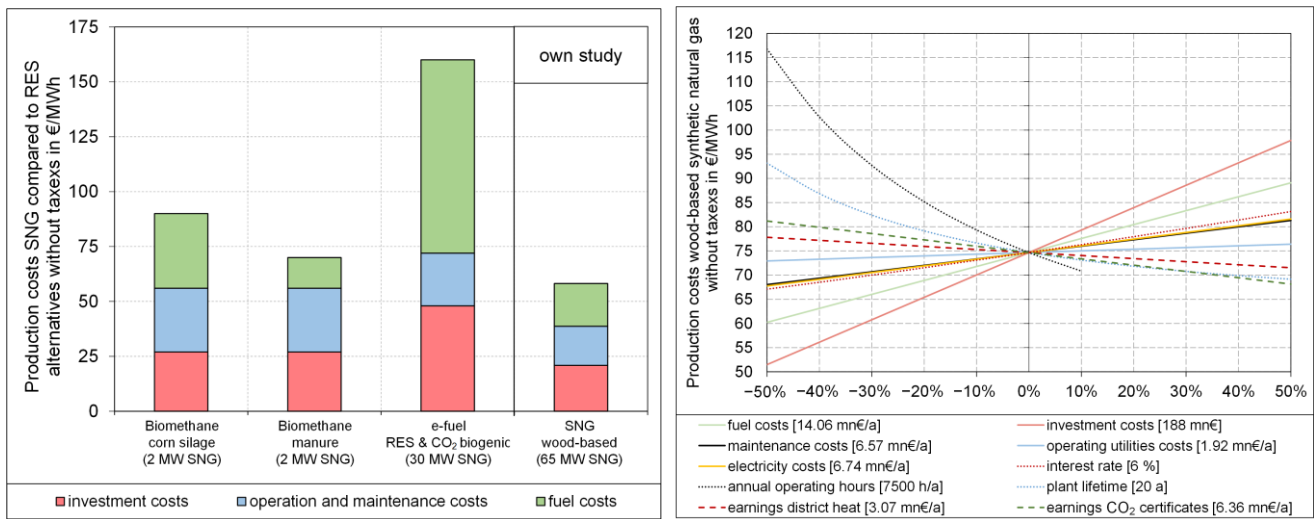


Figure 4. Comparison of production costs of wood-based SNG with RES alternatives (left, base year 2019) [56,57] and sensitivity analysis of production costs of wood-based SNG (right, base year 2022).

In Figure 5, the FT diesel production costs are compared to the stock market and petrol station prices for fossil diesel based on the pre-crisis year 2019 and the crisis year 2022. The FT diesel production costs are in the range of the petrol station prices but above stock market prices for fossil diesel in both reference years. Furthermore, the FT diesel production costs comprise 20–23% fuel costs, 36–39% operation and maintenance costs, and 40–41% investment costs, dependent on the base year. The FT diesel production costs with taxes are approximately 1.31 EUR /L for 2019 and 1.89 EUR /L for 2022. The production costs increase from 2019 compared to 2022 is in the same range as mentioned for the SNG process route.

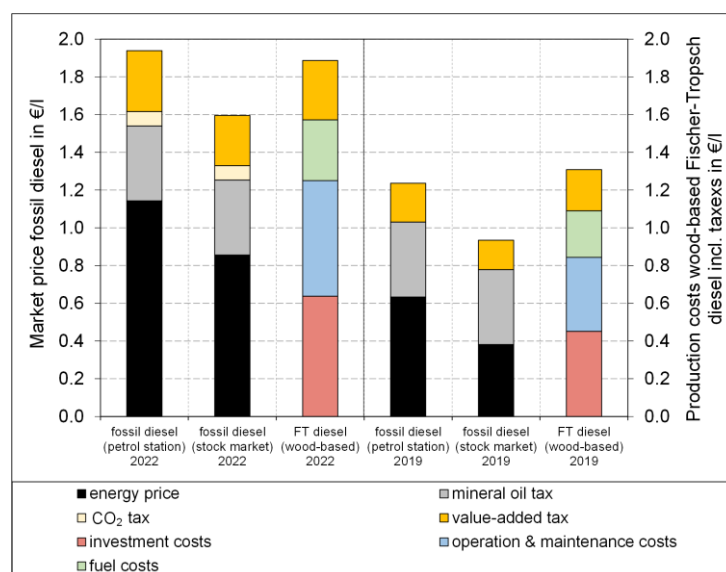


Figure 5. Comparison of wood-based FT diesel production costs with market price of fossil counterpart based on the years 2019 and 2022.

Additionally, the yearly operation and maintenance costs of the FT diesel route are 67–74% higher compared to the SNG route. This is because of the higher consumption of catalysts and electricity and higher maintenance needs. The investment costs of the FT diesel production route are approximately 70% higher than the investment costs of the SNG process route, while the fuel costs remain constant.

In Figure 6 (left), the FT diesel production costs excluding taxes, based on 2019, are compared with renewable alternative routes published by Maniatis et al. [58] and Pratschner et al. [59]. The biodiesel production routes fatty acid methyl ester (FAME) and hydroprocessed ester and fatty acid (HEFA) based on used cooking oil show production costs of 0.86–0.87 EUR /L and are approximately 26% cheaper than the wood-based FT diesel at 100 MW scale. The jatropha oil-based biodiesel from the HEFA route is more expensive than the FT diesel due to the higher fuel costs. E-fuels based on RES electricity and industrial CO₂ are approximately two to three times more expensive than wood-based FT diesel due to the high dependency on the electricity price.

The sensitivity analysis regarding the wood-based FT diesel production costs for 2022 is visualized in Figure 6 (right). Similar to the SNG route, the main influences are the annual operating hours, the plant lifetime, and the investment costs. However, the sensitivity to varying fuel costs is lower in comparison to the SNG route due to their lower share within the overall production costs.

If the techno-economics of the biomass-based SNG and FT diesel routes are compared in an energy-related manner, it is noticeable that the production costs of SNG at 70–91 EUR /MWh are much lower than FT diesel with 137–198 EUR /MWh. This results from the much higher investment costs for the production of FT diesel due to the significantly more complex product upgrading steps. Furthermore, the O&M are higher because more electricity is required for compression to a higher pressure level in synthesis and hydrogen is needed in upgrading.

3.3. Ecological Results of Commercial SNG and FT Production Plants

In analogy to the techno-economic, the ecologic assessment expressed by the CO₂ footprint of both process routes is conducted. The underlying methodology for determining the CO₂ footprint for wood-based SNG and FT diesel is explained in Section 2.3.

Figure 7 (left) shows a breakdown of the CO₂ footprint of the wood-based SNG production route. The CO₂ footprint per produced unit of SNG is 0.027 kgCO₂e/kWh_{SNG}. The direct and indirect emissions of wood are responsible for approximately 77% of the

total CO₂ footprint. About 10% are related to using rapeseed methyl ester as a scrubber solvent. All the other utilities, like steel, concrete, bed material, activated carbon, zinc oxide, nickel catalyst, amine, glycol, and green electricity, cause the remaining 13% of the overall CO₂ footprint. Regarding the CO₂ footprint for electricity, it must be mentioned that the calculation is based on the utilization of green electricity. If the CO₂ footprint of the Austrian electricity mix were chosen, the total CO₂ footprint of the produced SNG would increase by 37% to 0.037 kgCO₂e/kWh_{SNG}.

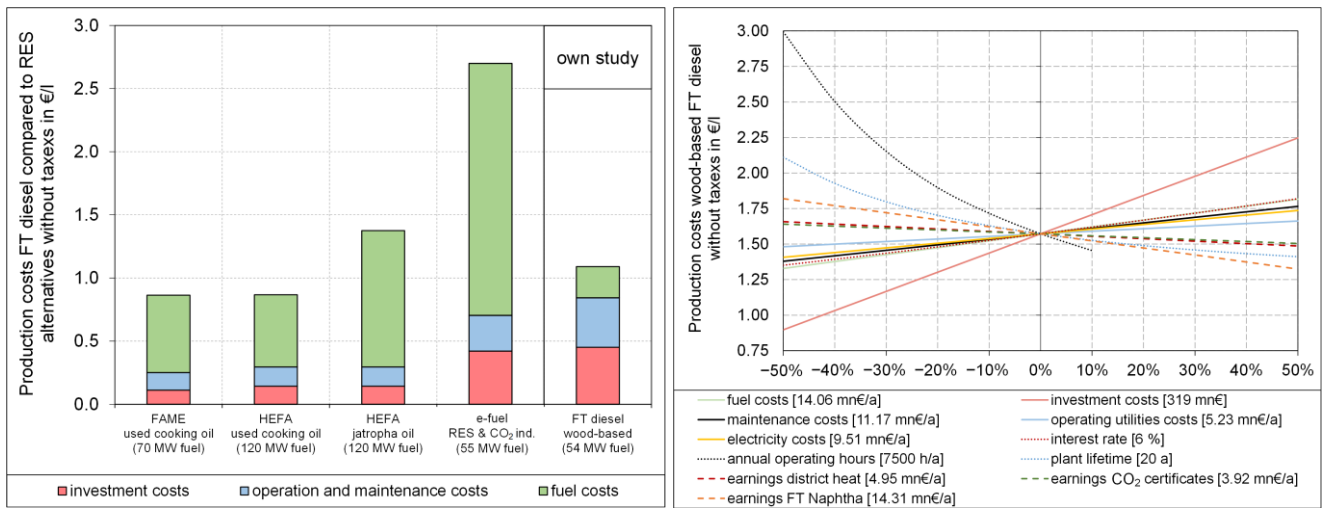


Figure 6. Comparison of wood-based FT diesel production costs with RES alternatives (left, base year 2019) [58,59] and sensitivity analysis of production costs FT diesel (right, base year 2022).

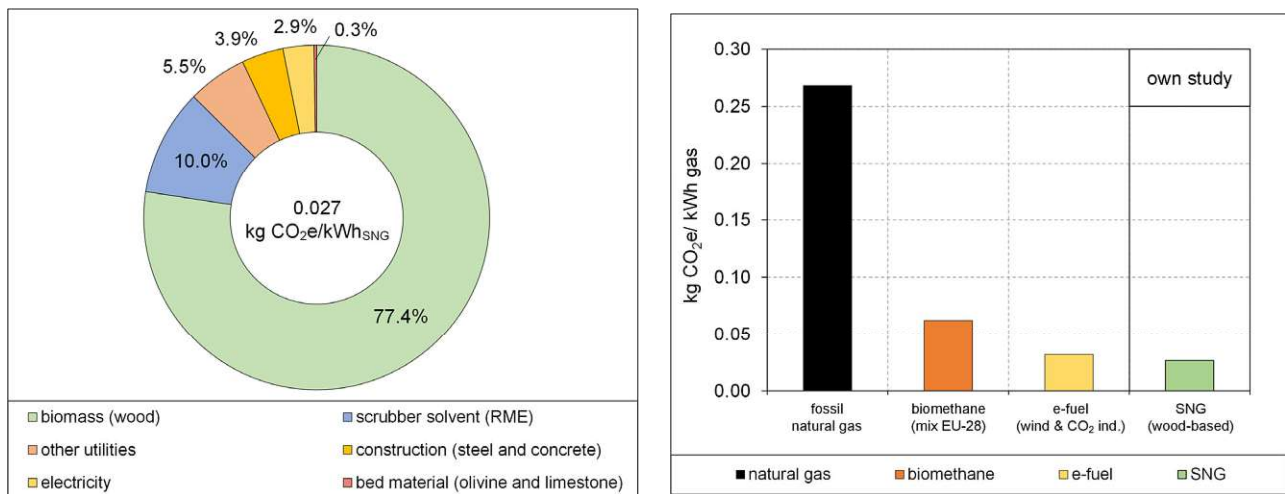


Figure 7. Breakdown of the CO₂ footprint of wood-based SNG (left) and comparison with fossil and RES alternatives (right) [30,49,60].

In Figure 7 (right), a comparison of the CO₂ footprint from wood-based SNG with that from fossil natural gas, according to Federal Environmental Agency Austria [49], and from RES alternatives, according to a study from Jungmeier et al. [30,60], is shown. Therein, it can be seen that using wood-based SNG at 100 MW scale instead of fossil natural gas can save 90% of CO₂ emissions. Furthermore, the CO₂ footprint of wood-based SNG is also lower compared to the renewable alternatives biomethane and e-fuel. The CO₂ footprint per kWh of biomethane, based on the average substrate mix within the European Union, is more than double as high as the value of synthetic natural gas, mostly caused by the emissions due to the use of corn silage or energy plants. The CO₂ footprint of e-fuels using

renewable electricity and biogenic CO₂ is also in the range of wood-based SNG and quite low. However, the CO₂ footprint of e-fuels using fossil electricity is much higher than that of fossil natural gas. Finally, it has to be mentioned that for the CO₂ footprint of the biomass-based SNG, the 6150 Nm³/h of captured CO₂ during gas upgrading are not considered. If this is considered a CO₂ sink, a negative CO₂ footprint of 0.127 kgCO₂e/kWh_{SNG} could be achieved, and thereby, a below zero emission technology is possible.

In Figure 8 (left), the breakdown of the CO₂ footprint for the wood-based FT diesel is shown. The CO₂ footprint of the wood-based FT diesel is 0.269 kgCO₂e/l_{FT diesel}. The distribution of CO₂ emissions is very similar to the SNG process route. Due to the larger consumption of different catalysts in the synthesis and upgrading step, the category “other utilities” has a slightly larger impact on the CO₂ footprint compared to the SNG route. The electricity consumption is also slightly higher due to the higher pressure level in the synthesis step. Additionally, hydrogen is required in the upgrading steps of the FT diesel, which also accounts for a small share of the CO₂ footprint. The CO₂ footprint of the electricity is based on green electricity. If the CO₂ footprint of the Austrian electricity mix were chosen for calculating the CO₂ footprint of electricity and hydrogen, the total CO₂ footprint of the produced FT diesel would increase by 64% to 0.440 kgCO₂e/l_{FT diesel}.

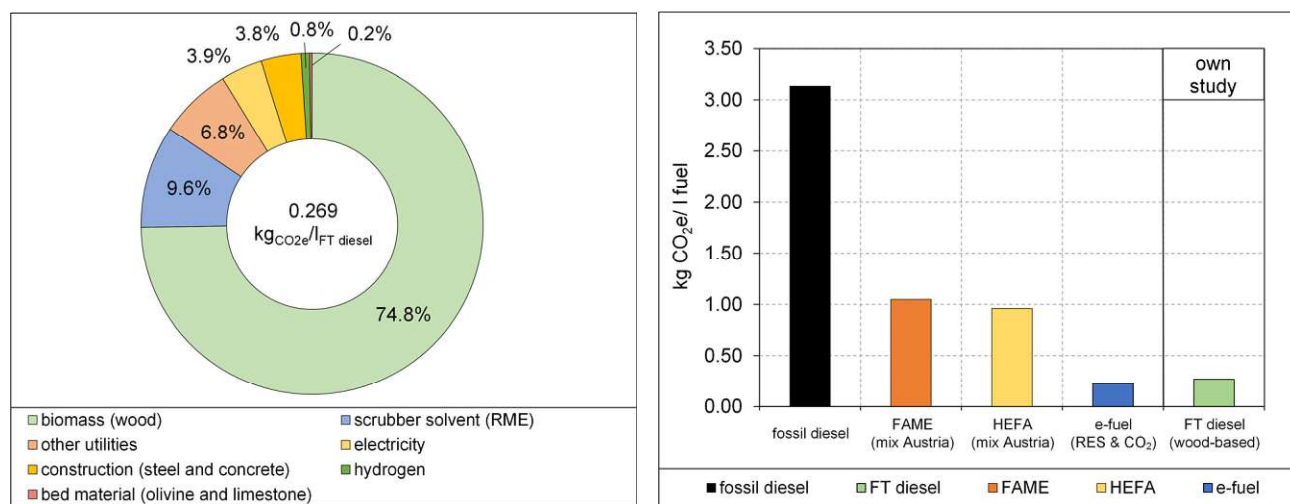


Figure 8. Breakdown of the CO₂ footprint of wood-based FT diesel (left) and comparison with fossil and RES alternatives (right) [49,61,62].

In Figure 8 (right), the CO₂ footprint of the wood-based FT diesel is compared with that of fossil diesel, according to Federal Environmental Agency Austria [49], and of RES alternatives, according to studies from Aichmayer et al. [61] and Pratschner et al. [62]. The CO₂ footprints of the wood-based FT diesel and the e-fuels, both based on green electricity, are the lowest and more than 90% lower compared to the CO₂ footprint of fossil diesel. If using fossil-based electricity as an energy source for e-fuels, the CO₂ footprint is much higher than the CO₂ footprint of fossil diesel. The CO₂ footprint of the FAME and HEFA process routes based on an Austrian fuel mix is 65–70% lower compared to the fossil diesel. If cooking oil is used as a feedstock for the FAME and HEFA processes, CO₂ footprints in the same range as those of e-fuels and wood-based FT diesel can be achieved. Similar to the SNG process route, the capturing of CO₂ is not considered. By taking the capture of approximately 3790 Nm³/h of CO₂ in the upgrading step into account as a CO₂ sink, a footprint of 0.657 kgCO₂e/l_{FT diesel} could be achieved.

If the CO₂ footprints of the two biomass-based products are compared, hardly any difference can be detected. The energy-related CO₂ footprint of FT diesel is 0.028 kgCO₂e/kWh_{FT diesel}, nearly the same as the SNG footprint of 0.027 kgCO₂e/kWh_{SNG}. The reason is that the same amount of biomass is used for the production of an energy-related product unit, with approximately the same energetic process efficiencies. In contrast to the techno-economy,

the higher electricity demand and the use of hydrogen have not as strong of an impact, since green electricity with a very low CO₂ footprint was assumed.

3.4. Integration of Biomass-Based SNG and FT Diesel in the Austrian Energy System

The biomass potential analysis (from Section 2.1) and the techno-economic (from Section 3.2) and ecological (from Section 3.3) results form the basis for discussing integration possibilities of biomass-based SNG and FT diesel in the Austrian energy system. Based on the biomass potential analysis, an additional biomass potential of 185 PJ/a can be determined in Austria in the year 2050. It should be mentioned that this potential does not consider competitive use by other biomass-based technologies. Considering the energetic efficiencies for the SNG and FT diesel process route, 120 PJ/a of SNG or 67.5 PJ/a of FT diesel can be produced out of the raised biomass potential. Additionally, the by-products of FT diesel, naphtha, district heat, and captured CO₂, are produced. In Figure 9, the annual Austrian energy demand for fossil natural gas and fossil diesel, distributed to six sectors related to the scenarios explained in Section 2.4, is compared to the biomass-based SNG and FT diesel potential in 2050. It can be seen that there is enough potential to substitute the whole natural gas demand in the energy sector or private and public sector, or nearly the whole industry sector. Instead of producing SNG, biomass-based FT diesel can substitute approximately half of the fossil diesel demand in private and public transport sectors or the heavy-duty traffic sector, or the whole demand in the heat and power sector.

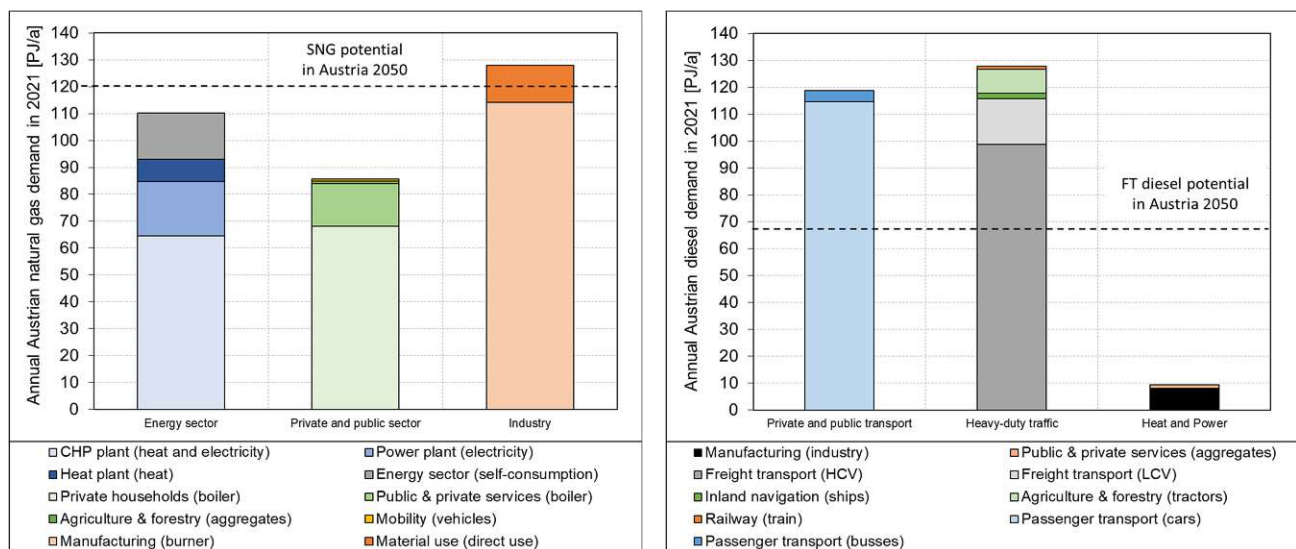


Figure 9. Annual Austrian energy demand for natural gas (left) and diesel (right) in 2021 compared to the SNG and FT diesel potential in 2050.

In Table 4, the six scenarios for the use of SNG and FT diesel as drop-in fuels in several sectors are summarized and compared. Therein, the substituted fossil natural gas and fossil diesel demands are compared with the change in the sectoral gross value added (GVA) for the pre-crisis year 2019 and crisis year 2022 and the CO₂ reduction potential of the sector.

It can be seen that the highest sectoral CO₂ reduction, 89%, can be reached in the energy sector through a nearly complete defossilization of the electricity and district heat mix with SNG. Regarding the economic impact, it can be seen in Figure 3 that the SNG production costs in the pre-crisis year 2019 were more than double and in the crisis year 2022, nearly on the same level compared to the related industrial natural gas market prices. This comparison shows that by integrating SNG into the energy sector, the electricity and heat price can be decoupled from the natural gas price. However, because cheaper alternative electricity and heat production technologies like wind power or solar PV exist, the SNG use in the energy sector should be focused on gas-fired power plants for the coverage of peak-loads.

Table 4. Comparison of possible implementation scenarios of biomass-based SNG and FT diesel in the Austrian energy system.

Implementation Scenarios	Natural Gas or Diesel Demand in 2050	Substituted Natural Gas or Diesel Demand in 2050	Additionally Produced by-Products	Sectoral CO ₂ Reduction Potential	Economic Competitiveness (Change of Sectoral GVA)		Possible Renewable Alternatives
					2019	2022	
SNG use in energy sector	110 PJ/a ¹	110 PJ/a	24 PJ/a district heat	89.1%	−12.4%	−0.5%	Peak-load power coverage <ul style="list-style-type: none"> increased interconnection to the European power grid additional storage facilities sector coupling Provision of district heat <ul style="list-style-type: none"> heat pumps biomass heating plants solar thermal systems waste heat utilization hydrogen
SNG use in private and public sector (without mobility)	85 PJ/a ¹	85 PJ/a	18.5 PJ/a district heat	70.6%	0%	8.6%	Provision of decentral heat <ul style="list-style-type: none"> heat pumps solar thermal systems wood-fired boilers district heat
SNG use in industry	128 PJ/a ¹	120 PJ/a	26.2 PJ/a district heat	30.3%	−2.0%	−0.1%	Provision of high-temperature heat <ul style="list-style-type: none"> waste heat recovery hydrogen high-temperature heat pumps

Table 4. Cont.

Implementation Scenarios	Natural Gas or Diesel Demand in 2050	Substituted Natural Gas or Diesel Demand in 2050	Additionally Produced by-Products	Sectoral CO ₂ Reduction Potential	Economic Competitiveness (Change of Sectoral GVA)		Possible Renewable Alternatives
					2019	2022	
FT diesel in private and public transport	61.5 PJ/a ²	61.5 PJ/a	38.4 PJ/a district heat and 29.6 PJ/a FT naphtha	40.2%	−0.2%	0.2%	Alternative mobility options <ul style="list-style-type: none"> • battery electric vehicles • fuel cell electric vehicles • hydrogenated vegetable oil • e-fuels
FT diesel in heavy-duty traffic	119 PJ/a ²	67.5 PJ/a	42.2 PJ/a district heat and 32.5 PJ/a FT naphtha	58.5%	−1.8%	−0.8%	Alternative mobility options <ul style="list-style-type: none"> • battery electric vehicles (limited) • fuel cell electric vehicles • hydrogenated vegetable oil • e-fuels • compressed natural gas vehicles
FT diesel in heat and power	9 PJ/a ³	9 PJ/a	5.5 PJ/a district heat and 4.2 PJ/a FT naphtha	2.6%	−0.1%	−0.1%	Provision of high-temperature heat <ul style="list-style-type: none"> • wood-fired boilers • waste heat recovery • hydrogen • high-temperature heat pumps (limited usability)

¹ gas demand remains constant until 2050. ² diesel demand for cars and LCV was reduced by half compared to 2021, because of vehicle fleet predictions [35]/diesel demand for busses and other heavy-duty traffic vehicles remain constant until 2050. ³ diesel demand for aggregates in public and private sector was reduced by half compared to 2021/diesel demand in manufacturing remains constant until 2050.

SNG use in the private and public sector also helps to reduce the sectoral CO₂ footprint by more than 70%, while raising the sectoral GVA. This would mean that using SNG in private households in times of crisis would help relieve household budgets. In comparison with alternative decentralized heat production technologies, it has to be mentioned that heat pumps and district heat should be used preferentially, because biomass-based SNG is not infinitely available. However, using SNG in private households, where no district heat or other renewable options are available, could be favorable.

Furthermore, the industry can use SNG to defossilize the gas demand for burners and direct material use without major changes in the process chains. In this way, nearly a third of the industrial CO₂ emissions can be reduced. The economic impact in this scenario is limited, with a sectoral GVA change of up to 2%. Consequently, the use of SNG could be a viable option in the defossilization process of the industry where the use of heat-pumps or waste heat cannot be realized.

In addition to the three integration scenarios for biomass-based SNG, three scenarios for integrating FT diesel in the Austrian energy system are discussed. According to the biomass potential, approximately half of the private and public transport diesel demand can be substituted with FT diesel. Consequently, according to future vehicle fleet predictions [35], it was assumed that only half of the diesel demand for cars could be replaced by synthetic fuels, thus leading to a sectoral CO₂ reduction of approximately 40%, while the sectoral GVA remains nearly constant. However, besides FT diesel, there are several alternative options for the public and private transport sector, first and foremost e-mobility.

The use of FT diesel in the heavy-duty traffic sector would be another option for using biomass-based products in the Austrian energy system. If the entire biomass potential is used to produce FT diesel for the heavy-duty traffic sector, the sectoral CO₂ footprint can be reduced by over 58%, while the sectoral GVA would be reduced by up to 2%. Furthermore, alternative options in this sector are, to date, limited; thus, the integration of FT diesel into the heavy-duty traffic sector is a promising solution. Moreover, it must be mentioned that the use of FT diesel in mobility can only take place if this fuel is approved for use in the most common diesel engines, regardless of the standard to be met.

The last scenario is based on the use of FT diesel in the heat and power sector, which comprises public and private heat production and the diesel demand in the manufacturing sector. The substitution of the diesel demand in this sector can only lead to a sectoral CO₂ reduction of 2–3%, much less than in the other scenarios. Consequently, it can be concluded that using high-quality FT diesel in the heat and power sector is not a viable option.

The scenarios examined aim to ensure that the released biomass can be used in either one sector or another. This means that several scenarios can only be implemented if the total amount of biomass used does not exceed the calculated biomass potential of 185 PJ/a.

4. Conclusions and Outlook

Based on a study from TU Wien [11], the Austrian Government could be convinced to fund the establishment of a 5 MW demonstration plant for the biomass-based production of SNG and FT diesel. The remaining knowledge gaps regarding the long-term behavior of different process units and utilities can be clarified within this demonstration phase. This includes exemplifying the technical investigation of the influence of fluctuating fuel qualities on product quality, the lifetime of catalysts and other utilities, and the required maintenance intervals with regard to plant availability. Furthermore, non-technical aspects, such as the examination of the all-season regional provision of biomass and the creation of social acceptance of the novel technology, should be investigated. In addition to the knowledge gaps described above, the competitive use of biomass must also be mentioned here as a possible limitation for the roll-out process.

After this demonstration phase, the lessons learned should be used to roll out the investigated technology commercially in Austria. This publication investigated the commercial scale concepts for producing wood-based SNG and FT diesel based on a 100 MW_{th} scale.

The simulation of both process routes showed that the energetic efficiency of the SNG process route is 79%, slightly higher compared to the 77% of the FT diesel process route. At the same time, it must be mentioned that within the SNG process, 65% of the chemical energy of the biomass can be converted to the main product, SNG. In comparison, within the FT process, only 36.6% of the biomass input is converted to the main product, FT diesel.

The techno-economic assessment showed that biomass-based SNG and FT diesel production costs can compete with the market prices of their fossil counterparts. The production costs of wood-based SNG related to the pre-crisis year 2019 are approximately 70 EUR /MWh. The market price range for fossil natural gas in the same year was 30–70 EUR /MWh, depending on the quantity purchased in industrial and household sectors. Based on the crisis year 2022, the SNG production costs were 91 EUR /MWh, slightly higher due to inflation. However, the market price for fossil natural gas increased to 89–150 EUR /MWh. Thus, it can be seen that the SNG production costs based on 2019 are in the range of the household prices, and when based on 2022, in the range of industrial market prices. Consequently, wood-based SNG production can help to decouple the domestic natural gas price level from the global market price level. The production costs for wood-based FT diesel are 1.31–1.89 EUR /L in the reference years 2019 and 2022. In comparison, the petrol station price level for fossil diesel was between 1.24–1.94 EUR /L. This comparison shows that the FT diesel production costs approximately match the petrol station price level, independent of the reference year. The economical comparison also showed that biomass-based SNG and FT diesel can compete with other renewable alternatives. The energy-related comparison of production costs for both biomass-based products shows that FT diesel, with 137–198 EUR /MWh, costs approximately twice as much as SNG, with 70–91 EUR /MWh. The reason for this is the much higher investment costs for the FT diesel route due to the more complex product upgrading and the additional costs for the higher electricity and hydrogen demand.

Furthermore, the CO₂ footprints of the wood-based SNG and FT diesel were determined. The CO₂ footprint for wood-based SNG is 0.027 kgCO₂e/kWh_{SNG}, and it is 0.269 kgCO₂e/l_{FT diesel} for wood-based FT diesel, which are more than 90% lower than their fossil counterparts. Compared to renewable alternatives, wood-based SNG and FT diesel are among the products with the lowest CO₂ footprint. The energy-related comparison of the two biomass-based products shows hardly any differences, since the higher consumption of electricity and hydrogen due to the use of green electricity is not significant. Moreover, it has to be mentioned that if the additional CO₂ capturing in both process routes were considered, the production of wood-based SNG and FT diesel would create a CO₂ sink.

Moreover, six integration scenarios for producing biomass-based SNG and FT diesel were investigated to find possible applications in the Austrian energy system. The biomass potential analysis, based on several literature studies, showed that, in 2050, an additional biomass potential of 185 PJ/a would be available. Hence, a potential for biomass-based SNG of 120 PJ/a or biomass-based FT diesel of 67.5 PJ/a can be assumed. The scenarios demonstrated the various application possibilities for biomass-based SNG and FT diesel. Therein, the sectoral change of gross value added and the CO₂ reduction potential were calculated to investigate the economic and ecological impacts. The most promising applications for biomass-based FT diesel and SNG are summarized below:

- SNG use for covering electricity peak loads in the energy sector → helps to prevent blackouts and to decouple the domestic electricity market from the gas market;
- SNG use in the industry sector for the provision of high-temperature heat → economically feasible and a good option, when no waste heat or heat pumps can be used;
- FT diesel in heavy-duty traffic → economically feasible and an excellent option to facilitate the defossilization of inland navigation, railway, freight transport, agriculture, and forestry.

Further, the use of biomass-based FT diesel in private and public transport, as well as the use of biomass-based SNG in the private and public heat provision sector, could

be an additional economically favorable option to accelerate the transition phase towards defossilization of these sectors. However, the sectoral view neglects the fact that individual enterprises and households certainly experience different economic and ecological impacts from transitioning to sustainable FT diesel and SNG, since the used energy sources and energy quantities can vary significantly.

To accelerate the rollout of the two biomass-based technologies, regulatory measures must be applied. The associated EU directive on the expansion of renewable energy sources in the EU (RED II) [63] already set mandatory quotas for the share of advanced biofuels, such as FT diesel, until 2030. Furthermore, the Austrian Renewable Energy Expansion Act [64] specifies that a fixed annual amount of biomethane, such as SNG, must be fed into the grid by 2030. A further increase in quotas with associated financial support measures would help to accelerate the roll-out process.

Besides determining the energetic efficiency, production costs, and CO₂ footprint, further sustainability indicators like the acidification potential, ground air quality, eutrophication, land use, payback time, or changes in gross domestic products should be investigated. Future research should focus on validating the calculated sustainability indicators after the scale-up to the demonstration plant. The process simulation focused mostly on each unit's mass and energy balances to define the main streams of the whole process unit. More detailed simulation models based on experimental test rigs can help to refine the whole process chain. In addition, future research should focus on biomass price changes caused by greater demand. The biomass price depends very much on the market situation and is dominated by supply and demand. Therefore, an increase in biomass use must be expected to lead to an increase in biomass price, unless regulatory measures follow. The continuous improvement of the sustainability criteria for the use of biomass must contribute to sustainable agriculture and forestry in Austria.

Summing up, the extensive investigation of biomass-based SNG and FT diesel production showed significant potential and enables the implementation of different defossilization strategies in the Austrian energy system. Nevertheless, the technical feasibility must first be tested within the framework of long-term trials in the planned demonstration plant.

Supplementary Materials: Supplementary data to this article can be found online at <https://www.mdpi.com/article/10.3390/en16166097/s1>. References [65–130] are cited in the Supplementary Materials.

Author Contributions: Conceptualization, M.H., A.B., F.B., M.V., S.P. and H.H.; methodology, M.H., A.B., F.B. and S.P.; validation, M.H., A.B. and S.P.; investigation, M.H., A.B., F.B. and S.P.; resources, M.H., A.B., S.P. and F.B.; writing—original draft, M.H. and A.B.; writing—review and editing, F.B., M.V., S.P., S.M. and H.H.; visualization, M.H. and A.B.; supervision, S.M. and H.H.; project administration, F.B. and H.H.; funding acquisition, F.B. and H.H. All authors have read and agreed to the published version of the manuscript.

Funding: Open Access Funding by TU Wien. The present work contains results of the project “Reallabor zur Herstellung von FT-Treibstoffen und SNG aus Biomasse und biogenen Reststoffen für die Land- und Forstwirtschaft” (101471), which is being conducted within the “DaFNE” research program funded and processed by the Federal Ministry for Sustainability and Tourism.

Data Availability Statement: Selected data that support the findings of this study are available from the corresponding author, M. Hammerschmid, upon reasonable request.

Acknowledgments: The authors acknowledge TU Wien Bibliothek for financial support through its Open Access Funding Programme.

Conflicts of Interest: The authors declare no conflict of interest.

Abbreviations

AC	activated carbon
AT	Austria
C ₁ –C ₃	gaseous short-chain hydrocarbons recycled in Fischer–Tropsch tailgas
C ₄ –C ₉	naphtha fraction (raw product for producing gasoline)
C ₁₀ –C ₁₉	middle distillate fraction (after upgrading equivalent to diesel)
C ₁₀₊	middle distillate fraction and long-chain waxes
C ₂₀₊	long-chain waxes
CH ₄	methane
CO	carbon monoxide
CO ₂	carbon dioxide
CO _{2e}	carbon dioxide equivalent
DE	Germany
DFB	dual fluidized bed
EC	economic competitiveness
FAME	fatty acid methyl ester
FT	Fischer–Tropsch
GEMIS	software tool with database for life cycle analysis
GVA	gross value added
H ₂	hydrogen
H ₂ O	water
H ₂ S	hydrogen sulfide
HCV	heavy commercial vehicles
HEFA	hydroprocessed ester and fatty acid
IEA	International Energy Agency
IPSEpro 8.0	software tool for process simulation from company SimTech GmbH
JP	Japan
LCOP	levelized costs of products
LCV	light commercial vehicles
MP	market prices
NH ₃	ammonia
O&M	operation and maintenance
PFD	process flow diagram
PG	product gas
PV	photovoltaic
raw-SNG	synthetic natural gas after methanation unit and before upgrading
RES	renewable energy sources
RME	rapeseed methyl ester
SE	Sweden
SNG	synthetic natural gas
TH	Thailand
TSA	temperature swing adsorption
ZnO	zinc oxide
Symbols:	
%	percent
CDF	cumulative discount factor
CEPCI ₂₀₁₉	Chemical Engineering Plant Cost Index based on 2019 or 2022
CEPCI ₂₀₂₂	Chemical Engineering Plant Cost Index based on 2019 or 2022
CEPCI _{base year}	Chemical Engineering Plant Cost Index based on base year of literature
C _{eq,base}	equipment costs based on base year and base scale of literature
C _{eq,design}	overall costs for installed equipment based on 2019 or 2022
CO _{2e,red,sector i}	carbon dioxide reduction potential in sector i
CO _{2e,tot,sector i}	total carbon dioxide equivalent in sector i
E	annual expenditures
EC _{sector i}	economic competitiveness in sector i based on 2019 or 2022

$E_{gas/diesel,sector\ i}$	substituted annual fossil gas or diesel demand in sector i
$FP_{fos.gas/diesel}$	carbon dioxide equivalent footprint of fossil natural gas or diesel
$FP_{SNG/FTdiesel}$	carbon dioxide equivalent footprint of biomass-based SNG or FT diesel
$GVA_{total,sector\ i}$	total gross value added in sector i based on 2019 or 2022
i	interest rate
I_0	total capital investment costs of plant
l	liter
$LCOP$	levelized costs of products
$LCOP_{SNG/FTdiesel}$	levelized costs of products for SNG or FT diesel based on 2019 or 2022
l_{Diesel}	liters of diesel
$MP_{fos.gas/diesel}$	market prices of fossil natural gas or diesel in 2019 or 2022
$M_{t,main\ prod.}$	annual quantity of the produced main product
MW	megawatt
MWh	megawatt hours
MWh_{th}	megawatt hours of thermal fuel power
MWh_{SNG}	megawatt hours of synthetic natural gas
n	plant lifetime
PJ/a	petajoule per year
r	scaling factor
$R_{sec.prod.}$	annual revenues of secondary products
S_{base}	base scale
S_{design}	desired scale
Z	overall installation factor

References

1. European Union. The European Green Deal. 2019. Available online: https://commission.europa.eu/system/files/2019-12/european-green-deal-communication_de.pdf (accessed on 2 July 2023).
2. Anderl, M.; Bartel, A.; Frei, E.; Gugele, B.; Gössl, M.; Mayer, S.; Heinfellner, H.; Heller, C.; Heuber, A.; Köther, T.; et al. *Klimaschutzbericht 2022*; Federal Environmental Agency: Vienna, Austria, 2022. Available online: <https://www.umweltbundesamt.at/fileadmin/site/publikationen/rep0816.pdf> (accessed on 2 July 2023).
3. Kaltschmitt, M.; Hartmann, H.; Hofbauer, H. *Energie aus Biomasse: Grundlagen, Techniken und Verfahren*, 3rd ed.; Springer Vieweg: Berlin/Heidelberg, Germany, 2016. [CrossRef]
4. Schmid, J.C.; Benedikt, F.; Fuchs, J.; Mauerhofer, A.M.; Müller, S.; Hofbauer, H. Syngas for biorefineries from thermochemical gasification of lignocellulosic fuels and residues—5 years' experience with an advanced dual fluidized bed gasifier design. *Biomass Convers. Biorefinery* **2021**, *11*, 2405–2442. [CrossRef]
5. Benedikt, F.; Schmid, J.C.; Fuchs, J.; Mauerhofer, A.M.; Müller, S.; Hofbauer, H. Fuel flexible gasification with an advanced 100 kW dual fluidized bed steam gasification pilot plant. *Energy* **2018**, *164*, 329–343. [CrossRef]
6. Bartik, A.; Benedikt, F.; Fuchs, J.; Hofbauer, H.; Müller, S. Experimental investigation of hydrogen-intensified synthetic natural gas production via biomass gasification: A technical comparison of different production pathways. *Biomass Convers. Biorefinery* **2023**. [CrossRef]
7. Thunman, H.; Seemann, M.; Berdugo Vilches, T.; Maric, J.; Pallares, D.; Ström, H.; Berndes, G.; Knutsson, P.; Larsson, A.; Breitholtz, C.; et al. Advanced biofuel production via gasification—Lessons learned from 200 man-years of research activity with Chalmers' research gasifier and the GoBiGas demonstration plant. *Energy Sci. Eng.* **2018**, *6*, 6–34. [CrossRef]
8. Cleantech Cluster. Erstes Produkt der Fischer-Tropsch-Pilotanlage in Wien-Simmering kommt in Flottentest zum Einsatz. 2023. Available online: <https://www.cleantech-cluster.at/partnerunternehmen-im-ctc/ctc-partnernews-umwelt/detail/news/erstes-produkt-der-fischer-tropsch-pilotanlage-in-wien-simmering-kommt-in-flottentest-zum-einsatz> (accessed on 28 May 2023).
9. Kadlez, D.; Benedikt, F.; Bartik, A.; Müller, S.; Hofbauer, H.; Karel, T.; Binder, M.; Huber, M.; Egger, A.; Hochstätger, D.; et al. First results of mass and energy balances of a 1 MW advanced dual fluidized bed steam gasification demonstration plant. In Proceedings of the Central European Biomass Conference, Graz, Austria, 18–20 January 2023.
10. Kuba, M.; Karel, T.; Fürsatz, K.; Binder, M.; Hannl, T.; Huber, M.; Hochstätger, D.; Egger, A.; Weber, G.; Haslinger, W.; et al. Second generation biomass gasification: The Syngas Platform Vienna—Current status and outlook. In Proceedings of the Central European Biomass Conference, Graz, Austria, 18–20 January 2023.
11. Hofbauer, H.; Mauerhofer, A.M.; Benedikt, F.; Hammerschmid, M.; Bartik, A.; Veress, M.; Haas, R.; Siebenhofer, M.; Resch, G. *Reallabor zur Herstellung von Holzdiezel und Holzgas aus Biomasse und Biogenen Reststoffen für die Land- und Forstwirtschaft*; TU Wien: Vienna, Austria, 2020; Available online: <https://dafne.at/projekte/ftsng-reallabor> (accessed on 2 July 2023).
12. Fuchs, J.; Schmid, J.C.; Müller, S.; Hofbauer, H. Dual fluidized bed gasification of biomass with selective carbon dioxide removal and limestone as bed material: A review. *Renew. Sustain. Energy Rev.* **2019**, *107*, 212–231. [CrossRef]

13. Schmid, M.; Beirow, M.; Schweitzer, D.; Waizmann, G.; Spörl, R.; Scheffknecht, G. Product gas composition for steam-oxygen fluidized bed gasification of dried sewage sludge, straw pellets and wood pellets and the influence of limestone as bed material. *Biomass Bioenergy* **2018**, *117*, 71–77. [CrossRef]
14. Schmid, M.; Hafner, S.; Scheffknecht, G. Experimental Parameter Study on Synthesis Gas Production by Steam-Oxygen Fluidized Bed Gasification of Sewage Sludge. *Appl. Sci.* **2021**, *11*, 579. [CrossRef]
15. Schweitzer, D.; Beirow, M.; Gredinger, A.; Armbrust, N.; Waizmann, G.; Dieter, H.; Scheffknecht, G. Pilot-Scale Demonstration of Oxy-SER steam Gasification: Production of Syngas with Pre-Combustion CO₂ Capture. *Energy Procedia* **2016**, *86*, 56–68. [CrossRef]
16. Karl, J.; Pröll, T. Steam gasification of biomass in dual fluidized bed gasifiers: A review. *Renew. Sustain. Energy Rev.* **2018**, *98*, 64–78. [CrossRef]
17. Kuba, M.; Benedikt, F.; Fürsatz, K.; Fuchs, J.; Demuth, M.; Aichernig, C.; Arpa, L.; Hofbauer, H. Integration of dual fluidized bed steam gasification into the pulp and paper industry. *Biomass Convers. Biorefinery* **2021**. [CrossRef]
18. Loipersböck, J.; Weber, G.; Rauch, R.; Hofbauer, H. Developing an adsorption-based gas cleaning system for a dual fluidized bed gasification process. In Proceedings of the International Conference on Polygeneration Strategies, Vienna, Austria, 18–20 November 2019; Hofbauer, H., Müller, S., Eds.; TU Wien: Vienna, Austria, 2019. [CrossRef]
19. Bardolf, R. Optimierung eines Produktgaswäschers bei der Biomassedampfergasung im Zweibettwirbelschichtverfahren. Ph.D. Thesis, TU Wien, Vienna, Austria, 2017.
20. Rehling, B. Development of the 1MW Bio-SNG Plant, Evaluation on Technological and Economical Aspects and Upscaling Considerations. Ph.D. Thesis, TU Wien, Vienna, Austria, 2012.
21. Schildhauer, T.J.; Biollaz, S.M.A. Reactors for Catalytic Methanation in the Conversion of Biomass to Synthetic Natural Gas (SNG). *Chimia* **2015**, *69*, 603–607. [CrossRef] [PubMed]
22. Seemann, M.C.; Schildhauer, T.J.; Biollaz, S.M.A. Fluidized Bed Methanation of Wood-Derived Producer Gas for the Production of Synthetic Natural Gas. *Ind. Eng. Chem. Res.* **2010**, *49*, 7034–7038. [CrossRef]
23. Gruber, H. Synthesis and Refining of Biomass-Derived Fischer-Tropsch Paraffin Waxes. Ph.D. Thesis, TU Wien, Vienna, Austria, 2020.
24. Sauciu, A.; Abosteif, Z.; Weber, G.; Potetz, A.; Rauch, R.; Hofbauer, H.; Schaub, G.; Dumitrescu, L. Influence of operating conditions on the performance of biomass-based Fischer-Tropsch synthesis. *Biomass Convers. Biorefinery* **2012**, *2*, 253–263. [CrossRef]
25. Guilera, J.; Díaz-López, J.A.; Berenguer, A.; Biset-Peiró, M.; Andreu, T. Fischer-Tropsch synthesis: Towards a highly-selective catalyst by lanthanide promotion under relevant CO₂ syngas mixtures. *Appl. Catal. A Gen.* **2022**, *629*, 118423. [CrossRef]
26. Müller, S.; Groß, P.; Rauch, R.; Zweiler, R.; Aichernig, C.; Fuchs, M.; Hofbauer, H. Production of diesel from biomass and wind power—Energy storage by the use of the Fischer-Tropsch process. *Biomass Convers. Biorefinery* **2018**, *8*, 275–282. [CrossRef]
27. Rauch, R.; Hrbek, J.; Hofbauer, H. Biomass gasification for synthesis gas production and applications of the syngas. *WIREs Energy Environ.* **2014**, *3*, 343–362. [CrossRef]
28. Thunman, H.; Gustavsson, C.; Larsson, A.; Gunnarsson, I.; Tengberg, F. Economic assessment of advanced biofuel production via gasification using cost data from the GoBiGas plant. *Energy Sci. Eng.* **2019**, *7*, 217–229. [CrossRef]
29. Neuling, U.; Kaltschmitt, M. Techno-economic and environmental analysis of aviation biofuels. *Fuel Process. Technol.* **2018**, *171*, 54–69. [CrossRef]
30. Jungmeier, G.; Canella, L.; Pucker-Singer, J.; Beermann, M. *Geschätzte Treibhausgasemissionen und Primärenergieverbrauch in der Lebenszyklusanalyse von Pkw-basierten Verkehrssystemen*; Joanneum Research Forschungsgesellschaft: Graz, Austria, 2019.
31. Österreichische Vereinigung für das Gas- und Wasserfach. *Richtlinie G B210—Gasbeschaffenheit: Gas Quality*; Österreichische Vereinigung für das Gas- und Wasserfach: Vienna, Austria, 2021; Available online: https://shop.austrian-standards.at/action/de/public/details/697809/OEVGW_G_B210_2021_06 (accessed on 2 July 2023).
32. *DIN EN 15940; Kraftstoffe—Paraffinischer Dieselmotortreibstoff aus Synthese oder Hydrierungsverfahren—Anforderungen und Prüfverfahren*. Beuth Verlag: Berlin, Germany, 2019. Available online: <https://www.beuth.de/de/norm/din-en-15940/309170058> (accessed on 2 July 2023).
33. Österreichischer Biomasseverband. *Basisdaten 2019 Bioenergie*; Österreichischer Biomasseverband: Vienna, Austria, 2019; Available online: https://www.biomasseverband.at/wp-content/uploads/Basisdaten_Bioenergie_2019.pdf (accessed on 2 July 2023).
34. Dißauer, C.; Rehling, B.; Strasser, C. *Machbarkeitsuntersuchung Methan aus Biomasse*; Bioenergy 2020+: Wieselburg, Austria, 2019; Available online: https://www.gruenes-gas.at/assets/Uploads/BioEnergy2020+_Machbarkeitsuntersuchung_Methan_aus_Biomasse.pdf (accessed on 2 July 2023).
35. Hammerschmid, M.; Konrad, J.; Werner, A.; Popov, T.; Müller, S. ENECO₂Calc—A Modeling Tool for the Investigation of Energy Transition Paths toward Climate Neutrality within Municipalities. *Energies* **2022**, *15*, 7162. [CrossRef]
36. Kranzl, L. *Bioenergy—A Key Option within all Energy Sectors*. VO Economic Perspectives of Renewable Energy Systems; Energy Economics Group (EEG), TU Wien: Vienna, Austria, 2020.
37. Kranzl, L.; Haas, R.; Kalt, G.; Diesenreiter, F.; Eltrop, L.; König, A.; Makkonen, P. *Strategien zur Optimalen Erschließung der Biomassepotenziale in Österreich bis zum Jahr 2050 mit dem Ziel einer Maximalen Reduktion an Treibhausgasemissionen*; Energy Economics Group (EEG), TU Wien: Vienna, Austria, 2008.
38. Alamia, A.; Gardarsdóttir, Ö.S.; Larsson, A.; Normann, F.; Thunman, H. Efficiency Comparison of Large-Scale Standalone, Centralized, and Distributed Thermochemical Biorefineries. *Energy Technol.* **2017**, *5*, 1435–1448. [CrossRef]

39. Förtsch, D.; Pabst, K.; Groß-Hardt, E. The product distribution in Fischer–Tropsch synthesis: An extension of the ASF model to describe common deviations. *Chem. Eng. Sci.* **2015**, *138*, 333–346. [CrossRef]
40. Pratschner, S.; Hammerschmid, M.; Müller, F.J.; Müller, S.; Winter, F. Simulation of a Pilot Scale Power-to-Liquid Plant Producing Synthetic Fuel and Wax by Combining Fischer–Tropsch Synthesis and SOEC. *Energies* **2022**, *15*, 4134. [CrossRef]
41. Hammerschmid, M.; Rosenfeld, D.C.; Bartik, A.; Benedikt, F.; Fuchs, J.; Müller, S. Methodology for the Development of Virtual Representations within the Process Development Framework of Energy Plants: From Digital Model to Digital Predictive Twin—A Review. *Energies* **2023**, *16*, 2641. [CrossRef]
42. Konstantin, P. *Praxisbuch Energiewirtschaft: Energieumwandlung, -Transport und -Beschaffung, Übertragungsnetzausbau und Kernenergieausstieg*, 4th ed.; VDI-Buch; Springer Vieweg: Berlin/Heidelberg, Germany, 2017; ISBN 978-3-662-49823-1.
43. Resch, G.; Kranzl, L.; Faninger, G.; Geipel, J. Block 1: Introduction: Energy & climate challenge and basics of economic assessment. In *VO Economic Perspectives of Renewable Energy Systems*; Energy Economics Group (EEG), TU Wien: Vienna, Austria, 2020.
44. Kost, C.; Shammugam, S.; Jülch, V.; Nguyen, H.-T.; Schlegl, T. *Stromgestehungskosten Erneuerbare Energien*; Fraunhofer-Institut für solare Energiesysteme (ISE): Freiburg, Germany, 2018.
45. Veress, M. Optimization of a Process Concept for the Industrial Production of Bio-SNG from Low-Grade Fuels. Master’s Thesis, TU Wien, Vienna, Austria, 2020.
46. Peters, M.S.; Timmerhaus, K.D. *Plant Design and Economics for Chemical Engineers*, 4th ed.; McGraw-Hill Chemical Engineering Series; McGraw-Hill: New York, NY, USA, 1991; ISBN 0-07-049613-7.
47. Wulf, C.; Kaltschmitt, M. Hydrogen Supply Chains for Mobility—Environmental and Economic Assessment. *Sustainability* **2018**, *10*, 1699. [CrossRef]
48. Lichtblau, G.; Pölz, W.; Stix, S.; Winter, R. *Ökobilanzen Ausgewählter Biotreibstoffe: Projekt proVISION*; Umweltbundesamt Österreich: Vienna, Austria, 2012; Available online: <https://www.umweltbundesamt.at/fileadmin/site/publikationen/rep0360.pdf> (accessed on 2 July 2023).
49. Federal Environmental Agency Austria. *Berechnung von Treibhausgas (THG)-Emissionen verschiedener Energieträger*; FEA: Vienna, Austria, 2022. Available online: <https://secure.umweltbundesamt.at/co2mon/co2mon.html> (accessed on 20 March 2023).
50. Federal Environmental Agency Germany. *ProBas—Prozessorientierte Basisdaten für Umweltmanagementsysteme*; FEA Germany: Dessau-Roßlau, Germany, 2015. Available online: <https://www.probas.umweltbundesamt.de/php/index.php> (accessed on 2 July 2023).
51. INAS GmbH, Version 4.94. Globales Emissions-Modell Integrierter Systeme (GEMIS). Internationales Institut für Nachhaltigkeitsanalysen und -Strategien: Freiburg, Germany, 2018.
52. Gollner, M. *Gesamtenergiebilanz Österreich 1970 bis 2021*; Statistik Austria: Vienna, Austria, 2022; Available online: https://www.statistik.at/web_de/statistiken/energie_umwelt_innovation_mobilitaet/energie_und_umwelt/energie/energiebilanzen/index.html (accessed on 2 July 2023).
53. Resch, G.; Burgholzer, B.; Totschnig, G.; Lettner, G.; Auer, H.; Geipel, J.; Haas, R. *Stromzukunft Österreich 2030: Analyse der Erfordernisse und Konsequenzen eines Ambitionierten Ausbaus von Erneuerbaren Energien*; Energy Economics Group (EEG), TU Wien: Vienna, Austria, 2017; Available online: <https://www.igwindkraft.at/mmedia/download/2017.07.10/1499698755049626.pdf> (accessed on 2 July 2023).
54. Kranzl, L.; Müller, A.; Büchele, R. *Wärmezukunft 2050: Anforderungen an die Gebäudesanierung: Endbericht*; Energy Economics Group (EEG), TU Wien: Vienna, Austria, 2018; Available online: <https://www.igwindkraft.at/mmedia/download/2018.02.05/1517825327514183.pdf> (accessed on 2 July 2023).
55. Baumann, M.; Fazeni-Fraisl, K.; Kienberger, T.; Nagovnak, P.; Pauritsch, G.; Rosenfeld, D.; Sejkora, C.; Tichler, R. *Erneuerbares Gas in Österreich 2040: Quantitative Abschätzung von Nachfrage und Angebot*; Bundesministerium für Klimaschutz, Umwelt, Energie, Mobilität, Innovation und Technologie: Vienna, Austria, 2021. Available online: <https://www.bmk.gv.at/themen/energie/publikationen/erneuerbares-gas-2040.html> (accessed on 2 July 2023).
56. Terlouw, W.; Peters, D.; van Tilburg, J.; Schimmel, M.; Berg, T.; Cihlar, J.; Ur Rehman Mir, G.; Spöttle, M.; Staats, M.; Lejaretta, A.V.; et al. *Gas for Climate: The Optimal Role for Gas in a Net-Zero Emissions Energy System*; Navigant: Utrecht, The Netherlands, 2019; Available online: <https://gasforclimate2050.eu/wp-content/uploads/2020/03/Navigant-Gas-for-Climate-The-optimal-role-for-gas-in-a-net-zero-emissions-energy-system-March-2019.pdf> (accessed on 2 July 2023).
57. Götz, M.; Lefebvre, J.; Mörs, F.; Koch, A.M.; Graf, F.; Bajohr, S.; Reimert, R.; Kolb, T. Renewable Power-to-Gas: A technological and economic review. *Renew. Energy* **2016**, *85*, 1371–1390. [CrossRef]
58. Maniatis, K.; Landäl, I.; Waldheim, L.; van den Heuvel, E.; Kalligeros, S. *Final Report—Building up the Future: Sub Group on Advanced Biofuels—Sustainable Transport Forum*; European Commission: Luxembourg, 2017; ISBN 978-92-79-69010-5.
59. Pratschner, S.; Hammerschmid, M.; Müller, S.; Winter, F. Converting CO₂ and H₂O into Fischer–Tropsch Products—A Techno-economic assessment. In Proceedings of the 27th International Symposium for Chemical Reaction Engineering—ISCRE 27, Quebec City, QC, Canada, 11–14 June 2023.
60. Jungmeier, G. Umweltbilanz von E-Fuels—Vergleich mit anderen Treibstoffen im Lebenszyklus. In Proceedings of the ÖGEW/DGMK Onlinekonferenz „Innovative Energieversorgung“, Graz, Austria, 13 November 2020; Available online: <https://www.wko.at/site/oegew/veranstaltungen/umweltbilanz-von-e-fuels.pdf> (accessed on 2 July 2023).

61. Aichmayer, S.; Mitterhuemer, R.; Winter, R. *Biokraftstoffe im Verkehrssektor 2021*; Bundesministerium für Klimaschutz, Umwelt, Energie, Mobilität, Innovation und Technologie: Vienna, Austria, 2021; Available online: https://www.biokraft-austria.at/media/18119/biokraftstoffbericht_2021.pdf (accessed on 2 July 2023).
62. Pratschner, S.; Hammerschmid, M.; Müller, S.; Winter, F. CO₂ Footprint of Fischer-Tropsch Products produced by a Power-to-Liquid Plant. In Proceedings of the 15th Mediterranean Congress of Chemical Engineering—MECCE 2023, Barcelona, Spain, 30 May–2 June 2023.
63. European Union. Directive (EU) 2018/2001 of the European Parliament and of the Council of 11 December 2018 on the Promotion of the Use of Energy from Renewable Sources, RED II. *Off. J. Eur. Union* **2018**, L 328/82. Available online: <https://eur-lex.europa.eu/legal-content/DE/TXT/?qid=1575559881403&uri=CELEX:32018L2001> (accessed on 12 May 2021).
64. Bundesrepublik Österreich. Erneuerbaren-Ausbau-Gesetz, EAG. 2021. Available online: https://www.parlament.gv.at/PAKT/VHG/XXVII/I/I_00733/index.shtml (accessed on 12 August 2021).
65. Ringhofer, T. Evaluierung des Biomassetrockners der Kraft-Wärme-Kopplungsanlage Oberwart. Bachelor's Thesis, TU Wien, Vienna, Austria, 2011.
66. Müller, S. Hydrogen from Biomass for Industry—Industrial Application of Hydrogen Production Based on Dual Fluid Gasification. Ph.D. Thesis, TU Wien, Vienna, Austria, 2013.
67. Benedikt, F.; Fuchs, J.; Schmid, J.C.; Müller, S.; Hofbauer, H. Advanced dual fluidized bed steam gasification of wood and lignite with calcite as bed material. *Korean J. Chem. Eng.* **2017**, *34*, 2548–2558. [CrossRef]
68. Benedikt, F.; Müller, S.; Hofbauer, H. 1 MW scale-up of the advanced fuel flexible dual fluidized bed steam gasification process by process simulation. In Proceedings of the ICPS19—International Conference on Polygeneration Strategies, Vienna, Austria, 18–20 November 2019; ISBN 978-3-9503671-1-9.
69. Wolfesberger, U. Profiling Tar Behavior in Dual Fluidized Bed Biomass Steam Gasification. Ph.D. Thesis, TU Wien, Vienna, Austria, 2013.
70. Hofbauer, H.; Rauch, R.; Bosch, K.; Koch, R.; Aichernig, C. Biomass CHP plant Güssing—A success story. In Proceedings of the Pyrolysis and Gasification of Biomass and Waste—Expert Meeting, Strasbourg, France, 30 September–1 October 2002.
71. Pröll, T.; Siefert, I.G.; Friedl, A.; Hofbauer, H. Removal of NH₃ from Biomass Gasification Producer Gas by Water Condensing in an Organic Solvent Scrubber. *Ind. Eng. Chem. Res.* **2005**, *44*, 1576–1584. [CrossRef]
72. Stidl, M. Prozesssimulation von spezifischen Anwendungsfällen der Zweibett-Wirbelschicht-Dampfvergasungs-Technologie für die Papier- und Zellstoffindustrie. Ph.D. Thesis, TU Wien, Vienna, Austria, 2012.
73. Sadegh, A.M.; Worek, W.M. *Marks' Standard Handbook for Mechanical Engineers*, 12th ed.; McGraw-Hill Education: New York, NY, USA, 2018; ISBN 9781259588518.
74. Broer, K.M.; Woolcock, P.J.; Johnston, P.A.; Brown, R.C. Steam/oxygen gasification system for the production of clean syngas from switchgrass. *Fuel* **2015**, *140*, 282–292. [CrossRef]
75. Bartik, A.; Fuchs, J.; Pacholik, G.; Föttinger, K.; Hofbauer, H.; Müller, S.; Benedikt, F. Experimental investigation on the methanation of hydrogen-rich syngas in a bubbling fluidized bed reactor utilizing an optimized catalyst. *Fuel Process. Technol.* **2022**, *237*, 107402. [CrossRef]
76. Li, K.; Leigh, W.; Feron, P.; Yu, H.; Tade, M. Systematic study of aqueous monoethanolamine (MEA)-based CO₂ capture process: Techno-economic assessment of the MEA process and its improvements. *Appl. Energy* **2016**, *165*, 648–659. [CrossRef]
77. Günther, L. *Biomethanreinigung mit der Drucklosen Wäsche zur Herstellung von Biomethan und Kohlendioxid*. Fachtagung "Innogas"; DGE GmbH Presentation: Wittenberg, Germany, 2007; Available online: <https://www.dge-wittenberg.de/vortraege/DGE%20Fachtagung%20WB%202006.pdf> (accessed on 2 July 2023).
78. Neagu, M.; Cursaru, D.L. Technical and economic evaluations of the triethylene glycol regeneration processes in natural gas dehydration plants. *J. Nat. Gas Sci. Eng.* **2017**, *37*, 327–340. [CrossRef]
79. Kidnay, A.J.; Parrish, W.R.; McCartney, D.G. *Fundamentals of Natural Gas Processing*; CRC Press: Boca Raton, FL, USA, 2019; ISBN 9780429464942.
80. Gruber, H.; Groß, P.; Rauch, R.; Reichhold, A.; Zweiler, R.; Aichernig, C.; Müller, S.; Ataimisch, N.; Hofbauer, H. Fischer-Tropsch products from biomass-derived syngas and renewable hydrogen. *Biomass Convers. Biorefinery* **2019**, *48*, 22. [CrossRef]
81. De Klerk, A. *Fischer-Tropsch Refining*; Wiley-VCH Verlag GmbH & Co. KGaA: Weinheim, Germany, 2011; ISBN 9783527635603.
82. Schädel, B.T.; Duisberg, M.; Deutschmann, O. Steam reforming of methane, ethane, propane, butane, and natural gas over a rhodium-based catalyst. *Catal. Today* **2009**, *142*, 42–51. [CrossRef]
83. Ali, S.; Sørensen, K.; Nielsen, M.P. Modeling a novel combined solid oxide electrolysis cell (SOEC)—Biomass gasification renewable methanol production system. *Renew. Energy* **2020**, *154*, 1025–1034. [CrossRef]
84. Clariant International Ltd. *Catalysts and Adsorbents for Syngas*; Clariant International Ltd.: Muttenz, Switzerland, 2017; Available online: <https://de.scribd.com/document/477562978/Clariant-Brochure-Catalysts-And-Adsorbents-For-Syngas-2017-EN-1> (accessed on 2 July 2023).
85. Petersen, A.M.; Chireshe, F.; Okoro, O.; Gorgens, J.; van Dyk, J. Evaluating refinery configurations for deriving sustainable aviation fuel from ethanol or syncrude. *Fuel Process. Technol.* **2021**, *219*, 106879. [CrossRef]
86. Fahim, M.A. *Fundamentals of Petroleum Refining*; Elsevier Science & Technology: Oxford, UK, 2010; ISBN 978-0-444-52785-1.
87. De Klerk, A. Can Fischer-Tropsch Syncrude Be Refined to On-Specification Diesel Fuel? *Energy Fuels* **2009**, *23*, 4593–4604. [CrossRef]

88. Kang, J.; Ma, W.; Keogh, R.A.; Shafer, W.D.; Jacobs, G.; Davis, B.H. Hydrocracking and Hydroisomerization of n-Hexadecane, n-Octacosane and Fischer–Tropsch Wax Over a Pt/SiO₂–Al₂O₃ Catalyst. *Catal. Lett.* **2012**, *142*, 1295–1305. [CrossRef]
89. Murali, C.; Voolapalli, R.K.; Ravichander, N.; Gokak, D.T.; Choudary, N.V. Trickle bed reactor model to simulate the performance of commercial diesel hydrotreating unit. *Fuel* **2007**, *86*, 1176–1184. [CrossRef]
90. Busca, G. *Heterogeneous Catalytic Materials*; Elsevier: Amsterdam, The Netherlands, 2014; ISBN 978-0-444-59524-9.
91. Mauerhofer, A.M.; Schmid, J.C.; Benedikt, F.; Fuchs, J.; Müller, S.; Hofbauer, H. Dual fluidized bed steam gasification: Change of product gas quality along the reactor height. *Energy* **2019**, *173*, 1256–1272. [CrossRef]
92. Schmid, J.C. Technoökonomische Fallstudien als Entscheidungsunterstützung für das Strategische Management. Master's Thesis, Fachhochschule Burgenland, Eisenstadt, Austria, 2016.
93. E-Control. *Gaspreisentwicklung*; E-Control: Vienna, Austria, 2022. Available online: <https://www.e-control.at/statistik/gas/marktstatistik/preisentwicklung> (accessed on 10 August 2022).
94. E-Control. *Strom- und Gaspreise in Österreich*; E-Control: Vienna, Austria, 2022; Available online: <https://www.e-control.at/preismonitor> (accessed on 10 August 2022).
95. Bundesministerium für Klimaschutz, Umwelt, Energie, Mobilität, Innovation und Technologie. Treibstoffpreise aktuell. Bundesministerium für Klimaschutz, Umwelt, Energie, Mobilität, Innovation und Technologie: Vienna, Austria, 2022. Available online: https://www.bmk.gv.at/themen/energie/preise/aktuelle_preise.html (accessed on 15 October 2022).
96. *Deutsche Börse*; Diesel: Frankfurt, Germany, 2022; Available online: <https://www.boerse.de/charts/Dieselpreis/XC0009677813> (accessed on 15 October 2022).
97. Statistik Austria. Erzeugerpreisindex Produzierender Bereich—Österreich. Vienna, Austria; 2022. Available online: <https://www.statistik.at/statistiken/volkswirtschaft-und-oeffentliche-finanzen/preise-und-preisindizes/erzeugerpreisindex-produzierender-bereich> (accessed on 10 August 2022).
98. Meehan, J. Europe Monoethanolamine Prices Move Down on Import Pressure. 2013. Available online: <https://www.icis.com/explore/resources/news/2013/06/19/9680122/europe-monoethanolamine-prices-move-down-on-import-pressure/> (accessed on 13 December 2019).
99. Billig, E. DBFZ Report Nr. 26. Ph.D. Thesis, Universität Leipzig, Helmholtz-Zentrum für Umweltforschung, Leipzig, Germany, 2016.
100. Thrän, D.; Pfeiffer, D. Methodenhandbuch: Stoffstromorientierte Bilanzierung der Klimagaseffekte. *Energetische Biomassenutzung* **2013**, *2013*, 4.
101. European Energy Exchange AG (EEX). *EEX EUA Spot Market—CO₂ Emission Allowances*; EEX: Leipzig, Germany, 2022; Available online: <https://www.eex.com/de/marktdaten/umweltprodukte/spot> (accessed on 15 October 2022).
102. E-Control. *Strompreisentwicklung*; E-Control: Vienna, Austria, 2022; Available online: <https://www.e-control.at/statistik/strom/marktstatistik/preisentwicklung> (accessed on 10 August 2022).
103. Godula-Jopek, A.; Stolten, D. *Hydrogen Production: By Electrolysis*, 1st ed.; Wiley-VCH: Weinheim, Germany, 2015; ISBN 9783527676507.
104. Goritschnig, M.; Kreuter, K.; Novakovits, P.; Pomper, M.; Zweiler, R. *Winddiesel_klienIF: Untersuchung des Lastwechselverhaltens eines Slurryreaktors zur Einkopplung von H₂ und Produktion von FT-Diesel*. Güssing Energy Technologies. 2017. Available online: https://www.winddiesel.at/images/Downloads/13003-BB008a_Winddiesel_kurzfassung.pdf (accessed on 15 October 2022).
105. Perry, R.H.; Green, D.W.; Maloney, J.O. *Perry's Chemical Engineers' Handbook*, 7th ed.; McGraw-Hill: New York, NY, USA, 1997; ISBN 0070498415.
106. Batidzirai, B.; Shotman, G.S.; van der Spek, M.W.; Junginger, M.; Faaij, A.P.C. Techno-economic performance of sustainable international bio-SNG production and supply chains on short and longer term. *Biofuels Bioprod. Biorefining* **2019**, *13*, 325–357. [CrossRef]
107. Brasington, R.D.; Haslbeck, J.L.; Kuehn, N.J.; Lewis, E.G.; Pinkerton, L.L.; Turner, M.; Varghese, E.; Woods, M. *Cost and Performance Baseline for Fossil Energy Plants: Volume 2, Coal to Synthetic Natural Gas and Ammonia*; DOE/NETL-2010/1402; Report for the U.S. Department of Energy; National Energy Technology Laboratory by the Research and Development Solutions, LLC (RDS): Morgantown, WV, USA, 2011.
108. Heyne, S.; Harvey, S. Impact of choice of CO₂ separation technology on thermo-economic performance of Bio-SNG production processes. *Int. J. Energy Res.* **2014**, *38*, 299–318. [CrossRef]
109. Arvidsson, M.; Morandin, M.; Harvey, S. Biomass gasification-based syngas production for a conventional oxo synthesis plant—Greenhouse gas emission balances and economic evaluation. *J. Clean. Prod.* **2015**, *99*, 192–205. [CrossRef]
110. Holmgren, K.M. *Investment Cost Estimates for Gasification-Based Biofuel Production Systems*; IVL Swedish Environmental Research Institute: Stockholm, Sweden, 2015; Available online: <https://www.ivl.se/download/18.694ca0617a1de98f472a45/1628413810159/FULLTEXT01.pdf> (accessed on 2 July 2023).
111. Federal Environmental Agency Germany. *ProBas—Xtra-AbbauQuarzsand-DE-2030*; Federal Environmental Agency Germany: Dessau-Roßlau, Germany, 2008. Available online: <https://www.probas.umweltbundesamt.de/php/prozessdetails.php?id=%7b843DA94D-BDA7-442E-A9A3-B80D8B40E66F%7d> (accessed on 20 March 2023).

112. Federal Environmental Agency Germany. *ProBas—LKW oder Lastzug*; Federal Environmental Agency Germany: Dessau-Roßlau, Germany, 2010. Available online: <https://www.probas.umweltbundesamt.de/php/prozessdetails.php?id=%7b539f70d8-e544-fe35-bbca-700578003269%7d> (accessed on 20 March 2023).
113. Federal Environmental Agency Germany. *ProBas—BioRaff-IIRME-DE-2020/brutto*; Federal Environmental Agency Germany: Dessau-Roßlau, Germany, 2011. Available online: <https://www.probas.umweltbundesamt.de/php/prozessdetails.php?id=%7b50476e3a-c90a-4ae4-a1fb-3bc08579e219%7d> (accessed on 20 March 2023).
114. Jekel, M.; Baur, N.; Böckelmann, U.; Dünnbier, U.; Eckhardt, A.; Gnirß, R.; Grummt, T.; Hummelt, D.; Lucke, T.; Meinel, F.; et al. *Anthropogene Spurenstoffe und Krankheitserreger im Urbanen Wasserkreislauf*; Universitätsverlag der TU Berlin: Berlin, Germany, 2016; ISBN 978-3-7983-2815-0.
115. Federal Environmental Agency Germany. *ProBas—Zink*; Federal Environmental Agency Germany: Dessau-Roßlau, Germany, 2008. Available online: <https://www.probas.umweltbundesamt.de/php/prozessdetails.php?id=%7b50476e3a-c90a-4ae4-a1fb-3bc08579e219%7d> (accessed on 20 March 2023).
116. Federal Environmental Agency Germany. *ProBas—MetallNickel-DE-2020*; Federal Environmental Agency Germany: Dessau-Roßlau, Germany, 2008. Available online: <https://www.probas.umweltbundesamt.de/php/prozessdetails.php?id=%7b65c51f09-9f88-4d3c-8858-cfbcacf98d53%7d> (accessed on 20 March 2023).
117. Federal Environmental Agency Germany. *ProBas—AufbereitungTonerde-DE-2020*; Federal Environmental Agency Germany: Dessau-Roßlau, Germany, 2010. Available online: <https://www.probas.umweltbundesamt.de/php/prozessdetails.php?id=%7b9dfe17e4-264f-459f-90d0-8edf677f1bc0%7d> (accessed on 20 March 2023).
118. Federal Environmental Agency Germany. *ProBas—Kobalt*; Federal Environmental Agency Germany: Dessau-Roßlau, Germany, 2008. Available online: <https://www.probas.umweltbundesamt.de/php/prozessdetails.php?id=%7b81a717dc-da5b-4edc-a754-03331a829e4f%7d> (accessed on 20 March 2023).
119. Federal Environmental Agency Germany. *ProBas—EdelmetallPt-primär-mix-Welt*; Federal Environmental Agency Germany: Dessau-Roßlau, Germany, 2008. Available online: <https://www.probas.umweltbundesamt.de/php/prozessdetails.php?id=%7b0e0b2a95-9043-11d3-b2c8-0080c8941b49%7d> (accessed on 20 March 2023).
120. Federal Environmental Agency Germany. *ProBas—Quarz, Quarzite*; Federal Environmental Agency Germany: Dessau-Roßlau, Germany, 2008. Available online: <https://www.probas.umweltbundesamt.de/php/prozessdetails.php?id=%7b9e9c7d4e-6240-4bf8-823a-d80c0f0c257b%7d> (accessed on 20 March 2023).
121. Federal Environmental Agency Germany. *ProBas—Trimethylamin*; Federal Environmental Agency Germany: Dessau-Roßlau, Germany, 2008. Available online: <https://www.probas.umweltbundesamt.de/php/prozessdetails.php?id=%7b44c6c-8eda-74119209c218%7d> (accessed on 20 March 2023).
122. Federal Environmental Agency Germany. *ProBas—Chem-OrgPEG+DPM (Hochrein)*; Federal Environmental Agency Germany: Dessau-Roßlau, Germany, 2011. Available online: <https://www.probas.umweltbundesamt.de/php/prozessdetails.php?id=%7b150efbab-dba6-4752-bf86-fb34f95a1b3c%7d> (accessed on 20 March 2023).
123. NREL. *H2A: Hydrogen Analysis Production Models: Case Studies 2018*; National Renewable Energy Laboratory: Denver, CO, USA, 2018. Available online: <https://www.nrel.gov/hydrogen/h2a-production-models.html> (accessed on 28 June 2021).
124. Federal Environmental Agency Germany. *ProBas—MetallStahl-Profil-85%Recycling-Welt-2005*; Federal Environmental Agency Germany: Dessau-Roßlau, Germany, 2012. Available online: <https://www.probas.umweltbundesamt.de/php/prozessdetails.php?id=%7b0e0b2a95-9043-11d3-b2c8-0080c8941b49%7d> (accessed on 20 March 2023).
125. Federal Environmental Agency Germany. *ProBas—Stahl*; Federal Environmental Agency Germany: Dessau-Roßlau, Germany, 2008. Available online: <https://www.probas.umweltbundesamt.de/php/prozessdetails.php?id=%7b19e7d6cb-2337-4ed1-a096-3df3961dda87%7d> (accessed on 20 March 2023).
126. Federal Environmental Agency Germany. *ProBas—Beton*; Federal Environmental Agency Germany: Dessau-Roßlau, Germany, 2012. Available online: <https://www.probas.umweltbundesamt.de/php/prozessdetails.php?id=%7b07e23ca-304f-485c-83a6-90c0a0f1baa6%7d> (accessed on 20 March 2023).
127. Wirtschaftskammer Österreich. *Statistisches Jahrbuch 2023*; Wirtschaftskammer Österreich: Vienna, Austria, 2023; Available online: <https://www.wko.at/service/zahlen-daten-fakten/statistisches-jahrbuch.html> (accessed on 2 July 2023).
128. Gollner, M. *Nutzenergieanalyse 1993–2021*; Statistik Austria: Vienna, Austria, 2022; Available online: <https://www.statistik.at/statistiken/energie-und-umwelt/energie/nutzenergieanalyse> (accessed on 2 July 2023).
129. Turner, J.; Winkler, G.; Swoboda, G. *Statistiken Sonderheft: Einkommen, Konsum und Vermögen der Haushalte—Sektorale Volkswirtschaftliche Gesamtrechnungen in den Letzten 20 Jahren*; Oesterreichische Nationalbank: Vienna, Austria, 2022. Available online: <https://www.oenb.at/Publikationen/Statistik/Statistiken-Sonderhefte/2022/sectorale-vgr.html> (accessed on 2 July 2023).
130. Fichtinger, M.; Grohall, G.; Helmenstein, C.; Schitnig, H.; Sengschmid, E.; Zalesak, M. *Die volkswirtschaftliche Bedeutung des österreichischen Logistiksektors: Studie im Auftrag der Wirtschaftskammer Österreich—Sparte Transport und Verkehr, der Vereinigung der Österreichischen Industrie und des Zentralverbandes Spedition & Logistik*; Economica GmbH: Vienna, Austria, 2022. Available online: <https://news.wko.at/news/oesterreich/221115-Logistik-Studienbericht-Economica.G.pdf> (accessed on 2 July 2023).

Disclaimer/Publisher's Note: The statements, opinions and data contained in all publications are solely those of the individual author(s) and contributor(s) and not of MDPI and/or the editor(s). MDPI and/or the editor(s) disclaim responsibility for any injury to people or property resulting from any ideas, methods, instructions or products referred to in the content.

Paper VI

ENECO₂Calc – A Modeling Tool for the Investigation of Energy Transition Paths toward Climate Neutrality within Municipalities

Hammerschmid, M., Konrad, J., Werner, A., Popov, T., Müller, S.
Energies, 2022, 15(19), 7162, SI Environmental Assessment and
Optimization of Energy Systems and Technologies

<https://doi.org/10.3390/en15197162>

Article

ENECO₂Calc—A Modeling Tool for the Investigation of Energy Transition Paths toward Climate Neutrality within Municipalities

Martin Hammerschmid ^{1,*}, Johannes Konrad ², Andreas Werner ³, Tom Popov ¹ and Stefan Müller ¹

¹ Institute of Chemical, Environmental and Bioscience Engineering, TU Wien, Getreidemarkt 9/166, 1060 Vienna, Austria

² Institute for Powertrains and Automotive Technologies, TU Wien, Getreidemarkt 9/315, 1060 Vienna, Austria

³ Institute of Energy Systems and Thermodynamics, TU Wien, Getreidemarkt 9/302, 1060 Vienna, Austria

* Correspondence: martin.hammerschmid@tuwien.ac.at

Abstract: The paper focuses on developing an energy-modeling tool called ENECO₂Calc, which allows the determination of current ecologic and economic footprints based on calculating the final energy demand within several sectors for municipalities. Furthermore, different energy transition paths until 2050 can be investigated and compared to the business-as-usual reference scenario. ENECO₂Calc is the first municipality-based energy-modeling tool that allows the development of meaningful scenarios until 2050 by considering climate policy goals and RES potentials, and it involves the mobility emission forecast tool “PROVEM”. ENECO₂Calc is exclusively based on consistent statistical datasets. Additionally, the energy-modeling process was demonstrated as exemplary for the Austrian municipality St. Margareten im Rosental. For the selected municipality, three different scenarios were investigated. It could be concluded that a mix of decentral RES technologies and central cogeneration units in the heat sector, a mix of solar PV and cogeneration units in the electricity sector, and the use of synthetic biofuels coupled with a higher share of electrification in the fuel sector seemed to be most promising in the considered region. ENECO₂Calc is a helpful energy-modeling tool toward climate neutrality to support municipalities in developing appropriate economic and ecological footprint strategies.

Keywords: energy modeling; municipalities; economic and ecologic footprint; energy communities; digital twin



Citation: Hammerschmid, M.; Konrad, J.; Werner, A.; Popov, T.; Müller, S. ENECO₂Calc—A Modeling Tool for the Investigation of Energy Transition Paths toward Climate Neutrality within Municipalities. *Energies* **2022**, *15*, 7162. <https://doi.org/10.3390/en15197162>

Academic Editors: Carlos Pozo and Ángel Galán Martín

Received: 4 August 2022

Accepted: 16 September 2022

Published: 29 September 2022

Publisher's Note: MDPI stays neutral with regard to jurisdictional claims in published maps and institutional affiliations.



Copyright: © 2022 by the authors. Licensee MDPI, Basel, Switzerland. This article is an open access article distributed under the terms and conditions of the Creative Commons Attribution (CC BY) license (<https://creativecommons.org/licenses/by/4.0/>).

1. Introduction

In the year 2018, the EU-27 emitted 3764 million tons of greenhouse gas emissions [1]. Within the same period, Austria was responsible for 79 million tons of carbon dioxide equivalent (CO₂e), which amounted to a share of 2% compared to the total emissions of the EU-27 [2]. The Paris Agreement [3] set out a global framework to reduce climate change by limiting global warming to well below 2 °C compared to the pre-industrial level. The European Union responded to the Paris Agreement with the 2030 Climate and Energy Framework [4], implemented by the Renewable Energy Directive (RED II) [5]. The key targets are reducing greenhouse gas emissions, raising the share of renewable energy carriers, and improving energy efficiency. RED II [5] and the national implementation in the Austrian Renewable Energies Act [6] allow the establishment of renewable energy communities (RECs) and citizen energy communities (CECs). The COVID-19 epidemic destabilized the world economy and energy markets. Model calculations have shown that coal and crude oil prices are interconnected [7,8]. Subsequently, it is essential to raise the cost security of supply by increasing the share of renewable energy carriers. To increase energy autonomy, RECs and CECs can be established to enable local initiatives by citizens, communities, and businesses. RECs are defined as legal entities [5] with

natural persons, small- or medium-sized enterprises, or local authorities as shareholders or members [5]. The primary purpose of RECs is to ensure environmental, economic, or social community benefits for the shareholders and members, as well as for the respective local areas, rather than financial profits [5]. RECs are allowed to produce, consume, store, and sell products based on renewable energies [9,10]. CECs are open for any legal entity and are technology-neutral [11]. CECs are independent of location. In addition to REC activities, CECs are also allowed to distribute, supply, and aggregate electricity, as well as provide energy services [9,10]. This sharing-economy approach should raise public acceptance through active participation and mobilize private capital for the energy transition process. Further effects are the economic strengthening of the domestic economy, the growing independence of energy providers, and the diversification of actors within the energy market. RECs and CECs are supposed to relieve the existing grid load by local balance of supply and demand [9,10,12]. For the successful implementation of energy communities within the national energy market, assurances of ecologic, economic, and social advantages for members and shareholders of CECs and RECs, as well as a cost-oriented network charge system, are essential [9,10]. Further details regarding the designing, potential, economic and ecologic viability, regulatory challenges, and opportunities of energy communities, as well as blockchain-based trading with RECs and CECs, can be found in [13–21].

In addition to RED II, the European Green Deal [22] shall generate further efforts regarding climate protection. The core of the European Green Deal is the European Climate Law [23]. This law shall be the basis for climate neutrality until 2050 in the European Union. The CO₂e emissions in the EU-27 are mainly caused by energy supply, industry, transport, residential sources, agriculture, waste, shipping, and aviation. Therefore, the broad range of CO₂ emitters requires a complete transition and global energy system optimization. The global optimum toward climate neutrality in the energy system can only be a mix of centralized and decentralized RES-based energy systems because of different requirements [2], from private consumers in households up to heavy industry. More than 50% of European and Austrian greenhouse gas emissions refer to decentral emissions within municipalities, such as heat and electricity consumption, passenger and freight transport, or energy use within agriculture and forestry [2]. Therefore, the energy transition process toward climate neutrality on the decentralized regional level can only work effectively by considering the specific requirements of the different municipalities. To conclude, an interdisciplinary approach between energy transition and spatial planning with a focus on environmental, economic, and social impacts is crucial to reach the notified climate goals [24,25]. Municipality-based energy models can support this interdisciplinary approach.

Numerous researchers, institutions, and companies have developed energy models with a wide range of different applications. The energy models can be classified according to [26] in econometric, macro-economic, economic equilibrium, optimization, simulation, spreadsheet, backcasting, and multicriteria models. Based on this classification scheme, it is evident that energy modeling is always a tradeoff between spatial-, temporal-, and content-related resolution and, further, between energy security, energy equity, and environmental sustainability, called the energy trilemma [27–29]. Many different energy models are available that differ, among other things, in terms of geographical and sectoral coverage [30]. Energy models used for national energy-system-modeling approaches are, for example, EnergyPLAN from Aalborg University [31], MARKAL/TIMES from IEA-ETSAP [32], PRIMES from NTUA [33], or MESSAGE from IIASA [34]. Modeling approaches regarding district heat and electricity grid simulations can be investigated, for example, with EDisOn [35] or the Hotmaps dispatch model [36], both developed by the EEG at TU Wien. Electricity market simulation can be conducted with ELMOD [37] or Green-X [35]. Energy modeling on the municipality level has to be applied to consider the necessary interdisciplinary approach between energy transition and spatial planning. For this approach, energy-modeling software tools such as HOMER [38] or TRNSYS18 [39] can be used. Most community-based holistic energy models require a significant amount of

input data. Content and spatial relations have to be implemented manually [28,40]. The ELAS calculator [41], published in 2011, was the first holistic energy model to determine an Austrian municipality's energy-related ecologic, economic, and social impact mainly using statistical data from publicly accessible sources or predefined surveys [41]. In 2019, the Energy Mosaic Austria [28] was published, representing an ELAS-based nationwide energy and greenhouse gas inventory on the municipal level in high spatial and contextual resolution. Detailed information regarding energy models can be found in [27,30,42–45].

Summing up, there are a lot of energy models for different applications available. Nevertheless, no local energy model exists that supports municipalities within their energy transition processes. For the development of such a tool, it is important to create a user-friendly support instrument that can handle present and predictive investigations. In addition to calculating the current energy demand within the considered region based on generally available statistical datasets, the energy-modeling tool should be able to analyze different energy transition scenarios toward climate neutrality. For this, a vast database for different renewable-energy-source (RES) technologies with their mass and energy balances, as well as ecologic and economic footprints, has to be available. Furthermore, these technology-specific values should also be available for future energy transition scenarios. Additionally, the energy-modeling tool should be able to consider further implications on the future energy balance of the municipality, such as decrease in the heat demand through renovation or increase in the electricity demand through digitalization or electrification. Finally, each region's future energy transition scenarios should be based on local RES potentials and national climate policy goals. The results of the future scenarios should be compared with the present base scenario and visualized.

All these thoughts are gathered in the novel holistic energy model called ENECO₂Calc, which is first introduced in this work. ENECO₂Calc is based on the determination of a final energy demand using consistent statistical datasets [46,47] regarding the heat, electricity, and fuel of a selected municipality in Austria. Based on the final energy demand, a holistic, energy-related ecologic and economic footprint can be determined. Furthermore, different energy transition scenarios can be investigated in the municipality's energy production, distribution, and infrastructure sectors until 2050. The involvement of the emission forecast tool "PROVEM" [48] allows the development of different scenarios regarding energy transition in the mobility sector. Thus, the methodology can be applied to reach the global optimum of an energy system considering the regional specificities, e.g., individual municipalities. Additionally, the decentral potentials of renewable energy technologies from RegioEnergy [49] and calculations based on consistent statistical datasets [46,47] support the development of realistic energy transition scenarios. Moreover, a wide range of different renewable energy technologies is integrated within the energy model. Additionally, ENECO₂Calc enables the integration of RECs and CECs, considering the related benefits of energy communities. The holistic approach of ENECO₂Calc enables the comparison of different energy transition paths regarding ecologic and economic footprints in terms of energy production, distribution, and infrastructure until the year 2050. Furthermore, the visualization of related energy flows within a municipality is possible. Therefore, a holistic economic and ecologic footprint approach can be created, with suggestions for CO₂ taxes and regional subsidies. Finally, the integration of renewable and citizen energy communities according to RED II [5] and the electricity market directive [11] within regions and municipalities is conducted. It offers excellent potential for the energy transition process on the local level.

Energy transition paths regarding climate neutrality in the whole world look different. Every region and municipality is faced with different energy consumption distributions and industry sectors [28]. Furthermore, every region and municipality has different possibilities for establishing RES technologies. Therefore, the need for a regional-based energy-modeling tool for planning regional energy transitions becomes evident to find appropriate energy transition scenarios for every region. This gap can be closed by the development of ENECO₂Calc. In the first development stage, which is the objective of this

study, ENECO₂Calc is built to deal with all the municipalities (2095 in total) in Austria [28]. Therefore, in the present stage, the methodology is focused on dealing with consistent statistical datasets from Austrian municipalities. In the future, the methodology can be extended to also deal with statistical datasets from the municipalities of other countries. The holistic approach of ENECO₂Calc is reached through an interdisciplinary approach between the research areas of energy systems and thermodynamics, chemical engineering, and powertrains and automotive technology. Moreover, ENECO₂Calc is user-friendly and expandable, and it can support the regional energy transition process.

First of all, the present paper describes the methodology of ENECO₂Calc and discusses the following sections:

- General purpose and approach of the novel tool;
- Methodology for the calculation of the final energy demands of municipalities;
- Methodology for the distribution of the final energy demands and energy capacities;
- Methodology for the monthly discretization of the final energy demand and supply;
- Ecologic and economic evaluation framework;
- Development framework regarding energy transition scenarios.

Furthermore, ENECO₂Calc is applied to build up energy transition scenarios for St. Margareten im Rosental, a municipality in Carinthia. Therein, the present energy demand and the ecologic and economic footprint of the raised municipality are shown. Additionally, the possible energy transition scenarios and the predictions of the future energy demand, as well as the ecologic and economic footprint, are visualized.

2. Concept and Methodology of ENECO₂Calc

For answering the research questions, the systematic approach of ENECO₂Calc is explained. The methodology ranged from calculating the final energy demand based on consistent statistical datasets to developing energy transition scenarios until 2050.

2.1. General Purpose and Approach of ENECO₂Calc

ENECO₂Calc is the first energy-modeling tool for developing energy transition scenarios for the defossilization of municipalities. In the first evolution stage, which is the objective of this study, ENECO₂Calc is able to develop energy transition paths for all the Austrian municipalities. ENECO₂Calc helps to estimate a municipality's ecologic and economic footprint after integrating new energy technologies, with a particular focus on RECs and CECs. ENECO₂Calc is an artificial word to express the connection of the ENergetic, ECOlogic, and ECONomic footprint. In Figure 1, the methodology of ENECO₂Calc is illustrated. ENECO₂Calc delivers, based on consistent statistical datasets for a selected municipality in Austria, the final annual energy demand in terms of space heat, hot water, electricity, and fuels. Afterward, this final annual energy demand is distributed regarding energy technologies and energy capacities. The monthly discretization of energy demand and supply leads to the monthly surplus energy being fed into the Austrian grid, and the monthly deficit energy obtained from the national energy system.

A broad database of emission and cost factors allows the economic and ecologic footprint to be divided into energy production, energy distribution, and infrastructure. The scenario development until 2050 is based on predicted national and regional potentials and energy system targets to reach the energy transition concerning legislative targets within the next three decades. ENECO₂Calc is based on a variety of MS Excel spreadsheets with around 6500 specific and absolute preset values based on studies, as well as around 1000 user-based set values to define the municipality. These parameters can be obtained from consistent statistical datasets, such as Statistik Austria or open-source databases. The modular methodology allows the implementation of statistical datasets and, thus, the extension of ENECO₂Calc to analyze further countries.

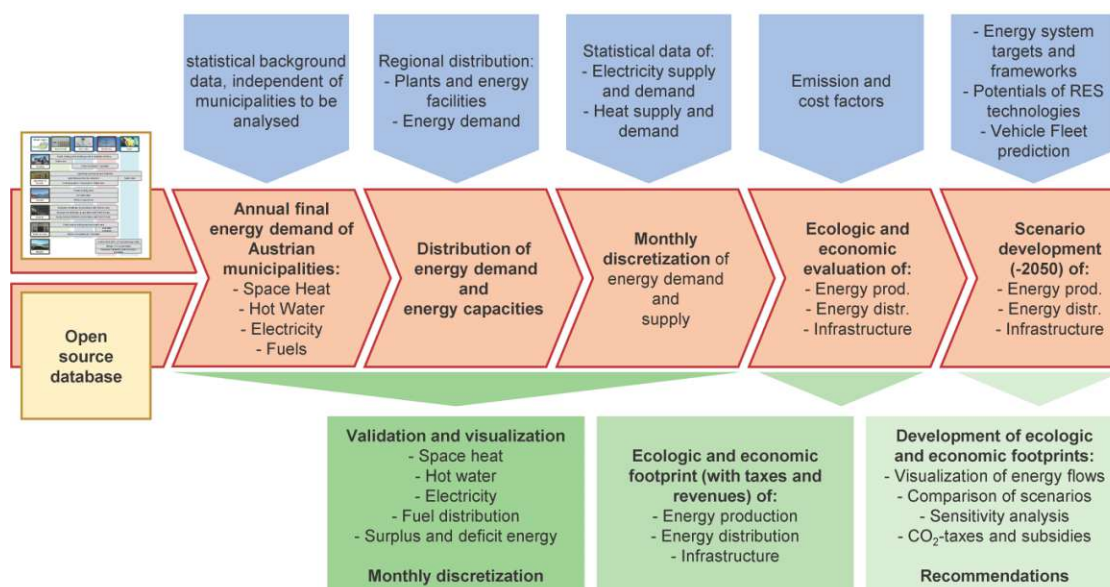


Figure 1. Methodology of ENECO₂Calc.

2.2. Calculation of Final Energy Demand of Municipalities

The first step within ENECO₂Calc is the calculation of the final energy demand of a selected municipality. Determining the final annual energy demands of municipalities in Austria per year are based on a mixture of bottom-up and top-down approaches [26]. The reasons are different requirements and dependencies in various sectors. In Figure 2, the methodology with the essential input data is illustrated. All the visualized input data are based on consistent statistical datasets or open-source databases to ensure a widely applicable municipality-based energy-modeling tool. For calculating the final energy demand of a selected municipality in Austria, the space heat, hot water, electricity, and fuel demand are calculated. The demands of these energy carriers are determined in the residential building, agriculture and forestry, tourism, industry, public services, and mobility sectors. The space heat demand is calculated in all the mentioned sectors except the mobility sector. The hot water demand is estimated for the residential building, tourism, industry, and public services sectors. The space heat and hot water demands within the industry sector are calculated together as the total heat demand. The electricity demand is determined in all the industries. The fuel demand for tractors is assigned to the agriculture and forestry sector according to Austrian sectoral CO₂e distribution [2]. The fuel demand due to passenger cars, light commercial vehicles (LCV), medium commercial vehicles (MCV), and heavy commercial vehicles (HCV) is considered in the mobility sector. Within the calculation of the fuel demand, the vehicle stock and consumption rates of different technologies are fed from PROVEM [48]. The integration of the institute-owned emission forecast tool PROVEM into ENECO₂Calc enables the determination of vehicle fleets and fuel consumptions in the considered municipality.

The final energy demand in the residential building sector is based on the inhabitant structure, building period, commuter balance, population, and specific energy demands, which could be defined as a classic bottom-up approach. The public services sector is considered similarly to the residential building sector based on a bottom-up approach related to the usable area. Exemptions are hospitals and sewage sludge plants. The bottom-up approach within the sewage treatment sector refers to the population equivalent, the design basis for sewage treatment plants. The use of hospital bed numbers calculates the energy demand for hospitals. A mixed approach calculates the energy demand of the agriculture and forestry sector. Therefore, the heat and electricity demand is proportional to the agricultural and forestry land distribution, animal population, and the number of animal owners for the municipality in the dedicated state. The fuel demand is determined

by the land distribution of the municipality and specific fuel demands per agricultural land. The energy demand within the tourism sector is calculated using a bottom-up approach based on tourism building stock and the number of seasonal guest beds, with related specific energy demands. The primary and secondary industry sectors, such as the manufacturing goods or construction sectors, are based on a top-down approach according to different frameworks for the related state. The tertiary industry sectors, such as trading enterprises, are based on a bottom-up approach.

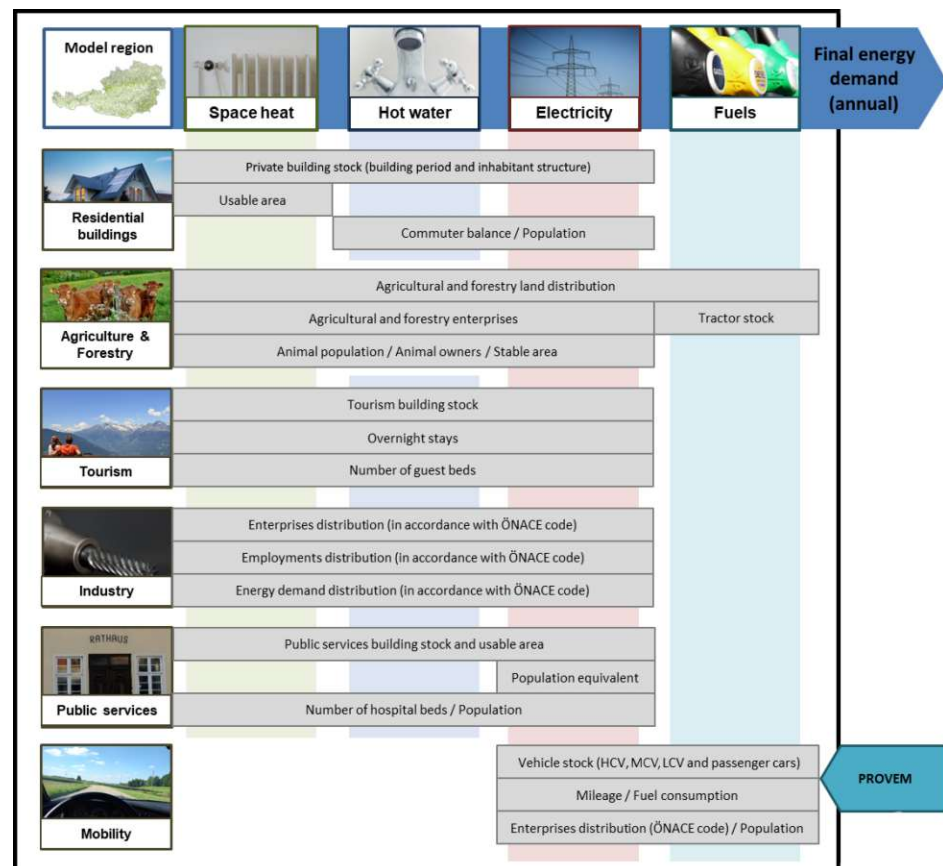


Figure 2. Methodology for calculation of final energy demand for municipalities.

The calculation of the final energy demand within the mobility sector is determined using a top-down approach. Therefore, the determination of the vehicle stock of passenger cars is based on comparing the population of the dedicated federal state and the municipality. The calculation of the vehicle stocks of LCV, MCV, and HCV are based on the number of enterprises. This approach is supported by implementing PROVEM [48], a forecasting tool for emissions within the mobility sector. Therefore, an extensive database on Austrian vehicle stock and consumption numbers is accessible. After the calculation of the final energy demand, a validation of the results is possible. Therein, a comparison of the calculated values with results from EMA [28] or other specific literature could be made.

Another way to feed ENECO₂Calc with final energy demand numbers is to import analysis results from EMA [28], which provides data with similar sectoral distributions for every municipality in Austria.

Summing up, the determination of the final energy demand is only based on consistent statistical datasets, which are structured in the same way for all the municipalities in Austria. Therefore, ENECO₂Calc is able to determine the final energy demand of all 2095 municipalities in Austria in the current development phase. The modular structure of ENECO₂Calc allows an easy adaption of the methodology to deal in the future with municipality-based statistical datasets from other countries.

2.3. Distribution of Final Energy Demand and Energy Capacities

Based on the final annual energy demand, the space heat, hot water, electricity, and fuel demands are determined via a distribution regarding energy supply technologies within the selected region. Therefore, several energy supply technologies are implemented for decentral and central heat and electricity production, as well as several mobility options. In Table 1, an overview of the energy supply technologies and mobility options is given. The assumed energy source mix, technology, plant size, and annual average efficiency factors are listed. Most decentral heat production technologies are based on solid or liquid energy sources converted in a boiler to heat, as shown in [50]. A technology distribution of 50% flat plate and 50% vacuum tube collector for solar thermal systems is assumed. Ambient heat systems are mainly based on air heat according to the Austrian market distribution [51]. Combined heat and power plants, such as fossil fuel or waste-based plants, are supra-regional supply technologies and, therefore, influence the Austrian electricity mix due to feeding into the Austrian grid. Biomass, biogas, or cogeneration plants are considered energy supply technologies for regional application within municipalities. According to the Austrian energy mix, hydropower plants are allocated by 75% run-off river plants and 25% pump storage plants [52]. In ENECO₂Calc, a lot of mobility options for the distribution of the final fuel demand are available. The mobility options are classified as internal combustion engine technologies, gas engines based on compressed natural gas, plug-in hybrid electric vehicles, battery electric vehicles, and fuel-cell electric vehicles. The use of diesel and gasoline is assumed with the Austrian biofuel share. For diesel, a biofuel share of 5.9% FAME [53] and, for gasoline, a biofuel share of 3.1% bioethanol [53] is considered, based on the European production mix. Further mobility options for internal combustion engines are the application of bioethanol or FAME. The related adaption of internal combustion engines for this approach is currently not considered. Further options are the use of biomass-to-liquid (BtL) or power-to-liquid (PtL) biofuels. In addition to fossil natural gas, synthetic natural gas (SNG) options based on biogas or biomass gasification plants are listed for gas engines. Typically, demand distributions for plug-in hybrid electric vehicles, according to [54], are assumed. The Austrian electricity mix or RES technologies, such as wind power, water power, solar PV, and biomass as fuel energy sources, can be considered for battery electric vehicles. Fuel-cell electric vehicles can be powered by biomass-based or electricity-based hydrogen.

2.4. Monthly Discretization of Final Energy Demand and Supply

The monthly discretization of the calculated and distributed final energy demand and supply is the next step within the ENECO₂Calc methodology. Therefore, the heat demand, which represents the sum of hot water and space heat, is discretized according to the monthly reference load profiles used within the Hotmaps dispatch model [36,55]. The electricity demand is discretized according to Austria's average monthly electricity demands from 2017 to 2020 [56]. The fuel demand and supply are not discretized because of equal distribution over the year. Therefore, it is assumed that a model region's fuel demand and supply are uniformly distributed over a year. The same assumption is applied for non-volatile energy supply technologies, such as biomass-based cogeneration plants. For the monthly discretization of volatile electricity supply technologies, such as solar, wind, and hydro, monthly distributions [57] are used based on mean values from 1986 to 2016. Therefore, the discretization of the heat demand enables the definition of possible central heat production technologies. The discretization of the electricity demand and supply delivers a deficit or surplus of electricity, which has to be imported from or exported to the Austrian electricity grid.

The energy distribution and discretization enable the visualization of energy flows in and connected with a selected municipality. Therefore, a direct link between the MS-Excel-based ENECO₂Calc and e!Sankey [58], a tool for visualizing energy flows, is used. The connection with ENECO₂Calc allows the visualization of all the energy flows connected to a municipality.

Table 1. Overview of heat and electricity supply technologies and mobility options within ENECO₂Calc.

Energy Supply Technology	Energy Source	Technology Specification	Unit Size	Annual Efficiency * [kWh _{Output} /kWh _{Input}]	Literature
Heat Production Technologies					
Coal boiler	coal	boiler	<15 kW _{th} (decentral)	80% _{th}	[59,60]
Oil boiler	oil	boiler		85% _{th}	[59–61]
Gas-fired boiler	gas	boiler		90% _{th}	[59–61]
Electricity heater	electricity (AT mix)	heater		100% _{th} **	[59]
Wood-fired boiler	firewood	boiler		85% _{th}	[53,59–61]
Wood pellet boiler	wood pellets	boiler		90% _{th}	[53,59–61]
Wood chip boiler	wood chips	boiler		90% _{th}	[53,59–61]
Solar thermal system	solar power	50% flat plate 50% vacuum tube collector		50% _{th}	[62]
Ambient heat system	70% air/25% ground/ 5% water heat	heat pump	2.8 (COP)	[51,59,62,63]	
Combined heat and power production technologies					
Coal-fired power plant	coal	steam power plant	50–500 MW _{el}	48% _{th} /42% _{el}	[35,63–66]
Oil-fired power plant	heating oil	steam power plant	0.05–1 GW _{el}	45% _{th} /45% _{el}	[35,63–65]
Gas-fired power plant	gas	gas turbine plant	0.05–1 GW _{el}	47% _{th} /45% _{el}	[35,63–66]
Combined-cycle gas power plant	gas	gas turbine and steam power plant	0.05–1 GW _{el}	35% _{th} /60% _{el}	[35,63–66]
Waste incineration plant	waste	steam power plant	5–30 MW _{el}	67% _{th} /23% _{el}	[67,68]
Biomass power plant	33% wood residue 33% industrial wood residue 33% wood pellets	steam power plant	2–20 MW _{el}	65% _{th} /25% _{el}	[35,63–65]
Biogas plant	33% energy crops 33% manure 33% waste	anaerobic digestion plant	0.1–8 MW _{el}	45% _{th} /30% _{el}	[35,63–65]
Cogeneration power plant	50% wood pellets 50% wood chips	air gasification and gas engine	0.05–5 MW _{el}	55% _{th} /25% _{el}	[35,63–65]
Electricity production technologies					
Rooftop PV system	solar power	crystalline silicon solar cells (rooftop)	<15 kW _{pel} (decentral)	18% _{el}	[35,62–64,66]
Wind turbine	wind power	onshore	>500 kW _{el}	45% _{el}	[35,62–64,66]
Hydropower plant	water power	75% run-off river 25% pump storage	250 kW _{el} – 250 MW _{el}	85% _{el}	[35,62–64,66]
Ground-mounted PV system	solar power	crystalline silicon solar cells (ground-mounted)	>500 kW _{pel} (central)	18% _{el}	[35,62–64,66]

Table 1. Cont.

Energy Supply Technology	Energy Source	Technology Specification	Unit Size	Annual Efficiency * [kWh _{Output} /kWh _{Input}]	Literature
Mobility options					
ICE—Diesel	5.9% FAME (EU mix) 94.1% fossil diesel	internal combustion engine			[53,69–77]
ICE—Biodiesel	FAME (EU mix)	internal combustion engine			[60,69–79]
ICE—FT Diesel (BtL)	wood-based diesel (DFB)	internal combustion engine			[60,70,73,76,78,80,81]
ICE—PtL Diesel	hydrogen (EU mix) and CO ₂ (EU mix)-based diesel	internal combustion engine	-	-	[78,80–82]
ICE—Gasoline	3.1% bioethanol (EU mix) 96.9% fossil gasoline	internal combustion engine			[53,70–77]
ICE—Bioethanol	bioethanol (EU mix)	internal combustion engine			[53,70–79,83]
ICE—FT Gasoline (BtL)	wood-based gasoline (DFB)	internal combustion engine			[60,70,73,76,80,81]
ICE—PtL Gasoline	hydrogen (EU mix) and CO ₂ (EU mix)-based gasoline	internal combustion engine			[80–82]
CNG—Fossil	natural gas	compressed natural gas			[74,76,81,84]
CNG—SNG from Biogas	SNG from biogas plant (AT mix)	compressed natural gas			[63,70,72–74,76,78–81,84]
CNG—SNG from Biomass	SNG from wood (DFB)	compressed natural gas			[60,73,80]
PHEV—Diesel	63% electricity (AT mix) 2.2% FAME (EU mix) 34.8% fossil diesel	plug-in hybrid electric vehicle			[74,76,85]
PHEV—Gasoline	63% electricity (AT mix) 1.1% bioethanol (EU mix) 35.9% fossil gasoline	plug-in-hybrid electric vehicle			[74,76]
BEV—AT mix	electricity (AT mix)	battery electric vehicle			[53,76,77,81,82,85]
BEV—Mix RES technologies	electricity (mix RES)	battery electric vehicle			[53,76,82,85]
FCEV—H ₂ electrolysis	hydrogen from electricity (mix RES) (electrolysis)	fuel-cell electric vehicle			[70,73,74,76,80–82,86,87]
FCEV—H ₂ from Biomass	hydrogen from wood (DFB)	fuel-cell electric vehicle			[70,73,80,87]

* Assumed parameter for the year 2020 (present)/annual COP for ambient heat system; ** Assumption: no losses due to the conversion from electricity to heat.

2.5. Ecologic and Economic Evaluation

For the definition of a municipality's ecologic footprint, the direct and indirect emissions of the energy production, energy distribution, and infrastructure are calculated. Therein, the direct and indirect emissions due to the heat and electricity supply are considered through emission factors according to Table 2. The implemented emission factors are mean values from different sources, as listed in Table 2. The same applies to the economic evaluation based on levelized production cost factors. All the economic factors were scaled to 2020 by applying the Austrian consumer price index (CPI) [88]. Emissions due to operation are considered within the direct emissions. Indirect emissions are linked to the preceding chain, such as preparation and transport of fuel, plant manufacturing, and auxiliary electrical energy [63]. The ecologic footprint of the mobility sector is determined by applying ecologic factors according to Table 2. The lifecycle approach to vehicles is implemented to generate the ecological footprint of the mobility options. Therefore, the direct emissions of the mobility sector contain the direct and indirect emissions of the fuel production process and the direct emissions within the conversion of fuel or energy in vehicles. The indirect fuel emissions are linked to the emissions of the vehicle-manufacturing process [89]. Therefore, within the ecologic footprint, all greenhouse gas emissions due to energy production are considered. By applying grid loss factors for heat and electricity, the energy distribution process considers the ecologic footprint. The emissions due to the construction of district heating systems, grids, filling stations, and the renovation of buildings are currently not considered.

Table 2. Ecologic and economic factors of supply technologies within ENECO₂Calc for the year 2020.

Energy Supply Technologies	Indirect CO ₂ e Emissions * [kg CO ₂ e/kWh _{output}]		Direct CO ₂ e Emissions * [kg CO ₂ e/kWh _{output}]		Levelized Production Costs * [€/kWh _{output}]		Literature
Heat Production Technologies							
Coal boiler	0.060		0.415		0.161 ***		[59,60,63,90]
Oil boiler	0.061		0.279		0.157		[53,59,60,63,91,92]
Gas-fired boiler	0.077		0.215		0.153		[53,59,60,63,93,94]
Electricity heater	0.258				0.226		[53,93]
Wood-fired boiler	0.016		0.007		0.129		[53,59,60,63,95,96]
Wood pellet boiler	0.030		0.007		0.147		[53,59,60,63,95,97]
Wood chip boiler	0.016		0.007		0.123		[53,59,60,63,95,96]
Solar thermal system	0.020		0.000		0.134		[53,59,63,94]
Ambient heat system	0.112		0.000		0.217		[63,65,94,97]
Combined heat and power production technologies							
Output type	Heat	Elec.	Heat	Elec.	Heat	Elec.	
Coal-fired power plant	0.045	0.089	0.307	0.613	0.060	0.073	[63,65,66,90,94]
Oil-fired power plant	0.066	0.132	0.268	0.536	-	0.237	[53,63,91,94]
Gas-fired power plant	0.053	0.107	0.150	0.301	0.042	0.110	[35,53,63,65,66,94]
Combined-cycle gas power plant	0.046	0.091	0.129	0.258	0.042	0.076	[35,53,60,63,66]
Waste incineration plant	0.153 (heat)/0.306 (elec.) **				0.041	0.082	[65,68,94]
Biomass power plant	0.018	0.036	0.005	0.011	0.053	0.107	[35,53,59,63,94]
Biogas plant	0.069	0.139	0.049	0.098	0.058	0.138	[35,53,62,63,66,98]
Cogeneration power plant	0.019	0.038	0.005	0.010	0.084	0.159	[77]

Table 2. Cont.

Energy Supply Technologies	Indirect CO ₂ e Emissions * [kg CO ₂ e/kWh _{output}]	Direct CO ₂ e Emissions * [kg CO ₂ e/kWh _{output}]	Levelized Production Costs * [€/kWh _{output}]	Literature
Electricity production technologies				
Rooftop PV system	0.062	0.000	0.106	[35,53,63,66,92,93]
Wind turbine	0.010	0.000	0.063	[35,53,63,66,93]
Hydropower plant	0.007	0.000	0.056	[35,53,63]
Ground-mounted PV system	0.062	0.000	0.077	[35,53,63,66]
Fuel production technologies/Mobility options				
ICE—Diesel	0.054	0.289	0.058	[60,73,81,89]
ICE—Biodiesel	0.054	0.159	0.072	[60,70,73,80,89]
ICE—FT Diesel (BtL)	0.054	0.052	0.117	[60,73,80,89]
ICE—PtL Diesel	0.054	0.123	0.410	[81,82]
ICE—Gasoline	0.047	0.337	0.059	[60,81,89]
ICE—Bioethanol	0.047	0.256	0.074	[60,70,73,80,89]
ICE—FT Gasoline (BtL)	0.047	0.052	0.117	[60,73,80,89]
ICE—PtL Gasoline	0.047	0.106	0.410	[81,82]
CNG—Fossil	0.044	0.254	0.032	[81,89,93]
CNG—SNG from Biogas	0.044	0.062	0.080	[60,70,73,89,93]
CNG—SNG from Biomass	0.044	0.045	0.072	[60,73,89,93]
PHEV—Diesel	0.110	0.279	0.066	[54,60,73,77,81,89,93]
PHEV—Gasoline	0.101	0.313	0.066	[54,60,77,81,89,93]
BEV—AT mix	0.274	0.327	0.070	[53,77,89,93]
BEV—Mix RES technologies	0.274	0.020	0.100	[35,53,66,89,93]
FCEV—H ₂ electrolysis	0.144	0.050	0.125	[73,87,89,99]
FCEV—H ₂ from Biomass	0.144	0.046	0.082	[73,87,89,99]

* Assumed parameter for the year 2020 (present); ** emissions not separated into indirect and direct emissions; *** investment and O&M costs assumed to be equal to wood-fired boiler.

For the determination of the economic footprint of a municipality, fuel, operation and maintenance (O&M), and investment costs are considered in terms of energy production, energy distribution, and infrastructure. The energy production costs for energy supply within the model region are calculated for the heat, electricity, and fuel supply technologies by applying the levelized production cost factors from Table 2. These levelized production costs are split into investment, O&M, and fuel costs.

ENECO₂Calc represents the first municipality-based modeling tool that enables the simultaneous determination of economic and ecologic footprints exclusively based on statistical datasets. In the current development phase, ENECO₂Calc is built to deal with all Austrian municipalities. Therefore, the ecologic and economic factors are based on Austrian sources. In the future, the tool could be extended to analyze further countries.

The levelized energy production costs are raised by costs for the monthly-based deficit electricity. The Austrian electricity mix covers the deficit electricity by applying energy price mean values from 2020 [100]. Further natural gas costs are calculated, similar to the costs for the Austrian electricity mix, by applying energy price mean values from 2020 [101].

The energy distribution costs include the transportation or grid costs for the provision of heat, electricity, and fuels except for the transportation costs of liquid fuels to filling stations, which are already covered by the levelized fuel production costs. The hydrogen

distribution costs to filling stations are added by applying a fixed share compared to the total provision cost rate according to [86]. The distribution costs for central district heat systems are calculated by assuming a total length of the district heating system under the consideration of an investment cost factor [102]. Other costs for the district heating system, such as consumer stations, are considered by applying a fixed cost ratio between the grid investment costs and the total costs for the district heating system. Distribution costs for electricity and gas are calculated by applying grid cost factors according to [100,101]. The assumption is that only 50% of the electricity grid costs are offset for RECs. This is based on the claims of several experts in this field [9,10] regarding cost-orientated grid charges. The reduced cost factor of 50% grid costs for RECs is the result of comparing grid cost factors within the different grid levels in Austria. Therefore, the grid costs for level 5 to level 7, which are for low- and medium-voltage grid systems, are about half of the grid charges of the superordinate levels [103].

For the infrastructure costs, different sources are applied. The filling station costs are based on [85] and [104]. The vehicle costs for passenger and commercial vehicles (LCV, MCV, and HCV) are based on consumer prices without taxes according to [53]. The costs for conventional diesel-powered tractors were determined by comparing manufacture sale prices. The costs of alternative-powered tractors are assumed to be proportional to HCV prices. Further infrastructure costs are considered due to the renovation of buildings in the heating sector. For this, cost factors per square meter usable area of buildings [59] are implemented.

Additionally, revenues and ecological taxes are considered for the calculation of the economic footprint of a municipality. Revenues are considered due to the month-based surplus electricity that is exported to the Austrian electricity grid [105]. Therein, market value factors according to [35] are implemented to consider the fluctuating seasonal electricity market conditions. Finally, ecological taxes, such as CO₂ emission certificate costs for the production of the Austrian electricity mix [106] and mineral oil tax for diesel, gasoline, and heating oil [91,107], as well as coal tax [90] for energy production, are considered.

Several assumptions are made for the economic and ecologic footprint prediction until the year 2050, which is the basis for building future scenarios (see Section 2.6). To determine future direct emission factors and indirect preceding chain factors within the years 2030, 2040, and 2050, an efficiency increase of 0.35%/year is assumed for renewable-based heat and electricity supply technologies [92], which results in lower emission factors. For the indirect emissions, due to electrical auxiliary energy use, the factors are based on the electricity mix of the model region within the year. For fossil-based energy technologies, no efficiency increase was assumed. Predicting future direct and indirect emission factors within the mobility sector is based on [89]. Investment, O&M, and fuel cost parameter assumptions are the basis of the implemented economic factors. The investment costs are scaled to 2050 by applying technological learning rates [65,108–110]. The O&M costs until the year 2050 are predicted by applying the CPI [88]. For this assumption, the yearly mean CPI value in 1999–2019 was extrapolated to 2050. Further, for renewable-based energy supply technologies, the prediction of the O&M costs relies on the mean CPI value reduced by the above-mentioned yearly efficiency increase of 0.35%. The applied scaling method for the fuel costs is very similar to the scaling of the O&M costs. Instead of the CPI, the energy price index (EPI) [97] is used. The cost factors for the distribution costs are scaled by applying the CPI. The building renovation cost factors are scaled according to learning rates from [98]. Finally, energy supply technologies' annual future investment costs are calculated by the total investment costs for the analyzed period, divided by the technology lifetime [35,59,102]. The lifetime factors of vehicle stock are implemented according to [99]. The predictions for other infrastructure investment cost factors, such as vehicles or filling stations, are based on studies from the literature.

Finally, the ecologic footprint can be validated with specific literature according to the climate model regions [47] or EMA [28] within ENECO₂Calc. For the validation of the economic footprint, no database on the municipality level is currently available.

2.6. Scenario Development Regarding Energy Transition

Using the knowledge of the current energy carrier distribution and the methodology explained beforehand, it is possible to determine the overall energy demand and the economic and ecologic footprint of a specific Austrian municipality of interest for 2020 using ENECO₂Calc. Based on the 2020 data, different scenarios for possible energy transitions until 2050 for a given municipality could be investigated, whereby three major frameworks are considered for the scenario development. First and foremost, the European and national climate policy goals needed to be reached. Second, realizable potentials of RECs within the municipality and CECs regarding biomass-based technologies are considered. Third, future heat, electricity, and fuel demands until 2050 are predicted.

With the European Green Deal [22] in combination with the European Climate Law [23], the EU has set a legal framework to reach climate neutrality by 2050. To meet these climate ambitions, the European Commission recently adopted a package of comprehensive and interconnected proposals for the next decade called “Fit for 55” [111] to ensure the necessary acceleration and to tackle a reduction of greenhouse gas emissions by at least 55% by 2030 compared to the year 1990. Furthermore, the share of renewable energy carriers in the EU should reach 32% by 2030 [5]. Austria has even more vital ambitions and wants to reach climate neutrality by 2040 [112], with a share of renewable energy carriers between 46% and 50% by 2030 [113].

Raising the share of RECs based on biomass and other renewable technologies within municipalities can help reach the set targets. Therefore, in this work, potentials for RECs and CECs were defined as reduced technical potentials [114,115] and comprised today’s possible proceeds of current “state-of-the-art” energy conversion technologies by considering the possible competition for land between energetic and non-energetic forms of use, as well as competition between different forms of renewable energy technologies. Moreover, and especially crucial in terms of biomass-based energy carriers from forestry biomass, a reduced technical potential in this work always implied sustainable forest management. Different works have investigated the potential to substitute fossil gas and fuels over the coming years by converting biomass from woody, agricultural, and other biogenic residues, as well as waste, into synthetic natural gas (SNG), synthetic Fischer–Tropsch (FT) fuels, or hydrogen (H₂) [73,116–119]. Based on these literature studies, Figure 3 shows a comparison between the Austrian annual energy demand of 2020 and biomass-based RES potential for 2050. The potential of biomass-to-gas (BtG) in 2050 to produce SNG could come close to one-half of the annual gas demand in 2020 if SNG were produced from the biomass potential. BtG in terms of hydrogen (H₂) and biomass-to-liquid (BtL) to produce Fischer–Tropsch fuels had a potential share in 2050 of nearly one-third of the 2020 annual energy demand in gasoline and diesel if H₂ or FT fuels would be produced from the biomass potential.

Furthermore, for the definition of potentials of RES technologies within the selected Austrian municipality, average reduced technical potential data from REGIO Energy [49,115] were considered for solar PV, solar thermal heat, wind power, and heat pump technologies. They were scaled down from the district level to the municipality level. Despite REGIO Energy being a study from 2010 defining potentials for all Austrian municipalities, it was assumed that potentials concerning the mentioned RES technologies would not change significantly up to 2050. According to [115], the most hydropower potential was based on revitalizing existing hydropower plants. For the defossilization of the Austrian electricity mix, a hydropower potential of 5 TWh was predicted [115]. This potential was about 10% of the existing hydropower supply capacity. Therefore, a hydropower potential of 10% for the selected municipality compared to the existing hydropower plant capacity in the region was foreseen. The biomass-based RES potentials results from our own investigations. The potential of biomass within the municipality could be categorized into two groups: forestry and agriculture biomass.

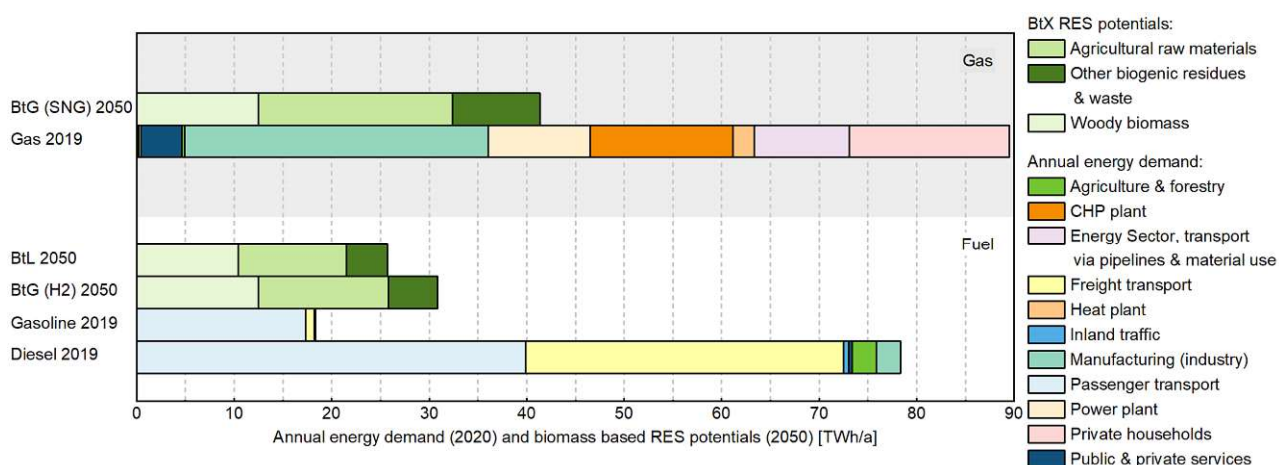


Figure 3. Central realizable potential regarding biomass-based synthetic gas and fuel products produced in CECs within the year 2050 compared with the current annual energy demand of natural gas, diesel, and gasoline in Austria.

For the forestry biomass, two different potentials were defined. These were the potential of unused forest area in 2020 and unused growth within harvested forest area in 2020. Just a share of the overall forest area of a municipality was considered as the harvested forest area. Depending on the municipality, these shares could vary significantly for different reasons, for example, challenging topographies in mountainous regions, making harvest technically or economically unreasonable. By comparing data for the share of the harvested forest area for the selected municipality with those of directly adjacent municipalities with similar topographies [46], forestry biomass potentials for the selected municipality could be raised. Based on data from [120], the potential of unused forest growth was defined as the difference between the annual growth within the harvested forest area and the current annual harvested amount within the forest. It was assumed that sustainable forest management could be fulfilled when, on average, the annual harvest did not overcome the annual growth, which meant that the forestry mass would not change over the years. Based on these potentials, it was possible to define the potential surplus amount of wood from harvested forests that could be generated for 2020. Furthermore, for the wood potential in 2050, the following scenarios were considered. According to [73], for the last 30 years, the share of hardwood has increased, while the share of softwood has constantly decreased within Austrian forests and the species being harvested. Hardwood is mainly used as energy wood, while softwood is primarily used in the sawmill and general industries [73]. This trend should lead to an increase of energy wood in the coming years and is being pursued until 2050. Wheat straw and corn cobs as agriculture residue, as well as miscanthus and short-rotation wood (e.g., willow and poplar), as energy plants have been investigated for their agricultural potentials. For the potential in 2020, data from [46] for cultivation areas of the investigated species were considered. For the potential in 2050, different scenarios were applied. Average change rates from [121,122] for wheat and corn cultivation areas in 2010 to 2020 being pursued before 2050 were assumed for corresponding areas. Furthermore, change rates for the general agricultural area in the municipality until 2050 and potential shares of miscanthus and short-rotation wood in 2050 according to scenario A (base scenario) in [60] were applied. Based on the corresponding areas of different species, annual harvest yields for wheat straw according to [123,124], as well as miscanthus, short-rotation wood, and corn cobs according to [125], could be calculated. To maintain sustainable use of wheat straw, only one-third was considered for energy conversion, according to [121]. For corn cobs, miscanthus, and short-rotation wood, no restrictions had to be considered.

The following methodology was implemented to predict the future heat, electricity, and fuel demands for 2050 in the analyzed Austrian municipality. Based on [59], it was

possible to predict the future energy demand for space heating and warm water supply based on the assumed renovation rate for the housing sector. The Austrian annual change rate from the last 20 years [122] was pursued until 2050 and applied to the municipality for the future electricity demand. Regarding the future fuel demand, it was assumed that the number of vehicles would not change in the given Austrian municipality until 2050, although efficiency enhancement was considered.

After developing scenarios, the energy flows for selected scenarios can be visualized within an energy flow diagram. Furthermore, a sensitivity analysis can be developed and visualized by adjusting ecologic and economic factors.

With regard to the present energy crisis related to the COVID-19 pandemic [7,8] and other disruptive events, it is essential to investigate possible negative and positive effects related to the economic and ecologic key parameters. The applied data are mostly from 2019 and 2020. Consequently, the effects of COVID-19 are considered depending on available data for the status quo of 2020.

Comparing the different scenarios with the status quo enables the recommendation of an energy transition path for the considered municipality regarding the regional conditions and frameworks. As a result, recommendations for applicable CO₂ taxes and subsidies could be made.

Summing up, ENECO₂Calc is a municipality-based energy-modeling tool, which is exclusively based on statistical datasets and open-source databases. ENECO₂Calc is the first municipality-based energy-modeling tool that allows the combined determination of the final energy demand, CO₂ footprint, and energy costs for all Austrian municipalities. The novel implementation of the mobility emission forecast tool “PROVEM” enables the determination of vehicle fleets and fuel consumption on the municipality level. Furthermore, the integration of PROVEM facilitates the consideration of a vast amount of mobility options and the development of realistic energy transition scenarios by 2050 due to modeling the future Austrian vehicle fleet. Thus, ENECO₂Calc delivers a novel approach to investigate municipality-based energy transition scenarios to support municipalities toward the way to climate neutrality.

3. Results and Discussion

In the first evolution stage, which is the objective of this study, ENECO₂Calc is able to develop energy transition paths for all Austrian municipalities. To show the extensive possibilities, ENECO₂Calc was applied to develop several transition paths of a selected municipality in the following chapter. For that, St. Margareten im Rosental, located within Carinthia near Klagenfurt in Austria, was chosen. The municipality area is about 43.98 km² and is characterized mainly by forest area. At the beginning of 2020, 1084 inhabitants [46] were living in St. Margareten im Rosental. The industry sector consisted primarily of tertiary service enterprises, such as gastronomy and other service-orientated SMEs. For the primary and secondary industry sectors, only the mechanical engineering sector was relevant [77].

Subsequently, the present final energy demand results and the investigated scenarios for the year 2050 developed with ENECO₂Calc are shown. The scenarios show possible ways to reach climate neutrality within St. Margareten im Rosental within the next three decades.

3.1. Present Annual Energy Demand and Ecologic and Economic Footprint

The determination of the current final annual energy demand was the first step in the ENECO₂Calc methodology, as mentioned in Section 2.2. In Figure 4, the final annual energy demand of St. Margareten im Rosental divided into defined sectors is shown. In the considered municipality, the final energy demand within the year 2020 was about 22.7 GWh. Figure 4 shows that the residential building sector with space heat demand and the mobility sector with fuel demand are the biggest energy consumers. The industry and residential building sectors mainly determined the electricity demand. In addition, the

fuel and space heat demands within the agriculture and forestry sectors are relevant. The validation of the calculated final energy demand results within ENECO₂Calc can be seen in Table 3. The comparison of the calculations with the literature results showed a deviation of no more than $\pm 29\%$.

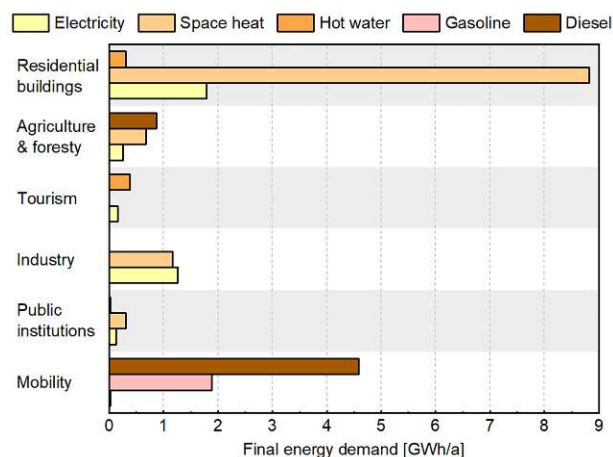


Figure 4. Final energy demand distribution of St. Margareten im Rosental for the year 2020.

Table 3. Validation of present annual energy demand and CO_{2e} emissions of St. Margareten im Rosental for the year 2020 with the literature data.

Validation of Results	ENECO ₂ Calc	Austrian Heat Map [126]	EMA Austria [28]	Carnica Rosental Study *** [127]
Final heat demand [GWh _{th} /a]	11.69	10.75 (−8%) *	11.21 (−4%) *	11.70 (+0.1%) *
Final electricity demand [GWh _{el} /a]	3.63	-	4.23 (+17%) *	3.92 (+8%) *
Final fuel demand [GWh/a]	7.34	-	9.46 (+29%) *	5.45 ** (−26%) *
Total CO _{2e} emissions [M kg CO _{2e} /a]	5.12	-	5.71 (+11%) *	4.62 (−10%) *

* Compared to ENECO₂Calc result; ** without freight traffic; *** heat demand scaled by the total floor area of buildings/electricity and fuel demand scaled by inhabitants.

In Figure 5, the energy flow diagram of St. Margareten im Rosental regarding the current annual energy demand is visualized. Therein, all the energy flows that are connected with the municipality are shown. The primary energy sources, listed as sources from the municipality, the state (Austria), or abroad, can be seen on the left. The energy conversion processes within abroad, Austria, and municipality categories are listed from left to right after the primary energy sources. The final energy demands distributed to the residential building, agriculture and forestry, tourism, industry, public services, and mobility sectors are visualized on the right side. The visualization of the energy flows associated with the municipality showed that, within the year 2020, around 30% of the Austrian electricity mix, which was imported into the municipality, was based on imports from abroad. Therefore, significant amounts of oil- and coal-based electricity were imported. The decentral heat demand was covered mainly through biomass-based and oil-based heating boilers. Furthermore, a small district heating grid driven by a cogeneration unit was in use. Other decentral heat generation technologies within the municipality were heat pump systems and electric heaters. The present heat and electricity demand distribution of 2020 is also shown in Figure 7 (reference case in the year 2020–2020 RF). The electricity demand within the present reference case was mainly based on imports from the Austrian electricity mix. In addition to the cogeneration unit, there were also some decentral rooftop PV systems

and small hydropower plants. The current fuel demand was based three-quarters on diesel and one-quarter on gasoline. The biogenic shares of biodiesel within diesel and bioethanol within gasoline were based on the Austrian mix, with about 5.9% biodiesel and 3.1% bioethanol. Figure 8 (2020 RF) also visualizes the current fuel demand.

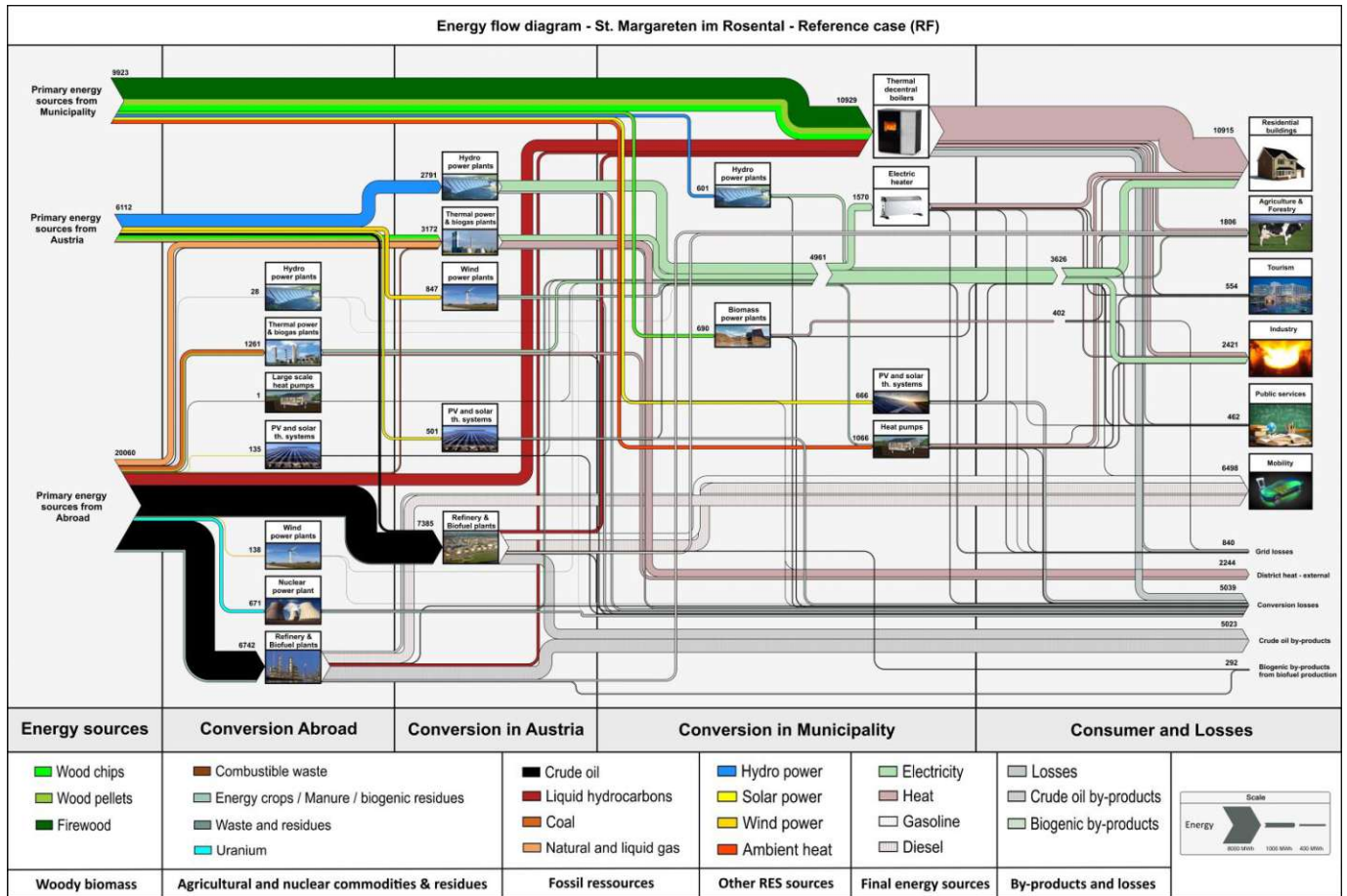


Figure 5. Energy flow diagram of present annual energy demand of St. Margareten im Rosental from reference case (2020 RF).

The annual CO₂e emissions and energy costs were calculated based on the previously described final energy demand. The present CO₂e emissions distributed to the heat, electricity, and fuel sectors are visualized in Figure 9 (2020 RF). The total annual CO₂e emissions of St. Margareten im Rosental were about 5.12 M kg CO₂e/a and can be seen in Figure 11 (2020 RF). Therein, it is highlighted that the most direct CO₂e emissions were caused by diesel and gasoline consumption in the mobility sector and electricity and oil consumption in the heating sector. Furthermore, electricity consumption was responsible for 15% of the total CO₂e emissions. The indirect emissions within the fuel sector, which were around 7% of the total emissions, were based on the manufacturing of vehicles. Additionally, the indirect emissions for transport and the extraction of heating oil and biomass, as well as indirect emissions caused by the Austrian electricity mix, were relevant for the ecologic footprint of the municipality.

The CO₂e emissions within the present reference case were also validated with the literature data in Table 3. Therein, it can be concluded that the ENECO₂Calc results were close to the literature data, with a deviation of ±11%. The calculated annual energy costs for St. Margareten are visualized sectorally distributed in Figure 10, and a total perspective is given in Figure 11 (2020 RF). The sectorally distributed annual energy costs in Figure 10 show that the most annual energy costs were based on fuel and O&M costs in the heating

sector. Additionally, fuel costs and taxes of the mobility sector were relevant. The results of the energy costs could not be validated because of a lack of data from the literature.

3.2. Scenario Development for St. Margareten im Rosental in 2050

Subsequent energy transition scenarios for St. Margareten im Rosental were investigated and compared with the reference case. Different frameworks had to be considered to develop a broad range of scenarios, as mentioned in Section 2.6. These frameworks were the national climate targets, central and decentral potentials for RES technologies, and possible prediction methodologies regarding the municipality's heat, electricity, and fuel demands. The heat, electricity, and fuel demand predictions for all the developed scenarios were applied. Therefore, the final heat demand was decreased by around 27% by 2050 compared to 2020, which assumed an ambitious renovation rate of 3% [59]. The final balanced annual electricity demand increased in all the scenarios by 31%, according to the trend of the past two decades of the total energy balance of Austria [122]. The fuel demand predictions were based on the assumption that the number of vehicles remains constant within the next three decades in the municipality. Therefore, the fuel demand decreased depending on the mobility option mix due to efficiency improvements. In addition to reaching the climate targets, which meant no fossil energy consumption by 2050, the explained central biomass potentials (see Section 2.6) and decentral RES technology potentials were the framework for the scenario development. The central biomass potentials showed several promising options to use biomass for the central production of synthetic natural gas, synthetic biofuels (FT fuels), or hydrogen. The decentral RES potentials for St. Margareten im Rosental are visualized in Figure 6. The reduced technical-biomass-based potential combined with forestry and agriculture potentials used in biomass CHP plants are plotted as a solid line. The dashed line shows the additional potential if it was assumed that the 2020 used wood in heating boilers in St. Margareten im Rosental could also be used in biomass CHP plants. According to REGIO Energy [49,114], solar thermal energy had the most significant potential and could cover nearly three times the 2020 thermal energy demand. The reduced technical potential of biomass CHP plants could cover up to half of the 2020 heat demand. Using the additional biomass potential, substituting existing biomass-based heating boilers could increase this share to over 80%. Solar PV showed the biggest electricity potential in 2050 and could reach over three times the electricity demand in 2020. The reduced technical potential of biomass CHP plants reached one-third of the electricity demand. The overall electricity demand could be covered entirely by using the additional wood from household heating boilers in biomass CHP plants. St. Margareten im Rosental already has a hydropower plant, and it was assumed that revitalization could increase the efficiency by 10%. Nevertheless, hydropower potential showed a small share of the overall electricity demand. According to [127], St. Margareten im Rosental show no development potential for wind energy.

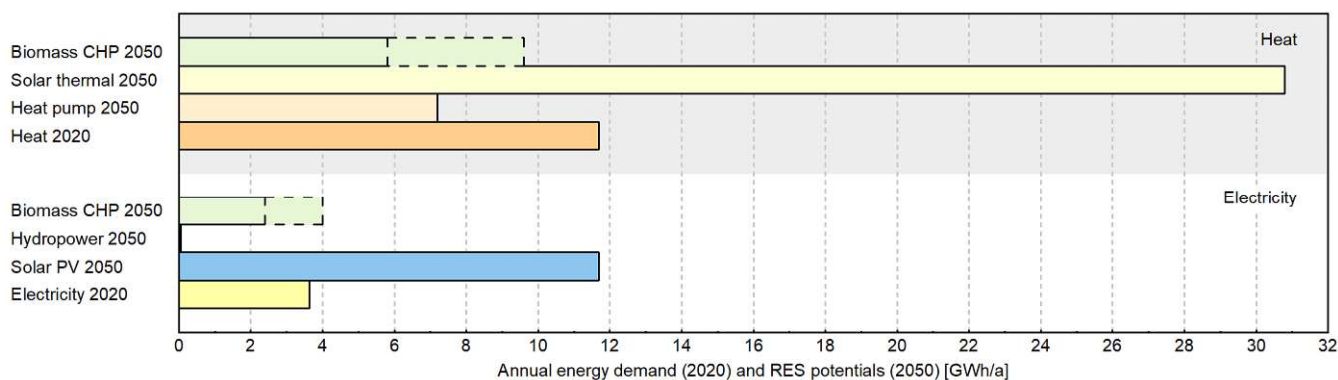


Figure 6. Decentral realizable heat and electricity potentials regarding RECs in the year 2050 compared with the current annual heat and electricity demand in St. Margareten im Rosental.

Based on the central Austrian biomass and decentral RES potentials of St. Margareten im Rosental, different scenarios were investigated to substitute fossil energy carriers with renewables. In summary, the greatest potential within the municipality could be provided with solar PV, biomass-based technologies, and heat pumps. In the total Austrian view, there were also huge biomass potentials to substitute significant amounts of natural gas with SNG or diesel and gasoline with synthetic biomass-based fuels or hydrogen. These considerations led to the assumed scenarios for the energy transition process within St. Margareten im Rosental by 2050 shown in Table 4. Scenario 0 represents the business-as-usual (BAU) scenario. Therein, the same energy distribution from the present reference case (2020 RF) was assumed. Scenario 1 is called biomass-to-mobility (BtM). Therein, the biomass was used centrally to produce synthetic biofuels. As a consequence, a lot of ICE vehicles were still in the vehicle fleet. Furthermore, the heating sector was defossilized by solar thermal collectors and heat pumps and the electricity sector mainly by the expansion of solar PV. Scenario 2 is called biomass to combined heat and power plants (BtCHP), which meant that the biomass was used in the municipality to produce heat and electricity within cogeneration units. Therefore, the heating sector was defossilized by the construction of a huge district heating system. The electricity sector was supplied half through the electricity from cogeneration units and half through solar PV plants. Furthermore, a strong focus on electrification, especially BEV, was placed within this scenario. Scenario 3 is called biomass-to-gas (BtG), which aimed to defossilize the Austrian electricity mix by substituting natural gas with biomass-based SNG within gas-fired power plants. Furthermore, the biomass was also used for the central production of hydrogen. Therefore, within scenario 3, there was a strong focus on FCEV. The heating sector was defossilized by solar thermal collectors and heat pumps.

In summary, the developed scenarios represent the possible development paths of the energy system. Therefore, on the one hand, the defossilization of the energy system could be reached by a focus on decentralized energy production enabled through local initiatives by citizens, communities, and businesses, supported by authorities to increase energy autonomy. On the other hand, the defossilization of the energy system could be based on the centralized production of synthetic biofuels, natural gas, hydrogen, and renewable electricity to strengthen the national and global economies. The considered scenario frameworks related to the possible trends regarding distributed or global energy production are underpinned by the Ten-Year Network Development Plan from the European Network of Transmission System Operators for Gas and Electricity [128].

3.3. Prediction Energy Demand and Ecologic and Economic Footprint in 2050

The scenarios in Section 3.2 were the basis for predicting the energy demand, as well as ecologic and economic footprint, in 2050. First of all, the results regarding heat and electricity demand compared with the present reference case are shown in Figure 7. The comparison of heat demand showed that the assumed building renovation rate of 3% decreased the final annual heat demand by around one-third. Furthermore, the heat distribution of the BtCHP scenario was dominated by cogeneration units and the BtG scenario by ambient heat systems. Within the BtM scenario, only the fossil oil and coal boilers were substituted with solar thermal collectors and heat pumps. The final annual electricity demand distribution, which included the electricity demands in the heating and mobility sectors, showed that the electricity demand increased within all the scenarios due to the underlying assumptions (see Section 3.2). Therefore, comparing the BAU scenario with the present reference case (RF) visualized the assumed increase according to the electricity demand. Based on the assumption that all the monthly deficit energy had to be covered by the AT electricity mix, the total final annual electricity demand was highest within the BtM scenario, according to the highest share of volatile energy technologies. Within the BtG scenario, the high share of ambient heat systems led to increased electricity demand due to the high amounts of auxiliary electric energy. Within the BtCHP scenario, only the low share of heat pumps led to a slight increase in the final electricity demand.

Table 4. Overview of investigated scenarios for St. Margareten for the year 2050.

Development of Energy Transition Scenarios	Scenario 0 (Business-as-Usual—BAU)	Scenario 1 (Biomass-to-Mobility—BtM)	Scenario 2 (Biomass to Combined Heat and Power Plants—BtCHP)	Scenario 3 (Biomass-to-Gas—BtG)
Heating sector		coal and oil boilers were substituted by solar thermal collectors and heat pumps	thermal decentral fossil- and renewable-based boilers and electrical heaters were substituted by the expansion of the existing district heating system driven by several cogeneration units	thermal decentral fossil- and renewable-based boilers were substituted by solar thermal collectors and heat pumps
Electricity sector		AT mix was substituted mainly through solar PV and small amounts of hydropower due to the revitalization	AT mix was substituted uniformly by cogeneration units and solar PV	AT mix was defossilized by the use of synthetic natural gas instead of fossil natural gas in central gas power plants
focus scenario:	no changes in energy distribution compared to the reference case (2020 RF)	strong focus on synthetic fuels	strong focus on BEV	strong focus on FCEV
cars and LCV:		ICE (54%) + BEV (36%) + PHEV (6%) + FCEV (4%)	ICE (23%) + BEV (61%) + PHEV (2%) + FCEV (14%)	ICE (33.5%) + BEV (36%) + PHEV (2.5%) + FCEV (28%)
MCV:		ICE-D (100%)	BEV (100%)	FCEV (100%)
HCV:		ICE-D (100%)	ICE-D (40%) + FCEV (60%)	FCEV (100%)
tractors:		ICE-D (95%) + BEV (5%)	ICE-D (52%) + BEV (14%) + FCEV (34%)	ICE-D (18%) + BEV (21%) + FCEV (61%)
ICE fuel:		BtL (33.5%) + PtL (66.5%)	PtL (100%)	PtL (100%)
hydrogen:		H ₂ electrolysis (100%)	H ₂ electrolysis (100%)	H ₂ from Biomass (33.5%) + H ₂ electrolysis (66.5%)

* Scenarios are based on mobility distribution scenarios according to [48] (cars and LCV) and [54] (MCV and HCV); for tractors, our own estimations following the distribution of HCV according to [54] are implemented.

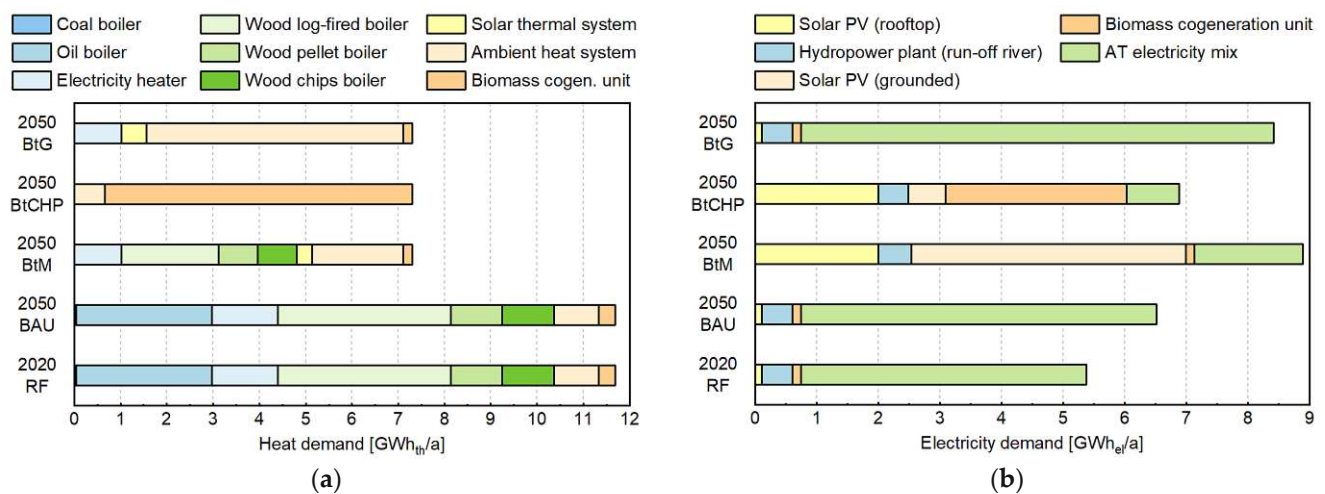


Figure 7. Comparison of final heat (a) and electricity (b) demands of the reference case (2020) with assumed scenarios (2050).

In Figure 8, the comparison of the annual final fuel demand of the present reference case (2020 RF) with alternative future scenarios can be seen. Due to the assumption that the number of vehicles was constant over the next 30 years and an assumed efficiency increase in the mobility sector, the final fuel demand decreased in all the alternative scenarios compared to the reference case. By comparing the final fuel demand within BAU and RF, the assumed efficiency increase for ICE could be seen. Within the scenario of BtCHP, with the highest electrification share in the mobility sector, the final fuel demand was the lowest due to the high efficiency of the vehicle fleet. The final fuel demand in the BtM scenario was higher than in the other scenarios because of the high share of ICE. The BtG final fuel demand was also deficient because of the high efficiency of fuel-cell vehicles in this scenario.

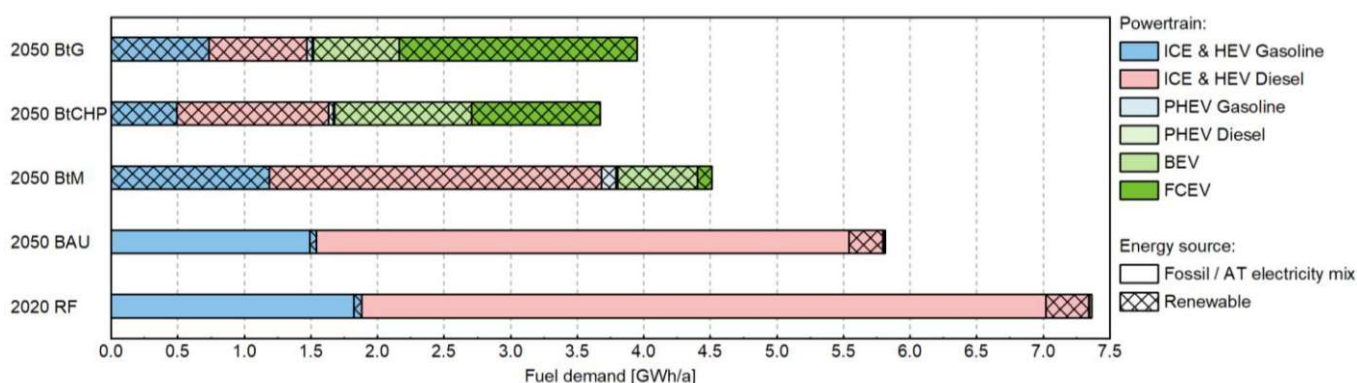


Figure 8. Comparison of final fuel demand of the reference case (2020) with assumed scenarios (2050).

The results regarding annual CO_{2e} emissions are visualized in Figure 9. Therein, it can be seen that the substitution of fossil fuels and electric heaters in the heating sector led to a huge reduction in CO_{2e} emissions. The CO_{2e} emissions in the heating sector of the BtM scenario were slightly higher than in the other alternative scenarios because of the electrical-based indirect emissions due to solar PV, which could also be seen in the electricity sector. In the BtG scenario, there were very low direct emissions in the heating sector because of the substitution of all thermal heating boilers. The electricity CO_{2e} emissions within the BtG scenario were the lowest because of the defossilization within the Austrian electricity mix through the use of biomass-based SNG in existing centralized gas-fired power plants instead of fossil natural gas. The substitution of fossil fuels with alternative technologies or synthetic biofuels showed the highest potential concerning CO_{2e} emission savings in the fuel sector. By comparing the indirect emissions of the alternative scenarios regarding fuel, it could be concluded that the higher indirect emissions of BEV and FCEV were balanced through the high efficiencies of the mobility systems. Therefore, the CO_{2e} emissions in the BtM scenario focused on synthetic biofuels caused more direct emissions due to the higher CO_{2e} footprint of PtL fuels than renewable-based electricity in BEV or H₂ in FCEV.

In Figure 10, the comparison of annual energy costs for the reference case and within the assumed scenarios is shown. In the heating sector, the renovation costs (infrastructure and investment costs) were much lower than the savings due to less heat demand. The heating costs in the BtCHP scenario were the lowest because of the central production of heat. The investment costs due to the expansion of the district heating grid (energy distribution and investment costs) were lower than the savings due to cheaper heat production costs. The heating costs within the BtG scenario were the highest because of the high O&M costs for heat pumps. The annual costs for the electricity sector were lower than the costs for the fuel and heating sectors. Within the BtM and BtCHP scenarios, the revenues due to surplus energy overtook the tax costs. The BtM scenario with huge amounts of solar PV cells had the lowest electricity costs because of the marginal fuel costs. The electricity costs in the BtCHP scenario were slightly higher than the others due to cogeneration units' higher electricity production costs than solar PV. The BtG scenario regarded electricity costs in the

range of the BtCHP scenario. The defossilization of the Austrian electricity mix increased the energy costs for electricity imports in the municipality. In the fuel sector, it was evident that the annual investment costs for vehicles overtook the fuel costs. The comparison of the scenarios showed that the higher costs of FCEV and BEV compared to ICE were meaningful. The lower fuel costs in the BtCHP scenario due to the high electrification rate balanced the higher investment costs of BEV. Compared with the BAU scenario, the higher fuel costs of synthetic biofuels in the BtM scenario could be balanced due to the reduced mineral oil tax exemption.

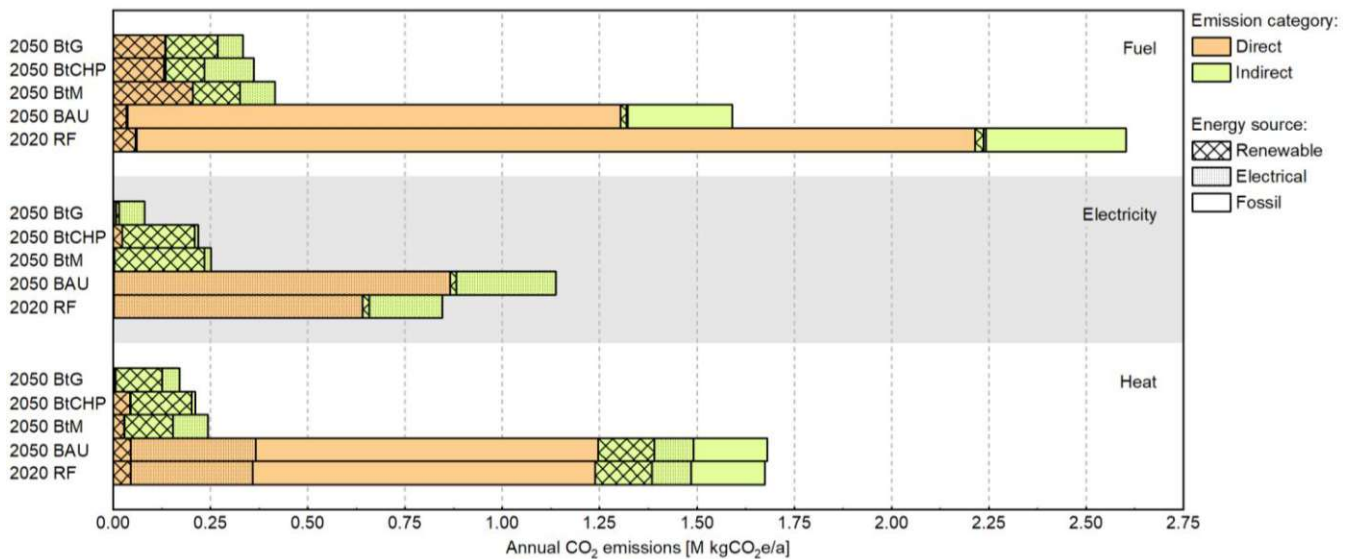


Figure 9. Comparison of annual CO₂e emissions of the reference case (2020) with assumed scenarios (2050).

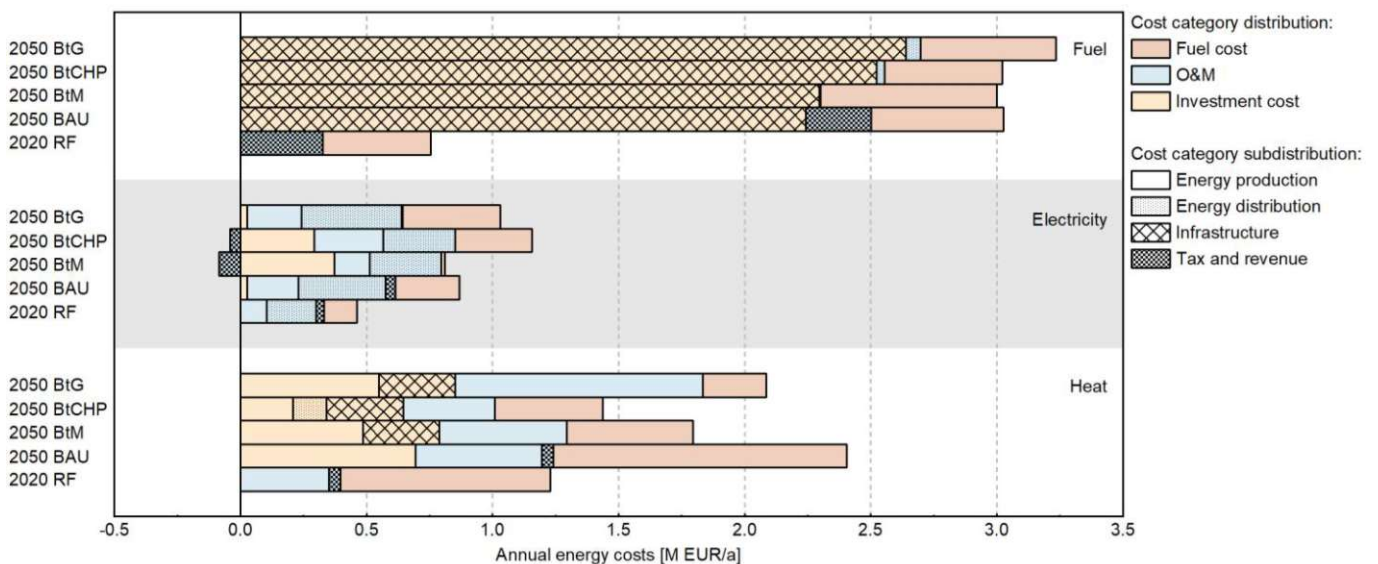


Figure 10. Comparison of annual energy costs of the reference case (2020) with assumed scenarios (2050).

The total annual CO₂e emissions and energy costs can be seen in Figure 11. It can be seen that the lowest CO₂e emissions were reached in the BtG scenario due to the low electricity emissions. Therein, the total CO₂e emissions could be reduced by around 85% in comparison to the BAU scenario. The total energy costs were nearly the same in the BtM and BtCHP scenarios. By comparison, the higher electricity costs in the BtCHP scenario

were balanced by the lower heat costs. The total energy costs within these two scenarios were about 12% lower than those within the BAU scenario. The reason was the much lower heat costs due to the ambitious renovation rate. The BtG scenario was in the BAU scenario range due to the fuel sector's higher costs with a focus on FCEV. The reference case, which represented the status quo of 2020, caused more emissions than the BAU scenario. However, the energy costs were much lower due to the missing investment costs. The comparability is to be discussed.

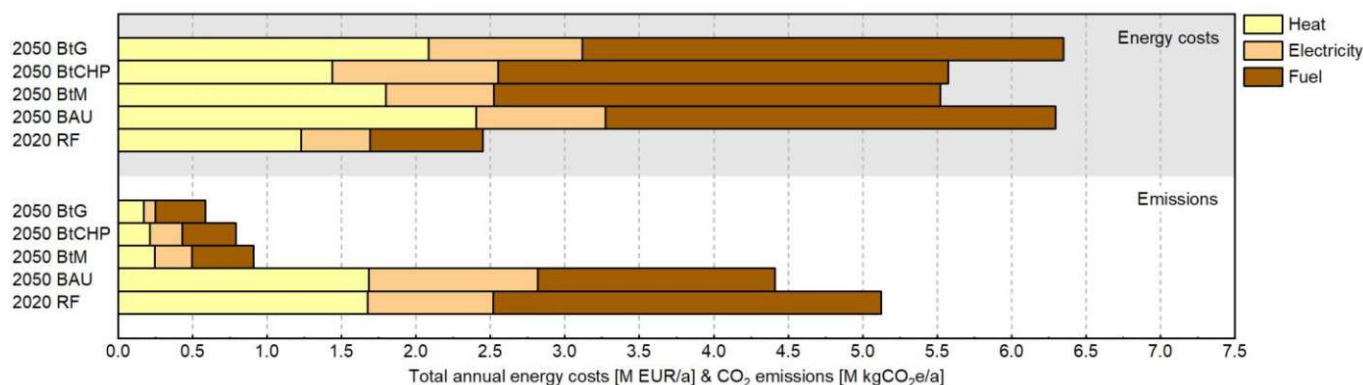


Figure 11. Comparison of total annual CO₂e emissions and costs of the reference case (2020) with assumed scenarios (2050).

It can be concluded that the fuel sector in St. Margareten im Rosental, due to the high number of vehicles, especially tractors, had the most impact on the total CO₂e emissions and energy costs. The fuel sector's lowest emissions were calculated by applying a high share of FCEV (BtG scenario). BEV vehicles (BtCHP scenario) caused more indirect emissions than FCEV. ICE vehicles (BtM scenario) caused more direct emissions due to the conversion of synthetic fuels than BEV or FCEV. The total energy costs in the fuel sector were lowest within the ICE-based (BtM) and BEV-based (BtCHP) scenarios because of the lower investment costs in comparison to FCEV (BtG). The greatest CO₂e emission reduction in the electricity sector could be reached by the defossilization of the Austrian electricity mix by substituting natural gas with biomass-based synthetic natural gas within the BtG scenario. The decentral defossilization of the municipality electricity mix could be reached by expanding solar PV (BtM) or biomass-based cogeneration plants (BtCHP). Despite higher electricity demand, the electricity costs were lowest within the solar PV (BtM) scenario. The heat costs were lowest when implementing central heat production with cogeneration plants within the BtCHP scenario. The BtG scenario, which was based on heat pumps, was the most expensive one, but the emissions were lowest because of the elimination of direct emissions.

Therefore, through a comparison of the total emissions and energy costs within the different scenarios, it could be recommended that, within the fuel sector, a mix of high electrification due to BEV in passenger transport and synthetic biofuels in freight transport and agriculture, could be a good compromise between energy costs and CO₂e emissions. In the heat sector, the lowest energy costs could be reached by the expansion of cogeneration plants. Therefore, it could be concluded that the existing district heating system should be extended and combined with decentral heat pumps. In the electricity sector, cogeneration plants combined with solar PV could perfectly defossilize the electricity demand. The electrification would increase in the fuel and heating sectors due to the expansion of heat pumps. Increasing the CO₂e emission certificate price to a level of 100–150 €/tCO₂e would help support biomass-based technologies for electricity, gas, and biofuel production to achieve more market penetration. The market premium schemes in Austria to support electricity RES technologies could also help balance the additional costs in the energy transition process.

In summary, ENECO₂Calc in the present evolutionary stage is able to develop energy transition paths for all 2095 municipalities in Austria based on consistent statistical datasets. Furthermore, ENECO₂Calc is the first municipality-based energy-modeling tool that allows the combined determination of the final energy demand, CO₂ footprint, and energy costs. ENECO₂Calc delivers results for the status quo, which is based on the year 2020, and helps to develop appropriate energy transition scenarios until the year 2050. Additionally, ENECO₂Calc enables the investigation of a sensitivity analysis to quantify examples of the impact of changes in energy resource cost factors caused by crisis.

The exemplary investigation of the Austrian municipality of St. Margareten im Rosental delivered results for the final energy demand and CO₂ footprint, as well as energy costs based on 2020. The results for the final energy demand and CO₂ footprint were in line with several other studies from the literature. It is underlined that ENECO₂Calc is the first municipality-based energy-modeling tool that enables the determination of the economic footprint for the reference year 2020. Additionally, ENECO₂Calc is the first tool for determining the economic and ecologic footprint for several energy transition scenarios based on realistic frameworks, such as potential analysis, and climate goals for the year 2050. Finally, ENECO₂Calc is coupled with the energy flow diagram software eSankey to visualize all the energy flows connected to the municipality. The investigation of energy transition scenarios for St. Margareten im Rosental showed that a mix of decentral RES technologies and central cogeneration units in the heat sector, a mix of solar PV and cogeneration units in the electricity sector, and the use of synthetic biofuels coupled with a higher share of electrification in the fuel sector seemed to be most promising in the considered region.

The modular methodology also allows the extension of ENECO₂Calc to deal with statistical datasets from municipalities of other countries in the future.

4. Conclusions and Outlook

This publication's scope was to set up and investigate an energy-modeling tool on the regional level that allows the prediction of energy transition scenarios for selected municipalities and projected the upcoming economic and ecologic footprint. Furthermore, the energy-modeling tool should allow the integration of energy communities within the municipality. With the development of ENECO₂Calc, it is possible to determine the current energy flows and the economic and ecologic footprint within a selected Austrian municipality. For this, a broad database of economic and ecologic factors of different energy supply technologies is provided with ENECO₂Calc. Furthermore, the final energy demand determination is exclusively based on consistent statistical datasets, such as Statistik Austria or other open-source databases. The distribution of the final energy demand and supply can be specified based on the present annual final energy demand. Additionally, a monthly discretization of the final energy demand and supply can cover seasonal differences in volatile energy supply technologies. As a result, the selected municipality's present economic and ecologic footprint can be determined. ENECO₂Calc also enables the prediction of different energy transition paths on the municipality level. Therefore, the European and national climate policy goals, the determination of future decentral and central RES potentials, and the prediction of the future heat, electricity, and fuel demands until 2050 build the framework for developing meaningful scenarios. Furthermore, ENECO₂Calc enables the implementation of RECs and CECs within the energy model, which considers the direct sale of final energy to the end-consumers on the levelized production cost level and savings concerning electricity network fees. The implementation of renewable energy technologies in ENECO₂Calc requires high-fidelity monthly distributed mass and energy balances enabled through the integration of digital twins.

The application of ENECO₂Calc within the Carinthian municipality of St. Margareten im Rosental proved the huge possibilities of the energy-modeling tool. The results showed that the final energy demand in St. Margareten im Rosental was mainly based on the residential building and mobility sectors. The validation of the calculated final energy demand was in line with several references. Due to the huge amount of forest area, the

municipality was suitable for integrating different biomass-based supply technologies. For the development of energy transition scenarios, three different ways toward a fossil-free municipality were set up and compared. The BtG scenario, with the defossilization of the heat sector by integrating solar thermal collectors and heat pumps coupled with the defossilization of the Austrian electricity mix by the central production of synthetic natural gas, resulted in the lowest ecologic footprint but also implied the highest energy costs. The BtCHP scenario, primarily based on biomass-based cogeneration units, and the BtM scenario, primarily based on a mix of decentral RES technologies in the heat and solar PV in the electricity sector, predicted much lower energy transition costs but also slightly higher greenhouse gas emissions. In the mobility sector, defossilization by synthetic biofuels in the BtM scenario and electrification via BEV in the BtCHP scenario were the most promising options for an affordable and sustainable energy transition within St. Margareten im Rosental.

ENECO₂Calc provides the first municipality-based energy-modeling tool for determining the present economic footprint, as well as the final energy demand and CO₂ footprint. Additionally, ENECO₂Calc offers the novel possibility to provide several energy transition paths for a selected municipality regarding their ecologic and economic impacts until the year 2050 based on realistic frameworks, such as a potential analysis and climate goals. Further development of ENECO₂Calc should focus on different final energy calculation approaches in the industry sector. Due to the general top-down approach, bigger inaccuracies could arise in industrialized municipalities. Additionally, the tool could be expanded by the cooling demand. Moreover, further discretization of the final energy demand would enable the consideration of storage and flexibility demand. In addition, the energy-modeling tool could be extended by implementing other technologies or ecologic characterization categories, such as water consumption or ozone depletion. Furthermore, the determination of the ecologic and economic footprint could be extended by social impact, such as the regional added value. Additionally, the economic and ecologic factors could be extended by regional dependencies, such as the implementation of regional distributed solar irradiation or wind speed. The prediction of cost factors for energy resources, such as crude oil or biomass, could be combined with energy market models to implement possible dynamic effects due to crisis. Furthermore, the methodology could be extended to also deal with statistical datasets from other countries than Austria. Finally, the usability of ENECO₂Calc could be improved by developing automatic data import processes and a user interface. In conclusion, ENECO₂Calc can support municipalities in finding the best strategy regarding economic and ecological footprint toward climate neutrality. In the present development stage of ENECO₂Calc, the methodology is focused on dealing with consistent statistical datasets from all 2095 Austrian municipalities. In the future, the methodology can easily be extended to also deal with statistical datasets from the municipalities of other countries.

Author Contributions: Conceptualization, M.H., J.K., A.W. and S.M.; methodology, M.H., J.K., A.W., T.P. and S.M.; software, M.H. and J.K.; validation, M.H., J.K. and S.M.; formal analysis, M.H., J.K., A.W. and T.P.; investigation, M.H., J.K., A.W. and T.P.; resources, M.H., J.K. and A.W.; data curation, M.H. and J.K.; writing—original draft preparation, M.H. and T.P.; writing—review and editing, J.K., T.P., and S.M.; visualization, M.H. and J.K.; supervision, S.M.; project administration, J.K. and S.M.; funding acquisition, J.K. and S.M. All authors have read and agreed to the published version of the manuscript.

Funding: The authors acknowledge TU Wien Bibliothek for financial support through its Open Access Funding Program. Open Access Funding by TU Wien.

Institutional Review Board Statement: Not applicable.

Informed Consent Statement: Not applicable.

Data Availability Statement: Selected data that support the findings of this study are available from the corresponding author, M. Hammerschmid, upon reasonable request.

Acknowledgments: The present work contains results of the project “Studie Modellregion”, funded by GLOCK Technology GmbH.

Conflicts of Interest: The authors declare no conflict of interest.

Abbreviations

2020 RF	reference case scenario for the present state based on the year 2020
AT mix	Austrian mix
BAU	business-as-usual
BEV	battery electric vehicle
BtCHP	biomass to combined heat and power plants
BtG	biomass-to-gas
BtL	biomass-to-liquid
BtM	biomass-to-mobility
CEC	citizen energy community
CHP	combined heat and power
CNG	compressed natural gas
CO ₂	carbon dioxide
CO ₂ e	carbon dioxide equivalent
CPI	consumer price index
DFB	dual fluidized bed steam gasification
e!Sankey	software for the development of energy flow diagrams
EDisOn	energy-modeling tool from the EEG at TU Wien
EEG	Energy and Economics Group at TU Wien
ELAS	energy-modeling tool for municipality level
ELMOD	energy-modeling tool for electricity market simulations
EMA	energy mosaic Austria
ENECO ₂ Calc	energy-modeling tool investigated in this paper
EnergyPLAN	energy-modeling tool from Aalborg University
EPI	energy price index
EU	European Union
EU-27	member states of the European Union (since February 2020)
EU mix	European Union mix
FAME	fatty acid methyl ester
FCEV	fuel-cell electric vehicle
FT	Fischer–Tropsch
Green-X	energy-modeling tool for electricity market simulations
H ₂	hydrogen
HCV	heavy commercial vehicle
HOMER	energy-modeling tool from LCC Homer
ICE	internal combustion engine
ICE-D	internal combustion engine powered with diesel
IEA-ETSAP	energy technology systems analysis program from the International Energy Agency
IFA	Institute for Powertrains and Automotive Technology at TU Wien
LCV	light commercial vehicle
MARKAL/TIMES	energy-modeling tool from IEA-ETSAP
MCV	medium commercial vehicle
MS Excel	spreadsheet software from Microsoft
O&M	operation and maintenance
ÖNACE	classification of economic activities
PHEV	plug-in hybrid electric vehicle
PROVEM	emission forecast tool from the IFA at TU Wien
PtL	power-to-liquid
PV	photovoltaic
REC	renewable energy community
RED II	Renewable Energy Directive

REGIO Energy	potential analysis of renewable energy sources on the district level
RES	renewable energy sources
RF	reference case
SME	small- and medium-sized enterprise
SNG	synthetic natural gas
TRNSYS18	energy-modeling tool from the University of Wisconsin-Madison
Symbols	
%/year	percent of energy per year
% _{th}	percent of energy based on thermal energy
% _{el}	percent of energy based on electrical energy
COP	coefficient of performance
GW _{el}	gigawatt of electrical power
GWh	gigawatt hours of energy
km ²	square kilometer
kW _{el}	kilowatt of electrical power
kW _p _{el}	kilowatt peak of electrical power
kWh _{Input}	kilowatt hours of energy on the educt side
kWh _{Output}	kilowatt hours of energy on the product side
M EUR	millions of euros
M kg	millions of kilograms
MW _{el}	megawatt of electrical power
t CO _{2e}	tons of carbon dioxide equivalent

References

- Umweltbundesamt Deutschland. Treibhausgas-Emissionen in der Europäischen Union. 2021. Available online: <https://www.umweltbundesamt.de/daten/klima/treibhausgas-emissionen-in-der-europaeischen-union#gase> (accessed on 22 October 2021).
- Anderl, M.; Geiger, K.; Gugele, B.; Gössl, M.; Haider, S.; Heller, C.; Köther, T.; Krutzler, T.; Kuschel, V.; Lampert, C.; et al. *Klimaschutzbericht 2020*; Umweltbundesamt GmbH: Vienna, Austria, 2020; ISBN 978-3-99004-558-9. Available online: https://www.umweltbundesamt.at/studien-reports/publikationsdetail?pub_id=2340&cHash=04535f1c207c6ac8814ee0edb3809750 (accessed on 22 October 2021).
- United Nations. The Paris Agreement—UNFCCC. 2015. Available online: https://unfccc.int/sites/default/files/english_paris_agreement.pdf (accessed on 22 October 2021).
- European Union. 2030 Climate and Energy Policy Framework. 2020. Available online: https://ec.europa.eu/clima/eu-action/climate-strategies-targets/2030-climate-energy-framework_en (accessed on 22 October 2021).
- European Union. DIRECTIVE (EU) 2018/2001 of the European Parliament and of the Council of 11 December 2018 on the Promotion of the Use of Energy from Renewable Sources, RED II. Official Journal of the European Union, 2018. Available online: <https://eur-lex.europa.eu/legal-content/DE/TXT/?qid=1575559881403&uri=CELEX:32018L2001> (accessed on 12 May 2021).
- Bundesrepublik Österreich. Erneuerbaren-Ausbau-Gesetz, EAG. 2021. Available online: https://www.parlament.gv.at/PAKT/VHG/XXVII/I/I_00733/index.shtml (accessed on 12 August 2021).
- Wang, Q.; Su, M. A preliminary assessment of the impact of COVID-19 on environment—A case study of China. *Sci. Total Environ.* **2020**, *728*, 138915. [CrossRef] [PubMed]
- Wang, Q.; Yang, X.; Li, R. The impact of the COVID-19 pandemic on the energy market—A comparative relationship between oil and coal. *Energy Strat. Rev.* **2022**, *39*, 100761. [CrossRef]
- Frieden, D.; Türk, A.; Neumann, C. *Energiegemeinschaften: Neue Geschäftschancen für Die Grüne Energiezukunft*; Green Tech Cluster Styria GmbH, Joanneum Research Forschungsgesellschaft mbH: Graz, Austria, 2020.
- Neubarth, J. *Energiegemeinschaften im Zukünftigen Österreichischen Strommarkt: Erforderliche Rahmenbedingungen für Eine Erfolgreiche Umsetzung*; E3 Consult: Innsbruck, Austria, 2020.
- European Union. DIRECTIVE (EU) 2019/944 of the European Parliament and of the Council of 5 June 2019 on Common Rules for the Internal Market for Electricity and Amending Directive 2012/27/EU. Official Journal of the European Union, 2019; volume 2019. Available online: <https://eur-lex.europa.eu/legal-content/DE/TXT/?uri=CELEX:32019L0944> (accessed on 12 May 2021).
- E-Control. Energiegemeinschaften. 2021. Available online: <https://www.e-control.at/energiegemeinschaften> (accessed on 17 May 2021).
- Azarova, V.; Cohen, J.; Friedl, C.; Reichl, J. Designing local renewable energy communities to increase social acceptance: Evidence from a choice experiment in Austria, Germany, Italy, and Switzerland. *Energy Policy* **2019**, *132*, 1176–1183. [CrossRef]
- Dóci, G.; Vasileiadou, E.; Petersen, A.C. Exploring the transition potential of renewable energy communities. *Futures* **2015**, *66*, 85–95. [CrossRef]
- Fina, B.; Auer, H. Economic Viability of Renewable Energy Communities under the Framework of the Renewable Energy Directive Transposed to Austrian Law. *Energies* **2020**, *13*, 5743. [CrossRef]

16. Fina, B.; Auer, H.; Friedl, W. Cost-optimal economic potential of shared rooftop PV in energy communities: Evidence from Austria. *Renew. Energy* **2020**, *152*, 217–228. [CrossRef]
17. Inês, C.; Guilherme, P.L.; Esther, M.-G.; Swantje, G.; Stephen, H.; Lars, H. Regulatory challenges and opportunities for collective renewable energy prosumers in the EU. *Energy Policy* **2020**, *138*, 111212. [CrossRef]
18. Karunathilake, H.; Hewage, K.; Mérida, W.; Sadiq, R. Renewable energy selection for net-zero energy communities: Life cycle based decision making under uncertainty. *Renew. Energy* **2019**, *130*, 558–573. [CrossRef]
19. Lowitzsch, J.; Hoicka, C.E.; van Tulder, F.J. Renewable energy communities under the 2019 European Clean Energy Package—Governance model for the energy clusters of the future? *Renew. Sustain. Energy Rev.* **2020**, *122*, 109489. [CrossRef]
20. Stefan, M.; Zehetbauer, P.; Cejka, S.; Zeilinger, F.; Taljan, G. *Blockchain-Based Self-Consumption Optimization and Energy Trading in Renewable Energy Communities: CIRED 2020 Berlin Workshop*; Austrian Institute of Technology GmbH, Siemens AG, Energienetze Steiermark GmbH: Berlin, Germany, 2020.
21. Soeiro, S.; Dias, M.F. Renewable energy community and the European energy market: Main motivations. *Heliyon* **2020**, *6*, e04511. [CrossRef]
22. European Union. The European Green Deal. 2019. Available online: https://ec.europa.eu/info/sites/default/files/european-green-deal-communication_en.pdf (accessed on 22 October 2021).
23. European Union. Regulation of the European Parliament and of the Council Establishing the Framework for Achieving Climate Neutrality and Amending Regulation (EU) 2018/1999—European Climate Law: Proposal. 2018. Available online: <https://eur-lex.europa.eu/legal-content/EN/TXT/PDF/?uri=CELEX:52020PC0080&from=EN> (accessed on 22 October 2021).
24. Hayley, T.; Bardos, P.; Smith, J.; Evans, F.; Haslam, A.; Howard, T.; Boyle, R.; Thomas, A.; Lewis, R.; Dent, V.; et al. *Supplementary Report 2 of the SuRF-UK Framework: Selection of Indicators/Criteria for Use in Sustainability Assessment for Achieving Sustainable Remediation*; CL: AIRE Publications: Haddenham, UK, 2020; ISBN 978-1-905046-34-8.
25. Stoglehner, G.; Neugebauer, G.; Erker, S.; Narodoslawsky, M. *Integrated Spatial and Energy Planning: Supporting Climate Protection*; SpringerBriefs in Applied Sciences and Technology; Springer: Berlin/Heidelberg, Germany, 2016; ISBN 3319318683.
26. van Beeck, N.M.J.P. Classification of Energy Models. FEW Research Memorandum. *Oper. Res.* **1999**, *777*, 1–26.
27. Pfenninger, S.; Hawkes, A.; Keirstead, J. Energy systems modeling for twenty-first century energy challenges. *Renew. Sustain. Energy Rev.* **2014**, *33*, 74–86. [CrossRef]
28. Abart-Heriszt, L.; Erker, S.; Stoglehner, G. The Energy Mosaic Austria—A Nationwide Energy and Greenhouse Gas Inventory on Municipal Level as Action Field of Integrated Spatial and Energy Planning. *Energies* **2019**, *12*, 3065. [CrossRef]
29. The World Energy Council. World Energy Trilemma Index 2018. London, UK, 2018. Available online: <https://www.worldenergy.org/assets/downloads/World-Energy-Trilemma-Index-2018.pdf> (accessed on 22 October 2021).
30. Hall, L.M.; Buckley, A.R. A review of energy systems models in the UK: Prevalent usage and categorisation. *Appl. Energy* **2016**, *169*, 607–628. [CrossRef]
31. Aalborg University. EnergyPLAN: Advanced Energy System Analysis Computer Model. 2021. Available online: <https://www.energyplan.eu/> (accessed on 11 May 2021).
32. International Energy Agency. MARKAL/TIMES: Energy Technology Systems Analysis Programme. 2021. Available online: <https://iea-etsap.org/> (accessed on 11 May 2021).
33. National Technical University of Athens. PRIMES: Energy-Economics-Environment Modelling Laboratory Research and Policy Analysis. 2021. Available online: <http://www.e3mlab.eu/e3mlab/> (accessed on 11 May 2021).
34. International Institute for Applied Systems Analysis. MESSAGE: Energy Modelling Framework: Model for Energy Supply Strategy Alternatives and Their General Environmental Impact. 2021. Available online: <https://webarchive.iiasa.ac.at/Research/ENE/model/message.html> (accessed on 11 May 2021).
35. Resch, G.; Burgholzer, B.; Totschnig, G.; Lettner, G.; Auer, H.; Geipel, J.; Haas, R. *Stromzukunft Österreich 2030: Analyse der Erfordernisse und Konsequenzen Eines Ambitionierten Ausbaus von Erneuerbaren Energien*; Energy Economics Group (EEG), Technische Universität Wien: Vienna, Austria, 2017.
36. Hasani, J.M.F. Hotmaps Dispatch Model: District-Heating Supply Dispatch. Energy Economics Group, Technische Universität Wien. 2021. Available online: <https://wiki.hotmaps.eu/en/CM-District-heating-supply-dispatch> (accessed on 11 May 2021).
37. Leuthold, F.U.; Weigt, H.; Von Hirschhausen, C. A Large-Scale Spatial Optimization Model of the European Electricity Market. *Networks Spat. Econ.* **2012**, *12*, 75–107. [CrossRef]
38. Homer Energy LCC. HOMER. 2021. Available online: <https://www.homerenergy.com/> (accessed on 11 May 2021).
39. University of Wisconsin-Madison. A TRAnSient SYStems Simulation Program. Version 18. 2021. Available online: <https://sel.me.wisc.edu/trnsys/> (accessed on 11 May 2021).
40. Keirstead, J.; Jennings, M.; Sivakumar, A. A review of urban energy system models: Approaches, challenges and opportunities. *Renew. Sustain. Energy Rev.* **2012**, *16*, 3847–3866. [CrossRef]
41. Stöglehner, G.; Narodoslawsky, M.; Baaske, W.; Mitter, H.; Weiss, M.; Neugebauer, G.C.; Niemetz, N.; Kettl, K.-H.; Eder, M.; Sandor, N.; et al. *ELAS—Energetische Langzeitanalysen von Siedlungsstrukturen: Projektendbericht*; Gefördert aus Mitteln des Klima- und Energiefonds, des Landes Oberösterreich, des Landes Niederösterreich und der Stadtgemeinde Freistadt: Vienna, Austria, 2011.
42. Lyden, A.; Pepper, R.; Tuohy, P.G. A modelling tool selection process for planning of community scale energy systems including storage and demand side management. *Sustain. Cities Soc.* **2018**, *39*, 674–688. [CrossRef]

43. Lopion, P.; Markewitz, P.; Robinius, M.; Stolten, D. A review of current challenges and trends in energy systems modeling. *Renew. Sustain. Energy Rev.* **2018**, *96*, 156–166. [CrossRef]
44. Connolly, D.; Lund, H.; Mathiesen, B.; Leahy, M. A review of computer tools for analysing the integration of renewable energy into various energy systems. *Appl. Energy* **2010**, *87*, 1059–1082. [CrossRef]
45. Pfenninger, S.; Hirth, L.; Schlecht, I.; Schmid, E.; Wiese, F.; Brown, T.; Davis, C.; Gidden, M.; Heinrichs, H.; Heuberger, C.; et al. Opening the black box of energy modelling: Strategies and lessons learned. *Energy Strat. Rev.* **2018**, *19*, 63–71. [CrossRef]
46. Statistik Austria. Ein Blick auf die Gemeinde. Vienna, 2020. Available online: https://www.statistik.at/web_de/services/ein_blick_auf_die_gemeinde/index.html (accessed on 17 May 2020).
47. Klima und Energiefonds. Klima- und Energiemodellregionen: Wir Gestalten Die Energiewende. Kommunalkredit Public Consulting. 2021. Available online: <https://www.klimaundenergiemodellregionen.at/> (accessed on 17 May 2021).
48. TU Wien, Institut für Fahrzeugantriebe. PROVEM: Emissionsprognose-Tool. Vienna, 2019. Available online: <http://www.ifa.tuwien.ac.at/en/research-development/research-projects/miscellaneous/emission-forecasts/> (accessed on 11 May 2021).
49. Stanzer, G.; Novak, S.; Dumke, H.; Plha, S.; Schaffer, H.; Breinesberger, J.; Kirtz, M.; Biermayer, P.; Spanring, C. Regio Energy: Regionale Szenarien erneuerbarer Energiepotentiale in den Jahren 2012/2020, ÖIR, Mecca Environmental Consulting, AGRAR PLUS, TU Wien/Energy Economics Group, Vienna, St. Pölten. 2010. Available online: <http://regioenergy.oir.at/> (accessed on 17 May 2021).
50. Statistik Austria. Nutzenergieanalyse Österreich 2019. 2020. Available online: http://www.statistik.at/web_de/statistiken/energie_umwelt_innovation_mobilitaet/energie_und_umwelt/energie/nutzenergieanalyse/index.html (accessed on 17 May 2020).
51. Biermayr, P.; Kristöfel, C.; Enigl, M.; Strasser, C.; Schmidl, C.; Wopienka, E.; Leonhartsberger, K.; Fechner, H.; Weiß, W.; Eberl, M.; et al. *Innovative Energietechnologie in Österreich Marktentwicklung 2015: Berichte aus Energie- und Umweltforschung 6/2016*; Bundesministerium für Verkehr, Innovation und Technologie: Vienna, Austria, 2016.
52. Losch, M.; Streitner, J.; Gary, W.; Berger, P. *Energie in Österreich 2020: Zahlen, Daten, Fakten. Bundesministerium für Klimaschutz, Umwelt, Energie, Mobilität; Innovation und Technologie (BMK): Vienna, Austria, 2020.*
53. Umweltbundesamt Österreich. Berechnung von Treibhausgas (THG)-Emissionen Verschiedener Energieträger, Vienna. 2020. Available online: <https://secure.umweltbundesamt.at/co2mon/co2mon.html> (accessed on 7 June 2021).
54. Bründlinger, T.; König, J.E.; Frank, O.; Gründig, D.; Jugel, C.; Kraft, P.; Krieger, O.; Mischinger, S.; Prein, P.; Seidl, H.; et al. *Dena-Leitstudie Integrierte Energiewende: Impulse für die Gestaltung des Energiesystems bis 2050*; Deutsche Energie-Agentur (DENA): Berlin, Germany, 2018.
55. Aydemir, A.; Schilling, D. CM Wärmelastprofile. Hotmaps-Wiki. 2020. Available online: <https://wiki.hotmaps.eu/de/CM-Heat-load-profiles#license> (accessed on 28 June 2021).
56. Austrian Power Grid. Monatlicher Stromverbrauch in Österreich von Januar 2017 bis Mai 2021. Statista GmbH. Hamburg. 2021. Available online: <https://de.statista.com/statistik/daten/studie/1108164/umfrage/woechentlicher-stromverbrauch-in-oesterreich/> (accessed on 2 June 2021).
57. Huneke, F.; Perez, C.L.; Heidinger, P. *Österreichs Weg Richtung 100% Erneuerbare: Eine Analyse von 2030 mit Ausblick 2050*; Austrian Power Grid AG: Berlin, Germany, 2019.
58. Institut für Umweltinformatik Hamburg GmbH. e!Sankey. Version 4 Pro. 2017. Available online: <https://www.ifu.com/de/e-sankey/> (accessed on 22 October 2021).
59. Kranzl, L.; Müller, A.; Maia, I.; Büchele, R.; Hartner, M. *Wärmezukunft 2050: Erfordernisse und Konsequenzen der Dekarbonisierung von Raumwärme und Warmwasserbereitstellung in Österreich*; Endbericht, Technische Universität Wien, Energy Economics Group: Vienna, Austria, 2018.
60. Kranzl, L.; Haas, R.; Kalt, G.; Diesenreiter, F.; Eltrop, L.; König, A.; Makkonen, P. *Strategien zur optimalen Erschließung der Biomassepotenziale in Österreich bis zum Jahr 2050 mit dem Ziel einer maximalen Reduktion an Treibhausgasemissionen: Berichte aus Energie- und Umweltforschung, Bundesministerium für Verkehr; Innovation und Technologie, Technische Universität Wien, Institut für elektrische Anlagen und Energiewirtschaft: Vienna, Austria, 2008.*
61. Thermondo GmbH. Wirkungsgrad der Heizung—Wichtige Kennzahl für die Effizienz des Heizgeräts. Berlin, 2019. Available online: <https://www.thermondo.de/info/rat/vergleich/wirkungsgrad-der-heizung/> (accessed on 2 June 2021).
62. Kranzl, L.; Hasani, J. *Renewable Heating and Cooling. Economic Perspectives of Renewable Energy Systems*; Technische Universität Wien, Energy Economics Group: Vienna, Austria, 2020.
63. Lauf, T.; Memmler, M.; Schneider, S. *Emissionsbilanz erneuerbarer Energieträger: Bestimmung der vermiedenen Emissionen im Jahr 2018*; Umweltbundesamt Deutschland: Dessau-Roßlau, Germany, 2019.
64. Hofbauer, H. *Bewertung von Energiebereitstellungssystemen. Lecture Script; Brennstoff- und Energietechnologie*, Technische Universität Wien, Institut für Verfahrenstechnik: Vienna, Austria, 2019.
65. Alberici, S.; Boeve, S.; van Breevoort, P.; Deng, Y.; Förster, S.; Gardiner, A.; van Gastel, V.; Grave, K.; Groenenberg, H.; de Jager, D.; et al. *Subsidies and Costs of EU Energy: Final Report*; Ecofys: Utrecht, The Netherlands, 2014.
66. Kost, C.; Shammugam, S.; Jülch, V.; Nguyen, H.-T.; Schlegl, T. *Stromgestehungskosten Erneuerbarer Energien*; Fraunhofer-Institut: Freiburg, Germany, 2018.
67. Böhmer, S.; Kügler, I.; Stoiber, H.; Walter, B. *Abfallverbrennung in Österreich: Statusbericht 2006*; Umweltbundesamt Österreich: Vienna, Austria, 2007.

68. Schwarzböck, T. *Bestimmung der fossilen Kohlendioxidemissionen aus Österreichischen Müllverbrennungsanlagen (BEFKÖM): Endbericht, Bundesministeriums für Land- und Forstwirtschaft, Umwelt und Wasserwirtschaft*; Technische Universität Wien, Institut für Wassergüte, Ressourcenmanagement und Abfallwirtschaft: Vienna, Austria, 2015.
69. Dufour, J.; Iribarren, D. Life cycle assessment of biodiesel production from free fatty acid-rich wastes. *Renew. Energy* **2012**, *38*, 155–162. [CrossRef]
70. Fachagentur Nachwachsende Rohstoffe e.V. *Biokraftstoffe—Eine Vergleichende Analyse*; Fachagentur Nachwachsende Rohstoffe e.V.: Berlin, Germany, 2006.
71. Rauch, A.; Thöne, M. *Biofuels—At What Cost? Mandating Ethanol and Biodiesel Consumption in Germany*; Universität Köln, International Institute for Sustainable Development, FiFo Institut: Köln, Germany, 2012.
72. Lichtblau, G.; Pölz, W.; Stix, S.; Winter, R. *Ökobilanzen ausgewählter Biotreibstoffe: Projekt proVISION*; Umweltbundesamt Österreich: Vienna, Austria, 2012.
73. Hofbauer, H.; Mauerhofer, A.; Benedikt, F.; Hammerschmid, M.; Bartik, A.; Veress, M.; Haas, R.; Siebenhofer, M.; Resch, G. *Reallabor zur Herstellung von Holzdieisel und Holzgas aus Biomasse und biogenen Reststoffen für die Land- und Forstwirtschaft, Bundesministerium für Nachhaltigkeit und Tourismus*; Institut für Verfahrenstechnik, Umwelttechnik & Technische Biowissenschaften, Institut für Energiesysteme und Elektrische Antriebe, TU Wien: Vienna, Austria, 2020.
74. Bell, M.; Kollamthodi, S.; Hill, N.; Greaney, A. *The Net Zero Challenge—Life Cycle Impacts on Propulsion System Technologies, Supply Chains & the Regulatory Landscape, 41*; Internationales Wiener Motorensymposium: Vienna, Austria, 2020.
75. OMV Refining & Marketing GmbH. Raffinerie Schwechat: Geschichte und Standort, Schwechat. 2016. Available online: https://ahgroup.at/user_files/SE-&-VO/UNT.044_Industrieexkursion/OMV_Raffinerie-Schwechat.pdf (accessed on 25 October 2021).
76. Alt, R.; Antrekowitsch, H.; Baumann, M.; Borrmann, J.; Brandauer, W.; Egger, L.; Eichlseder, H.; Eichlseder, W.; Fichtinger, M.; Geringer, B.; et al. *Expertenbericht Mobilität & Klimaschutz 2030, ÖAMTC, ARBÖ*; Economica Institut für Wirtschaftsforschung: Vienna, Austria; Montanuniversität Leoben: Leoben, Austria; Österreichische Energieagentur: Vienna, Austria; TU Graz: Graz, Austria; TU Wien: Vienna, Austria; PIERER Industrie AG: Wels, Austria; Joanneum Research Forschungsgesellschaft mbH: Graz, Austria; Eurotax Österreich GmbH: Vienna, Austria, 2018.
77. Bruckmüller, T.; Graf, J.; Konrad, J.; Scharinger-Urschitz, G.; Werner, A.; Hammerschmid, M.; Hofbauer, H.; Lehr, M.; Müller, S.; Geringer, B. *Ökologische und ökonomische Analyse der Energieversorgung und Mobilität einer Referenzregion und deren Entwicklungspotentiale bis 2030*; Institut für Fahrzeugantriebe und Automobiltechnik; Institut für Energietechnik und Thermodynamik; Institut für Verfahrenstechnik, Umwelttechnik und & Technische Biowissenschaften, Technische Universität Wien: Vienna, Austria, 2019.
78. Neuling, U.; Kaltschmitt, M. Techno-economic and environmental analysis of aviation biofuels. *Fuel Process. Technol.* **2018**, *171*, 54–69. [CrossRef]
79. Mitterhüemer, R.; Winter, R. *Biokraftstoffe im Verkehrssektor 2020*; Bundesministerium für Klimaschutz, Umwelt, Energie, Mobilität, Innovation und Technologie (BMK): Vienna, Austria, 2020.
80. Kalligeros, S.; van Heuvel, E.; Waldheim, L.; Landälv, I.; Maniatis, K. *Building Up the Future: Sub Group on Advanced Biofuels: Final Report*; Publications Office: Luxembourg, 2017; ISBN 978-92-79-69010-5.
81. Mottschall, M.; Kasten, P.; Kühnel, S.; Minnich, L. *Sensitivitäten zur Bewertung der Kosten Verschiedener Energieversorgungsoptionen des Verkehrs bis zum Jahr 2050: Abschlussbericht*; Umweltbundesamt Deutschland, Öko-Institut: Berlin, Germany, 2019.
82. Jungmeier, G. *Umweltbilanz von E-Fuels—Vergleich mit anderen Treibstoffen im Lebenszyklus*; Innovative Energieversorgung; ÖGEW/DGMK Onlinekonferenz, Joanneum Research Forschungsgesellschaft mbH: Graz, Austria, 2020.
83. Nielsen, P.H.; Wenzel, H. *Environmental Assessment of Ethanol Produced from Corn Starch and Used as an Alternative to Conventional Gasoline for Car Driving*; The Institute for Product Development, Technical University of Denmark: Lyngby, Denmark, 2005.
84. Geiger, J. *Erdgas als alternativer Kraftstoff: Ein Potenzial zur Reduktion von Treibhausgasemissionen*; Technologie-Highlights aus dem FEV-Arbeitsspektrum; Sonderausgabe: Aachen, Germany, 2013.
85. Bruckmüller, T. *Entwicklung einer Methodik zur Bewertung des Ladeinfrastrukturbedarfs für Elektrofahrzeuge hinsichtlich Anzahl, Kosten und Auswirkungen auf die Energieversorgung am Beispiel Österreichs bis 2030*. Ph.D. Thesis, Technische Universität Wien, Vienna, Austria, 2020.
86. Bundestag, D. *Kosten der Produktion von Grünem Wasserstoff*; Dokumentation: Berlin, Germany, 2020.
87. Wulf, C.; Kaltschmitt, M. Hydrogen Supply Chains for Mobility—Environmental and Economic Assessment. *Sustainability* **2018**, *10*, 1699. [CrossRef]
88. Statistik Austria. Consumer Price Index. 2021. Available online: http://statistik.at/web_en/statistics/Economy/Prices/consumer_price_index_cpi_hcpi/index.html (accessed on 29 June 2021).
89. Jungmeier, G.; Canella, L.; Pucker-Singer, J.; Beermann, M. *Geschätzte Treibhausgasemissionen und Primärenergieverbrauch in der Lebenszyklusanalyse von Pkw-basierten Verkehrssystemen*; ÖAMTC, ADAC, FIA, Joanneum Research Forschungsgesellschaft mbH: Graz, Austria, 2019.
90. Wirtschaftskammer Österreich. *Energiebesteuerung—Die Kohleabgabe: Lieferant oder Verbraucher hat die Abgabe zu entrichten*. 2021. Available online: https://www.wko.at/service/steuern/Energiebesteuerung_-_Die_Kohleabgabe.html (accessed on 29 June 2021).
91. ÖAMTC. Mineralölsteuer. Vienna, 2018. Available online: <https://www.oeamtc.at/thema/verkehr/mineraloelsteuer-17914742>. (accessed on 29 June 2021).

92. Graus, W.; Blomen, E.; Worrell, E. Global energy efficiency improvement in the long term: A demand- and supply-side perspective. *Energy Effic.* **2011**, *4*, 435–463. [CrossRef]
93. IINAS GmbH. *Globales Emissions-Modell Integrierter Systeme (GEMIS)*. Internationales Institut für Nachhaltigkeits-Analysen und -Strategien; Version 4.94; IINAS GmbH: Darmstadt, Germany, 2018.
94. Müller, A.; Biermayer, P.; Kranzl, L.; Haas, R.; Friedl, G.; Haslinger, W.; Ohnmacht, R.; Weiss, W.; Bergmann, I.; Heimrath, R.; et al. *Heizen 2050: Systeme zur Wärmebereitstellung und Raumklimatisierung im österreichischen Gebäudebestand: Technologische Anforderungen bis zum Jahr 2050*; Energy Economics Group (EEG), Technische Universität Wien: Vienna, Austria, 2010.
95. Resch, G.; Kranzl, L.; Faninger, G.; Geipel, J. *Block 1: Introduction: Energy & Climate Challenge and Basics of Economic Assessment*; VO Economic Perspectives of Renewable Energy Systems, Energy Economics Group (EEG), Technische Universität Wien: Vienna, Austria, 2020.
96. Resch, G.; Liebmann, L.; Ortner, A.; Busch, S.; Panzer, C.; Del Rio, P.; Ragwitz, M.; Steinhilber, S.; Klobasa, M.; Winkler, J.; et al. *Design and Impact of a Harmonised Policy for Renewable Electricity in Europe: Final Report of the beyond 2020 Project—Approaches for a Harmonisation of RES(-E) Support in Europe*; Energy Economics Group (EEG), Technische Universität Wien: Vienna, Austria, 2014.
97. Austrian Energy Agency. Zahlen & Fakten: Energiepreisindex (EPI) der Österreichischen Energieagentur. 2021. Available online: <https://www.energyagency.at/fakten-service/energiepreise/httpswwwenergyagencyatepi.html> (accessed on 29 June 2021).
98. Pehnt, M.; Mellwig, P.; Claus, L.; Blömer, S.; Brischke, L.-A.; von Oehsen, A.; Künz, C.; Voss, K.; Heinze, M.; Spars, G.; et al. *100% Wärme aus Erneuerbaren Energien? Auf dem Weg zum Niedrigstenergiehaus im Gebäudebestand. Endbericht Band 2: Szenarien und Perspektiven des Gebäudebestandes*; Institut für Energie- und Umweltforschung Heidelberg: Heidelberg, Germany, 2013.
99. Siegemund, S.; Trommler, M.; Kolb, O.; Zinnecker, V.; Schmidt, P.; Weindorf, W.; Zittel, W.; Raksha, T.; Zerhusen, J. “E-Fuels” Study: The Potential of Electricity-Based Fuels for Low-Emission Transport in the EU, Deutsche Energie-Agentur (DENA); Ludwig-Bölkow-Systemtechnik GmbH: Berlin, Germany, 2017.
100. E-Control. Preisentwicklungen—Strom: Berichtsjahr 2020. 2021. Available online: <https://www.e-control.at/statistik/strom/marktstatistik/preisentwicklung> (accessed on 28 June 2021).
101. E-Control. Preisentwicklungen—Gas: Berichtsjahr 2020. 2021. Available online: <https://www.e-control.at/statistik/gas/marktstatistik/preisentwicklung> (accessed on 28 June 2021).
102. Eltrop, L.; Härdtlein, M.; Jenssen, T.; Henßler, M.; Kruck, C.; Özdemir, E.D.; Poboss, N.; Scheffknecht, G.; Hartmann, H. *Leitfaden Feste Biobrennstoffe, Fachagentur Nachwachsende Rohstoffe E.V.*; Universität Stuttgart: Stuttgart, Germany, 2014.
103. Kalab, O. Systemnutzungsentgelte für Strom werden angehoben. WKO Oberösterreich. 2020. Available online: <https://www.wko.at/service/ooe/umwelt-energie/Die-Strom-Netztarife-2021-im-Detail.pdf> (accessed on 25 October 2021).
104. Kasten, P.; Mottschall, M.; Köppel, W.; Degünther, C.; Schmied, M.; Wüthrich, P. *Erarbeitung einer Fachlichen Strategie zur Erarbeitung einer Fachlichen Strategie zur Energieversorgung des Verkehrs bis zum Jahr 2050*; Umweltbundesamt Deutschland: Berlin, Germany; Öko-Institut Berlin: Berlin, Germany; DVGW-Forschungsstelle am Engler-Bunte-Institut am KIT: Karlsruhe, Germany; INFRAS AG Bern: Bern, Switzerland, 2016.
105. EXAA. Die EXAA Strombörse: Historische Marktdaten. Energy Exchange Austria, Vienna. 2021. Available online: <https://www.exaa.at/marktdaten/historische-marktdaten/> (accessed on 10 March 2021).
106. European Energy Exchange AG. Spotmarkt: EEX EUA SPOT. Leipzig, 2021. Available online: <https://www.eex.com/de/marktdaten/umweltprodukte/spotmarkt> (accessed on 4 December 2021).
107. Republik Österreich. Mineralölsteuergesetz 1995: Bundesgesetz, mit dem die Mineralölsteuer an das Gemeinschaftsrecht angepaßt wird. Rechtsinformationssystem des Bundes. 2021. Available online: <https://www.ris.bka.gv.at/GeltendeFassung.wxe?Abfrage=Bundesnormen&Gesetzesnummer=10004908> (accessed on 29 June 2021).
108. Schmidl, C. Bioenergielösungen im Neubau. Broschüre Erneuerbare Wärme des Österreichischen Biomasseverband, Ed.: 05/2013, Graz. 2014. Available online: https://www.waermeausholz.at/fileadmin/content/downloads/Schmidl_Bioenergie_im_Nebau_erweitert.pdf (accessed on 25 October 2021).
109. Terlouw, W.; Peters, D.; van Tilburg, J.; Schimmel, M.; Berg, T.; Cihlar, J.; Mir, G.U.R.; Spöttle, M.; Staats, M.; Lejaretta, A.V.; et al. *Gas for Climate: The Optimal Role for Gas in a Net-Zero Emissions Energy System*; Navigant Netherlands B.V.: Utrecht, The Netherlands, 2019.
110. NREL. H2A: Hydrogen Analysis Production Models: Case Studies 2018. National Renewable Energy Laboratory, Denver. 2018. Available online: <https://www.nrel.gov/hydrogen/h2a-production-models.html> (accessed on 28 June 2021).
111. European Union. ‘Fit for 55’: Delivering the EU’s 2030 Climate Target on the Way to Climate Neutrality, Communication from the Commission to the European Parliament, the Council, the European Economic and Social Committee and the Committee of the Regions. Brussels. 2021. Available online: <https://eur-lex.europa.eu/legal-content/EN/TXT/PDF/?uri=CELEX:52021DC0550&from=EN> (accessed on 25 October 2021).
112. Bundeskanzleramt Österreich. Aus Verantwortung für Österreich: Regierungsprogramm Die neue Volkspartei und Die Grünen 2020–2024, Vienna. 2020. Available online: https://www.dieneuevolkspartei.at/Download/Regierungsprogramm_2020.pdf (accessed on 25 October 2021).
113. Bundesministerium für Nachhaltigkeit und Tourismus. *Integrierter Nationaler Energie- und Klimaplan für Österreich: Periode 2021–2030. gemäß Verordnung (EU) 2018/1999 des Europäischen Parlaments und des Rates über das Governance-System für die Energieunion und den Klimaschutz, Bundesministerium für Nachhaltigkeit und Tourismus*; Bundesministerium für Nachhaltigkeit und Tourismus: Vienna, Austria, 2019.

114. Kranzl, L. *Bioenergy—A Key Option within all Energy Sectors*; VO Economic Perspectives of Renewable Energy Systems, Energy Economics Group (EEG), Technische Universität Wien: Vienna, Austria, 2020.
115. Stanzer, G. *Regio Energy: Potentiale*. Österreichisches Institut für Raumplanung, Vienna. 2010. Available online: <https://regioenergy.oir.at/methodik/potenziale2008> (accessed on 25 October 2021).
116. Dißauer, C.; Rehling, B.; Strasser, C. *Machbarkeitsuntersuchung Methan aus Biomasse, Bioenergy 2020+, Fachverband der Gas- und Wärmeversorgungsunternehmen*; Österreichischer Biomasseverband: Wieselburg, Austria, 2019.
117. Lindorfer, J.; Tichler, R.; Steinmüller, H. *Erhöhung des Einsatzes von erneuerbarem Methan im Wärmebereich: Modul 1 und Modul 2*; Johannes Kepler Universität Linz: Linz, Austria, 2017.
118. Höher, M.; Holzmann, A.; Strimitzer, L. *Netzeinspeisung von erneuerbarem Gas: Volkswirtschaftliche Effekte des Ausbaus von Erzeugungskapazitäten für erneuerbare Gase und deren Einspeisung in das Gasnetz*; Fachverband der Gas- und Wärmeversorgungsunternehmen: Vienna, Austria, 2019.
119. Kienberger, T. *Technisches Potenzial an Synthetischem Methan aus Biogenen Ressourcen*. Montanuniversität Leoben; Lehrstuhl für Energieverbundtechnik: Leoben, Austria, 2018.
120. Bundesforschungs- und Ausbildungszentrum für Wald, Naturgefahren und Landschaft, 2018. Österreichische Waldinventur (ÖWI). Vienna. 2018. Available online: <http://bfw.ac.at/rz/wi.home> (accessed on 25 October 2021).
121. Münch, J. *Nachhaltig Nutzbares Getreidestroh in Deutschland*; Institut für Energie- und Umweltforschung Heidelberg (ifeu): Heidelberg, Germany, 2008.
122. Gollner, M.; Sterzl, J.G. *Gesamtenergiebilanz Österreich 1970 bis 2019*, Vienna. 2020. Available online: https://www.statistik.at/web_de/statistiken/energie_umwelt_innovation_mobilitaet/energie_und_umwelt/energie/energiebilanzen/index.html (accessed on 25 October 2021).
123. Statistik Austria. *Feldfrüchte: Feldfruchternte 2020*. Vienna, 2020. Available online: http://www.statistik.at/web_de/statistiken/wirtschaft/land_und_forstwirtschaft/agrarstruktur_flaechen_ertraege/feldfruechte/index.html (accessed on 25 October 2021).
124. Statistik Austria. *Feldfruchtproduktion ab 1970: STATcube*. Statistik Austria—Direktion Raumwirtschaft—Pflanzliche Produktion. Vienna, 2020. Available online: <https://statcube.at/statistik.at/ext/statcube/jsf/dataCatalogueExplorer.xhtml> (accessed on 25 October 2021).
125. Kaltschmitt, M.; Hartmann, H.; Hofbauer, H. *Energie aus Biomasse: Grundlagen, Techniken und Verfahren, 3. Aktualisierte und Erweiterte Auflage*; Springer Vieweg: Berlin/Heidelberg, Germany, 2016; ISBN 3662474379.
126. Büchele, R.; Haas, R.; Hartner, M.; Hirner, R.; Hummel, M.; Kranzl, L.; Müller, A.; Ponweiser, K.; Bons, M.; Grave, K.; et al. *Endbericht—Bewertung des Potenzials für den Einsatz der hocheffizienten KWK und effizienter Fernwärme- und Fernkälteversorgung*; Austrian Heat Map, Energy Economics Group (EEG), Institut für Energietechnik und Thermodynamik, Technische Universität Wien; Ecofys, Vienna. 2015. Available online: <http://www.austrian-heatmap.gv.at/ergebnisse/> (accessed on 25 October 2021).
127. Bostjančič-Feinig, A. *Umsetzungskonzept der Klima- und Energie-Modellregion Carnica Rosental: Die Energiediversitätsregion—B569605, Klima- und Energie-Modellregion 2015*; Carnica Rosental: Ferlach, Austria, 2016.
128. ENTSO-E; ENTSG. *TYNDP 2022—Scenario report*, Brussels. 2022. Available online: https://entsos-tyndp-scenarios.eu/wp-content/uploads/2022/04/TYNDP2022_Joint_Scenario_Full-Report-April-2022.pdf (accessed on 22 August 2022).

Curriculum Vitae

Dipl.-Ing. Martin Hammerschmid

Date and place of birth: [REDACTED]
Address: [REDACTED]
Place of residence: [REDACTED]
Telephone number: [REDACTED]
E-mail address: [REDACTED]
Citizenship: [REDACTED]



Professional career

04/2019 - 12/2023

TU Wien, 1060 Vienna

Project assistant (PhD) at Institute of Chemical, Environmental and Bioscience Engineering

Research Area „Industrial Plant Engineering & Application of Digital Methods”

- Processing and Leading of industry-related research projects
 - o „Digital Twins“ of thermo-chemical energy plants
 - o Techno-economic and ecological assessment of renewable energy technologies
 - o Process simulation

09/2017 - 03/2019

Energy & Chemical Engineering GmbH, 1140 Vienna

Process engineer

- Process simulation
- Basic Engineering of energy plants

08/2016

Federation of Austrian Industries, 1030 Vienna

Trainee Resources & Infrastructure / Innovation & Technology

- Collaboration in the preparation of a statement on the Green Paper of the integrated energy & climate strategy of the BMWWF
- Writing briefings on biofuels

Education

04/2019 - Present

TU Wien

Doctoral program chemical engineering with focus on digital twins in the process development

10/2016 - 02/2019

TU Wien

Master program chemical engineering
Specialization Apparatus & Plant Engineering with focus on Environment & Resources

03/2016 - 02/2019

WU Wien

Participation in selected courses

01/2017 - 06/2017

KTH Stockholm

Semester abroad
Industrial Engineering & Management

10/2013 - 10/2016

TU Wien

Bachelor program chemical engineering

Professional Skills

MS Office (very good knowledge – Outlook, Word, Excel, PowerPoint, Visio, Publisher, Teams, Project, OneNote, OneDrive)

CAD (very good knowledge – AutoCAD, Inventor, Creo, Catia)

Prozesssimulation (very good knowledge – IPSEpro, SysCAD, Aspen Plus, HSC Chemistry)

Programmieren (good knowledge – VBA, Python, MATLAB)

Cloud Computing (basic knowledge – Microsoft Azure)



Dipl.-Ing. Martin Hammerschmid

Professional career

03/2013 - 09/2013

TU Wien, 1060 Vienna

Project assistant at Institute of Chemical, Environmental and Bioscience Engineering

Research Area „Sustainable Energy Technologies“

- Design and implementation of a warehousing concept
- Procurement of plant components
- Preparation of construction drawings
- Commissioning and supervision of the manufacture of plant components
- Conference Organization & Project Marketing

08/2011

ITT Austria, 2000 Stockerau

Trainee Design department

- Design of a pump test bench
- Preparation of construction drawings

07/2011

Voith Paper GmbH, 3100 St. Pölten

Trainee Process development

- Standardization of crossbars (CAD)
- Database implementation

Additional qualifications

Various rethoric and teambuilding seminars

Certificate as environmental officer (ISO 14001 and EMAS)

Certificate as waste management officer (AWG 2002)

Training as paramedic

Language skills

German (mother tongue)

English (business fluent)

Semester abroad in Stockholm

Swedish (basics)

Semester abroad in Stockholm

Voluntary engagement

07/2016 - present

Head of youth department

soccer club Röschitz

(Foundation youth soccer project

„Fußballnachwuchs Wein4tel West“)

01/2022 - 12/2023

Board member SAVT

(Association for students and graduates of process engineering)

09/2017 - 06/2019

Project Lernblitz

(Learning support for children with cancer)

09/2007 - 12/2021

Member music association Röschitz

11/2010 - 11/2013

District chairman Landjugend NÖ

(Medal of honor LJ NÖ)

Social Media Links

